Experimental Condensed Matter Physics Principal Investigators' Meeting–2015

September 28–30, 2015

Hilton Washington DC North/Gaithersburg, Gaithersburg, MD

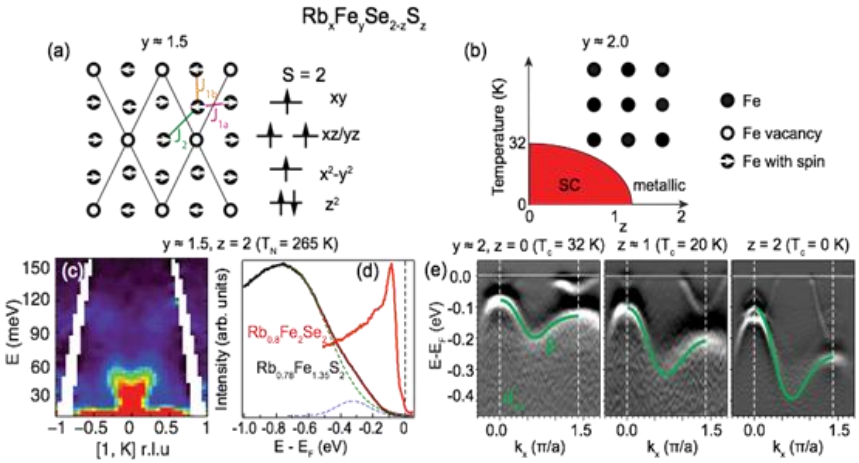

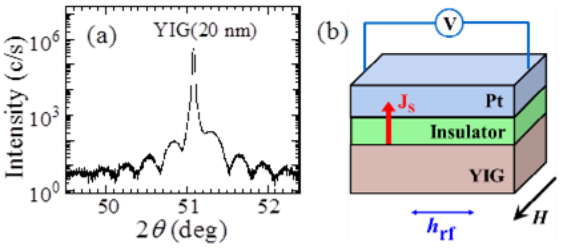

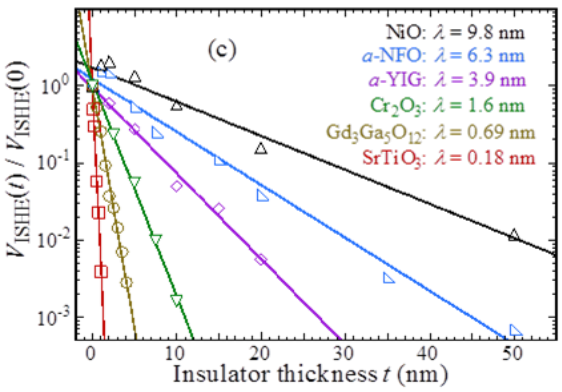

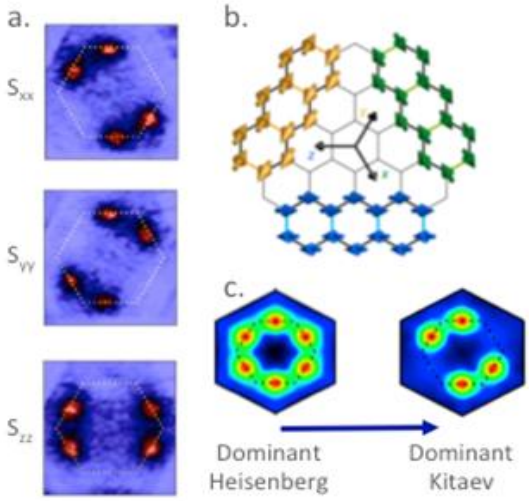

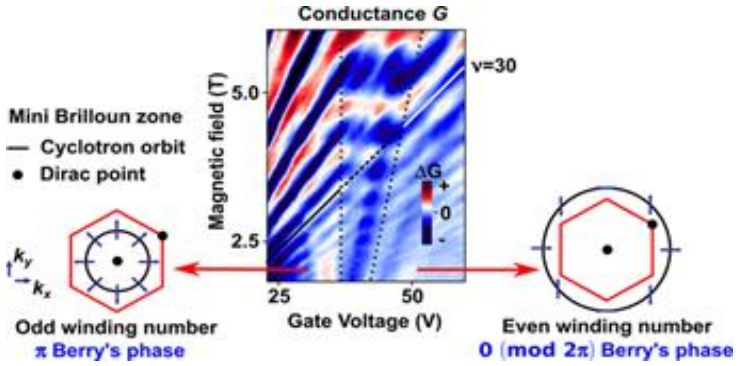

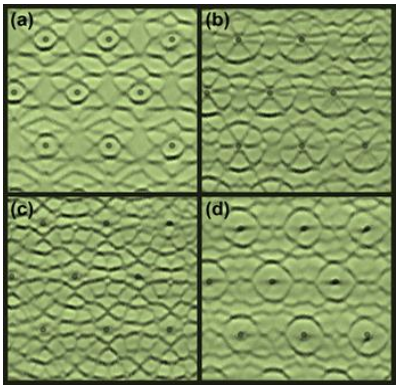

U.S. DEPARTMENT OF ENERGY | Office of Science

Office of Basic Energy Sciences
Materials Sciences and Engineering Division

On the Cover

Shown are selected figures from abstracts submitted to the ECMP PI Meeting and contained in this book. They are, with abbreviated descriptive titles (clockwise from upper left):

- Phases in Quantum Materials. Joe Orenstein, lead PI. Lawrence Berkeley National Laboratory.
- Antiferromagnonic Spin Transport. Fengyuan Wang, lead PI. Ohio State University.
- Conductivity of Graphene/Hexagonal Boron Nitride Superlattices. Jeanie Lau, PI. UC – Riverside.
- Dynamic Mode MFM of Superconducting Islands on Metal. Nadya Mason, lead PI. University of Illinois.
- Kitaev Interactions in Honeycomb Iridates. John Mitchell, lead PI. Argonne National Laboratory.

This document was produced under contact number DE-AC05-06OR23100 between the U.S. Department of Energy and Oak Ridge Associated Universities.

The research grants and contracts described in this document are supported by the U.S. DOE Office of Science, Office of Basic Energy Sciences, Materials Sciences and Engineering Division.

Foreword

This book contains abstracts for presentations made at the 2015 Experimental Condensed Matter Physics Principal Investigators' Meeting sponsored by the Materials Sciences and Engineering Division of the US Department of Energy, Office of Basic Energy Sciences (DOE-BES). The meeting convenes scientists supported by the DOE-BES program in Experimental Condensed Matter Physics to present the most exciting, new research accomplishments and proposed future research directions in their BES supported projects. The meeting also affords PIs in the program an opportunity to see the full range of research currently being supported. We hope the meeting fostered a collegial environment to (1) stimulate the discussion of new ideas and (2) provide unique opportunities to develop or strengthen collaborations among PIs. In addition, the meeting provides valuable feedback to DOE-BES in its assessment of the state of the program and in identifying future programmatic directions. The meeting was attended by approximately 100 scientists presenting their research in a mix of oral and poster sessions.

The Experimental Condensed Matter Physics program covers a broad range of research activities supporting experimental research with the goal of fundamentally understanding the relationships between intrinsic electronic structure and the properties of complex materials. The program focus is largely on systems whose static and dynamic behavior derives from strong electron correlation effects, competing or coherent quantum interactions, effects of interfaces, defects, anisotropy and reduced dimensionality. Scientific themes include superconductivity, magnetism, low-dimensional electron systems, and nanoscale systems. The program also supports studies of materials under extreme conditions such as ultra-low temperatures and ultra-high magnetic fields. In the last few years the program has increased support for research in the areas of quantum materials, spin physics, topological materials, materials far from equilibrium, and highly anisotropic materials to provide new insights into the evolution of correlated electron behavior in condensed matter systems. Improving understanding of the electronic behavior of complex materials on the atomic, nano and mesoscopic scales is relevant to the DOE mission, as these materials offer enhanced properties potentially leading to dramatic improvements in wide-ranging technologies needed for efficient energy generation, conversion, storage, delivery, and use.

The meeting was organized into ten oral and two poster sessions covering the range of activities supported by the program. These areas included research on correlated electrons, superconductivity, magnetism, spin physics, nano-systems, semiconductors, photonic systems and two-dimensional electron systems. We thank all the participants for their investment of time and for their willingness to share their ideas with the meeting participants. We also want to gratefully acknowledge the excellent support provided by Ms. Linda Severs of the Oak Ridge Institute for Science and Education and by Ms. Teresa Crockett of BES, for their efforts in organizing the meeting.

Dr. Michael (Mick) Pechan
Program Manager, Condensed Matter and Materials Physics
Division of Materials Sciences and Engineering
Basic Energy Sciences

Table of Contents

Experimental Condensed Matter Physics
Principal Investigators' Meeting Agenda

Monday, September 28, 2015

7:30–8:15am	*****Breakfast*****
8:15–8:40am	*Introductory Remarks* **Mick Pechan**
Session I	Chair: **Philip Kim**, Harvard University
8:40–9:00am	**Pablo Jarillo-Herrero** – Massachusetts Institute of Technology *Quantum transport in topological insulator nanoelectronic devices*
9:00– 9:20am	**Jeanie Lau**, University of California, Riverside *Spontaneous and field-induced symmetry breaking in low dimensional nanostructures*
9:20–9:40am	**Ramesh Mani,** Georgia State University *Magnetotransport studies of low-dimensional electron systems based on GaAs/AlGaAs heterostructures and graphene*
9:40–10:00am	**Bob Westervelt**, Harvard University *Imaging electrons in atomically layered materials*
10:00–10:30am	*****Break*****
Session II	Chair: **Tom Lemberger**, Ohio State University
10:30–10:50am	**Luis Balicas,** Florida State University *Novel and unconventional superconductors: quantum critically and possible field-induced superconducting states*
10:50–11:10am	**Girsh Blumberg** – Rutgers University *The chirality density wave of the "hidden order" phase in URu_2Si_2*
11:10–11:30am	**Ian Fisher** – SLAC National Accelerator Laboratory *Correlated materials – synthesis and physical properties*
11:30-11:50am	**Johnpierre Paglione,** University of Maryland *Non-centrosymmetric topological superconductivity*
11:50–12:10pm	**Brian Maple**, University of California, San Diego *Superconductivity and magnetism in d- and f-electron materials*
12:10–1:35pm	*****Working Lunch***** *(Meeting Discussions)*
Session III	Chair: **Axel Hoffman,** Argonne National Laboratory
1:35–2:10pm	**Linda Horton**, Director of Materials Science & Engineering *DMSE Overview*

2:10–2:30pm	**Geoff Beach**, Massachusetts Institute of Technology *Interface-driven chiral magnetism in ultrathin metallic ferromagnets: towards skyrmion spintronics*
2:30-2:50pm	**Frances Hellman,** Lawrence Berkeley National Laboratory *Non-equilibrium magnetism: materials and phenomena*
2:50-3:10pm	**FengyuanYang,** Ohio State University *Novel regimes of spin transport: pure spin currents in antiferromagnets and time-resolved studies of spin dynamics*
3:10-3:40pm	*****Break*****
Session IV	Chair: **Jan Musfeldt,** University of Tennessee
3:40-4:00pm	**Ted Hodapp,** American Physical Society *APS conference for undergraduate women in physics*
4:00–4:20pm	**Dave Sellmyer,** University of Nebraska *Physics of nanoscale magnets*
4:20–4:40pm	**Adam Kaminski,** Ames Laboratory (**Paul Canfield FWP)** *Complex states, emergent phenomena, and superconductivity in intermetallic and metal-like compounds*
4:40–5:00pm	**Michael McGuire,** Oak Ridge National Laboratory (**Brian Sales FWP)** *Correlated and complex materials*
5:00–5:20pm	**Poster Session I Introductions**
5:20–5:40pm	*****Free Time*****
5:40–7:00pm	*****Working Dinner***** (Scientific Highlights of the day: Discussion and Input from Attendees)
7:00–9:00pm	**Poster Session I**

Tuesday, September 29, 2015

7:30–8:30am	*****Breakfast*****
Session V	Chair: **Mansour Shayegan,** Princeton University
8:30-8:50am	**Lloyd Engel**, Florida State University *High magnetic field microwave spectroscopy of two-dimensional electron systems in GaAs and graphene*
8:50-9:10am	**Aron Pinczuk**, Columbia University *Artificially structured semiconductors to model novel quantum phenomena*

9:10-9:30am	**Michael Zudov**, University of Minnesota *Emergent phenomena in quantum hall systems far from equilibrium*
9:30-9:50am	**Wei Pan,** Sandia National Laboratories *Quantum electronic phenomena and structures*
9:50-10:10am	**Ray Ashoori**, Massachusetts Institute of Technology *Novel temperature limited tunneling spectroscopy of quantum hall systems*
10:10-10:40am	*****Break*****
Session VI	Chair: **Jun Kono**, Rice University
10:40-11:00am	**Dragomir Davidovic**, Georgia Tech *Electronic manipulation of magnetization in zero-dimensional magnets*
11:00-11:20am	**Nadya Mason**, University of Illinois, Champaign *Controlling superconductivity via tunable nanostructure arrays*
11:20-11:40am	**Ali Yazdani**, Princeton University *Probing correlated superconductors and their phase transitions on the nanometer scale*
11:40-12:00pm	**Alex Zettl**, Lawrence Berkeley National Laboratory *Novel sp2-bonded materials and related nanostructures*
12:00-1:30pm	*****Working Lunch***** *(Meeting Discussions)*
Session VII	Chair: **John Mitchell**, Argonne National Laboratory
1:30-1:50pm	**Dennis Drew**, University of Maryland *Infrared hall effect in correlated electronic materials*
1:50-2:10pm	**Gunter Luepke**, College of William and Mary *Time-resolved spectroscopy of insulator-metal transitions: exploring low-energy dynamics in strongly correlated systems*
2:10-2:30pm	**Jon Simon,** University of Chicago *Dynamics of emergent crystallinity in photonic quantum materials*
2:30-2:50pm	**Gleb Finkelstein**, Duke University *Symmetries, interactions and correlation effects in carbon nanotubes*
2:50-3:20pm	*****Break*****
Session VIII	Chair: **Ilya Krivorotov,** University of California, Irvine
3:20-3:40pm	**Wai-Kwong Kwok**, Argonne National Laboratory *Superconductivity and magnetism*
3:40-4:00pm	**Leonardo Civale,** Los Alamos National Laboratory *Towards a universal description of vortex matter in superconductors*

4:00-4:20pm	**Joe Orenstein**, Lawrence Berkeley National Laboratory *Quantum materials*
4:20-4:40pm	**Ivan Schuller**, University of California, San Diego *Nanostructured materials: from superlattices to quantum dots*
4:40-5:00pm	**Poster Session II Introductions**
5:00-5:20pm	*****Free Time*****
5:20-7:00pm	*****Working Dinner***** Scientific Highlights of the day: Discussion and Input from Attendees)
7:00-9:00pm	**Poster Session II**

Wednesday, September 30, 2015

7:30-8:30am	*****Breakfast*****
Session IX	Chair: **Leonid Rokhinson,** Purdue University
8:30-8:50am	**Milind Kunchur**, University of South Carolina *Dissipative and fast-timescale phenomena in superconductors*
8:50-9:10am	**Lu Li,** University of Michigan *Probing high temperature superconductors with magnetometry in ultrahigh magnetic fields*
9:10-9:30am	**Ni Ni**, University of California, Los Angeles *Exploring superconductivity at the edge of magnetic or structural instabilities*
9:30-9:50am	**Leonid Butov,** University of California, San Diego *Cold exciton gases in semiconductor heterostructures*
9:50-10:20am	*****Break*****
Session X	Chair: **Doug Natelson**, Rice University
10:20-10:40am	**Anand Bhattacharya,** Argonne National Laboratory *Digital synthesis - a pathway to create and control novel states of condensed matter*
10:40-11:00am	**Greg MacDougall**, University of Illinois, Champaign *Establishing the consequences of intertwined order parameters in spatially modulated superconductors*
11:00-11:20am	**Min Ouyang**, University of Maryland *Exploring photon-coupled fundamental interactions in colloidal semiconductor based hybrid nanostructures*
11:20-12:00pm	*Open Discussion on Future Program Topics and Concluding Comments* **Mick Pechan**
12:00pm	**Meeting Adjourns**

Session I

Project Title: Quantum Transport in Topological Insulator Nanoelectronic Devices
Prof. Pablo Jarillo-Herrero
Massachusetts Institute of Technology, Department of Physics

i. Program Scope

This program aims to explore and understand quantum transport in topological insulator (TI) materials. TI-based electronic devices are attractive as platforms for spintronic applications[1], and for detection of emergent properties such as Majorana excitations[2], electron-hole condensates[3], and the topological magneto-electric effect[4]. Most theoretical proposals envision geometries consisting of a planar TI device integrated with materials of distinctly different physical phases (such as ferromagnets and superconductors). Experimental realization of physics tied to the surface states is challenging due to the ubiquitous presence of bulk carriers in most TI compounds as well as surface degradation during device fabrication.

In the past, we approached these challenges by developing two alternative device fabrication approaches: the first approach is based on contacting Bi_2Se_3 flakes exfoliated from a single crystal, which we employed for establishing that the surface channel supports electronic transport[5], that its density is tunable by a gate voltage, and that the surface-state's spin-helicity allows for a polarization-dependent photocurrent[6]. The second approach is based on patterning thin-films of Bi_2Se_3 grown in an ultra-high vacuum chamber. We investigated the nature of coherent transport in the TI system[7], where weak antilocalization (WAL) emerges as a consequence of the strong spin-orbit coupling in the system. Using low carrier density films we demonstrated that the contribution of both surfaces to coherent transport phenomena can be separated from each other as the system is tuned so that the bulk is largely removed. This principle, the additivity of phase coherent phenomena, is now widely acknowledged as an intrinsic property of multi-channel transport systems and is used as a measure of surface-dominated transport in TI systems.

ii. Recent Progress

Our work more recently focused on surface-sensitive probes which include tunneling spectroscopy and dual-gated transport. These are implemented in exfoliated devices of Bi_2Se_3 and $Bi_{1.5}Sb_{0.5}Te_{1.7}Se_{1.3}$ (BSTS), respectively. In both cases, we continue to use our development of an advanced fabrication technique based on exfoliated thin film transfer, which allows us to integrate TI layers into heterostructures including hexagonal Boron-Nitride (h-BN) and graphene. Here we focus on dual-gated transport in h-BN—TI heterostructures, through which we can begin to understand transport without bulk electrons.

Dual-Gated Devices

For this thrust, we continued development of a TI device architecture where both surfaces are separately controlled by gates (Figure 1(a)). Full control over both surfaces allows us to study the interplay between quantum oscillations on both surfaces, effects of Coulomb interactions between two TI surfaces, and potentially exciton condensations[8].

Obtaining a high quality dielectric suitable for dual-gating exfoliated TI crystals was a known challenge[5], which we addressed by adapting a mechanical transfer technique originally developed for graphene devices[9] to interface TI flakes with h-BN (see Fig. 1(a)). Not only is h-BN a robust dielectric, it may encapsulate the underlying layer, protecting it from contamination and reactions later in the fabrication process.

By utilizing this fabrication technique with the quaternary TI compound BSTS, we obtained fully surface-dominated behavior. In the bulk form, this material shows extremely low bulk electron density and mobility, resulting in strong indications of surface transport[10]. In thin exfoliated devices, evidence for surface-dominated transport was found, but the absence of bulk states was not confirmed[11,12]. Here, we fabricated dual-gated devices from BSTS and found clear evidence of transport through two surface states that are separately modulated by the top and bottom gate electrodes, as evidenced by the distinct resistance peaks found when modulating each gate (see Fig. 1(c)). For the first time, we observe independently tunable surface states on both the top and bottom surfaces.

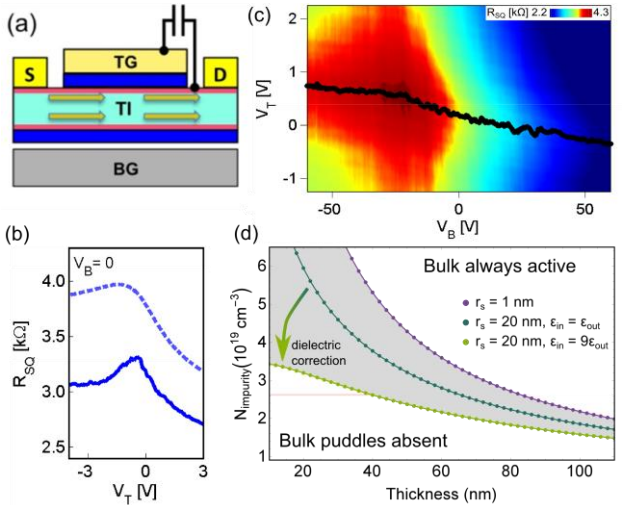

Figure 1: h-BN gated TI devices. (a) Cross-sectional schematic of a double-gated TI device. (b) Representative resistance vs top gate voltage trace. Lower curve at 4K, upper curve at room temperature. (c) Resistance (color) vs both gate voltages, with the upper surface resistance peak highlighted by black dots. (d) Theoretical modeling showing the boundary between regions of film thickness and impurity density in which bulk puddles do or do not exist. The three curves are for the strong screening limit (purple), weak screening with dielectric matching between the TI and environment (teal), and weak screening with realistic dielectric mismatch between the TI and environment (green).

In thin devices (~40 nm thick), the top surface resistance peak is clearly affected by voltages applied to *both* gate electrodes, which means that the surfaces are electrostatically coupled (see Fig. 1(c)) yet separately tunable. This implies that bulk electronic states are likely absent in thin devices (see next section). We have shown that the trajectory of the upper surface resistance peak in the space of both gate voltages contains information about the density of states of the lower surface state, which partially screens the electric field from the bottom gate. We developed an electrostatic model which allows us to linearly transform the gate-gate trajectory of the upper surface resistance peak into the energy-density relationship of the lower surface state. In Fig. 2(a), we show a fit of this data to a model for the surface state dispersion independently derived from angle-resolved photoemission spectroscopy. From this fit, we extract the bulk dielectric constant (ε_r~35) and the initial doping levels of the two surface states.

Additionally, we find the bottom gate couples much more strongly to the upper surface state at high magnetic field. This anomalous behavior implies the opening of a surface state band gap due to time-reversal symmetry breaking. Indeed, by using the same linear transformation, we find that the relationship between energy and density for the lower surface state develops a large "jump" near zero density, similar to that of a gapped system (Fig. 2(a)). This is corroborated by the temperature dependence of the resistance at total charge neutrality, which indicates a magnetic-field induced metal-insulator transition. If confirmed, this experiment would be the first direct observation of band-gap opening via externally induced time-reversal symmetry breaking. We additionally find that this

magnetic field-effect is still strong at high temperatures (Fig. 2(b)). The interlayer capacitance is somewhat diminished at high temperature (Fig. 2(c)), but the magnetic field effect on the density of states is roughly constant (Fig. 2(d)). More detailed studies are necessary to fully understand the behavior in this system at high magnetic fields. The majority of the work noted in this section has been published in Physical Review Letters.

Understanding Field Penetration in Thin Films

For a thicker device (80nm thick) we found that there was no electric field penetration through the bulk of the sample. We can understand this from a theoretical framework developed to explain the anomalously small energy gap measured in transport of macroscopic samples of compensation-doped materials like BSTS[13]. Since materials like BSTS have come to the forefront of surface-state dominated transport, understanding the effect of charged impurities in thin nanodevices is crucial. We expect that charged impurities in thick devices lead to bulk charge puddles that screen electric fields and contribute to transport. For thin devices, the surface-states screen the charged impurities, thereby reducing the disorder potential to the point that the bulk charge puddles no longer form. That means that as thickness increases there will be a crossover from a truly surface-state-only system to a bulk-active system, which we can see via electric field penetration. To this end, we have begun extending theories of charged impurities in TI surface states to the thin-film regime. Comparing the model with already-measured devices, we estimate the density of charged impurities to roughly 2.5 x 10^{19} cm^{-3} for our samples (see Fig. (1d)). A more thorough experimental thickness dependence coupled should enable us to deduce the true impurity density.

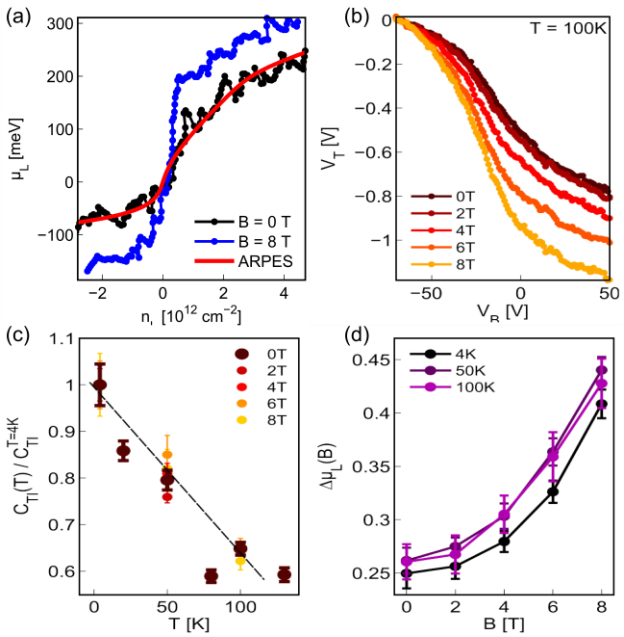

Figure 2: (a) Fit of the transport data to the ARPES-derived model of the band-structure, as well as the transformation of transport data at high magnetic field using the interlayer capacitance value found at B=0. (b) Offset gate-gate curves of R_{peak} at 100K, showing the significant magnetic field effect at high temperature. (c) Interlayer capacitance vs temperature, normalized to the low temperature value at a given magnetic field. The temperature dependence is the same for all magnetic fields. Dashed line is a guide to the eye. (d) Given a fixed capacitance (calibrated at B=0), we find that effect of magnetic field on the total chemical potential change is the same over a wide range of temperature.

iii. Future Plans

Thickness Limits of Electric Field Penetration

As mentioned in the text, we will continue to model the full TI system with disorder to fully understand the limits by which surface states can screen charged impurities to render a true bulk gap in a highly disordered TI.

Exploration of 2D Topological Semimetal WTe_2

Recent theoretical work has predicted specific transition metal dichalcogenide materials to be 2D topological insulators in the monolayer limit[14]. Experimentally, only WTe_2 has the correct structural polymorph in the bulk, which has already shown remarkable behavior in transport, including high mobility and precise matching of electron and hole densities[15]. Studying these properties in the 2D limit

in addition to searching for quantum spin Hall effects are of significant scientific interest, and we are well equipped to meet the challenges of this material in the monolayer form.

iv. References

1. Yazyev, O. V., Moore, J. E. & Louie, S. G. Spin Polarization and Transport of Surface States in the Topological Insulators Bi2Se3 and Bi2Te3 from First Principles. *Phys. Rev. Lett.* **105,** 266806 (2010).
2. Fu, L. & Kane, C. Superconducting Proximity Effect and Majorana Fermions at the Surface of a Topological Insulator. *Physical Review Letters* **100,** (2008).
3. Seradjeh, B., Moore, J. E. & Franz, M. Exciton Condensation and Charge Fractionalization in a Topological Insulator Film. *Phys. Rev. Lett.* **103,** 066402 (2009).
4. Qi, X.-L., Hughes, T. L., Raghu, S. & Zhang, S.-C. Time-Reversal-Invariant Topological Superconductors and Superfluids in Two and Three Dimensions. *Phys. Rev. Lett.* **102,** 187001 (2009).
5. Steinberg, H., Gardner, D. R., Lee, Y. S. & Jarillo-Herrero, P. Surface State Transport and Ambipolar Electric Field Effect in Bi2Se3 Nanodevices. *Nano Lett.* **10,** 5032–5036 (2010).
6. McIver, J. W., Hsieh, D., Steinberg, H., Jarillo-Herrero, P. & Gedik, N. Control over topological insulator photocurrents with light polarization. *Nat Nano* **7,** 96–100 (2012).
7. Steinberg, H., Laloë, J.-B., Fatemi, V., Moodera, J. S. & Jarillo-Herrero, P. Electrically tunable surface-to-bulk coherent coupling in topological insulator thin films. *Phys. Rev. B* **84,** 233101 (2011).
8. Gorbachev, R. V. *et al.* Strong Coulomb drag and broken symmetry in double-layer graphene. *Nat Phys* **8,** 896–901 (2012).
9. Dean, C. R. *et al.* Boron nitride substrates for high-quality graphene electronics. *Nat Nano* **5,** 722–726 (2010).
10. Ren, Z., Taskin, A. A., Sasaki, S., Segawa, K. & Ando, Y. Optimizing $Bi_{2-x}Sb_xTe_{3-y}Se_y$ solid solutions to approach the intrinsic topological insulator regime. *Phys. Rev. B* **84,** 165311 (2011).
11. Lee, J., Park, J., Lee, J.-H., Kim, J. S. & Lee, H.-J. Gate-tuned differentiation of surface-conducting states in $Bi_{1.5}Sb_{0.5}Te_{1.7}Se_{1.3}$ topological-insulator thin crystals. *Phys. Rev. B* **86,** (2012).
12. Xia, B. *et al.* Indications of surface-dominated transport in single crystalline nanoflake devices of topological insulator $Bi_{1.5}Sb_{0.5}Te_{1.8}Se_{1.2}$. *Phys. Rev. B* **87,** 085442 (2013).
13. Skinner, B., Chen, T. & Shklovskii, B. I. Effects of bulk charged impurities on the bulk and surface transport in three-dimensional topological insulators. *J. Exp. The. Phys.* **117,** 579–592 (2013).
14. Qian, X., Liu, J., Fu, L. & Li, J. Quantum spin Hall effect in two-dimensional transition metal dichalcogenides. *Science* **346,** 1344–1347 (2014).
15. Ali, M. N. *et al.* Large, non-saturating magnetoresistance in WTe2. *Nature* **514,** 205–208 (2014).

v. List of Papers

1. Ferhat Katmis, Valeria Lauter, Flavio S. Nogueira, et al. "Achieving high-temperature ferromagnetic topological insulating phase by proximity coupling." Under review in *Nature*.
2. Hadar Steinberg, Lucas E. Orona, Valla Fatemi, Javier Sanchez-Yamagishi, Pablo Jarillo-Herrero. "Transport Through Graphene-Topological Insulator Interfaces." Under review in *PRL*.
3. Yi-Hua Wang, John R. Kirtley, Ferhat Katmis, et al. "Observation of chiral currents at the magnetic domain boundary of a topological insulator." *Science* 349, 6251, pp. 948-952 (2015)
4. Fatemi, Valla, Benjamin Hunt, Hadar Steinberg, et al. "Electrostatic Coupling between Two Surfaces of a Topological Insulator Nanodevice." *Physical Review Letters* 113, 20 206801 (2014)
5. Yi-Hua Wang, Hadar Steinberg, Pablo Jarillo-Herrero, Nuh Gedik. "Observation of Floquet-Bloch States on the Surface of a Topological Insulator." *Science* 342, 6157, pp. 453-457 (2013)

Spontaneous and Field-Induced Symmetry Breaking in Low Dimensional Nanostructures

PI: Chun Ning (Jeanie) Lau
co-PI: Marc Bockrath
Department of Physics and Astronomy, University of California, Riverside, CA 92521

Program Scope

Electron-electron interactions can strongly modify the qualitative properties of low-dimensional materials. For example, one-dimensional (1D) systems exhibit Luttinger liquid behavior instead of Fermi liquid behavior, while two-dimensional (2D) systems exhibit the fractional quantum Hall effect. The goal of this program is to investigate and understand strongly correlated electron behavior using carbon nanotubes and graphene, which has emerged as archetypal 1D and 2D nanostructures. These systems will be studied via low temperature transport experiments and nanoelectromechanical measurements. The research program focuses the following projects: (1). symmetry-broken phases and quantum phase transitions in ultra-clean bilayer graphene (BLG); (2). symmetry-breaking, phase diagrams and stacking-order dependent transport of trilayer graphene (TLG); and (3). multicomponent quantum Hall ferromagnetism and phase transitions in the quantum Hall regime. Taken together, these proposed experiments will provide an in-depth investigation of how electron-electron interactions affect the properties of these exciting materials.

The first 2 projects are motivated by the instability of few-layer graphene to the formation of a correlated electron ground state[1-3]. A variety of states have been theoretically proposed, such as a gapped anomalous Hall state[4], a layer antiferromagnetic state[5] and gapless nematic states with reduced rotational symmetry[6, 7]; however, the exact nature of the ground state is under intense experimental and theoretical debate. We plan to investigate and establish the nature of the ground state in BLG and TLG, using dual-gated suspended devices with mobility as high as 300,000 cm^2/Vs. The devices' electrical properties will be measured as functions of electric field, perpendicular and parallel magnetic fields, charge density, disorder and temperature. Furthermore, since the various correlated states are in principle energetically comparable, we plan to explore possible quantum phase transitions among the phases and systematically map the phase diagram.

In the quantum Hall (QH) regime, the competing spin, valley and orbital symmetries in few-layer graphene allow various ordering possibilities and transitions via externally controlled parameters. This underlies exciting new quantum Hall and many body physics afforded by few-layer graphene as a quantum hall system. Yet, the nature of the symmetry-broken states is poorly understood and often under intense theoretical debate. We plan to investigate the integer QH states in BLG, explore their energy gaps and inter-Landau level transitions. Finally, improved mobility and device geometry should allow us to observe fractional quantum Hall states and examine their evolution with temperature and magnetic and electric fields.

For TLG, the presence of an extra layer affords additional symmetry and an intriguing parameter – stacking order. We have recently demonstrated that ABA-stacked TLG remains metallic at the Dirac point, whereas ABC-stacked TLG develops a spontaneous gap due to interactions[8]. We plan to explore the different ground states and phase diagrams in TLG with both stacking orders and transport across stacking domains. Comparison of the results with those found in BLG will provide us with fundamental insight into correlated electron phenomena in low dimensions.

Recent Progress

In the past two years, we have made significant progress in our studies of ultra-clean low dimensional nanostructures, focusing on ultra-clean graphene devices that are either suspended or supported on hexagonal BN substrates. Some of the works are highlighted below.

A. Distinct, Competing Ordered Filling Factor Two States In Bilayer Graphene

The quantum Hall effect, in which a two-dimensional sample's Hall conductivities become quantized, is commonly observed at strong magnetic fields. However, it may also appear at zero magnetic field if time reversal symmetry is broken. Charge-neutral bilayer graphene is unstable to a variety of competing and closely related broken symmetry states, some of which have non-zero quantized Hall conductivities. In this experiment we explore those states by stabilizing them with an external magnetic field. Transport spectroscopy measurements reveal two distinct states that have two quantum units of Hall conductivity, stabilized by large magnetic and electric fields, respectively. The majority spins of both phases form a quantum anomalous Hall state; the minority spins constitute a Kekulé state with spontaneous valley coherence for phase I, and a quantum valley Hall state for phase II. Our results shed light on the rich set of competing ordered states in bilayer graphene. This work is published by *Nature Communications.*

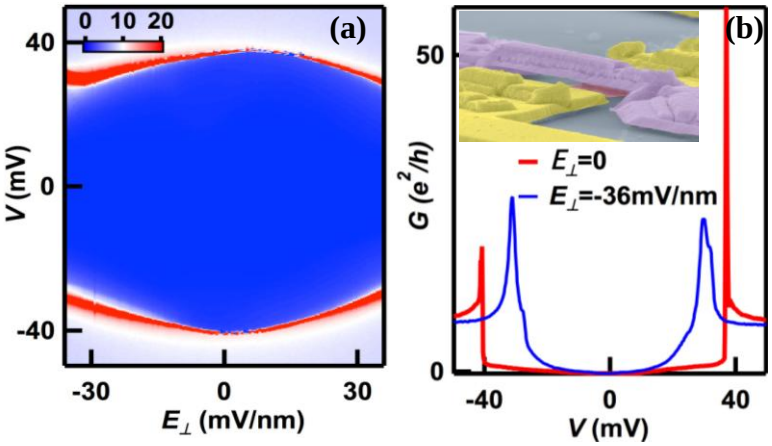

Fig. 1. (a) Conductance (color) in units of e^2/h *vs.* source-drain bias (vertical axis) and applied electric field $E_\perp$ (horizontal axis). The dark blue region represents an insulating gap, which is being closed symmetrically by $E_\perp$. (b). *G(V)* line traces at $E_\perp$=0 and -36mV/nm, respectively. Inset: an SEM image of a graphene sheet (red) suspended between electrodes (yellow) below a top gate (purple).

B. Giant Interaction-Induced Gap in Trilayer Graphene

ABC-stacked TLG, which is found in ~15% of all TLG sheets, has an unusual *cubic* dispersion relation, with the energy $E \sim k^3$, where k is the wavevector. This produces a very high density of states at the charge neutrality point, making it highly unstable to electronic interactions. Such inclination towards interaction-induced phases with broken symmetries is similar to, but even more so than that in bilayer graphene. Recently we have been able to fabricate dual-gated suspended ABC-stacked TLG devices (Fig. 1b inset) with mobility up to 150,000 cm^2/Vs. We found a strongly insulating state at the charge neutrality point, with a gap ~42 meV (Fig. 1). This gap can be partially suppressed by an interlayer potential, a parallel magnetic field or a critical temperature ~36K. Among the proposed correlated phases with spatial uniformity, our results are most consistent with a layer antiferromagnetic state with broken time reversal symmetry. These results reflect the interplay between externally induced and spontaneous symmetry breaking whose relative strengths are tunable by external fields, and provide insight into other low dimensional systems. This work was published by *Nature*

Communications. Such a large interaction-induced gap is exceedingly interesting for condensed matter physics, and may also be useful for THz technologies.

C. Moiré Superlattices in Graphene-hBN Heterostructures

We have recently made Graphene-hexagonal BN (hBN) heterostructure devices with the graphene and BN lattices aligned[9-11]. Due to the lattice constant mismatch between the two materials, this creates a lattice moiré pattern which produces a superlattice periodic potential within the graphene sheet. Our transport data on this system (Fig. 2) show many intriguing features, such as Hofstadter quantization and additional electron and hole states not present in ordinary graphene. The interplay between the quantizing magnetic field and the periodic lattice yields much new area for exploration. For example, much interesting behavior occurs for densities near the secondary Dirac points that occur at magnetic field B=0 on the electron and hole sides. Fig. 1 shows two-terminal conductance data versus gate voltage and magnetic field taken near the secondary Dirac point on the electron side. We observe a π phase shift in the Berry's phase associated with the electron orbits due to a change in topological winding number induced by the periodic potential. This shows how the Hofstadter butterfly spectrum can be altered by a topological number. The interplay between the quantizing magnetic field and the periodic lattice yields much new area for exploration. The manuscript describing this work has been submitted to *Nano Letters*.

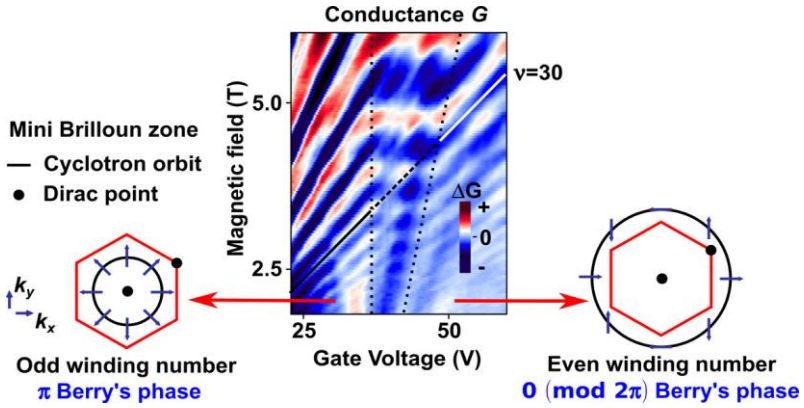

Fig. 2. Conductivity of a graphene/hBN superlattice device vs gate and magnetic field. The quantum oscillations show a shift in phase at constant filling factor ν, as shown by the line at ν=30 crossing through the transition region enclosed by the two dotted lines. This occurs when the cyclotron orbit size is tuned by the gate voltage to enclose the entire mini Brillouin zone, which results from a change in the topological winding number associated with the number of Dirac points enclosed by the reciprocal space orbit.

D. Fractional Quantum Hall Effect in Bilayer Graphene

We have recently observed fractional quantum Hall effect in suspended bilayer graphene tunable by an out-of-plane electric field $E_\perp$. Using bias spectroscopy, we are able to measure the Landau level gap of the state at filling factor ν=2/3 at finite $E_\perp$, which scales with magnetic field with a slope of ~0.16 meV/T. This fractional state, however, is only observed at non-zero electric field. A manuscript describing this work is in preparation.

Future Plans

Apart from the general direction outlined in the first section, our immediate plans for the next year include:

Symmetry-Broken Quantum Hall States in Trilayer Graphene

The band structure of ABA-stacked trilayer graphene is a combination of the linear dispersion of monolayer graphene and the quadratic dispersion of bilayer graphene. At the charge

neutrality point, the quantum Hall state at filling factor ν=0 has diverging longitudinal and transverse resistance. We plan to investigate evolution of this insulating state under out-of-plane electric field and in-plane magnetic field.

Away from the charge neutrality point, the monolayer and bilayer branches induces Landau level crossings, which can be modified by the application of electric field that breaks the mirror inversion symmetry. We plan to investigate the nature of the symmetry-broken quantum Hall states along the crossings. In high mobility samples, we also seek to explore fractional quantum Hall states and its dependence on electric field; since an out-of-plane electric field hybridizes the monolayer and bilayer branches, it is expected to have qualitatively different effect than in BLG.

Transport across stacking ABA-ABC stacking domains

Using Raman spectroscopy mapping, we are able to map and identify ABA-ABC stacking domains in individual TLG sheets. We would be able to fabricate devices to study transport across the stacking domain soon.

References

[1] M. Kharitonov, Phys. Rev. Lett. **109**, 046803 (2012).
[2] F. Zhang *et al.*, Phys. Rev. Lett. **106**, 156801 (2011).
[3] R. T. Weitz *et al.*, Science **330**, 812 (2010).
[4] R. Nandkishore, and L. Levitov, Phys. Rev. B **82**, 115124 (2010).
[5] J. Velasco *et al.*, Nature Nanotechnol. **7**, 156 (2012).
[6] Y. Lemonik *et al.*, Phys. Rev. B **82**, 201408 (2010).
[7] A. S. Mayorov *et al.*, Science **333**, 860 (2011).
[8] W. Bao *et al.*, Nat. Phys. **7**, 948 (2011).
[9] C. R. Dean *et al.*, Nature **497**, 598 (2013).
[10] L. A. Ponomarenko *et al.*, Nature **497**, 594 (2013).
[11] B. Hunt *et al.*, Science **340**, 1427 (2013).

Publications Supported by BES

1. J. Velasco Jr., Y. Lee, Z. Zhao, L. Jing, P. Kratz, M. Bockrath, and C. N. Lau, Transport Measurement of Landau level Gaps in Bilayer Graphene with Layer Polarization Control, Nano Lett. 14, 1324 (2014).

2. H. Zhang, J.-W. Huang, J. Velasco Jr., K. Myhro, M. Maldonado, D. Tran, Z. Zhao, F. Wang, Y. Lee, G. Liu, W. Bao, and C. N. Lau, Transport in suspended monolayer and bilayer graphene under strain: A new platform for material studies, Carbon 69, 336 (2014).

3. Y. Lee, D. Tran, K. Myhro, J. V. Jr., N. Gilgren, Y. Barlas, C. N. Lau, J. M. Poumirol, D. Smirnov and F. Guinea, "Competition Between Spontaneous Symmetry Breaking and Single Particle Gaps in Trilayer Graphene", *Nature Communications*, 5, 5656 (2014).

4. J. Velasco Jr., Y. Lee, F. Zhang, K. Myhro, D. Tran, M. Deo, D. Smirnov, A. H. MacDonald, C.N. Lau, "Observation of Distinct Competing Ordered □=2 States in Bilayer Graphene", *Nature Communications*, 5,4550 (2014).

5. T. Miao, S. Yeom, P. Wang, B. Standley, and M. Bockrath, Graphene Nanoelectromechanical Systems as Stochastic-Frequency Oscillators, *Nano Letters*, 2982-2987 (2014).

6. Juan Aguilera-Servin, Tengfei Miao and Marc Bockrath, "Nanoscale pressure sensors realized from suspended graphene membrane devices", *Applied Physics Letters*, 106, 083103 (2015).

Project Title: Magnetotransport Studies of Low Dimensional Electron Systems Based on GaAs/AlGaAs Heterostructures and Graphene

Principal Investigator: R. G. Mani
Mailing Address: Dept. of Physics, Georgia State University, Atlanta, GA 30303
E-mail: rmani@gsu.edu

Program Scope

Magneto-transport studies of low dimensional electron systems have contributed to exciting advances in condensed matter physics such as the discoveries of the integral and fractional quantum Hall effects in the Si-MOSFET and the GaAs/AlGaAs heterostructure systems, respectively, and the identification of Dirac fermions in sheets of carbon known as graphene. This research is concerned, in part, with comparing magneto-transport under equilibrium conditions with magnetotransport under steady-state non-equilibrium conditions attained under microwave- and terahertz- photoexcitation in such low dimensional electron systems. An aim of this research is to uncover novel emergent phenomena. Another aim of the research is to elucidate the electronic properties of such 2D materials.

Recent Progress

1. Size dependent giant magnetoresistance in millimeter-scale GaAs/AlGaAs device

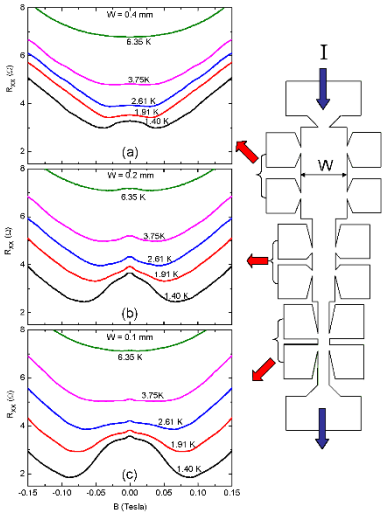

Fig. 1) Right: A sketch of the GaAs/AlGaAs Hall bar sample with three sections, with width W = 0.4, 0.2, and 0.1mm, respectively. (a) This panel shows R_{xx} [left-ordinate] and R_{xy} [right-ordinate] vs. the magnetic field, B, for the W = 0.4 mm section . (b) R_{xx} vs. B for the W = 0.2 mm section. (c) R_{xx} vs. B for the W = 0.1 mm section. The parameter appearing next to the data traces is the temperature, T , as indicated. These data suggest that a bell-shape magneto-resistance becomes wider with decreasing W, at each T.

Giant magnetoresistance is interesting from both the sensing-application-[1] and basic-physics- perspectives.[2] physically, semiconductor - magnetoresistance is interesting because it can provide insight into localization and scattering in disordered 2D electronic systems. Noteworthy topics here include weak localization, weak anti-localization, electron-electron interaction-induced magnetoresistance, metal-insulator transitions induced by a magnetic field.[2] Here, we examine a "bell-shape" negative GMR effect confined to B < 0.1 Tesla that grows in magnitude with decreasing temperatures, T, in the high mobility GaAs/AlGaAs 2DES. In devices sharing the same material characteristics at a constant temperature, T, we show that the span on the magnetic field, B, axis of the negative magnetoresistance increases with decreasing device width, W, without concurrent Hall resistance corrections, in millimeter-sized devices. A multi-conduction model captures the essential features of experiment. The results suggest that a "non-ohmic" temperature- and size- dependent negative diagonal conductivity term, possibly due to boundary-scattering-induced transport-constriction, might be responsible for the observed negative GMR effect. The results also serve to propose the possibility of novel zero-resistance states arising from such a negative magnetoresistance effect. Figure 1 exhibits the diagonal magnetoresistance, R_{xx}, of a triple Hall bar device, that is

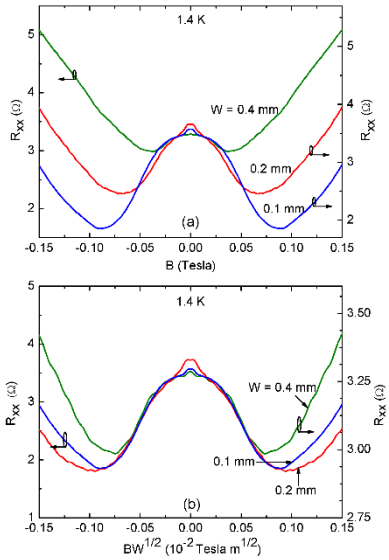

Fig. 2) (a) This panel compares the R_{xx} vs. B for W = 0.4, 0.2, and 0.1 mm sections at 1.4K. The panel suggests a monotonic increase in the full-width at half-maximum of the bell-shape magneto-resistance, with decreasing W. (b) At 1.4K, R_{xx} has been plotted vs. $BW^{1/2}$ in order to convey the size scaling observed for W = 0.4, 0.2, and 0.1 mm-wide Hall bars.

illustrated on the right side of Fig. 1. The length-to-width ratio L/W = 1 for each section. Panels (a), (b), and (c) of Fig. 1 show R_{xx} vs. B, over the temperature range $1.4 < T < 6.35$ K, for the W = 0.4, 0.2, and 0.1mm-wide devices, respectively. In all three panels, a positive magnetoresistance is evident at the highest temperature. As T is reduced, the R_{xx} at B = 0 Tesla decreases, and at the same time, negative magnetoresistance contributions become stronger with decreasing temperature. A close examination of the data indicates that two distinct negative magnetoresistance terms are discernable in Fig. 1(b) and (c). A first, small, negative magnetoresistance term, which will be examined in greater detail elsewhere, is restricted to $B < 0.01$ Tesla. A larger second term, which is the focus of this study, spans a wider B field range, $-0.1 < B < 0.1$ Tesla in Fig. 1(c), and exhibits the greater magnetoresistive contribution at the lowest T. For W = 0.1 mm, this term produces a nearly 50 per-cent reduction in R_{xx} over $B < 0.1$ Tesla. A comparison of panels (a), (b), and (c) also shows that, at a constant T, the typical width of this negative magnetoresistance contribution becomes larger at smaller device widths. Thus, these results empirically establish a size-dependent negative magnetoresistance effect in this high mobility GaAs/AlGaAs system.

Figure 2(a) exhibits a direct comparison of the R_{xx} for the three Hall bar sections of Fig. 1 at T = 1.4K. The striking feature observable in Fig. 2(a) is that the characteristic field scale for the "bell shape" negative magnetoresistance is strongly dependent upon the device width, as mentioned above. In order to illustrate that the functional form of the magnetoresistance is the same in the three devices, we re-plot in Fig. 2(b) the data of Fig. 2(a) as R_{xx} vs $BW^{1/2}$, where W is the device width. In Fig. 2(b), there is observable data collapse onto the same bell shape envelope. We have examined this effect is great detail and utilized a model to understand the observations.

2. Distribution of neutrality potentials, vanishing Hall effect, and the residual carrier density across the gate-controlled n←→p transition in graphene

The zero-bandgap in monolayer graphene allows for the gate-induced carrier type conversion, from holes to electrons, without crossing a bandgap.[3,4,5] When the Fermi level is placed at the Dirac point in monolayer graphene, one expects the density of carriers, n_q, i.e., electrons (n_e) and holes (n_h), to vanish, leading to a divergent Hall resistance, R_{xy}, and a diverging resistivity ρ_{xx}, since R_{xy} and ρ_{xx} are $\sim 1/n_q$. Remarkably, experiment has reported a finite, nearly quantized $\rho = \sigma^{-1} \sim h/4e^2$.[3] Here, we examine a Hall effect compensation over the p ←→ n transition, in CVD graphene,[6] which is characterized by vanishing- instead of diverging- Hall effect, in addition to $R_{xy} \rightarrow 0$ as $\rho_{xx} \sim h/4e^2$ at the nominal Dirac point. We reproduce these characteristics in an ambipolar conduction model with a parabolic distribution $f(V_N)$ of neutrality potentials, V_N. The results serve to extract the electron- and hole- densities as a function of the gate voltage, and

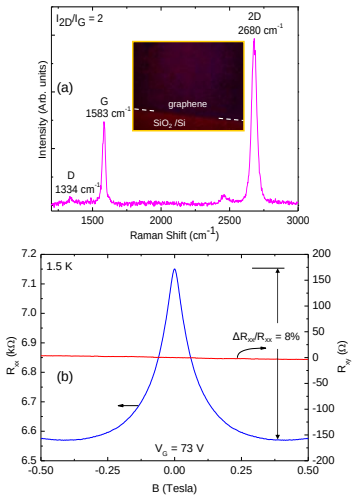

Fig. 3) (a) The Raman spectrum for graphene-on-SiO_2/Si-substrate. The D-, G-, and 2D-peaks have been marked. (b) The diagonal resistance, R_{xx}, and the Hall resistance, R_{xy}, have been plotted vs. the magnetic field, B, for a gate-voltage V_G = 73 V, close to the nominal neutrality point.

suggest that the applied current could be simultaneously carried by electrons and holes within spatially separated current domains.

Monolayer graphene was prepared using the CVD technique and processed into mm-scale devices. The inset of Fig. 3(a) shows the graphene on SiO_2/Si, while figure 3(a) exhibits the Raman spectrum. Here, the D-peak is small and the 2D-to-G intensity ratio, I_{2D}/I_G=2, suggests monolayer graphene. Figure 3(b) shows the diagonal resistance, R_{xx}, and R_{xy} vs. the magnetic field, B, at a back gate-voltage V_G = 73 V, close to the nominal neutrality voltage, ν = 72.8 V, for this specimen. The $|R_{xy}|$ = 3.7 Ω at B=0.5 Tesla suggests, in a single carrier model, that $n_e = 8.5 \times 10^{13}$ cm^{-2} at V_G = 73 V, while one expects $n_e < 1 \times 10^{12}$cm^{-2}.

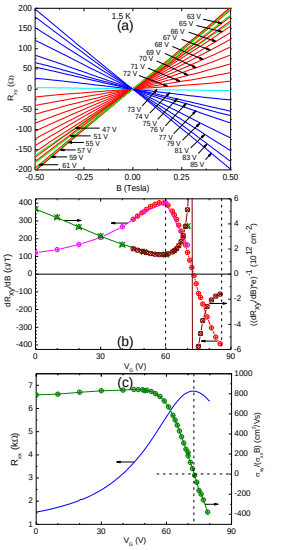

Fig. 4) (a) The Hall resistance, R_{xy}, is exhibited vs. B. (b) dR_{xy}/dB evaluated from panel (a) are plotted vs. V_G. The green and brown symbols show $((dR_{xy}/dB)e)^{-1} = n_q$ in a single carrier model. (c) The diagonal resistance R_{xx} (blue trace) is plotted vs. V_G The evaluated $\sigma_{xy}/\sigma_{xx}B$ (green symbols), would, in a single carrier model, suggest a precipitous drop in the hole mobility over the range 55 < V_G < 72V.

Figure 4 shows the overview of the approach of the vanishing Hall effect state at V_G=ν. dR_{xy}/dB evaluated from Fig. 4(a) are plotted vs. V_G in Fig. 4(b). Also shown with the green and brown symbols in Fig. 4(b), is $((dR_{xy}/dB)e)^{-1}$, which would equal the carrier density for single carrier conduction. The associated trace shows that $((dR_{xy}/dB)e)^{-1}$ decreases up to V_G ~ 50V as expected for hole depletion with increasing positive V_G. The trace then deviates from expectations as $((dR_{xy}/dB)e)^{-1}$ increases with increasing V_G between 60 < V_G < 72V, although one expects further hole depletion. The R_{xx} vs. V_G data, shown as the blue trace in Fig. 4(c), indicate R_{xx} = 6.5 kΩ ~ h/4e^2 at V_G = ν. The green trace in Fig. 4(c) shows $\sigma_{xy}/\sigma_{xx}B$ vs. V_G. A single carrier interpretation of this trace suggests, unphysically, that the mobility changes with V_G. In modeling the results, a two carrier Drude model including uniform, but gate-voltage dependent, electron and hole densities did not help to produce good fits of the data. Thus, we introduced a distribution function f(V_N), to produce a gradation in the neutrality potentials across the specimen, assumed the same mobility for electrons and holes, and summed the conductances of strips at different V_N. Expressions were then obtained for σ_{xx} and σ_{xy}; the resistivities were obtained by inverting the conductivity tensor. Using this model, we evaluated R_{xx} and dR_{xy}/dB. A least squares data-fit was carried out with ν and the width of f(V_N) as the fitting parameters. The analysis indicated that (a) for a broad range of V_G about ν= 72.8 V, there is non-vanishing n_e and n_h, unlike the expectations for ideal graphene, and (b) at ν, $n_h = n_e = 0.49 \times 10^{12}$ cm^{-2}. Thus, this approach helps us to determine the residual densities of electrons and holes at the nominal neutrality point with vanishing Hall effect.

Future Plans

(a) Install a helium-3 system to obtain lower temperature capability.
(b) In the GaAs/AlGaAs system, investigate size effect in giant magnetoresistance in higher mobility material.
(c) Examine overlap of radiation-induced zero-resistance states and quantum Hall effect.
(d) Examine influence of circularly polarized radiation on microwave induced magneto-resistance oscillations.
(e) Fabricate layered 2D systems using graphene, boron nitride, and MoS_2.
(f) Carry out equilibrium and non-equilibrium transport studies on these 2D systems.

References

1) J. Heremans, J. Phys. D: Appl. Phys. 26, 1149 (1993).
2) P. A. Lee and T. V. Ramakrishnan, Rev. Mod. Phys. 57, 287(1985)
3) A. K. Geim and K. Novoselov, Nat. Mat'l. 6, 183 (2007).
4) A. H. Castro-Neto et al., Rev. Mod. Phys. 81, 109 (2009).
5) S. Das Sarma, S. Adam, E. H Hwang, and E. Rossi, Rev. Mod. Phys, 83, 407 (2011).
6) X. Li et al., Science 324, 1312 (2009).

Publications (SUPPORTED BY BES)

1) Size-dependent giant-magnetoresistance in millimeter scale GaAs/AlGaAs 2D electron devices, R. G. Mani, A. Kriisa, and W. Wegscheider, Scientific Reports 3, 2747 (2013).
2) Magnetotransport characteristics of a 2D electron system driven to negative conductivity by microwave photoexcitation, R. G. Mani and A. Kriisa, Scientific Reports 3, 3478 (2013).
3) Remote sensor response study in the regime of the microwave radiation-induced magnetoresistance oscillations, T. Ye, R. G. Mani, and W. Wegscheider, Appl. Phys. Lett. 103, 192106 (2013).
4) Microwave reflection study of ultra-high mobility GaAs/AlGaAs 2D electron system at large filling factors, T. Ye, R. G. Mani, and W. Wegscheider, MRS Proc. 1635, pp 69-74 (2014).
5) Combined study of microwave-power/linear polarization dependence of the microwave radiation-induced magnetoresistance oscillations in GaAs/AlGaAs devices, T. Ye, H-C. Liu, W. Wegscheider, and R. G. Mani, Phys. Rev. B 89, 155307 (2014).
6) Evolution of the linear-polarization-angle-dependence of the radiation-induced magnetoresistance-oscillations with microwave power, T. Ye, R. G. Mani, and W. Wegscheider, Appl. Phys. Lett. 105, 191609 (2014).
7) Interaction of microwave radiation with the high mobility two-dimensional electron system in GaAs/AlGaAs heterostructures, A. N. Ramanayaka, T. Ye, H-C. Liu, W. Wegscheider, and R. G. Mani, Physica B 453, 43 (2014).
8) Frequency dependent polarization-angle-phase-shift in the microwave-induced magnetoresistance oscillations, H-C. Liu, T. Ye, W. Wegscheider, and R. G. Mani, J. Appl. Phys. 117, 064306 (2015).
9) Comparative study of microwave radiation-induced magnetoresistance oscillations induced by circularly and linearly polarized photo-excitation, T. Ye, H-C. Liu, Z. Wang, W. Wegscheider, and R. G. Mani, Scientific Reports (in press).

Program Title: Imaging Electrons in Graphene

Principal Investigator: Robert M. Westervelt, Co-PI: David Bell
Mailing Address: School of Engineering and Applied Sciences, Harvard University
29 Oxford Street, Cambridge MA 02138
Email: westervelt@seas.harvard.edu

Program Scope

Graphene is a promising new material with a long mean free path that permits the design and construction of ballistic electronics devices. In order to visualize the motion of electrons through graphene devices, we use a cooled scanning probe microscope (SPM) in Westervelt's lab [1-4] in conjunction with a high-resolution transmission electron microscope (TEM) in the Center of Nanoscale Systems (CNS) at Harvard, managed by David Bell.

Recent Progress - Imaging the Cyclotron Orbit of Electrons in Graphene

In a perpendicular applied magnetic field B, electrons in graphene travel in circles along cyclotron orbits with diameter:

$$d_c = (2\hbar/eB)\sqrt{\pi n} \qquad (1)$$

where e is the electronic charge and n is the electron density [5]. Magnetic focusing occurs in the flow between two point contacts, because electrons entering at the first contact bunch together again at the far side of the cyclotron orbit. A peak in transmission between the two point contacts occurs when $d_c = L$, where L is their separation separation. Additional peaks can occur when L is an integer multiple of d_c, because the electrons can bounce off the edge of the sample. Magnetic focusing has been previously imaged in a two-dimensional electron gas in a GaAs/AlGaAs device using our cooled SPM [3].

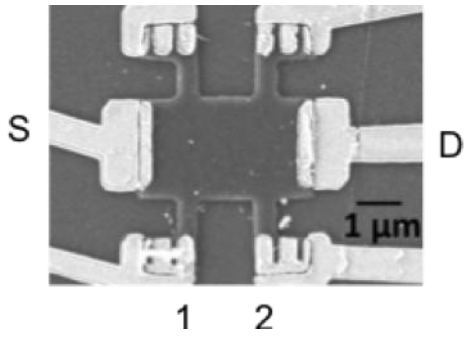

Fig. 1 High-mobility BN/graphene/BN sample with large end contacts and two narrow contacts 1 and 2 along each side.

Through a collaboration with Philip Kim, we studied the graphene Hall bar sample shown in Fig. 1. To increase the mobility, both sides of the graphene atomic layer are covered with hexagonal boron nitride (BN) sheets which are 30 nm thick. Magnetic focusing is sensed by injecting a small current I_i between point contact 1 and the grounded source (S) contact. Electrons circle around in a perpendicular applied magnetic field B and pile up at point contact 2, increasing the local chemical potential V_c. The measured voltage determines the transresistance $R_m = V_c / I_i$ which is proportional to the transmission coefficent for electrons travelling from point contacts 1 to 2. A heavily doped silicon substrate acts as a backgate to change the electron density.

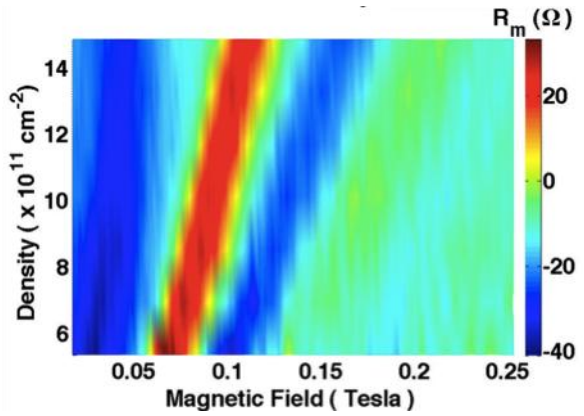

Fig. 2 Magnetic focusing in the transmission between point contacts 1 and 2 in Fig. 1.

Figure 2 displays magnetic focusing peaks for electrons flowing between point contacts 1 and 2 over a range of magnetic fields B and electron densities n. The first magnetic focusing peak is clearly shown (red stripe) and the second peak is also visible. The cyclotron diameter equals the point contact spacing along the first magnetic focusing peak.

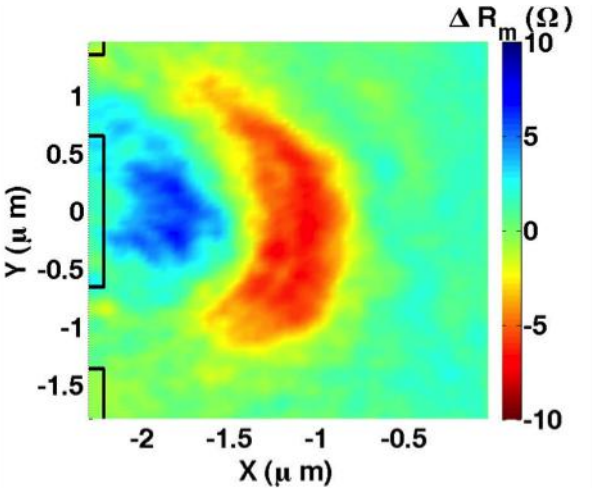

Fig. 3 SPM image of the cyclotron orbit at 4.2 K for electrons passing between contacts 1 and 2 on the first magnetic focusing peak for density n = 1.5 x 10^{12} cm^{-2} and B = 125 mT

Figure 3 shows a SPM image of the cyclotron orbit in graphene that connects the two point contacts (shown by the dark lines) on the first magnetic focusing peak. The image was recorded using our cooled scanning probe microscope [1-4] to image the path of electrons between point contacts 1 and 2. The SPM tip is held at a height h ~ 40 nm above the graphene, above the top BN layer. The tip charge creates an image charge in the graphene below with halfwidth ~ h, and the corresponding potential energy scatters electrons. In this way, the tip throws a downstream shadow in the flow of electrons past the tip location that reduces the electron transmission from point contact 1 to 2 and the corresponding transresistance R_m. An image of electron flow is obtained by displaying the change ΔR_m, as the tip is raster scanned above the sample. We first used this technique to image magnetic focusing in the 2DEG inside a GaAs/AlGaAs heterostructure [3].

In Fig. 3, the circular cyclotron orbit connecting the two point contacts is clearly shown in the red region - scattering by the tip knocks electrons away from their original path, reducing the transmission. When the tip is near the edge between the two contacts in the blue region of the image, it increases transmission by bouncing electrons that would not have reached the second point contact back into the sample.

Figure 4 presents SPM images of the cyclotron orbit connecting the two point contacts that was recorded at a series of density / magnetic-field combinations along the first magnetic focusing peak. Their form is quite similar, providing a strong verification of our interpretation. The effect of the tip's image charge is proportionally greatest at low density, as expected.

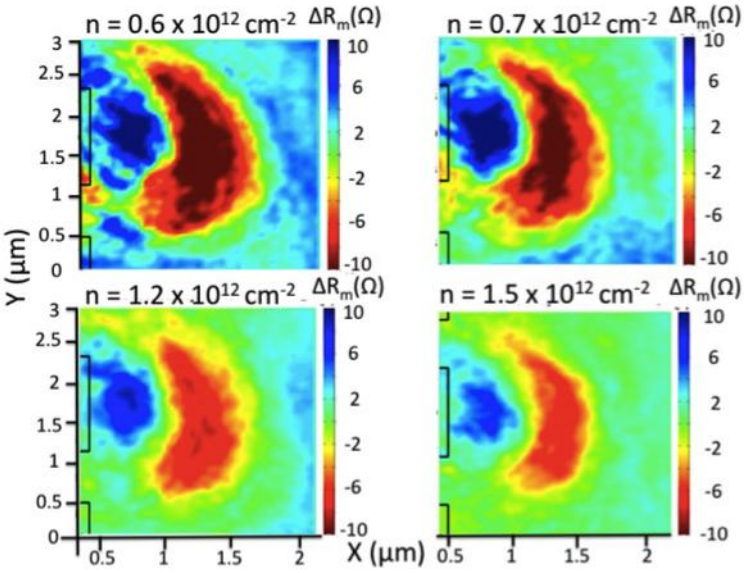

Fig. 4 SPM images of the cyclotron orbit densities along the first magnetic focusing peak with magnetic field B = 89 mT, 99 mT, 107 mT, and 125 mT.

Figure 5 presents SPM images that tile the position of the first magnetic

focusing peak as we vary the electron density *n* and the magnetic field *B*. The presence of the focusing peak is clearly shown. In addition there are alternations between decreased (blue) and enhanced (red) transmission between contacts that we plan to study using ray tracing simulations.

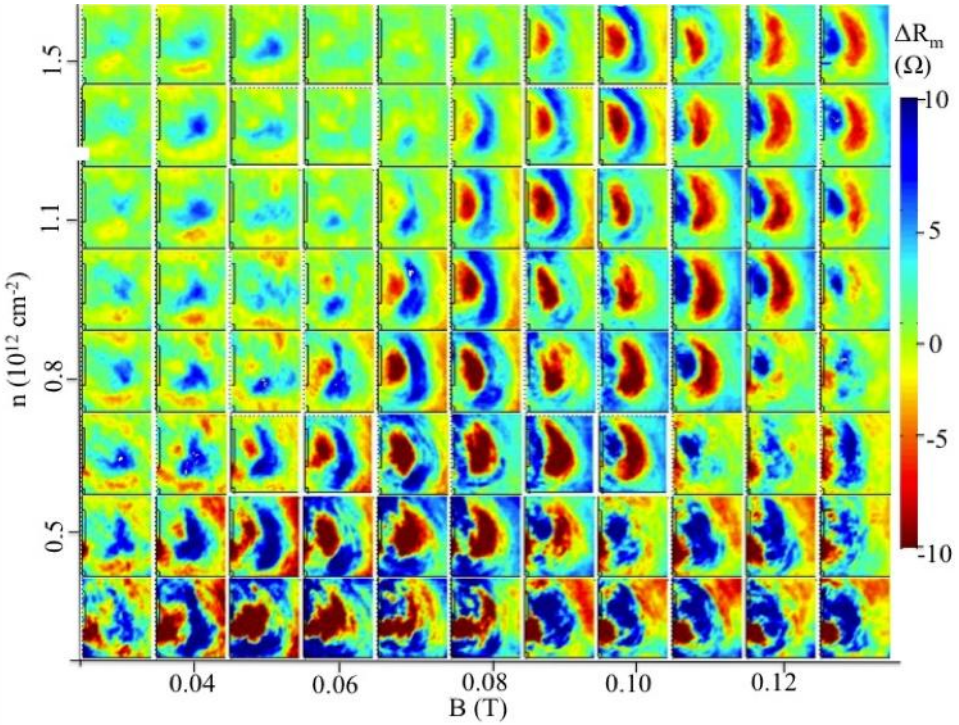

Fig. 5 Tiled images of electron flow as we vary B and n. For values that correspond to the first focusing peak in Fig. 2, cyclotron orbits are seen.

The data shown here are some of the first SPM images of electron flow in graphene. By visualizing the spatial flow of electrons inside devices made from graphene and other atomic layer materials, SPM images promise to provide valuable information for the development of future atomic-scale electronic devices.

Future Plans

Sagar Bhandari obtained his PhD degree in May 2015. He is continuing his work on this DOE research project in Westervelt's lab as a postdoctoral associate in 2015-2016.

We plan to continue our collaboration with Philip Kim's group - they are experts in the assembly of high mobility BN/graphene/BN sandwiches that allow ballistic transport over micron-scale distances. Using facilities of the Center for Nanoscale Systems at Harvard, we can shape the BN/graphene/BN layers into a wide variety of nanoscale structures and devices.

We have begun collaboration with Eric Heller - his group will carry out a theoretical study of magnetic focusing in graphene, including simulations of our experimental SPM images. We have worked closely with Heller, since our initial imaging experiments in 2001, and his knowledge and insights are very valuable.

Specific projects imaging electron flow include:

Imaging interference due to coherent electron flow in graphene structures. We plan to extend studies of electron interference in SPM images of GaAs/AlGaAs 2DEGs, including flow from a quantum point contact [1], and imaging electron interferometer [2], and magnetic focusing [3], as well as imaging of universal conductance fluctuations in graphene [4].

Imaging electron flow in BN/graphene/BN sandwiches with superconducting contacts to examine currents due to Andreev scattering.

References

[1] M.A. Topinka, B.J. LeRoy, R.M. Westervelt, S.E.J. Shaw, R. Fleischmann, E.J. Heller, K.D. Maranowski and A.C. Gossard, Nature **410**, 183 (2001).

[2] B.J. LeRoy, A.C. Bleszynski, K.E. Aidala, R.M. Westervelt, A. Kalben, E.J. Heller, K.D. Maranowski and A.C. Gossard, "Imaging electron interferometer", Phys. Rev. Lett. **94**, 126801 (2005).

[3] Katherine E. Aidala, Robert E. Parrott, Tobias Kramer, R. M. Westervelt, Eric J. Heller, Micah P. Hanson, Arthur C. Gossard, "Imaging Magnetic Focusing of Coherent Electron Waves", Nature Physics **3**, 464 (2007).

[4] J. Berezovsky, M.F. Borunda, E.J. Heller and R.M. Westervelt, Nanotech Special issue **21,** 274014 (2010).

[5] T. Taychatanapat, K. Watanabe, T. Taniguchi and P. Jarillo-Herrero, Nature Physics **9**, 225 (2013).

Publications

S. Bhandari, A. Lin, A. Klales, E.J. Heller, G-H Lee, P. Kim and R.M. Westervelt, "Imaging Electron Cyclotron Orbits in Graphene," in preparation (2015).

S. Bhandari and R.M. Westervelt, "Low-Temperature Scanning Capacitance Probe for Imaging Electron Motion," Proc. LT27 Int. Conf. Low Temperature Physics, Buenos Aires, Argentina, August 6-13 (2014).

Wei Li Wang, E. J. G. Santos, B. Jiang, E. D. Cubuk, C. Ophus, A. Centeno, A. Pesquera, A. Zurutuza, J. Ciston, R.M. Westervelt, and E. Kaxiras, "Dynamics of a long-lived single-atom catalyst chiseling atomic structures in graphene," Nano Letters **14** (2), 450–455 (2014).

Session II

Program Title: Novel and unconventional superconductors: quantum criticality and possible field-induced superconducting states

Principal Investigator: Luis Balicas
Mailing Address: National High Magnetic Field Lab – Florida State University, 1800, E. Paul Dirac Dr., Tallahassee-FL, 32310
E-mail: balicas@magnet.fsu.edu

1. Project Scope

We proposed a detailed extensive effort in understanding the properties of unconventional superconducting states and their interplay with quantum criticality. For example, $CeCu_2Ge_2$ displays superconductivity under hydrostatic pressure, presumably around the spin-density wave quantum critical (QC) pressure. Its superconducting transition temperature is observed to increase around a structural transition seen at higher pressures which is associated with a valence transition. In $CeCu_2Ge_2$ we found evidence for a complex magnetic-field temperature phase diagram bearing a potentially rich QC-behavior. We propose to expose its properties around field-induced quantum criticality associated with the suppression of a spin-density wave, and in so doing gather a better understanding on its interplay with superconductivity. URu_2Si_2 is characterized by a "hidden-order state" having very pronounced magnetic and superconducting fluctuations, hence suggesting proximity to a QC point, from which superconductivity emerges. All experimental evidence collected so far points to a rather exotic superconducting pairing symmetry, with possibly unique topological properties. We intend to expose these through thermal measurements, which have the potential to unveil the pairing symmetry of this compound. Quantum criticality has also been shown to be relevant for the Fe pnicitides/chalcogenides, In the Fe pnictides the proximity to this TRSB state has been predicted to lead to an exotic superconducting pairing symmetry, i.e. containing a triplet component, when both order parameters coexist in a certain region of their phase diagram. We intend to experimentally verify this claim in already synthesized single crystals. Finally, we found new Pd and chalcogenide based anisotropic, multiband superconductors whose metallic state is anomalous suggesting interplay with charge/magnetic order and perhaps related quantum criticality. We propose to clarify their pairing symmetry and the interplay of superconductivity with such underlying order.

2. Recent Progress

Recently, we performed a detailed study on the temperature and angular dependence of the Shubnikov-de-Haas (SdH) effect observed on the semi-metal WTe_2. This compound was recently shown to display a very large non-saturating magnetoresistance which was attributed to nearly perfectly compensated densities of electrons and holes. We observed four fundamental SdH frequencies and attributed them to spin-orbit split, electron- and hole-like, Fermi surface (FS) cross-sectional areas. Their angular dependence seems consistent with ellipsoidal FSs with volumes suggesting a modest excess in the density of electrons with respect to that of the holes. We show that density functional theory (DFT) calculations fail to correctly describe the FSs of WTe_2. When their cross-sectional areas are adjusted to reflect the experimental data, the resulting volumes of the electron/hole FSs obtained from the DFT calculations would imply a pronounced imbalance between the densities of electrons and holes. We find evidence for field-dependent Fermi surface cross-sectional areas by fitting the oscillatory component superimposed onto the magnetoresistivity signal to several Lifshitz-Kosevich components. We also observe a pronounced field-induced renormalization of the effective masses. Taken together, our observations suggest that the electronic structure of WTe_2 evolves with the magnetic field. This evolution might be a factor contributing to its pronounced magnetoresistivity. Our interest in WTe_2 is partially fueled by recent calculations concerning its electronic structure which predict the existence of a particular type of Weyl like Fermion acting as source and drains of Berry phase curvature. Its physics connects with our interests in URu_2Si_2 which has also been proposed to be a compensated semi-metal.

Concerning pronounced magnetoresistive effects, we have observed a hitherto unreported magnetoresistive effect in ultra-clean layered metals. We detected a negative longitudinal magnetoresistance that is capable of overcoming their very pronounced (positive) orbital magnetoresistance. We show that this effect is correlated with the inter-layer coupling, and disappears for fields applied along the so-called Yamaji angles where the inter-layer coupling vanishes. Therefore, this effect seems to be intrinsically associated with the existence of Fermi points in the field-induced, quasi-one-dimensional electronic dispersion. We suggest that this effect results from the axial anomaly among Fermi points, and in analogy for the prediction of an axial anomaly among Weyl points. In its original formulation the anomaly leads to the violation of separate number conservation laws for left- and right-handed chiral, or Weyl-fermions. For a certain class of gapless semiconductors, it was predicted to induce a large suppression of the electrical resistivity, as observed here. The observation of this effect in $PdCoO_2$, $PtCoO_2$ and Sr_2RuO_4 suggests that it would be generic to clean metals (or semi-metals) near the quantum limit.

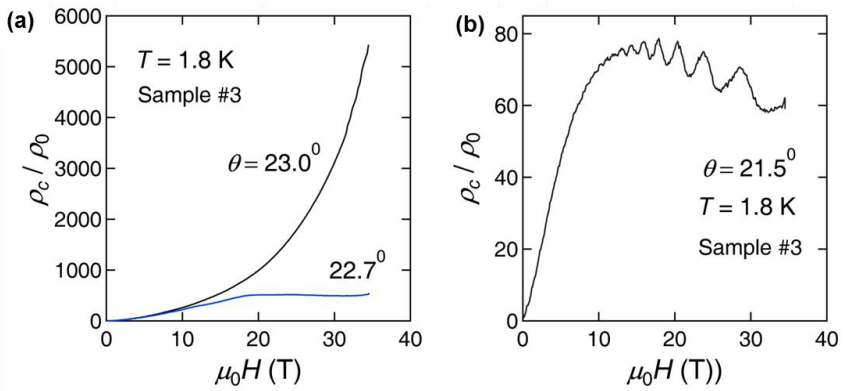

Fig. 1 (a) Inter-planar resistivity ρ_c of $PdCoO_2$ normalized by its zero-field value ρ_0 as a function of H, at $T = 1.8$ K and for two angles, i.e. the so-called Yamaji value $\theta_{n=1} = 23.0^o$ and for $\theta = 22.7^o$. Notice how the pronounced positive magnetoresistivity observed at $\theta_{n=1}$ is strongly suppressed when H is rotated by just $\Delta\theta \cong 0.3^o$ leading to the saturation of the magnetoresistance. (b) ρ_c as a function of H under $T = 1.8$ K and for $\theta = 21.5^o$. Notice how ρ_c, after increasing by several orders of magnitude, displays negative magnetoresistivity at higher fields thus indicating a clear competition between the orbital magnetoresistivity and another mechanism which suppresses it. Very similar results are obtained for $PtCoO_2$.

Along the same lines of magnetoresistive systems characterized by an anomalous electronic structure predicted to lead to Weyl like singularities, we have successfully synthesized NbAs, NbP, TaAs and TaP. These tetragonal compounds are non-centrosymmetric and are characterized by a strong spin-orbit coupling. In the phosphide compounds we systematically observe oscillations in the resistivity (Shubnikov de Haas) at high frequencies, which are not observable in the magnetization (de Haas van Alphen). At the moment we are speculating that discrepancy between both effects might be ascribed to the existence of surface states which are detectable in transport measurements but not in thermodynamic ones. This will require the analysis of samples of varying geometry.

Finally, we have characterized the field as a function of temperature phase diagram for $Ta_4Pd_3Te_{16}$, and of for $Nb_3Pd_{0.6}Se_7$ (but having a considerably higher T_c than previously reported by us) indicating a very anomalous temperature dependence for their upper-critical field(s).

3. Future Plans

Quantum criticality in $CeCu_2Ge_2$: We plan to fully expose and to characterize the quantum critical behavior detect by us in $CeCu_2Ge_2$. We plan to explore the possibility of observing quantum tri-critical their relation with quantum critical end points, and the existence of possible quantum critical lines in this compound. Currently we are studying the evolution of the exponent in the resistivity as a function temperature, field and angle. We also intend to study the evolution of the quasiparticle effective mass,

through the de Haas van Alphen effect, upon approaching the critical field required to suppress its spin-density wave ground state. Finally, we intend to explore the observation of the Wiedemann-Franz law along all fields, and angles required to suppress the AF in $CeCu_2Ge_2$

Time reversal symmetry broken (TRSB) superconducting in URu_2Si_2: we propose to explore the possibility of detecting an anomalous magneto electric response in its superconducting state, which would result from Weyl fermion like properties intrinsic to the most plausible pairing symmetries. This could clarify the nature of its superconducting pairing symmetry. Currently, we are developing a thermal Hall effect set-up which should be sensitive to the Berry phase curvature (and predicted existence of a Chern number) of the nodal quasiparticles in this compound.

New superconductors: To search for new transition metal and chalcogenide based multiband superconductors hoping to detect higher transition temperatures with respect to the compounds discovered by us so far, e.g. $Nb_2Pd_{0.81}S_5$, and to continue to unveil the physical properties of the discovered compounds. In collaboration with other groups we are performing penetration depth measurements as a function of the temperature, hoping to detect an anomalous temperature dependence that could provide clues about the nature of its pairing symmetry.

Quest for time reversal symmetry broken superconducting states in Fe pnictides: We will explore the properties of the superconducting state, in the vicinity of the spin-density wave phase, of the $(Ba,Sr)Fe_2(As_xP_{1-x})_2$ series with the goal of detecting evidence for a TRSB superconducting state as predicted theoretically. Notice, that the zone of coexistence between antiferromagnetism and superconductivity has been shown by the Meingast group to be complex, with the existence of more than one antiferromagnetic phase. In bulk FeSe, orbital order is suppressed upon application of pressure stabilizing an antiferromagnetic state. Measurements, by other groups, unveil a dramatic enhancement of the upper critical field for the superconducting state coexisting with superconductivity although T_c does not vary much under pressure. Our intention is to confirm similar observations in $(Ba,Sr)Fe_2(As_xP_{1-x})_2$ and proceed with thermal conductivity and NMR spin-lattice relaxation rate measurements looking anomalous exponents.

4. A list of publications resulting from DOE sponsored research that have been published in 2013 - 2015

1. *Unconventional Fermi surface in an insulating state*. B. S. Tan, Y. -T. Hsu, B. Zeng, M. Ciomaga Hatnean, N. Harrison, Z. Zhu, M. Hartstein, M. Kiourlappou, A. Srivastava, M. D. Johannes, T. P. Murphy, J.-H. Park, L. Balicas, G. G. Lonzarich, G. Balakrishnan, and S. E. Sebastian. *Science* **349**, 287 (2015)
2. *Field-induced quadrupolar quantum criticality in PrV_2Al_{20}*. Y. Shimura, M. Tsujimoto, B. Zeng, L. Balicas, A. Sakai, S. and Nakatsuji. *Phys. Rev. B (RC)* **91**, 241102(R) (2015).
3. *Spin-orbital liquid and quantum critical point in $Y_{1-x}La_xTiO_3$*. Z. Y. Zhao, O. Khosravani, M. Lee, L. Balicas, X. F. Sun, J. G. Cheng, J. Brooks, H. D. Zhou, and E. S. Choi. *Phys. Rev. B (RC)* **91**, 161106(R) (2015).
4. *$CeCu_2Ge_2$: Challenging our understanding of quantum criticality*. B. Zeng, Q. R. Zhang, D. Rhodes, Y. Shimura, D. Watanabe, R. E. Baumbach, P. Schlottmann, T. Ebihara, and L. Balicas. *Phys. Rev. B* **90**, 155101 (2014).
5. *Quantum Oscillations in $EuFe_2As_2$ single crystals.* P. F. S. Rosa, B. Zeng, C. Adriano, T. M. Garitezi, T. Grant, Z. Fisk, L. Balicas, M. D. Johannes, R. R. Urbano, P. G. Pagliuso. *Phys. Rev. B* **90**, 195146 (2014).
6. *Field induced charge order in the heavy fermion compound $CeRhIn_5$*. P.J.W. Moll, B. Zeng, L. Balicas, S. Galeski, F.F. Balakirev, E.D. Bauer, F. Ronning, *Nature Comm.* **6**, 6663 (2015).
7. *Critical Current Oscillations in the Intrinsic Hybrid Vortex State of SmFeAs(O,F)*. Moll, P.

J. W.; Balicas, L.; Zhu, X.;Wen, H.-H.; Zhigadlo, N. D.; Karpinski, J.; Batlogg, B. *Phys. Rev. Lett.* **113**, 186402 (2014).

8. *$CeCu_2Ge_2$: Challenging our understanding of quantum criticality*. Zeng, B.; Zhang, Q. R.; Rhodes, D.; Shimura, Y.; Watanabe, D.; Baumbach, R. E.; Schlottmann, P.; Ebihara, T. and Balicas, L. *Phys. Rev. B* **90**, 155101 (2014).
9. *Entropy of the quantum soliton lattice and multiple magnetization steps in $BiCu_2PO_6$.* Kohama, Y.; Mochidzuki, K.; Terashima, T.; Miyata, A.; DeMuer, A.; Klein, T.; Marcenat, C.; Dun, Z. L.; Zhou, H. D.; Li, G.; Balicas, L.; Abe, N.; Matsuda, Y.H.; Takeyama, S.; Matsuo, A.; Kindo, K., *Phys. Rev. B* **90**, 060408 (2014).
10. *Manifestation of magnetic quantum fluctuations in the dielectric properties of a multiferroic*. Kim, J. W.; Khim, S.; Chun, S. H.; Jo, Y.; Balicas, L.; Yi, H. T.; Cheong, S. W.; Harrison, N.; Batista, C. D.; Han, J. H.; Kim, K. H. *Nature Comm.* **5**, 4419 (2014).
11. *Magnetic field-tuned localization of the 5f-electrons in URu_2Si_2.* Harrison, N.; Moll, P.J.W.; Sebastian, S. E.; Balicas, L.; Altarawneh, M. M.; Zhu, J. X.; Tobash, P. H.; Ronning, F.; Bauer, E. D.; Batlogg, B. *Phys. Rev. B* **88**, 241108 (2013).
12. *Surface electronic structure of the topological Kondo-insulator candidate correlated electron system SmB_6.* Neupane, M.; Alidoust, N.; Xu, S. Y.; Kondo, T.; Ishida, Y.; Kim, D. J.; Liu, C.; Belopolski, I.; Jo, Y. J.; Chang, T. R.; Jeng, H. T.; Durakiewicz, T.; Balicas, L.; Lin, H.; Bansil, A.; Shin, S.; Fisk, Z.; Hasan, M. Z. *Nature Comm.* **4**, 2991 (2013)
13. *Small and nearly isotropic hole-like Fermi surfaces in LiFeAs detected through de Haas-van Alphen effect*. Zeng, B.; Watanabe, D.; Zhang, Q.R.; Li, G.; Besara, T.; Siegrist, T.; Xing, L.Y.; Wang, X. C.; Jin, C. Q.; Goswami, P.; Johannes, M. D.; Balicas, L. *Phys. Rev. B* **88**, 144518 (2013)
14. *Bulk evidence for a time-reversal symmetry broken superconducting state in URu_2Si_2.* Li, G.; Zhang, Q.; Rhodes, D.; Zeng, B.; Goswami, P.; Baumbach, R. E.; Tobash, P. H.; Ronning, F.; Thompson, J. D.; Bauer, E. D.; Balicas, L. *Phys. Rev. B* **88**, 134517 (2013).
15. *Anomalous metallic state and anisotropic multiband superconductivity in $Nb_3Pd_{0.7}Se_7$.* Zhang, Q. R.; Rhodes, D.; Zeng, B.; Besara, T.; Siegrist, T.; Johannes, M. D.; Balicas, L. *Phys. Rev. B* **88**, 024508 (2013).
16. *Superconductivity with extremely large upper critical fields in $Nb_2Pd_{0.81}S_5$.* Zhang, Q.; Li, G.; Rhodes, D.; Kiswandhi, A.; Besara, T.; Zeng, B.; Sun, J.; Siegrist, T.; Johannes, M. D.; Balicas, L. *Sci. Rep.* **3**, 1446 (2013).
17. *Vortex lock-in transition and evidence for transitions among commensurate kinked vortex configurations in single-layered Fe arsenides*. Li, G.; Grissonnanche, G.; Conner, B. S.; Wolff-Fabris, F.; Putzke, C.; Zhigadlo, N. D.; Katrych, S.; Bukowski, Z.; Karpinski, J.; Balicas, L. *Phys. Rev. B* **87**, 100503 (2013).
18. *Transition from slow Abrikosov to fast moving Josephson vortices in iron pnictide superconductors*. Moll, P. J. W.; Balicas, L.; Geshkenbein, V.; Blatter, G.; Karpinski, J.; Zhigadlo, N. D.; Batlogg, B. *Nature Mater.* **12** , 134-138 (2013).
19. *Anomalous hysteresis as evidence for a magnetic-field-induced chiral superconducting state in LiFeAs*. Li, G.; Urbano, R. R.; Goswami, P.; Tarantini, C.; Lv, B.; Kuhns, P.; Reyes, A. P.; Chu, C. W.; Balicas, L. *Phys. Rev. B* **87**, 024512 (2013).

Program Title: **Raman spectroscopy of pnictide and other unconventional superconductors**

Principle Investigator: **Girsh Blumberg**
Mailing Address: **Department of Physics & Astronomy, Rutgers University, 136 Frelinghuysen Road, Piscataway NJ 08854-8019**
E-mail: **girsh@physics.rutgers.edu**

PROGRAM SCOPE

The objectives of this project are to investigate the manner in which charge, spin, orbital and lattice coupling and dynamics evolve through various low temperature phases of "strongly correlated materials" by employing electronic Raman scattering spectroscopy, and to clarify the microscopic origin of collective behavior like unconventional superconductivity induced in these compounds by electron correlations. Among the anticipated outcomes of this project are (i) the elucidation of the microscopic origin of superconductivity in the iron-pnictide family of materials, including the evaluation of the role of electronic correlations in both normal and superconducting states, the role of proximity to a magnetically ordered state, the mechanisms of formation of the superconducting order parameter and its symmetry; (ii) insights into how to design new materials with enhanced superconducting properties; and (iii) determination of a spectrum of collective excitation in superconductors and in heavy fermion materials with "hidden orders".

RECENT PROGRESS

Heavy Fermions. Many novel electronic ground states have been found to emerge from the hybridization between localized *d*- or *f*-electron states and conduction electron states in correlated electron materials. The heavy fermion (HF) compound URu_2Si_2 exhibits the coexistence of two such ground states: so called hidden order (HO) below T_{HO}=17.5 K and superconductivity below T_c =1.5 K. The PI and his collaborators used polarization resolved Raman spectroscopy to identify the symmetry of low energy excitations above and below the HO transition and to uncover the hidden order parameter. These excitations involve transitions between interacting uranium *5f* orbitals, responsible for the broken symmetry in the HO phase. From the symmetry analysis of the discovered collective mode, the PI and collaborators determined that the HO parameter breaks local vertical and diagonal reflection symmetries at the uranium sites, resulting in states with distinct chiral properties, which order to a commensurate chirality-density-wave ground state. As a continuation of this work, the PI will study the effects of substituting of Fe for Ru which provides chemical pressure and drives the system into antiferromagnetic (AF) phase.

Multiband pnictide superconductors. Iron-pnictides present a new paradigm of multi-band superconductivity in proximity to nematic transition and spin density wave (SDW) order. Most FeAs compounds share a common phase diagram which in the underdoped region is marked by a

structural transition at temperature T_S from tetragonal to orthorhombic phase followed by an SDW transition at T_{SDW}, slightly below T_S. The orthorhombic distortion at T_S breaks C_4 rotational symmetry while the translational symmetry is broken due to doubling of the unit cell either at or above T_{SDW}. The system provides exceptional setting to study coexistence or competition between quadrupole fluctuations, superconductivity, and density-wave phases.

During this project we performed multiple series of polarized low-temperature Raman scattering studies of phononic, electronic, inter-band and magnetic excitations on many following families of compounds: $CaFe_2As_2$, $(Sr_2VO_3)_2Fe_2As_2$, $Fe_{1+x}(TeSe)$, $K_{0.75}Fe_{1.75}Se_2$, $BaFe_{1.9}Pt_{0.1}As_2$, $Ca(Co_xFe_{1-x})_2As_2$, $Na_{1-x}FeCo_xAs$, $Ba_{1-x}K_xFe_2As_2$ and others.

I will highlight the following results:

1. Evolution of the nematic fluctuations and the evidences for new Pomeranchuk-like charge/orbital order below T_S.

2. Evolution of the structural and magnetic order of the parent materials. Spectroscopy of SDW gap.

3. Evolution of the superconducting order, superconducting gaps in the multi-band materials, evidences for s+- order parameter, competition between the ordered magnetic and superconducting phases.

4. In-gap collective excitations in the superconducting phase. Evidences for sub-dominant pairing in d-wave channel. Observation of Pomeranchuk-like and Bardasis-Schrieffer collective modes (excitons).

We will continue spectroscopic study of the oxypnictide compounds across the phase diagram as a function of carrier concentration, temperature, and magnetic field.

ACKNOWLEDGMENTS

The work is done in collaboration with P. Dai, B.S. Dennis, K. Haule, A. Ignatov, H.-H. Kung, A. Mialitsin, J. Paglione, V.K. Thorsmolle, N.L. Wang, S.F. Wu, Z. Yin, W.-L. Zhang, C. Zhang. Research was supported by U.S. DOE, Office of BES, Award DE-SC0005463.

PUBLICATIONS AND SELECTED PRESENTATIONS

1. Kung, H.H., Baumbach, R.E., Bauer, E.D., Thorsmolle, V.K., Zhang, W.L., Haule, K., Mydosh, J.A. and G. Blumberg. Chirality density wave of the 'hidden order' phase in URu2Si2 . Science, 347, 1339 (2015
2. Ziemak, S., Kirshenbaum, K., Saha, S.R., Hu, R., Reid, J.-P., Gordon, R., Taillefer, L., Evtushinsky, D., Thirupathaiah, S., Borisenko, S.V., Ignatov, A., Kolchmeyer, D., Blumberg, G. and Paglione, J. Isotropic multi-gap superconductivity in BaFe1.9Pt0.1As2 from thermal transport and spectroscopic measurements. Superconductor Science and Technology, 28, 014004 (2015). Invited submission for focus issue on Multicomponent Superconductivity.
3. Khodas, M., Chubukov, A.V. and Blumberg G. Collective modes in multiband superconduc- tors: Raman scattering in iron selenides. Phys. Rev. B, 89, 245134 (2014).
4. Ignatov A., Kumar A., Lubik P., Yuan R.H., Guo W.T., Wang N.L., Rabe K., Blumberg G. Structural phase transition below 250 K in superconducting K0.75Se1.75Fe2. Editor's suggestion. Phys. Rev. B, 86, 134107 (2012).
5. Thorsmolle, V. K., Khodas, M., Yin, Z. P., Zhang, C., Carr, S. V., Dai, P., and Blumberg, G. (2014) Critical Charge Fluctuations in Iron Pnictide Superconductors. Research article under evaluation with Science Advances. ArXiv e-prints http://arxiv.org/abs/1410.6456.
6. Zhang, W.-L., Richard, P., Ding, H., Sefat, A. S., Gillett, J., Sebastian, S. E., Khodas, M., and Blumberg, G. On the origin of the electronic anisotropy in iron pnictide superconductors. Under evaluation with Phys. Rev. Lett. ArXiv e-prints http://arxiv.org/abs/1410.6452.
7. Zhang, W.-L., Richard, P., Ding, H., Sefat, and Blumberg, G. Raman scattering study of the spin density wave induced anisotropic electronic properties in AFe_2As_2 (A=Ca, Eu). In preparation.
8. Zhang, W.-L., Richard, P., Ding, H., Sefat, and Blumberg, G. Self-energy effects and electronphonon coupling in FeAs superconductors. In preparation.
9. Kung, H.H., Baumbach, R.E., Bauer, Haule, K., Mydosh, J.A. and G. Blumberg. Chiral fluctuations observed in the paramagnetic state of URu_2Si_2. In preparation.
10. Mialitsin, A.V., Solov'yov, I.A., Toth, A.I., Mazin, I.I., Nevidomskyy, A.H., Dennis, B.S., and Blumberg G. Raman-scattering measurements of the electronic structure of $NbSe_2$: Evidence of a combined order parameter for charge-density-wave and superconducting states. In preparation.
11. Mialitsin, A.V., and Blumberg G. Raman sum rules in superconductors. In preparation.
12. A. Ignatov, R.H. Yuan, and N.L. Wang, and G. Blumberg, "Phononic, magnetic, and inter-band Raman scattering in $K_{0.75}Fe_{1.75}Se_2$ superconductor." Contribution at APS March meeting. Boston, Massachusetts, Feb 27 - March 2, 2012.
13. G. Blumberg, "Raman spectroscopy of iron based superconductors." Low Energy Electrodynamics in solids (LEES 2012). Napa, California, July 22 - 27, 2012.
14. G. Blumberg, "Raman spectroscopy of iron based superconductors." International Seminar and Workshop on Quantum Matter from the Nano- to the Macroscale. Dresden, Germany, June 18 - July 6, 2012.
15. S. Ziemak, K. Kirshenbaum, S.R. Saha, R. Hu, J. Paglione, J.-Ph. Reid, R. Gordon, L.

Taillefer, A. Ignatov, D. Kolchmeyer, G. Blumberg, D. Evtushinsky, S. Thirupathaiah, S.V. Borisenko, "Investigation of Pairing Symmetry in Pt-Substituted $BaFe_2As_2$" Contribution at APS March meeting. Baltimore, MD, March 18 - 22, 2013.

16. G. Blumberg, "The phase diagram of pnictide superconductors – competing orders." International Summer School on Superconductivity – Theory, Experiments, and Phenomena." Cargèse, France, August 5-17, 2013.
17. G. Blumberg, "Raman spectroscopy of multiband superconductors." International Workshop on Recent developments in Fe-based high-temperature superconductors Riverhead, Long Island, New York. 2-6 September 2013.
18. G. Blumberg, "Polarized Electronic Raman Scattering Study of the Heavy Fermion Compound URu_2Si_2." Hidden Order, Superconductivity, and Magnetism in URu_2Si_2 at the Lorentz Center, Leiden, The Netherlands, 4-8 November, 2013.
19. W.-L. Zhang, "Nematic charge fluctuations and electron-phonon coupling in $EuFe_2As_2$ and $SrFe_2As_2$." APS March meeting. Denver, CO, March, 2014.
20. H.H. Kung. "The Hidden Order gap and in-gap excitation mode in URu_2Si_2 revealed by electronic Raman scattering." APS March meeting. Denver, CO, March, 2014.
21. V.K. Thorsmolle, "Origin of electronic nematicity in the iron pnictide $NaFe_{1-x}Co_xAs$ Superconductor." APS March meeting. Denver, CO, March, 2014.
22. G. Blumberg, "Chiral Density Wave of the 'Hidden Order' phase in URu_2Si_2." Low Energy Electrodynamics in solids (LEES 2014). France. June 29-July 4, 2014.
23. H.H. Kung. "Chiriality density wave of the hidden order phase in URu_2Si_2." Gordon research Conference, Superconductivity. Invited. Hong Kong, May 24 - 29, 2015.
24. G. Blumberg, "Critical Charge Fluctuations in Iron Pnictide Superconductors" Gordon research Conference, Superconductivity. Hong Kong, May 24 - 29, 2015.
25. G. Blumberg, "Chiriality density wave of the hidden order phase in URu_2Si_2." The 20th International Conference on Magnetism. Invited. Barcelona, July 5 - 10, 2015.
26. G. Blumberg, "Critical Quadrupole Fluctuations and collective modes in Iron Pnictide Superconductors" Invited. Quantum Design, International Seminar and Workshop. Dresden, July 13 - 24, 2015.
27. H.H. Kung. "Chiriality density wave of the hidden order phase in URu_2Si_2." Summer school on new physics due to Spin-Orbit coupling in correlated electron systems. Cargèse, France, August 4-14, 2015.
28. G. Blumberg, "Raman spectroscopy of unconventional superconductors" Invited. School and Workshop on Strongly Correlated Electronic Systems - Novel Materials and Novel Theories. Trieste, August 10 - 21, 2015.
29. G. Blumberg, "Critical charge fluctuations in iron pnictide superconductors" Invited. School and Workshop on Strongly Correlated Electronic Systems - Novel Materials and Novel Theories. Trieste, August 10 - 21, 2015.
30. G. Blumberg, "Chiriality density wave of the hidden order phase in URu_2Si_2." The 11th International Conference on Materials and Mechanisms of Superconductivity. Invited. Geneva, August 23 - 28, 2015.
31. G. Blumberg, "Critical charge fluctuations in iron pnictide superconductors." The 11th International Conference on Materials and Mechanisms of Superconductivity. Geneva, August 23 - 28, 2015.

Program Title: Correlated Materials - Synthesis and Physical Properties

Principle Investigators: I. R. Fisher, T. H. Geballe, A. Kapitulnik, S. A. Kivelson, and K. A. Moler
Institution: Geballe Laboratory for Advanced Materials, and Departments of Applied Physics and Physics, Stanford University, and the Stanford Institute for Materials & Energy Science, SLAC National Accelerator Laboratory.
Emails: irfisher@stanford.edu, geballe@stanford.edu, aharonk@stanford.edu, kivelson@stanford.edu, kmoler@stanford.edu

Program Scope

The overarching goal of our research is to understand, and ultimately control, emergent behavior in strongly correlated quantum materials. Our research combines synthesis, measurement and theory to coherently address questions at the heart of these issues. We use cutting edge, often unique, experimental probes to uncover novel forms of electronic order in a variety of complex materials. Our theoretical work provides a framework to understand the rich variety of possible ordered states, and guides our ongoing measurements and synthesis efforts. Big questions that we collectively address include;

- What are the rules and organizing principles governing emergent behavior in quantum materials?
- What is the nature of the coexisting and competing phases in high temperature superconductors, and how do they determine/limit the maximum critical temperature?
- Is there an associated quantum critical point beneath the superconducting dome, and if so what is its nature?
- How does disorder affect quantum phase transitions in strongly correlated materials?
- How should we understand electronic and thermal transport in the quantum critical regime, and, more generally, in "bad metals"?

Our research addresses these challenging questions in the context of a range of complex quantum materials.

Recent Progress

1. Broken symmetry phases in high temperature superconductors

A major emphasis of our recent and ongoing work involves broken symmetry phases in the underdoped regime of both cuprate and Fe-based superconductors. During FY13-15, our experiments focused primarily on Polar Kerr effect and elastoresistivity measurements. In both cases, our experimental work has been strongly tied to theoretical advances, both in terms of developing a detailed understanding of the measurements, and in terms of our results motivating further theoretical treatment. Our crystal growth activities have also supported several collaborative projects based on these and related materials.

During the last few years we have developed a new experimental technique based on differential elastoresistance measurements, which directly reveals the *nematic* susceptibility of a material [1, 13, and arXiv:1503.00402]. Our results based on this new technique definitively establish that the structural phase transition in the Fe-based superconductors is driven by electronic nematic order (i.e. is driven by electronic correlations). Further, we find that nematic fluctuations are prevalent across the superconducting region of the phase diagram, being strongest in the vicinity of an associated quantum phase transition [9] near optimal doping. These observations raise the question of what role nematic fluctuations might play in the superconducting pairing interaction in these materials and possibly beyond. This problem can be analyzed theoretically (using conventional Eliashberg theory) in the limit in which the coupling between the nematic fluctuations and the low energy electronic excitations of the metal is weak: we find that nematic fluctuations enhance the strength of whatever pairing tendencies are already present, regardless of the favored channel (i.e. s-, s±, d-, or p-wave, etc.); this enhancement grows upon approach to the nematic quantum critical point, and this effect is stronger in 2d than in 3d.

In addition, high-resolution polar Kerr effect (PKE) measurements of $La_{1.875}Ba_{0.125}CuO_4$ (LBCO) single crystals, using our highly sensitive zero area loop Sagnac interferometer (ZALSI), revealed a Kerr signal arising below an onset temperature T_K that roughly coincides with the charge ordering onset temperature T_{CO} measured with x-rays [10]. These observations are suggestive that there is some form of chiral order which onsets above T_c in LBCO, while similarities to other cuprates suggest that it might be a universal property of the pseudogap regime.

2. Broken Symmetry Phases in Heavy Fermion Materials

In the absence of a detailed understanding of the microscopic origins of heavy-Fermion (HF) superconductivity, descriptions of the superconducting states in these materials seek to identify the internal structure of the order parameter. Key questions include whether HF superconductors possess multi-component order parameters, and whether the respective phases preserve or break time-reversal symmetry. Similarly, for materials that suffer additional phase transitions prior to the superconducting transition, identifying the symmetry of the ordered state is crucial in determining the superconducting order parameter. With our Zero Area Loop Sagnac Interferometer (ZALSI), we investigated UPt_3[14], URu_2Si_2[20], $CeCoIn_5$, and $PrOs_4Sb_{12}$. We have also investigated the symmetry of the Hidden Order phase in URu_2Si_2 via differential elastoresistance measurements, finding that the HO phase breaks 4-fold rotational symmetry [19]. These investigations have involved a close collaboration between theory and experiment.

3. New insight into the Superconductor-Insulator Transition

Quantum phase transitions (QPT) continue to attract intense theoretical and experimental interest. In the past few years we revisited experiments done on thin superconducting films, which with the application of magnetic field (the tuning external parameter) undergo a Superconductor-Insulator transition (SIT). Focusing on the magnetic-field tuned SIT of two-

dimensional amorphous indium-oxide films, we combined measurements of the longitudinal and Hall resistances in the $T \to 0$ limit to obtain the full resistivity tensor (and hence, also the conductivity tensor). We found that the transition exhibits signatures of self-duality, and separates the superconducting state from a "Hall-insulator" phase [arXiv:1504.08115].

4. Imaging currents in strongly correlated and topological materials

We developed methods to image current flow in strongly correlated and topological materials with our scanning SQUID. Our work imaging the two known quantum spin Hall (QSH) insulators provides images of edge conduction [4, 15]. It is well known that the quantum spin Hall insulator should carry dissipationless current at the edge, and well known among experts that real devices nevertheless show dissipation. We used a scanning SQUID to image magnetic fields to map current flow. Using a SQUID allowed us to determine the edge current even in the presence of bulk conductivity, where traditional transport measurements are complicated to interpret. The measured temperature dependence disagrees with known theories, indicating that further work is required. We also applied this technique to the interface between the insulators $LaAlO_3$ and $SrTiO_3$. We imaged the field produced by the current and reconstructed the 2D current density in many samples grown by multiple collaborators. We found that twinning in the $SrTiO_3$ substrate greatly affects the conductivity [7].

Future Plans

For FY16-18, our proposed research focuses primarily on broken symmetry phases and quantum phase transitions in strongly correlated materials. A major component of our research involves the design and implementation of new types of experiment that probe the (often subtle) types of emergent order in these materials. In particular, motivated by questions associated with nematicity, we incorporate the ability to exert anisotropic strain (which acts as a field on electronic nematic fluctuations) in our transport, optical and scanning SQUID measurements. Other developments include measurement of the photogalvanic effect, and of thermal diffusivity. The experiments and associated theoretical work described in our proposal focus specifically on the closely related themes of (1) Bad metals and incoherent transport in correlated electron fluids; (2) Electronic nematicity in Fe-based and cuprate superconductors; (3) Broken time reversal symmetry in the pseudogap regime of the cuprates; (4) Numerical and analytic studies of quantum phase transitions; (5) Quadrupolar effects in heavy Fermion systems; and (6) Topological materials systems and superconductivity.

Selection of publications resulting from DOE sponsored research between Aug 2013 and August 2015

1) *Measurement of the elastoresistivity coefficients of the underdoped iron arsenide* $Ba(Fe_{0.975}Co_{0.025})_2As_2$, Hsueh-Hui Kuo, Maxwell C. Shapiro, Scott C. Riggs, and Ian R. Fisher, Phys. Rev. B **88**, 085113 (2013) – Published 12 August 2013
2) *Band structure effects on superconductivity in Hubbard models,* W-J. Cho, R. Thomale, S. Raghu, and S. A. Kivelson, Phys. Rev. B **88**, 64505 (2013) – Published 12 August 2013
3) *Emerging Weak Localization Effects on Topological Insulator-Insulating Ferromagnet (Bi2Se3-EuS) Interface* Qi I. Yang, Merav Dolev, Li Zhang, Jinfeng Zhao, Alexander D. Fried, Elizabeth Schemm, Min Liu, Alexander

Palevski, Ann F. Marshall, Subhash H. Risbud, Aharon Kapitulnik, Phys. Rev. B **88**, 081407(R) – Published 28 August 2013

4) *Imaging currents in HgTe quantum wells in the quantum spin Hall regime*, Katja C. Nowack, Eric M. Spanton, Matthias Baenninger, Markus König, John R. Kirtley, Beena Kalisky, C. Ames, Philipp Leubner, Christoph Brüne, Hartmut Buhmann, Laurens W. Molenkamp, David Goldhaber-Gordon, Kathryn A. Moler Nature Materials **12**, pp 787–791– Published 01 September 2013
5) *Field theory of a quantum Hall nematic transition,* J. Maciejko, B. Hsu, S. A. Kivelson, Y. Park, and S. L. Sondhi, Phys. Rev. B **88**, 125137 – Published 27 September 2013
6) *Evidence from tunneling spectroscopy for a quasi-one dimensional origin of superconductivity in Sr_2RuO_4*, I. A. Firmo, S. Lederer, C. Lupien, A. P. Mackenzie, J. C. Davis and S. A. Kivelson, Phys. Rev. B **88**, 134521 (2013) – Published 28 October 2013
7) *Locally enhanced conductivity due to tetragonal domain structure in $LaAlO_3/SrTiO_3$ heterointerfaces*, Beena Kalisky , Eric Spanton, Hilary Noad , John Kirtley, Katja Nowack , Christopher Bell , Hiroki Sato , Masayuki Hosoda , Yanwu Xie , Yasuyuki Hikita , Carsten Woltmann , Georg Pfanzelt , Rainer Jany , Christoph Richter, Harold Hwang, Jochen Mannhart, Kathryn Moler *Nature Materials* **12**, pp 1091-1095 – Published 1 December 2013
8) *Correlations and renormalization of the electron-phonon coupling in the honeycomb Hubbard ladder and superconductivity in polyacene,* G. Karakonstantakis, L. Liu, R. Thomale, and S. A. Kivelson, Phys. Rev. B **88**, 224512 (2013) – Published 27 December 2013
9) *Transport near a quantum critical point in $BaFe_2$ $(As_{1-x}P_x)_2$*, James G. Analytis, H-H. Kuo, Ross D. McDonald, MarkWartenbe, P. M. C. Rourke, N. E. Hussey and I. R. Fisher, Nature Physics **10**, 194–197 (2014) [4 pages] – Published online 19 January 2014
10) *Evidence of Chiral Order in the Charge-Ordered Phase of Superconducting $La_{1.875}Ba_{0.125}CuO_4$ Single Crystals Using Polar Kerr-Effect Measurements,* Hovnatan Karapetyan, Jing Xia, M. Hucker, G. D. Gu, J. M. Tranquada, M.M. Fejer, A. Kapitulnik, Phys. Rev. Lett **112**, 047003 (2014) – Published 30 January 2014
11) *Pulsed Laser Deposition of High-Quality Thin Films of the Insulating Ferromagnet EuS* Qi I. Yang, Jinfeng Zhao, Li Zhang, Merav Dolev, Alexander D. Fried, Ann F. Marshall, Subhash H. Risbud, Aharon Kapitulnik, Appl. Phys. Lett. **104**, 082402 (2014) – Published 25 February 2014.
12) *Quenched disorder and vestigial nematicity in the pseudo-gap regime of the cuprates,* L Nie, G. Tarjus, and S. A. Kivelson, Proceedings of the National Academy of Sciences, **111**, 7980-7985 (2014) – Published 3 June 2014
13) *Effect of Disorder on the Resistivity Anisotropy Near the Electronic Nematic Phase Transition in Pure and Electron-Doped $BaFe_2As_2$* Hsueh-Hui Kuo and Ian R. Fisher, Phys. Rev. Lett **112**, 227001 (2014) [5 pages] – Published 4 June 2014
14) *Observation of Broken Time-Reversal Symmetry in the B Phase of the Heavy Fermion Superconductor UPt_3* E. R. Schemm, W. J. Gannon, C. Wishne, W. P. Halperin, A. Kapitulnik, Science **345**, 190-193 (2014) – Published 11 July 2014
15) *Images of edge current in InAs/GaSb quantum wells,* Eric M. Spanton, Katja C. Nowack, Lingjie Du, Gerald Sullivan, Rui-Rui Du, Kathryn A. Moler Physical Review Letters, **113**, 026804 (2014) – Published 11 July 2014
16) *Notes on Constraints for the Observation of Polar Kerr Effect in Complex Materials*, Aharon Kapitulnik, Physica B **460**, 151-158 (2015). doi:10.1016/j.physb.2014.11.059 – Published online 24 November 2014
17) *Theory of disordered unconventional superconductors,* A. Keles, A. V. Andreev, S. A. Kivelson, and B.Z. Spivak, JETP **119(**6), 1109 (2015) – Published 1 December 2014
18) *High Temperature Superconductivity in the Cuprates,* B. Keimer, S. A. Kivelson, M. Norman, S. Uchida, and J. Zaanen, Nature **518**, 179-186 (12 February 2015) doi: 10.1038/nature14165 – Published 11 February 2015
19) *Evidence for a nematic component to the hidden-order parameter in URu_2Si_2 from differential elastoresistance measurements,* Scott C. Riggs, M.C. Shapiro, Akash V Maharaj, S. Raghu, E.D. Bauer, R.E. Baumbach, P. Giraldo-Gallo, Mark Wartenbe & I.R. Fisher, Nature Communications **6**, 6425 (2015) doi:10.1038/ncomms7425 [6 pages] – Published 06 March 2015
20) *Evidence for broken time-reversal symmetry in the superconducting phase of URu_2Si_2*, E. R. Schemm, R. E. Baumbach, P. H. Tobash, F. Ronning, E. D. Bauer, A. Kapitulnik,Phys. Rev. B **91**, 140506(R) – Published 30 April 2015
21) *Colloquium: Theory of Intertwined Orders in High Temperature Superconductors,* Eduardo Fradkin, Steven A. Kivelson, and John M. Tranquada, Reviews of Modern Physics **87**, 457 (2015) – Published 26 May 2015.

Project Title: Non-Centrosymmetric Topological Superconductivity
Principal Investigator: Johnpierre Paglione
Institution: University of Maryland
Email address: paglione@umd.edu

Project Scope

Topological insulator (TI) materials are distinguished from ordinary insulators by the so-called Z_2 topological invariants associated with the bulk band structure [1]. Several intriguing and potentially technologically useful properties make the TI states of particular interest beyond fundamental curiosities. In particular, TIs possess a surface state with a Dirac electronic dispersion similar to graphene, topologically protected against localization by time-reversal-invariant (i.e. non-magnetic) disorder. Spin and momentum are perfectly coupled in the chiral TI surface state, leading to novel magnetoelectric effects and much potential for advanced applications [2,3]. Furthermore, the realization of a condensed-matter version of Majorana quasipaticles, fermions that are their own anti-particle [4], has driven an entire field of interest in coupling TI states with superconductivity. First shown by Kitaev in the context of spinless $p_x + ip_y$ superconducting quantum wire [5], the possibility of localizing Majorana fermions at the boundaries of a topological superconductor – for instance at the edges of a wire or inside a vortex core – has great potential in realizing the next generation of fault-tolerant quantum computation [6].

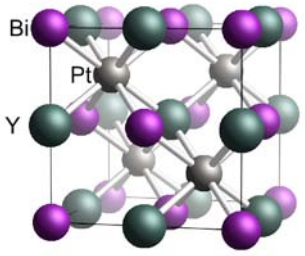

Figure 1: non-centrosymmetric crystallo-graphic half-Heusler structure in YPtBi.

The major experimental efforts over the past several years have been conducted primarily these non-interacting bismuth-based "first generation" TI materials, and have focused on refining both growth and measurement techniques in order to detect signatures of surface states. Large families of new topological materials are waiting to be discovered in small-gap semiconductor systems and semimetals with high-Z elements [7], and true materials exploration is the only route to finding them. To move beyond the problems of the first generation of TI materials, we have focused on the synthesis, characterization and optimization of a new family of topological superconductors to help elucidate the scientific and technological potential of this second generation of topological insulator materials. We have identified a new family of superconducting topological insulator compounds in the ternary half-Heusler system (Fig. 1) that not only show promise to realize TI states in stable, stoichiometric materials, but also to combine non-trivial topologies of both electron band structure and odd-parity superconducting states to produce a truly new realm of topological materials.

A non-trivial band structure that exhibits band ordering analogous to that of the known 2D and 3D TI materials was predicted in a variety of 18-electron half-Heusler compounds using first principles calculations [8,9]. The band structures of these compounds are very sensitive to the electronegativity difference of the constituents, resulting in semiconducting band gaps that can vary from zero (LaPtBi) to 4 eV (LiMgN) [8]. A subset of these compounds possess an inverted band structure, with the top of an *s*-type orbital-derived valence band lying below a *p*-type conduction band, with both centered at the high-symmetry Γ point and with no other bands crossing the Fermi level elsewhere in the Brillouin zone. Because such a band inversion changes the parity of the wavefunction, it provides the proper condition for the TI state, yielding a handy indicator of the potential for specific compounds to be TIs. This can be quantified by calculating the band structure and measuring the degree of band inversion; in the half-Heuslers, a sensitive tuning of band inversion is possible due to the tunable lattice constants [8,9]. With the ability to tune the energy gap and set the desired band inversion by appropriate choice of compound with appropriate hybridization strength (i.e., lattice constant) and magnitude of spin-orbit coupling (i.e.,

nuclear charge), the half Heusler family shows much promise for realizing the next generation of TI materials.

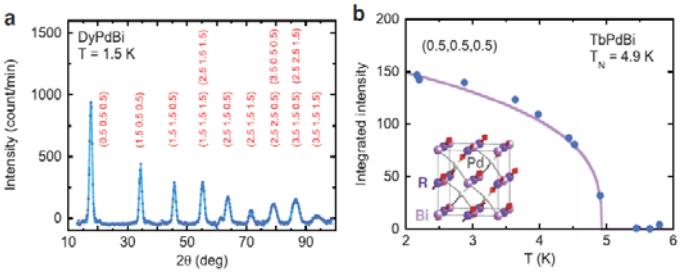

Figure 2: Neutron diffraction study of AFM order in a) DyPdBi and b) TbPdBi obtained from the intensity of the (0.5,0.5,0.5) magnetic Bragg peak. Solid curve is a mean-field fit to the data, and the inset presents a schematic of the antiferromagnetic spin structure [Nakajima *et al*, Science Advances (2015)].

Superconductors are among the most fascinating systems for realizing topological states, either via a proximity effect, or intrinsically via an odd-parity, time-reversal-invariant pairing state. Alongside the usual signature supercurrents arising from Cooper pair coherence, a direct analogy exists between superconductors and insulators: since the Bogoliubov-de Gennes (BdG) Hamiltonian for the quasiparticles of a superconductor is essentially analogous to that of a band insulator, one can consider the interesting possibility of TI surface states arising due to a superconducting "band gap". Similar to TI systems, a topological superconductor (TSC) thus has a fully gapped bulk band structure and gapless surface Andreev bound states. Thus the search for TSCs in materials with strong band inversion is a promising direction. In the case of time-reversal-invariant (centrosymmetric) systems, a material is a TSC if it is an odd-parity, fully gapped superconductor and its Fermi surface encloses an odd number of time-reversal-invariant momenta in the Brillouin zone [10].

Superconductors without inversion symmetry, or non-centrosymmetric superconductors, promise a much more robust route to realizing TSC states. With inversion symmetry being one of two key symmetries for Cooper pairing (time reversal being the other), its absence has profound implications on the formation of Cooper pairs. With a non-trivial topology of the Bogoliubov quasiparticle wavefunction resulting in protected zero-energy boundary states analogous to those of TI systems, the promise of TSC in NC superconductors is very strong. With strong band inversion, the RPtBi and RPdBi ternary half-Heusler compounds are candidate TI systems as explained above. As NC superconductors, the also have the potential to harbor mixed-parity states and are therefore unique in that they are simultaneously both TI and TSC candidate systems.

Recent Progress

We have completed a thorough study of the palladium-based rare earth-bismuthide (RPdBi) half-Heusler family, synthesizing high-quality crystalline specimens and fully characterizing their normal, superconducting and magnetic states in an effort to reveal their potential for realizing the next generation of topological insulators and superconductors. We synthesized the series of heavy-R compounds, including Sm, Gd, Tb, Dy, Ho, Er, Tm magnetic rare earths as well as Y and Lu non-magnetic elements. Electrical resistivity and magnetic susceptibility measurements of the RPdBi series has been performed down to 20 mK temperatures, revealing an interesting progression of superconducting phase transitions that evolves with rare earth species. We have found that superconductivity exists in most of these compounds, with a maximum transition T_c = 1.6 K found in the non-magnetic Y- and Lu-based compounds, and is systematically suppressed with increasing strength of magnetism from the magnetic rare earth species. Neutron scattering experiments performed in collaboration with Dr. Jeff Lynn at NIST Gaithersburg have confirmed long-ranged antiferromagnetic order as shown in Figure 2, which presents a representative scan of magnetic peaks in DyPdBi (T_N=3.5 K) and the AFM order parameter in TbPdBi (T_N=4.9 K). The R local moment sublattice leads to long-range antiferromagnetic (AFM) order in R=Sm, Gd, Tb, and Dy, as evidenced by abrupt drops in susceptibility. Low-temperature specific heat measurements confirm the thermodynamic AFM transitions, and reveal low-temperature ordering in HoPdBi and ErPdBi at 1.9 K and 1.0 K respectively. We also observe a precursor of magnetic order in

TmPdBi, as evidenced by a huge divergence of heat capacity reaching 10 J/mol K^2 at the lowest measured temperatures. Furthermore, superconductivity coexists with long-range magnetic order as shown in Figure 3, as determined by neutron scattering experiments on TbPdBi, DyPdBi and HoPdBi, which all undergo antiferromagnetic ordering transitions before entering a superconducting state at a lower temperature. This presents two rather interesting aspects that warrant further investigation: coexistence of superconductivity with potential spin-triplet non-trivial topology along with a new type of proposed topological insulator system, the antiferromagnetic topological insulator. Besides the exotic collective modes, antiferromagnetism breaks time reversal and translational symmetries but preserves the combination of both symmetries, leading to a new, as yet unrealized type of topological system. *This work appeared in Science Advances in June 2015*.

Because the non-centrosymmetry of the half-Heusler crystal structure forces an automatic mixing of singlet and triplet pairing states in the superconductivity, we are interested in determining the possibility of a complex superconducting gap function in this and related compounds. Such a gap function could lead to very unique excitations involved in the Majorana fermions in topological superconductors by controlling the singlet and triplet contributions. It is hoped in the half-Heusler series that the ability to fine-tune the lattice parameters, and hence aspects of the electronic band structure, one can tune the spin parity of the gap function from singlet dominant to triplet dominant as has been shown in other non-centrosymmetric systems.

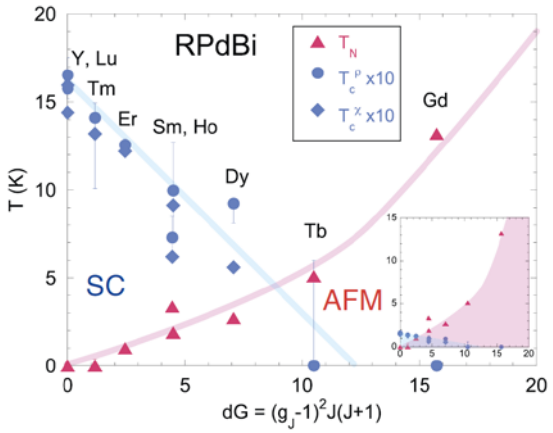

Figure 3: Phase diagram of RPdBi series, indicating evolution of superconducting (SC) and antiferromagnetic (AFM) ground states as a function of magnetic de Gennes factor. The plotted T_c is scaled by a factor of 10, and solid lines are guides to the eye. [Nakajima *et al*, Science Advances (2015)]

We have been working in collaboration with Joseph Stroscio at NIST Gaithersburg on scanning tunneling spectroscopy experiments on the platinum-based member YPtBi in order to search for signatures of unconventional superconductivity. With Dr. Stroscio's milliKelvin STM system, we have been working to characterize the nature of the superconducting energy gap, and hence the nature of Cooper pairing in these systems and whether evidence of spin-triplet pairing is evident. Difficulties in cleaving single crystal samples have hampered progress on this project, however the Stroscio group has made several breakthroughs in the last year leading to exciting results. Taking advantage of a local annealing technique that creates nanostructured superconductor islands by partial crystallization of an amorphous layer that results from the cleave process, we were able to create islands with diameters in the range of 100 nm, and characterize the superconducting island properties by scanning tunneling spectroscopic measurements to determine the gap energy, critical temperature and field, coherence length, and vortex formations. These results show unique properties of a confined superconductor and demonstrate that this new method holds promise to create tailored superconductors for a wide variety of nanometer scale applications. *This work is to be published in Physical Review B.*

Future Plans

We continue to explore the unusual normal and superconducting state properties of this family of compounds to understand the nature of the normal and superconducting states, using our full arsenal of probes in combination with a systematic growth program aimed at comparing properties of the RPtBi and RPdBi series. The peculiar normal state properties will be studied by probing their sensitivity to crystalline and sample surface quality by using different growth and treatment techniques (flux/melt

growth, Bridgman temperature gradient growth, arc melting growth, annealing, acid etching, high-temperature quench, etc.). Furthermore, with the availability of various rare earth substituents at our disposal, we plan to substitute varying amounts of magnetic and non-magnetic rare earth elements (e.g., $Y_{1-x}R_xPtBi$) to study the effects of magnetic impurities on both the TI surface states as well as the superconducting state.

A collaboration with Prof. Ruslan Prozorov at Ames National Lab continues to investigate the superconducting state of YPtBi by using milliKelvin TDR London penetration depth measurements, yielding a very interesting linear temperature dependence that is indicative of the presence of line nodes in the superconducting energy gap of YPtBi with moderate impurity scattering. With theoretical support from Prof. Daniel Agterberg at UM Wisconsin and Dr. Philip Brydon at U Maryland, we are developing a model to understand the nature of the pairing state in this material. In addition, we are collaborating with Dr. Jonathan Denlinger at Lawrence Berkeley National Lab to perform angle-resolved photoemission spectroscopy to map the electronic band structure of this material and further confirm the validity of our pairing model. Future work will extend this approach (both theoretical and experimental) to the RPdBi series, including understanding the interplay between magnetism and superconductivity.

References

1. C. L. Kane and E. J. Mele, "Z2 Topological Order and the Quantum Spin Hall Effect," Phys. Rev. Lett. 95, 146802 (2005); L. Fu and C. L. Kane, "Time reversal polarization and a Z2 adiabatic spin pump," Phys. Rev. B 74, 195312 (2006).
2. J. E. Moore, "The birth of topological insulators," Nature 464, 194 (2010).
3. M. Z. Hasan and C.L. Kane, Topological insulators, Rev. Mod. Phys. 82, 3045 (2010); X.-L. Qi and S.-C. Zhang, Topological insulators and Superconductors, Rev. Mod. Phys. 83, 1057 (2011).
4. F. Wilczek, "Majorana returns," Nature Phys. 5, 614 (2009).
5. A. Y. Kitaev, "Unpaired Majorana fermions in quantum wires", Phys.-Usp. 44, 131 (2001).
6. C. Nayak, S. H. Simon, A. Stern, M. Freedman, S. Das Sarma, "Non-Abelian anyons and topological quantum computation," Rev. Mod. Phys. 80, 1083 (2008).
7. B. Yan, S.-C. Zhang, "Topological Materials," Rep. Prog. Phys. 75, 096501 (2012).
8. S. Chadov *et al.*, "Tunable multifunctional topological insulators in ternary Heusler compounds," Nature Mater. 9, 541 (2010).
9. H. Lin *et al.*, "Half-Heusler ternary compounds as new multifunctional experimental platforms for topological quantum phenomena," Nature Mater. 9, 546 (2010); D. Xiao *et al.*, "Half-Heusler Compounds as a New Class of Three-Dimensional Topological Insulators" Phys. Rev. Lett. 105, 096404 (2010); W. Feng *et al.*, "Half-Heusler topological insulators: A first-principles study with the Tran-Blaha modified Becke-Johnson density functional," Phys Rev B 82, 235121 (2010); W. Al-Sawai *et al.*, "Topological electronic structure in half-Heusler topological insulators," Phys Rev B 82, 125208 (2010).
10. L. Fu, E. Berg, "Odd-Parity Topological Superconductors: Theory and Application to CuxBi2Se3", Phys. Rev. Lett. 105, 097001 (2010).

Publications

Y. Nakajima, R. Hu, K. Kirshenbaum, A. Hughes, P. Syers, X. Wang, K. Wang, R. Wang, S.R. Saha, D. Pratt, J.W. Lynn, and J. Paglione, "*RPdBi half-Heusler semimetals: a new family of non-centrosymmetric magnetic superconductors*", Science Advances 1, e1500242 (2015).

H. Baek, J. Ha, D. Zhang, B. Natarajan, J. P.Winterstein, R. Sharma, R. Hu, K. Wang, S. Ziemak, J. Paglione, Y. Kuk, N. B. Zhitenev, and J. A. Stroscio, "*Creating Nanostructured Superconductors by Local Current Annealing of the Half-Heusler Alloy YPtBi*", Phys. Rev. B – in press.

Project Title: Superconductivity and magnetism in *d*- and *f*-electron materials

Principal Investigator: M. Brian Maple
Mailing Address: Department of Physics, University of California, San Diego, La Jolla, CA 92093
Email: mbmaple@ucsd.edu

Project Scope

The emphasis of this project is on the physics of strongly correlated electron phenomena in novel transition metal, rare earth, and actinide based oxides and intermetallic compounds with a focus on the growth of high quality single crystals. These phenomena include superconductivity, novel types of magnetic and charge order, heavy fermion behavior, non-Fermi liquid behavior, quantum criticality, metal-insulator transitions, etc. The types of materials investigated include iron-based high temperature superconductors, layered BiS_2-based superconductors, uranium-based superconductors, magnetically ordered rare earth compounds, heavy fermion *f*-electron materials, transition metal oxides and intermetallic compounds. The approach involves the synthesis and characterization of bulk and thin film materials, with emphasis on single crystals, coupled with the investigation of their transport, thermal, and magnetic properties as a function of temperature, magnetic field and pressure. This approach completes the feedback loop between materials synthesis and properties measurements and thereby facilitates efforts to identify underlying mechanisms of correlated electron phenomena in new materials and modify materials of interest to optimize their properties. A wide variety of sample synthesis techniques are employed including solid-state reaction, arc-melting, pulsed laser deposition, optical floating zone growth, Czochralski crystal growth, and molten metal flux growth. Electrical/thermal transport, specific heat, and magnetization measurements can be performed in our laboratory at UCSD to temperatures as low as 20 mK, in magnetic fields up to 10 T, and pressures into the megabar range. More specialized measurements to study electronic and magnetic structures and excitations are carried out in the laboratories of collaborators and at national laboratory facilities for high magnetic field, synchrotron light source, and neutron scattering research.

Recent Progress

Our recent research has been focused on several topics, which include: Superconductivity in Bi-sulfide, Fe-pnictide, and LnT_4X_{12} filled skutterudite compounds; Yb valence fluctuations, quantum criticality, and superconductivity in the $Ce_{1-x}Yb_xCoIn_5$ system; hidden order, magnetism, and superconductivity in URu_2Si_2 and it alloys; rare earth transition metal cadmium "cage" compounds, and investigation of strontium iridates at high pressure. In the following, we briefly describe highlights in five of these areas.

Superconductivity in Bi-sulfide compounds

Polycrystalline samples of F-substituted $LnOBiS_2$ (*Ln* = La, Ce, Pr, Nd, Yb) compounds were synthesized by solid-state reaction. The compounds were found to exhibit superconductivity with superconducting critical temperatures T_c in the range 1.9 – 5.4 K; prior to this study, superconductivity had only been reported for the compound with Ln = La [12]. These materials belong to a new family of BiS_2-based superconductors that have layered crystal structures similar to those of high T_c cuprate and Fe-based superconductors [15]. We discovered a new method of inducing superconductivity in $LaOBiS_2$ by increasing the charge-carrier density (electron doping) via substitution of tetravalent Th^{4+}, Hf^{4+}, Zr^{4+}, and Ti^{4+} ions for trivalent La^{3+} (rather than substitution of F for O) [11]. The $LaOBiS_2$ and $ThOBiS_2$ parent compounds, which behave as bad metals, can be rendered superconducting by electron doping with T_c values reaching 2.85 K.

Electrical resistivity measurements under pressure to ~2.8 GPa on $LnO_{0.5}F_{0.5}BiS_2$ (*Ln* = La, Ce, Pr, Nd) compounds revealed a transition from a low-pressure superconducting phase to a high-pressure superconducting phase with a higher T_c (highest T_c = 10 K for La) at a critical pressure P_c that increases with *Ln* atomic number. A structural transition at P_c from tetragonal to monoclinic occurs for La (and probably the other *Ln* ions). Measurements of the electrical resistivity between 1 K and 300 K at pressures up to ~3 GPa on the four superconducting compounds $LnO_{0.5}F_{0.5}BiS_2$ (*Ln* = La, Ce, Pr, Nd) revealed a continuous transition from semiconducting towards nearly metallic behavior at $P \approx P_c$. The pressure dependence of the resistivity and the evolution of T_c with pressure are both remarkably consistent among all four compounds [3,9].

Yb valence fluctuations, quantum criticality, and superconductivity in the $Ce_{1-x}Yb_xCoIn_5$ system

The $Ce_{1-x}Yb_xCoIn_5$ system exhibits an Yb valence transition, suppression of the quantum critical field, and a Fermi-surface reconstruction at a nominal Yb concentration $x \approx 0.2$ (the actual composition is ~1/3 of the nominal concentration x up to $x \sim 0.5$) [4,8]. In collaboration with Professor Ruslan Prozorov's group at Iowa State University, the London penetration depth $\lambda(T)$ was measured in single crystals of $Ce_{1-x}R_xCoIn_5$ (R = La, Nd, and Yb) down to $T_{min} \approx 50$ mK ($T_c/T_{min} \sim 50$) using a tunnel-diode resonator (Kim *et al.* [6]). In the cleanest samples, $\Delta\lambda(T)$ is best described by a power law $\Delta\lambda(T) \propto T^n$, with $n \sim 1$, consistent with the existence of line nodes in the superconducting gap. Substitutions of La, Nd, and Yb for Ce lead to similar monotonic suppressions of T_c; however, the effects on $\Delta\lambda(T)$ differ. While La and Nd substitution leads to an increase in the exponent n and saturation at $n \sim 2$, as expected for a dirty nodal superconductor, Yb substitution leads to $n > 3$, suggesting a change from nodal to nodeless superconductivity. This change in superconducting gap structure occurs in the Yb concentration range where there are changes in the Fermi-surface topology, implying that the nodal structure and Fermi-surface topology are related.

Hidden order, magnetism and superconductivity in URu_2Si_2 and its alloys

The compound URu_2Si_2 undergoes a transition into a so-called "hidden order" (HO) phase at 17.5 K whose identity remains to be established after three decades of intense experimental and theoretical effort. The HO phase coexists with superconductivity below $T_c \approx 1.5$ K at atmospheric pressure [17]. The application of pressure results in a temperature T vs pressure P phase diagram in which superconductivity is suppressed and a transition from the HO phase to an antiferromagnetic (AFM) phase occurs at a pressure of about 1.5 GPa along the HO/AFM transition temperature T_o vs P phase boundary and ~0.8 GPa near 0 K. We have found that the substitution of Fe for Ru yields a T vs Fe concentration x phase diagram that resembles that of T vs P phase diagram of URu_2Si_2 when the Fe concentration is converted to "chemical pressure" P_{ch}, with a two-fold increase of the HO/AFM phase boundary $T_o(x)$ [2,5]. The chemical pressure P_{ch} is associated with the decrease in volume arising from the substitution of the smaller Fe atoms for Ru atoms. These results provide information that will be useful in developing theoretical candidates for the HO phase and provide an opportunity to apply spectroscopic techniques to probe the electronic structure and investigate the HO phase that cannot be employed under pressure, such as infrared reflectance (IR), angle-resolved photoemission spectroscopy (ARPES), and scanning tunneling microscopy (STM). Such investigations may yield the identity of the elusive HO phase in URu_2Si_2. Recent neutron diffraction measurements on the $URu_{2-x}Fe_xSi_2$ system have revealed that the magnetic moment increases rapidly with x in the HO regime to a maximum value of $\sim 0.8\ \mu_B$ and then decreases slowly with x in the AFM regime [2].

Rare earth transition metal cadmium "cage" compounds

We have a long standing interest in various classes of "cage compounds" such as filled skutterudites [18] and "1-2-20" compounds of the form RT_2X_{20}, where R is a rare-earth element, T is a transition metal, and X is an *s-p* metal like Al or Zn. Recently, we synthesized eleven new Cd-based compounds with chemical formulas RNi_2Cd_{20} (R = Y, La–Nd, Sm, Gd, Tb) and RPd_2Cd_{20} (R = Ce, Pr, and Sm) in single crystalline form [1,13,14,19]. These compounds crystallize in the $CeCr_2Al_{20}$-type structure in which the R and T crystallographic sites have cubic and trigonal point group symmetries, respectively. The coordination for the R site is a Frank–Kasper polyhedron with coordination number 16 (CN-16) and the T atoms occupy a site with icosahedral Cd coordination (CN-12). The Cd ions have three distinct crystallographic sites. These compounds contain both *f*- and *d*-electron ions, each of which can generate correlated electron behavior, that may act in concert to produce new types of emergent quantum phenomena. Our results show that $NdNi_2Cd_{20}$ orders antiferromagnetically with Néel temperatures T_N = 1.5 K, while $SmNi_2Cd_{20}$, $GdNi_2Cd_{20}$, and $TbNi_2Cd_{20}$ order ferromagnetically with Curie temperatures T_C = 7.2 K, 13.8 K, and 7.5 K, respectively.

The RT_2Cd_{20} compounds with R = Ce, Pr and T = Ni, Pd do not show any evidence of magnetic order above 2 K. Magnetization measurements on CeT_2Cd_{20} (T = Ni, Pd) reveal the presence of localized magnetic moments, which are favored by the large separations of ~ 6.7– 6.8 Å between Ce ions. The strength of the Ruderman–Kittel–Kasuya–Yosida exchange interaction between the localized moments is severely limited by the large Ce–Ce separations and by weak hybridization between localized Ce 4*f* and itinerant electron states. Measurements of electrical resistivity performed down to 0.14 K were unable to provide evidence of magnetic

order; however, magnetically ordered ground states with very low transition temperatures are still expected in these compounds despite the isolated nature of the localized magnetic moments [19]. Magnetization measurements suggest that Pr ions assume a nonmagnetic Γ_1 singlet or non-Kramers Γ_3 doublet ground state. A broad peak, identified as a Schottky anomaly, is observed in the specific heat at low temperature. Low-lying excitations involving the 4*f* electrons persist down to 2 K for both $PrNi_2Cd_{20}$ and $PrPd_2Cd_{20}$ and related features are also observed in the magnetization and electrical resistivity [14].

Investigation of strontium iridates at high pressure

High-temperature superconductivity, colossal magnetoresistance, and many other important phenomena have been observed among transition metal oxides that form with a perovskite crystal structure. While such compounds containing transition metal elements with 3*d* electrons are often electrically insulating, metallic ground states are expected for 5*d* transition metal oxides. This is a consequence of a combination of wide bands associated with 5*d* electrons and small Coulomb interactions *U*. However, the 5*d*-electron compound Sr_2IrO_4 is an electrical insulator as a result of strong spin-orbit coupling that induces a Mott instability. This mechanism results in a localized effective total angular momentum $J_{\text{eff}} = 1/2$ state in the strong spin-orbit coupling limit. The Mott energy gaps associated with this state are expected to be relatively small, so we performed measurements of the electrical resistance of single crystals of Sr_2IrO_4 and $Sr_3Ir_2O_7$ under pressure in an attempt to induce a metallic state in these compounds. We found that pressures up to 55 GPa were insufficient to close the relatively pressure-independent energy gap in Sr_2IrO_4. On the other hand, the application of pressures up to 60 GPa caused the electrical resistance of $Sr_3Ir_2O_7$ at 10 K to decrease by five orders of magnitude (Mott energy gap was significantly reduced). However, further increases in pressure up to 100 GPa were unable to completely close the Mott energy gap and induce a metallic state [16].

Future plans

Some of our future research plans are briefly described in the following:

Yb valence fluctuations, quantum criticality, and superconductivity in the $Ce_{1-x}Yb_xCoIn_5$ system

As a follow up to the recent penetration depth measurements on the $Ce_{1-x}Yb_xCoIn_5$ system which indicate that a nodal to nodeless transition in the superconducting energy gap occurs at $x \approx 0.2$, we plan to perform detailed measurements of the specific heat and thermal conductivity as a function of temperature and angular dependence of magnetic field to probe the superconducting energy gap with several groups of collaborators. Inelastic neutron scattering measurements to probe the magnetic excitations involved in the superconducting electron pairing in $Ce_{1-x}Yb_xCoIn_5$ in collaboration with Professor Pengcheng Dai of Rice University are currently underway. We will continue an investigation of the related $Ce_{1-x}Yb_xRhIn_5$ system to determine whether Yb undergoes a valence transition as a function of *x* and how this affects the physical properties of this system as a function of temperature, magnetic field and pressure.

Rare earth transition metal cadmium "cage" compounds

The new series of compounds generated by filling the *X* position in RT_2X_{20} with Cd ions opens this family to further investigations of new quantum phases and phenomena that may not be present in the *X* = Al, Zn series of compounds. We plan to investigate the RT_2Cd_{20} compounds with *R* = Ce, Pr and *T* = Ni, Pd at low temperatures in the mK region in high magnetic fields to determine the ground states of the *R* ions and to study magnetic or quadrupolar order that will presumably occur at low temperatures. These compounds may exhibit an unconventional form of superconductivity mediated by magnetic, quadrupolar, or valence fluctuations at low temperatures and high pressures due to the increase in hybridization under pressure. Ultrasound measurements are planned in collaboration with Professor T. Yanagisawa of Hokkaido University.

Hidden order, magnetism, quantum criticality, and superconductivity in URu_2Si_2 and its alloys

We will continue our efforts to grow single crystals of $URu_{2-x}T_xSi_2$ (*T* = Fe, Os, Re) pseudoternary compounds for studies of HO, magnetism, quantum criticality, and superconductivity in these systems. Further measurements will be performed to establish a detailed *T* vs Fe concentration phase diagram in the $URu_{2-x}Fe_xSi_2$ system. Transport, thermal and magnetic measurements will be carried out on $URu_{2-x}Fe_xSi_2$ single crystals, some at high pressures and in high magnetic fields; e.g., electrical resistivity, Hall effect,

magnetoresistance, magnetization, specific heat, thermoelectric power, thermal expansion, and differential electroresistance. Spectroscopic studies that are planned include inelastic neutron scattering, infrared spectroscopy, Raman spectroscopy, ultrafast optical spectroscopy, NMR, ARPES, and STM. Many of these studies will be carried out with collaborators who are experts in performing, and interpreting the results of, these types of measurements. In addition, we will conduct exploratory research on other $URu_{2-x}T_xSi_2$ systems.

Selected Publications (which acknowledge DOE support)

[1] V. W. Burnett, D. Yazici, B. D. White, N. R. Dilley, A. J. Friedman, B. Brandom, and M. B. Maple, "Structure and physical properties of RT_2Cd_{20} (R = rare earth, T = Ni, Pd) compounds with the $CeCr_2Al_{20}$-type structure," *J. Solid State Chem.* **215**, 114 (2014).

[2] P. Das, N. Kanchanavatee, J. S. Helton, K. Huang, R. E. Baumbach, E. D. Bauer, B. D. White, V. W. Burnett, M. B. Maple, J. W. Lynn, and M. Janoschek, "Chemical pressure tuning of URu_2Si_2 via isoelectronic substitution of Ru with Fe," *Phys. Rev. B* **91**, 085122 (2015).

[3] Y. Fang, D. Yazici, B. D. White, and M. B. Maple, "Enhancement of superconductivity in $La_{1-x}Sm_xO_{0.5}F_{0.5}BiS_2$," *Phys. Rev. B* **91**, 064510 (2015).

[4] T. Hu, Y. P. Singh, L. Shu, M. Janoschek, M. Dzero, M. B. Maple, and C. C. Almasan, "Non-Fermi liquid regimes with and without quantum criticality in $Ce_{1-x}Yb_xCoIn_5$," *Proc. Nat. Acad. Sci.* **110**, 7160 (2013).

[5] N. Kanchanavatee, B. D. White, V. W. Burnett, and M. B. Maple, "Enhancement of the hidden order/large moment antiferromagnetic transition temperature in the $URu_{2-x}Os_xSi_2$ system," *Phil. Mag.* **94**, 3681 (2014).

[6] H. Kim, M. A. Tanatar, R. Flint, C. Petrovic, R. Hu, B. D. White, I. K. Lum, M. B. Maple, and R. Prozorov, "Nodal to Nodeless Superconducting Energy-Gap Structure Change Concomitant with Fermi-Surface Reconstruction in the Heavy-Fermion Compound $CeCoIn_5$," *Phys. Rev. Lett.* **114**, 027003 (2015).

[7] L. Shu, D. E. MacLaughlin, C. M. Varma, O. O. Bernal, P.-C. Ho, R. H. Fukuda, X. P. Shen, and M. B. Maple, "Landau Renormalizations of Superfluid Density in the Heavy-Fermion Superconductor $CeCoIn_5$," *Phys. Rev. Lett.* **113**, 16640 (2014).

[8] B. D. White, J. D. Thompson, and M. B. Maple, "Unconventional superconductivity in heavy-fermion compounds," *Physica C* **514**, 246 (2015).

[9] C. T. Wolowiec, D. Yazici, B. D. White, K. Huang, and M. B. Maple, "Pressure induced enhancement of superconductivity and suppression of semiconducting behavior in $LnO_{0.5}F_{0.5}BiS_2$ (Ln = La, Ce) compounds," *Phys. Rev. B* **88**, 064503 (2013).

[10] C. T. Wolowiec, B. D. White, and M. B. Maple, "Conventional magnetic superconductors," *Physica C* **514**, 113 (2015).

[11] D. Yazici, K. Huang, B. D. White, I. Jeon, V. W. Burnett, A. J. Friedman, I. K. Lum, M. Nallaiyan, S. Spagna, and M. B. Maple, "Superconductivity induced by electron doping in $La_{1-x}M_xOBiS_2$ (M = Ti, Zr, Hf, Th)," *Phys. Rev. B* **87**, 174512 (2013).

[12] D. Yazici, K. Huang, B. D. White, A. H. Chang, A. J. Friedman, and M. B. Maple, "Superconductivity of F-substituted LnOBiS2 (Ln = La, Ce, Pr, Nd, Yb) compounds," *Phil. Mag.* **93**, 673 (2013).

[13] D. Yazici, B. D. White, P.-C. Ho, N. Kanchanavatee, K. Huang, A. J. Friedman, A. S. Wong, V. W. Burnett, N. R. Dilley, and M. B. Maple, "Investigation of magnetic order in $SmTr_2Zn_{20}$ (Tr = Fe, Co, Ru) and $SmTr_2Cd_{20}$ (Tr = Ni, Pd)," *Phys. Rev. B* **90**, 144406 (2014).

[14] D. Yazici, T. Yanagisawa, B. D. White, and M. B. Maple, "Nonmagnetic ground state in the cubic compounds $PrNi_2Cd_{20}$ and $PrPd_2Cd_{20}$," *Phys. Rev. B* **91**, 115136 (2015).

[15] D. Yazici, I. Jeon, B. D. White, and M. B. Maple, "Superconductivity in layered BiS_2-based compounds," *Physica C* **514**, 218 (2015).

[16] D. A. Zocco, J. J. Hamlin, B. D. White, B. J. Kim, J. R. Jeffries, S. T. Weir, Y. K. Vohra, J. W. Allen, and M. B. Maple, "Persistent non-metallic behavior in single- and bi-layered iridates Sr_2IrO_4 and $Sr_3Ir_2O_7$ at high pressures," *J. Phys.: Condens. Matter* **26**, 255603 (2014).

[17] L. A. Wray, J. Denlinger, S. Huang, H. He, N. P. Butch, M. B. Maple, Z. Hussain, and Y. Chuang, "Spectroscopic Determination of the Atomic f-Electron Symmetry Underlying Hidden Order in URu_2Si_2," *Phys. Rev. Lett.* **114**, 236401 (2015).

[18] J. Zhang, D. E. MacLaughlin, A. D. Hillier, Z. F. Ding, K. Huang, M. B. Maple, and L. Shu, "Broken time-reversal symmetry in superconducting $Pr_{1-x}Ce_xPt_4Ge_{12}$," *Phys. Rev. B* **91**, 104523 (2015).

[19] B. D. White, D. Yazici, P-C. Ho, N. Kanchanavatee, N. Pouse, Y. Fang, A. J. Breindel, A. J. Friedman, and M. B. Maple, "Weak hybridization and isolated localized magnetic moments in the compounds CeT_2Cd_{20} (T = Ni, Pd)," *J. Phys: Condens. Matter* **27**, 315602 (2015).

Session III

Interface-Driven Chiral Magnetism in Ultrathin Metallic Ferromagnets: Towards Skyrmion Spintronics

Geoffrey Beach, Department of Materials Science and Engineering, Massachusetts Institute of Technology, Cambridge, MA 02135; Email: gbeach@mit.edu

Program Scope

Magnetic skyrmions [1-3] are localized chiral magnetic textures in the form of nanoscale vortices or bubbles that are topologically protected from being 'unwound'. Their topological nature gives rise to rich behaviors including ordered lattice formation, emergent electrodynamics and robust current-driven displacement at remarkably low current densities. However, magnetic skyrmions have so far been restricted to just a few materials and observed only at low temperatures, limiting the experimental accessibility and technological application of these unique topological objects. This project aims to realize magnetic skyrmions at room temperature in ultrathin ferromagnetic transition metal films in which interfaces with heavy metals generate a strong chiral Dzyaloshinskii-Moriya interaction (DMI) that can stabilize topological spin textures [4,5]. This project focuses on ultrathin magnetic heterostructures that are engineered and patterned into laterally-confined nanostructures in which skyrmions can be stabilized, manipulated, and detected under ambient conditions. Specific aims of this project include

- Developing a fundamental understanding of the mechanisms to optimally engineer interfacial Dzyaloshinskii-Moriya exchange interactions at ferromagnetic/heavy metal interfaces in order to stabilize individual skyrmions and chiral magnetic ground states.
- Elucidating the static and dynamic properties and interactions of individual skyrmions and skyrmion lattices through x-ray imaging, and magnetotransport studies.
- Understanding charge/spin transport in the presence of skyrmions in ultrathin films, including phenomena such as emergent electrodynamics and topological electromotive forces, and exploiting spin-transfer and spin-orbit torques, and interface-driven mechanisms, to control skyrmions in nanoscale devices.

Recent Progress

During the past year, we have observed stable magnetic skyrmions and their current-driven motion in a thin transition metal ferromagnet at room temperature, using high-resolution magnetic transmission x-ray microscopy (MTXM) at ALS and scanning transmission x-ray microscopy (STXM) at BESSY II Berlin. In the work described below, we have 1) quantitatively determined the strength of the interfacial DMI in polycrystalline Pt/Co/Ta multilayer films through its influence on domain structure and the domain wall (DW) energy; 2) examined magnetic skyrmions in laterally-confined geometries, and demonstrated dynamical switching between a worm domain state and an ordered hexagonal skyrmion lattice that is stable in the absence of a field; 3) created trains of skyrmions in a magnetic strip and characterized their current-driven dynamics, providing the first experimental demonstration of a skyrmion racetrack.

Our studies have focused on $[Pt(3nm)/Co(0.9nm)/Ta(4nm)]_{15}$ multilayer stacks with perpendicular magnetic anisotropy (PMA). Our prior work has shown that Pt/ferromagnet interfaces exhibit very strong DMI, while Ta/ferromagnet interfaces generate very weak DMI, so that a strong net DMI is expected in this heterostructures. Moreover, both Pt and Ta have large spin Hall angles, with opposite signs, so that they generate spin Hall currents that are additive, enhancing the spin torque efficiency.

Determining DMI strength from domain spacing. MTXM was used to image the domain structure in continuous Pt/Co/Ta multilayers, from which the DMI was quantified for the fist time through purely static measurement. At remanence, the film exhibits a demagnetized labyrinth domain structure, where the domain width reflects the balance between the decreased demagnetizing energy and increased domain wall (DW) energy in the multidomain state. The latter scales with the DW surface energy density $\sigma_{DW} = 4\sqrt{AK_{u,eff}} - \pi|D|$, with A the exchange stiffness, $K_{u,eff}$ the effective uniaxial anisotropy constant, and D the DMI constant. Hence, σ_{DW} is lowered and domain formation is more favorable whenever D is finite. The high spatial resolution (~25 nm) of MTXM allowed measurement of the widths of up and down domains, respectively, as a function of increasing field. Analytical and micromagnetic modelling of the data yield σ_{DW} = 1.3±0.2 mJ/m^2, much smaller than $4\sqrt{AK_{u,eff}} \approx 5.3$ mJ/m^2 expected in the absence of DMI. From this we compute a large DMI with $|D|$ = 1.3±0.2 mJ/m^2, far exceeding the threshold required to stabilize homochiral Neel domain walls.

Stabilization of a skyrmion lattice phase in geometrically-confined structures. Recent simulations [4] suggest that in thin films with strong DMI, lateral confinement can act to stabilize skyrmions through topological edge repulsion. We therefore examined the influence of geometrical constraint on domain structure in Pt/Co/Ta disks of varying diameter. Figure 1a shows STXM images of the domain structure in a 2 μm diameter Pt/Co/Ta disk during minor loop cycling of the out-of-plane field B_z. The left panel shows a parallel stripe phase at B_z = -6 mT (favoring down, or light-contrast domains), which transforms spontaneously into a symmetric hexagonal skyrmion lattice when the field is quasistatically swept to +2 mT, favoring up (dark-contrast) domains. Figure 2b summarizes experiments that have examined the dynamical transformation of a labyrinth stripe domain phase into a hexagonal skyrmion lattice, using a lithographically patterned microcoil to apply large, fast-risetime field pulses. When

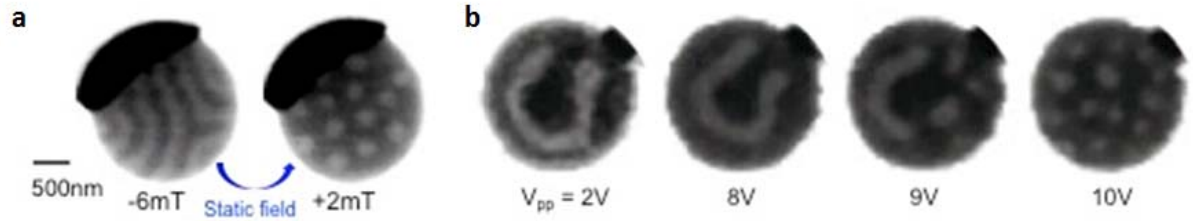

Fig. 1. a, STXM images of the domain state in a 2 μm Pt/Co/Ta disk at B_z = -6 mT (left) and after subsequently applying B_z = 2 mT (right). b**,** Sequence of STXM images after applying bipolar pulse trains (peak-to-peak voltage amplitude V_{pp}) with a microcoil, showing transformation from labyrinth stripe domain into skyrmion lattice.

formed, these skyrmion lattices remain stable at zero field. Detailed micromagnetic simulations (were performed to understand magnetic phase diagram and skyrmion lattice stability.

Current-driven motion of skyrmions in a track. Recent simulations suggest that skyrmions in ultrathin films might be driven with high efficiency by the spin Hall effect, which can occur when charge current flows in an adjacent heavy metal. As the spin Hall effect-direction of motion of a skyrmion depends on its topology, observations of current-induced displacement can moreover serve to verify the topology and chirality of the skyrmions in this system. Fig. 2b shows a sequence of STXM images of a train of four skyrmions stabilized by a small field B_z. Each image was acquired after injecting 20 current pulses with current-density amplitude $j_a = 2.2 \times 10^{11}$ A/m^2 and duration 20 ns, with the polarity indicated in the figure. Three of the four skyrmions move freely along the track, and can be displaced back and forth by current, while the left-most skyrmion remains immobile, evidently pinned by a defect. The propagation direction is along the current flow direction (against electron flow), and this same directionality was observed for skyrmions of opposite polarity. Our micromagnetic simulations show that the observed unidirectional spin-Hall driven displacement is consistent with Néel skyrmions with left-handed chirality, confirming the topological nature of the skyrmions in this material.

We found that the skyrmions move at different average speeds in different regions of the track, suggesting a significant influence of pinning on the skyrmion motion in this current regime. At the highest current density used, we find that pinned skyrmions can be annihilated, as in the last image of Fig. 2b, where only three skyrmions remain, and the leftmost skyrmion becomes pinned at the same location as was the annihilated skyrmion. The average velocity of the most mobile skyrmion versus current density is shown in Fig. 2c, with the narrow range determined by the critical propagation threshold and the maximum pulse amplitude experimentally available.

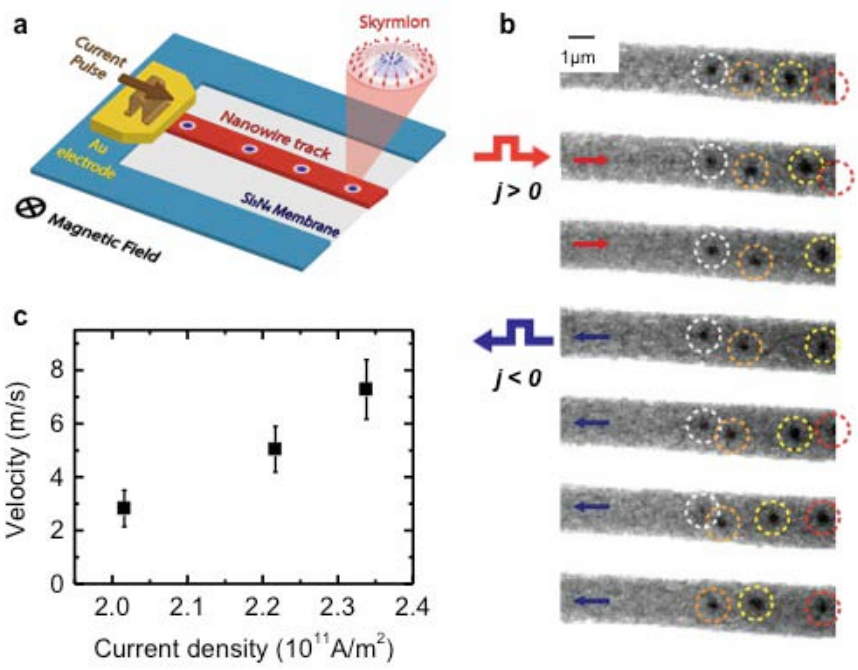

Fig. 2. **a,** Schematic of magnetic track on Si_3N_4 membrane with current contacts and skyrmions stabilized by a down-directed applied magnetic field. **b,** Sequential STXM images showing skyrmion displacement after injecting 20 unipolar current pulses along the track, with an amplitude $j_a = 2.2 \times 10^{11}$ and polarity as indicated. Individual skyrmions are outlined in colored circles for clarity. **c,** Average velocity versus current density for the skyrmion circled in yellow in **b**

We find velocities that are significantly lower than calculated for a defect-free sample, in contrast to recent micromagnetic studies that predict high skyrmion mobility even in the presence of defects. Micromagnetic simulations suggest that dispersion in the local DMI due to interface disorder causes skyrmion pinning and reduced velocities qualitatively consistent with experiments.

Future Plans

1. We will continue our magnetic transmission x-ray microscopy efforts to image the recently-discovered skyrmion lattice phase in geometrically confined structures of heavy metal/ferromagnet multilayers, varying stacking materials and structures to determine the phase space for lattice stability. Micromagnetic simulations will be used to provide insight into the energy landscape of stripe and lattice phases and the mechanisms for dynamical transformations
2. Current-driven skyrmion dynamics will be examined in detail, using both x-ray microscopy and magneto-optical Kerr effect studies. The primary aim will be to reach a velocity regime corresponding to dynamical flow (as opposed to the depinning regime) and to perform pump-probe measurements of skyrmion velocity and trajectory. Results will be modeled micromagnetically to provide insight into gyrotropic dynamics of skyrmion dynamics.
3. Initial work will begin to search for signatures of topological Hall effects in metallic ferromagnets supporting individual skyrmions and a skyrmion lattice phase. Lithographic processes to prepare optimized dots on Hall cross structures with integrated excitation coil will be developed, and electrical measurements performed under conditions informed by microscopy experiments that confirm the presence of a skyrmion lattice in the device.

References

1. Rößler, U. K., Bogdanov, A. N. & Pfleiderer, C. Spontaneous skyrmion ground states in magnetic metals. Nature 442, 797–801 (2006).
2. Mühlbauer, S. et al. Skyrmion Lattice in a Chiral Magnet. Science 323, 915–919 (2009).
3. Heinze, S. et al. Spontaneous atomic-scale magnetic skyrmion lattice in two dimensions. Nat. Phys. 7, 713–718 (2011).
4. Emori, S., Bauer, U., Ahn, S.-M., Martinez, E. & Beach, G. S. D. Current-driven dynamics of chiral ferromagnetic domain walls. Nat. Mater. 12, 611–616 (2013).
5. Fert, A., Cros, V. & Sampaio, J. Skyrmions on the track. Nat. Nanotechnol. 8, 152–156 (2013).

Publications

1. S. Woo, K. Litzius, B. Krüger, M.-Y. Im, L. Caretta, K. Richter, M. Mann, A. Krone, R. Reeve, M. Weigand, P. Agrawal, P. Fischer, M. Kläui, and G. S. D. Beach, "Observation of room temperature magnetic skyrmions and their current-driven dynamics in ultrathin Co films," submitted (2015).

Program Title: Non-Equilibrium Magnetism: Materials and Phenomena
Principle Investigator: Frances Hellman; Co-PIs Jeff Bokor, Peter Fischer, Steve Kevan, Sayeef Salahuddin, Lin-Wang Wang; Materials Sciences Division, LBNL
Email: fhellman@berkeley.edu or fhellman@lbl.gov

i) Program Scope

This new program focuses on fundamental science of non-equilibrium magnetic materials and phenomena with emphasis on those enabled by interfaces and spin-orbit coupling. It encompasses design, fabrication, measuring, and modeling of static and dynamic magnetic properties of thin film materials exhibiting strong spin-orbit interactions and inversion symmetry breaking due to interfaces. The research addresses three interrelated sub-projects in these heterostructure materials:

- **i)** Dynamics and thermodynamics of static and quasi-static novel thin film spin structures such as skyrmions and chiral magnetic textures and domain walls
- **ii)** Strong spin accumulation, spin transfer, and consequent control of magnetization created by interfaces between ferromagnet/non-magnet with strong spin-orbit coupling
- **iii)** Highly non-equilibrium magnetic states produced through electron or optical pumping at time scales ranging from nsec to fsec

Through strategic choice of materials and utilizing a collective expertise in growth, magnetic, electrical, optical, and thermodynamic characterization, spectromicroscopy, and theoretical modeling, the NEMM team aims to control the strength of the critical underlying, sometimes competing, interactions (spin-orbit, exchange, single ion anisotropy, Dzyaloshinskii-Moriya, Coulomb, disorder) within and between dissimilar materials in proximity to each other, enabling development of models for resulting magnetic states and their dynamics. Theoretical modeling provides a basis for understanding the structure (atomic, electronic, magnetic) and dynamics (electron and spin transport, magnetization response) of these states, and guides exploration of the multidimensional space of new material systems. Our initial focus is on B20 phase compounds and RE-TM alloys, with high SOC metals including Pt, Ta, W and their alloys, with comparison oxide structures to separate charge from spin transport effects.

ii) Recent Progress

a) Local spin configuration at Domain Walls in Co-Pt Multilayers

XMCD-spectromicroscopy using magnetic transmission soft x-ray microscopy (MTXM) at the Co L_3 and L_2 edges in a (Co 0.3nm/Pt 0.5nm)x30 PtCo multilayer film indicates a significant reduction of L/S at the domain walls (Fig. 1) [P3]. This can be explained by a deviation from the spin texture in a Bloch wall, where close to the surface of the film, the spins form more Neel-type walls. An analogous phenomenon has been observed as Neel caps, which occur in in-plane

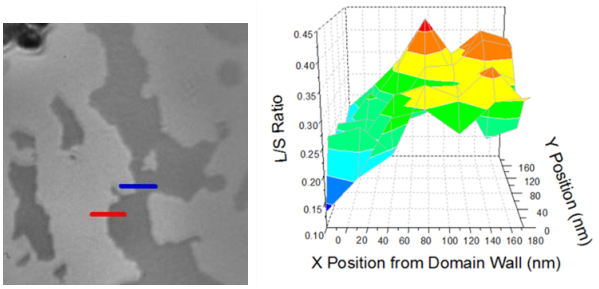

Fig. 1: Left: MTXM image at the Co L_3 edge. Lines indicate two intensity profiles across the domain wall where the L_3/L_2 values are derived. Right: 3dim representation of the L_3/L_2 profile as a function of distance to the domain.

magnetized nanostructures [1]. Such canting of spins across the thickness of a film could aide the formation of skyrmions in thin films and a fundamental understanding of their formation will have impact to domain wall engineering for spin torque transfer (STT) devices. We have developed DFT code with spin-orbit coupling and noncollinear magnetism, enabling us to define the parameter space for the experiments and to interpret our experimentally observed data.

b) Room Temperature Dipole-induced Skyrmion Phases in Amorphous Gd-Fe Films

Using resonant soft x-ray scattering (RSXS), MTXM, and Lorentz transmission electron microscopy (LTEM), we have discovered intriguing, tunable skyrmion phases in *a*-Gd-Fe that extend to 300K. Fig. 2 (left) presents a room temperature LTEM image showing a single skyrmion in a sea of biskyrmions [2,3], and room temperature RSXS results (right) that indicate how a phase with aligned stripe domains at low field (a) transforms to a two-fold symmetric diffraction pattern indicative of a biskyrmion phase at higher field (b), and then to a hexagonal phase at still higher field (c), and finally to a uniform phase (not shown). These behaviors can be tuned by varying the field protocol, and are very sensitive to film composition and thickness. Based on LTEM, we developed a model for how the spin textures evolve and for the internal structures of the skyrmions and biskyrmions. The phases are net achiral, and we conclude that the skyrmion phases are driven primarily by competition between exchange, anisotropy and dipolar interactions; surface or bulk chiral interactions are not necessary to explain our results.

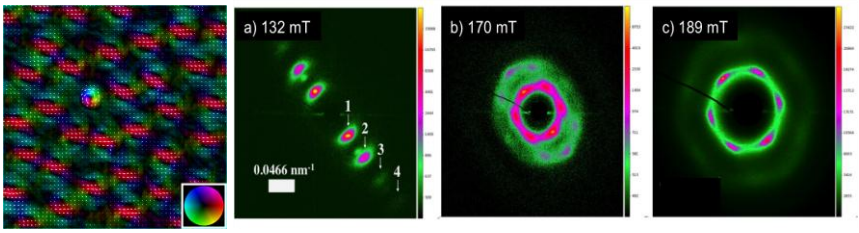

Fig 2 LTEM image (left), RSXS (right) at various fields showing skyrmion phases in a-Gd-Fe films at 300K.

c) Imaging magnetization dynamics in imprinted skyrmionic textures

Imprinting magnetic vortices from permalloy disks into an out-of-plane magnetized Co/Pd multilayer stack has been shown to produce chiral spin textures with a skyrmion number that can be manipulated by tuning interlayer exchange coupling via the thickness of an interspacer Pd layer [P10]. We have studied the nsec spin dynamics of such non-collinear textures using time-resolved MTXM in a pump-probe setup [P11]. We have described the observed dynamics analytically within the Thiele equation taking into account an enlarged core size of the imprinted donut state with respect to regular magnetic vortices. We find a clear dependence of the gyrofrequency on the interlayer exchange coupling strength that offers an indirect access to the core diameter via its dynamic mass.

d) Temperature driven skyrmion and domain wall motion

Beyond field driven control of magnetic textures, we are investigating both the static and dynamics of spin textures upon local heating with the goal to understand coupling of heat to spin currents. Although first studies indicate the possibility to drive domain walls by thermal

gradients [4], a microscopic understanding of these processes is still lacking. Specifically, the question as to whether the observed motion is purely temperature driven or whether there are additional spin currents involved is far from experimentally confirmed. To that end, we have developed a membrane-based heater stage with high (100K/μm) controlled thermal gradient to measure thermoelectric and thermodynamic effects in skyrmion structures and perform magnetic x-ray imaging studies, with about 20nm spatial resolution of the position of domain walls and skyrmionic textures before and after the application of tailored heat pulses.

e) Spin Hall heterostructures.

We have shown that spin currents generated by dissimilar materials do not add algebraically, and that bulk Spin Hall Effect cannot be the only source of the spin current. Fig. 3 shows switching current density vs Ta thickness for a CoFeB/Ta/Pt heterostructure where the total thickness of Ta+Pt is 10 nm. As the Ta thickness is reduced, one would expect Pt to dominate the total spin current accumulated at the CoFeB/Ta interface and hence the switching current to go up. Surprisingly, the opposite is observed, showing that the spin current from Pt and Ta do not add algebraically and the CoFeB/Ta interface dominates the sign of the magnetic switching. [P12]

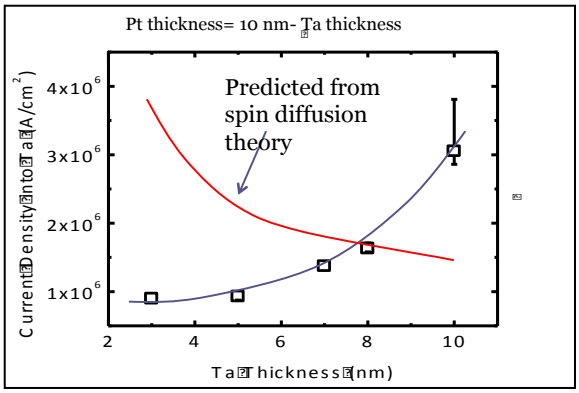

Fig 3. Switching current density plotted as a function of Ta thickness. [P12]

iii) **Future Plans**

a) Skyrmion studies: We will experimentally and theoretically construct the thickness–composition–field-temperature phase diagram in the *a*-Gd-Fe system and related RE-TM alloys, particularly those with different magnetic anisotropy and high SOC overlayers hence controlled DMI. We will study the *motion* of skyrmion and biskyrmions, driven by an electrical or thermal current, using TXM and LTEM. As a first example, skyrmions of opposite helicity should accelerate in opposite directions, so this will allow separation of the biskyrmion and mixed-helicity skyrmion phases into macroscopically separated chiral domains. We will conduct studies of temperature dependent domain wall motion in RE-TM systems to investigate thermally induced spin torque domain wall motion. This would indicate a thermal current that induces a pure spin current (see Spin-Seebeck, Spin Nernst, Spin-Peltier effects). We will investigate effects on this of chiral walls resulting from high SOC metal overlayers and varying anisotropy.

b) Optical magnetic second harmonic generation to study dynamics of buildup of spin accumulation in SOC metals (Pt, Ta, Au, W). By optical magnetic second harmonic generation we have directly detected surface spin accumulation (see Figure 4) and will now turn to the dynamics of buildup of spin accumulation and spin-Hall angle in the absence of the ferromagnet by calibrating to spin polarization in the normal metal

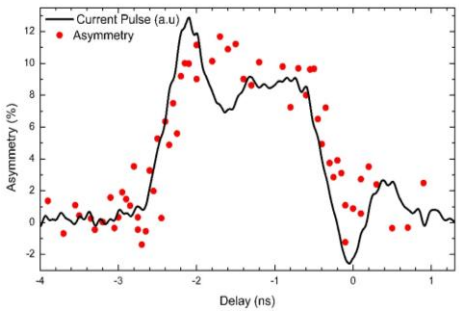

Fig 4: Time resolved MSHG for 10 nm Pt

induced by external magnetic field. We will explore the mechanism of spin transport across interface(s), laser-induced depolarization of spins in normal metal and exchange coupling across interface under non-equilibrium conditions, and use quantum transport calculations at the interface with SOC to calculate directly spin accumulation.

c) Time-resolved magneto-optic Kerr effect (MOKE) with ultrafast electrical and optical pulse excitation, to study highly non-equilibrium magnetic states produced and studied through electron, optical and x-ray pump/probe techniques at time scales ranging from nsec to fsec, focusing on heterostructures of TM and RE-TM alloys with high SOC normal metals (Pt, Ta, W), and using rt-TDDFT calculation on the SOC PEtot code to understand demagnetization processes after laser excitation; the goal is to understand the underlying physics so as to control magnetism via this non-equilibrium regime. We have reproduced the puzzling, controversial, and poorly understood phenomenon of helicity-independent all-optical switching in amorphous GdFeCo [5]. We will now explore the dynamics of the process, including testing other triggering mechanisms such as direct electron injection, to provide crucial constraints on theoretical models. We also developed an improved code (incorporating the SOC PEtot version with the rt-TDDFT version), used in some preliminary runs for ultrafast demagnetization.

iv) ***References***

1) F. Cheynis et al, Phys. Rev. Lett. 102, 107201 (2009).
2) X. Z. Yu, Y. Tokunaga, Y. Kaneko, W. Z. Zhang, K. Kimoto, Y. Matsui, Y. Taguchi, and Y. Tokura, Nat Commun 5 (2014);X. Yu et al, PNAS 109, 8856 (2012).
3) N. Nagosa and Y. Tokura, Nature Nanotechnology 8, 899 (2013).
4) R. Tolley, T. Liu, Y. Zu, S. Le Gall, M. Gottwald, T. Hauet, M. Hehn,. F. Montaigne, E.E. Fullerton, and S. Mangin, Appl Phys Lett 106, 242403 (2015)
5) I. Radu, H. A. Durr, et al., Nature, vol. 472, pp. 205-208, Apr 2011.

i) ***Publications*** (work supported by the DOE since program started Aug. 2014)

P1) P. Fischer, *Frontiers in imaging magnetism with polarized x-rays*, Front. in Phys. 2:82 (2014)
P2) P. Fischer, *X-ray imaging of magnetic structures*, IEEE Trans. Magn. 51 0800131 (2015)
P3) M.J. Robertson, Ch.J. Agostino, A.T. N'Diaye, G. Chen, M.-Y. Im, and P. Fischer, *Quantitative XMCD mapping with high spatial resolution full-field magnetic transmission soft x-ray spectro-microscopy*, J Appl Phys 117 17D145 (2015)
P4) P. Fischer and H. Ohldag, *X-rays and magnetism: a review of program in magnetic studies with polarized soft x-rays*, Report on Progress in Physics 78 094501 (2015)
P5) M. Charilaou and F. Hellman, *Surface-induced phenomena in uncompensated collinear antiferromagnets,* J. Phys.: Cond Matter 27, 086001 (2015).
P6) M. Charilaou and F. Hellman, *Roughness effects in uncompensated antiferromagnets*, J. Appl. Phys. 117, 083907 (2015)
P7) J. Karel, J. Juraszek, J. Minar, C. Bordel, K.H. Stone, Y. N. Zhang, J. Hu, R. Q. Wu, H. Ebert, J.B. Kortright and F. Hellman, *Effect of Chemical Order on the Magnetic and Electronic Properties of Epitaxial, Off-Stoichiometry FexSi1-x Thin Films*, Phys. Rev. B 91, 14402 (2015)
P9) C. Baldasseroni, C. Bordel, C. Antonakos, A. Scholl, K. Stone, J. Kortright, F. Hellman, *Temperature-driven growth of antiferromagnetic domains in thin-film FeRh,* J. Phys.: Cond. Matt. (2015).
P10) R. Streubel, L. Han, M.-Y. Im, F. Radu,R. Abdrudan, U. K. Roessler, G. Lin, O. G. Schmidt, P. Fischer, D. Makarov, *Manipulating Topological States by Imprinting Non-Collinear Spin Textures*, Sci Rep 5 8787 (2015).
P11) R. Streubel, P. Fischer, M. Kopte, O.G. Schmidt, and D. Makarov, *Magnetization Dynamics of Imprinted Non-collinear Spin Textures,* Appl Phys Lett (2015) accepted.
P12) D. Bhowmik, N. Kent, L-W. Wang, P. Fischer, S. Salahuddin, *Interface-induced SOT efficiency in spin Hall heterostructure*, preprint

Project Title: **Novel Regimes of Spin Transport: Pure Spin Currents in Antiferromagnets and Time-Resolved Studies of Spin Dynamics**

Principle Investigator: **Fengyuan Yang; Co-PI: Ezekiel Johnston-Halperin**
Mailing Address: Department of Physics, The Ohio State University, Columbus, OH 43210
Email: fyyang@physics.osu.edu

Project Scope:

This research project focuses on the generation, propagation and detection of pure spin currents without an accompanying charge current in antiferromagnetic (AF) insulators and the magnetic dynamics responsible for spin transport. The generation and manipulation of spin currents has been the central focus of spintronics in the past two and half decades. In recent years, pure spin transport driven by ferromagnetic resonance (FMR) spin pumping or a thermal gradient has attracted intense interest and become one of the most active frontiers in condensed matter physics. In both of these regimes a dynamic excitation of the magnetization results in the transfer of spin angular momentum in the absence of net charge flow, a long-sought goal for the field. Extensive research efforts over the last few years have demonstrated pure spin currents in a broad range of materials, including nonmagnetic (NM) metals and semiconductors, ferromagnetic (FM) and AF metals and insulators. These advances significantly enrich our understanding of dynamically-driven spin transport in heterostructures and open new paradigms for energy-efficient, spin-based information processing, data storage and sensing applications.

Eliminating the need for charge currents in spin transport has a paradigm-shifting impact on spintronics. For example, pure spin currents can be carried by either the spin degree of freedom of charge carriers or magnetic excitations in both FMs and AFs, opening entirely new classes of materials for exploration. Most interestingly, AF insulators, which have been largely absent in charge-based spin transport, become a desirable choice of materials for pure spin transport due to their intrinsically high resonance frequencies (THz) and high efficiency of spin conversion at interfaces. In addition, the inherently dynamic nature of this process drives the need for a comprehensive understanding of the dynamic interplay between spin, charge and magnetic excitations in FM, AF, and NM heterostructures. Ultrafast optical pump-probe techniques provide an ideal platform for pursuing these investigations. Building on our recent experimental demonstration of robust spin transport in AF insulators, established track records in spin pumping using high quality $Y_3Fe_5O_{12}$ (YIG) thin films, and expertise in microwave to terahertz spin dynamics, we will perform a collaborative research project with the following thrusts:

1. Investigate dynamically generated pure spin currents in AF insulators excited by FMR and thermally driven spin pumping in YIG/AF/Pt trilayers to reveal mechanisms of spin transfer in AF insulators and across interfaces.
2. Study the dynamics and coupling of non-equilibrium spin excitations in heterostructures of FMs, AFs, semiconductors, and NM metals using time-resolved Kerr rotation (TRKR) and ultra-fast excitation to probe the magnetic dynamics and pure spin currents in the time domain.

Recent Progress

- Antiferromagnonic spin transport in YIG/AF/Pt trilayer structures. We demonstrated growth of epitaxial YIG thin films of state-of-the-art crystalline quality (Fig. 1a) using a unique off-axis sputtering technique. Through collaboration with Prof. Hammel at Ohio State, the high quality YIG films enabled us to observe highly efficient dynamic spin injection from YIG into NiO, an AF insulator with a high AF ordering temperature, which is detected by a top Pt layer via the

inverse spin Hall effect (ISHE), as schematically shown in Fig. 1b. Robust spin propagation in NiO up to 100-nm thickness mediated by its AF spin correlations is observed in the Pt/NiO/YIG trilayers. Strikingly, the insertion of a thin NiO layer between YIG and Pt significantly enhances the spin currents driven into Pt, suggesting exceptionally high spin transfer efficiency at both YIG/NiO and NiO/Pt interfaces.[1] We then systematically studied spin transport in a serious of AF insulators having a wide range of ordering temperatures (Fig. 1c).[2] Our results show a strong correlation between spin propagation lengths in the AF insulators with the AF ordering temperatures. An excellent linear relationship between the spin decay length in the AF insulators and the damping enhancement in YIG was observed, which suggests the critical role of magnetic correlations in the AF insulators as well as at the AF/YIG interfaces for spin transport in magnetic insulators. This offers a powerful platform for studying AF spin transport and AF dynamics as well as for exploration of spin manipulation in tailored structures comprising metallic and insulating FMs, AFs, and NMs. This work was published in Physical Review Letters[1] and Physical Review B as a Rapid Communication.[2]

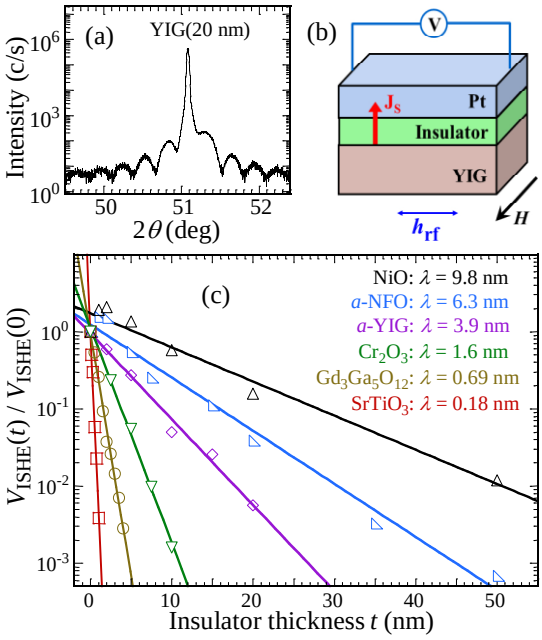

Fig. 1. (a) An x-ray diffraction scan of a 20-nm YIG epitaxial film on $Gd_3Ga_5O_{12}$(111). (b) Schematic of ISHE measurement on Pt/insulator/YIG structures. (c) Semilog plots of V_{ISHE} as a function of the insulator thickness for the six series normalized to the values for the corresponding Pt/YIG bilayers, where the straight lines are exponential fits to each series, from which the spin decay lengths λ are determined.[1,2]

- Damping of confined spin-wave modes in a uniform YIG film: angular momentum transfer across a nanoscale field-defined interface. Studies of spin transport in uniform materials offer the opportunity to study spin transport across the cleanest possible interfaces: the interface distinguishing the pumping volume from the receiving volume in the same YIG film is defined by a magnetic field gradient. This approach has been applied to continuous paramagnetic and FM materials. While the details are quite different, fundamental similarities are revealed. Through collaboration with Prof. Hammel, we observe a dependence of the damping of a confined spin-wave mode of precessing YIG magnetization on the size of the mode.[3] The micron-scale spin-wave mode is created within an extended, unpatterned YIG film by means of the intense local dipolar field of a micromagnetic tip. We find that the damping of the confined mode scales like the surface-to-volume ratio of the mode (Fig. 2), indicating an interfacial

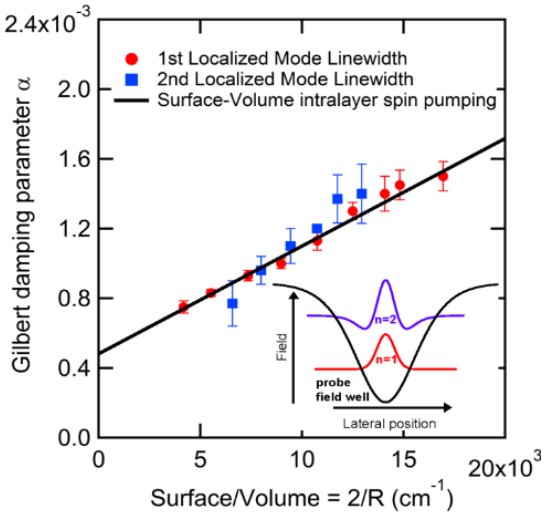

Fig. 2. Comparison of the measured size-dependent Gilbert damping parameter α of the first two localized modes with theory. The solid black line is a linear fit to confined-mode intralayer spin pumping that scales with the surface-volume ratio of the mode.[3]

damping effect (as in spin pumping) due to the transfer of angular momentum from the confined spin-wave mode to the equilibrium spin sink provided by the YIG film in the surrounding area. Though unexpected for insulating systems, the magnitude of the intralayer spin-mixing conductance demonstrates efficient intralayer angular momentum transfer. This work was published in Physical Review Letters.[3]

- Systematic variation of spin-orbit coupling with *d*-orbital filling in 3*d* transition metals. Spin-orbit coupling (SOC) is an intriguing fundamental interaction which is the underlying mechanism for numerous novel electronic and magnetic phenomena such as topological insulators, spin Hall effect (SHE), and magnetocrystalline anisotropy. It is generally believed that SOC scales with Z^4 (Z: atomic number) and is significant only in heavy elements, and hence that SOC in 3*d* transition metals should be negligible. Through collaboration with Prof. Hammel, we used dynamic spin pumping in YIG/3d-metal bilayers to uncover a systematic evolution of the spin Hall angle (θ_{SH}) with *d*-orbital filling in a series of 3*d* metals[4], as shown in Fig. 3. In particular, Cr and Ni show very large θ_{SH}, indicating that *d*-orbital filling plays a critical role in SHE. This result enriches the understanding of SHE and broadens the scope of materials available for exploring the rich phenomena enabled by SOC as well as presenting a guidepost for testing theoretical models of SOC in transition metals. This work was published in Physical Review B as a Rapid Communication.[4]

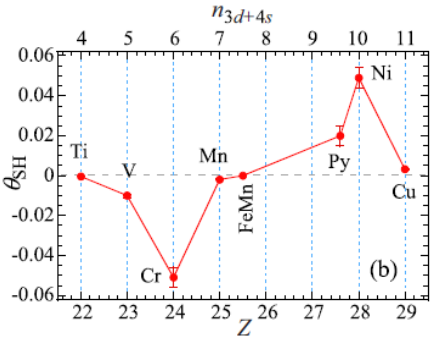

Fig. 3. Atomic number Z dependence of the spin Hall angle θ_{SH} of 3*d* metals shows a surprisingly large variation of θ_{SH} with electron count n_{3d+4s}.[4]

- Experimental and numerical understanding of localized spin-wave mode behavior in broadly tunable, spatially complex magnetic configurations. Spin-wave modes confined in an FM film by the spatially inhomogeneous magnetic field generated by a scanned micromagnetic tip of a ferromagnetic resonance force microscope (FMRFM) enable microscopic imaging of the internal fields and spin dynamics in nanoscale magnetic devices. Through collaboration with Prof. Hammel, we report a detailed study of spin-wave modes in a thin YIG film localized by magnetic field configurations frequently encountered in FMRFM experiments, including geometries in which the probe magnetic moment is both parallel and antiparallel to the applied uniform magnetic field. We demonstrate that characteristics of the localized modes, such as resonance field and confinement radius, can be broadly tuned by controlling the orientation of the applied field relative to the film plane. Micromagnetic simulations accurately reproduce our FMRFM spectra allowing quantitative understanding of the localized modes. These results reveal a general method of generating tightly confined spin-wave modes in various geometries with excellent spatial resolution that significantly facilitates the broad application of FMRFM. This work was published in Physical Review B.[5]

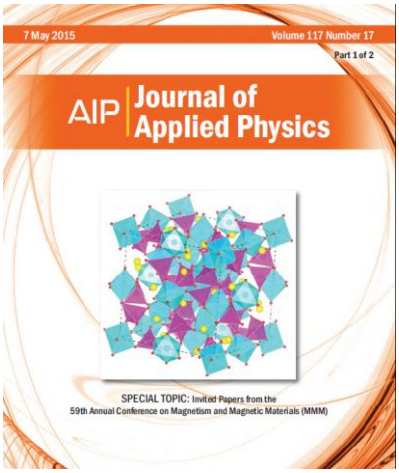

Fig. 4. Cover article of J. Appl. Phys. on our YIG spin pumping.[7]

- Supported by this DOE grant, we have published five more papers[6-10], including one in Applied Physics Letters[6] and one as a Featured Article and Issue Cover of Journal of Applied Physics (see Fig. 4).[7] In addition, Yang gave an invited talk in the 59th. Magnetism and Magnetic Materials Conference in November

2014 and an invited talk in the American Physical Society (APS) March Meeting 2015.

Future Plans

We focus on a group of antiferromagnetic 3*d* transition metal monoxides, NiO, CoO, FeO, and MnO, for the investigation of dynamic spin transport in AF insulators on YIG thin films excited by ferromagnetic resonance and thermal gradient. These four AF insulators are among the most studied AF insulators with substantial prior knowledge about their structural and magnetic properties. Their AF ordering temperatures span a broad range between 122 and 523 K, which allow probing the roles of AF ordering and excitations in spin transport. They also share the same rock-salt crystal structure and can be grown epitaxially on YIG. We will study AF spin transport in the AF insulators using Pt/AF/YIG trilayers as a function of temperature, FMR excitation frequency, crystal orientations, and excitation source (FMR or thermal). The thermally-driven spin transport study in AF insulators will complement the FMR spin pumping results for understanding the role of AF excitations in determining the magnitude of spin currents and spin decay lengths in the four AF oxides at various temperatures and frequencies.

References: publications which acknowledge DOE support (2014 and 2015)

1. H. L. Wang, C. H. Du, P. C. Hammel and F. Y. Yang, "Antiferromagnonic Spin Transport from $Y_3Fe_5O_{12}$ into NiO," *Phys. Rev. Lett.* **113**, 097202 (2014).
2. H. L. Wang, C. H. Du, P. C. Hammel, and F. Y. Yang, "Spin transport in antiferromagnetic insulators mediated by magnetic correlations," *Phys. Rev. B Rapid Comm.* **91**, 220410(R) (2015).
3. R. Adur, C. H. Du, H. L. Wang, S. A. Manuilov, V. P. Bhallamudi, C. Zhang, D. V. Pelekhov, F. Y. Yang, and P. C. Hammel, "Damping of confined modes in a ferromagnetic thin insulating film: Angular momentum transfer across a nanoscale field-defined interface," *Phys. Rev. Lett.* **113**, 176601 (2014).
4. C. H. Du, H. L. Wang, F. Y. Yang, and P. C. Hammel, "Systematic variation of spin-orbit coupling with d-orbital filling: surprisingly large inverse spin Hall effect in 3*d* transition metals," *Phys. Rev. B Rapid Comm.* **90**, 140407(R) (2014).
5. C. H. Du, R. Adur, H. L. Wang, S. A. Manuilov, F. Y. Yang, D. V. Pelekhov, and P. C. Hammel, "Experimental and Numerical Understanding of Localized Spin Wave Mode Behavior in Broadly Tunable Spatially Complex Magnetic Configurations," *Phys. Rev. B* **90**, 214428 (2014).
6. S. A. Manuilov, C. H. Du, R. Adur, H. L. Wang, V. P. Bhallamudi, F. Y. Yang, and P. C. Hammel, "Spin pumping from spinwaves in thin film YIG," *Appl. Phys. Lett.* **107**, 042405 (2015).
7. C. H. Du, H. L. Wang, P. C. Hammel and F. Y. Yang, "$Y_3Fe_5O_{12}$ Spin Pumping for Quantitative Understanding of Pure Spin Transport and Spin Hall Effect in a Broad Range of Materials (Invited)," *J. Appl. Phys.* **117**, 172603 (2015).
8. R. Adur, C. H. Du, J. Cardellino, N. Scozzaro, C. S. Wolfe, H. L. Wang, M. R Herman, V. P. Bhallamudi, D. V. Pelekhov, F. Y. Yang, P. C. Hammel, "Microscopic studies of nonlocal spin dynamics and spin transport," *J. Appl. Phys*. **117**, 172604 (2015).
9. R. Adur, C. H. Du, S. A. Manuilov, H. L. Wang, F. Y. Yang, D. V. Pelekhov, P. C. Hammel, "The Magnetic Particle in a Box: Analytic and Micromagnetic Analysis of Probe-Localized Spin Wave Modes," *J. Appl. Phys.* **117**, 17E108 (2015).
10. Y.-H. Chiu, N. G. Minutillo, R. E. A. Williams, G. J. Smith, D. W. McComb, J. A. Carlin, E. Johnston-Halperin, F. Y. Yang, "Photoluminescence Evolution in GaAs/AlGaAs Core/Shell Nanowires Grown by MOCVD: Effects of Core Growth Temperature and Substrate Orientation," *J. Cryst. Growth* **429**, 1 (2015).

Session IV

PROJECT TITLE: APS CONFERENCES FOR UNDERGRADUATE WOMEN IN PHYSICS

PI: THEODORE HODAPP, AMERICAN PHYSICAL SOCIETY, COLLEGE PARK, MD
EMAIL: hodapp@aps.org

1) PROGRAM SCOPE

The APS Conferences for Undergraduate Women in Physics (CUWiP), held annually since 2006, provide female physics majors with information, resources, and motivation to support their pursuit of an undergraduate physics degree, graduate education, and a career in physics. These conferences offer (i) inspirational talks by female physicists; (ii) student presentation sessions; (iii) workshops and panel discussions on summer research, graduate school, physics careers, professional development, and issues facing underrepresented minority women and first-generation college students; and (iv) ample opportunities for networking and informal mentoring. The conferences have an amplification effect by producing student "ambassadors" for physics when the participants return to their home institutions.

The long-term vision of the CUWiP organizers is to increase the number of women who complete their undergraduate degree and pursue graduate school and/or a career in physics. To best carry out this vision, the project leadership makes a special effort to choose sites for the conferences in diverse areas of the country, to recruit participants from underrepresented groups, including at community colleges, and to design the conferences to meet these student's needs as effectively as possible.

2) RECENT PROGRESS

The number of conferences has grown from six in 2013 to eight broadly geographically distributed conferences in 2014 and 2015, and will be expanding to nine in 2016. The number of participants has shown remarkable growth, increasing from 29 students in the first year to about 900 in 2013. During the time period of this award, the participation has increased to about 1100 in 2014, 1200 in 2015, and we expect 1300 participants in 2016. Conference attendance has more than tripled since APS first became involved following the 2011 conferences.

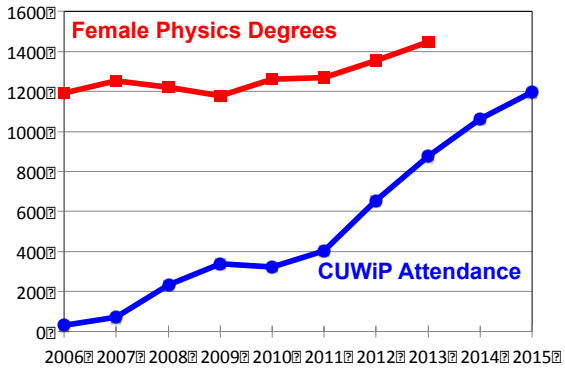

The conferences have also recently inspired replication of the events in Canada (hosting its 3rd conference in 2016), and the UK (planning its second this coming year). Discussions with Canadian leaders are exploring the idea of unifying the events to allow Canadian events to become a part of these APS-sponsored meetings, with a likely first unified conference in 2017.

Major achievements in the project include developing infrastructure that makes the conferences more sustainable and efficient to organize -- by implementing a national student

application and registration process with administrative support from APS, by developing a repository of online materials to help future local organizing committees host effective conferences that satisfy the goals of APS CUWiP, and by introducing a host-site application process, also through APS.

The organizational details of each conference were handled by Local Organizing Committees (LOC). A National Organizing Committee (NOC) met by phone approximately monthly to guide the overall organization of the conferences, specification of the content of the application and registration forms, etc. Members of the NOC include a three-person chair line, current and past heads of LOCs, several APS staff members, and the assessment team.

This project included formal assessment by Professors Eric Brewe and Zahra Hazari at Florida International University, who have described their findings in a report based on pre- and post-conference surveys. The assessment team designed pre-conference and post-conference surveys that were implemented by APS and administered online. The assessment report made several recommendations that were implemented for the 2015 conferences, and assessment in 2015 revealed gains in several areas including student's sense of how to progress as a physicist, and their interest in pursuing various employment tracks.

To select future sites, APS and the NOC implemented a national host-site application process that was used for 2015 host-site proposals and was fine-tuned to improve the process for 2016. Details can be seen at: http://www.aps.org/programs/women/workshops/cuwip-host.cfm.

All conferences organized panel discussions or workshops on topics such as applying for summer research, graduate school or employment in industry, and on the breadth of physics-related career opportunities. Many of the conferences included tours of laboratories -- from small departmental labs to large national laboratories. Some participants had the opportunity to present their own research results in poster sessions or presentations. In addition to the conference activities for undergraduates, a couple of the conferences offered short parallel programs for local high school students, with some sessions overlapping with the undergraduate program.

As an aid to improving the quality of the conference experience, we have, for the past two years, held a leadership gathering at APS headquarters in College Park, MD in late May. Here we bring together past and future site leaders, project leadership, and the project's assessment personnel. Site leaders indicate this meeting as extremely valuable in understanding resources available from APS and other sources, and for planning an effective timeline. Site leaders often leave having thrown out portions of their existing plans and having replaced them with a clearer sense of how to assemble the various pieces of a conference that will better achieve their goals.

3) FUTURE PLANS

We are currently organizing the 2016 APS CUWiP at nine sites – Black Hills State University, Georgia Institute of Technology, Old Dominion University/Jefferson Lab, Ohio

State University, Oregon State University, Syracuse University, University of California, San Diego, University of Texas, San Antonio/Southwest Research Institute, and Wesleyan University. We are also preparing for site selection for 2017 sites. We will continue to incorporate the recommendations from our assessment efforts. We are planning a repeat of the Leadership Gathering in May 2016, and are updating our assessment instruments to probe other questions including a measure of sexual harassment witnessed or experienced by participants. We expect several publications to result from the data we are gathering at these conferences.

Project leadership (NOC leadership) meets regularly to consider strategic directions for the events, and to handle any issues that arise. One important role is to reach out to universities in geographic areas that are less well covered, and to universities that have fewer financial resources to encourage them to consider hosting a future event. They and APS staff also speak to various audiences to continue to improve the messages presented at conferences, professional development opportunities available, and to invite groups to consider bringing their message to these energetic young women.

Program Title: Physics of Nanoscale Magnets

Principal Investigator: David J. Sellmyer; Co-PI: Ralph Skomski, in collaboration with PI: George Hadjipanayis (University of Delaware)
Mailing Address: Nebraska Center for Materials and Nanoscience and Department of Physics, University of Nebraska, Lincoln, NE 68588-0298
E-mail: dsellmyer@unl.edu

Program Scope

The *goal* of this research is to develop novel nanoscale magnets with characteristic dimensions of 1-100 nm, which are important in magnetism and several areas of nanoscience and nanotechnology. First, low-dimensional and quantum confinement effects can be combined in a unique way to improve magnetic properties by controlling the grain size and dimensions. Second, the nonequilibrium synthetic processes used for clusters, particles, and films can stabilize new and metastable compounds and often lead to new crystal and spin structures. Third, this research can offer basic-science challenges involving the spin-polarized quantum mechanics of many-electron systems containing 10-10,000 atoms. Finally, the nanomaterials under study may have potential impacts in advanced applications including ultra-strong permanent magnets, extremely high-density magnetic recording, nanoscale spintronics, magneto-optical devices, and biomedical imaging.

Our project is focused on new cluster, thin-film, and nanocomposite structures for developing nanoscale magnets that consist of rare-earth-free or rare-earth-lean Co- and Mn-rich compounds and exhibit high anisotropy, large magnetization, and high Curie temperature. We also expanded our research towards Heusler-type magnetic alloys and nanostructured compounds showing novel phenomena like spin-gapless semiconducting behavior and skyrmion-type spin structures. In addition, it is also essential for both basic science and technological reasons to understand the ground-state electronic structure including spin polarization in objects at length scales smaller than 20 nm. For example, competing exchange, phenomena involving spin-orbit coupling such as magnetic anisotropy and Dzyaloshinsky-Moriya (DM) interactions, and magnetostatic interactions can yield novel skyrmion-like spin textures in nanostructured magnets with reduced feature dimensions.

The research is based on a continuing collaboration in experimental and theoretical work between groups at the Universities of Nebraska and Delaware. A broad set of experiments is performed including structural characterization by x-ray diffraction and analytical and high-resolution electron microscopy, and magnetic and transport measurements between 4.2 and 1000 K using SQUID and PPMS magnetometry. The experimental results are correlated with first-principle density functional theory (DFT) and analytical simulations to study anisotropies, magnetization reversal mechanisms, spin polarizations, and magnetic interactions.

Recent Progress

Background: Our recent work has focused on the synthesis and properties of nanoclusters and nanostructures of magnetic compounds having new or metastable crystal structures as well as known structures. We have used a variety of growth routes including non-equilibrium processes such as cluster deposition, sputtering, e-beam evaporation, and rapid quenching from the melt. Additional methods have included wet-chemical, mechanochemical, and sonochemical

processes. A few examples of our recent research are explained below to highlight the important physics and technological aspects of these nanoclusters and nanostructured magnetic materials [1-30].

1. Spin Correlations in Nanoclusters [1-9]

Discussion: Co_2Si nanoclusters exhibit average magnetic moments of up to 0.70 μ_B/Co at 10 K and 0.49 μ_B/Co at 300 K, in sharp contrast to the nearly vanishing bulk magnetization as shown in Fig. 1a [1]. DFT and analytical calculations demonstrate a large spin polarization at the nanocluster surface that subsequently polarizes the very weak itinerant core as revealed by Fig. 1b and Fig. 1c, respectively. The underlying spin correlations are also associated with a strong size-dependence of the magnetic moment of Co_2Si (Fig. 1d). Recently, we have also produced FeGe nanocluster films having cubic B20-type structure that show a peak/feature around 0.4 kOe at 200 K in the dc susceptibility curve, which is similar to the signature of a skyrmion-like spin structure [2].

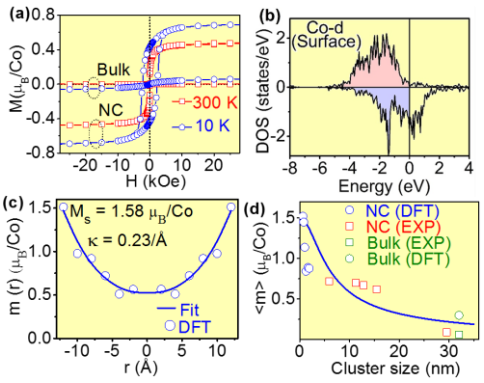

Figure 1. (a) Hysteresis loops of Co_2Si bulk and nanoclusters (NC). (b) Density of states of surface atoms, (c) radial-distribution of magnetic moments, and (d) size-dependent magnetic moment for nanoclusters. The solid line in (a) and (b) represents the fitting using an analytical model

Significance: The results demonstrate how atomic-scale exchange phenomenon can be controlled and exploited in nanoscale magnets to substantially improve magnetic properties.

2. Nanostructures with High-Anisotropy and Interesting Spin-Electronic Properties [6-28]

Discussion: We have used the cluster-deposition method to fabricate various high-anisotropy Co-rich nanoclusters [6, 7]. Recently we produced Co_3Si nanoclusters, a new rare-earth-free magnetic material, crystallizing in the $CdMg_3$-type hexagonal structure and exhibiting an effective magnetocrystalline anisotropy constant with a magnitude of 64 Mergs/cm^3 (6.4 MJ/m^3). This strong anisotropy leads to high coercivities (H_c = 5.0 kOe at 300 K and 20 kOe at 10 K) in field-aligned Co_3Si nanoclusters and appreciable saturation magnetic polarizations (J_s = 8.3 kG at 300 K and 9.6 kG at 10 K). Nanostructured materials designed from Co- and Fe-rich building blocks are required to preserve good permanent-magnet properties at elevated temperatures for many applications. We achieve this goal via effective nanostructuring of exchange-coupled $HfCo_7$:Fe-Co hard-soft composite films that exhibit an energy product of 17.1 MGOe at 180 °C [8], a record value for critical rare-earth- or expensive Pt- free materials. Analysis based on a model structure indicates that the soft-phase addition improves the performance of the hard magnetic material by mitigating Brown's paradox in magnetism. Employing other synthetic methods, we also have fabricated $L1_0$-FePt-based nanoparticles [9-15], Mn- and Co-based alloys with anisotropic structures and interesting spin-electronic properties including spin-gapless semiconducting behavior [17-22], and RCo_5 nanocrystalline powders (R = Y, Sm, La) having high room-temperature coercivities up to 41.5 kOe [23-28], and Fe and Co nanoparticles [29, 30].

Significance: Our approach provides useful insights for developing next-generation materials for permanent magnets and spin-electronics devices.

Future Plans

We will continue to produce new nanostructured Co- and Mn-based magnetic compounds of fundamental and technological importance. A further investigation will be carried out to understand the effects of size confinement on the ground-state electronic structure and associated spin correlations in nanoclusters and nanostructured materials in which complex interactions including DM effects may exist.

References Acknowledging DOE Support

1. B. Balasubramanian, P. Manchanda, R. Skomski, P. Mukherjee, B. Das, T.A. George, G.C. Hadjipanayis, and D. J. Sellmyer, "Unusual Spin Correlations in a Nanomagnet," Appl. Phys. Lett. **106**, 242401 (5 pages) (2015).
2. D. J. Sellmyer, B. Balamurugan, B. Das, P. Mukherjee, R. Skomski, and G. C. Hadjipanayis, "Novel Structures and Physics of Nanomagnets (invited)," J. Appl. Phys. **117**, 172609 (6 pages) (2015).
3. M. Koten, P. Manchanda, B. Balamurugan, R. Skomski, D.J. Sellmyer, and J.E. Shield, "Ferromagnetism in Laves-Phase WFe_2 Nanoparticles," APL Mat. **3**, 076101 (6 pages) (2015).
4. P. Mukherjee, P. Manchanda, P. Kumar, L. Zhou, M.J. Kramer, A. Kashyap, R. Skomski, D.J. Sellmyer, and J.E. Shield, "Size-Induced Chemical and Magnetic Ordering in Individual Fe-Au Nanoparticles," ACS Nano **8**, 8113-8120 (2014).
5. P. Manchanda, P. Kumar, B. Balasubramanian, P. Mukherjee, A. Kashyap, D.J. Sellmyer, and R. Skomski, "Magnetic Silicon Nanoparticles" IEEE Trans. Magn. **50**, 2303604 (4 pages) (2014).
6. B. Balamurugan, B. Das, W.Y. Zhang, R. Skomski, D.J. Sellmyer, "Hf-Co and Zr-Co Alloys for Rare-Earth-Free Permanent Magnets," J. Phys.: Condens. Matter **26**, 064204 (8 pages) (2014).
7. B. Balamurugan, B. Das, P. Mukherjee, and D.J. Sellmyer, "Development of Nanoparticle-Based Permanent-Magnet Materials: Challenges and Advances," Proc. REPM' 14, p. 429-432 (2014).
8. B. Balasubramanian, P. Mukherjee, R. Skomski, P. Manchanda, B. Das, and D.J. Sellmyer, "Magnetic Nanostructuring and Overcoming Brown's Paradox to Realize Extraordinary High-Temperature Energy Products," Sci. Rep. **4**, 6265 (6 pages) (2014).
9. Y. Yu, P. Mukherjee, Y. Tian, X.-Z.Li, J.E. Shield, and D.J. Sellmyer, "Direct Chemical Synthesis of $L1_0$-FePtAu Nanoparticles with High Coercivity," Nanoscale **6**, 12050-12055 (2014).
10. X. C. Hu, A. Capobianchi, R. Gallagher, and G. C. Hadjipanayis, "Influence of Ball Milling and Annealing Conditions on the Properties of $L1_0$ FePt Nanoparticles Fabricated by a New Green Chemical Synthesis Method," J. Appl. Phys. **115**, 17A732 (3 pages) (2014).
11. R. Choudhary, P. Kumar, P. Manchanda, Y. Liu, A. Kashyap, D.J. Sellmyer, R. Skomski, "Atomic Magnetic Properties of Pt-Lean FePt and CoPt Derivatives," Proc. REPM'14, Annapolis 2014, p. 289-291.
12. X.C. Hu, G.C. Hadjipanayis, D.J. Sellmyer, "Annealing Effect on $L1_0$ FePt Nanoparticles Prepared by Ball Milling of Layered Crystal $Fe(H_2O)_6PtC_{l6}$," Proc. REPM'14, Annapolis 2014, p. 99-101.
13. Y. Yu, Y. Liu, and D.J. Sellmyer, "Novel FePt-Based Nanostructures: Synthesis and Magnetic Properties," Magnetics Technology International, UKIP Media & Events, Ltd., p. 10-16 (2014).

14. X. C. Hu, E. Agostinelli, C. Ni, G. C. Hadjipanayis and A. Capobianchi, "A Low Temperature and Solvent-free Direct Chemical Synthesis of $L1_o$ FePt Nanoparticles With Size Tailoring," Green Chem. **16**, 2292-2297 (2014).
15. D.J. Sellmyer, Y. Liu, W.Y. Zhang, P. Kharel, "Nanostructuring and Properties of Strong Permanent-Magnet Films," Proc. REPM'14, Annapolis 2014, p. 69-73.
16. P. Manchanda, V. Sharma, H. Yu, D.J. Sellmyer, and R. Skomski, "Magnetism of Ta Dichalcogenide Monolayers Tuned by Strain and Hydrogenation," Appl. Phys. Lett. **107**, 032402 (5 pages) (2015).
17. W.Y. Zhang, P. Kharel, S. Valloppilly, R. Skomski, and D.J Sellmyer, "Synthesis and Magnetism of Single-phase Mn-Ga Films," J. Appl. Phys. **117**, 17E306 (4 pages) (2015).
18. Y. Huh, P. Kharel, A. Nelson, V.R. Shah, J. Pereiro, P. Manchanda, A. Kashyap, R. Skomski, D.J. Sellmyer, "Effect of Co Substitution on the Magnetic and Eectron-Transport Properties of Mn_2PtSn," J. Phys.: Condens. Matter **27**, 076002 (7 pages) (2015).
19. R. Fuglsby, P. Kharel, W.Y. Zhang, S. Valloppilly, Y. Huh, D.J. Sellmyer, "Magnetism of Hexagonal $Mn_{1.5}X_{0.5}Sn$ (X= Cr, Mn, Fe, Co) Nanomaterials," J. Appl. Phys. **117**, 17D115 (4 pages) (2015)
20. A. Nelson, P. Kharel, Y. Huh, R. Fuglsby, J. Guenther, W. Zhang, B. Staten, P. Lukashev, S. Valloppilly, and D.J. Sellmyer, "Enhancement of Curie temperature in Mn_2RuSn by Co Substitution," J. Appl. Phys. **117**, 153906 (6 pages) (2015).
21. P. Kharel, W. Zhang, R. Skomski, S. Valloppilly, Y. Huh, R. Fuglsby, S. Gilbert, and D.J. Sellmyer, "Magnetism, Electron Transport and Effect of Disorder in CoFeCrAl," J. Phys. D: Appl. Phys. **48**, 245002 (6 pages) (2015).
22. P. Kharel, Y. Hu, N Al-Aqtash, V.R. Shah, R.F. Sabirianov, R. Skomski, and D.J. Sellmyer, "Structural and Magnetic Transitions in Cubic Mn_3Ga," J. Phys.: Condens. Matter **26**, 126001 (8 pages) (2014).
23. R. Madugundo, D. S. Jaramillo, J. M. Barandiaran, and G. C. Hadjipanayis, "High Coercivity in Rare Earth Lean Nanocomposite Magnets by Grain Boundary Infiltration", J. Magn. Magn. Mater. (2015); doi:10.1016/j.jmmm.2015.07.019; (in press).
24. A.M. Gabay and G. C. Hadjipanayis, "Application of Mechanochemical Synthesis to Manufacturing of Permanent Magnets," JOM, **67**, 1329-1335 (2015).
25. W.Y. Zhang, X.Z. Li, S. Valloppilly, "Effect of Sm Content on Energy Product of Rapidly Quenched and Oriented $SmCo_5$ Ribbons," Appl. Phys. A **118**, 1093 - 1097 (2015).
26. W.Y. Zhang, R. Skomski, X.Z. Li, S. Vallopilly, J. Shield, and D.J. Sellmyer, "Effect of Quench Rate on Nanostructure and Magnetic Properties of $PrCo_5$," J. Appl. Phys. **115**, 17A731 (3 pages) (2014).
27. A.M. Gabay, X. C. Hu and G. C. Hadjipanayis, "Preparation of YCo_5, $PrCo_5$ and $SmCo_5$ Anisotropic High-Coercivity Powders via Mechanochemistry," J. Magn. Magn. Mater. **368**, 75-81 (2014).
28. A.M. Gabay and G. C. Hadjipanayis, "Mechanochemical Synthesis of $LaCo_5$ Magnetically Hard Anisotropic Powder," J. Phys. D: Appl. Phys. **47**, 182001 (4 pages) (2014).
29. W. Q. Liu, X. C. Hu, G. C. Hadjipanayis and M. Yue, "Fabrication and Characterization of Fe Nanoparticles by Sonochemistry Method," Mater. Lett. **131**, 266-268 (2014).
30. F. M. Abel, V. Tzitzios, G. C. Hadjipanayis, "New Approach for Direct Synthesis of Hexagonal Co Nanoparticles," J. Magn. Magn. Mater. (2015); doi:10.1016/j.jmmm.2015.07.051; (in press).

Program Title: Complex States, Emergent Phenomena, and Superconductivity in Intermetallic and Metal-Like Compounds

Principle Investigator: Paul Canfield (FWP leader), Sergei Bud'ko, Yuji Furokawa, David Johnston, Adam Kaminski, Vladimir Kogan, Marakiy Tanatar, Ruslan ProzorovDivision of Materials Science and Engineering, Ames Laboratory, Iowa State University, Ames, IA 50011

Program Scope

Our FWP focuses on discovering, understanding and ultimately controlling new and extreme examples of complex states, emergent phenomena, and superconductivity. Materials manifesting specifically clear or compelling examples (or combinations) of superconductivity, strongly correlated electrons, quantum criticality, and exotic, bulk magnetism are of particular interest given their potential to lead to revolutionary steps forward in our understanding of their complex, and potentially energy relevant, properties. The experimental work consists of new materials development and crystal growth, combined with detailed and advanced measurements of microscopic, thermodynamic, transport and electronic properties, at extremes of pressure, temperature, magnetic field, and resolution. The theoretical work will focus on understanding and modeling transport, thermodynamic and spectroscopic properties using world-leading, phenomenological approaches to superconductors and modern, quantum many-body theory.

The priority of this FWP is the development and understanding of model systems combined with agile and flexible response to, and leadership in, a rapidly-changing materials landscape. To accomplish this goal, three highly intermeshed classes of activities will operate both in series and in parallel. This work supports the DOE mission by directly addressing the Grand Challenge of understanding the Emergence of Collective Phenomena: Strongly Correlated Multiparticle Systems and is a key contributor to fulfilling the Ames Laboratory Scientific Strategic Plan for preeminence in solid-state materials discovery, synthesis, and design; this FWP will design, discover, characterize and understand systems that shed light on how remarkable properties of matter emerge from complex correlations of the atomic or electronic constituents and, as a result, provide better control of these properties.

Recent Progress

<u>High temperature superconductivity in cuprates</u>: One of the outstanding questions in cuprates is the relation between the superconducting gap and pseudogap. In past years we were able to demonstrate that pseudogap is a signature of an ordered state that competes with superconductivity [1-3]. Presence of pseudogap leads to formation of Fermi arcs – disconnected segments of the Fermi surface that defy conventional concept of Fermi surface as a closed contour in the momentum space [4]. Few recent reports concluded however that above Tc the parts considered to be arcs are not truly gapless [5]. To address this issue in detail, we developed new methodology that allows detection of very small energy gaps. Using this approach we were

able to demonstrate that real, gapless Fermi arcs do form, but only above temperature T~150K that is significantly higher than Tc. The length of these "real" arcs remains constant over an extended temperature range from below T*~250 K to ~150 K. Below ~150 K pre-formed pairs start to form [6] and this causes collapse of the gapless arcs to point nodes of a d-wave superconductor. The constant length of these arcs is a very strong argument for the pseudogap being an ordered state. Our data identifies the characteristic vectors connecting the tips of the arcs related to CDW order [7].

The role of interactions with collective excitations in conventional and unconventional superconductivity: In most known case of the superconductivity the pairing arises due to interaction with collective excitations. Therefore detailed knowledge of this interaction is essential for understanding of superconductivity and design of new families of superconductors. Surprisingly, there is very sparse ARPES data about the signatures of collective modes in classical superconductors. To fill this gap we conducted detail studies of the electronic properties of MgB_2 – a phonon mediated multiband superconductor. We were able to observe the signatures of interaction of electrons with E_2g phonon mode that is responsible for pairing and study its temperature dependence. Our ultra high resolution data also revealed another very low energy mode. Its characteristics strongly suggest that it is a Leggett mode – due to phase excitation of the two superfluid condensates. These findings build a foundation for interpretation of spectroscopic features in novel, unconventional superconductors[8, 9].

Future Plans

Having invested significant effort in building a laboratory-based, tunable, high resolution, laser ARPES system over the past several years [10], we will enhance further its capabilities to low temperatures (<5K) and use this system to address a number of key question about superconductivity. For example, the order parameter is the most important characteristic of a SC because it contains key information about the pairing mechanism. ARPES is the only technique that can directly measure the momentum dependence of the SC gap. There are several areas where the unique capabilities of the tunable, high resolution laser ARPES system can lead to significant breakthroughs. We propose to study the order parameter of iron arsenic superconductors in 3-dimensional momentum space with higher precision than it was done previously. Surprisingly, after 6 years of intensive research, this issue still remains elusive, with a number of seemingly contradictory results. The problem with direct measurements of the SC gap in the pnictides is that most of the synchrotron facilities do not have sufficient energy resolution in order to make accurate measurements along kz. Measurements of the superconducting gap with traditional laser ARPES systems are performed at fixed photon energy and thus lack critical kz information. We will use our tunable laser ARPES spectrometer [10] to address this key issue using single crystals of $(Ba_{1-x}K_x)Fe_2As_2$. Our measurements will focus on the 3-dimensional momentum dependence of the SC gap across the phase diagram. Such information is absolutely critical in order to firmly establish the symmetry of the order parameter

across the phase diagram in iron arsenic high temperature SC and identify the correct pairing mechanism.

The role of impurities (especially in newly discovered materials) often impedes our understanding of the intrinsic properties and the mechanism of pairing. Building on our recent success in measuring the electronic properties of pure MgB2 with unprecedented precision [8, 9] we will use our laser ARPES system to study the effect of impurities on the momentum dependence of the SC gap – one of key unresolved questions in the field of superconductivity. We will use MgB2 for these studies since it is a prototypical multiband superconductor. Defects and impurities will be introduced to the material using magnetic and non-magnetic substitution as well as by neutron, and possibly electron and proton, irradiation. Measurements of the changes in the momentum dependence of the SC gap will be compared to theory and will guide interpretation of the penetration depth and thermal conductivity measurements.

References

1. Lee, W. S., et al., Abrupt onset of a second energy gap at the superconducting transition of underdoped Bi2212. Nature 450, 81-84 (2007).
2. Kondo, T., Takeuchi, T., Kaminski, A., Tsuda, T., and Shin, S. Evidence for Two Energy Scales in the Superconducting State of Optimally Doped (Bi,Pb)2(Sr,La)2CuO6+x Phys. Rev. Lett. 98, 267004 (2007).
3. Kondo, T., Khasanov, R., Takeuchi, T. , Schmalian, J., and Kaminski, A. Competition between the pseudogap and superconductivity in the high-Tc copper oxides. Nature 457, 296-300 (2009).
4. Kanigel, A. et\ al. Evolution of the pseudogap from Fermi arcs to the nodal liquid Nature Physics **2**, 447 – 451 (2006).
5. Reber, T. J., Plumb, N. C., Sun, Z., Cao, Y., Wang, Q., McElroy, K., Iwasawa, H., Arita, M., Wen, J. S., Xu, Z. J., Gu, G., Yoshida, Y., Eisaki, H., Aiura, Y., Dessau, D. S., The origin and non-quasiparticle nature of Fermi arcs in $Bi_2Sr_2CaCu_2O_{8+\delta}$. Nature Physics **8**, 606-610 (2012)
6. Kondo, T. et al., Disentangling Cooper-pair formation above the transition temperature from the pseudogap state in the cuprates. Nature Physics **7**, 21 (2011).

Publications

The FWP published 82 papers in 2014 and 2015 and their list will not fit within allocated space. This includes 5 papers published in Physical Review Letters 31 in Physical Review B and 2 in Nature Communications. Below we list few selected papers published in this period.

7. Kondo, T., Palczewski, A. D., Hamaya, Y., Takeuchi, T., Wen, J. S., Xu, Z., J., Gu G., Kaminski, A., Formation of Gapless Fermi Arcs and Fingerprints of Order in the Pseudogap State of Cuprate Superconductors, Phys. Rev. Lett. **111**, 157003 (2013)
8. Mou, D., Jiang, R., Taufour, V., Flint, R., Bud'ko, S. L., Canfield, P. C., Wen, J. S., Xu, Z. J., Gu, G., Kaminski, A., Strong interaction between electrons and collective excitations in the

multiband superconductor MgB_2, Phys. Rev. B **91**, 140502(R) (2015)
9. Mou, D., Jiang, R., Taufour, V., Bud'ko, S. L., Canfield, P. C., Kaminski, A. Momentum dependence of the superconducting gap and in-gap states in MgB2 multiband superconductor. Phys. Rev. B 91, 214519 (2015)
10. Dhaka R. S., Jiang, R., Ran. S., Bud'ko, S. L., Canfield, P. C., Harmon, B. N., Tomi`c, M., Valent´i. R., Kaminski, A., Dramatic changes in the electronic structure upon transition to the collapsed tetragonal phase in $CaFe_2As_2$. Phys. Rev. B **89**, 020511RC (2014)
11. Jiang, R., Mou, D., Wu, Y., Huang, L., McMillen, C. D., Kolis, J., Giesber III, H. G., Egan, J. J., Kaminski, A., Tunable vacuum ultraviolet laser based spectrometer for angle resolved photoemission spectroscopy, Review of Scientific Instruments **85**, 033902 (2014)
12. Anand, V. K., Dhaka, R. S., Lee, Y., Harmon, B. N., Kaminski, A., Johnston, D. C., Physical properties of metallic antiferromagnetic $CaCo_{1.86}As_2$ single crystals, Physical Review B **89**, 214409 (2014)
13. A. Kaminski, T. Kondo, T. Takeuchi, and G. Gu, Pairing, pseudogap and Fermi arcs in cuprates, Philosophical Magazine **95**, 453 (2015)
14. Jiang, R., Mou, D., Liu, C., Zhao, X., Yao, Y., Ryu, H., Petrovic, C., Ho, K.-M., Kaminski, A., Electronic structure of Ce_2RhIn_8: A two-dimensional heavy-fermion system studied by angle-resolved photoemission spectroscopy, Phys. Rev. B **91**, 165101 (2015)
15. Kim, H., Tanatar, M. A., Flint, R., Petrovic, C., Hu, R., White, B. D., Lum, K. M., Maple, B., Prozorov, R., Nodal to Nodeless Superconducting Energy-Gap Structure Change Concomitant with Fermi-Surface Reconstruction in the Heavy-Fermion Compound $CeCoIn_5$, Physical Review Letters **114**, 027003 (2015)
16. Zhang, Q., Fernandes, R. M., Lamsal, J., Yan, J., Chi, S., Tucker, G. S., Pratt, D., K., Lynn, J. W., McCallum, R. W., Canfield, P. C., Lograsso, T. A., Goldman, A. I., Vaknin, D., McQueeney, R. J. Neutron-Scattering Measurements of Spin Excitations in LaFeAsO and$Ba(Fe_{0.953}Co_{0.047})_2As_2$: Evidence for a Sharp Enhancement of Spin Fluctuations by Nematic Order. Physical Review Letters, **114**, 057001 (2015)
17. Hodovanets, H., Bud'ko, S. L., Straszheim, W. E., Taufour, V., Mun, E. D., Kim, H., Flint, R., Canfield, P. C., Remarkably Robust and Correlated Coherence and Antiferromagnetism in $(Ce_{1-x}La_x)Cu_2Ge_2$. Physical Review Letters **114**, 236601 (2015)
18. Prozorov, R., Konczykowski, M., Tanatar, M. A., Thaler, A., Bud'ko, S. L., Canfield, P. C., Mishra, V., Hirschfeld, P. J., Effect of Electron Irradiation on Superconductivity in Single Crystals of $Ba(Fe_{1-x}Ru_x)_2As_2$ (x=0.24). Physical Review X **4**, 041032 (2015)
19. Jesche, A., McCallum, R. W., Thimmaiah, S., Jacobs, J. L., Taufour, V., Kreyssig, A., Houk, R. S., Bud'ko, S. L., Canfield, P. C., Giant magnetic anisotropy and tunnelling of the magnetization in $Li_2(Li_{1-x}Fe_x)N$. Nature Comm. **5** 3333 (2014)

Program Title: Correlated and Complex Materials

Principle Investigator: B. C. Sales; Co PIs: L. A. Boatner, C. Cantoni, D. Mandrus, A. F. May, M. A. McGuire, J.-Q. Yan
Mailing Address: Materials Science and Technology Division, Oak Ridge National Laboratory, Oak Ridge, TN 37831
E-mail: salesbc@ornl.gov

Program Scope

This program aims to attain a predictive understanding of the behavior of key correlated and complex materials (CCM). Virtually all of the diverse topics and materials to be investigated involve some aspect of magnetism associated with partially filled d or 4f shells. These include the role of magnetic fluctuations in iron-based superconductors, the behavior of layered and cleavable ferromagnets, the effects of spin orbit coupling in 4*d*/5*d* transition metals, and the conduction of heat by magnetic excitations. Many of the spectacular properties of CCM are believed to result from competing ground states that are close in energy, and hence CCM are often responsive to small changes in composition, temperature, pressure, electric, or magnetic fields. The experimental tools of materials synthesis, compositional tuning, and crystal growth are used to address cutting edge issues in the physics of these systems, with particular focus on the discovery and investigation of novel cooperative phenomena and new forms of order in CCM. A substantial fraction of the effort is devoted to the discovery of innovative materials and the growth of large single crystals of fundamental interest to materials physics. Single crystals are prepared using a variety of techniques, including flux growth, vapor transport, Bridgman, and optical-floating-zone growth, including a new high-pressure optical floating zone furnace. The ability to prepare synthetically challenging and sometimes unique single crystals is a major strength of this project. The program works to identify and synthesize "model compounds" that are complicated enough to exhibit the properties of interest but simple enough to be amenable to both theory and experiment. The effects of compositional tuning on the basic physics of the materials are studied by measurement of X-ray and neutron diffraction, magnetization, specific heat, electrical and thermal transport, scanning transmission electron microscopy, and electron energy loss spectroscopy. Once the materials have been prepared and a basic understanding of their behaviors has been developed, in-depth experiments such as inelastic neutron scattering, photoemission, and scanning tunneling microscopy are performed (through collaborations) in order to obtain a deeper understanding of the relevant physics. Some of the materials investigated are promising for energy-related applications, such as superconductors for grid applications and thermoelectrics and permanent magnets for energy conversion.

Recent Progress

The van der Waals bonded ferromagnet CrI_3: Chromium triiodide (CrI_3) is a van der Waals bonded ferromagnet, making it attractive for studying magnetism in very thin crystals and potentially monolayers. Development of such ultra-thin magnetic materials may help enable continued advancement in miniaturization and performance enhancement of electronic devices, either as electronically active components themselves, or through interfacing with materials like graphene. This experimental and theoretical study, [1] enabled by the growth of large single crystals, revealed the detailed crystallographic properties and magnetic behavior of CrI_3. Results are summarized in Figure 1. The material is made up of

three-atom-thick layers, which are weakly bound to one another. As a result, the material is easily cleaved into very thin sheets. Calculations using a van der Waal density functional showed the strength of the interlayer bonding is similar to that of graphite, which can be easily cleaved into graphene. Weak interlayer bonding makes the total binding energy relatively insensitive to the stacking sequence, resulting in the first-order crystallographic phase transition that is observed to occur near 200K. Cr magnetic moments align ferromagnetically below the Curie temperature of 61K, directed normal to the layers and displaying strong anisotropy. Initial calculations show that this ferromagnetism is favored even in single CrI_3 layers, motivating study of ultrathin samples.

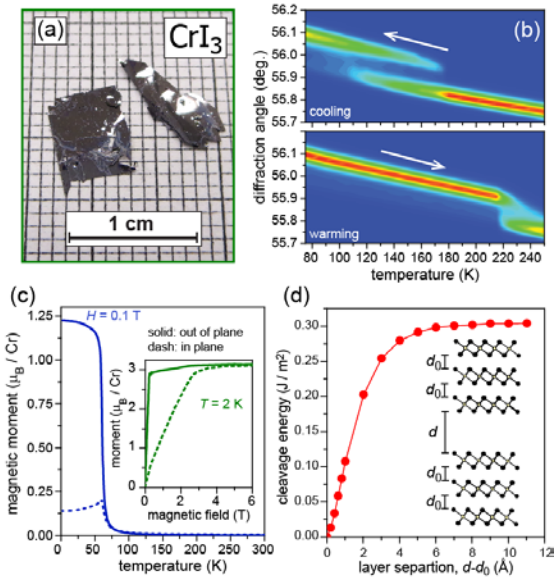

Figure 1. (a) CrI_3 single crystals. (b) A first order crystallographic phase transition occurs near 200K. (c) Ferromagnetism develops in the low T structure at 61K. (d) Calculations predict easy cleavage, and suggest that magnetism may persist in very thin samples.

$SrRu_2O_6$, a 4d compound with unusually strong magnetic interactions: The layered strontium ruthenium oxide $SrRu_2O_6$ (Hiley et al., 2014) was identified as a promising model platform for investigating the origin of unusually strong magnetic correlations in 4*d* compounds. An understanding of magnetism in 4*d* compounds that order well above room temperature may lead to new high-performance electronic devices, as well as possible new routes to high temperature superconductivity.

The combined experimental and theoretical study [2] indicated in-plane antiferromagnetic interactions between Ru^{5+} ions similar in strength to those found in the cuprate superconductors, and equivalent to a temperature of about 1200K. Relatively weak inter-plane coupling results in three-dimensional G-type antiferromagnetic order at T_N = 565K (see Figure 2). Empirically, the strong magnetic interactions in this 4*d* compound are related to the Ru $4d^3$ electronic configuration in an octahedral environment. $SrRu_2O_6$ is the first layered 4*d* oxide to be identified with this d^3 electronic configuration. New and interesting physics may emerge upon doping charge carriers into this Mott insulator, in analogy with the cuprate superconductors.

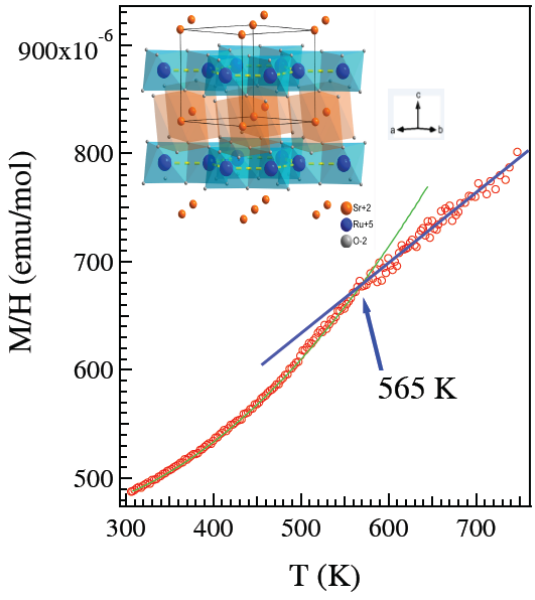

Figure 2. Magnetization measurements reveal the Neel temperature of $SrRu_2O_6$. The hexagonal crystal structure is shown in the inset, and contains magnetic Ru^{5+} ions on a honevcomb net.

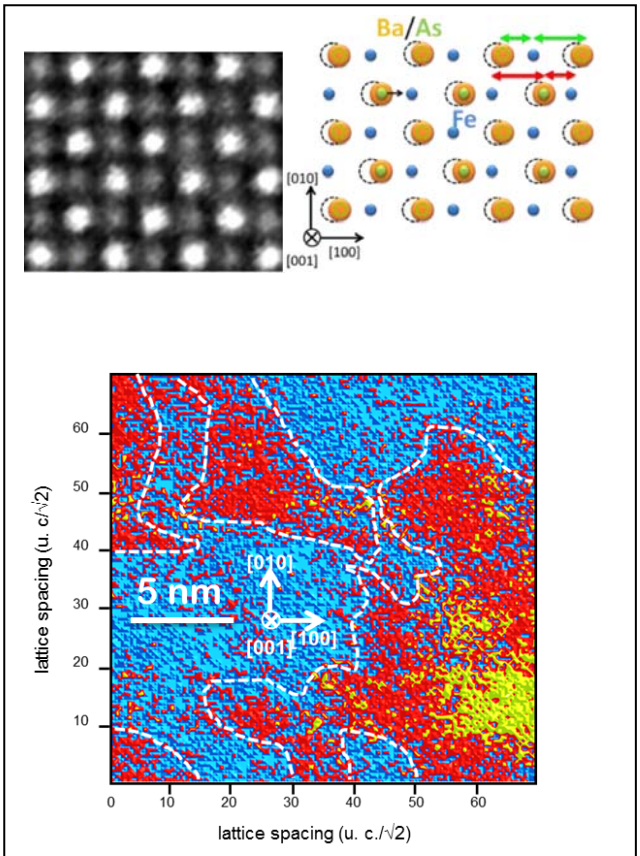

Figure 3. Room temperature, real-space, atomic resolution image shows subtle off-centering of atomic columns in $Ba(Fe_{1-x}Co_x)As_2$. As simple model describes this as an orthorhombic distortion in the *ab*-plane. Displacements can happen along [100] or [010], producing domains indicated as red and blue in the distortion map.

Orthorhombic distortion at room temperature in $Ba(Fe_{1-x}Co_x)_2As_2$: High-resolution microscopy revealed an unexpected room-temperature crystal structure of the '122' $Ba(Fe_{1-x}Co_x)_2As_2$ superconductors, with domains similar to those in ferroelectrics but with nanometer size. [3] This finding provides direct evidence that crystal structure and magnetism are coupled in these materials and that both are important for superconductivity. The domains form because in some regions atoms undergo a displacement in the [100] direction while in others the displacement is along [010]. The displacements and domains are shown in Figure 3. Domains are only a few nanometers in size, and previous x-ray and neutron experiments have sampled data over both domain types simultaneously, probing only the average structure. The size of the domains is found to correlate with both the fluctuating local magnetic moment at room temperature and the superconductivity at low temperature. At the optimal doping for superconductivity, the magnetic fluctuations are large and the domains are large (up to 15 nm in size). When superconductivity and magnetic fluctuations are weak, the domains are smaller. Our study demonstrates that aberration-corrected scanning transmission electron microscopy (STEM) can reveal atomic-scale structural irregularities that would otherwise be missed when less spatially resolved techniques average data.

Future Plans

Ongoing and future work within this program include efforts to dope charge carriers into the Mott insulator $SrRu_2O_6$. This is complicated by the limited stability of this compound at high temperatures, and a variety of doping strategies and synthetic routes will have to be examined. In addition, transition metal compounds adopting structures based on the Fe_2P structure type will be investigated. This family of materials is known to include superconductors and magnetic materials with extreme sensitivity to composition and chemical order. We will examine possible relationships between the magnetism and (potentially unconventional) superconductivity in these non-centrosymmetric materials. We are also currently studying, in addition to CrI_3, other van der Waals bonded magnetic materials, including Fe_3GeTe_2. The magnetism in this layered ferromagnet can be controlled by chemical substitutions and tuning of the Fe content. We have produced thoroughly characterized large single crystals of some compositions, and will continue with doping studies and neutron scattering experiments.

References

C.I. Hiley et al., "Ruthenium(V) Oxides from Low-Temperature Hydrothermal Synthesis", Angew. Chem. Int. Ed. 53, 4423 (2014).

Selected Publications 2014-2015

[1] M.A. McGuire, H. Dixit, V.R. Cooper, and B.C. Sales, "Coupling of Crystal Structure and Magnetism in the Layered, Ferromagnetic Insulator CrI_3," Chem. Mater. 27, 612 (2015).

[2] W.Tian, C. Svoboda, M. Ochi, M. Matsuda, H.B. Cao, J.-G. Cheng, B.C. Sales, D.G. Mandrus, R. ARita, N. Trivedi, J.-Q. Yan, "High antiferromagnetic transition temperature of a honeycomb compound $SrRu_2O_6$" Phys. Rev. B Rapid, accepted (2015).

[3] C. Cantoni, M. A. McGuire, B. Saparov, A. F. May, T. Keiber, F. Bridges, A. S. Sefat, B. C. Sales, "Room-Temperature $Ba(Fe_{1-x}Co_x)_2As_2$ is not Tetragonal: Direct Observation of Magnetoelastic Interactions in Pnictide Superconductors," Advanced Materials, 27, 2715 (2015).

[4] J.-Q. Yan, M. A. McGuire, A. F. May, D. Parker, D. G. Mandrus, B. C. Sales, "Fragile Structure Transition in Mo_3Sb_7" Phys. Rev. B 92, 064507 (2015).

[5] H. B. Cao, Z. Y. Zhao, M. Lee, E. S. Choi, M. A. McGuire, B. C. Sales, J. –Q. Yan and D. G. Mandrus, "High pressure floating zone growth and structural properties of ferrimagnetic quantum paraelectric $BaFe_{12}O_{19}$" APL Materials 3, 062512 (2015).

[6] D. S. Parker, A. F. May, D. J. Singh, "Benefits of Carrier-Pocket Anisotropy to Thermoelectric Performance," Physical Review Applied 3, 064003 (2015).

[7] G. Aivazian, Z. Gong, A.M. Jones, R-L. Chu, J. Yan, D.G. Mandrus, C. Zhang, D. Cobden, W. Yao, and X. Xu, "Magnetic control of valley pseudospin in monolayer WSe_2," Nature Phys. 11, 148 (2015).

[8] O. Delaire, I.I. Al-Qasir, A.F. May, C.W. Li, B.C. Sales, J.L. Niedziela, J. Ma, M. Matsuda, D.L. Abernathy, T. Berlijn, "Heavy-impurity resonance, hybridization, and phonon spectral functions in $Fe_{1-x}M_xSi$ (M = Ir, Os)," Phys. Rev. B 91, 094307 (2015).

[9] M.J. Neish, M.P. Oxley, J. Guo, B.C. Sales, L.J. Allen, and M.F. Chisholm, "Local Observation of the Site Occupancy of Mn in a MnFePSi Compound," Phys. Rev. Lett. 114, 106101 (2015).

[10] J.-Q. Yan, S. Nandi, B. Saparov, P. Čermák, Y. Xiao, Y. Su, W.T. Jin, A. Schneidewind, Th. Brückel, R.W. McCallum, T.A. Lograsso, B.C. Sales, and D.G. Mandrus, "Magnetic and structural transitions in $La_{0.4}Na_{0.6}Fe_2As_2$ single crystals," Phys. Rev. B 91, 024501 (2015).

[11] C. Cantoni, J. E. Mitchell, A. F. May, M. A. McGuire, J.-C. Idrobo, T. Berlijn, E. Dagotto, M. F. Chisholm, W. Zhou, S. J. Pennycook, A. S. Sefat, and B. C. Sales, "Orbital Occupancy and Charge Doping in Iron-Based Superconductors," Adv. Mater. 26, 6193 (2014).

[12] A. F. May, M. A. McGuire, and B. C. Sales, "Effect of Eu Magnetism on the Electrical Properties of the Candidate Dirac Materials $EuMnBi_2$," Phys. Rev. B 90, 075109 (2014).

[13] M. A. McGuire, V. O. Garlea, A. F. May, and B. C. Sales, "Competing magnetic phases and field-induced dynamics in DyRuAsO," Phys. Rev. B 90, 014425 (2014).

[14] J. M. Farmer, L. A. Boatner, B. C. Chakoumakos, M.–H. Du, M. J. Lance, C. J. Rawn, and J. C. Bryan, "Structural and Crystal Chemical Properties of Rare-Earth Titanate Pyrochlores," J. Alloy. Compd. 605, 63 (2014).

Session V

High magnetic field microwave spectroscopy of two-dimensional electron systems in GaAs and graphene

Lloyd W. Engel, National High Magnetic Field Laboratory, Florida State University, engel@magnet.fsu.edu

Scope of project

The project is to perform microwave spectroscopy on two dimensional electron systems (2DES) exhibiting the quantum Hall effects in GaAs/$Al_xGa_{1-x}As$ heterostructures, and also in graphene. The focus of the work is on electron solids in high magnetic field. The simplest such solid is the Wigner crystal [1-3] a triangular lattice of individual carriers. Microwave spectroscopy is of value in studying an electron solids because they exhibit a striking resonance, which is understood as a pinning mode [4-7], in which pieces of the solid oscillate within the confining potential of the residual disorder of the sample. Fig. 1a illustrates the transmission-line-based measuring set-up that we use to obtain such spectra.

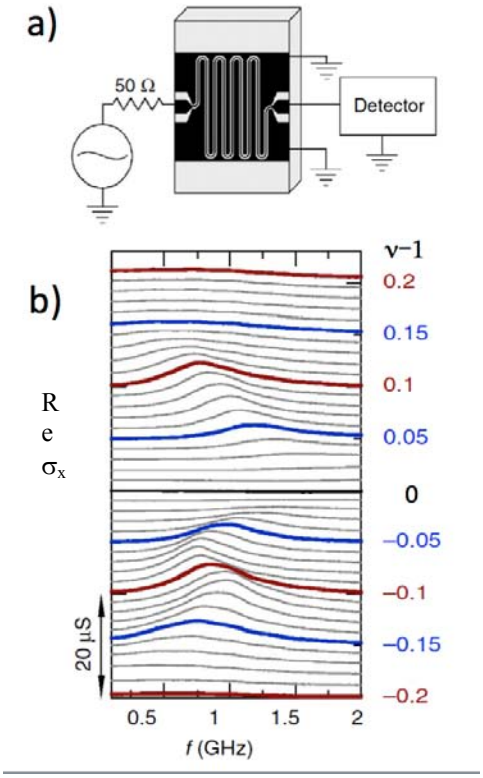

Figure 1. a) Schematic of GaAs/$Al_xGa_{1-x}As$ sample with transmission line pattern, metal film shown as black. b) Spectra, Re σ_{xx} vs frequency f, taken for many Landau fillings ν near 1. ν-1 is marked at right. Spectra are offset upward proportional to ν. The sample was a WQW with width w= 65 nm and density n= 1.39x10^{11} cm^{-2}.

There is an exciting variety of solids of 2DES in high B. As judged by the resonance, solids exist at the low Landau filling (ν) termination of the fractional quantum Hall effect (FQHE) series [5-7], Pinned electron solids are also present [8] in GaAs-hosted 2DES within the ν ranges of the integer quantum Hall effect (IQHE) plateaus, near but not just at integer filling. These integer quantum Hall Wigner crystals (IQHWC) are composed of quasiparticles or holes in the partially filled Landau level. We have also experimentally identified pinned solid within the 1/3 FQHE [10]. Theories indicate that electron solids can be lattices of composite fermions (CFs) [9], or of skyrmions [11,12].

The microwave spectroscopy is used to search for new types of solids in GaAs, and to examine transitions between distinct solids and between solids and liquids. Study of the solids at smaller length scales is also under way. Microwave spectroscopy in

graphene is in progress to search for electron solids, such as an IQHWC, in graphene, and also to search for low lying modes predicted [13] particularly in bilayers.

Recent Progress

In collaboration with M. Shayegan, we have recently been successful in finding multiple distinct types of electron solid in wide quantum wells (WQWs), and observing transitions between these different solids. WQWs offer an interplay between subband, CF-Landau and spin levels, and can support bilayer as well as single-layer states, depending on the well width, *w*, and on the overall density, *n,* of the carriers in the well. To date we have studied electron solid phases in WQWs in three different regimes.

i) **Single-layer near ν=1.** (Hatke *et al.,* Nature Commun., 2014) An example of data showing these solids appears in Fig. 1b. For ν >1, the pinning mode resonance frequency, f_{pk} , decreases as ν goes above 1, as is normal for an IQHWC resonance. As ν goes below 1, f_{pk} first decreases the same way, but then shows an upward jump, which is taken to be evidence for a transition to a different type of solid. We refer to the solid found further from ν =1 as S2, and the solid closer to ν =1 as S1. Using in-plane magnetic field as well as *n* dependence (paper in preparation), we find S2 exists for intermediately large Zeeman energy. S2 is interpreted, like the nearby 4/5 FQHE state [14,15], as having a one partly filled plus one fully filled CF Landau level, each of the same spin. At even higher in-plane field or *n*, S2 disappears, though the reason for this has yet to be determined.

ii) **Low ν bilayer electron solid**. (Hatke *et al.,* Nature Commun., 2015) Electron solids form in a WQW when ν is sufficiently low, at the termination of the FQHE series. The ν at which the transition to solid occurs depends on whether the electrons are in bilayer or single- layer states. A measure of the tendency of the charge in a WQW to separate into two layers is $\gamma \equiv (e^2/4\pi\varepsilon_0\varepsilon l_B)/\Delta_{SAS}$ where $l_B = (\nu/2\pi n)^{1/2}$ is the magnetic length. Δ_{SAS} is the interlayer tunneling gap, which depends on *n*. $e^2/4\pi\varepsilon_0\varepsilon l_B$ is the Coulomb energy. Figure 2a shows

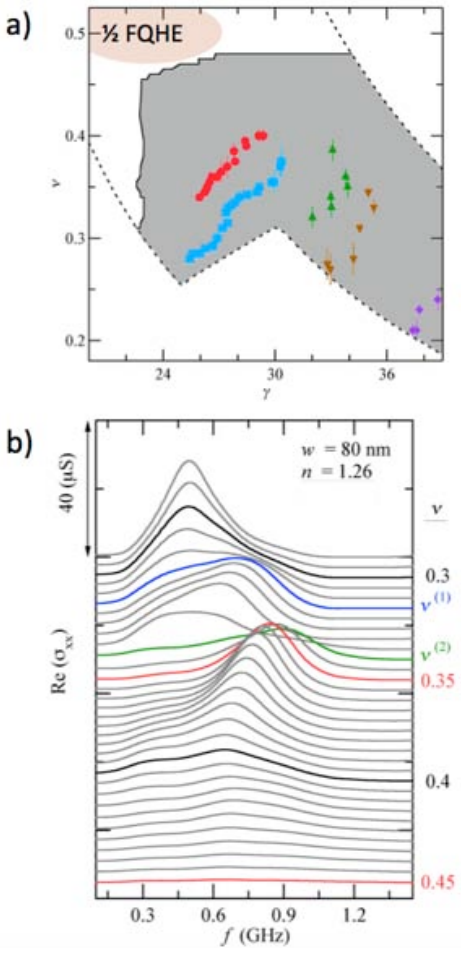

Figure 2 a) Diagram on γ-ν plane (see text) of occurrence of a pinning mode, shown as grey shading, for an 80 nm WQW. The dotted lines show experimental limits due to *n* and maximum magnetic field. The colored symbols indicate transitions within the solid, as indicated by changes in the pinning mode. b) Spectra for the same sample at $n = 1.26 \times 10^{11}$ cm^{-2}, Re σ_{xx} vs frequency *f*, taken for many Landau fillings ν, marked at right. Spectra are vertically offset proportional to ν. Abrupt changes in the pinning mode are seen at fillings $\nu^{(1)}$ and $\nu^{(2)}$.

a phase diagram in the γ-ν plane. The grey area shows where there is a pinning mode, and is similar to earlier plots [16] of dc insulating behavior. Consistent with a bilayer solid, the resonance is observed for ν much larger than the ~1/5 transition seen in single-layer, narrow well samples [17].

Figure 2b shows the evolution of spectra at fixed *n*, with changing ν. The turn-on of the resonance is clear, but at certain ν within the solid range the spectrum abruptly changes. These abrupt changes are interpreted as due to transitions between solid phases. Systematic study of the pinning mode in the low solid regime reveals multiple transitions, marked by colored symbols in Fig 2a. The trajectories of the transitions on the γ-ν plane do not follow expected patterns either for changes in CF type [9] or in bilayer crystal lattice type [18].

iii) **Solid of quasiholes of ½ FQHE** (Hatke *et al.*, arXiv:1504.08182) The microwave spectra of a WQW for ν just below 1/2, under bilayer conditions for which the 1/2 FQHE [19] is present, show two resonances. The lower-f_{pk} is resonance has the same f_{pk} resonance as is found in the insulator at lower ν. The higher-f_{pk} resonance exhibits intensity variations in striking agreement with that expected for a pinning mode of Wigner solid of the quasiholes of this FQHE state. This resonance is also quite sensitive to asymmetrization of the growth-direction charge distribution in the quantum well by gate bias, as is the ½ FQHE in dc [20]. The presence of the two resonances shows the sample is capable of forming states with multiple components.

Future Plans

While we have established that there are a variety of solids in WQWs, we still do not understand the nature of these solids or of the transitions between them. We plan to address this by systematic studies varying temperature, growth-direction asymmetry, in-plane field and the well width.

In addition in GaAs, we plan to study samples of much smaller length scales, and are developing sample geometries to do this. This could reveal some of the behavior of the electron solids at finite wave vector.

Finally, in collaboration with C. Dean of Columbia, we are working on measuring graphene samples encapsulated in BN. These samples could have IQHWCs with pinning modes. Particularly in bilayers [13] they may have other accessible intra Landau level modes.

References Cited

1. Y. E. Lozovik and V. I. Yudson, JETP Letters 22, 11 (1975).
2. P. K. Lam and S. M. Girvin Phys. Rev. B **30** 473 (1984).
3. D. Levesque, J. J. Weis, and A. H. MacDonald, Phys. Rev. B **30** 1056 (1984).
4. H. Fukuyama and P. A. Lee, Phys. Rev. B, **18** 6245 (1978).
5. E. Y. Andrei, G. Deville, D. C. Glattli, F. I. B. Williams, E. Paris, and B. Etienne, Phys. Rev. Lett. **60**, 2765 (1988).
6. F. I. B. Williams, P. A. W. and R. G. Clark, E. Y. Andrei, G. Deville, D. C. Glattli, O. Probst, B.

Etienne, C. Dorin, C. T. Foxon, and J. J. Harris,Phys. Rev. Lett. 66, 3285 (1991).
7. P. D. Ye, L. W. Engel, D. C. Tsui, R. M. Lewis, L. N. Pfeiffer, and K. West, Phys. Rev. Lett. **89**, 176802 (2002).
8. Yong Chen, R. M. Lewis , L. W. Engel , D. C. Tsui , P. D. Ye , L.N. Pfeiffer and K. W. West, Phys. Rev. Lett. **89**, 016801 (2003).
9. A. C. Archer, K. Park, and J. K. Jain, Phys. Rev. Lett. 111, 146804 (2013).
10. Han Zhu, Yong P. Chen, P. Jiang, L. W. Engel, D. C. Tsui, L. N. Pfeiffer, and K. W. West Phys. Rev. Lett. **105**, 126803 (2010).
11. R. Côté, A. H. MacDonald, Luis Brey, H. A. Fertig, S. M. Girvin, and H. T. C. Stoof, Phys. Rev. Lett. 78, 4825 (1997).
12. Han Zhu, G. Sambandamurthy, Yong P. Chen, P. Jiang, L. W. Engel, D. C. Tsui, L. N. Pfeiffer, and K. W. West, Phys.Rev. Lett. **104**, 226801 (2010).
13. Y. Barlas, R. Cote, K. Nomura, and A. H. MacDonald, Phys. Rev. Lett. **101** 097601 (2008).
14. Yang Liu, C. G. Pappas, M. Shayegan, L. N. Pfeiffer, K. W. West, and K. W. Baldwin Phys. Rev. Lett. **109**, 036801 (2012).
15. Yang Liu, D. Kamburov, S. Hasdemir, M. Shayegan, L. N. Pfeiffer, K. W. West, and K. W. Baldwin Phys. Rev. Lett. **113,** 246803 (2014) .
16. H. C. Manoharan, Y. W. Suen, M. B. Santos, and M. Shayegan, Phys. Rev. Lett. 77, 1813 (1996).
17. H. W. Jiang, R. L. Willett, H. L. Stormer, D. C. Tsui, L. N. Pfeiffer, and K. W. West, Phys. Rev. Lett. **65**, 633 (1990).
18. S. Narasimhan and T.-L. Ho, Phys. Rev. B **52**, 12291 (1995).
19. Y. W. Suen L. W. Engel, M. B. Santos, M. Shayegan, and D. C. Tsui, Phys. Rev. Lett. **68**, 1379 (1992).
20. Y. W. Suen, H. C. Manoharan, X. Ying, M. B. Santos, and M. Shayegan Phys. Rev. Lett. **72**, 3405 (1994).

Publications resulting from DOE sponsored research, 2014-2015

B.-H. Moon, L. W. Engel, D. C. Tsui, L. N. Pfeiffer, and K. W. West, “Pinning modes of high-magnetic-field Wigner solids with controlled alloy disorder", Phys. Rev. B **89**, 075310 (2014).

A. T. Hatke, Yang Liu, B. A. Magill, B. H. Moon, L. W. Engel, M. Shayegan, L. N. Pfeiffer, K. W. West, and K. W. Baldwin, “Microwave spectroscopic observation of distinct electron solid phases in wide quantum wells", Nature Communications **5**, 4154 (2014).

S. Chakraborty, A. T. Hatke, L. W. Engel, J. D. Watson, and M. J. Manfra, “Multiphoton processes at cyclotron resonance subharmonics in a two-dimensional electron system under dc and microwave excitation”, Phys. Rev. B **90**, 195437 (2014).

A. T. Hatke, Y. Liu, L. W. Engel, M. Shayegan, L. N. Pfeiffer, K. W. West and K. W. Baldwin, “Microwave spectroscopy of the low- filling-factor bilayer electron solid in a wide quantum well”, Nature Communications **6**, 7071 (2015).

B.-H. Moon, L. W. Engel, D. C. Tsui, L. N. Pfeiffer, and K. W. West, “Microwave pinning modes near Landau filling $\nu = 1$ in two-dimensional electron systems with alloy disorder”, Phys. Rev. B **92**, 035121 (2015).

Program Title: Artificially Structured Semiconductors to Model Novel Quantum Phenomena.
Principal Investigator: A. Pinczuk; Co-PIs: S. J. Wind and V. Pellegrini.
Mailing Adress: Dept. of Applied Physics and Applied Mathematics, Columbia University, New York, NY 10027.
E-mail: ap359@columbia.edu

1. Program Scope

In this project we seek the design and exploration of novel electron states and associated collective phases in controllable artificial structures that are realized in semiconductor quantum structures by advanced nanofabrication methods. The fabricated devices belong to a class of scalable quantum simulators of novel quantum states in which the main actors are many electron systems in high quality semiconductor structures. A primary goal is to reveal striking interplays between fundamental electron interactions and geometrical constraints (topology). These interactions should be venues for novel quantum states that could, eventually, lead to new device concepts.

To achieve milestones in this research we strive to advance the state-of the-art of nanofabrication to create new electronic states in semiconductors. High-resolution nanolithography and inductively-coupled-plasma reactive-ion-etching (ICP-RIE) are used to impose a potential on a high quality modulation doped GaAs/AlGaAs quantum wells (QWs) grown by molecular-beam-epitaxy. The honeycomb topology, or 'artificial graphene' (AG), is a benchmark of the research [1,2]. AG lattices should support the formation of a band structure with linear energy-momentum dispersion, known as massless Dirac fermions (MDFs), and with interactions that are tunable by design and by external fields. In semiconductors with strong spin-orbit coupling AG lattices should enable access to novel topological phases [3].

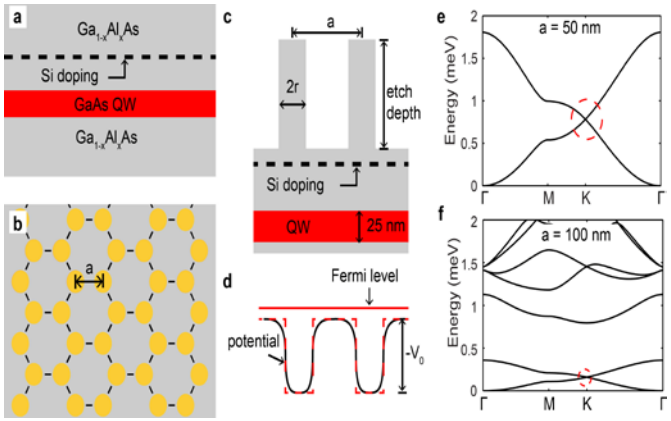

Figure 1. **Description of an AG lattice in a modulation doped GaAs QW**. (a) Layer sequence in the QW sample. (b) Schematic of the etch mask with honeycomb topology. (c) Illustration of sample profile after etching. (d) Schematic of the periodic potential induced by AG pattern (black solid line). In the evaluation of AG band structures a muffing-tin potential is used (red dashed line). (e) Lowest two AG bands for a=50nm, Vo=-10meV and r=8.5nm. (f) AG band structure for a=100nm, Vo=-2meV and r=17nm. Panels (e) and (f) show that the linear dispersion range, highlighted by the dashed circles, is increased by about a factor of 4 by the reduction in lattice constant a.

2. Recent Progress

Figures1(a)-1(d) describe steps in the creation of an AG lattice superimposed on a modulation doped GaAs QW. Figures 1(e) and 1(f) visualize the impact of the reduction of lattice constant, showing that the lower lattice period results in greater definition of the range of massless MDFs.

Figures 2(a) and 2(c) schematically describe the key nanofabrication steps. Figures 2(b) and 2(d) are actual SEM images of recent achievements in nanofabrication of AG. Figure 2(b) demonstrates the creation of a honeycomb lattice mask with lattice constant a=40nm, and Fig. 2(d) shows the high quality AG lattice created after ICP-RIE etching.

Since the start of the project in September 2013 we have achieved two significant milestones:
1. Fabrication of sub-50 nm pitch honeycomb lattices in a AlGaAs/GaAs heterostructure with excellent uniformity and long range order.
2. Observation by Resonant Inelastic Light Scattering (RILS) of evidence for the existence of massless Dirac fermions (MDFs) in a tunable, engineered semiconductor system.
These results suggest new, highly tunable pathways for the exploration of the fundamental interplay between quantum mechanics and topology. Nano-patterned semiconductors with strong spin-orbit coupling should enable access to topological phases in low dimensional electron systems.
Previous work on nano-patterned AG lattices on GaAs QW structures found no evidence of MDFs because of the relatively large lattice periods [2,4,5]. Theoretical estimates such as those in Figs. 1(e) and 1(d) indicate that well-defined MDFs already occur in AG lattices of period below 60nm. The results in Figs. 2(b) and 2(d) show our achievement of AG patterns of lattice constants of 40 – 50nm. In our current work the AG lattices have been experimentally studied at zero magnetic field by photoluminescence (PL) and RILS [6].
RILS spectra of inter-AG-band transitions shown in Fig. 3(b) and 3(c) should be proportional to the joint density of states (JDOS) for vertical transitions (no wave vector change). The calculated JDOS peak shown in Fig. 3(c), which very precisely overlaps the relatively narrow peak E_L, is largely due to transitions in the regions of wave vector space marked as 1 and 2 in Figs. 3c) and 3(d). In region 1, the c_{01} and c_{02} bands are nearly parallel, which results in a maximum in the JDOS. Transitions in region 2 of the JDOS initiate at the Dirac cones formed at K and K' points. Transitions in region 3 are mainly from transitions around the M point in the BZ, where the c_{01} and c_{02} bands have fairly different k-dispersion, generating a broader peak E_H. The excellent agreement between measured RILS spectra and calculated JDOS is strong evidence that well-defined AG bands are formed under the periodic potential generated in the fabricated AG lattice patterns.
Transitions from region 2 are of particular interest since they originate from the segments of the reciprocal lattice BZ near the K and K' points where MDFs are formed. To focus on contributions

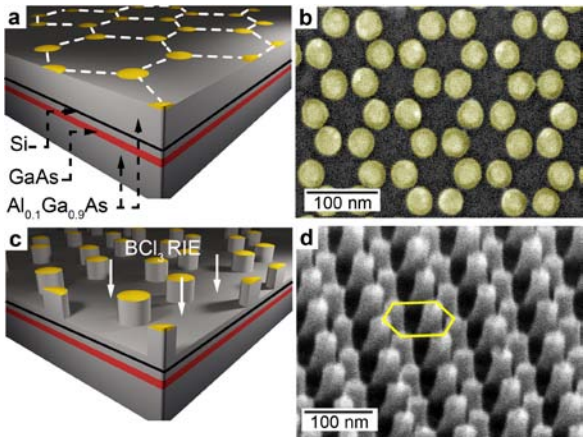

Figure 2. **Nanofabrication of an AG pattern on a modulation doped GaAs QW**. (a) Illustration of the etch-mask consisting of an array of metal nano-disks arranged in a honeycomb lattice on the surface of a QW. (b) SEM micrograph of the mask of gold nano-disks with a=40nm (false color). (c) Cartoon representing the AG nano-pattern obtained through a mask using a BCl_3 – based gas mixture. (d) SEM image of an AG lattice of a=50nm after the ICP-RIE dry etch of the sample and removal of the metal mask. The etch depth is 50nm.

from region 2 in the E_L band of the RILS spectra we take advantage of resonance enhancement of RILS. Region 2 transitions that occur at the high-energy cutoff of the E_L peak in the upper RILS spectrum displayed in Fig. 4, obtained using the lower incident photon energy, where the E_L peak mainly results from transitions around the Dirac points because these transitions are selectively enhanced in RILS spectra [6]. The low energy tail of the E_L peak (grey area) likely arises from non-vertical transitions due to disorder as indicated in the inset to the figure. The sharp high-energy

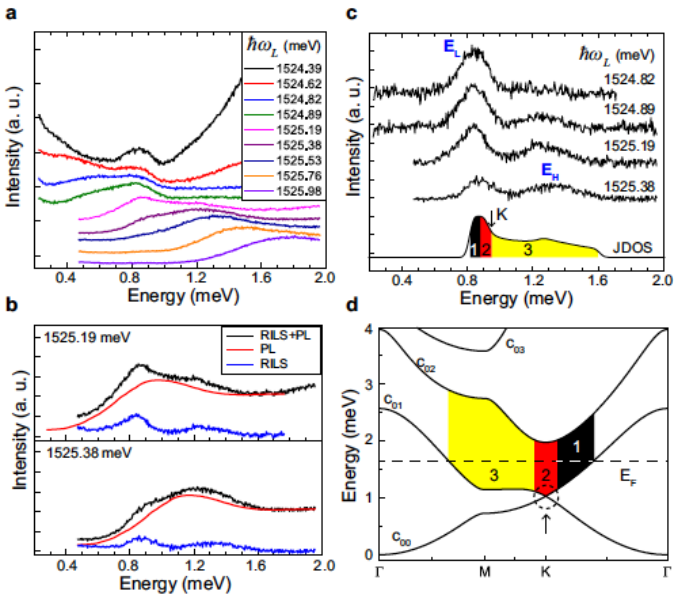

Figure 3. **Low-lying inter-AG-band transitions from an AG lattice with a=50nm**. (a) Spectra of low-lying excitations at different incident photon energies. The RILS signal overlaps with PL. (b) Subtraction of the PL (red) reveals RILS (blue) of low-lying excitations. (c) RILS after the removal of the PL. Two peaks are identified at E_L = 0.85 meV and E_H = 1.3 meV. (d) Illustration of the electronic transitions associated with the observed RILS spectra. The AG bands have been calculated with a = 50 nm, r = 8.5 nm, and V_0=-6.4meV. The dashed circle highlights the linear dispersion range in the c_{00} and c_{01} bands. Three regions of the reciprocal space are identified with different colors. In (c) the calculated joint density of states (JDOS) of the inter-AG-band transitions between the c_{01} and c_{02} bands for the transitions in each region shown in (d) are in agreement with the measured spectra.

cutoff seen in the asymmetric E_L peak present in the upper spectrum in Fig. 4 is interpreted as the cutoff of the JDOS due to MDFs around the K and K' points. These results provide evidence of the presence of a minimum of JDOS at the K and K' points, which indicate well-defined MDF's.

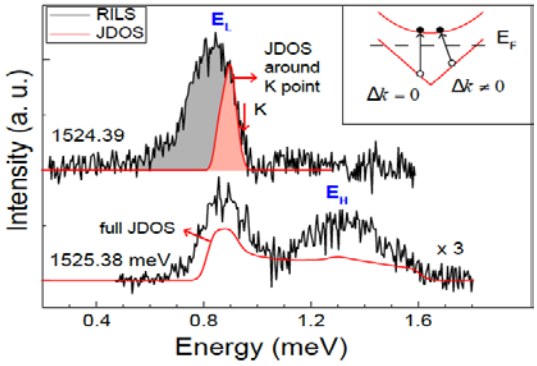

Figure 4. **Exploration of MDFs in RILS spectra: AG lattice with a=50nm.** RILS spectra at two different incident photon energies labeled in meV. The inset shows vertical ($\Delta k = 0$) and non-vertical ($\Delta k \neq 0$) transitions between the c_{01} and c_{02} AG bands. The upper spectrum is largely from transitions close to the K and K' points. The JDOS from transitions near the K and K' points (red line) accurately interprets the line shape of the high-energy cutoff due to the vanishing DOS at the Dirac point. The lower spectrum, taken at higher incident photon energy, showing bands at E_L and E_H is interpreted with JDOS (in red) with contributions from a larger range of k space.

3. Future plans

In the 24 months since the start of this project, we have achieved the creation of 2D honeycomb lattices (AG) on modulation doped AlGaAs/ GaAs QWs of very small lattice constant by means of nano-fabrication using advanced e-beam lithography and ICP-RIE. We have demonstrated excellent long-range order, short-range uniformity and anisotropic etching profile. RILS spectra measured in the sample with lattice constant a=50nm reveal transitions of occupying states of AG bands with well-defined massless Dirac fermions (MDFs). We are now well positioned to seek further milestones in this realm of study. Among our top priorities is the achievement of high quality patterns of smaller lattice period. We now understand how to create high quality patterns of smaller lattice constant by slight changes in the design of the modulation doping AlGaAs/GaAs QW that supports the AG pattern and by optimization of the depth of ICP-RIE etching. At this time time we are optimizing patterns with a=40nm.

Our next goals include:

-- the realization of AG patterns with lattice constants of a=35nm and smaller. Here, reaching of milestones require that we optimize fabrication protocols that are at the frontiers of the state-of-the-

art. We have also modeled an "anti-dot" lattice that would allow well-defined MDF's.
-- The velocity of MDF's, tuned by changes in lattice constant, will be probed by RILS measurements in intra-AG-band transitions at energy proportional to the velocity.
-- We are currently getting ready for studies of fabricated AG lattices in high magnetic fields and very low temperatures in the laboratory of the PI. These experiments probe key properties of MDF's.

AG patterns of such very small period in a diverse group of compound semiconductors could access new physics of MDFs that may not be accessible in natural graphene. Among our priorities is to initiate AG studies in semiconductor systems that have larger spin-orbit coupling to seek emergence of topological protection of MDF's.

4. References

1. Making Massless Dirac Fermions from a Patterned Two-Dimensional Electron Gas, Cheol-Hwan and Steven G. Louie, *Nano Letters* **9**, 1793-1797 (2009).
2. Engineering Artificial Graphene in a Two-dimensional Electron Gas, Marco Gibertini, Achintya Singha, Vittorio Pellegrini, Marco Polini, Giovanni Vignale, Aron Pinczuk, Loren N. Pfeiffer, and Ken W. West, *Physical Review B* **79**(R), 241406 (2009).
3. Quantum Spin Hall Effect in Graphene, C. L. Kane and E. J. Mele*Physical Review Letters* **95,** 226801 (2005).
4. Two-dimensional Mott-Hubbard Electrons in an Artificial Honeycomb Lattice, A. Singha, M. Gibertini, B. Karmakar, S. Yuan, M. Polini, G. Vignale, M.I. Katsnelson, A. Pinczuk, L.N. Pfeiffer, K.W. West, and V. Pellegrini, *Science* **332**, 1176-1179 (2011).
5. From Laterally Modulated Two-dimensional Electron Gas Towards Artificial Graphene, L Nadvornik, M. Orlita, N. A. Goncharuk, L. Smrcka, V. Novak, V. Jurka, et al, *New Journal of Physics*, **14**, 053002 (2012).
6. Observation of Dirac Bands in Artificial Graphene Realized in Small Period Nano-patterned GaAs Quantum Wells, Sheng Wang, Diego Scarabelli, Yuliya Y. Kuznetsova, Loren N. Pfeiffer, Ken West, Michael J. Manfra, Geoff C. Gardner, Vittorio Pellegrini, Shalom J. Wind, and Aron Pinczuk, submitted for publication in *Nature Nanotechnology,* June 2015.

5. Papers that acknowledge support from this DOE grant

1. Fabrication of Artificial Graphene in an Engineered Semiconductor System, Diego Scarabelli, Sheng Wang, Antonio L. Levy, Loren Pfeiffer, Ken West, Vittorio Pellegrini, Michael J. Manfra, Aron Pinczuk, and Shalom J. Wind, *Journal of Vacuum Science and Technology B*, undergoing requested revisions.
2. Observation of Dirac Bands in Artificial Graphene Realized in Small Period Nano-patterned GaAs Quantum Wells, Sheng Wang, Diego Scarabelli, Yuliya Y. Kuznetsova, Loren N. Pfeiffer, Ken West, Michael J. Manfra, Geoff C. Gardner, Vittorio Pellegrini, Shalom J. Wind, and Aron Pinczuk, *Nature Nanotechnology*, undergoing requested revisions.

Project Title: Emergent Phenomena in Quantum Hall Systems Far From Equilibrium
Principle Investigator: Michael Zudov
Mailing address: School of Physics and Astronomy, University of Minnesota, Minneapolis, Minnesota 55455, USA
Email: zudov@physics.umn.edu

Program Scope

The focus of the project is on magnetotransport properties of semiconductor nanostructures, especially when these structures are driven away from equilibrium by microwave or dc electric fields [1]. In particular, the project explores nonequilibrium phenomena in a new experimental regime of separated Landau levels in two-dimensional electron gas (2DEG) in GaAs/AlGaAs quantum wells, e.g., photoresistance in the regime of Shubnikov-de Haas oscillations (SdHOs). In addition, the project searches for nonequilibrium and other novel phenomena in new 2D systems, e.g., a two-dimensional hole gas (2DHG) hosted in strained Ge/SiGe quantum wells.

Recent Progress

SdHOs in a 2DEG in GaAs/AlGaAs quantum wells under sub-THz radiation – Extending photoresistance experiments to high frequencies f and low temperatures T allows to explore the regime of SdHO. Our recent measurements at f up to 0.4 THz revealed strong, and totally unexpected, correlation between SdHO and microwave-induced resistance oscillations (MIROs).

When a 2DEG is subject to sub-THz radiation and low T, its magnetoresistivity $\rho(B)$ exhibits both MIROs and SdHOs: $\rho = \rho_{sm} + \delta\rho_{MIRO} + \delta\rho_{SdHO\omega}$. Here, ρ_{sm} is the smooth part of the resistivity and $\delta\rho_{MIRO} = -2\pi\rho_0\varepsilon P\eta\lambda^2\sin(2\pi\varepsilon)$, where ρ_0 is the zero-field resistivity, $\varepsilon = \omega/\omega_c$, $\omega = 2\pi f$ is the radiation frequency, ω_c is the cyclotron frequency, P is the radiation intensity, η is the dimensionless scattering rate [1], and λ is the Dingle factor. Without radiation, $\delta\rho_{SdHO} = -A\cos(\pi\nu)$, where $A = 4\rho_0\lambda D$, $D = X/\sinh(X)$, $X = 2\pi^2 k_B T/\hbar\omega_c$, and ν is the filling factor. Under irradiation, one could expect modulation of A, with the minima at integer or half-integer ε, due to magneto-absorption [2] or direct modification of A through the displacement mechanism [3].

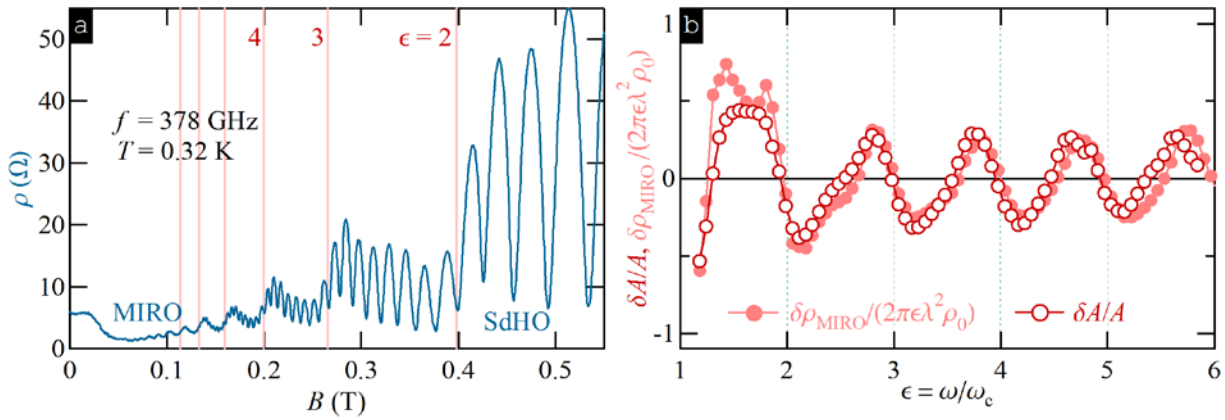

Fig. 1. (a) ρ vs magnetic field B at $f = 378$ GHz and $T = 0.32$ K. (b) $\delta\rho_{MIRO}/(2\pi\varepsilon\lambda^2\rho_0)$ and $\delta A/A$ vs $\varepsilon = \omega/\omega_c$.

Surprisingly, our experimental findings are inconsistent with either of the above scenarios [4]. In Fig. 1(b) we present the radiation-induced correction to the SdHO amplitude, $\delta A/A$, along with $\delta\rho_{\mathrm{MIRO}}/(2\pi\varepsilon\lambda^2\rho_0)$, both obtained from $\rho(B)$ shown in Fig. 1(a), as a function of ε. Remarkably, both quantities show excellent agreement not only in the period, but also in the phase. However, in contrast to theoretical predictions [2,3], the minima in A occur at neither integer nor half-integer ε, but rather at $\varepsilon \approx n + 1/4$. Even more surprising is the quantitative agreement between these two quantities which allows us to obtain an empirical relation for the radiation-induced correction to A, namely $\delta A \approx -AP\eta\sin(2\pi\varepsilon)$. While it is well established that oscillations of the order $O(\lambda^2)$ can mix with each other, the correlation between MIRO ($\sim\lambda^2$) and SdHO ($\sim\lambda$) is totally unexpected, revealing that our understanding of nonequilibrium 2DEG is still lacking.

Magnetotransport in a high-mobility 2DHG in strained Ge/SiGe quantum wells – Our recent studies in a new material system, a high-mobility 2DHG in a Ge/SiGe quantum well, revealed both MIROs [5] and Hall field-induced resistance oscillations (HIROs) [6], which were previously exclusive to 2DEG in GaAs, and the first observation of the fractional quantum Hall effect in this system [7]. The most unexpected finding, however, is an incredibly strong transport anisotropy [8] which, to our knowledge, has not yet been observed in any material system.

In contrast to 2DEG in GaAs, which is known for transport anisotropies in high Landau levels due to stripes [9], our 2DHG in Ge (mobility $\approx 1 \times 10^6$ cm^2/Vs, density $\approx 2.8 \times 10^{11}$ cm^{-2}) shows no significant anisotropy in perpendicular field $B_\perp$ down to $T \approx 50$ mK. However, when an *in-plane magnetic field* $B_{||}$ is added, R_{xx} increases almost everywhere, except at the quantum Hall states, whereas R_{yy} decreases. As shown in Fig. 2, even at a modest tilt angle of $\theta = 72^\circ$ and a rather high temperature $T = 0.3$ K, the ratio R_{xx}/R_{yy} exceeds 2000 at $\nu = 9/2$. Remarkably, this ratio is determined entirely by θ and is nearly independent of the Landau level index up to $\nu \approx 40$. The hard (easy) direction is always parallel (perpendicular) to $B_{||}$. In addition, the anisotropy is remarkably robust against T. While R_{xx}/R_{yy} decreases with T [Fig. 2(a) and (b)], it remains significant, $R_{xx}/R_{yy} \approx 150$, even at $T = 1.5$ K [Fig. 2 (c)]. The easy tunability by θ, the robustness against T, and the absence of significant anisotropy in pure $B_\perp$ (or pure $B_{||}$) point towards a novel mechanism of transport anisotropy.

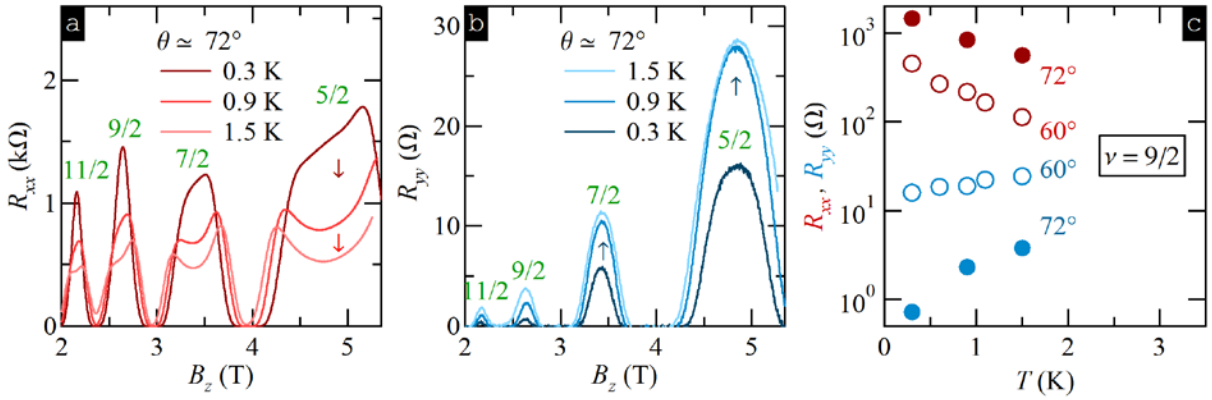

Fig. 1. (a)[(b)] R_{xx} [R_{yy}] vs B_z at θ = 72° and T = 0.3, 0.9, 1.5 K. (c) R_{xx}, R_{yy} vs T at ν = 9/2, θ = 60° and 72°.

Future Plans

2DEG in GaAs/AlGaAs quantum wells at sub-THz frequencies – Our recent measurements in the SdHO regime revealed a large number of sharp photoresistance features which appear in a rather wide range of B in the vicinity of the cyclotron resonance. These features are roughly periodic in B and are best observed at low temperatures. We now plan to test whether or not such sharp features could originate from very high harmonics of the magneto-plasmon resonance.

2DHG hosted in strained Ge/SiGe quantum wells in tilted magnetic fields – To single out the origin of strong transport anisotropy discussed above, we will extend studies to much higher T and much higher ratios of $B_{||}/B_{\perp}$. The main goal of these experiments is to determine whether the anisotropy relies on Landau and/or spin quantization or can survive in the semi-classical regime.

Photoresistance in an ultrahigh quality 2DEG in GaAs/AlGaAs – We have recently started investigations of microwave photoresistance in an ultrahigh quality 2DEG, in which transport and *quantum* mobilities exceed 3×10^7 and 1×10^6 cm^2/Vs, respectively. In such a device, MIROs persist to incredibly low magnetic fields, well below 0.01 T. We have already detected very unusual features which we now plan to investigate in detail.

Transport in 2DEG with alloy disorder – Disorder plays a central role in quantum transport, controlling the quality of both high- and low-field phenomena. To better understand its role, we will study how non-equilibrium and equilibrium transport is modified by an alloy disorder which is controllably introduced by adding a small mole fraction of Al into the otherwise pure GaAs channel. Our preliminary data already revealed its interesting effect on both MIROs and HIROs.

References

[1] I. A. Dmitriev, *et al.*, Rev. Mod. Phys. **84**, 1709 (2012).
[2] I. A. Dmitriev *et al.*, Phys. Rev. Lett. **91**, 226802 (2003); Phys. Rev. B **70**, 165305 (2004).
[3] X. L. Lei, Phys. Rev. B **79**, 115308 (2009); I. A. Dmitriev, J. Phys. Conf. Ser. **334**, 012015 (2011).
[4] Q. Shi *et al.*, Phys. Rev. B **92**, 081405(R) (2015).
[5] M. A. Zudov, *et al.*, Phys. Rev. B **89**, 125401 (2014).
[6] Q. Shi *et al.*, Phys. Rev. B **90**, 161301(R) (2014).
[7] Q. Shi *et al.*, Phys. Rev. B **91**, 241303(R) (2015).
[8] Q. Shi *et al.*, Phys. Rev. B **91**, 201301(R) (2015).
[9] M. P. Lilly *et al.*, Phys. Rev. Lett. **82**, 394 (1999); R. R. Du, *et al.*, Solid State Commun. **109**, 389 (1999); A. A. Koulakov *et al.*, Phys. Rev. Lett. **76**, 499 (1996).

Publications (2013-2015)

(i) Q. Shi, P. D. Martin, A. T. Hatke, M. A. Zudov, J. D. Watson, G. C. Gardner, M. J. Manfra, L. N. Pfeiffer, and K. W. West "Shubnikov–de Haas oscillations in a two-dimensional electron gas under subterahertz radiation", Phys. Rev. B – Rapid Commun. **92**, 081405(R) (2015)

(ii) M. A. Zudov, "Comment on "Theory of microwave-induced zero-resistance states in two-dimensional electron systems" and on "Microwave-induced zero-resistance states and second-harmonic generation in an ultraclean two-dimensional electron gas"", Phys. Rev. B **92**, 047301 (2015)
(iii) Q. Shi, M. A. Zudov, C. Morrison, and M. Myronov, "Spinless Composite Fermions in an Ultra-high Quality Strained Ge Quantum Well", Phys. Rev. – Rapid Commun. **91**, 241303(R) (2015)
(iv) Q. Shi, M. A. Zudov, C. Morrison, and M. Myronov, "Strong Transport Anisotropy in a Ge/SiGe Quantum Well in Tilted Magnetic Fields", Phys. Rev. B – Rapid Commun. **91**, 201301(R) (2015)
(v) Q. Shi, Q. A. Ebner, and M. A. Zudov, "Hall field-induced resistance oscillations in Ge/SiGe quantum wells", Phys. Rev. B – Rapid Commun. **90**, 161301(R) (2014)
(vi) M. A. Zudov, O. A. Mironov, Q. A. Ebner, P. D. Martin, Q. Shi, and D. R. Leadley, "Observation of microwave-induced resistance oscillations in strained Ge/SiGe quantum wells", Phys. Rev. B **89**, 125401 (2014)
(vii) Q. Zhang, T. Arikawa, E. Kato, J. L. Reno, Wei Pan, J. D. Watson, M. J. Manfra, M. A. Zudov, M. Tokman, M. Erukhimova, A. Belyanin, and J. Kono, "Superradiant decay of cyclotron resonance of two-dimensional electron gases", Phys. Rev. Lett. **113**, 047601 (2014)
(viii) Q. Shi, P. D. Martin, Q. A. Ebner, M. A. Zudov, L. N. Pfeiffer, and K. W. West, "Colossal negative magnetoresistance in a 2D electron gas", Phys. Rev. B – Rapid Commun. **89**, 201301(R) (2014)
(ix) Q. Shi, M. Khodas, A. Levchenko, and M. A. Zudov, "Phase-sensitive bichromatic photoresistance in a two-dimensional electron gas", Phys. Rev. B **88**, 245409 (2013)
(x) A. Bogan, A. T. Hatke, S. A. Studenikin, A. S. Sachrajda, M. A. Zudov, L. N. Pfeiffer, and K. W. West, "Effect of an in-plane magnetic field on microwave photoresistance and Shubnikov-de Haas effect in high-mobility GaAs/AlGaAs quantum wells", J. Phys. Conf. Ser. **456**, 012004 (2013)
(xi) A. T. Hatke, M. A. Zudov, J. D. Watson, M. J. Manfra, L. N. Pfeiffer, and K. W. West, "Effective mass from microwave photoresistance measurements in GaAs/AlGaAs quantum wells", J. Phys. Conf. Ser. **456**, 012040 (2013)
(xii) A. T. Hatke, M. A. Zudov, L. N. Pfeiffer, and K. W. West, "Shubnikov-de Haas oscillations at very high tilt angles", J. Phys. Conf. Ser. **456**, 012041 (2013)
(xiii) M. A. Zudov, "Microwave-induced Nonequilibrium Phenomena" in Z. F. Ezawa, Quantum Hall Effects: Recent Theoretical and Experimental Developments, pp. 754-778, World Scientific, Singapore, ISBN: 978-981-4360-75-3 (2013)
(xiv) A. T. Hatke, M. A. Zudov, J. D. Watson, M. J. Manfra, L. N. Pfeiffer, and K. W. West, "Evidence for effective mass reduction in GaAs/AlGaAs quantum wells", Phys. Rev. B – Rapid Commun. **87**, 161307(R) (2013)

Program Title: Quantum Electronic Phenomena and Structures

Principle Investigator: W. Pan; Co-PIs: M.P. Lilly, J.L. Reno, T.M. Lu, E. Nielsen, G.T. Wang, E.A. Shaner, R. Prasankumar, and D.C. Tsui
Mailing Address: P.O. Box 5800, MS 1086, Sandia National Labs, Albuquerque, NM 87185
E-Mail: wpan@sandia.gov

Program Scope

This project is to discover and understand emerging quantum phenomena and states in novel electronic device structures that are governed by the laws of quantum mechanics. The project includes research of quantum transport studies in low dimensional electron systems, carrier transport dynamics, optical properties, and high quality materials synthesis. We investigate electron physics at the nano and mesoscopic scales that occurs due to strong electron-electron and electron-disorder interactions, and focus on important areas, such as novel fractional quantum Hall physics, exotic many-body states in coupled quantum structures, the impact of disorder in strongly correlated ground states, topological transport properties in Dirac materials, the valley degree of freedom in high quality Si/SiGe quantum wells, and THz quantum Hall effects in two dimensional electron/hole systems. These research topics are at the frontier of the field of condensed matter physics and will undoubtedly yield new discoveries and new understanding of emergent quantum states and behaviors.

Recent Progress:

Second Generation Fractional Quantum Hall Effect: The search for novel fractional quantum Hall effect (FQHE) states, for example, non-abelian FQHE states, continues to attract a great deal of interest since they were first discovered in 1982. To date, studies on non-Abelian FQHE states have mostly been limited to the second Landau level. A little over ten years ago, observation of the signature of the FQHE at ν=4/11, however, generated new excitements on the existence of non-Abelian FQHE states in the lowest Landau level. Several theoretical proposals have been made. Among them, the numerical simulations by Wójs, Yi, and Quinn (WYQ) showed that a spin-polarized 4/11 state is an unconventional FQHE state of composite fermions (CFs) and, possibly, a new non-Abelian state.

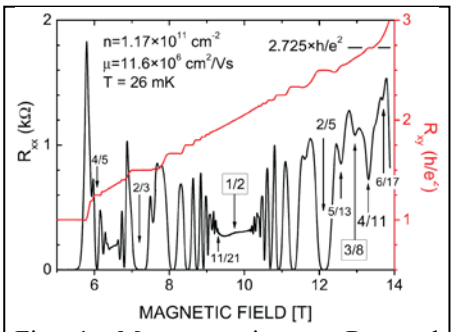

Fig. 1: Magneto-resistance R_{xx} and Hall resistance R_{xy}. A quantized plateau is observed at ν=4/11.

Despite a significant amount of theoretical work on this novel 4/11 FQHE state, experimentally, a definitive observation of an accurately quantized Hall plateau with activated longitudinal resistance has been lacking. Recently, with new improvements in wafer growth, a high electron mobility of ~ 12×10^6 cm^2/vs has been achieved at an electron density of ~ 1.2×10^{11} cm^{-2}. In this high-quality low-density sample, we observed at ν=4/11 activated magnetoresistance R_{xx} and quantized Hall resistance R_{xy}. Our results thus confirm that the 4/11 state is a true FQHE state. Furthermore, we studied the spin polarization of this new FQHE state, utilizing the well-developed in-situ tilt magnetic field technique. Results from two quantum well samples of different well thickness (40 nm versus 50 nm) show that the 4/11 state is most likely spin polarized in the density range of n~1×10^{11} cm^{-2}, consistent with previous numerical results [Barlam et al, PRB **91**, 045109 (2015)]. Our results thus suggest that the 4/11 state is a WYQ state, a new non-Abelian state in the lowest Landau level. [Pub #09]

Terahertz magneto-optical spectroscopy of two-dimensional hole system: Two-dimensional hole systems (2DHS) are known to have an advantage in their use in the burgeoning areas of quantum computing and spintronics, as the *p*-type hole valence band has a reduced hyperfine interaction with the nuclei, leading to longer spin coherence times for holes. We have performed the first temperature-dependent THz magneto-optical spectroscopic measurements on 2DHS, revealing significant differences in the dependence of the cyclotron frequency on magnetic field as compared to the more commonly studied two-dimensional electron systems, particularly at higher temperatures. We then built upon these results by performing ultrafast optical microscopy, providing new insight into carrier relaxation in radial multiple quantum well systems. [Pub #10]

Electron bilayers in undoped Si/SiGe double quantum wells: Additional degrees of freedom often bring about new physical phenomena in the quantum Hall regime. Spins and valleys have both been shown to play an important role in integer and fractional quantum Hall states. Layers are another degree of freedom that can be engineered into a 2D electron system. In GaAs this has led to a plethora of inter-layer correlation effects, the most famous one being the Bose-Einstein condensation of excitons. A bilayer system also serves as the platform for building coupled quantum wires. This architecture has long been employed to study Luttinger liquid physics in 1D electron gas.

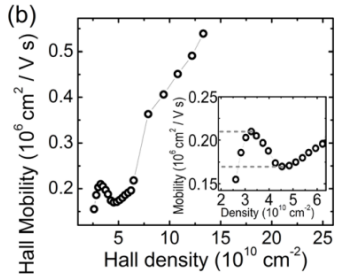

Fig. 2: Mobility dip indicating the onset of population of the second layer.

In Si/SiGe, no high-mobility electron bilayer system has been reported. The main difficulty is in material growth, since dopants can travel along the growth front and are incorporated throughout the structure, spoiling the mobility. We circumvent this difficulty by employing a dopantless architecture. By carefully choosing the barrier and quantum well thicknesses, two layers of electrons can be capacitively induced and coexist under certain gate bias conditions. As shown in Fig. 2, a mobility dip is observed with increasing electron density, a signature of the onset of inter-layer scattering. It occurs at a density consistent with our self-consistent Schrodinger-Poisson simulations, thus proving the existence of an electron bilayer system in Si. We also observed a $\nu=2$ integer quantum Hall state. We think this state could arise from inter-layer correlation but inter-layer tunneling could render the state single-layer-like. [Pub #11]

Reversible Bandgap Tuning in GaN Nanowire Lasers: We demonstrated dynamic and continuous tuning of single nanowire lasers by application of hydrostatic pressures up to ~7 GPa. A wide ~30 nm range of reversible wavelength tuning was achieved in a single GaN nanowire laser. The wavelength tuning is caused by an increase in the direct bandgap of GaN with increasing pressure and is precisely controllable to subnanometer resolutions. The observed pressure coefficients of the NWs are ~40% larger compared with GaN microstructures fabricated from the same material or from reported bulk GaN values, revealing a nanoscale-related effect that significantly enhances the tuning range using this approach. [Pub #16]

Future Plans:

Fractional quantum Hall effect at $\nu=3/8$: Surprisingly, very little experimental data are available for this possible even-denominator fractional quantum Hall state in the lowest Landau level. On the other hand, numerical calculations have revealed many possible exotic ground states at this filling factor. Thus, a better understanding of the nature of this novel FQHE is needed. We plan to systematically study this state in our ultra-high mobility two-dimensional electron systems.

We will explore its spin polarization utilizing the tilted magnetic field technique. In particular, we will examine whether there exists a spin transition as predicted in numerical calculations.

Si/SiGe bilayer material: We will perform low-temperature magneto-transport studies on the new Si/SiGe bilayer material with suppressed inter-layer tunneling and search for evidence of inter-layer correlation. An electron bi-wire Si/SiGe sample has been fabricated and is ready to be measured. We will study 1D-1D tunneling and 1D-1D drag in this system with a valley degree of freedom. We are also working toward selective modulation doping through STM-based hydrogen lithography, which will allow us to introduce position correlation in the remote charge layer. Theoretically this should lead to higher 2DEG mobilities than with a random distribution of ionized donors.

Terahertz magneto-optical spectroscopy: We have re-optimized our ultrafast optical microscopic setup and will perform ultrafast optical microscopy measurements on InN nanowires in the near future. We are also adapting our system to perform ultrafast optical Faraday rotation measurements on single nanowires, with the goal of exploring spin-orbit coupling in these systems. We have also begun optical-pump, THz probe experiments in a magnetic field on 2DEG and 2DHG, revealing novel photo-induced quantum states.

Topological properties in Dirac materials: We will begin a new synthesis effort in topological materials. Our initial focus will be on SnTe nanostructures, which have been predicted to have topological states on the high symmetry facets. We will explore the growth of SnTe nanostructures by thermal vapor deposition, examining the effects of substrate, metal catalyst, and growth conditions on nanostructure formation. Quantum transport properties of topological surface states in these materials will be studied. In addition, high frequency transport studies, which have extensively been used to manifest quantum phases and phase transitions, will be carried out in understanding quantum properties in topological nanostructures coupled with photons. We have begun THz magneto-optical measurements on other 2D nanosystems, including MoS2, topological insulators, and Dirac/Weyl semimetals. Finally, we plan to theoretically explore the effect of realistic disorder on the current-carrying edge modes of a topological insulator. We will use actual measured device geometries, where appropriate, in numerical simulations to compare candidate disorder models with the results of experiment.

Publications intellectually led by this FWP (October'13 to September'15):

1) G.C. Dyer, G.R. Aizin, S.J. Allen, A.D. Grine, D. Bethke, J.L. Reno, and E.A. Shaner, *Induced transparency by coupling of Tamm and defect states in tunable terahertz plasmonic crystals*, Nature Photonics **7**, 925 (2013).
2) W. Pan, A. Serafin, J.S. Xia, L. Yin, N.S. Sullivan, K.W. Baldwin, K.W. West, L.N. Pfeiffer, and D.C. Tsui, *Competing quantum Hall phases in the second Landau level in low density limit*, PRB **89**, 241302(R) (2014).
3) G.C. Dyer, G.R. Aizin, S.J. Allen, A.D. Grine, D. Bethke, John L. Reno, Eric A. Shaner, *Interferometric measurement of far infrared plasmons via resonant homodyne mixing*, Optics Express **22**, 16254 (2014).
4) D. Laroche, G. Gervais, M.P. Lilly, and J.L. Reno, *1D-1D Coulomb Drag Signature of a Luttinger Liquid*, Science **343**, 631 (2014).
5) N. S. Selby, M. Crawford, L.A. Tracy, J.L. Reno, and W. Pan, *in-situ Biaxial Rotation at Low-Temperatures in High Magnetic Fields*, Rev. Sci. Instrum. **85**, 095116 (2014).
6) S.K. Lyo and W. Pan, *Miniband transport in a two-dimensional electron gas with a strong periodic unidirectional potential modulation,* Solid State Communications **196**, 51 (2014).

7) W. Pan, E. Dimakis, G.T. Wang, T.D. Moustakas, and D.C. Tsui, *Two-dimensional electron gas in monolayer InN quantum wells*, Appl. Phys. Lett. **105**, 213503(2014).
8) Brian L. Brown, Julia S. Bykova, Austin R. Howard, A. A. Zakhidov, Mark Lee, and Eric A. Shaner, *Microwave AC Conductance of Carbon Nanotube Sheets*, Appl. Phys. Lett. **105** , 263105 (2014).
9) W. Pan, K.W. Baldwin, K.W. West, L.N. Pfeiffer, and D.C. Tsui, *Fractional Quantum Hall Effect at Landau Level Filling nu=4/11*, Phys. Rev. B **91**, 041301(R) (2015).
10) N. Kamaraju, W. Pan, U. Ekenberg, D. M. Gvozdić, S. Boubanga-Tombet, P. C. Upadhya, J. Reno, A. J. Taylor, and R. P. Prasankumar, *Terahertz magneto-optical spectroscopy of two-dimensional hole and electron systems*, Appl. Phys. Lett. **106** , 031902 (2015).
11) D. Laroche, S.-H. Huang, Erik Nielsen, C. W. Liu, J.-Y. Li, and T. M. Lu, *Magneto-transport of an electron bilayer system in an undoped Si/SiGe double quantum well heterostructure*, Appl. Phys. Lett. **106**, 143503 (2015).
12) P.C. Upadhya, J.A. Martinez, Q. Li, George T. Wang, B.S. Swartzentruber, A.J. Taylor, and Rohit P. Prasankumar, *Space-and-time-resolved spectroscopy of single GaN nanowires*, Appl. Phys. Lett. **106** , 263103 (2015).
13) X. Shi, W. Pan, K.W. Baldwin, K.W. West, L.N. Pfeiffer, and D.C. Tsui, *Impact of modulation doping layer on the 5/2 anisotropy*, Phys. Rev. B **91**, 125308 (2015).
14) B.L. Brown, P. Martinez, Anvar A. Zakhidov, E.A. Shaner, and Mark Lee, *Microwave Conductance Properties of Aligned Multiwall Carbon Nanotube Textile Sheets*, J. Appl. Phys**. 118**, 014308 (2015).
15) X. Shi, W. Yu, S. D. Hawkins, J. F. Klem, and W. Pan, *McMillan-Rowell Like Oscillations in a Superconductor-InAs/GaSb-Superconductor Junction*, Appl. Phys. Lett. 107, 052601 (2015).
16) S. Liu, C. Li, J. J. Figiel, S. R. Brueck, I. Brener, G. T. Wang , *Continuous and dynamic spectral tuning of single nanowire lasers with subnanometer resolution using hydrostatic pressure*, Nanoscale **7**, 9581 (2015).

Collaborative publications (October'13 to September'15)

17) O. Mitrofanov, W. Yu, R.J. Thompson, Y. Jiang, I. Brener, W. Pan, C. Berger, W.A. de Heer, and Z. Jiang, *Probing terahertz surface plasmon waves in graphene structures*, APL. **103**, 111105 (2013).
18) H.A. Quintana, E. Song, G.T. Wang, and J. A. Martinez, *Heat Transport in Novel Nanostructured Materials and their Thermoelectric Applications*, Chem Eng Process Tech **1**, 1008 (2013).
19) M. A. Seo, S. Boubanga-Tombet, J. Yoo, Z. Ku, A. V. Gin, S. T. Picraux, S. R. J. Brueck, A. J. Taylor, and R. P. Prasankumar, *Ultrafast optical wide field microscopy*, Optics Express **21**, 8763 (2013)
20) Qi Zhang, T. Arikawa, E. Kato, J.L. Reno, W. Pan, J.D. Watson, M.J. Manfra, M.A. Zudov, M. Tokman, M. Erukhimova, A. Belyanin, and J. Kono, *Superradiant Nature of Cyclotron Resonance Decoherence in Two-Dimensional Electron Gases*, Phys. Rev. Lett. **113**, 047601 (2014).
21) C.S.F. Cobaleda, X.Y. Xiao, D.B. Burckel, Ronen Polsky, D. Huang, E. Diez, and W. Pan, *Superconducting properties in Tantalum decorated three-dimensional graphene and carbon structures*, Appl. Phys. Lett. **105**, 053508 (2014).
22) W. Yu, Y. Jiang, X. Chen, Z. Jiang, S.D. Hawkins, J.F. Klem, and W. Pan, *Superconducting proximity effect in inverted InAs/GaSb QW structures with Ta electrodes*, APL **105**, 192107 (2014).
23) L.V. Frolova, I.V. Magedov, A. Harper, S. K. Jha, M. Ovezmyradov, G. Chandler, Jill Garcia, Donald Bethke, Eric A. Shaner, Igor Vasiliev, Nikolai G. Kalugin, *Tetracyanoethylene oxide-functionalized graphene and graphite characterized by Raman and Auger spectroscopy*, Carbon **81**, 216 (2015).
24) O. Sydoruk, K. Choonee, and G.C. Dyer, *Transmission and Reflection of Terahertz Plasmons in Two-Dimensional Plasmonic Devices*, IEEE Transactions on THz Science and Technology **5**, 486 (2015).
25) B. Zhang , P. Lu, H. Liu, L. Jiao, Z. Ye, M. Jaime, F.F. Balakirev, H. Yuan, H.Z. Wu, W. Pan, and Y. Zhang, *Quantum oscillations in a two-dimensional electron gas at the twisted zincblende/rocksalt interface of CdTe/PbTe (111) heterostructures*, Nano Letters **15**, 4381 (2015).
26) O. Wolf, S. Campione, A. Benz, A.P. Ravikumar, S. Liu, T.S. Luk, E.A. Kadlec, E.A. Shaner, J.F. Klem, M.B. Sinclair, and I. Brener, *Phased-array sources based on nonlinear metamaterial nanocavities*, Nature Communications **6**, 7667 (2015).

Project Title: **Novel Temperature Limited Tunneling Spectroscopy of Quantum Hall Systems**

Principal Investigator (PI): **Raymond Ashoori**

Mailing Address: Dept. of Physics, Room 13-2053, Massachusetts Institute of Technology, Cambridge, MA 02139

Program Scope

Spectroscopic methods involving injection or ejection of electrons in materials have unique power in probing the electronic structure and interactions between electrons. The "single particle" spectrum obtained from techniques such as photoemission or tunneling spectroscopy is among the most fundamental quantities in theories of highly interacting systems, answering the question, "at which energies can electrons be added to (or removed from) the system?" For example, in ordinary superconductors, comparison of features in this spectrum with theory proved to be one of the primary experimental signatures validating the BCS theory of superconductivity.

In a number of scientifically exciting and technologically important electronic systems, it has proven very difficult to achieve accurate quantitative determination of this single-particle spectrum. Among these is the two-dimensional (2D) electron system in semiconductors, host to the remarkable quantum Hall effects. This system continues to produce fascinating results as scientists discover new ways in which electrons that strongly repel one another correlate their motions to minimize the energy of this repulsion. Stunningly, these correlations give rise to "quasi-particles" that have a charge that is a fraction of that of the constituent electrons in the system. Another electronic system of great scientific and technological interest is graphene. The motion of electrons in this material is governed by the Dirac equation rather than the Schrödinger equation, leading to remarkable new electrical properties that may enable ultrahigh frequency transistors and novel electronic devices. A means of spectroscopy that injects single electrons can reveal how a newly added electron is incorporated in the dance that produces novel electronic properties in these systems.

This work aims to study the behavior of electrons in high magnetic fields both in semiconductors and graphene using of a fundamentally new spectroscopic technique, time domain capacitance spectroscopy (TDCS). TDCS injects or ejects electrons from the system of interest by means of inducing electron tunneling from hundreds of thousands of small electrical pulses. It measures the single-particle spectrum of the 2D electron system with negligible electron heating, even when the in-plane conductivity of the system vanishes.

This work applies TDCS to a number of quantum Hall systems and develops a new charge detection scheme for TDCS using single electron transistors. This new method can provide high-resolution spectra of small graphene samples in the quantum Hall regime and in the recently observed "Hofstadter Butterfly". TDCS will also be used to study the very low temperature behavior of the semiconductor two-dimensional electron systems in high magnetic fields in the regime of the fractional quantum Hall effect. This will allow study of "charge stripe" and "bubble phases" and the 5/2 fractional quantum Hall state as well as probing "Wigner Crystal" state of the 2D-hole system. TDCS will also be used to monitor single electron additions to quantum dots for a direct measurement of the thermodynamics of the 5/2-state. Finally, TDCS

detection will be adapted and used to search for Josephson plasma oscillations in quantum Hall bilayers.

Recent Progress – Observation of a Wigner Crystal with Long-Range Order

In the last year, we have discovered a new and extremely sharp tunneling feature that very likely reveals the formation of Wigner Crystal in the 2D electronic system. We have also come close to creating viable samples for studying Josephson plasma excitations in double-quantum-well samples thought to contain an excitonic superfluid. We have been working to measure single electron to very clean GaAs quantum dots, and we have built aluminum single electron transistors for measuring tunneling in graphene samples.

Observation of a Wigner Crystal in a 2D system using TDCS

We have discovered a clear signature of a Wigner crystal with long range correlation in hole-doped GaAs quantum well (QW) sample using TDCS. This discovery was facilitated by performing our TDCS measurements in a newly installed dilution refrigerator with base electron temperature of ~20 mK in high magnetic fields.

Theories predict that a Wigner crystal of quasiparticles exists near integer quantum Hall states as an insulating phase [1] with the expected transition temperature in the range of a few hundred millikelvin or below. This state of broken translational symmetry under a perpendicular magnetic field is expected to show exotic tunneling spectrum as one tunes the inter-particle spacing and magnetic field strength [2,3].

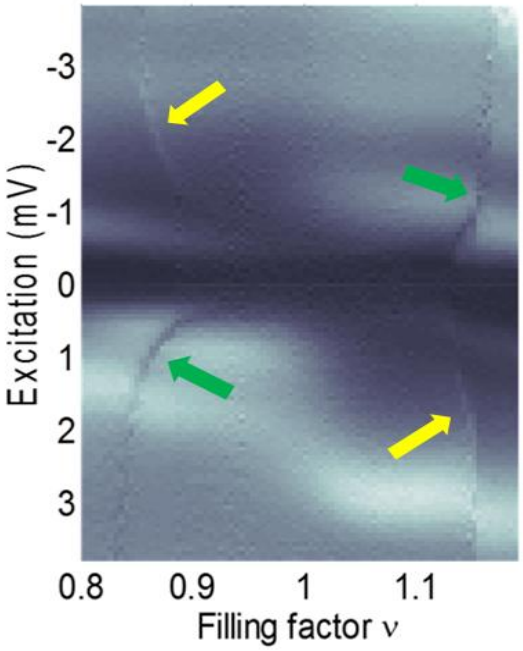

Fig.1 Tunneling density of states of hole doped GaAs quantum well at B=8 T and T=20 mK. Notice the antisymmetric structure of the resonances.

We have used Time Domain Capacitance Spectroscopy (TDCS) to measure the tunneling density of states (TDOS) of a hole-doped 2D QW under high perpendicular magnetic fields at low temperature. The measurement at 8 Tesla and 20 mK showed very sharp resonances (see Fig. 1), whose FWHM is as small as 0.3 meV, located anti-symmetrically around Fermi energy and filling factor $\nu = 1$ of quantum Hall state. This feature is strongly carrier (hole) filling factor dependent, which signifies the origin of the feature as carrier-carrier interaction. The similar anti-symmetric (odd-parity in energy) resonances in TDOS around Fermi energy were previously reported [4] and extensively studied in planar tunneling junctions between normal metal and semiconductor; the electron-phonon (or more generally electron-boson) interaction is known to influence the tunneling process and gives the anti-symmetric features. However, the emergence of the corresponding feature in TDOS in our hole-doped sample under quantum Hall regime is rather surprising because the charged carriers

in this system are "effectively" decoupled with lattice dynamics; no strong DOS of an ionic phonon exists in the scale of the cyclotron energy (a few meV or less). More importantly, the strong filling factor dependence of the resonance feature obviously rules out the case for the interaction with ionic phonons.

Instead, we propose an interaction with the magneto-phonon of a magnetic-field-induced Wigner crystal formed by quantum Hall quasiparticles near integer filling factors, responsible for the electron-boson coupling modifying TDOS. Near the Brillouin zone boundary, the magneto-phonon dispersion displays van Hove singularities making the phonon DOS peaked accordingly; this leads to the resonance in TDOS at the corresponding excitation energies. As the filling factor deviates from $\nu = 1$, the system is populated with quasiparticles, thus shortening the inter-particle distance of the quasiparticle crystal. As a result, the phonon mode stiffens and the energy of the van Hove singularity would increase, resulting as shown in Fig. 1. It is important to note that the tunneling spectrum is the reflection of the dynamics between two kinds of quasiparticles: localized ones forming the crystal and mobile ones located mainly at interstitial sites.

In order to further investigate the nature of the resonance, we also studied the temperature dependence. As temperature is increased from base temperature of 20 mK in a step of ~50 mK, the resonances seems to disappear almost completely above 250 mK (Fig. 2). This observation is consistent with the thermal melting of the Wigner crystal of quasiparticles, and the resulting disappearance magneto-phonons [5]. Interestingly, in this picture, the increase of the density of quasiparticles, by changing the filling factor away from $\nu = 1$, also drives the crystal into the quantum mechanical melting transition. The filling factor needed to melt the crystal is $|\nu - 1| \sim 0.15$, which is in qualitative agreement with the expected values for Wigner crystal melting under quantum Hall regime [5].

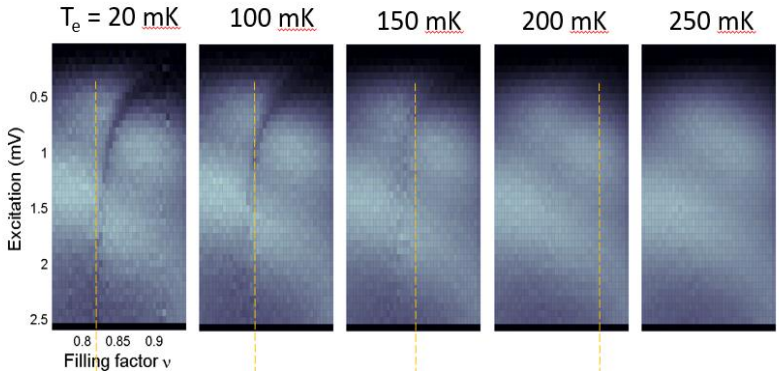

Fig 2. Temperature dependence of the resonance feature. The vertical dotted line (yellow) is a guide to the eye for disappearance of the feature.

The sharpness of the resonance attests to the long-range correlation in the Wigner Crystal. A rough calculation, considering the energy of the resonance and the width of the resonance indicates that the crystal is ordered over a length scale of at least 10 lattice spacings. Finally, we have also observed features from Wigner Crystals at low filling factors and at filling factor 2. We have also seen that electron samples do not display the feature near filling factor ν=1 unless we apply a strong in-plane field. This suggests that there is a competition with Skyrmions that form in the electron system. The in-plane field increases the spin-splitting and disfavors Skyrmion formation.

References

[1] D. Levesque, J. J. Weis, and A. H. MacDonald, "Crystallization of the incompressible quantum-fluid state of a two-dimensional electron gas in a strong magnetic field," *Phys. Rev. B*, vol. 30, no. 2, pp. 1056–1058, Jul. 1984.

[2] D. R. Hofstadter, "Energy levels and wave functions of Bloch electrons in rational and irrational magnetic fields," *Phys. Rev. B*, vol. 14, no. 6, pp. 2239–2249, Sep. 1976.

[3] H. A. Fertig, "Properties of the Electron Solid," in *Perspectives in Quantum Hall Effects*, S. D. Sarma and A. Pinczuk, Eds. Wiley-VCH Verlag GmbH, 1996, pp. 71–108.

[4] L. C. Davis and C. B. Duke, "Analysis of the Tunneling Measurement of Electronic Self-Energies Due to Interactions of Electrons and Holes with Optical Phonons in Semiconductors," *Phys. Rev.*, vol. 184, no. 3, pp. 764–779, Aug. 1969.

[5] Y. P. Chen, G. Sambandamurthy, Z. H. Wang, R. M. Lewis, L. W. Engel, D. C. Tsui, P. D. Ye, L. N. Pfeiffer, and K. W. West, "Melting of a 2D quantum electron solid in high magnetic field," *Nat Phys*, vol. 2, no. 7, pp. 452–455, Jul. 2006.

Publications acknowledging DOE support:

1. S. L. Tomarken, A. F. Young, S. W. Lee, R. G. Gordon, and R. C. Ashoori, "Torque magnetometry of an amorphous-alumina/strontium-titanate interface" Phys. Rev. B 90, 201113(R – Rapid Communications) – Published 24 November 2014

2. A.F. Young, J.D. Sanchez-Yamagishi, B. Hunt, S.H. Choi, K. Watanabe, T. Taniguchi, R.C. Ashoori, and P. Jarillo-Herrero "Tunable Symmetry Breaking and Helical Edge Transport in a Graphene Quantum Spin Hall State", Nature Vol. 505, Pages: 528-532, JAN 23, 2014

3. B. Hunt, J.D. Sanchez-Yamagishi, A.F. Young, M. Yankowitz, B.J. LeRoy, K. Watanabe, T. Taniguchi, P. Moon, M. Koshino, P. Jarillo-Herrero, R.C. Ashoori "Massive Dirac Fermions and Hofstadter Butterfly in a van der Waals Heterostructure" SCIENCE Volume: 340 Issue: 6139 Pages: 1427-1430 Published: JUN 21 2013

Session VI

Program Title: Electronic Control of Magnetic Switching in Extremely Small Ferromagnets

Principle Investigator: Dragomir Davidovic
Mailing Address: School of Physics, Georgia Institute of Technology
837 State Street, Atlanta, GA 30332
E-mail: dragomir.davidovic@physics.gatech.edu

Program Scope

The project goal is to study how the magnetization of a nanomagnet can be electronically manipulated in the limit of a very small nanomagnet volume. In recent years, the miniaturization of magnets has led to an increased interest into the properties of extremely small ferromagnets, such as nm-scale magnetic particles and magnetic molecules. While there are many measurement techniques for determining the magnetic state of such magnets, electron transport through single magnets is particularly important for integrating the magnets into a microelectronic system. The reduced dimensions of molecules pose both challenges and advantages. A primary challenge is due to the fact that the energy barrier for magnetic switching (E_B) is suppressed in proportion with the volume of the nanomagnet, which weakens the directional stability of the magnetization due to thermal or electronic perturbations. However, the weakened barrier could also be viewed as an advantage if the external perturbations are properly controlled to manipulate magnetic switching. As an example, consider spin-transfer torque (STT) switching in a nanomagnet, which is normally a current-driven effect. The critical current for magnetization switching due to STT is proportional to E_B [1-3]. In larger magnets E_B is large and the resulting critical current can be associated with large power dissipation, which is a well known issue for applications. By reducing the size to the molecular scale, E_B is significantly reduced, leading to the possibility of a much lower critical current. The challenge that we are addressing is to understand if STT can be controlled in such limit, and if so, how such manipulation can be used to make a device.

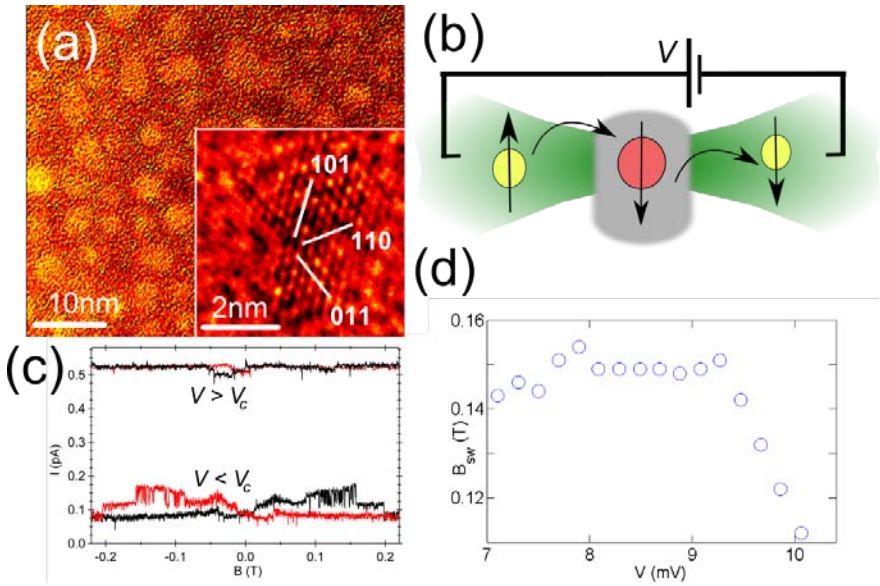

Figure 1 – (a) Transmission Electron Micrograph of Ni particles used in our samples. Crystal facets visible in inset. (b) Illustration of double-tunnel junction geometry in our experiments. (c) Current hysteresis curves as a function of applied magnetic field in the low bias ($V < V_c$) and high bias ($V > V_c$) regimes, where V_c is the critical voltage for magnetic switching. Red (black) corresponds to field sweep in negative (positive) directions. (d) Data of magnetic switching field as a function of bias voltage in a representative Ni sample.

Recent Progress

Discovery of Magnetization Blockade. We discuss the breakdown of magnetic hysteresis in nanomagnets due to voltage-bias, as opposed to the familiar case of current-bias. In particular, we investigate magnetic properties of individual nanometer scale Ni particles of diameter ~2nm, examples are shown in Fig. 1A. Fig. 1B displays a schematic of the device that we measure, showing such a single Ni particle in weak tunnel contact with two leads. At this time, the leads are normal metals (Al). Prior experimental work was done using Co particles, which showed robust magnetic hysteresis in tunneling current versus applied magnetic field. By contrast, we find that the Ni particles have especially fragile magnetic hysteresis; in fact, we find many Ni particles do not display any hysteresis at all, regardless of the voltage bias or temperature. Our main finding is that in those Ni particles that do exhibit magnetic hysteresis at milli-Kelvin temperature, that hysteresis is fragile and can be tuned out by the bias voltage. As shown in Fig. 1C, sample 1 has clear hysteresis at low voltage, and vanishing hysteresis in current vs magnetic field at higher voltage. Fig. 1D displays the corresponding magnetic switching field versus bias voltage. We find that the suppression of the magnetic hysteresis is not a heating effect [4]. Rather, the hysteresis suppression demonstrates an example of a voltage-biased magnetization control; this phenomenon is fundamentally different from more familiar current-driven magnetization dynamics in STT-physics.

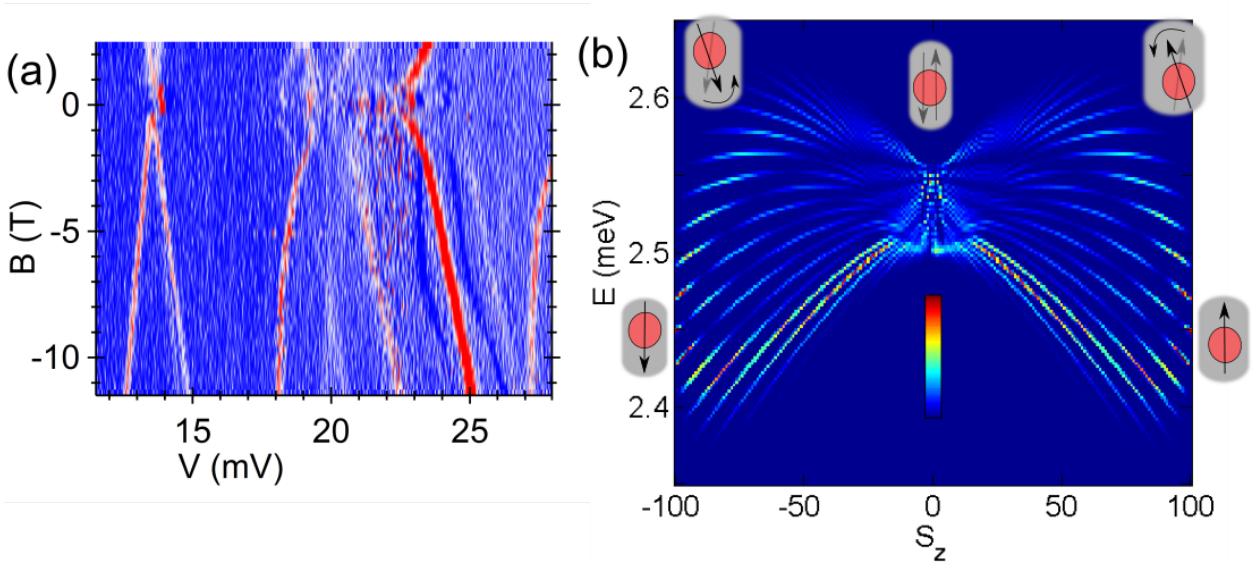

Figure 2—(a) Differential conductance tunneling spectra of a Ni sample exhibiting Zeeman splitting and level curvature. The color scale ranges from blue to white to red as the differential conductance varies from 0 to 0.5 nS. (b) Simulated tunneling Density of States (DOS). The inset color scale indicates a range from blue to red as the DOS varies from a minimum to a maximum value. The regions of stability are illustrated by the red magnetic particles, with a magnetization in the direction indicated by the arrows. At low bias values, the particle magnetization will remain localized near the positions $M_{\downarrow}$ or $M_{\uparrow}$. However, if the bias is raised past 2.58 meV, the magnetization direction can be changed using bias voltage.

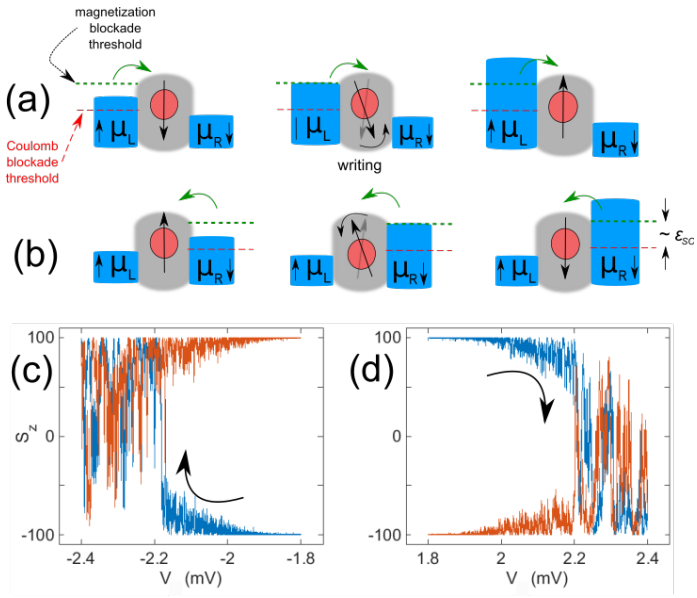

Figure 2— Writing the magnetic state with spin-polarized leads. (a) Illustration of the variation of the electrochemical potential of the left lead (μ_L) for the forward writing process ($M_\downarrow \rightarrow M_\uparrow$), implying a negative *V*. Long red dashed line is the threshold for sequential electron tunneling. When the writing threshold (smaller green dotted line) is reached, the particle magnetization flips directions. (b) Illustration of reverse state writing process ($M_\uparrow \rightarrow M_\downarrow$). Green arrows indicate electron tunneling direction. (c) Simulation of magnetization vs voltage during forward magnetic state writing process illustrated in (a). (d) Magnetization vs voltage for reverse magnetic state writing process as illustrated in (b). In both (c) and (d), blue (orange) correspond to magnetization during positive (negative) magnitude ramp of bias.

Voltage bias driven magnetization dynamics arises from the effect that we named magnetization blockade. The crucial role is played by the spin-orbit energy shifts of the discrete energy levels of the particle, which vary with the direction of the magnetization. Magnetization blockade arises from electron tunneling transitions with energies that increase as the particle magnetization is displaced from the easy axis. The origin of magnetization blockade can be precisely related to the energy spectra of magnetic Hamiltonians in the presence of spin-orbit shifts. Fig. 2A displays the measured tunneling spectrum of a typical Ni sample, showing discrete levels in conductance vs voltage, lack of hysteresis, and Zeeman splitting that indicates the ergodic nature of the particle magnetization. Fig. 2B displays a simulated butterfly-shaped tunneling density of states for the magnetic transitions, indicating the regions of stability and instability of the magnetization. The relationship between the spectra in Fig. 2 and the magnetic hysteresis will be discussed in the talk.

Future Plans

In future work, we plan to observe and study voltage-biased STT effects in nanomagnets. The schematic of the proposed device is in Fig. 1B. For the leads we will use ferromagnets, and the soft magnetic layer in the middle will be either a Ni nanoparticle or a magnetic molecule. Figure 3A illustrates the expected Coulomb blockade threshold and the magnetization blockade threshold of this device. When the electrochemical potential of the lead is raised above the first blockade, sequential electron transport is initiated as indicated by the curved green arrows, and the magnetization direction will be measured noninvasively from the magnetoresistance. When the electrochemical potential is increased above the magnetization blockade threshold, the spin-polarized leads initiate the particle magnetization state writing process. When the electrochemical potential in the right lead reaches the reverse writing threshold, the magnetization of the particle will flip into the $M_\downarrow$ state. Fig. 3C and D displays the simulated forward and reverse writing process of the states $M_\uparrow$ and $M_\downarrow$, respectively, which are governed by the sign of the applied bias voltage.

The relevance of the future work: in the proposed device, the control of magnetization dynamics is bias-voltage driven, which is a fundamentally different effect from that in conventional, current-driven spin-transfer torque devices. The work presents a possibility to significantly decrease power dissipation in spin-transfer torque switching in magnetic particles.

References

1. Berger, L., *Emission of spin waves by a magnetic multilayer traversed by a current.* Physical Review B, 1996. **54**(13): p. 9353.
2. Slonczewski, J.C., *Current-driven excitation of magnetic multilayers.* Journal of Magnetism and Magnetic Materials, 1996. **159**(1): p. L1-L7.
3. Ralph, D. and M.D. Stiles, *Spin transfer torques.* Journal of Magnetism and Magnetic Materials, 2008. **320**(7): p. 1190-1216.
4. Gartland, P., W. Jiang, and D. Davidović, *Voltage control of magnetic hysteresis in a nickel nanoparticle.* Physical Review B, 2015. **91**(23): p. 235408.

Publications (which acknowledge DOE support)

- P. Gartland and D. Davidovic. Voltage-Driven Spin-Transfer Torque in a Magnetic Particle. *Applied Physics Letters*. (currently under review)
- D. Deniz, P. Gartland , and D. Davidovic. Emerging Magnetic Effects of Au Break Junctions with Embedded Ni Nanoparticles. *J Nanosci Adv Tech*, 1.2 (2015).
- P. Gartland, W. Jiang, and D. Davidovic. Voltage control of magnetic hysteresis in a nickel nanoparticle. *Phys. Rev. B*, ***91***, *235408* (2015)
- P. Gartland, F. T. Birk, W. Jiang, and D. Davidovic. Giant electron-spin g factors in a ferromagnetic nanoparticle. *Phys. Rev. B*, **88**, 075303 (2013)
- W. Jiang, P. Gartland, and D. Davidovic. Size-dependence of magneto-electronic coupling in Co nanoparticles. *J. Appl. Phys*., **113**, 223703 (2013)
- W. Jiang, F. T. Birk, and D. Davidovic. Effects of confinement and electron transport on magnetic switching in single Co nanoparticles. *Sci. Rep*., **3**:1200 (2013)

Program Title: Controlling Superconductivity via Tunable Nanostructure Arrays

Principle Investigator: Nadya Mason; Co-PIs: Raffi Budakian, Taylor Hughes
Mailing Address: Department of Physics, University of Illinois at Urbana-Champaign, Urbana IL 61801
Email: nadya@illinois.edu

Program Scope:

The goal of this program is to use proximity-coupled nanostructure arrays to understand and control how collective behavior emerges in superconducting systems. The outcome of this research will be the discovery and characterization of exotic phases in superconducting systems, a better understanding of how microscopic parameters lead to macroscopic behavior in key materials systems, and an improved ability to control interactions to manipulate the electronic properties of superconductors.

The program is based on the idea that superconducting islands placed on a thin conductor at a separation smaller than the normal metal coherence length can support a finite Josephson coupling between the islands, where the strength of the coupling depends on the length and conductance of the intervening material. By adjusting the size, configuration, and type of islands, the correlated states, as well as the competition between them, can be precisely tuned. This allows for the clear determination of how superconductors' critical properties can be enhanced or diminished. We also aim to determine how controlling these parameters can lead to novel phase regimes, such as pseudogap-like phases, 2D metallic states and FFLO phases.

In previous, DOE-supported work, we demonstrated that the array systems behave as 2D superconductors, and showed how junction length controlled the transition [1]. More significantly, our measurements of these samples [2] provided evidence of the long sought-after 2D metallic state [3] as a function of well-understood parameters (e.g., island spacing, a parameter of dissipative coupling). In more recent measurements of superconducting transitions in individual, granular, mesoscopic Nb islands, we observed an anomalous suppression of the superconducting transition temperature T_c at large island diameters (compared to the coherence length), which we can explain as a rare region effect, where superconducting order first appears in unusually large grains [4].

Further, we have recently used the clear vortex signatures in the array system to determine the effects of interactions and dissipation on vortex dynamics. In a joint theoretical and experimental study, we have used the current-driven voltage response to demonstrate interactions in the vortex flux creep regime as well as the importance of time-correlated dissipative forces in the transition to vortex flux-flow [5]. The transport and theoretical studies are complemented by new magnetic force microscopy (MFM) techniques that enable the imaging of both individual and collective vortex *dynamics* at high resolution. MFM images of vortex dynamics in Nb island arrays under various magnetic field and island configurations are compared to transport results for similar samples, and analyzed using numerical simulations of interacting vortices.

The research combines temperature- and field-dependent transport measurements with magnetic resonance force microscopy measurements of local vortex spatial structure and surface currents, as well as accurate phenomenological modeling, to provide complete characterization of the collective behavior of the samples.

Recent Progress: Unusual dynamics and dissipation in vortex transport

Vortices play a central role in determining the properties of superconducting thin films and Josephson junction arrays, yet many aspects of vortex transport and dynamics are still unknown. We have performed joint theoretical and experimental studies of arrays of Nb islands on Au, having an applied perpendicular magnetic field which induces flux lines penetrating as vortices. In these systems, we were able to understand an unusually wide range of vortex-dominated transport behavior, and demonstrate the unusual influence of dissipation on the system.

The motion of vortices is a source of dissipation in superconductors, and the amount of this dissipation can vary in complex ways depending on the properties of the superconductor. Island array systems in the current experiments offer exceptional tunability for the systematic study of vortex motion. For example, they enable the exploration of the role of diffusive transport in the metallic substrate, which can be enhanced by varying the distance between the islands. In our experiments, the current-driven voltage response is used to map the vortex evolution of the system from pinned to vortex creep to flux flow. Figure 1a shows a schematic of the vortex transport regimes, while Figure 1b shows experimental results of vortex de-pinning to flux flow. Unusual physics is observed, particularly a significant deviation from predicted linear drag behavior in the flux flow regime, leading to the absence of a differential resistance peak near the de-pinning transition.

To explain this behavior, we proposed a phenomenological model that describes the dissipative behavior of this system at low vortex densities, and also medium vortex densities where vortex-vortex interactions become important. We determined that modeling the vortex dynamics requires unexpected sources of dissipation that have not been discussed before in the literature. We successfully modeled these sources of dissipation as time-delayed forces that act on the vortices as they propagate throughout the system. The numerical simulations, including these new time-delayed forces, qualitatively reproduce the voltage characteristics obtained in the experiments, as can be seen in Figure 1c. In addition to this, we provided a theoretical understanding of the behavior of the critical current of this system when the vortex density is finite, finding that diffusive transport can suppress significantly the sensitivity of the critical current to variations in the vortex density.

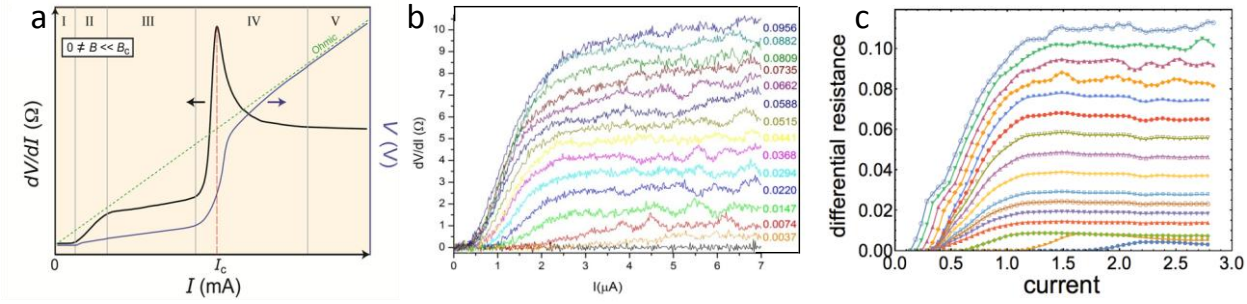

Figure 1: Current-induced vortex de-pinning (**a**) Schematic of the array transition from pinned vortices in region I to freely flowing vortices in III. Above a critical junction current, I_c, the array exhibits Ohmic behavior. (**b**) Differential resistance *dV/dI* for an array of 390-nm spaced islands under a current bias for *I* in different, weak magnetic fields. Measurements correspond to regions I,II,III in (a). The data was taken at T = 17 mK; adjacent numbers indicate the frustration Φ/Φ_o associated with each curve. (**c**) Simulations of differential resistance obtained from numerically solving the generalized Langevin equation, and including delayed dissipation effects. The units of each axis are arbitrary.

While it is useful to infer vortex dynamics from collective behavior in transport, an even better understanding can be gained by directly imaging individual vortices. Thus, we developed a magnetic force microscopy (MFM) method for high resolution imaging of the vortex *dynamics* in the Nb-island arrays. This new technique enables the unprecedented ability to model both individual and collective vortex dynamics at high resolution.

For this technique, a micron-size SmCo magnetic particle is attached to the tip of a cantilever and scanned several hundred nanometers over the surface of the array. At particular positions of the tip, the energy barrier separating certain vortex configurations is reduced, so that thermal fluctuations can cause the system to rapidly switch between degenerate vortex configurations. The fluctuating surface currents surrounding the vortex cores interacts with the magnetic moment on the cantilever, and lowers the cantilever frequency. Figure 2 shows images of the cantilever frequency as a function of position over the array. The darker contours in each image represent regions of lower cantilever frequency, and define locations where the energy of two or more vortex configurations becomes nearly degenerate. By changing the field profile under the tip, either by varying the tip-surface separation or by adding a uniform external magnetic field, different symmetries emerge.

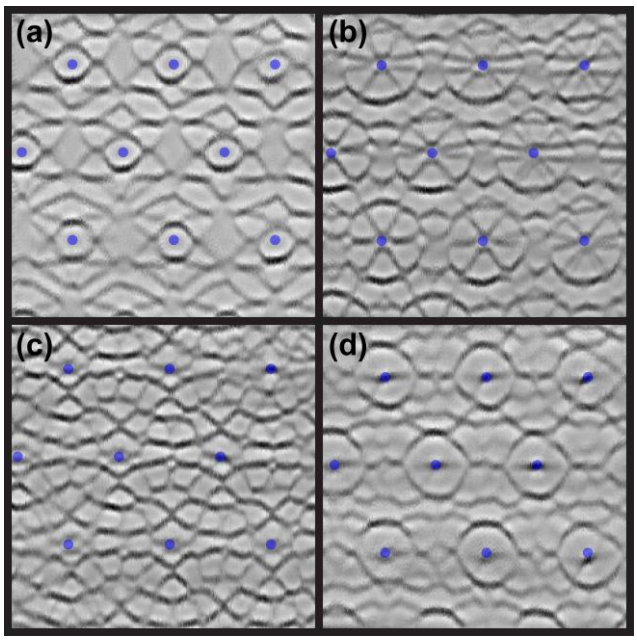

Figure 2: Dynamic mode MFM images of Nb-island arrays patterned on gold. The Nb islands are 80-nm thick, 200-nm in diameter, and have a center-to-center spacing of 500 nm; the gold film is 10-nm thick. The blue dots in the images indicate the center location of each island. The images were taken at 3.7 K at a tip-surface separation of 245 nm. In each of the four images, a uniform external field was applied in the opposite direction to the tip field. The following external fields were used: (a) 224 Oe, (b) 239 Oe, (c) 259 Oe, (d) 274 Oe.

We are working closely together to model the underlying vortex configurations that give rise to the observed images. We are currently running numerical simulations of interacting vortices, to attempt to reproduce the experimental measurements. Through the insights gained from the theoretical modeling of the data, we hope to understand the energy, stability, and dynamics of different vortex configurations.

Future Plans

Our future plans for this project include:

1. Integrated experimental design and theoretical framework for analyzing the MFM imaging of vortex dynamics, and determining novel physics. Complete manuscript on initial results.

2. Integrated theoretical, transport, and imaging techniques to study arrays of superconducting and magnetic islands on graphene and topological insulators, for exploring unconventional

superconducting states. Initial experiments will focus on the systematic effects of disorder for islands on graphene, to gain insight into disorder-driven phase transitions.

References

1. S. Eley, S. Gopalakrishnan, P.M. Goldbart, and N. Mason, "Dependence of global superconductivity on inter-island coupling in arrays of long SNS junctions," *J. Phys.: Condens. Matter* **25**, 445701 (2013).
2. S. Eley, S. Gopalakrishnan, P.M. Goldbart, and N. Mason "Approaching zero-temperature metallic states in mesoscopic superconductor-normal-superconductor arrays," *Nature Physics*, **8**, 59 (2012).
3. B. Spivak et al, "Theory of quantum metal to superconductor transitions in highly conducting systems," *Phys. Rev. B* **77**, 214523 (2008).
4. M. Durkin, S. Gopalakrishnan, R. Garrido-Menacho, R. Mansbach, J. Zuo, N. Mason, "Rare-region establishment of superconductivity in mesoscopic, disordered systems," manuscript in preparation.
5. M. Durkin, I.M. Shem, S. Eley, T.L. Hughes, N. Mason, "Dissipative vortex dynamics in two-dimensional superconductors," manuscript in preparation.

Manuscripts from 2014-2015 which acknowledge DOE support

- M. Durkin, S. Gopalakrishnan, R. Garrido-Menacho, R. Mansbach, J. Zuo, **N. Mason**, "Rare-region establishment of superconductivity in mesoscopic, disordered systems," manuscript in preparation.
- M. Durkin, I.M. Shem, S. Eley, **T.L. Hughes**, **N. Mason**, "Dissipative vortex dynamics in two-dimensional superconductors," manuscript in preparation.
- A. Kogar, S. Vig, A. Thaler, M.H. Wong, Y. Xiao, D. Reigi-Plessis, G.Y. Cho, T. Valla, Z. Pan, J. Schneeloch, R. Zhong, G. Gu, **T.L. Hughes**, G.J. MacDougall,T.-C. Chiang, P. Abbamonte, "Surface collective modes in the topological insulators Bi_2Se_3 and $Bi_{0.5}Sb_{1.5}Te_{3-x}Se_x$," arXiv:1505.03784 (2015).

Probing Correlated Superconductors and their Phase Transitions on the Nanometer Scale

Ali Yazdani
Department of Physics
Princeton University, Princeton, NJ 08544
Grant #: DE-FG02-07ER46419
Program Monitors: Dr. Michael Pechan and Dr. Jane Zhu
Reporting Period: May 2014-May 2015

Program Scope:

Our experimental program provides an atomic scale perspective of unconventional superconductivity — how it evolves from an unconventional conducting state and how it competes with other forms of order in correlated electronic systems. Such phenomena are at the heart of some of the most debated issues in condensed matter physics. Understanding these phenomena is an intellectual driver for many of the DOE-BES projects for the development of novel materials, including the search for higher temperature superconductivity. Our aim is to provide a microscopic view of these exotic materials and their phase transitions into the superconducting state using some of the most sophisticated scanning tunneling microscopy (STM) and spectroscopy techniques. The results of the experiments proposed here will provide important evidence that will help constrain theoretical models of unconventional superconductivity, the normal states from which it emerges from, and electronic states with which it competes.

Our program is divided into three parts. The first part is focused on examining how heavy electron states emerge in compounds in which localized *f* orbitals interact with more itinerate electronic states and the process by which such heavy electronic states give rise to unconventional superconductivity. Although heavy fermions do not superconduct at very high temperatures, their transition temperature is a substantial fraction of the heavy electron state bandwidth, hence making these materials among the most strongly correlated superconductors discovered to date. More importantly, the parallels between the puzzles in heavy fermions and high-*Tc* cuprates superconductors suggest that heavy fermions might provide important clues for a more general understanding of correlated electronic states and their superconductivity. For example, like cuprates or Fe-based superconductors, superconductivity in a heavy fermion system is often found in the vicinity of anti-ferromagnetism in the phase diagrams of these systems.

The second part of our program is focused on how charge ordering competes with superconductivity in high-*Tc* cuprates. One of the key questions is to determine whether there is universality in the way charge ordering occurs in doped Mott insulators and to study the connection between different forms of charge ordering now observed in dissimilar cuprate families. Overall, the precise determination of charge ordering in Bi-based compounds as a function of temperature will be examined in our program, and contrasting the results of such studies with experiments on other cuprates will establish the universality of charge ordering in the cuprates.

The third part of this program is focused on the development of techniques for local Josephson tunneling with superconducting STM tips at millikelvin temperatures. Development of such techniques can provide important details about the nature of the superfluid response and phase of the superconducting order parameter on the nanoscale, with broad applicability for the study of superconductivity in a wide range of materials. The three components of the proposed program provide a broad attack on some of the most important problems in the physics of correlated materials and the emergence of superconductivity in these systems.

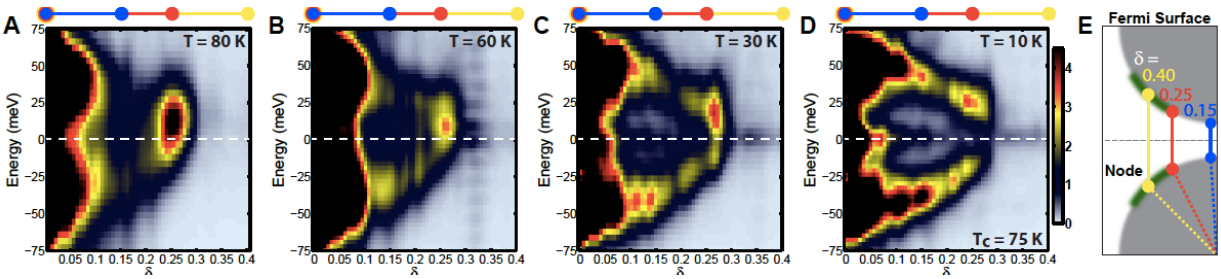

Figure 1. **(A-D)** Energy-momentum structure of the modulations seen in the STM along the Cu-O bond direction, extracted from line cuts along the (2π/a, 0) direction of the discrete Fourier transforms for an underdoped T_c =75 sample measured at selected temperatures. The data shows the opposite temperature dependence between the particle-hole symmetric BdG-QPI and the particle-hole asymmetric charge order. (**E**) Schematic layout of the Fermi surface in Bi-2212 UD75 sample. The green segment represents the Fermi arc as determined by ARPES above Tc. The vertical lines (also reproduced horizontally in **A-D**) correspond to QPI wavevectors connecting with the Fermi surface (consistent with ARPES, seen at different regions. From [1].

Highlights of breakthroughs under DOE grant in this funding cycle:

- Visualizing the formation of heavy fermions in a Kondo lattice (Nature 2012;Nature Physics 2013)
- Direct visualization of d-wave pairing in a heavy fermion superconductor (Nature Physics 2013)
- Demonstrating the ubiquity of charge ordering and its interplay with superconductivity in cuprates (Science 2014)
- Creating a nanoscale topological superconductor with Majorana fermion end modes (Science 2014) (partial support)

Recent Progress:

Ubiquitous Interplay Between Charge Ordering and High Temperature Superconductivity in Cuprates, Science 2014 and covered in Perspective [1]

During each of the past several years our group has achieved a major breakthrough in understanding the properties of high-Tc cuprates superconductors. This past year, our group had significant experimental results showing the ubiquity of charge ordering in cuprates and its competition with superconductivity. To put this work in context, we should first note that in 2004 (Vershinin et al. Science 2004), our group reported the first observation of a charge-ordering signal in the temperature range above T_c in underdoped Bi-based cuprates. In the interim years, we also established that this signal can be first detected at the onset of the pseudogap state at T* and has the strongest signal near 1/8 doping—similar to the stripe phase in La-based cuprates found in the late 1990s by Tranquada. During the last few years, resonant x-ray scattering has also been used to find charge ordering in Y-based cuprates and has shown that cooling the sample into the superconducting state weakens the charge ordering signal.

In a recent study of charge ordering that combined high-resolution, temperature dependent spectroscopic mapping provided by the STM with resonant elastic x-ray scattering (REXS) on the same sample, we have made several important findings. First, we established that the charge ordering observed with the STM is present at the same wavevector in the REXS measurements. Depending upon the doping, we find this wavevector to be the same as that of Y-based cuprates or La-based cuprates, thereby establishing a universality of charge ordering mechanism across all families of cuprates. Second, we found that both the STM and REXS signals confirmed that the charge ordering competes with superconductivity as it becomes weaker with decreasing temperature below Tc, where superconductivity becomes stronger. Third, using the energy resolution of the STM together with its ability to obtain information about the momentum of the quasi-particles using their interference, we established a

connection between the end of the arcs of the pseudogap in momentum space and the charge ordering wavevector (Figure 1). Finally, by demonstrating that charge ordering signatures in the STM measurements is particle-hole asymmetric, we have shown that it is likely caused by the organization of holes and is very much connected to Mott physics as opposed to a weak-coupling nesting mechanism.

New Technique: Josephson STM

Over the last year, we have developed the ability to perform Josephson tunneling between a superconducting tip and a superconducting sample on the atomic scale. This has been one of the long standing goals in the scanning probe and superconductivity community as the Josephson effect directly probes the strength of pairing interactions and its local measurement can be a valuable technique in the study of superconducting states in complex materials. For example, a number of novel superconducting states such as FFLO states proposed in the heavy fermion superconductors are expected to have spatially modulated pairing. Josephson STM techniques will have the unique capability to probe such modulations and prove the existence of such novel phases of matter.

The strength of Josephson coupling and associated supercurrent is a strong function of the size of the junction, which makes performing such measurements with the atomic scale junctions in STM particularly challenging. To achieve the conditions necessary to observe Josephson coupling (Figure 2), we have carried out such experiments in a dilution fridge at millikelvin temperatures. We have so far been able to perform such experiments using Pb tips on a Pb(110) single crystal surface. At these temperatures we have been able to obtain signatures of a Josephson supercurrent, which appears as a peak in the dI/dV curves of Figure 2a at zero bias, at an STM junction resistance of less than 1MΩ. Signals in this STM junction resistance range can be understood within a phase diffusive model of Josephson effect in small junctions, where thermal fluctuations still play a role and suppress the supercurrent from its ideal value. Regardless of non-ideal value of critical current, we have been able to map the strength of the Josephson current as a function of position on the surface of superconducting Pb on the atomic scale.

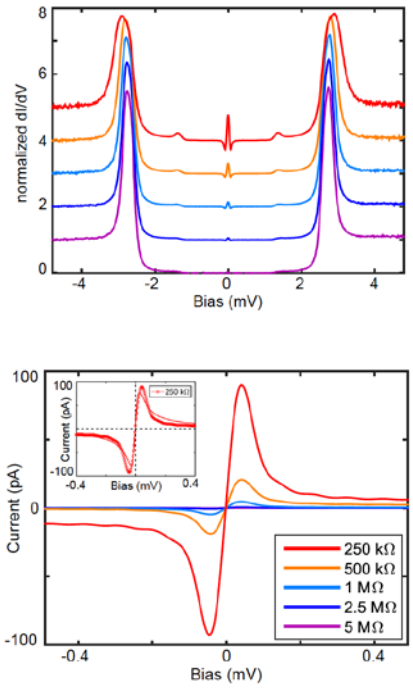

Figure 2. **(Top)** Tunneling conductance as a function of tip-sample resistance (values shown in the bottom inset). The peak at zero is an indication of the Josephson current when there is sufficient coupling between tip and sample at low junction resistance. **(Bottom)** The integrated current shows the size of Josephson super-current as a function of junction.

A first test of the capability of the Josephson STM to probe spatial variation of the superconducting order parameter on the atomic scale has been carried out by measuring the strength of the Josephson signal in the vicinity of individual magnetic impurities on the surface of Pb. It is well known that magnetic impurities locally suppress the superconducting order parameter on the atomic scale; however, evidence for such an effect has thus far been obtained indirectly through observation of impurity-induced bound states, so-called Shiba states, in local tunneling

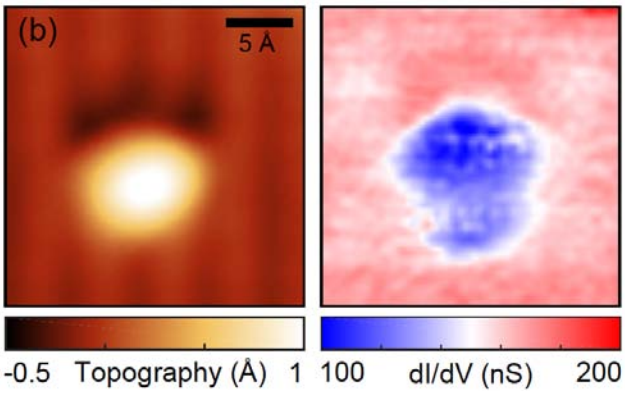

Figure 3. **(Left)** Topograph of a single magnetic defect (Fe) on the surface of Pb(110). (Right) is the strength of dI/dV single at zero energy which is direction related to the Josephson current.

density of states. As shown in Figure 3, a Josephson current between the superconducting Pb tip and Pb surface is locally suppressed on the atomic scale near individual magnetic impurities (Fe atoms deposited at low temperature on the Pb surface). The direct observation of this suppression and its recovery within a few angstroms away from the individual impurities on the Pb surface is indeed consistent with the theoretical expectation of spatial variation of the superconducting order parameter near individual magnetic impurities in BCS superconductors. We are currently working on a manuscript describing these finding that demonstrate the power of Josephson STM as a local probe of the pairing interactions on the atomic scale.

Future Plans:

We will continue to explore the physics of correlated superconductors through various experiments on heavy fermions and cuprates superconductors, with an emphasis on understanding the competition between superconductivity and other types of ordering phenomena that are possible in these systems. One area of focus will be to study the so-called Q-phase in the 115 compound in which anti-ferromagnetism (AFM) and superconductivity co-exist and there is the possibility that there is an FFLO state with pairing at a finite wavelength. Another focus will be study of superconductivity in URu_2Si2, which has an exotic superconducting phase emerging from the so-called hidden order phase. Finally, we plan to apply the Josephson STM technique described above to these exotic superconductors and probe situations in which pairing interaction is expected to vary spatially in correlated superconductors.

Publications Supported by the DOE-BES (2013-2014):

In addition to publications directly related to DOE-BES projects, the DOE funding that supports the instrumentation in our lab have assisted other projects. The publications from these projects benefiting from DOE support are also included in the list below (marked as partially supported by DOE).

1. E. H. da Silva Neto, P. Aynajian, A. Frano, R. Comin, E. Schierle, E. Weschke, A. Gyenis, J. Wen, J. Schneeloch, Z. Xu, S. Ono, G. Gu, M. Le Tacon, and A. Yazdani, "Ubiquitous Interplay between Charge Ordering and High-Temperature Superconductivity in Cuprates," Science, **343**, 393 (2014). (Also covered in Perspective). Fully supported by DOE.
2. A. Yazdani, E. H. da Silva Neto, and P. Aynajian, "Spectroscopic Imaging of Strongly Correlated Electronic States," Invited review for Annual Review of Condensed Matter Physics to appear 2015. Fully supported by DOE.
3. P. Aynajian, E. H. da Silva Neto, B. B. Zhou, S. Misra, R. E. Baumbach, Z. Fisk, J. Mydosh, J. D. Thompson, E. D. Bauer, and A. Yazdani, "Visualizing Heavy Fermion Formation and their Unconventional Superconductivity in *f*-Electron Materials," Journal of the Physical Society of Japan **83**, 061008 (2014), invited review paper. Fully supported by DOE.
4. I. K. Drozdov, A. Alexandradinata, S. Jeon, S. Nadj-Perge, H. Ji, R. J. Cava, B. A. Bernevig, and A. Yazdani, "One-dimensional topological edge states of bismuth bilayers," Nature Physics **10**, 664-669 (2014). Partial support by DOE.
5. S. Jeon, B. B. Zhou, A. Gyenis, B. E. Feldman, I. Kimchi, A. C. Potter, Q. D. Gibson, R. J. Cava, A. Vishwanath, A. Yazdani, "Landau quantization and quasiparticle interference in the three-dimensional Dirac semimetal Cd_3As_2," Nature Materials **13,** 851-856 (2014). Partial support by DOE.
6. S. Nadj-Perge, I. K. Drozdov, J. Li, H. Chen, S. Jeon, J. Seo, A. H. MacDonald, B. A. Bernevig, A. Yazdani, "Observation of Majorana fermions in ferromagnetic atomic chains on a superconductor," Science **346**, 6209 (2014). Partial support by DOE.

Novel sp2-Bonded Materials and Related Nanostructures

Alex Zettl (lead PI), Marvin Cohen, Michael Crommie, Alessandra Lanzara, Steven Louie, Feng Wang (to join FY 2016). Affiliations: Lawrence Berkeley National Laboratory, UC Berkeley

Program Scope

Ab-initio quantum mechanical calculations to predict new materials structures and relate them to electronic structure and mechanical and thermal properties. Experimental synthesis of novel sp2-bonded and MX2 materials including functionalized nanostructures, and characterization using SEM, TEM, STM, AFM, XRD, ARPES, mechanical properties, and transport. Nanoscale device fabrication and testing. Strong connection between theory and experiment.

Recent Progress

New high-volume method developed to produce BN nanotubes and nanoribbons; new architectures for nanostructured photovoltaic devices; mechanical properties of graphene examined at atomic scale using AFM and TEM; tunable phonon polaritons observed in sp^2-bonded hybrids; ARPES used to characterize charge screening in graphene; grain boundaries atomically characterized in graphene and hBN; ultra-clean edges of graphene nanoribbons produced and characterized, including switching between metastable states; 3D structure of individual nanocrystals in solution by TEM; electronic structure, spin orbit coupling and interlayer interaction in MoS_2, WS_2, and $MoSe_2$; topological valley transport at bilayer graphene domain walls; bandgap renormalization and excitonic effects studied in monolayer MX_2; graphene/hBN heterostructures studied for charge traps and artificial nuclei.

Future Plans

Study of C_{60} overlayers on graphene via transport, ARPES, and theory; STM of 2D quantum dots constructred from graphene/BN interfaces; metal filling of BN nanotubes; $NbSe_2$ monolayers studied via magnetotransport and STM; mechanical properties of suspended hBN and MX_2; continued valley transport in grain boundaries; stacking sequences in MoS_2 layers grown on hBN and other substrates studied via STM. Chemical activity of graphene and BN aerogels.

Publications

A. Gibb, N. Alem, and A. Zettl, "Low pressure chemical vapor deposition synthesis of hexagonal boron nitride on polycrystalline metal foils", *Physica Status Solidi B.* **250,** 12 pp2727-2731 (2013).
H.I. Rasool, C. Ophus, W.S. Klug, A. Zettl, and J.K. Gimzewski, "Measurement of the intrinsic strength of crystalline and polycrystalline graphene," *Nature Commun*. **4,** 2811 (2013).
K. Kim, S. Coh, C. Kisielowski, M.F. Crommie, S.G. Louie, M.L. Cohen, and A. Zettl, "Atomically perfect torn graphene edges and their reversible reconstruction," *Nature Commun*. **4**, 2723 (2013).

K. Liu, X. Hong, Q. Zhou, C. Jin, J. Li, W. Zhou, J. Liu, E. Wang, A. Zettl, and F. Wang, "High-throughput optical imaging and spectroscopy of individual carbon nanotubes in devices," *Nature Nanotech*. **8**, 917–922 (2013).
L.R. Comolli, C.E. Siegerist, S.H. Shin, C.R. Bertozzi, W. Regan, A. Zettl, and J. De Yoreo, "Conformational Transitions at an S-Layer Growing Boundary Resolved by Cryo-TEM," Angewandte Chemie-Int'l Ed., **52,** 18, pp4829-4832 (2013).
M.S. Chen, O.P. Lee, J.R. Niskala, A.T. Yiu, C.J. Tassone, K. Schmidt, P.M. Beaujuge, S.S. Onishi, M.F. Toney, A. Zettl, and J.M.J. Frechet, "Enhanced solid-state order and field-effect hole mobility through control of nanoscale polymer aggregation," *J. Am. Chem. Soc.* **135(51),** 19229–19236 (2013).
Q. Zhou, S. Coh, M.L. Cohen, S.G. Louie, and A. Zettl, "Imprint of transition metal d orbitals on a graphene Dirac cone," *Phys. Rev. B* **88**, 235431 (2013).
S. Coh, L.Z. Tan, S.G. Louie, and M.L. Cohen, "Theory of the Raman Spectrum of Rotated Double-layer Graphene," *Phys. Rev. B* **88**, 165431 (2013).
S.H. Shin, L.R. Comolli, R. Tscheliessnig, C. Wang, K.T. Nam, A. Hexemer, C.E. Siegerist, J.J. De Yoreo, and C.R. Bertozzi, "Self-Assembly of "S-Bilayers", a Step Toward Expanding the Dimensionality of S-Layer Assemblies," ACS Nano **7,** 6 pp 4946-4953 (2013).
X. Zhang, O.V. Yazyev, J. Feng, L. Xie, C. Tao, Y-C Chen, L. Jiao, Z. Pedramrazi, A. Zettl, S.G. Louie, H. Dai, and M.F. Crommie,"Experimentally Engineering the Edge Termination of Graphene Nanoribbons," ACS Nano **7**, 198 (2013).
Y. Wang, D. Wong, A.V. Shytov, V.W. Brar, S. Choi, Q. Wu, H-Z Tsai, W. Regan, A. Zettl, R.K. Kawakami, S.G. Louie, L.S. Levitov, and M.F. Crommie, "Observing Atomic Collapse Resonances in Artificial Nuclei on Graphene," Science **340**, 734 (2013).
Z. Fei, A.S. Rodin, W. Gannett, S. Dai, W. Regan, M. Wagner, M.K. Liu, A.S. McLeod, G. Dominguez, M. Thiemens, A.H. Castro Neto, F. Keilmann, A. Zettl, R. Hillenbrand, M.M. Fogler, and D.N. Basov, "Electronic and plasmonic phenomena at graphene grain boundaries," *Nature Nanotech*. **8**, 821-825 (2013).
A. Fathalizadeh, T. Pham, W. Mickelson, and A. Zettl, "Scaled Synthesis of Boron Nitride Nanotubes, Nanoribbons, and Nanococoons Using Direct Feedstock Injection into an Extended-Pressure, Inductively-Coupled Thermal Plasma," *Nano Lett.*, **14(8),** 4881-4886 (2014).
A. Sinitskii, K.J. Erickson, W. Lu, A.L. Gibb, C. Zhi, Y. Bando, D. Golberg, A.Zettl, and J.M. Tour, "High-Yield Synthesis of Boron Nitride Nanoribbons via Longitudinal Splitting of Boron Nitride Nanotubes by Potassium Vapor," *ACS Nano* **Online** (2014).
A.P. Goldstein, W. Mickelson, A. Machness, G. Lee, M.A. Worsley, L. Woo, and A. Zettl. Simultaneous Sheet Cross-Linking and Deoxygenation in the Graphene Oxide Sol-Gel Transition, Journ. Phys. Chem. C **2014,** 118 (49), pp 28855–28860, doi: 10.1021/jp5092027 (2014).
C. Hwang, D. Young Kim, D. A. Siegel, K. T. Chan, J. Noffsinger, A. V. Fedorov, M. L. Cohen, B. Johansson, J. B. Neaton, A. Lanzara. Ytterbium-driven strong enhancement of electron-phonon coupling in graphene. *Physical Review B* **90**, 115417 (2014).
D.N. Basov, M.M. Fogler, A. Lanzara, F. Wang, and Y.B. Zhang, "Colloquium: Graphene Spectroscopy," Rev. Modern Phys, **86,** 3, pp 959-994 (2014).
S. Dai, Z. Fei, Q. Ma, A. S. Rodin, M. Wagner, A. S. McLeod, M. K. Liu, W. Gannett, W. Regan, K. Watanabe, T. Taniguchi, M. Thiemens, G. Dominguez, A. H. Castro Neto, A. Zettl, F. Keilmann, P. Jarillo-Herrero, M. M. Fogler, and D. N. Basov, "Tunable phonon polaritons in atomically thin van der Waals crystals of boron nitride," *Science* **343**, 1125 (2014).
G. Samsonidze, F.J. Ribeiro, M.L. Cohen, and S.G. Louie, "Quasiparticle and Optical Properties of Polythiophene-derived Polymers," *Phys. Rev. B* **90**, 035123 (2014).
H.I. Rasool, C. Ophus, Z. Zhang, M.F. Crommie, B.I. Yakobson, and A. Zettl. Conserved atomic bonding sequences and strain organization of graphene grain boundaries. Nano Lett 14, 12, pp 7057-7063, doi: 10.2021/nl503450r (2014).

J-H. Chen, G. Autès, N. Alem, F. Gargiulo, A. Gautam, M. Linck, C. Kisielowski, O. V. Yazyev, S. G. Louie and A. Zettl, "Controlled growth of a line defect in graphene and implications for gate-tunable valley filtering," *Phys. Rev. B.* **89**, 121407 1-5 (2014).
J. Chang, Q. Zhou, and A. Zettl. Facile electron-beam lithography technique for irregular and fragile substrates. App. Physics Letters *105,* 17, 173109, doi: 10.1063/1.4900505 (2014).
K.H. Liu, C.H. Jin, X.P. Hong, J. Kim, A. Zettl, E.G. Wang, and F. Wang. Van der Waals-coupled electronic states in incommensurate double-walled carbon nanotubes. Nature Phys. 10 pp 737–742 doi: 10.1038/nphys3042 (2014).
K.H. Liu, L.M. Zhang, T. Cao, C.H. Jin, D. Qiu, Q. Zhou, A. Zettl, P.D. Yang, S. Louie, and F. Wang. Evolution of interlayer coupling in twisted molybdenum disulfide bilayers. Nat. Comm., **5** 4966 (2014).
L. Ju, J. Velasco Jr, E. Huang, S. Kahn, C. Nosiglia, Hsin-Zon Tsai, W. Yang, T. Taniguchi, K. Watanabe, Y. Zhang, G. Zhang, M. Crommie, A. Zettl & F. Wang, "Photoinduced doping in heterostructures of graphene and boron nitride," *Nature Nanotech.* **9**, 348–352 (2014).
M. M. Ugeda, A. J. Bradley, S.-F. Shi, F. H. da Jornada, Y. Zhang, D. Y. Qiu,W. Ruan, S.-K. Mo, Z. Hussain, Z.-X. Shen, F. Wang, S. G. Louie and M. F. Crommie, "Giant bandgap renormalization and excitonic effects in a monolayer transition metal dichalcogenide semiconductor," *Nature Materials* **Online** (2014).
M.A. Worsley, T.T. Pham, A.M. Yan, S.J. Shin, J.R.I. Lee, M. Bagge-Hansen, W. Mickelson, and A. Zettl. Synthesis and Characterization of Highly Crystalline Graphene Aerogels. ACS Nano, **8,** 10, pp 11013-11022 doi: 10.1021/22505335u (2014).
M.G. Menezes, R.B. Capaz, and S.G. Louie, "*Ab Initio* Quasiparticle Band Structure of ABA- and ABC-stacked Graphene Trilayers," *Phys. Rev. B* **89**, 035431 (2014).
O. Vazquez-Mena, J.P. Bosco, O. Ergen, H.I. Rasool, A. Fathalizadeh, M. Tosun, M. Crommie, A. Javey, H.A. Atwater, and A. Zettl, "Performance Enhancement of a Graphene-Zinc Phosphide Solar Cell Using the Electric Field-Effect," *Nano Lett.,* **14(8),** 4280-4285 (2014).
P. Bai, J. Kao, J.-H. Chen, W. Mickelson, A. Zettl, and T. Xu, "Nanostructures on graphene using supramolecule and supramolecular nanocomposites," *Nanoscale* **6**, 4503-4507 (2014).
S.-F. Shi, T.-T. Tang, B. Zeng, L. Ju, Q. Zhou, A. Zettl, and F. Wang, "Controlling Graphene Ultrafast Hot Carrier Response from Metal-like to Semiconductor-like by Electrostatic Gating," *Nano Lett.* **14(3),** 1578–1582 (2014).
S.-W. Nam, I.Choi, C.-C. Fu, K. Kim, S.-G. Hong, Y. Choi, A. Zettl, and L.P. Lee, "Graphene Nanopore with a Self-Integrated Optical Antenna," *Nano Lett.* **Article ASAP**, (2014).
Y. Sun, K. Liu, X. Hong, M. Chen, J. Kim, S. Shi, J. Wu, A. Zettl, and F. Wang, "Probing Local Strain at MX_2-Metal Boundaries with Surface Plasmon-Enhanced Raman Scattering," *Nano Lett*. **14(9),** 5329-5334 (2014).
Y. Yamada, K. Murota, R. Fujita, J.Kim, A. Watanabe, M. Nakamura, S. Sato, K. Hata, P. Ercius, J. Ciston, C.-Y. Song, K. Kim, W. Regan, W. Gannett, and A. Zettl, "Subnanometer vacancy defects introduced on graphene by oxygen gas," *J Am Chem Soc* **136(6)**, 2232-2235 (2014).
S.F. Shi, B. Zeng, H.L. Han, X. Hong, H.Z. Tsai, H.S. Jung, A. Zettl, M.F. Crommie, and F. Wang. Optimizing Broadband Terahertz Modulation with Hybrid Graphene/ Metasurface Structures. Nano Letters. 15, 1, pp 372-377. doi: 10.1021/nl503670d (2015).
A. J. Bradley, M. M. Ugeda, F. H. da Jornada, D. Y. Qiu, W. Ruan, Y. Zhang, S. Wickenburg, A. Riss, J. Lu, S.-K. Mo, Z. Hussain, Z.-X. Shen, S. G. Louie, and M. F. Crommie, "Probing the Role of Interlayer Coupling and Coulomb Interactions on Electronic Structure in Few-Layer $MoSe_2$ Nanostructures", *Nano Letters* **15**, 2594 (2015).
D. Wong, J. Velasco, Jr., L. Ju, J. Lee, S. Kahn, H.-Z. Tsai, C. Germany, T. Taniguchi, K. Watanabe, A. Zettl, F. Wang, and M. Crommie. Characterization and manipulation of individual defects in hexagonal boron nitride using scanning tunnelling microscopy. Nat. Nanotech. Doi: 10.1038/nnano.2015.188 (2015).

D.W. Latzke, W.T. Zhang, A. Suslu, T.R. Chang, H. Lin, H.T. Jeng, S. Tongay, J.Q. Wu, A. Bansil, and A. Lanzara, "Electronic structure, spin-orbit coupling, and interlayer interaction in bulk MoS2 and WS2," Phys. Rev. B, **91,** 23, 235202 (2015).
H. S. Jung, H.-Z. Tsai, D. Wong, C. Germany, S. Kahn, Y. Kim, A. S. Aikawa, D. K. Desai, G. F. Rodgers, A. J. Bradley, J. Velasco, Jr, K. Watanabe, T. Taniguchi, F. Wang, A. Zettl, and M. F. Crommie, "Fabrication of gate-tunable graphene devices for scanning tunneling microscopy studies with Coulomb impurities." *J. Vis. Exp.* **101,** e52711 (2015).
H.I. Rasool, C. Ophus, and A. Zettl. Atomic defects in two-dimensional materials. Adv. Mater. doi: 10.1002/adma.201500231 (2015).
J. Park, H. Elmlund, P. Ercius, J.-M. Yuk, D.T. Limmer, Q. Chen, K. Kim, S.H. Han, D.A. Weitz, A. Zettl, and A.P. Alivisatos. 3D structure of individual nanocrystals in solution by electron microscopy. Science, 349, 6245, pp 290-295 doi: 10.1126/science.aab1343 (2015).
L. Ju, Z. Shi, N. Nair, Y Lv, C. Jin, J. Velasco Jr., C. Ojeda-Aristizabal, H.A. Bechtel, M.C. Martin, A. Zettl, J. Analytis, and F. Wang. Topological valley transport at bilayer graphene domain walls. Nature **520,** 650-655 doi: 10.1038/nature14364 (2015).
O. Ergen, A. Gibb, O. Vazquez-Mena, W.R. Regan, and A. Zettl. Metal insulator semiconductor solar cell devices based on a Cu_2O substrate utilizing h-BN as an insulating and passivating layer. App Phys Let, 106, 103904, doi: 10.1063/1.4914181 (2015).
Q. Zhou, A. Sussman, J. Chang, J. Dong, A. Zettl, and W. Mickelson. Fast response integrated MEMS microheaters for ultra low power gas detection. Sensors & Actuators A 223, pp 67-75; doi: 10.1016/j.sna.2014.12.005 (2015).
W.C. Lee, K. Kim, J. Park, J. Koo, H.Y. Jeong, H. Lee, D.A. Weitz, A. Zettl, and S. Takeuchi. Graphene-templated directional growth of an inorganic nanowire. Nature Nanotech, 10 (4), pp 423-428 doi: 10.1038/nnano.2015.36 (2015).
X.Q. Huang, Z.P. Zhao, L. Cao, Y. Chen, E.B. Zhu, Z.Y. Lin, M.F. Li, A.M. Yan, A. Zettl, Y.M. Wang, X.F. Duan, T. Mueller, and Y. Huang. High-performance transition metal-doped Pt3Ni octahedra for oxygen reduction reaction. Science, **348,** 6240, pp 1230-1234 doi: 10.1126/science.aaa8765 (2015).

Session VII

Program title: Infrared magneto-optics of correlated electronic materials
Principle Investigator: H. Dennis Drew, Co-PI: Gregory Jenkins
Physics Department, University of Maryland, College Park, MD 20742
hdrew@physics.umd.edu

i. Program Scope

The goal of the program is to use optical and magneto-optical techniques to develop an understanding of the electronic structure of important novel electronic materials and search for novel new effects. The focus is on strongly interacting materials including cuprates and 5d transition metal oxides and especially materials in which topological effects are new expected. These include Dirac and Weyl semimetals as well as topological insulators. FTIR spectroscopy from 10 cm^{-1} to 50,000 cm^{-1} and polarization rotation and ellipticity measured by polarization modulation techniques using IR lasers in the 10 cm^{-1} to 1000 cm^{-1} range are used. The goal in the work on the cuprates is to elucidate the reconstructed Fermi surfaces in the charge ordered state of underdoped Bi(2201) and to compare the Hall masses with ARPES data[1,6]. In the 3D Dirac and Weyl semimetals optical characterization is the first goal. Probing the chiral pumping effect through the Faraday rotation and circular dichroism also planned. In general the use of the Kerr rotation measurements are used to detect broken time reversal symmetry states in these novel materials.

ii. Recent Progress

Dirac semimetals

We have extended our study of topological materials to encompass the recently discovered 3D Dirac materials. These include Dirac and Weyl semimetals. The materials studied include Dirac materials Cd_3As_2 and Na_3Bi and the Weyl semimetal $Eu_2Ir_2O_7$.[3,4,5] In addition to 3D Dirac bands in the bulk, they possess exotic "Fermi arc" states on their surfaces.[8,9] When either inversion or time reversal symmetry is broken in such systems, the Dirac states are decomposed into pairs of Weyl states with non-degenerate Dirac states. $Eu_2Ir_2O_7$ has broken time reversal symmetry in the antiferromagnetic state. Other important recently discovered material systems that exhibit semimetallic behavior include quantum spin liquids[10,11] and layered 2D materials akin to graphene. We have made preliminary optical studies on several of these mew materials. We have also performed IR measurements on the spin liquid system, Herbertsmithite in search of evidence for the spinon Fermi sea.[5,12]

Iridates – Weyl state

A Weyl semimetallic state with pairs of nondegenerate Dirac cones in 3D was recently predicted to occur in the antiferromagnetic state of the pyrochlore iridates.[8,9] We have performed temperature dependent IR reflectance studies on single crystals of $Eu_2Ir_2O_7$.[4] As shown in

Figure1, the extracted conductivity shows a broad semimetalic band extending from zero to 2.5 eV, and a free carrier-like Drude response that weakens in the antiferromagnetic insulating state below the antiferromagnetic transition at T_N =110 K. Transmission measurements at low temperatures reveal a THz conductivity increasing with frequency. These experiments represent experimental evidence for the Weyl state.[4] The temperature dependence of the free carrier response is in good agreement with theoretical calculations assuming purely thermal excitations in the Weyl state. The data give a Fermi velocity v_F =4x10^7 cm/s, and a logarithmic renormalization scale Λ_L=600 K and require a T = 0 doping E_F =100 K to account for the low temperature optical response and DC resistivity. The transmission data is also consistent with a Weyl semimetal with a Fermi velocity comparable with the value deduced from the high temperature reflectance data. This work has been submitted for publication in Physical Review Letters.[4]

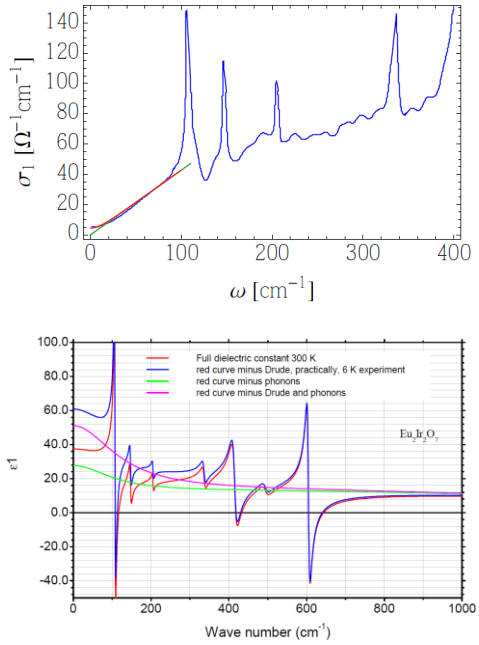

Figure 1. Top panel: Optical conductivity of $Eu_2Ir_2O_7$ single crystal. Blue curve – fit to experiment, red line – theory for 3D Dirac electrons. Bottom panel: various contributions to the dielectric constant at room temperature and at 6 K.

Cd_3As_2, Na_3Bi – Dirac materials

Our study of 3D Dirac state systems has been expanded to several newly discovered systems of great current intyerest. These include Cd_3As_2 and Na_3Bi which have been observed to have a Dirac spectrum by ARPES. We have observed the Pauli blocking interband edge for the Dirac bands in both materials.

As shown in Figure 2 the reflection spectrum of Cd_3As_2 displays, an observed frequency onset of Dirac cone interband transitions is observed in the vicinity of 1600 cm^{-1} that characterizes the chemical potential and the anisoptropy of the interband transition energy within the Dirac cone.[3] The feature has a strong temperature dependence due to the thermal broadening of the Fermi surface. Below these frequencies, our data is consistent with known IR active phonons.[3] Lower frequency measurements in other crystals show a dip in reflection at the plasma frequency associated with the Dirac cone carriers.

The high reactivity of Na_3Bi with water and oxygen prohibit atmospheric exposure. We have developed

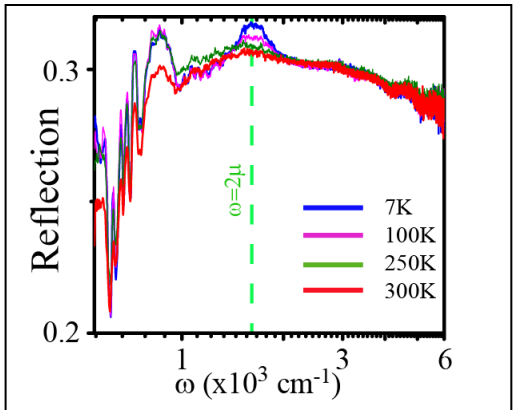

Figure 2: Cd3As2 reflection spectrum shows a sharp feature at around 1600 cm-1 upon cooling and a roll-off at higher frequency consistent with the onset of Dirac cone interband transition at twice the Fermi level and a linear dispersing interband conductivity. The peak is explained by a broadened logarithmic divergence associated with the interband transition edge prevalent in ϵ_1. Other interband transitions are the likely observed features below 1000 cm-1.

methods to avoid atmospheric exposure while allowing optical measurements.[3]

These broadband FTIR reflection measurements were performed on two samples across the entire spectrum shown in Figure 3. The phonon spectrum is similar to Cd_3As_2 with the lowest lying active phonon at about 50 cm^{-1}.[3] The large number of observed phonons implies a lower symmetry than has been assumed in band structure calculations.[3] The plasma edge associated with the large reststrahlen band between 600 cm^{-1} and 1500 cm^{-1} is sensitive to the changes in $\boldsymbol{\varepsilon}$ due to the interband transtions within the Dirac cone. A strong decrease in the strength of the interband transitions is observed with temperature, suggesting an electronic phase transition at 125K. These data are being compared with DFT band structure calculations of Bansil et al. These data represent the first measurement of the IR phonons and electronic optical response in Na_3Bi.[3]

iii. Future plans

During the coming year we plan IR Hall Effect measurements on cuprates, Kerr rotation measurements on broken time reversal ground states in topological insulators and magneto-optical measurements and cyclotron resonance in Dirac materials. The completion of the installation of a He recovery and reliquification system will greatly facilitate these cryogen intensive measurements.

The work on cuprates is driven by the recent observation of charge order in underdoped BSCCO by two groups.[1,6] These results indicate that the Fermi surface reconstruction in underdoped cuprates is driven by charge density wave order. We will address the question of hole pockets vs. electron pockets in the reconstructed Fermi surfaces using IR Hall measurements. The CDW results suggest electron pockets while ARPES data suggest hole pockets. We will also quantitatively compare our measurements of the Hall frequency with the ARPES data. This addresses questions of charge renormalization in the Hall Effect.

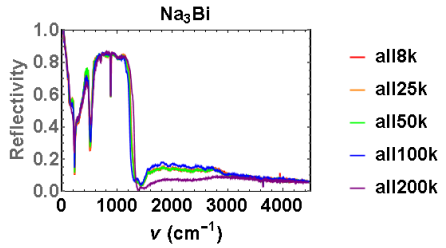

Figure 3: Na_3Bi spectrum was measured from 25 to 19,000 cm^{-1} and from 8 to 200K. The interband transition within the Dirac cone has an onset at 1600 cm^{-1}.

We plan extensive magneto-optical measurements on InSb/GaSb quantum wells.[7] Our main goal is to use magneto-optical spectroscopy to unravel the subband hybridization and the excitonic effects in this topological insulator system that shows great promise for practical Majorana states. The detection of broken time reversal ground states will be probed using THz Kerr rotation in zero magnetic field.

We will also study the magneto-IR response of the Dirac and Weyl state candidate systems: $Eu_2Ir_2O_7$, Cd_2As_3 and Na_3Bi. The main goal is the observation the THz magneto-optical manifestation of the chiral anomaly predicted in Weyl systems and the Fermi arc surface states predicted for these 3D Dirac systems.[11] We will also study cyclotron resonance of the Dirac cones and explore possible topological phenomena in these new opto-electronic materials.

iv. Publications

1. Dennis Drew, *IR Hall Effect for reconstructed Fermi surfaces*, Bulletin of the American Physical Society, 59, 1 (2014).

2. Jacob R. Colbert, H. Dennis Drew, and Patrick A. Lee *"Magneto-optical Faraday effect in spin-liquid candidates"* Phys. Rev. B 90, 121105(R) (2014).

3. Don C. Schmadel, Gregory S. Jenkins, Andrei B. Sushkov, Remington L. Carey, H. Dennis Drew, Jason W. Krizan, Satya Kushwaha, Quinn Gibson and Robert J. Cava, *Gated Terahertz Magneto-optical Measurements of 3D Dirac Semimetals,* Bulletin of the American Physical Society, 60, 1 (2015). Manuscript in preparation.

4. A.B. Sushkov, J.B, Hofmann, G.S. Jenkins, J. Ishikawa, S. Nakatsuji, S. Das Sarma and H.H. Drew, Optical Evidence for a Weyl semimetal state in $Eu_2Ir_2O_7$, submitted to Physical Reciew Letters.

5. Andrei Sushkov, Gregory Jenkins, Dennis Drew, Tian-Heng Han and Young Lee, *Infrared phonons as a probe of spin liquid in kagome antiferromagnet Herbertsmitite,* Bulletin of the American Physical Society, 60, 1 (2015). Manuscript in preparation.

6. Comin, R. *et al.* Charge Order Driven by Fermi-Arc Instability in Bi2Sr2−xLaxCuO6+δ. *Science* **343,** 390–392 (2014).

7. Pikulin, D. I. & Hyart, T. Interplay of Exciton Condensation and the Quantum Spin Hall Effect in InAs/GaSb Bilayers. *Phys. Rev. Lett.* **112,** 176403 (2014).

8. Wan, X., Turner, A. M., Vishwanath, A. & Savrasov, S. Y. Topological semimetal and Fermi-arc surface states in the electronic structure of pyrochlore iridates. *Phys. Rev. B* **83,** 205101 (2011).

9. Witczak-Krempa, W. & Kim, Y. B. Topological and magnetic phases of interacting electrons in the pyrochlore iridates. *Phys. Rev. B* **85,** 045124 (2012).

10. Ran, Y., Hermele, M., Lee, P. A. & Wen, X.-G. Projected-Wave-Function Study of the Spin-1/2 Heisenberg Model on the Kagomé Lattice. *Phys. Rev. Lett.* **98,** 117205 (2007).

11. Ashby, P. E. C. & Carbotte, J. P. Chiral anomaly and optical absorption in Weyl semimetals. *Phys. Rev. B* **89,** 245121 (2014).

12. Pilon, D. V. *et al.* Spin-Induced Optical Conductivity in the Spin-Liquid Candidate Herbertsmithite. *Phys. Rev. Lett.* **111,** 127401 (2013).

Time-Resolved Spectroscopy of Insulator-Metal Transitions: Exploring Low-Energy Dynamics in Strongly Correlated Systems

Gunter Luepke
Department of Applied Science, College of William & Mary,
Williamsburg, VA 23187, email: Luepke@wm.edu

Program Scope

This three-year research program focuses on the study of a variety of magnetoelectric (ME) coupling effects and coherent spin dynamics in a broad range of complex multiferroic (MF) oxide heterostructures using interface-specific and time-resolved nonlinear-optical techniques. A major innovation in this grant is the study of ME coupling effects in ferromagnetic (FM) manganite/ferroelectric (FE) oxide thin-film Schottky heterojunctions, including electron-doped $BaTiO_3$ and $BiFeO_3$. The coexistence of the FE phase and conductivity is interesting because such a conducting bistable material introduces new functionalities. Building on key advances of the previous award period, our program concentrates on two major themes: (i) to determine the interfacial ME coupling mechanism and its correlation with charge transfer, orbital states and strain states induced by the substrate or film thickness using the interface-specific magnetization-induced second-harmonic generation (MSHG) technique, and (ii) to investigate its effect on the coherent spin precession in these strongly correlated systems as a new path for fast magnetic switching utilizing the time-resolved magneto-optical Kerr effect (MOKE) technique. The goal of these studies is to elucidate the static and dynamic magnetic interactions and their correlations with the electronic structure and strain states at the valence and lattice mismatched interfaces, which can be artificially engineered. The science addresses issues of energy dissipation and the coupling between electronic and magnetic order in such advanced multifunctional materials, of fundamental importance to our understanding of solid-state properties and has numerous applications.

Recent Progress

<u>Interface Magnetic Transition via Minority Spin Injection</u>

Here we probe the $BaTiO_3/La_{0.7}Sr_{0.3}MnO_3$ (BTO/LSMO) interface magnetization, and discover a new interface ME effect. The injection of minority spins at the interface causes a sudden, reversible transition of the spin alignment of interfacial Mn ions from ferromagnetic to antiferromagnetic (AFM) exchange coupled, while the bulk magnetization remains unchanged. We attribute the emergent interfacial AFM interactions to weakening of the double-exchange mechanism caused by the strong Hund's rule coupling between injected minority spins and local magnetic moments. The effect is robust and may serve as a viable route for electronic and spintronic applications.

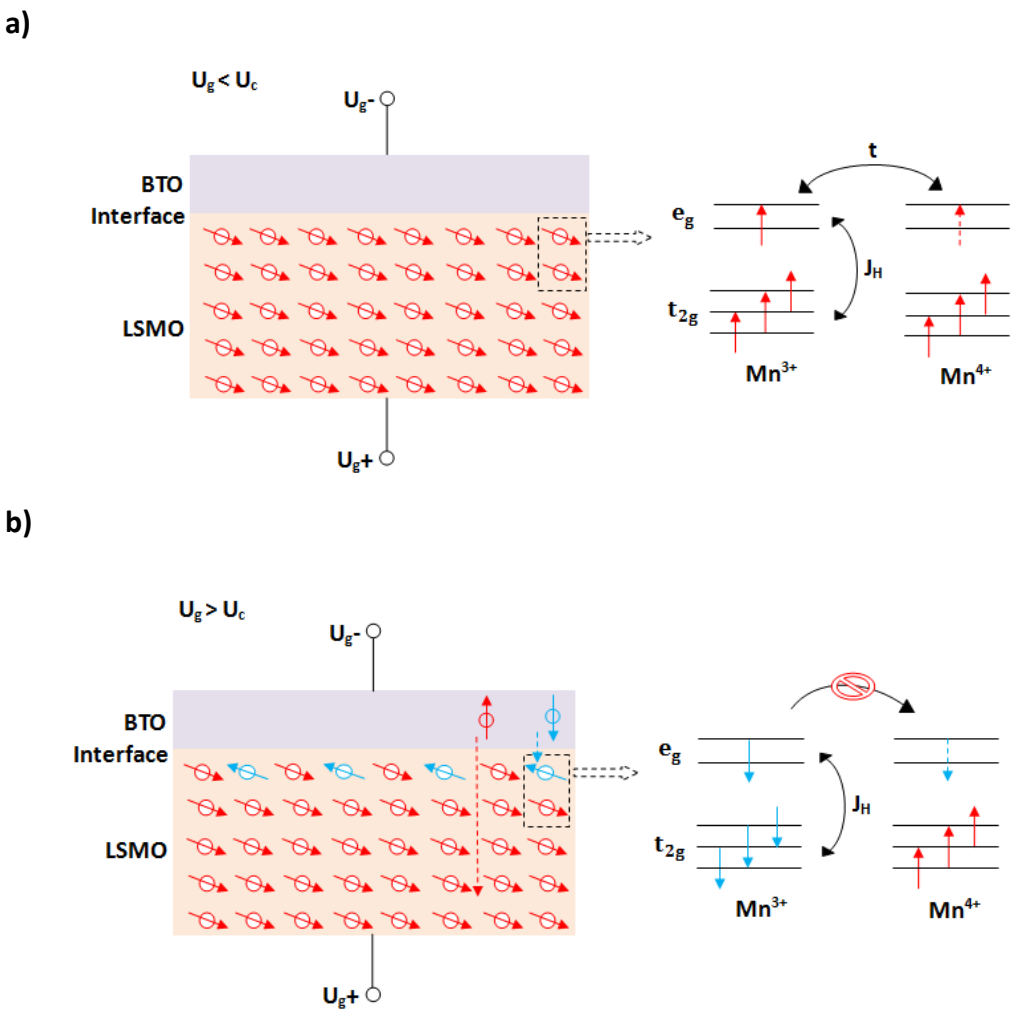

Figure 1: Model of spin alignment at the BTO/LSMO interface

(a) Below critical gate voltage U_c, majority spins (red arrows) of Mn^{3+} and Mn^{4+} ions are double-exchange coupled (right panel), leading to a ferromagnetic state of LSMO. (b) Above U_c, majority spins flow across the LSMO layer by spin-hopping process t. In contrast, the minority spins (blue arrows) will accumulate at the interface, since the spin-hopping process t is blocked by the strong interaction with the local spins due to the large Hund's rule coupling J_H (right panel). The AFM super-exchange interaction of t_{2g} electrons between neighboring Mn ions dominates, and the interfacial LSMO layer undergoes a FM-to-AFM phase transition.

As shown schematically in Fig. 1a, at the reverse gate voltage U_g, no spin injection current occurs at the BTO/LSMO interface. The nearby majority spins of Mn^{3+} and Mn^{4+} ions are double-exchange coupled, leading to a ferromagnetic state. When the forward bias voltage is applied, electron depletion at the interface reduces the number of e_g electrons per Mn ions, weakening the FM configuration due to less spin hopping. In this case, the most important process is the minority spin injection from BTO to LSMO layer near the interface, as depicted in Fig. 1b. The majority spins flow across the LSMO layer by spin-hopping process t. In contrast, the minority spin-down electrons will

accumulate at the interface, since the spin-hopping process t is blocked by the strong interaction with the local spins due to the large Hund's rule coupling J_H. Hence, the minority spins accumulate at the first layer near the interface rather than flowing across the LSMO layer as the majority spins. Thus, the super-exchange interaction of t_{2g} electrons between neighboring Mn ions favor the AFM configuration near the interface. At a critical gate voltage U_c, a FM-to-AFM phase transition occurs at the BTO/LSMO interface. In contrast, the bulk LSMO keeps the FM configuration due to the double-exchange interaction as the minority spins are confined to the interface.

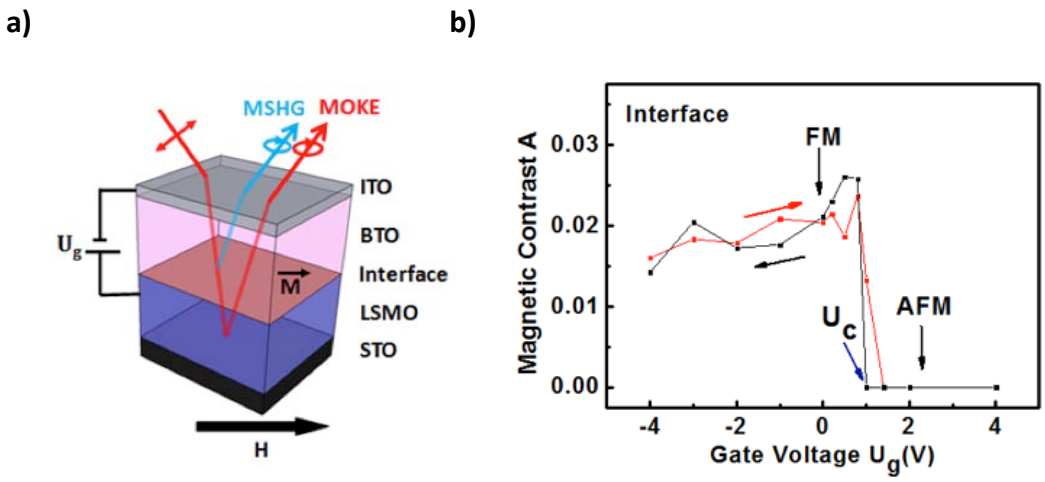

Figure 2: Measurement geometry and MSHG data

(a) Schematic of the optical measurements. MOKE measures the bulk magnetization of the LSMO film, while MSHG selectively probes the interface magnetization only. (b) Magnetic contrast A determined from MSHG measurements as a function of gate voltage U_g. The BTO/LSMO interface exhibits a FM-to-AFM phase transition at U_c, while the bulk LSMO remains unchanged in FM state. Decreasing (increasing) gate voltages are labeled in black (red).

Here, we use the MSHG technique to selectively probe the interface magnetization of the BTO/LSMO heterojunction as a function of gate voltage U_g (Fig. 2a). Figure 2b displays the magnetic contrast A obtained from the MSHG hysteresis loops as a function of U_g. For $U_g < U_c$ (+1 V), the interfacial LSMO is in the FM state since the magnetic contrast is obvious. Above U_c the magnetic contrast A suddenly vanishes. We attribute this sudden, reversible FM-to-AFM phase transition to an interface ME effect. In contrast, the magnetic contrast A obtained from the MOKE hysteresis loops remains constant, indicating that the magnetization of the LSMO bulk does not change.

The observed interfacial magnetoelectric coupling mechanism is conceptually different from those known previously, such as FE polarization-induced changes in the lattice strain or nature of chemical bonding, and/or charge (carrier) modulation at the multiferroic heterojunction. Both can affect the FM moments at the interface of LSMO layer, as expected from their critical phase-competitive nature in magnetism. Here, the injected minority spins through strong Hund's interaction with the local magnetic

moments cause a sudden and reversible magnetic transition at the LSMO interface. The results are important for the transport properties of magnetic tunneling junctions, because an interfacial magnetic transition may notably change the spin polarization of the tunneling current and thus be decisive for tunneling magnetoresistance.

Future Plans

In the future we will address the effect of the interfacial ME coupling on the coherent spin precession in the manganite layer with the time-resolved MOKE technique. The dynamic response of such structures based on ME coupling is not well investigated. Considering the future of ME coupling in magnetic storage, it is still a crucial question how fast magnetic states can response to a triggering E field for the purpose of switching. A coherent manipulation of the magnetization enhances the operational speed of these devices. The time-domain measurements also provide directly the damping constant which is a very important parameter in designing fast precessional switching devices. We plan to elucidate the mechanism of spin scattering by correlating the damping constant with the magnetic structure and interactions.

Publications

1. Wei Zheng, Aubrey T. Hanbicki, Berry T. Jonker, and Gunter Lüpke, Control of Magnetic Contrast with Nonlinear Magneto-Plasmonics, Nature Scientific Reports 4, 6191 (2014).
2. Y. Gong, Z. Zhang, D. Ascienzo, A. Abranyos, H. B. Zhao, G. Lüpke, Qi Li, and Y. H. Ren, Ultrafast optical detection of magnetic inhomogeneity in ferromagnetic $La_{0.67}Ca_{0.33}MnO_3$, Europhysics Letters 108, 17010 (2014).
3. X. Ma, P. He, L. Ma, G. Y. Guo, H. B. Zhao, S. M. Zhou, and G. Lüpke, Spin-Orbit Interaction Tuning of Perpendicular Magnetic Anisotropy in $L1_0$ FePdPt films, Appl. Phys. Lett. 104, 192402 (2014).
4. X. Ma, A. Kumar, S. Dussan, H. Zhai, F. Fang, H. B. Zhao, J. F. Scott, R. S. Katiyar, and G. Lüpke, Charge Control of Antiferromagnetism at $PbZr_{0.52}Ti_{0.48}O_3$ / $La_{0.67}Sr_{0.33}MnO_3$ Interface, Appl. Phys. Lett. 104, 132905 (2014).
5. Y. Fan, X. Ma, F. Fang, J. Zhu, Q. Li, T. P. Ma, Y. Z. Wu, Z. H. Chen, H. B. Zhao, and G. Lüpke, Photo-induced Spin Angular Momentum Transfer into Antiferromagnetic Insulator, Phys. Rev. B 89, 094428 (2014).
6. X. Ma, L. Ma, P. He, H. B. Zhao, S. M. Zhou, and G. Lüpke, Role of Anti-Site Disorder on Intrinsic Gilbert Damping in $L1_0$ FePt films, Phys. Rev. B, 91, 014438 (2015).
7. X. Ma, F. Fang, Q. Li, J. Zhu, Y. Yang, Y. Z. Wu, H. B. Zhao, and G. Lüpke, Ultrafast spin exchange coupling torque via photoexcited charge transfer processes, accepted in Nature Communications (2015).
8. Wei Zheng, Xiao Liu, Aubrey T. Hanbicki, Berend T. Jonker, and Gunter Lüpke, Nonlinear Magneto-Plasmonics, accepted in Optical Materials Express (2015).
9. F. Fang, H. Zhai, X. Ma, Y. W. Yin, Qi Li, J. D. Burton, E. Y. Tsymbal and G. Lüpke, Interface magnetic transition via minority spin injection, submitted to Nature Nanotechnology (2015).

Program Title: Dynamics of Emergent Crystallinity in Photonic Quantum Materials
Principle Investigator: J. Simon
Mailing Address: 929 East 57th Street, GCIS E207, Chicago Illinois 60637
E-mail: simonjon@uchicago.edu

Program Scope

The goal of this program is to employ a revolutionary cold atom/photon hybrid material that combines the advantages of cold atom and semiconductor approaches to materials science, to study quantum soft matter. By confining a thin layer of Rydberg-EIT dressed atoms in the waist of a confocal optical resonator, a new synthetic material will emerge, akin to an exciton-polariton gas, but with stronger interactions and exquisite control: In the resonator, photons and Rydbergs hybridize, producing quasi-particles whose low mass is inherited from photons, and strong interactions from the Rydbergs. These particles have adjustable mass, interactions, and confinement, allowing tuning from a BEC [1] to an unexplored regime expected to exhibit crystallinity [2]. By studying non-equilibrium evolution near this transition, it will be possible to investigate quantum dynamics in a non-classical crystal, where quantum zero-point motion is substantial. Such a regime offers a unique opportunity to probe the universality of quantum dynamics, and also to study, for the first time, a form of quantum "soft-matter", where the lattice structure is emergent, and competes with quantum fluctuations through the introduction of strongly interacting topological defects.

This work will build upon recent successes in harnessing the strong interactions between Rydberg atoms [3] to mediate interactions between photons [4, 5, 6]. These initial works were constrained by low optical depth per blockade radius (OD_B), limiting them to dissipative polariton-polariton interactions [7, 8, 9]. By employing an optical resonator, the achievable OD_B will be increased one hundredfold, thereby moving from a regime of 2-body loss to regime coherent 2-body interactions, enabling for the first time quantum *many*-body physics with Rydberg polaritons.

Recent Progress

We have now completed construction of the apparatus for studying the dynamics of intracavity Rydberg polaritons. This includes (1) a high-finesse resonator (Figure 1) with a 12 micron waist at the location where the atoms are stored, to allow for strong photon-photon interactions mediated by the Rydberg atoms; (2) a high-speed transport system capable of moving a laser-cooled atomic cloud the 2cm distance between the trapping location (MOT) and the cavity heterostructures, in 10ms (Figure 2); (3) an ultrastable laser system with linewidths below 30kHz for both the 5S to 5P transition at 780nm, and 5P-nS Rydberg transition near 480nm.

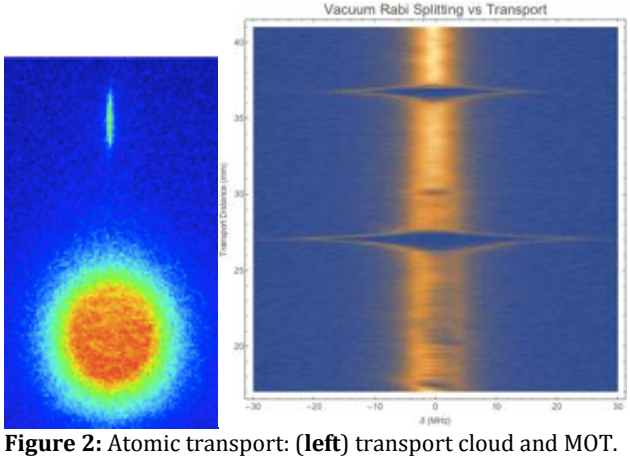

Figure 2: Atomic transport: (**left**) transport cloud and MOT. (**right**) vacuum rabi splitting vs transport distance

Figure 1: High Finesse Running-Wave Resonator

We have now employed this laser system to observe intra-cavity Rydberg EIT (Figure 3), featuring dark polaritons as narrow as ~200kHz. The central, narrow feature in the figure is the dark polariton resonance, which is primarily Rydberg-like, with almost no P-state component (as evidenced by the narrow linewidth, much below the P-state width of ~6MHz). The wider side-lobes are the bright polaritons, which are primarily P-state and photonic.

To date we have explored primarily single-mode characteristics of Rydberg polaritons. To simulate the impact of multiple resonator modes (and thus transverse polariton dynamics), we have varied the resonator detuning relative to the EIT line, observing the dependence of the dark resonance on detuning (Figure 4).

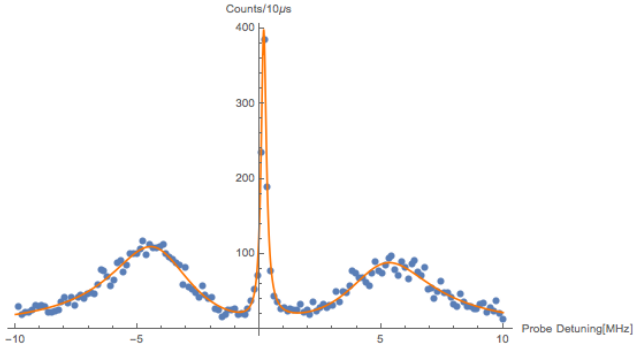

Figure 3: Cavity Rydberg EIT spectrum, showing near-perfect transparency window ~200kHz wide induced by the dark polariton mode, and vacuum rabi sidebands.

A central challenge to generating polaritonic synthetic materials with atomic gases has been broadening induced induced by atomic motion, and stray electric fields. We measure our stray fields to be of order 0.5V/cm, arising primarily from adsorbed Rubidium on the surface of an electric-field filter. We are now in the process of implementing field and gradient compensation electrodes, to suppress our stray fields and gradients down to ~mV/cm and ~mV/cm^2, respectively; more than sufficient for strongly interacting physics experiments with Rydberg polaritons.

To more carefully understand the role of inhomogeneous broadening, we have measured the loss-rate of the strongly-coupled dark polaritonic state, as a function of inhomogeneous linewidth of the uncoupled atoms, by varying the principal quantum number under investigation (which controls the DC polarizability). This data is shown in figure 5, and it indicates that there is a collective suppression of polariton loss, as evidenced by the quadratic, rather than linear dependence of the polariton loss rate on the inhomogeneous broadening. This is to be expected, because inhomogeneous broadening couples to the Rydberg component of the polaritonic state to another Rydberg collective (Dicke) state which is coupled to a similar P-state, but has no corresponding cavity mode—consequently the there is no dark polariton mode in the decoherent manifold, only two bright modes, which are shifted from the dark polariton mode; the decoherence coupling thus connects the dark polariton only off-resonantly to the bright counterparts, and the decoherence is suppressed.

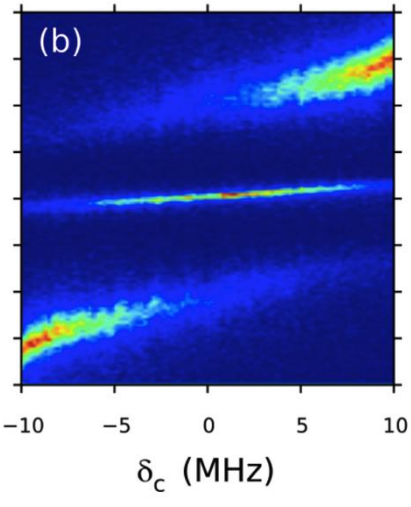

Figure 4: Cavity Rydberg EIT transmission vs. resonator detuning (x axis) and probe detuning (y-axis). The narrow dark-polariton resonance has a slope which is strongly reduced compared to that of the bare photon, due to the strong Rydberg admixture of the polariton state. The avoided crossing in the atomic state is reflected in the broad bright polariton resonances.

We have now also succeeded in demonstrating cavity Rydberg EIT in a two-mode system, paving the way for the extension to many resonator modes. As shown in Figure 6, the spacing between the corresponding dark polaritons becomes compressed as the control field power is reduced, as anticipated for dark polaritons.

Future Plans

Thus far we have carefully explored single polariton physics, primarily in isolated resonator modes. In the coming year we will implement E-field compensation plates which enable us to null the residual field within our optical resonator, thereby opening access to higher principal quantum number Rydberg states, and entering the strongly interacting regime. As a first step, we will probe blockade physics in a single isolated resonator mode. From there we will explore near-degenerate manifolds of modes, first in small systems, allowing for studies of small-system (eg, double-well) Bose-Hubbard-type experiments, and quickly expanding to larger, more continuous systems where we can investigate crystallization.

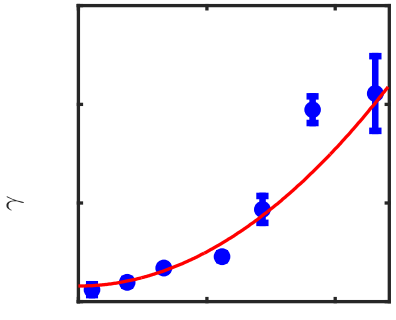

Figure 5: Impact of single-atom inhomogeneous broadening on collective polariton linewidth. By changing which Rydberg state we couple to, we are able to vary the single-atom polarizability (and hence single-atom inhomogeneous linewidth), over several orders of magnitude. We observe a quadratic dependence of the polariton linewidth on the inhomogeneous broadening, indicative of a collective suppression of the broadening.

In a separate effort, we have recently succeeded in generating synthetic magnetic fields for optical photons and observed the formation of photonic Landau levels as photon trapping is reduced to zero (see figure 7). We intend to add Rydberg-mediated interactions to this effort, to explore fractional quantum hall phases of photons.

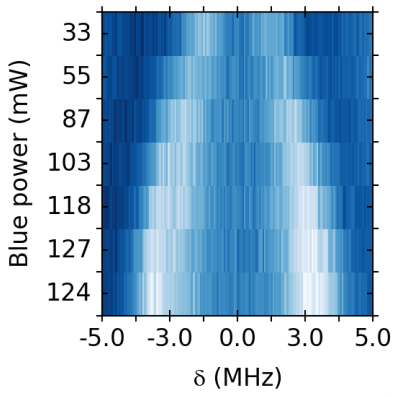

Figure 6: Two-mode Rydberg-EIT vs control field power. We plot the separation of two nearby dark polariton modes (TEM20 and TEM01) is plotted versus the blue control field intensity. As this intensity is reduced, the polaritons become more Rydberg-like, and the spectrum is spectrally compressed.

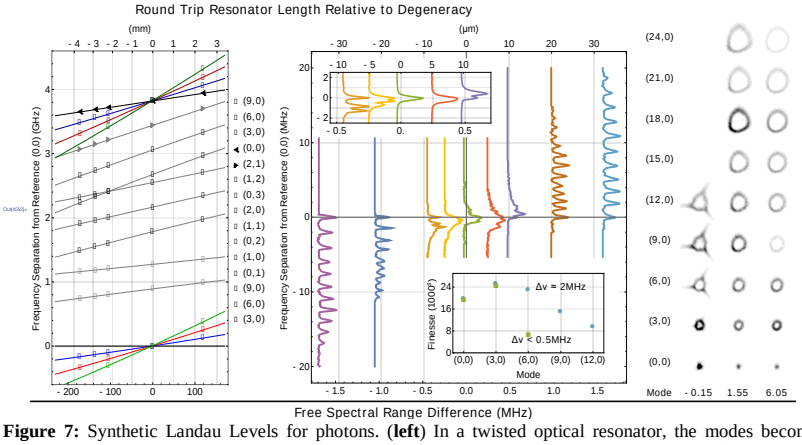

Figure 7: Synthetic Landau Levels for photons. (**left**) In a twisted optical resonator, the modes become degenerate when the twist per round-trip precisely compensates the mirror-curvature-induced refocusing per-roundtrip. At this point we observe a crossing of mode frequencies. (**center**) Zooming in on the crossing point, we observe the spectrum of the resonator as the modes become degenerate- there is a small avoided crossing right at the degeneracy point, resulting from disorder-induced coupling of the modes within the Lowest Landau Level. (**right**) We inject different modes into the resonator with a DMD array, and explore the cavity transmission at the various resonances. Away from degeneracy (right-most column), we observe that the transmitted modes essentially reflect the incident mode-shape. As we approach degeneracy, the modes begin to distort, due to disorder-induced couplings. At degeneracy, the modes are quite distorted due to disorder.

Other References

1. Nikoghosyan, G., Zimmer, F. E. & Plenio, M. B., Dipolar Bose-Einstein condensate of dark-state polaritons. *Phys. Rev. A. (In Press)* (2012).
2. Glaetzle, A. W., Nath, R., Zhao, B., Pupillo, G. & Zoller, P., Driven-dissipative dynamics of a strongly interacting Rydberg gas. *arXiv* **1207.2659** (2012).
3. Saffman, M., Walker, T. G. & Mølmer, K., Quantum information with Rydberg atoms. *Rev. Mod. Phys.* **82**, 2313-2363 (2010).
4. Peyronel, T. *et al.*, Quantum nonlinear optics with single photons enabled by strongly interacting atoms. *Nature* **488**, 57-60 (2012).
5. Dudin, Y. O. & Kuzmich, A., Strongly Interacting Rydberg Excitations of a Cold Atomic Gas. *Science* **18**, 887-889 (2012).
6. Parigi, V. *et al.*, Observation and measurement of "giant" dispersive optical non-linearities in an ensemble of cold Rydberg atoms. *arXiv:1209.1948* (2012).
7. Gorshkov, A. V., Otterbach, J., Fleischhauer, M., Pohl, T. & Lukin, M. D., Photon-Photon Interactions via Rydberg Blockade. *Phys. Rev. Lett.* **107** (133602) (2011).
8. Petrosyan, D. & Fleischhauer, M., Electromagnetically induced transparency and photon-photon interactions with Rydberg atoms. *J. Phys. Conf. Ser.* **350** (012001) (2012).
9. Maxwell, D. *et al.*, F. Bariani, Y. O. Dudin, T. A. B. Kennedy and A. Kuzmich, Phys. Rev. Lett. 108, 030501 (2012). *arXiv* **1207.6007** (2012).

References which acknowledge DOE support

This is a uniquely new, aggressive effort, which is only now reaching sufficient maturity to produce meaningful results. In the coming months, our exploration of cavity Rydberg polariton coherence will be submitted for, as will our observation of Landau levels for photons. Strong interactions should be demonstrated by year's end, and published shortly thereafter.

Project Title: Symmetries, interactions and correlation effects in carbon nanotubes

Principle Investigator: Gleb Finkelstein

Address: Physics Department, Duke University, Durham, NC 27708
E-mail: gleb@duke.edu

Program Scope

The role of the environment in quantum mechanics has captivated physicists' attention since the early days of the theory, resulting in the famous "paradoxes" at the interface of quantum and classical worlds. The environment of a quantum system is commonly modeled by an ensemble of oscillators, or a "bosonic bath", which in the classical context induces dissipation. In the case of quantum tunneling, these dissipative modes generally suppress the tunneling rate, with the degree of suppression depending on the bosonic density of states and the coupling strength. Tunneling with dissipation can be readily realized in a tunnel barrier contacted by resistive leads. In the simplest picture, the electromagnetic excitations in the leads provide a bosonic bath with a linear density of states (Ohmic environment); the dimensionless coupling strength $r \equiv Re^2/h$ is determined by the lead (*i.e.* environmental) resistance R and quantum conductance e^2/h. The key experimental observable is the electrical conductance through the barrier, which as a function of temperature T exhibits a power law suppression $G \propto T^{2r}$.

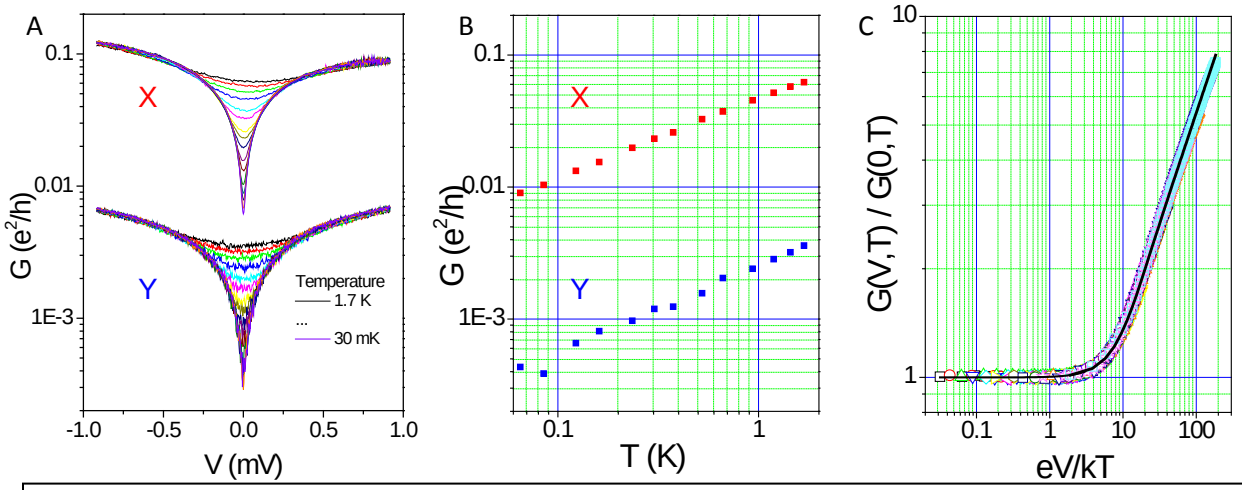

Figure 1: A) Differential conductance of a carbon nanotube G≡dI/dV measured vs. bias V. Gate voltage is fixed at two values, resulting in two sets of curves labeled X and Y. B) Zero-bias conductance G(V=0) vs. temperature T for the same two sets. Power law dependence is clearly seen. C) Conductance for set X scaled by zero-bias conductance plotted vs. bias scaled by temperature, same data as in (A). Black curve is the theoretical curve with dissipation strength r=0.3 [1].

The PI's group has developed a unique platform for studying the effects of dissipation and interactions on quantum impurity systems, which is based on a carbon nanotube quantum dot with dissipative leads (Figure 1). Tunneling in the Ohmic dissipative environment is known to emulate tunneling in the Luttinger liquid – an archetypical example of an interacting one-dimensional electron system. We have first studied resonant tunneling (i.e. tunneling through an intermediate resonance) in this system, and observed unitary resonances with vanishing width, predicted for the Luttinger liquid back in 1992. We have interpreted the observations in terms of a quantum critical transition enabled by dissipation [1].

Recent Progress

We have recently investigated the exotic state of electronic matter obtained by fine-tuning the system exactly to the quantum critical point (QCP) that we observed earlier. We have reported on several transport scaling laws both near and far from equilibrium, including a non-Fermi-liquid quasi-linear scattering rate at the QCP, interpreted in terms of a Majorana mode localized at the resonant level [2].

Figure 2 shows differential conductance maps $G(V) \equiv dI/dV$ measured near one of the resonant conductance peaks of the carbon nanotube. The three maps correspond to the different degrees of coupling asymmetry between the nanotube quantum dot and its two leads. For asymmetric couplings, note the clear zero-bias anomaly (ZBA)–a suppressed conductance at zero bias for all gate voltage values. The ZBA is eliminated only for symmetric tunnel couplings and only exactly at the center of the resonance (Figure 2A). This point – on-resonance and with symmetric coupling – corresponds to the QCP.

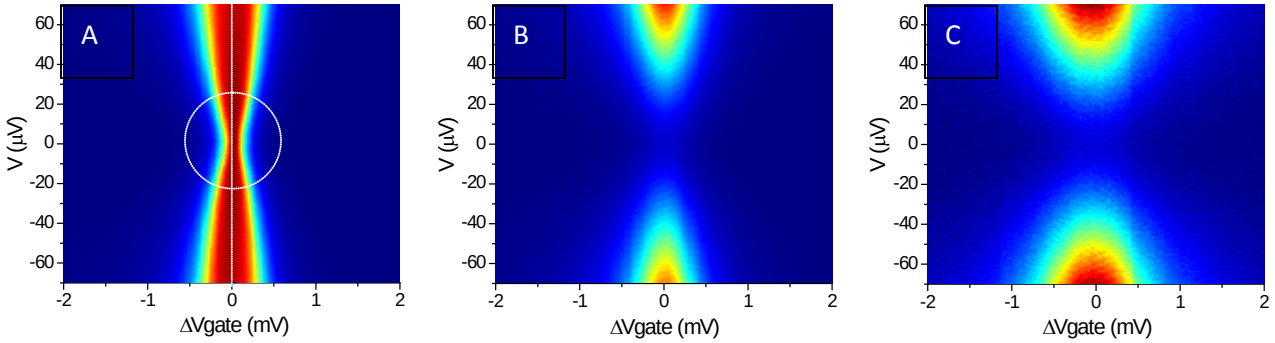

Figure 2: Differential conductance maps close to the QCP. The maps are obtained by sweeping bias V and backgate offset voltage ΔVgate (measured relative to the QCP) at T = 50 mK and B = 3 T. Conductance in the symmetric case (A) is followed by maps (B,C) showing progressively increasing barrier asymmetry, as controlled by the side gate voltages. The same color scale applies to all panels, but the small conductance in the maps B,C is multiplied by ×4 and ×40, respectively, to improve the contrast. The prominent zero-bias suppression of signal in the asymmetric cases (B,C) completely disappears when the system is tuned to the point of symmetric coupling and on resonance (A), indicating a QPT [2].

The dependence of the system conductance at the QCP on both the temperature and bias is shown in Figure 3A. Note the unusual cuspy dependence of conductance on bias, which gets progressively sharper as the temperature is lowered. At higher temperatures, this singularity is washed away, resulting in the $e^2/h - G \sim T$ dependence at $V = 0$ which theory ascribes to the Majorana modes. We have found that the data at different temperatures could be collapsed on the same universal curve (Figure 3B) if plotted in the form of $[1 - G(V,T)] / [1 - G(0,T)]$ *vs.* eV/kT. (Here, G is measured in units of e^2/h.) The overlaying curve represents an empirical dependence

$$\frac{1-G(V\neq 0,T)}{1-G(V=0,T)} = \frac{d}{dV}\{V|\frac{\Gamma(1+1/(1+r)+ieV/2\pi k_BT)}{\Gamma(1+ieV/2\pi k_BT)}|^2\}$$

This particular function was chosen because a similar functional form describes $G(V,T)/G(0,T)$ in a single barrier tunneling with dissipation (Figure 1C). Our recent preprint in collaboration with theorists accounts for this expression [7]. We have further collaborated with theoreticians on elucidating different aspects of the QCP. Specifically, we considered the non-equillibribrium effects [3] and the role of dissipative gate in tuning the properties of the QCP [4].

We have also conducted additional experimental projects. We observed a "bottleneck" in thermal transport between electrons and the substrate in graphene at mK temperatures, allowing for the electrons to be significantly hotter relative to the phonons. This effect may have important applications in ultra-sensitive cryogenic graphene-based detectors [5]. In collaboration with chemistry colleagues, we developed an alternative catalyst for growing carbon nanotubes that results in tighter control of the nanotube diameter [6].

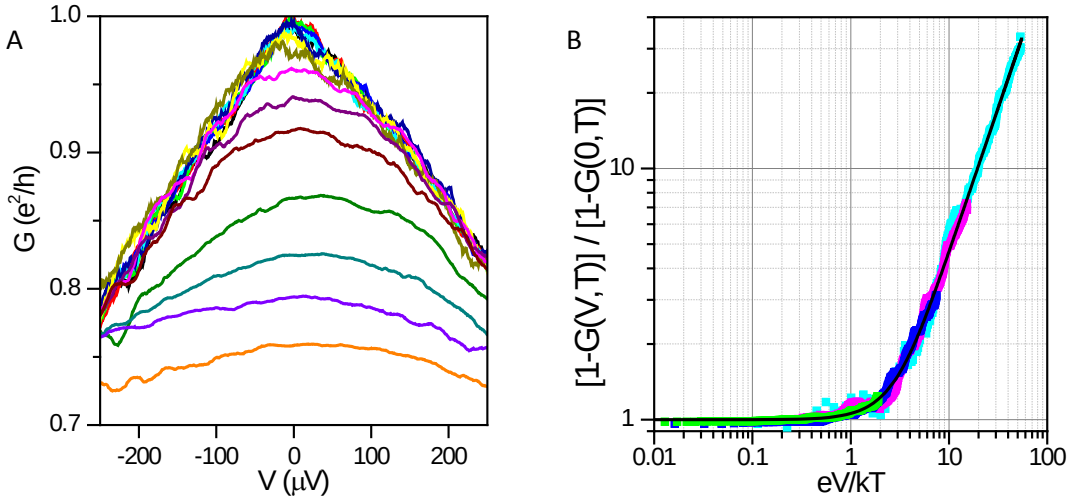

Figure 3: A) Differential conductance at the QCP as a function of bias V at different temperatures T, ranging from 2K (bottom) to 55 mK (top). Notice the upwards cusp developing at lowest temperatures. B) Select curves from (A) rescaled as described in the text and plotted vs. the dimensionless ratio of energies eV/kT. The overlaying curve is the heuristic formula [2,7].

Future Plans

Our work aims to enhance understanding of electronic interactions and dissipative phenomena in low-dimensional confined nanostructures, which naturally possess high degree of symmetry. One of the main topics of this project is to further develop the analogy between the dissipative environment and the Luttinger liquid, and experimentally realize many "quantum impurity" models with Luttinger leads, for which a rich body of theoretical knowledge has been accumulated, but experimental results are scarce or nonexistent. Building on our papers describing the Majorana modes in the dissipative resonant level [1-2], we plan to work on creating and probing strongly correlated quantum states of matter in nanostructures subject to dissipative environment, with a special emphasis on interactions, quantum phase transitions (QPT), and the non-Fermi liquid behavior. Specifically, we focus on the following major topics:

1) The charge localization transition in the dissipative resonant level.
2) Spinful resonant level with dissipation; Kondo effect with dissipation.
3) Double dot in dissipative environment: singlet to Kondo molecule QPT.

The experimental platform of tunneling with dissipation, which we have developed in the past few years, is uniquely suitable to address these challenging tasks.

References

1. H.T. Mebrahtu, I.V. Borzenets, D.E. Liu, H. Zheng, Y.V. Bomze, A.I. Smirnov, H.U. Baranger and G. Finkelstein, *Quantum phase transition in a resonant level coupled to interacting leads.* **Nature 488**, p. 61-64 (2012).

Publications since 2013

2. H.T. Mebrahtu, I.V. Borzenets, H. Zheng, Y.V. Bomze, A.I. Smirnov, S. Florens, H.U. Baranger and G. Finkelstein, *Observation of Majorana quantum critical behavior in a resonant level coupled to a dissipative environment.* **Nature Physics 9**, p. 732 (2013).
3. C.-H. Chung, K. Le Hur, G. Finkelstein, M. Vojta and P. Wölfle, *Nonequilibrium quantum transport through a dissipative resonant level.* **Phys. Rev. B 87**, p. 245310 (2013).
4. D.E. Liu, H. Zheng, G. Finkelstein and H.U. Baranger, *Tunable quantum phase transitions in a resonant level coupled to two dissipative baths.*
Phys. Rev. B 89, p. 085116 (2014).
5. I.V. Borzenets, U.C. Coskun, H.T. Mebrahtu, Y.V. Bomze, A.I. Smirnov and G. Finkelstein, *Phonon Bottleneck in Graphene-Based Josephson Junctions at Millikelvin Temperatures.* **Phys. Rev. Lett. 111**, p. 027001 (2013).
6. J. Li, C.-T. Ke, K. Liu, P. Li, S. Liang, G. Finkelstein, F. Wang and J. Liu, *Importance of Diameter Control on Selective Synthesis of Semiconducting Single-Walled Carbon Nanotubes.* **ACS Nano 8**, p. 8564-8572 (2014).
7. C.-H. Chung, H. Baranger, C.-T. Ke, C.-Y. Lin, G. Finkelstein, *Non-linear quantum critical conductance in resonant tunneling with dissipation.* Preprint.

Session VIII

Program Title: Superconductivity & Magnetism

Principle Investigators: W. –K. Kwok; Co-PIs: U. Welp, A. E. Koshelev, V. Vlasko-Vlasov, Z. L. Xiao

Mailing Address: Materials Science Division, Argonne National Laboratory, 9700 S. Cass Ave., Argonne IL 60439

E-mail: wkwok@anl.gov

Program Scope

This program undertakes experimental and theoretical investigations of novel superconducting and magnetic materials that are important for fundamental physics and applications. It explores new physical phenomena associated with superconductivity and its interplay with magnetism and determines the origins of these phenomena. We investigate phenomena on length scales ranging from macroscopic to nanoscale as well as in heterostructures using a wide range of sophisticated thermodynamic, dynamic and scanning probe characterization tools. One area of pursuit is the thermodynamic and dynamic studies of the mechanisms of novel superconductors, in particular, utilizing controlled particle irradiation to probe and/or alter the order parameter. Another area is the development of new strategies to control vortex dynamics by creating unique vortex pinscapes, combining nanoscale and magnetic structures to tailor their behavior. In addition, we continue to pursue research into the spectral character of THz radiation from high-temperature superconducting crystal micro-mesas, which have the potential for a new compact and portable continuous THz source. We maintain leading programs in experiment and theory, with each deriving strong benefit from close mutual cooperation.

Recent Progress

• *Phase diagram of iron-based superconductors:* Establishing the phase diagram, competing ground states and degrees of freedom is an essential step in unraveling the nature of superconductivity in Fe-based superconductors (FeSCs). Most of the parent compounds of FeSCs develop an antiferromagnetic ground state below a phase transition temperature T_N. This AFM transition is suppressed by doping, which eventually leads to superconductivity, and is preceded or coincident with a structural transition of the lattice from tetragonal to orthorhombic symmetry. A recent proposal challenged this evolution of phases by introducing a nematic transition as the 'true' phase transition leading from the tetragonal to the orthorhombic phase occurring at a temperature T* some 20 K (for $BaFe_2As_2$) above the structural transition [S. Kasahara *et al.*, Nature 486, 382 (2012)]. AC-microcalorimetry is the ideal tool to address these questions as it is a direct thermodynamic probe affording exquisite sensitivity, is not sensitive to the presence of twinning or grains and, at the same time, does not introduce perturbations such as mechanical strains or magnetic fields that could break symmetry. Figure 1 shows high-resolution specific heat measurements of $BaFe_2As_2$ crystals. Our results **[1]** demonstrate that there is no signature in the specific heat that would be consistent

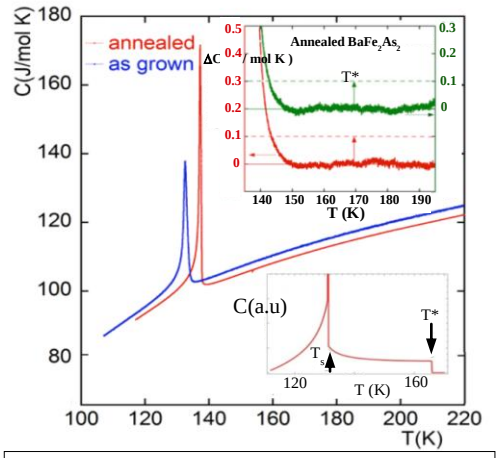

Figure 1 Specific heat of $BaFe_2As_2$ crystals obtained from microcalorimetry. Top inset: data measured on warming (red) and cooling (green), displayed on expanded scales. The vertical arrows indicate the size of the predicted specific heat signature at the nematic transition. Lower inset: specific heat simulation.

with the proposed nematic transition, and that reported features seen at T* are likely due to fluctuation phenomena and/or spurious symmetry breaking induced by the experimental procedure.

• *Vortex cutting and dynamic flux instabilities in anisotropic high temperature superconductors:* Vortices – magnetic field lines, each carrying a single flux quantum are responsible for the entire electromagnetic behavior of applied superconductors. These flux lines act like elastic strings and interact with each other and with the structural defects of the material to define the current carrying capacity of the superconductor. We discovered a first-order phase transition and novel vortex stripe domains in untwined $YBa_2Cu_3O_{7-d}$ under tilted magnetic fields **[2]**. In crossed-magnetic fields, the dynamic *vortex cutting* process is an unsolved problem that is of fundamental importance for understanding the collective behavior of vortex matter and for applications of high temperature superconductors (HTS) in rotating electric machinery and power cables. Through an extensive magneto-optical (MO) imaging study of $YBa_2Cu_3O_{7-d}$ under crossed fields and with large-scale time-dependent Ginzburg-Landau (TDGL) simulations, we reported the creation and dynamics of a high current-carrying magnetic flux front due to flux cutting and reconnection **[3,4]** (Fig. 2).

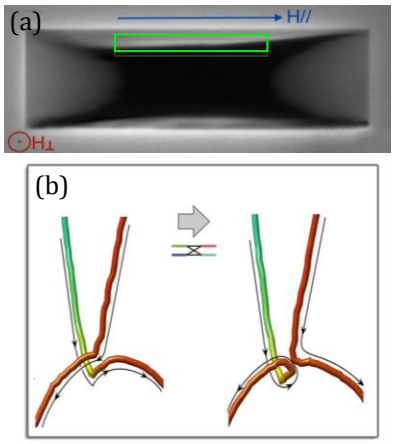

Figure 2 (a) MO image in crossed magnetic field (H// and H⊥) showing high critical current flux front (green box). (b) TDGL simulations of vortex cutting process at the flux front.

• *Enhancing critical current by randomness*: The key ingredient of high critical currents in a type-II superconductor is defect sites that pin vortices. We demonstrated that a random pinscape, an overlooked pinning system in nano-patterned superconductors, can lead to a substantially larger critical current enhancement at high magnetic fields than an ordered array of vortex pin sites **[5]**. We reveal that the better performance of a random pinscape is due to the variation of the local density of its pinning sites, which mitigates vortex-channeling motion. This is confirmed by achieving even higher enhancement of the critical current through a gradient mapped random pinscape, where the distribution of the local density of pinning sites is further enlarged (Fig. 3). Our findings highlight the potential of random pinscapes in enhancing the superconducting critical currents of applied superconductors in which random pin sites of nanoscale defects emerging in the materials synthesis process or through ex-situ irradiation are the only practical choice for large-scale production.

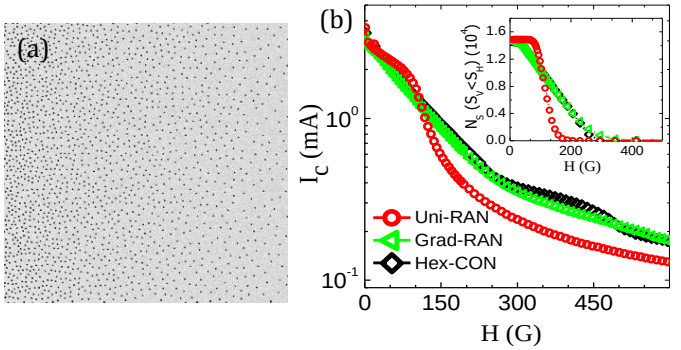

Figure 3 (a) SEM image of a MoGe film patterned with gradient-random holes. (b) Critical current of a sample with uniform (Uni-RAN), gradient (Grad-RAN) and conformal hexagonal array (Hex-CON) of holes. Inset: Voronoi analysis of number of pinning sites, N_s, corresponding to 'strong-pinning regions' as a function of magnetic field.

• *Hot-spot formation in BSCCO resonators for THz-emission*: The Josephson effect occurring intrinsically between the CuO_2-bilayers in $Bi_2Sr_2CaCu_2O_{8+\delta}$ (BSCCO) enables the fabrication of compact sources of coherent THz radiation. However, the layered structure and semiconducting c–axis resistivity of BSCCO cause thermal instabilities at bias conditions that are typical for THz-emission. Using thermo-luminescent microscopy that employs a coating of Eu-chelate as temperature sensor, we obtained direct images of the temperature distribution in the resonator **[6]** and revealed the formation of localized hot-spots, tens of micron in size, in which the temperature exceeds the surrounding by more than 50 K (Fig. 4). The hot-spots strongly affect the electro-magnetic properties of the BSCCO resonator as they draw up to half the bias current and cause hysteretic jumps in the current-voltage characteristics.

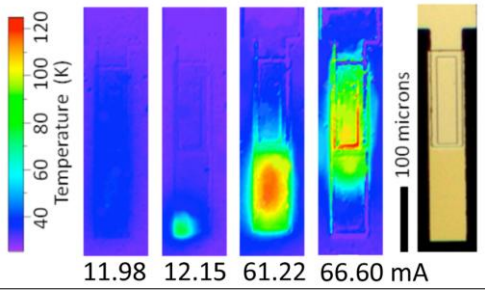

Figure 4 Temperature maps of the BSCCO resonator. A hot-spot nucleates in the lower left corner and jumps to the center on increasing bias current.

Future Plans

• *Phase diagrams and competing phases of unconventional superconductors:* We will investigate the interplay between charge density wave and superconducting ground states in under-doped LBCO using XRD, magneto-transport and specific heat measurements. We will use impurity scattering due to particle irradiation-induced defects as a probe to tune the competition between the ground states.

• *Vortex crossing in BSCCO and pnictide superconductors*: We will explore the effect of layered structure on the flux cutting phenomenon and emergence of helical and angular vortex instabilities in tilted fields using high speed magneto-optics measurements.

• *Controlling superconducting vortices using artificial spin ice nano-structures*: We recently designed a novel artificial spin ice structure with nanoscale ferromagnetic bars that could create several spin-ice ground states as a function of the in-plane magnetic field orientation. The transformation from one ground state to another can be locally tuned with a Magnetic Force Microscope (MFM). By combining such structures with a superconducting MoGe film, we plan to explore the mutual interaction between spin-ice structures and superconducting vortices.

• *THz-emission – synchronization of large-scale intrinsic Josephson junctions:* We will explore the non-linear collective states that arise from the interplay between the synchronization of large arrays of Josephson junctions and non-uniform temperature distribution by patterned heaters to control the formation of hot-spots and investigate their relation to high-power THz emission and the possibility to synchronize large resonator arrays capable of delivering higher emission power.

References which acknowledge DOE support

[1] X. Luo, V. Stanev, B. Shen, L. Fang, X. S. Ling, R. Osborn, S. Rosenkranz, T. M. Benseman, R. Divan, W.-K. Kwok, U. Welp, *Antiferromagnetic and nematic phase transitions in $BaFe_2(As_{1-x}P_x)_2$ studied by ac microcalorimetry and SQUID magnetometry*, Phys. Rev. B91, 094512 (2015)

[2] V. K. Vlasko-Vlasov, J. R. Clem, A. E. Koshelev, U. Welp, W. K. Kwok, *Stripe Domains and First Order Phase Transition in the Vortex Matter of Anisotropic High-temperature Superconductors*, Physical Review Letters 112, 157001 (2014)

[3] V. K. Vlasko-Vlasov, A. Glatz, A. E. Koshelev, U. Welp, W. K. Kwok, *Anisotropic superconductors in tilted magnetic fields*, Physical Review B91, 224505 (2015)

[4] V. K. Vlasko-Vlasov, A. Koshelev, A. Glatz, C. Phillips, U. Welp, and W. Kwok, *Flux cutting in high-Tc superconductors,* Physical Review B91, 014516 (2015)
[5] Y. L. Wang, L. R. Thoutam, Z. L. Xiao, B. Shen, J. E. Pearson, R. Divan, L. E. Ocola, G. W. Crabtree, and W. –K. Kwok, *Enhancing superconducting critical current by randomness*. *Proc Natl Acad Sci* (under review).
[6] T. M. Benseman, A. E. Koshelev, V. Vlasko-Vlasov, Y. Hao, W.-K. Kwok, U. Welp, C. Keiser, B. Gross, M. Lange, D. Kölle, R. Kleiner, H. Minami, C. Watanabe, and K. Kadowaki, *Current Filamentation in Large $Bi_2Sr_2CaCu_2O_{8+d}$ Mesa Devices Observed via Luminescent and Scanning Laser Thermal Microscopy,* Physical Review Applied 3, 044017 (2015)

Other Publications from Oct. 2013 – Oct 2015 which acknowledge DOE support

[7] L. Fang, Y. Jia, V. Mishra, C. Chaparro, V. K. Vlasko-Vlasov, A. E. Koshelev, U. Welp, G. W. Crabtree, S. Zhu, S. Katrych, N. D. Zhigadlo, J. Karpinski, and W. K. Kwok, *Huge Critical Current Density and Tailored Superconducting Anisotropy in $SmFeAsO_{0.8}F_{0.15}$ by Low Density Columnar-Defect Incorporation,* Nature Communications 4, 2655 (2013)
[8] E. Palacios, A. Chen, J. Foley, S. K. Gray, U. Welp, D. Rosenmann, V. K. Vlasko-Vlasov, *Ultra-confined modes in metal nanoparticle arrays for sub-wavelength light guiding and amplification,* Advanced Optical Materials 2, 394 (2014)
[9] Lei Fang and Wai-Kwong Kwok, *Quantum phenomena in transport measurements of topological insulator nanostructures,* Low Temperature Physics 40, 280 (2014)
[10] A. Petrean, L. Paulius, V. Tobos, H. Cronk, W. –K. Kwok, *Vortex dynamics in $YBa_2Cu_3O_{7-d}$ with in-plane columnar defects introduced by irradiation,* Physica C 505, 65 (2014)
[11] L. Fang, C. C. Stoumpos, Y. Jia, A. Glatz, D. Y. Chung, H. Claus, U. Welp, W. –K. Kwok and M. G. Kanatzidis, *Dirac fermions and superconductivity in the homologous structures $(Ag_xPb_{1-x}Se)_5(Bi_2Se_3)_{3m}$ (m=1,2),* Physical Review B90, 020504(R) (2014)
[12] L. Fang, J. Im, C. C. Stoumpos, F. Shi, V.Dravid, M. Leroux, A. J. Freeman, W.-K. Kwok, D. Y. Chung, and M. Kanatzidis, *Two-Dimensional Mineral $[Pb_2BiS_3][AuTe_2]$: High-Mobility Charge Carriers in Single-Atom-Thick Layers,* JACS 137, 2311 (2015)
[13] I. Lukyanchuk, V. M. Vinokur, A. Rydh, R. Xie, M. V. Milošević, U. Welp, M. Zach, Z. L. Xiao, G. W. Crabtree, S. J. Bending, F. M. Peeters & W. K. Kwok**,** *Rayleigh instability of confined vortex droplets in critical superconductors,* Nature Physics 11, 21 (2015)
[14] V. K. Vlasko-Vlasov, E. Palacious, D. Rosenmann, J. Pearson, Y. Jia, Y. L. Wang, U. Welp and W. -K. Kwok, *Self-healing patterns in ferromagnetic-superconducting hybrids,* SUST 28, 035006 (2015)
[15] N. Haberkorn, J. Kim, K. Gofryk, F. Ronning, A. S. Sefat, L. Fang, U. Welp, W. –K. Kwok and L. Civale, *Enhancement of the critical current density by increasing the collective pinning energy in heavy ion irradiated Co-doped $BaFe_2As_2$ single crystals,* SUST 28, 055011 (2015)
[16] B. Shen, M. Leroux, Y. L. Wang, X. Luo, V. K. Vlasko-Vlasov, A. E. Koshelev, Z. L. Xiao, U. Welp, W. K. Kwok, M. P. Smylie, A. Snezhko, and V. Metlushko, *Critical fields and vortex pinning in overdoped $Ba_{0.2}K_{0.8}Fe_2As_2$,* Physical Review B91, 174512 (2015)
[17] D. Campanini, Z. Diao, L. Fang, W.-K. Kwok, U. Welp, and A. Rydh, *Superconducting gap evolution in overdoped $BaFe_2(As_{1-x}P_x)_2$ single crystals through nanocalorimetry,* Physical Review B91, 245142 (2015)
[18] L. R. Thoutam, Y. L. Wang, Z. L. Xiao, S. Das, A. Luican-Mayer, R. Divan, G. W. Crabtree, and W. K. Kwok, *Temperature-dependent three-dimensional anisotropy of the magneto-resistance in WTe_2,* Physical Review Letters 115, 046602 (2015)

Towards a Universal Description of Vortex Matter in Superconductors

PI Leonardo Civale, Co-PI Boris Maiorov
Condensed Matter and Magnet Science,
Los Alamos National Laboratory, Los Alamos, NM 87545
e-mail: lcivale@lanl.gov

Program Scope

Vortex physics has been a topic of interest since the discovery of the oxide high temperature superconductors (HTS), driven both by fascinating new physics and the pursuit of technological uses.[1,2] The complex vortex phenomena in these materials, with several solid and liquid phases and fast non-equilibrium dynamics, arises from the presence of strong thermal fluctuations that are a consequence of the small coherence length (ξ, a few nm) and the large crystal anisotropy (γ).[2] On the other hand the fluctuations are the main obstacle for applications; moreover the problem is general and will also occur in any new-discovered superconductor (SC) operating at high temperatures. The control of vortex matter for performance enhancement requires the design of the pinning landscape by nano-engineering of the material disorder at the scale of ξ.[1,2]

To develop a universal description of vortex matter, we must note that modern vortex models have been created to describe the oxide HTS,[2] thus it is important to test them in other systems. **Our approach** is to perform comparative studies on several materials covering a broad spectrum of properties. Fe-based SC provide an opportunity to "bridge the gap" and check the validity of models in a new family of materials with broad ranges of T_c, ξ and γ. Other relevant SC for our scope are MgB_2, a chemically simple two-band SC, borocarbides that exhibit interactions of vortices with magnetic sublattices, and anisotropic low T_c superconductors (LTS) such as $NbSe_2$.

Recent Progress

Background: Thermal fluctuations in a SC allow vortices to jump out of the pinning centers, even for supercurrent densities (J) lower than the critical current density (J_c). This produces *flux creep*, a time decay of J that is characterized by the normalized relaxation rate $S=d\ln J/d\ln t$. The strength of the thermal fluctuations is given by the *Ginzburg number* $Gi = \frac{1}{2}(T_c/U_0)^2$ that measures the ratio of the thermal energy (T_c) to the condensation energy in an elementary SC volume ($U_0 = H_c^2\xi^3/\gamma$), where H_c is the thermodynamic critical field.[2] The values for NbTi and $YBa_2Cu_3O_7$ (YBCO) are $Gi \sim 10^{-8}$ and 10^{-2} respectively, easily accounting for the much higher S values in the later. A material that fits well into this picture is MgB_2, which has an intermediate $Gi \sim 10^{-5}$ to 10^{-4} (depending on how "clean" or "dirty" it is) and indeed exhibits intermediate S between those of LTS and HTS. In contrast, Fe-based SC do not follow this trend. For instance, several AFe_2As_2 compounds (the 122 family), with intermediate T_c, low γ and high upper critical field H_{c2} (i.e., small ξ), also have $Gi \sim 10^{-5}$ to 10^{-4}. However, they have S similar or even larger than YBCO.[3] One of the main goals that we set at the renewal of our BES program

three year ago was the resolution of this puzzle. Our recent studies have provided the answer: the large creep is due to extrinsic reasons (pinning landscape) rather than fundamental limitations.

Results: Fig. 1 displays examples of $S(T)$ curves from some of our studies. Fig. 1(a) shows $S(T)$ at $\mu_0 H$=1T for four YBCO films grown by different methods and with different pinning landscapes.[4] Fig. 1(b) shows $S(T)$ at several H for a relatively clean MgB_2 film (Gi~10^{-5}),[16] Fig. 1(c) shows data at $\mu_0 H$=1T for a $Na_{0.25}Ca_{0.75}Fe_2As_2$ single crystal (Gi~10^{-5}) before (red circles) and after (black squares) irradiation with protons to create random disorder.[12] Clearly, the rates in MgB_2 are much lower than in the other two cases, while YBCO and 122 are similar.

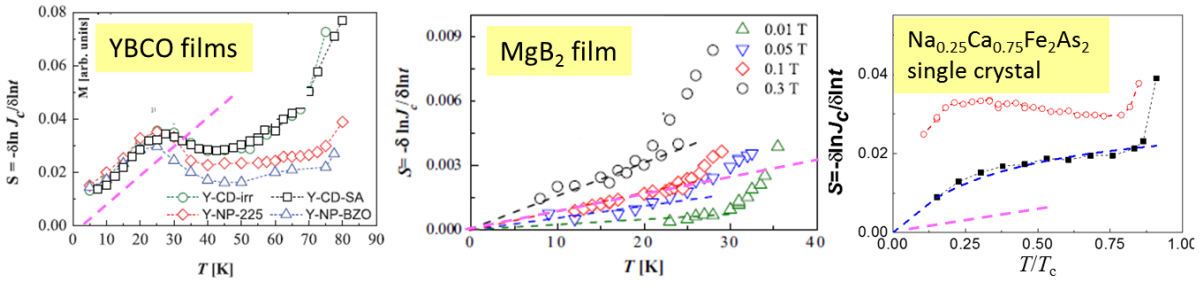

Fig. 1: $S(T)$ for (a) four YBCO films at $\mu_0 H$=1T; (b) a clean MgB_2 film at several H; (c) a $Na_{0.25}Ca_{0.75}Fe_2As_2$ single crystal at $\mu_0 H$=1T. In all cases **H**//c axis. The dashed magenta lines are estimates of $S \sim Gi^{1/2}(T/T_c)$.

In general $S(T,H)$ depends in a complex way on the pinning landscape as well as on the vortex elasticity and vortex-vortex interactions that produce collective effects.[2] But to get the basic idea, let's consider low enough T such that the pinning energy (U_p) is much larger than T, so we can use the Anderson-Kim (A.K.) model as a good approximation and $S \sim T/U_p$. If we assume that at low H the collective effects are small, which is true in the case of sparse strong defects, then U_p is associated to a single defect and we can estimate $U_p \sim U_0$. This leads to the simple scaling relation $S \sim Gi^{1/2}(T/T_c)$, shown in the three panels of Fig. 1. We conclude that the creep rates in MgB_2 and YBCO are close to the expected values, while in 122 they are well above them.

A clue to solve this puzzle comes from the post-irradiation data in Fig. 1(c) that shows a more than 2-fold S reduction due to the added pinning centers. In general, adding defects in MgB_2 or YBCO does not significantly reduce S, particularly in the A.K. regime. Our conclusion is that the large S in the 122 crystal is not due to a fundamental limit, but rather to a pinning landscape that is far from optimum. These are good news for the applications of Fe-based SC. We have strong additional evidence in support of this scenario. We irradiated $Ba(Fe_{1-x}Co_x)_2As_2$ with protons and also found a decrease in S.[5] Recently we irradiated other $Ba(Fe_{1-x}Co_x)_2As_2$ crystals with heavy ions (1.4 GeV Pb) to create discontinuous columnar defects (CD). This resulted in a decrease in S by more than a factor of 2 at low T/T_c, although still above the $S \sim Gi^{1/2}(T/T_c)$ limit.[17]

A very successful route to engineer strong pinning centers in YBCO films has been the incorporation of second phases, in particular $BaZrO_3$ (BZO), to create large defects such as nanorods and nanoparticles (NP). In collaboration with Dr. M. Miura (Seikei Univ.) we showed

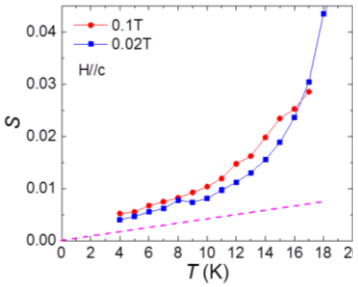

Fig. 2: $S(T)$ for $BaFe_2(As,P)_2$ film with $BaZrO_3$ nanoparticles. Dashed line: $S \sim Gi^{1/2}(T/T_c)$.

that the incorporation of BZO NP strongly enhances pinning in $BaFe_2(As_{0.66}P_{0.33})_2$ films,[8] and we are now exploring their creep. This is challenging because the films are very thin (δ~80nm) and thus the standard technique to obtain S fails. We have developed an alternative method to solve this limitation and the initial results are shown in Fig. 2. Not only is the $S(T)$ lower than in all our previous studies in 122 but it starts to approach the $S \sim Gi^{1/2}(T/T_c)$ line.

We also found that some LTS exhibit creep rates well above those expected from their small Gi. The common characteristic is that they are very clean single crystals with sparse and/or weak defects, so pinning is very low. We found surprisingly large flux creep rates (S~0.02 at T<1K) in single crystals of $ErNi_2B_2C$ (T_c~11K). The weak pinning allowed us to detect low energy interactions between vortices and spins, manifested as clear anomalies in S at the antiferromagnetic transition (T_N~6.3K), the weak ferromagnetic transition (T_{WFM}~2.2K), and a new one T~0.8K. The studies were made in the new ^{3}He probe (purchased with BES funds) that extends the range of our studies down to T ~ 0.43 K. We are exploring creep in $NbSe_2$ single crystals (T_c~7K) irradiated with heavy ions to create CD tilted away from the c-axis, which produce directional pinning. The initial results for the angular dependence of S are shown in Fig. 3. These data show two remarkable features. First, for **H** orientations far away from the CD (where their pinning is weak) S is as large as in YBCO, even though Gi ~ 10^{-7}. Second, for θ close to the CD orientation (θ~-27°) where pinning is highest, S decreased by a factor of ~ 20, providing clear proof-of-principle that creep can be reduced.

Future Plans

In the near future we will complete the $ErNi_2B_2C$ study, will finish the study of the P-doped 122 film and extend it to other NP concentrations. The work on $NbSe_2$ is just starting; we have only measured $S(\theta)$ at one T, H; we will complete it, extend it to ^{3}He and explore pristine crystals for comparison. We will use our new S measurement method and the ^{3}He probe to explore $CeCoIn_5$ crystals. In the longer term we want to better understand the requirements to reduce S to the $Gi^{1/2}(T/T_c)$ level or below, and extend that knowledge to higher T and H where pinning is collective. We will develop a general description of vortex dynamics due to NP. In particular, we want to establish if collective effects result in glassy dynamics.

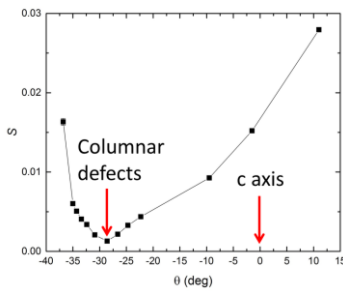

Fig. 3: S vs **H** angle (θ) for a $NbSe_2$ crystal with tilted CD.

References

1. "Basic Research Needs for Superconductivity", report of the Basic Energy Sciences Workshop on Superconductivity (Washington, DC, May 8-11, 2006).
2. G. Blatter *et al.*, Rev. Mod. Phys. **66**, 1125 (1994).
3. N. Haberkorn, M. Miura, B. Maiorov, G. Chen, W. Yu, L. Civale, PRB **84**, 094522 (2011).
4. N. Haberkorn, M. Miura, J. Baca, B. Maiorov, I. Usov,

P. Dowden, S. Foltyn, T. Holesinger, J. Willis, K. Marken, T. Izumi, Y. Shiohara and L. Civale, Phys. Rev. B, **85**, 174504 (2012).
5. N. Haberkorn, B. Maiorov, I. Usov, M. Weigand, W. Hirata, S. Miyasaka, S.Tajima, N. Chikumoto, K. Tanabe and L. Civale, Phys. Rev. B **85**, 014522 (2012).

Publications (since September 2013)

6. "Upper critical magnetic field and vortex-free state in very thin epitaxial delta-MoN films grown by polymer-assisted deposition", N Haberkorn, Y. Zhang, J. Kim, T. McCleskey, A. Burrell, R. Depaula, T. Tajima, Q.X. Jia, L. Civale, Supercond. Sci. Technol. **26**, 105023 (2013).
7. "Inversion of the upper critical field anisotropy in FeTeS films", B. Maiorov, P. Mele, S. Baily, M. Weigand, S.Z. Lin, F. Balakirev, K. Matsumoto, H. Nagayoshi, S. Fujita, Y. Yoshida, Y. Ichino, T. Kiss, A. Ichinose, M. Mukaida, and L. Civale, SuST **27**, 044005 (2014).
8. "Strongly enhanced flux pinning in one-step deposition of BaFe2($As_{0.66}P_{0.33}$)$_2$ superconductor films with uniformly dispersed BaZrO3 nanoparticles", M. Miura, B. Maiorov, T. Kato, T. Shimode, K. Wada, S. Adachi, and K. Tanabe, Nat. Commun. **4**, 2499 (2013).
9. "Observation of lock-in phenomena in heavy-ion-irradiated single crystal of $Ba(Fe_{0.93}Co_{0.07})_2As_2$", T. Taen, H. Yagyuda, Y. Nakajima, T. Tamegai, O. Ayala-Valenzuela, L. Civale, B. Maiorov, T. Kambara and Y. Kanai, Phys. Rev. B **89**, 024508 (2014).
10. "Interactive Growth Effects of Rare-Earth Nanoparticles on Nanorod Formation in $YBa_2Cu_3O_x$ Thin Films", F.J. Baca, T.J. Haugan, P.N. Barnes, T.G. Holesinger, B. Maiorov, R. Lu, X. Wang, J.N. Reichart, J.Z. Wu, Adv. Funct. Mater. **23**, 4826 (2013).
11. "Effect of lattice strain on the diameter of BZO nanorods in epitaxial YBCO films", J. Wu, J. Shi, J. Baca, R. Emergo, T. Haugan, B. Maiorov and T. Holesinger, SuST **27**, 044010 (2014).
12. "Increment of the collective pinning energy in $Na_{1-x}Ca_xFe_2As_2$ single crystals with random point defects introduced by proton irradiation", N. Haberkorn, Jeehoon Kim, B. Maiorov, I. Usov, G. F. Chen, W. Yu and L. Civale, Supercond. Sci. Technol. **27**, 095004 (2014).
13. "Vortex creep in TFA-YBCO nanocomposite films", V. Rouco, E. Bartolomé, B. Maiorov, A. Palau, L. Civale, X. Obradors and T. Puig, Supercond. Sci. Technol. **27**, 115008 (2014).
14. "Magnetic ordering in the frustrated J1-J2 Ising chain candidate $BaNd_2O_4$", A.A. Aczel, L. Li, V.O. Garlea, J.-Q. Yan, F. Weickert, M. Jaime, B. Maiorov, L. Civale, R. Movshovich, V. Keppens, and D. Mandrus, Phys. Rev. B **90**, 134403 (2014).
15. "Superconducting properties in heavily overdoped $Ba(Fe_{0.86}Co_{0.14})_2As_2$ single crystal", J. Kim, N. Haberkorn, K. Gofryk, M. Graf, L. Civale, F. Ronning, A. Sefat and R. Movshovich, Solid State Commun. **201**, 20 (2015).
16. "Strong magnetic field dependence of critical current densities and vortex activation energies in an anisotropic clean MgB_2 thin film" by J. Kim, N. Haberkorn, E. Nazaretski, R. de Paula, X. Xi, T. Tan, T. Tajima, R. Movshovich and L. Civale, Solid State Commun. **204**, 56 (2015).
17. "Enhancement of the critical current density by increasing the collective pinning energy in heavy ion irradiated Co-doped $BaFe_2As_2$ single crystals", N. Haberkorn, J. Kim, K. Gofryk, F. Ronning, A. Sefat, U. Welp, L. Fang, W.K. Kwok and L. Civale, SuST **28**, 055011 (2015).
18. "Vortex matter in the two-band superconductor MgB_2", L. Civale and A. Serquis, in Intermediate superconductors for applications: MgB2, ed. R. Flukiger, World Scientific, in press.
19. "Upward shift of the vortex solid phase in high-temperature-superconducting wires through high density nanoparticle addition", M. Miura, B. Maiorov, F. Balakirev, T. Kato, Y. Takagi, T. Izumi and L. Civale, submitted to Scientific Reports (2015).

Project Title: Quantum Materials

Principal Investigator: Joseph Orenstein; Co-PI's: RJ. Birgeneau, E. Bourret, A. Lanzara, DH Lee, JE Moore, R. Ramesh, A. Vishwanath, Lawrence Berkeley National Laboratory

Program Scope

The LBNL Quantum Materials program focuses on condensed matter systems in which quantum mechanics plays an essential role in determining the nature of phases and the transitions that take place between them. The goal of the program is to understand, manipulate, and control these phases. To achieve this goal, the Quantum Materials program brings together theorists and experimentalists with expertise in (i) thin film and bulk crystal fabrication, (ii) advanced characterization tools including ARPES, ultrafast optical pump/probe, neutron and X-ray scattering, (iii) fundamental and phenomenological theory. Currently the program is focused on three overlapping themes – high-temperature superconductivity, topological phases of matter, and systems in which strong-spin orbit coupling generates exotic magnetism. Specific material systems under investigation are transition metal oxides, such as cuprates and iridates, and iron-chalcogenide and iron-pnictide superconductors.

Recent Progress

1) Optical evidence for broken 4-fold symmetry in model iron-pnictide $Ba(As_{1-x}P_x)_2Fe_2$

The $Ba(As_{1-x}P_x)_2Fe_2$ system (P:Ba122) is a focus of research in iron-based superconductors because the isovalent substitution of P for As introduces a dome-like region of superconductivity in the T–x plane while introducing minimal disorder. This system is ideally suited for understanding the roles that antiferromagnetic and nematic order play in generating high-T_c superconductivity. The Analytis Lab at UCB/LBNL has provided the QM team with P:Ba122 samples from the parent $BaAs_2Fe_2$ phase to the overdoped (with P) regime. The phase diagram as revealed by their transport measurements is shown as open circles in Fig. 1 and is in agreement with previous work. Below the line labeled $T_s(x)$ lies a structural orthorhombic phase with stripe-like antiferromagnetic order. The termination of this phase near $x = 0.3$ has led to speculation that the P concentration for optimal superconductivity coincides with a nematic quantum critical point. However, torque magnetometry measurements complicate this picture, as evidence was found that C_4 symmetry is actually broken at a T much greater than $T_s(x)$, along a line that extends well above optimal doping [1].

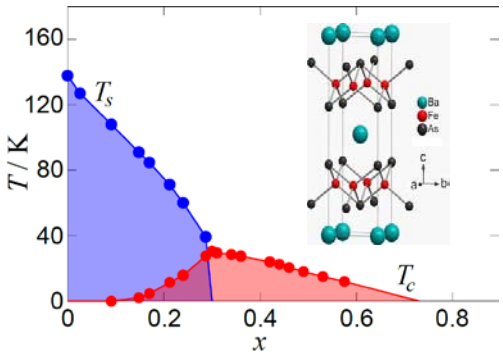

Figure 1: Phase diagram of $Ba(As_{1-x}P_x)_2Fe_2$ together with illustration of structure.

Our recently reported optical measurements provide additional evidence for C_4 breaking at optimal doping [2]. We have measured transient change in reflectivity at 1.5 eV, ΔR, induced by a weak pump pulse, in $Ba(As_{1-x}P_x)_2Fe_2$. Fig. 2a shows $\Delta R(t)$ traces obtained in a sample with $x = 0.31$, for probe electric field parallel to each of the orthogonal Fe-Fe bond directions. The T dependence of $\Delta R(t)$ near zero time-delay for the two probe field orientations, as presented in

Fig. 2c, shows the sharp onset of optical birefringence near 60 K, demonstrating that C_4 is clearly broken even in this nominally tetragonal, non-magnetic region of the phase diagram. The optical probe suggests the importance of an additional symmetry breaking field, perhaps orbital order, in the $Ba(As_{1-x}P_x)_2Fe_2$ system.

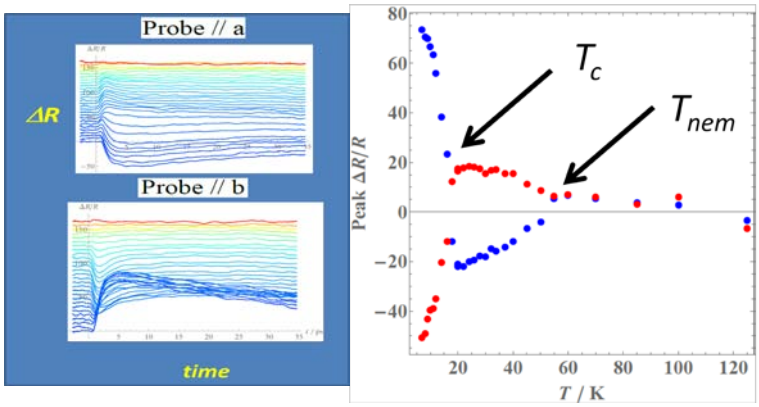

Figure 2: (a) Transient reflectivity as function of time for selected *T* between 5 and 120 K for two orthogonal probe polarizations; (b) Amplitude of ΔR near zero time delay showing onset of C_4 breaking at 60 K.

Future research: We will pursue two directions to characterize the onset of C_4 breaking. In the first, we are constructing a confocal pump/probe microscope to detect formation of orbitally ordered domains with lowering of temperature. In the second, we are adapting our optical microscope to include a device for applying variable strain, to measure if optical birefringence shows a diverging susceptibility near the onset of C_4 breaking.

(2) Phases in $A_xFe_ySe_{2-z}S_z$ system

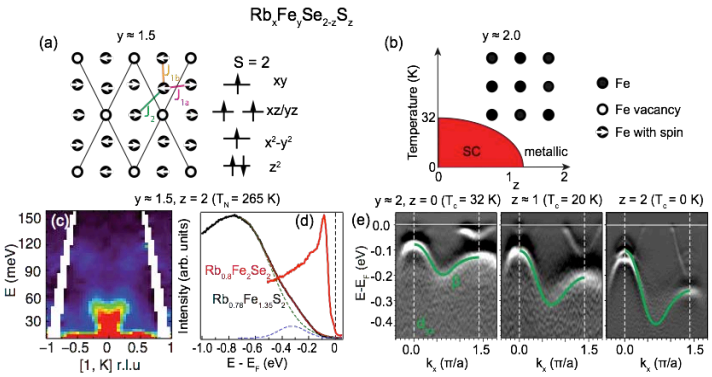

Figure 3 (a) Schematics of Fe-plane with stripe AF order and rhombic vacancy order and spin configuration. (b) Phase diagram of Fe-vacancy-free $Rb_xFe_2Se_{2-z}S_z$ vs. z (c) Spin wave spectrum of the stripe AF phase along the [1, K] direction. (d) ARPES energy distribution curves revealing a gap at Fermi level, with comparison to superconducting $Rb_{0.8}Fe_2Se_2$. (e) ARPES on the $Rb_xFe_2Se_{2-z}S_z$ system demonstrating variation in electron correlation with z.

Physical laws cannot simply explain the rule, they must account for the exceptions as well. Such was the role played by the $A_xFe_ySe_{2-z}S_z$ (A = alkali metals) system in the study of iron-based superconductors (FeSCs). Before the discovery of this system, it was nearly settled that optimal T_c in FeSCs required a favorable Fermi surface (FS) nesting condition between the hole and electron Fermi surfaces and close proximity to a spin density wave (SDW) phase. The $A_xFe_ySe_{2-z}S_z$ system defied both these rules – manifesting high-T_c without a hole pocket and SDW phase. This intriguing anomaly motivated us to study these materials to clarify the essential ingredients for high-T_c in the FeSCs.

To resolve this question, we grew $Rb_xFe_ySe_{2-z}S_z$ single crystals and utilized neutron scattering and angle resolved photoemission spectroscopy (ARPES) to identify complex phases and parameterize magnetic interactions. The main results are as follows:

- Discovery of a stripe antiferromagnetic (AF) phase, with a similar magnetic structure to previously known FeSCs, demonstrating that high-T_c in FeSCs occurs universally in proximity to magnetism [3].
- Inelastic neutron scattering studies of this stripe AF phase revealed a completely localized spin configuration S = 2, whose magnetic interactions are comparable to those in the itinerant iron pnictides [3].
- ARPES further revealed a large gap at the Fermi level which, combined with the finding of localized spin, demonstrates that the stripe phase is a Mott insulator—the first case found in the FeSCs. Hence, we have shown that high-T_c occurs in a regime of strong correlations in the FeSCs [4].
- ARPES measurements on $Rb_xFe_2Se_{2-z}S_z$ as a function of *z* showed that the evolution from superconducting $Rb_{0.8}Fe_2Se_2$ with T_c = 32 K to non-superconducting $Rb_{0.8}Fe_2S_2$ is accompanied by a dramatic decrease in electronic correlations [5].

Summarizing these results, we have arrived at a coherent overall phase diagram where the high-T_c phase of $Rb_xFe_2Se_2$ becomes a Mott insulator with increase of Fe vacancies and a non-superconducting metal with substitution of S for Se. These results demonstrate that the $Rb_xFe_ySe_{2-z}S_z$ family of materials lies in a moderate to strongly correlated regime situated between the more itinerant iron pnictides and the doped Mott insulators of the copper-based high-T_c superconductors.

Future research: We will study the role of Rb in the $Rb_xFe_ySe_{2-z}S_z$ system (with $y = 2$). The results will establish a phase diagram that connects FeSe and $Rb_{0.8}Fe_2Se_2$ superconductors, thus completing the multidimensional phase diagram in the space of *x, y,* and *z.* In addition we will study the $Rb_xFe_2Se_{2-z}Te_z$ system. As suggested by our ARPES measurements on the $Rb_xFe_2Se_{2-z}S_z$ samples, Te substitution will further enhance electronic correlations and may result in a spin-density-wave state. If so, we will establish a universal phase diagram that connects the iron chalcogenide system with the iron pnictide and copper-based superconductors.

References

[1] S. Kasahara et al. Nature 486, 382 (2012).
[2] E. Thewalt et al. arxiv: http://xxx.lanl.gov/abs/1507.03981
[3] M. Wang et al., Phys. Rev. B 90, 125148 (2014).
[4] M. Wang et al., Phys. Rev. B 92, 121101(R) (2015).
[5] M. Yi et al., arXiv:1505.06636.

Publication List (14 selected from total of 31 primary publications for 2014-2015)

1. Itamar Kimchi, James G. Analytis, and Ashvin Vishwanath, "Three-dimensional quantum spin liquids in models of harmonic-honeycomb iridates and phase diagram in an infinite-D approximation," Phys. Rev. B 90, 205126 (2014).
2. Jun Zhao, Yao Shen, R. J. Birgeneau, Miao Gao, Zhong-Yi Lu, D.-H. Lee, X. Z. Lu, H. J. Xiang, D. L. Abernathy, and Y. Zhao, "Neutron scattering measurements of spatially

anisotropic magnetic exchange interactions in semiconducting $K_{0.85}Fe_{1.54}Se_2$ (T_N=280 K)," Phys. Rev. Lett. 112, 177002 (2014).
3. K. A. Modic, Tess E. Smidt, Itamar Kimchi, Nicholas P. Breznay, Alun Biffin, Sungkyun Choi, Roger D. Johnson, Radu Coldea, Pilanda Watkins-Curry, Gregory T. McCandless, Julia Y. Chan, Felipe Gandara, Z. Islam, Ashvin Vishwanath, Arkady Shekhter, Ross D. McDonald and James G. Analytis, "Realization of a three-dimensional spin–anisotropic harmonic honeycomb iridate," Nature Communications 5, 4203 (2014).
4. R. Ramesh, "Electric field control of ferromagnetism using multi-ferroics: the bismuth ferrite story," Philosophical Transactions of the Royal Society A-Mathematical Physical and Engineering Sciences, 372, 1364-503X, 1471 (2014).
5. X. Marti, I. Fina, D. Yi, Jian Liu, J.-H. Chu, C. Rayan-Serrao, S. Suresha, J. Železný, T. Jungwirth, J. Fontcuberta, R. Ramesh, Anisotropic magnetoresistance in antiferromagnetic semiconductor Sr_2IrO_4 epitaxial heterostructure," Nat. Commun. 5, 4671 (2014).
6. Wentao Zhang, Choongyu Hwang, Christopher Smallwood, Tristan Miller, Gregory Affeldt, Koshi Kurashima, Chris Jozwiak, Hiroshi Eisaki, Tadashi Adachi, Yoji Koike, Dung-Hai Lee**,** and Alessandra Lanzara, "Ultrafast quenching of electron-boson interaction and superconducting gap in a cuprate superconductor," Nat. Comm. 5, 4959 (2014).
7. R. Vasseur, J. P. Dahlhaus, and J. E. Moore, "Universal nonequilibrium signatures of Majorana zero modes in quench dynamics," Phys. Rev. X 4, 041007 (2014). A. Biffin, R.D. Johnson, I. Kimchi, R. Morris, A. Bombardi, J.G. Analytis, A. Vishwanath, R. Coldea, "Non-coplanar and counter-rotating incommensurate magnetic order stabilized by Kitaev interactions in γ-Li_2IrO_3," Phys. Rev. Lett. 113, 197201 (2014).
8. J. P. Hinton, S. Patankar, E. Thewalt, A. Ruiz, G. Lopez, N. Breznay, A. Vishwanath, J. Analytis, and J. Orenstein, J. D. Koralek, I. Kimchi, "Photoexcited states of the harmonic honeycomb iridate γ–Li_2IrO_3," [Accepted Phys. Rev. B].
9. Shudan Zhong, Joseph Orenstein, and Joel E. Moore, "Optical gyrotropy from axion electrodynamics in momentum space," Phys. Rev. Lett. 115, 117403 (2015).
10. Meng Wang, Ming Yi, Huibo Cao, C. de la Cruz, S.K. Mo, Q.Z. Huang, E. Bourret-Courchesne, Pengcheng Dai, D.H. Lee, Z.X. Shen and R. J. Birgeneau, "Mott localization in a pure stripe antiferromagnet $Rb_{1-x}Fe_{1.5-y}S_2$," Phys. Rev. B, 92, 121101(R) (2015).
11. Meng Wang, P. Valdavia, Ming Yi, J.X. Chen, W.L. Zhang, R.A. Ewings, T.G. Perring, Yang Zhao, L.W. Harriger, J.W. Lynn, Pengcheng Dai, D.H. Lee, D.X. Yao, and R.J. Birgeneau, "Spin waves and spatially anisotropic exchange interactions in the S=2 stripe antiferromagnet $Rb_{0.8}Fe_{1.5}S_2$," Phys. Rev. B, 92, 041109(R) (2015).
12. Itamar Kimchi, Radu Coldea, and Ashvin Vishwanath, "Unified theory of spiral magnetism in the harmonic-honeycomb iridates α, β, and γ Li_2IrO_3," Phys. Rev. B 91, 245134 (2015).
13. Tristan L. Miller, Minna Arrala, Christopher L. Smallwood, Wentao Zhang, Hasnain Hafiz, Bernardo Barbiellini, Koshi Kurashima, Tadashi Adachi, Yoji Koike, Hiroshi Eisaki, Matti Lindroos, Arun Bansil, Dung-Hai Lee, and Alessandra Lanzara, "Resolving unoccupied electronic states with laser ARPES in bismuth-based cuprate superconductors," Phys. Rev. B 91, 085109 (2015).
14. Romain Vasseur and Joel E. Moore, "Multifractal orthogonality catastrophe in one-dimensional random quantum critical points," Phys. Rev. B 92, 054203 (2015).

Program Title: Nanostructured Materials: From Superlattices to Quantum Dots
PI: Ivan K. Schuller
Mailing Address: Physics Department, University of California-San Diego, La Jolla, Ca. 92093
E-mail: ischuller@ucsd.edu

Program Scope

The research performed under this grant relates to a number of current forefront research areas in nanomagnetism including: proximity effects between dissimilar materials, spin diffusion in non-magnetic materials and effect of nanostructuring in 1-3 dimensions on the properties of novel magnetic materials. This is a comprehensive study all the way from preparation, structural and chemical characterization and study of physical properties both in the lab of the PI and at major DOE funded facilities. Our results have shown that the invariably-present defects play a major role and therefore they have to be taken into consideration to understand the physical properties. We investigate a wide range of materials systems including elements, oxides, fluorides, and organics and perform detailed research to cover all aspects of research.

Recent Progress

During the last period we had major advances in several diverse material systems, published in the first-rate refereed literature, were recognized by major invitations at international scientific meeting. One of our accomplishments was recognized on the DOE Web site as the February 2015 highlight. This relates to the discovery of a Giant Enhanced Coercivity in Ferromagnetic-Oxide Heterostructures as illustrated in the figure below

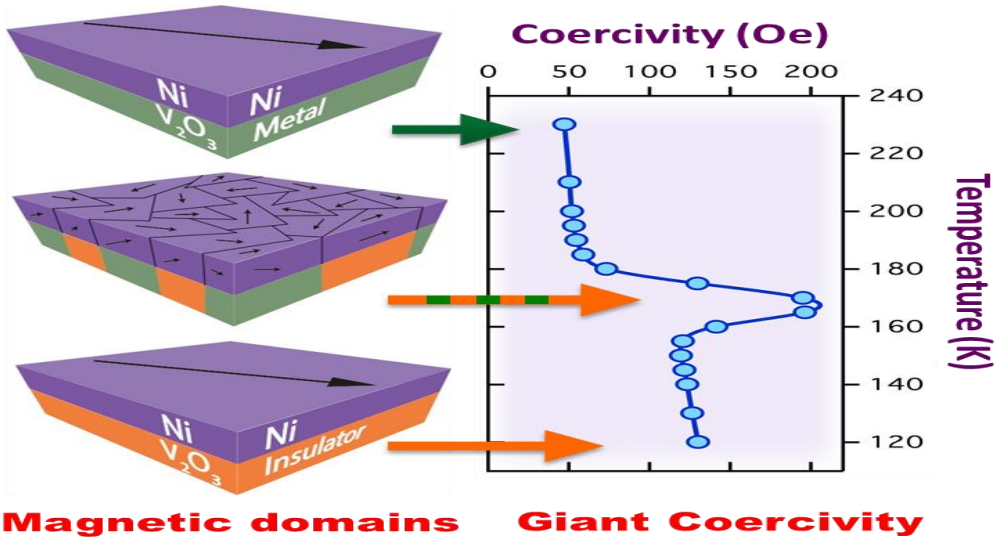

Figure 1. The magnetic coercivity, the resistance to change in the orientation of the magnetic domain structure for nickel (Ni), depends strongly on the crystal structure of the underlying oxide (vanadium oxide, V_2O_3) material. The maximum Ni coercivity occurs at the peak of the oxide's metal insulator transition.

Novel effects are increasingly being discovered when dissimilar materials are in contact ("hybrids"), often resulting in altogether new phenomena, materials with useful functionalities or the ability to sense or control important material properties. The focus of this investigation is a hybrid material consisting of a thin nickel (Ni) film on a vanadium oxide substrate which exhibits interesting and unusual magnetic properties unlike any other magnetic material. In this case, the magnetic coercivity of the nickel reveals insights concerning the metal-insulator transition of the vanadium oxide. In turn, the metal-insulator transition can be used to control the coercivity of the nickel. The vanadium oxide undergoes a (metal-insulator, MIT) transition from being an electrical conductor to becoming an insulator, which is coincidental with a structural change at a well-defined "transition" temperature. At the thermal midpoint of the transition, crystallites of both phases coexist in equal portions, resulting in maximal structural entropy. The oxide inhomogeneously stresses a Ni (or other magnetic) film deposited on top. This provides a strong link between the Ni coercivity and the disorder in the oxide. The coercivity is low when the oxide is structurally uniform (above and below the MIT) and high when it is maximally disordered in the middle of the transition. The magnetic properties of Ni therefore provides a window into the MIT process and in turn the MIT allows dramatic nonmagnetic control of the coercivity, which changes by several hundred percent within a narrow 10 K temperature range, unlike any other known magnetic material. Potential applications have been envisioned in two important, disparate energy related fields: as functional material for energy driven magnetic recording and self-healing current fault limiters.

Additional accomplishments from this research are extensively discussed in the manuscripts. Here we only include a brief description of the most important results:

a) We have performed extensive studies of proximity effects between ferromagnets and; oxides, fluorides or superconductors. These studies were performed in a variety of configuration including thin films and nanostructures.

b) Studies of the proximity effect between oxides and ferromagnetic materials have a produced a series of well recognized results. We developed a novel way of tuning the magnetic properties of magnetic materials by using the proximity effect between a ferromagnet and the structural phase transitions in Vanadium oxides. This has led to the discovery a Giant Enhanced Coercivity, a unique property unlike found in any other known magnetic material. This also showed that the creative use of intrinsic and extrinsic defects could lead to new functionalities and properties that do not exist in nature.

c) Extensive studies of Exchange Bias in a Ferromagnet (FM)/Antiferromagnet(AFM) fluoride showed that the magnetic structure along the ferromagnet plays a crucial role, unlike it was believed in the field for many years.

d) We used X-ray photoemission electron microscopy to show that a progressive spatial confinement of a FM, either through thickness variation or laterally via

patterning, actively controls the domains of uncompensated spins in the antiferromagnet (AF) in exchange biased systems.

e) We developed a novel laboratory based method for the detection of spin structure in magnetic hybrids. The planar Hall effect of nanostructured magnetic heterostructures contains striking information regarding the spin structure in the two constituents of the heterostructures. This combined with numerical calculations allows determining the magnetic structure of FMs when incorporated into an Exchange Biased configuration.

f) We performed extensive studies to investigate the magnetic properties and transport at the nanoscale of several metallo-phthalocyanines. We found an anomalous quadrupolar signal in X-ray magnetic circular dichroism (XMCD) at the Fe K-edge of iron phthalocyanine (FePc). All ground states previously suggested for FePc are incompatible with this experimental data. Based on ab-initio molecular orbital multiplet calculations of the isolated FePc molecule, we proposed a new model for the magnetic ground state of the FePc, which explains the XMCD data and reproduces the observed values.

g) Our development of high quality FeF_2 films allowed studies of diffusion of Li in these materials. The phase evolution and morphology of the solid state FeF_2 conversion reaction with Li has was characterized using angle-resolved x-ray photoelectron spectroscopy (ARXPS). These measurements provide insight into the atomistics and phase evolution of high purity FeF_2 conversion electrodes without contamination from electrolytes and binders. These results partially explain the capacity losses observed in cycled FeF_2 electrodes.

Future Plans

a) We will perform dynamical studies of hybrid FM/Oxide heterostructures which have produced the Giant Enhanced Coercivity (GEC). Novel results are to be expected also in the properties of the magnons.

b) Based on our discovery of the GEC we will start research on the development of a novel type of hybrid multiferroic in which a magnetic field will strongly affect the transport properties of an oxide.

c) We will perform further studies at synchrotron and neutron facilities to map out the 3 dimensional spin concentration when magnetic and non-magnetic materials are in proximity. This will include, magnetic-normal, magnetic-oxide, etc. heterostructures in a variety of configuration. This will be done in collaborations with scientists at major DOE facilities.

d) Many of the development we had last year are in the form of preprints which require extensive modifications during the publication period. We will devote considerable attention to these publications.

Publications (acknowledging DOE support)

1. *Coupling of Magnetism and Structural Phase Transitions by Interfacial Strain*, T. Saerbeck, J. de la Venta, S. Wang, J.G. Ramirez, M. Erekhinsky, I. Valmianski and Ivan K. Schuller, J. Mater. Res. **29**, 2353 (2015)

2. *Proximity Effects and Vortex Dynamics in Superconducting Heterostructures*, S.J. Carreira, V. Bekeris, Y.J. Rosen, C. Monton and Ivan K. Schuller, Proc. LT27, **568**, 022008 (2014)

3. *Resolving Transitions in the Mesoscale Domain Configuration in VO_2 Using Laser Speckle Pattern Analysis*, Katyayani Seal, Amos Sharoni, Jamie M. Messman, Bradley S. Lokitz, Robert W. Shaw, Ivan K. Schuller, Paul C. Snijders, Thomas Z. Ward, Sci. Rep., **4**, 6259 (2014).

4. *Effect of Co substitution on the Magnetic and Electron-transport properties of Mn_2PtSn*, Y. Huh, P. Kharel, A. Nelson, V.R. Shah, J. Pereiro, P. Manchanda, A. Kashyap, R. Skomski, and D.J. Sellmyer, submitted to J Appl Phys D: Condensed Matter (2014).

5. *Quadrupolar XMCD at the Fe K-edge in Fe Phthalocyanine film on Au: an insight into the Magnetic Ground State*, Juan Bartolome, Fernando Bartolome, Adriana I. Figueroa, Oana Bunau, Ivan K. Schuller, Thomas Gredig, Fabrice Wilhelm, Andrei Rogalev, Peter Kruger, and Calogero R. Natoli, Phys. Rev. Lett, Accepted (2015).

6. *Exchange Bias Phenomenon: The Role of the Ferromagnetic Spin Structure*, R. Morales, Ali C. Basaran, J.E. Villegas, D. Navas, N. Soriano, B. Mora, C. Redondo, X. Batlle, Ivan K. Schuller, Phys. Rev. Lett. **114**, 097202 (2014).

7. *Detection of In-depth Helical Spin Structures by Planar Hall Effect*, Ali C. Basaran, R. Morales, S. Guenon, and Ivan K. Schuller, submitted to Appl. Phys. Lett. (2015).

8. *Synthetic Magnetoelectric Coupling in a Nanocomposite Multiferroic*, P. Jain, Q. Wang, M. Roldan, A. Glavic, V. Lauter, C. Urban, Z. Bi, T. Ahmed, J. Zhu, M. Varela, Q.X. Jia & M.R. Fitzsimmons, Sci. Rep., Accepted (2015).

9. *Cobalt Phthalocyanine-based Submicrometric Field-effect Transistors*, F. Golmar, P. Stoliar, C. Monton, I. Valmianski, Ivan K. Schuller, L.E. Hueso and F. Cassanova, Phys. Status Solidi A, **212**(3), 607-611 (2015).

10. *The Solid State Conversion Reaction of Epitaxial FeF_2(110) Thin Films with Lithium Studied by Angle-Resolved X-Ray Photoelectron Spectroscopy*, R. Thorpe, S. Rangan, R.A. Bartynski, R. Whitcomb, A.C. Basaran, T. Saerbeck and Ivan K. Schuller, submitted to Phys. Chem. Chem. Phys. (2015).

11. *Molecular Tilting and Columnar Stacking of Fe Phthalocyanine Thin Films on Au(111)*, F. Bartolome, J. Bartolome, O. Bunau, L.M. Garcia, C.R. Natoli, M. Piantek, J.I. Pascual, I.K. Schuller, T. Gredig, F. Wilhelm, and A. Rogalev, J. Appl. Phys. **117**, Accepted (2015).

Session IX

Program Title: Dissipative and fast-timescale phenomena in superconductors
Principle Investigator: Milind N. Kunchur
Institution: Dept. of Physics and Astronomy, University of South Carolina, Columbia, SC 29208
Email: kunchur@sc.edu

Program Scope

Many new effects and regimes unfold in superconductors as they are pushed to extreme and unprecedented conditions of electrical transport, such as power densities of $jE > 10\,\mathrm{GW/cm^3}$ and vortex velocities of $v_\phi > 10$ km/s. Furthermore some of these effects (such as formation of phase slip processes and the acceleration of superfluid) are time dependent on time scales such as quasiparticle-phonon energy relaxation time and the gap relaxation time. The goal of this project is to use time-correlated pulsed current-voltage signals to access these high-dissipation regimes and observe directly in the time domain the temporal unfolding of these phenomena on sub-nanosecond time scales. Besides their own novelty, these phenomena yield independent information on many key parameters and properties of the superconducting state (such as gap anisotropy, electron-phonon coupling, charge-carrier concentration, normal-state scattering rates, thermodynamic critical field, interface coherence length, normal-state resistivity below T_C, etc.) and define its practical limits for technological applications.

This project has led to the discovery of unanticipated new effects and regimes in superconductors (the hot-electron instability, flux fragmentation—a superconducting analog of the semiconductor Gunn-effect, and quenched flux dynamics in MgB_2) and has experimentally verified for the first time some long-standing theoretical predictions (e.g., free flux flow, current induced pair breaking in HTS, real-time superfluid ballistic acceleration, and—most recently—the Likharev vortex explosion phenomenon). This group is one of few in the world that investigates these classes of phenomena and the techniques developed are unique.
As a result, these studies have been carried out in only in a few materials, thus far, and we actively seek collaborations to explore new systems.

Recent Progress

Current induced pair breaking in the Bi_2Te_3/FeTe interfacial superconductor and other systems:
Along with T_C and the upper-critical magnetic field B_{c2}, the depairing (pair-breaking) current density j_d represents one of the principal critical parameters of a type II superconductor. Of the three, j_d is the most difficult quantity to measure and therefore has not been measured in the vast majority of superconductors. In earlier work, our group was the first to report a measurement of j_d in any HTS and in MgB_2, and provided the most complete test of theories over the entire temperature range. Besides determining j_d for its own sake, j_d in combination with B_{c2} provides a reliable transport based estimation of λ that is not vulnerable to errors arising from magnetism, which may affect magnetic-induction based methods for measuring λ. Furthermore, in combination with the normal-state resistivity ρ_n one can obtain the carrier concentration n, superfluid density n_s, and normal-carrier scattering time τ, which are invaluable in understanding newly discovered systems. Besides its immunity from magnetism, this transport based approach also has the advantage of requiring very small quantities of the material and hence is ideal for investigating dimensionally limited systems, such as superconductivity at interfaces.

In the past two years, we investigated current induced pair breaking in two electron-doped cuprate systems—infinite-layer $Sr_{1-x}La_xCuO_2$ (SLCO) films and $Nd_{2-x}Ce_xCu0_{4-\delta}$ (NCCO) films—and more recently in the Bi_2Te_3/FeTe system. The interface of the Bi_2Te_3/FeTe heterostructure represents the first realization of superconductivity at the interface between a topological insulator (Bi_2Te_3) and an iron-chalcogenide (FeTe), with neither parent material a superconductor by itself. Many questions remain about this system. While the cause of this interfacial superconductivity is not fully understood, earlier work by our collaborators (Prof. Sou's group in Hong Kong) suggested the possibility that the robust topological surfaces states (TSS) may be doping

the FeTe and suppressing the antiferromagnetism in a thin region close to the interface, thus inducing the observed 2D superconductivity. Indeed, their observations of certain signatures of the Berezinski-Kosterlitz-Thouless (BKT) transition (with T_{BKT} ≈ 10 K), a square-root temperature dependence of the parallel upper critical field, and other observations indicate that the 2D superconductivity resides in a 7 nm thick layer near the interface (also confirmed by our vortex explosion studies as discussed below). Through our j_d measurements and related transport studies, we were able obtain estimates of λ, n, τ, and the mean free path *l*. In particular we were able to show that *l* (= 4.2 μm) was much greater than the thickness *d* of the superconducting interface. This implies that scattering from the faces that bound the superconducting layer is of a specular nature or is time-reversal invariant if the TSS play some role in the induced interfacial superconductivity. Also the normal-state resistivity of $\rho_n(T \rightarrow 0) \sim 200$ nΩ-cm represents an extraordinarily conductive normal state for a superconducting system. These $\rho_n(T)$ plots for two Bi_2Te_3/FeTe samples are shown in Fig. 1.

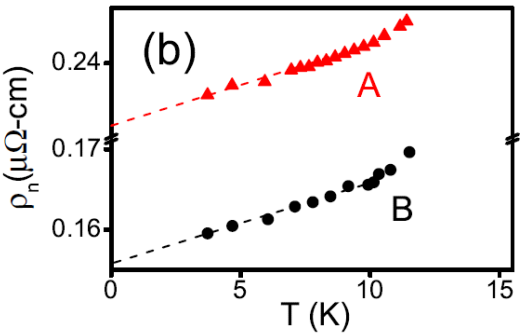

Fig. 1: *Intrinsic normal-state resistivity of the Bi_2Te_3/ FeTe topological-insulator/chacogenide interfacial superconductor obtained by destroying the superconductivity through current induced pair breaking (for two samples A and B). The normal state is unusually conductive for a superconductor.*

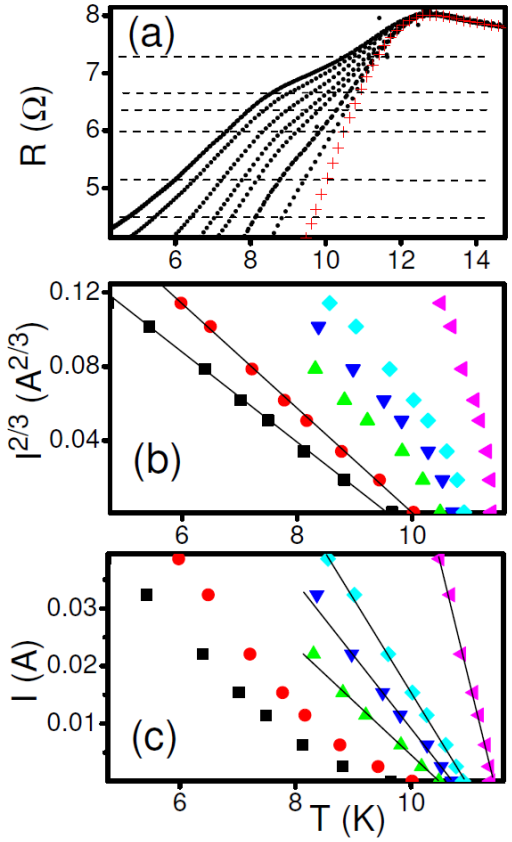

Figure 2: *(a) Resistive transitions for sample A in B=0 and various transport currents I; horizontal dashed lines show various resistance criteria R_C. (b) $I^{2/3}$ versus the T values where the curves in (a) intersect the R_C lines. (c) Same data plotted linearly as I vs T. In the limit of $R_C \rightarrow R_n$, we find that the steepest I vs T has an intercept of 0.23 A, in agreement with the theoretical estimate of 0.2A.*

The interplay between current-induced-pair-breaking and BKT behavior in Bi_2Te_3/FeTe leads to an interesting new cross over shown in Fig. 2. Panel (a) shows the resistive transitions in zero magnetic field at various applied transport currents. Panels (b) and (c) show graphs of the applied current *I* and its two-thirds power $I^{2/3}$ respectively; the abscissa shows the temperatures *T* where the *R(T)* curves in panel (a) intersect the horizontal dashed lines defining various resistance criteria R_C. The data follow the classic $I^{2/3} \alpha T$ depairing-current behavior below T_{BKT} (≈ 10 K) and a linear $I \alpha T$ behavior above T_{BKT}. A possible explanation for this is the following: With increasing current, resistance appears in a superconductor in zero external magnetic field chiefly through the two processes of pair breaking and vortices from the current's self field at the edges. This edge field (<10 mT) is dwarfed by B_{c2} and even exceeded by the lower critical field B_{c1} over most of the temperature range, so that pair breaking dominates over flux dissipation. As *T* is increased past T_{BKT}, the plasma of dissociated vortex-antivortex pairs suppresses the order parameter and reduces the threshold for self flux penetration. A rough estimate of the current level required for vortex penetration can be obtained from the energy balance between the work of the Lorentz force $\approx I\Phi_0 d/2w$ to form a vortex semi-loop of diameter *d* at the edge (*w* is the bridge width), and the corresponding self-energy of the vortex $\approx \Phi^2 d/4\pi\mu_0\lambda^2$. This leads to a linearly temperature dependent critical current: $I = I_0(1 - T/T_C)$ with $I_0 \approx w\Phi_0/2\mu_0\lambda^2(0) \approx 0.2$ A, in reasonable agreement with the observed intercept of 0.23 A (Fig. 2[c]).

The Likharev vortex core explosion:

The vortex-explosion effect, theoretically predicted by Likharev in 1979, was experimentally confirmed for the first time in any superconductor by our group in 2012 in amorphous MoGe films. More recently we observed it for a second time in the Bi_2Te_3/FeTe heterostructure. The gist of this effect is that when the sample dimension transverse to the vortex core is reduced, the circulating supercurrents get squeezed by the film surfaces causing the vortex core to become unstable and explode across the film thickness into a phase slip line. This explosion occurs when the thickness d falls below the critical value of $d = 4.4\xi(T_v)$, where T_v is the vortex-explosion temperature. In a thin-film bridge in B=0, a resistive state can arise from short vortices perpendicular to the film that are spontaneously generated by thermal fluctuations, either through the BKT unbinding of vortex-antivortex pairs in the interior or through the nucleation of single vortices at the film edge (unbinding from their antivortex images) as per the mechanism described by Gurevich and Vinokur (GV). For the geometry of our narrow bridges, the GV mechanism is favored over BKT. The presence/absence of parallel longitudinal vortex segments below/above T_v suppresses/facilitates the spontaneous generation of the perpendicular vortices. Thus the transition at T_v is reflected as a change in the *R(T)* characteristic, as can be seen in Fig. 3. Besides confirming the vortex explosion, we were also able to confirm details of the GV mechanism for the first time in that work (details are in reference 7.)

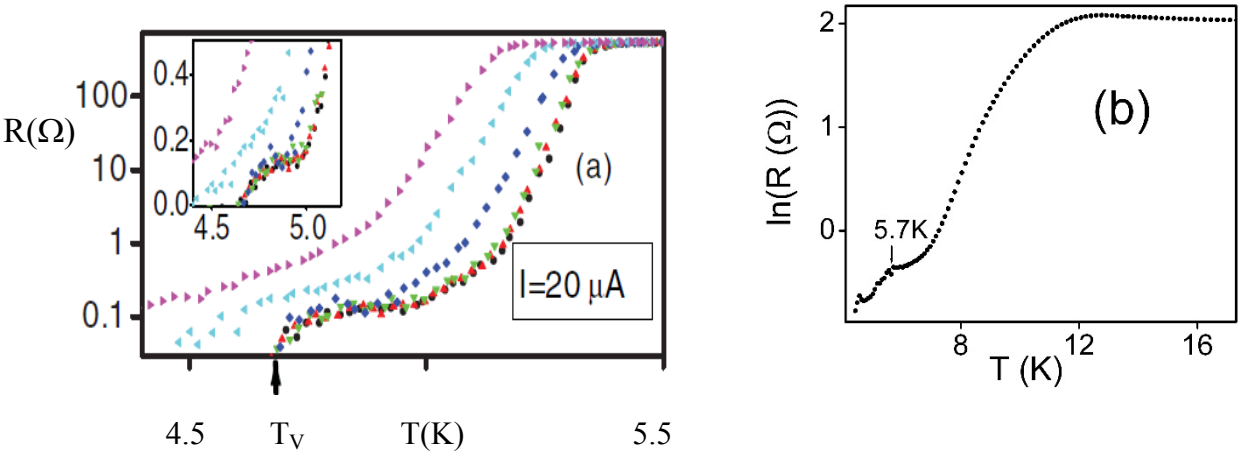

Figure 3: *Resistive transitions showing the vortex explosion feature—a "pause" in rising R(T) above a temperature T_V when $d = 4.4\xi(T_v)$. (a) MoGe microbridge in parallel fields B=0.05, 0.1, 0.2, 0.5, 0.8, 1.1T. (b) Bi_2Te_3/FeTe heterostructure in B=0; the inflection at 5.7K agrees with the $d = 4.4\xi(5.7)$ condition.*

Having tested the explosion concept and the critical condition $d = 4.4\xi(T_v)$ in MoGe—an amorphous isotropic system in which $\xi(T_v)$ is the same for both perpendicular and parallel orientations, and can be easily measured for the latter—this concept can now be applied to deduce d or ξ in situations when one of them is unknown. This was the case with the Bi_2Te_3/FeTe. Taking the d obtained from the parallel and perpendicular $B_{c2}(T)$ functions measured by He et al., our observation portrayed in Fig.3(b) can be taken as another confirmation of the explosion condition $d = 4.4\xi(T_v)$; on the other hand, assuming the condition to be true, our result can be taken as a second independent and valuable confirmation of the thickness d of the superconducting layer that forms at the interface of the heterostructure.

Future plans

The medium and long range future plans (full details are in the proposal) include the continued investigation of the vortex explosion, hot-electron flux instability and flux fragmentation, Cherenkov and phonon-spectrum effects in supersonic vortex motion, probing the nascent stage in vortex formation, gap anisotropy deduced through current induced pair breaking, and ballistic superfluid acceleration and superfluid suppression during acceleration. Some of the items in the above list represent new effects discovered or experimentally verified for

the first time by the PI's group in the past 10 years. Much work remains to be done as only a handful of groups around the world have repeated just a few of these experiments, and in only a limited number of materials. The initial observations were made—in some cases serendipitously—in less conventional systems; it is now worthwhile to better understand these phenomena by studying them in simpler low-T_C systems.

One near-term experiment is to study some of the above mentioned effects in NbTiN films (which we now have on hand) and other conventional superconductors. Another near-term (ongoing) experiment is the investigation of the in-plane anisotropy of the depairing current in the infinite-layer SLCO ($Sr_{1-x}La_xCuO_2$) system (Prof. Fruchter's group in France fabricated these samples). Earlier we attempted this experiment in YBCO ($YBa_2Cu_3O_7$) with mixed success—sample quality issues limited the accuracy of the data; however, that experiment did provide the confirmatory preliminary results shown in Fig. 4(a) (the theory predicts a $2^{1/2} = 41\%$ modulation with a 45° half-period, which is consistent with observations). Panels (b) and (c) show, respectively, the masks used for the experiment on YBCO and the ongoing experiment on SLCO. After completion in SLCO, the experiment will be redone in better quality YBCO and in newer systems whose symmetry is still unknown.

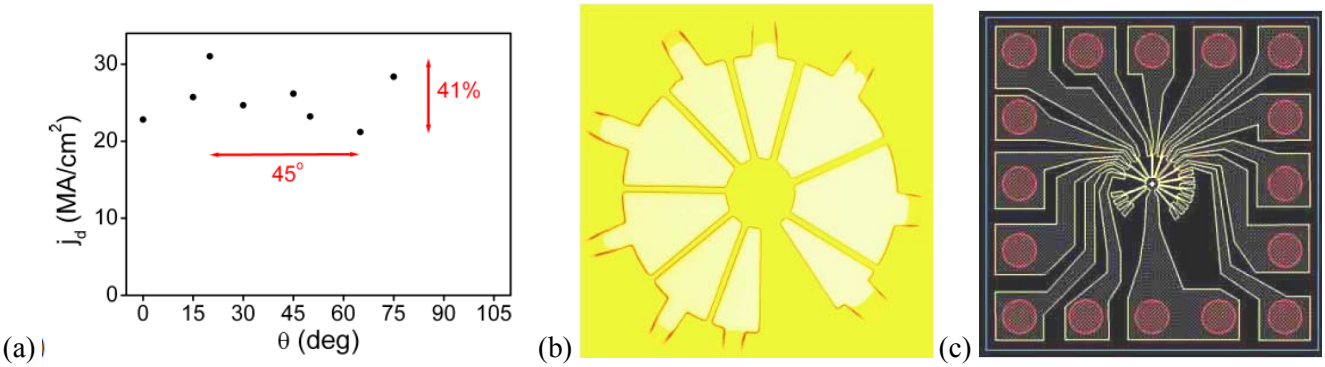

Figure 4: *(a) Preliminary j_d versus θ results on a YBCO film corresponding to the 8 bridges ("spokes of the wheel") shown in the photoresist mask in panel (b); although the data is noisy, minima and maxima appear to be separated by roughly 45°. (c) Lithography mask being used for the SLCO sample currently being measured.*

Besides the specific proposed experiments, discoveries of unexpected regimes and effects can expected because of the uncharted territories the measurements enter, as has been the case during the past history of this project.

DOE-BES sponsored references since 2012

1. *Current induced depairing in the Bi2Te3/FeTe interfacial superconductor*, M. N. Kunchur, C. L. Dean, N. Shayesteh Moghadam, J. M. Knight, Q. L. He, H. Liu, J. Wang, R. Lortz, I. K. Sou, and A. Gurevich, accepted for publication in Physical Reviw B (2015).
2. *Pinning mechanism in electron-doped HTS NdCe0CuO epitaxial films*, A Guarino, A Leo, G Grimaldi, N. Martucciello, C. Dean, M. N. Kunchur, S. Pace, and A Nigro, Supercond. Sci. Technol. 27, 124011 (2014).
3. *The mixed state in the confined geometry of parallel fields in thin films*, M. N. Kunchur, M. Liang, C. Dean, A. Gurevich, refereed book chapter in "Electron Correlation in Nanostructures"; Springer-Verlag, NATO Science Series; J. Bonca and S. Kruchinin (Eds.); 1st Edition, 2014.
4. *Depairing current density of Nd2-xCexCuO4-d superconducting films*, M. N. Kunchur, C. Dean, M. Liang, N. S. Moghaddam, A. Guarino, A. Nigro,G. Grimaldi, A. Leo, Physica C 495, 66 (2013).
5. *Depairing current density of infinite-layer Sr1-xLaxCuO2 superconducting films*, M. Liang, M. N. Kunchur, L. Fruchter, Z.Z. Li, Physica C 492, 178 (2013).
6. *The Vortex Explosion Transition,* M. N. Kunchur, M. Liang, A. Gurevich, AIP Conf. Proc. 1512, 19 (2013).
7. *Thermally activated dynamics of spontaneous perpendicular vortices tuned by parallel magnetic fields in thin superconducting films,* M. N. Kunchur, M. Liang, and A. Gurevich, Phys. Rev. B 86, 024521 (2012).

Program Title: Probing Strongly Correlated Materials with Magnetometry in Ultrahigh Magnetic Field

Program Investigator: Lu Li
Mailing Address: Department of Physics, University of Michigan, 450 Church St., Ann Arbor, MI 48105
Email: luli@umich.edu

Program Scope

The goal of the program is to investigate the high-field magnetic properties of strongly correlated materials. A good example of strongly correlated materials high temperature superconductors, in which strong electronic interaction makes the material conduct electricity without loss. High temperature superconductivity discovered in Fe-based [1, 2] and Cu-based materials [3] has been a treasure trove for condensed matter physicists. The relatively high transition temperature Tc, critical field, and critical currents indicate many possible applications in energy transfer and conservation. More importantly, the investigation of the origin of the superconductivity leads to various breakthroughs in fundamental physics. Currently, many key issues are under debate: for cuprates, whether they are a normal Fermi liquid with a hidden ordering state or an exotic phase coming out of a doped Mott Insulator; for Fe-based materials, what catches the essential physics in the parent compound - the "bad metal" seen in early discovered materials or the "Mott Insulator"? Direct answers to these questions will essentially determine the right approach to understanding the superconducting mechanism, i.e. whether it is a weak-coupling phenomenon or a strongly correlated effect. Moreover, in both cuprates and Fe-based materials, superconductivity arises by doping an antiferromagnetic state. Precise measurement of the magnetization M in ultrahigh magnetic fields will shed light on the magnetic ground state, the superconducting property, and the interaction between them.

To achieve the goal, torque magnetometry will be adapted to ultrahigh magnetic field up to 100 T in the pulsed magnetic field facilities in Los Alamos National Laboratory (LANL). Major challenges for research in the pulsed field facilities are 1) the vibrational and electrical noise, 2) difficulty stabilizing temperatures in elevated temperature ranges, and 3) short magnetic field pulses as narrow as milli-seconds. These conditions exclude some common approaches based on resonating oscillators or piezo resistors. Even the method using commercial capacitance bridge to track the cantilever deflection is challenging, since the measurement frequency of the commercial bridge is barely fast enough to catch the torque change in the milli-second pulse width. We propose several technical innovations to advance the high frequency capacitance bridge technique to precisely measure the magnetic torque in pulsed magnetic fields. The major innovations include, 1) home-built capacitance bridge working the best from 10 kHz to 10 MHz measurement frequencies, and 2) cold amplifier near the sample to eliminate the large shunt capacitance and to greatly enhance the bridge balancing signal.

Recent Progress

(1).Demonstrating the Dirac electronic surface states using quantum oscillations in topological Kondo insulator SmB_6. (Publication 1).

The discovery of topological insulators and possible topological superconductors opens a new area of study and brings hope to more exciting applications such as topological quantum computation. Strong electronic interaction usually prevents simple surface states from forming. However, on the surface of Kondo insulator Samarium Hexaboride SmB6, topologically protected surface states are predicted to exist as a result of a gap forming through the hybridization of the local orbital and the mobile electrons. The surface conductance has been demonstrated with non-local experiments in SmB_6. Our group has recently observed the dHvA effect in SmB6. The angular dependence of the oscillation period shows that the observed Fermi surfaces are two-dimensional, and exists on both the (101) surface and the (100) surface.

High-resolution torque magnetometry was used to measure the magnetic moment of the samples. Torque is measured by the change of the capacitance between a metal cantilever and a nearby metal plate. Using a rotator probe we were able to map the dHvA oscillation frequencies of SmB_6 as a function of angle. Our torque magnetometry is able to resolve the magnetic oscillation (de Haas – van Alphen effect). Using the 45 T hybrid magnet and a regular superconducting magnet, we mapped the angular dependence of the quantum oscillation frequencies. Fig.1 shows the Fast Fournier Transformation FFT spectra of the magnetic torque vs. 1/H curves of a single crystalline SmB6. Three set of Fermi surfaces and their higher harmonics are observed, and a strong angular dependence of oscillation frequencies indicates a strong anisotropy electronic state. Further analysis of the angular dependence shows that the frequencies are proportional to the inverse of sinusoidal functions, confirming the two-dimensional electronic state in SmB6.

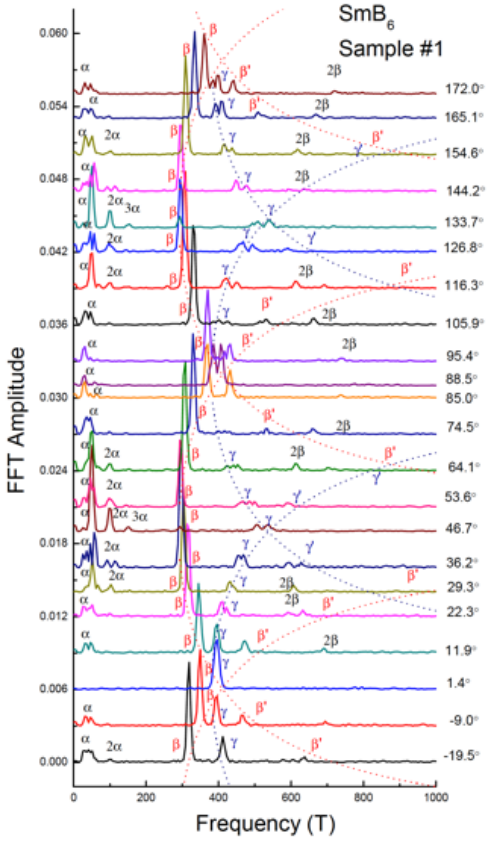

Fig. 1. The Fast Fourier Transformation (FFT) amplitude curves of the torque signal of SmB6 sample 1 at tilt angles expanding over 180 degrees. All the FFTs were taken on the torque curves measured in magnetic field up to 18 T at T = 300 mK.

Our result of resolving the Fermi surface is the first step to verify the topological nature of the Kondo insulator SmB6. We need to perform further tests to show the topological nature of the surface state. We have pushed the torque magnetometry measurement to 45 T to resolve the Landau level indexing plot. Like those in graphene and Bi2Te3, the interval of the index is about -1/2, which results from the Dirac nature of the electronic state.

An important aspect of these results is that we directly measured the magnetization of the single atomically layered surface states. Traditional experimental tools for studying surface states are photoemission, tunneling, and electrical transport. Thanks to our advanced magnetometry, we determined the magnetization of the surface state via torque for the first time. Our results open a new avenue for the detection of surface electronic states in novel materials.

(2). Revealing a charge-order-fluctuation transition in underdoped cuprate high temperature superconductors (Publication 2, preprint)

The magnetic torque of single crystalline high temperature superconductors $YBa_2Cu_3O_{6.55}$ (YBCO) samples were also measured using the 60 T pulsed-field solenoid at the Los Alamos National Laboratory. To eliminate torques induced by eddy currents, we fabricated insulating cantilevers with the bottom faces metalized for capacitive detection of the deflection. To make measurements within the pulse window of 100 msec, we built a capacitance bridge operating at a frequency of 20 kHz – 100 kHz.

An example of the magnetization curve taken on ortho- II YBCO is shown in Fig. 2. The torque curve at 4 K is plotted in comparison with that at 80 K, well above Tc. At T = 80 K the torque τ vs. magnetic field H curve is perfectly parabolic, reflecting the weak superconducting fluctuation diamagnetism at 80 K. By contrast, at T = 4 K, the sample is deep in the superconducting state. Below 20 T, we observed hysteresis caused by flux pinning. As shown in the insert in Fig. 2, the hysteresis ends at the melting field Hm ~20 T. At H > Hm, the τ −H curve at T = 4 K is smaller than that at 80 K.

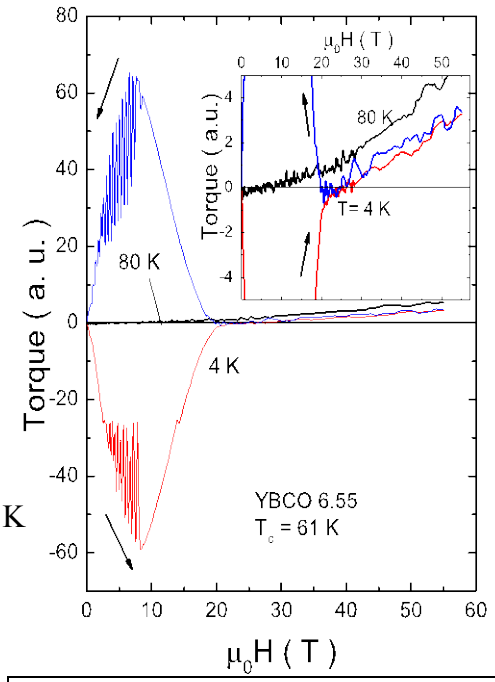

FIG. 2: Plots of the torque signal τ at 80 K and 4 K measured in ortho-II YBCO in a pulsed field up to 55 T, measured with θ ~10 degree. The curves of τ vs. H at 4 K is shown in red (H increasing) and blue (decreasing). Rapid oscillations below 10 T likely arises from collective flux motion. The trace at 80 K is shown in black. The insert displays the same data set in an expanded scale.

The difference between the torque curves at the two temperatures is the diamagnetic signal in vortex-liquid state. Furthermore, we observed that the torque signal shows a series of prominent spikes for H <10 T. These spikes may be caused by collective flux-bundle entry or exit (flux avalanches) within the vortex-solid state.

A detailed analysis shows that the measured M-H curves have a kink at H at ~ 15 T. We further carried detailed measurements of the diamagnetic signal Md using the 35 T DC magnetic field in National High Magnetic Field Laboratory (NHMFL). At low T, the kink signature of HK can be resolved in the differential susceptibility $\chi_d = dM_d/dB$. The curve of χ_d is initially featureless at 40 K. Below 40 K, a broad anomaly appears with a peak that grows with decreasing T. The peak occurs when the component of the field H equals 15 T. Such a kink feature in the magnetization, a thermodynamic measurement, suggests a magnetic-field-driven transition at a finite magnetic field around 15 T.

(3). High Field Magnetic Ground State of Kagome Lattice Spin Liquid Herbertsmithite (Publication 3)

An exciting field of modern condensed matter physics is the quantum spin liquid. The strong frustration leads to the lack of magnetic ordering and the emergence of novel physical phenomena in the ground state. Herbertsmithite $ZnCu_3(OH)_6Cl_2$ is a kagome lattice antiferromagnet with 1/2 spin and has been demonstrated to be a likely candidate of spin liquid by recent neutron scattering measurements. However, the direct determination of the magnetic

ground state at extremely low temperature has always been challenging because of two reasons: (a) The direct magnetization measurements are quite challenging to perform at extremely low temperatures; and (b) In the Zn plane, there are extra free Cu moments whose Curie-like paramagnetic signal dominates the magnetic response at low temperature. To solve the challenge, we applied torque magnetometry on single crystalline Herbertsmithite using high-resolution cantilever setups. Using high field torque magnetometry, we measured the angular dependence of the magnetic torque and the magnetization of Herbertsmithite at 20 mK < T < 40 K and in intense magnetic field. The intrinsic magnetization from the kagome lattice turns out to be linear with magnetic field, and the magnetic susceptibility is independent of temperature at 20 mK < T < 5 K.

Our results show that the high magnetic field phase of Herbertsmithite exists as a gapless spin liquid ground state. Such a state is not affected by the field-driven anomalies at 7 T – 15 T, which possibly originate from the interlayered Cu spins. Far from the gapped spin liquid state expected by theorists, our result is the first demonstration of the gapless spin liquid ground in Kagome-lattice quantum magnets.

Future Plans

We have succeeded in the magnetic torque measurement of copper oxide superconductors under a 60 T 200 ms generator-based magnet and a 65 T 20 ms capacitor-based magnet. We will continue our project measuring the magnetic torque of Fe-based superconductors using the same sets of magnets and extend our measurements to Copper oxide superconductors and topological Kondo insulator SmB_6. We will work to extend the ultrafast torque measurements under the 100 T pulsed magnet in LANL.

References

[1] Y. Kemihara et al. “Iron-based layered superconductors La[O1-xFx]FeAs (x = 0.05-0.12) with Tc = 26 K”, J. Am. Chem Soc. 103, 2396.
[2] X. H. Chen et al, “Superconductivity at 43 K in SmFeAsO1-xFx” Nature 453,761.
[3] Bednorz & Muller. “Possible High Tc Superconductivity in the Ba La Cu O System”, Z. Phys. B 64, 189.

Publications acknowledged the current DOE grant

1. G. Li, Z. Xiang, F. Yu, T. Asaba, B. Lawson, P. Cai, C. Tinsman, A. Berkley, S. Wolgast, Y. S. Eo, Dae-Jeong Kim, C. Kurdak, J. W. Allen, K. Sun, X. H. Chen, Y. Y. Wang, Z. Fisk and Lu Li "Two-dimensional Fermi surfaces in Kondo Insulator”. Science 346, 1208 (2014).
2. Fan Yu, Max Hirschberger, Toshinao Loew, Gang Li, Benjamin J. Lawson, Tomoya Asaba, J. B. Kemper, Tian Liang, Juan Porras, G. S. Boebinger, J. Singleton, B. Keimer, Lu Li, N. P. Ong "Diamagnetic response in under-doped YBa2Cu3O6.6 in high magnetic fields". arXiv:1402.7371. Nature Physics, under review.
3. Tomoya Asaba, Tian-Heng Han, B. J. Lawson, F Yu, C Tinsman, Z Xiang, G Li, Young S Lee, and Lu Li “High-field magnetic ground state in S=1/2 kagome lattice antiferromagnet ZnCu3(OH)6Cl2”. Physical Review B 90, 064417 (2014).
4. BJ Lawson, G Li, F Yu, T Asaba, C Tinsman, T Gao, W Wang, YS Hor, and Lu Li “Quantum oscillations in $Cu_xBi_2Se_3$ in high magnetic fields”. ”. Physical Review B 90, 195141 (2014).

Program Title: Exploring superconductivity at the edge of magnetic or structural instabilities

Principal Investigator: Ni, Ni

Mail: Department of Physics and Astronomy, 475 Portola Plaza, University of California, Los Angeles, 90024, CA

E-mail: nini@physics.ucla.edu

Project Scope:

Modern research of condensed matters devotes in understanding how properties of complex solids are determined by their structural and electronic degrees of freedom. Despite of the complicity in real materials where competing orders often exist, significant progress has been driven by the discovery of new materials with emergent ground states. The recent discovered Fe-based superconductors (FBS), together with the cuprates, are the only two high Tc superconducting families in the world. Although they differ in various ways, both of them are quasi two dimensional materials at the edge of structural/magnetic instabilities. The discovery and characterization of materials of this type can advance our understanding of high Tc superconductivity significantly. The objective of this research is to discover superconductors that lie at the edge of structural/magnetic instability using solid state reaction and crystal-growth methods, and to characterize them and examine their structure-property relations through thermodynamic, transport, X-ray, and neutron measurements.

Recent Progress:

1. We have successfully grown and characterized two new series of Fe-based superconductors, the Co and Ni doped 10-3-8 superconducting family. The structural/magnetic phase transitions in the parent compound were suppressed to lower temperature and superconductivity up to 15 K occurs. Single crystal quality has been significantly increased, indicating by a clear specific jump at Tc. The comparison between the two families shows rigid band approximation is applicable here. Tc is relatively lower in Ni doped 10-3-8, may be due to the strong impurity scattering from Ni atoms comparing to Co dopants.
2. We have successfully grown and characterized high quality single crystals of $Ca_{0.73}La_{0.27}FeAs_2$, the "parent" compound of the 112 superconducting family. The $Ca_{1-x}La_xFeAs_2$ (CaLa112) Fe based superconductors (FPS) shows the record bulk T_c up to 42 K in nonoxide FPS [1]. The breaking of C_4 rotational symmetry even at room temperature makes it unique among all FPS. The comparison of this CaLa112 with the other FPS will enable us to distill the important information on inducing high T_c. However, until now, no systematic study has been made on this system. Our comprehensive study of $Ca_{0.73}La_{0.27}FeAs_2$ single crystal established it is the parent compound of the CaLa112 FPS with structural/magnetic phase transitions. We unraveled the nature of both phase transitions and found a new stripe type magnetic structure.

What's more, by studying $Ca_{0.73}La_{0.27}FeAs_2$, we established that this CaLa112 family is characterized by the presence of metallic spacer layers and it is intrinsically structurally untwinned.

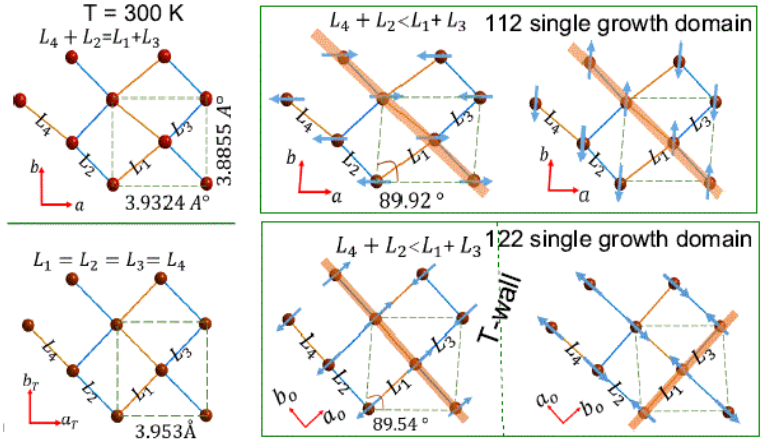

Electronic nematicity has been argued to exist in both cuprate and FBS, which lowers the rotational symmetry but keeps the translational symmetry. It has been argued to be the origin of the pseudogap in cuprate. In order to study the nematicity in FBS, uniaxial pressure/strain is usually used to detwin the sample. However, the external pressure itself already breaks the rotational symmetry, which has caused lots of debates on the origin of the observed in-plane anisotropy. The naturally detwinned 112 FBS provide a new avenue to examine the electronic nematicity in FBS. In addition, as the first tunable FBS with metallic layers, this material can also serve as a great platform to study the effect of metallic spacer layers on superconductivity.

The comparison of this material with the prototype 122 FPS is fruitful and revolutionary. The consensus of the Fe based superconductor is that the parent compound of the FPS is a semimetal with equal hole and electron carriers. The fact that the "parent" compound of CaLa112 is the apparently electron overdoped $Ca_{0.73}La_{0.27}FeAs_2$ is intriguing. A closer look into the ARPES data suggests a reasonable Fermi surface nesting exists in this electron-over doped material while the DMFT calculations indicate the Fermi surface nesting is enhanced when it is hole doped. This sheds light on the important role of both Fermi surface nesting and the superexchange interaction in the magnetism in FPS.

3. New 112 superconductors with Tc up to 20 K are discovered when Co substitutes Fe sites. This is a new route to realize SC in the 112 family. As the first controllable FPS with metallic spacer layers, we have systematically studied the $Ca_{0.73}La_{0.27}(Fe_{1-x}Co_x)As_2$ series using transport, thermodynamic and μSR measurements. The temperature-dopant phase diagram was mapped out where antiferromagnetism and superconductivity coexist at the underdoped region.
4. Elastic neutron scattering of $Ca_{0.73}La_{0.27}FeAs_2$ single crystals under magnetic field. Due to the existence of As chains in the crystal structure, this material is intrinsically structurally untwinned but magnetically "twinned" with spin rotation walls----this is unique in Fe pnictides. Without external field, a reasonable refinement of the single crystal neutron diffraction data requires two equal volumes with different spin orientations either along *a* or *b* axis. At 0.55T with the magnetic field along the *b* axis, our preliminary results show a reasonable refinement requires 86% of the volume with spin along the *a* axis and 14% of the volume with spins along the *b* axis. Therefore, external magnetic field can serve as an efficient way to wipe off S-walls in the CaLa112.

We also establish how large the external magnetic field is needed to wipe off the S-walls. This study provides the base of the future in-plane anisotropy study using external magnetic field.

5. We have tried to grow the $BaTi_2Bi_2O$ single crystals, which has CDW around 200 K and became SC at ~10 K when Na is doped. Although we failed in this trial, we discovered a new suboxide, $Ba_{1+\delta}Ti_{13-\delta}O_{12}$ ($\delta = 0.11$) [2]. It is a paramagnetic poor metal with hole carriers dominating the transport. Fermi liquid behavior appears at low temperature. The oxidization state of Ti obtained by the XAS is consistent with the metallic Ti^{2+} state. Local density approximation band structure calculations reveal the material is near the Van Hove singularity. The pseudogap behavior in the Ti-d band and the strong hybridization between the Ti-d and O-p orbitals reflect the characteristics of the building blocks of the Ti_{13} semi-cluster and the TiO_4 quasi-squares, respectively.

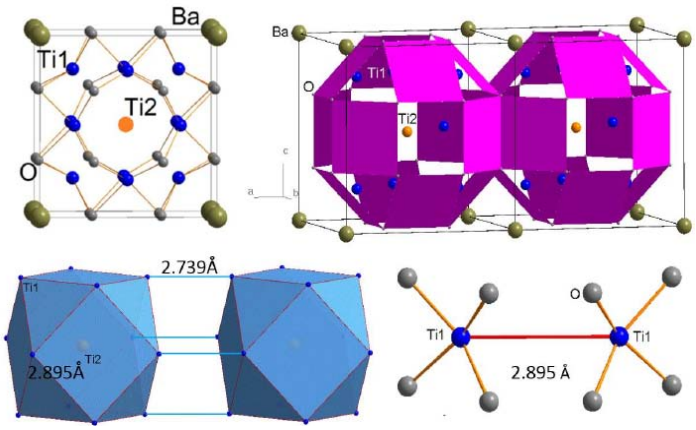

6. We have made high quality Cd_3As_2 sample for high pressure measurements [3]. Our collaboration with the high pressure group find that Cd_3As_2 undergoes a structural phase transition from a metallic tetragonal phase in space group I41/acd to a semiconducting monoclinic phase in space group P21/c at critical pressure 2.57 GPa, together with this structural phase transition, a metallic to semiconducting behavior is observed, indicating a breakdown of this 3D Dirac semimetal.
7. We have provided high quality $(Ca_{1-x}La_x)_{10}(Pt_3As_8)(Fe_2As_2)_5$ single crystals to study the doping-dependent superconducting gap structure by measuring the in-plane London penetration depth [4]. The gap is isotropic close to the optimal doping,—a trend commonly found in charge-doped FeSCs. While there is no evidence for the static microscopic coexistence of superconductivity and magnetism in the underdoped regime in this compound, the gap anisotropy increases dramatically in the underdoped regime which may suggest a possibility of either dynamic or much finer scale coexisting superconductivity and short-range magnetic correlations.

Future Plans:

1. The double doping study of $Ba(Fe_{1-x}Co_x)_2(As_{1-y}P_y)_2$. We will use Ba_2As_3 flux to grow single crystals of this kind to explore the quantum criticality of in this system. Transport and thermodynamic measurements will be performed.
2. The recent discovery of increased T_c in KFe_2As_2 under high pressure up to 20 Gpa has been argued to be due to the enhanced superconducting pairing in collapsed tetragonal FeAs phase. On the other hand, the collapsed tetragonal phase has been believed and proved to be harmful for spin fluctuation and thus superconductivity in $CaFe_2As_2$. Therefore, it is important to clarify the relation between superconductivity in collapsed

tetragonal phase. The $Na_{1-x}La_xFe_2As_2$ system has the potential to be a chemical-doping analog of the pressure-induced KFe_2As_2. We will grew single crystals and do systematic study of this series.

3. It has been a long-time debate if the magnetism in FBS is localized or itinerant. Recent study on the $Na(Fe_{1-x}Cu_x)As$ shows a Mott insulator phase at x=0.5 doping, providing strong evidence that FBS is near to Mott phase. We would like to investigate if this is in general for all FBS or just specific for NaFeAs system. We plan to study Cu doped 1038 to and use elastic neutrons scattering to study the possible magnetism inside.
4. The interplay between SC and magnetism in collapsed tetragonal phase in double doped $CaFe_2As_2$. $CaFe_2As_2$ is special in 122 because of the existence of collapsed tetragonal phase in it when chemical doping/pressure is applied, which is believed to be unfavorable for spin fluctuation and thus superconductivity. On the other hand, rare earth doped Ca122 shows trace superconductivity up to 45 K. We plan to use double doping trials to avoid the collapsed tetragonal phase and induced bulk superconductivity up to a record temperature.
5. The votex physics of 1038 FBS. As one of the most anisotropic FBS, the 1038 system is the only one that sizable single crystals can be obtained. We plan to study the vortex physics of the Co, Ni and La doped 1038FBS. Optimal doped samples will be irradiated by heavy ions to examine to vortex physics and to measure how the critical current be enhanced by the irradiation.

References since 2014 which acknowledge DOE support:

1. Shan Jiang, Chang Liu, Huibo Cao, Turan Birol, Jared M. Allred, Wei Tian, Lian Liu, Kyuil Cho, Matthew M. Krogstad, Jie Ma, Keith Taddei, Makariy A. Tanatar, Ruslan prozorov, Stephan Rosenkranz, Yasutomo J. Uemura, Gabriel Kotliar, Ni Ni, Naturally structurally detwinned Fe pnictide superconducting family with metallic spacer layers, in review (2015) arxiv 1505:05881
2. Costel R. Rotundu, Shan Jiang, Xiaoyu Deng, Yiting Qian, Saeed Khan,David G. Hawthorn, Gabriel Kotliar and Ni Ni, Physical properties and electronic structure of a new barium titanate suboxide $Ba_{1+\delta}Ti_{13-\delta}O_{12}$ ($\delta = 0.11$), APL Mat. **3**, 041517 (2015) Activity supported by this award: bulk sample growth, structure determination, bulk transport and thermodynamic measurements.
3. Shan Zhang, Qi Wu, Leslie Schoop, Mazhar N. Ali, Youguo Shi, Ni Ni, Quinn Gibson, Vladimir Sidorov, Jing Guo, Yazhou Zhou, Peiwen Gao, Dachun Gu, Chao Zhang, Sheng Jiang, Ke Yang, Aiguo Li, Yanchun Li, Xiaodong Li, Jing Liu, Xi Dai, Zhong Fang, Robert J. Cava, Liling Sun, Zhongxian Zhao, Breakdown of Three-dimensional Dirac Semimetal State in pressurized Cd_3As_2, PHYSICAL REVIEW B 91, 165133 (2015)
4. K Cho, M A Tanatar, N Ni and R Prozorov, Doping-evolution of the superconducting gap in single crystals of $(Ca_{1-x}La_x)_{10}(Pt_3As_8)(Fe_2As_2)_5$superconductor from London penetration depth measurements, Supercond. Sci. Technol. 27 104006 (2014)

Program Title: Cold Exciton Gases in Semiconductor Heterostructures

Principle Investigator: Leonid Butov

Mailing Address: University of California San Diego, Department of Physics, 9500 Gilman Drive, La Jolla, CA 92093-0319

E-mail: lvbutov@physics.ucsd.edu

Program Scope

An indirect exciton, IX, is a bound pair of an electron and a hole confined in spatially separated quantum well layers. IXs form a well-controlled platform for studying collective phenomena in a system of cold bosons. Long lifetimes of IXs allow them to cool down to low temperatures below the temperature of quantum degeneracy. This gives an opportunity to realize cold excitons. IXs have built-in dipole moments and, as a result, interact repulsively. This leads to strong correlations in a dipolar matter of IXs. Due to IX dipole moments, IX energy can be controlled by voltage. This gives an opportunity to create potential landscapes for IXs by voltage. The long lifetimes allow IXs to travel over large distances before recombination. This gives an opportunity to study exciton transport by imaging spectroscopy. The spatial separation between an electron and a hole in IX and the suppression of exciton scattering in a coherent exciton gas result to the suppression of spin relaxation. This allows the realization of long-range spin currents. The goal of this project is to explore these properties of IXs for studying cold excitons in periodic potential landscapes and for studying spin-related phenomena in cold excitons.

Recent Progress (2013-2015)

IX Correlations [1]

We developed a method for determining correlations in a system of IXs. The method involves subjecting the IXs to a periodic electrostatic potential that causes modulations of the IX density and photoluminescence (PL). Experimentally measured amplitudes of energy and intensity modulations of exciton PL serve as an input to a theoretical estimate of the IX correlation parameter. We demonstrated a proof-of-principle of the method and found strong correlations in a dipolar matter of IXs [1]. This method of determining correlations in an interacting gas is general and can be applied for a variety of other systems that can be subjected to lattice potentials and whose spatially modulated parameters can be measured, e.g. electron layers and cold atoms.

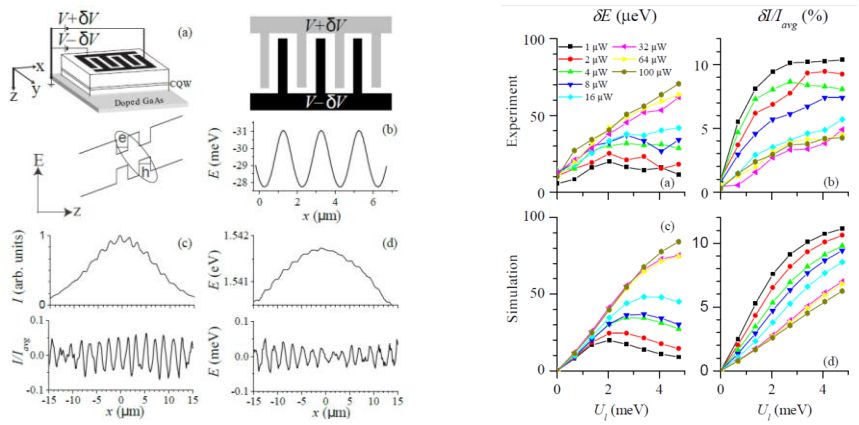

Fig. 1. Measurement of IX correlations using electrostatic lattices. Left: (a) CQW sample and its band diagram. (b) Voltage on interdigitated electrodes creates the lattice potential for IXs. (c,d) Measured PL intensity and energy profiles of IXs. The same data after subtraction of a smooth background are shown at the bottom. Right: Measured and simulated modulation of energy and PL intensity of IXs in a lattice vs the lattice depth for different excitation powers. From [1]

Stirring potential for IXs [2]

We demonstrated experimental proof of principle for a stirring potential for IXs. The azimuthal wavelength of this stirring potential is set by the electrode periodicity, the amplitude is controlled by the applied AC voltage, and the angular velocity is controlled by the AC frequency [2]. Stirring potentials can be used for studying rotating exciton matter.

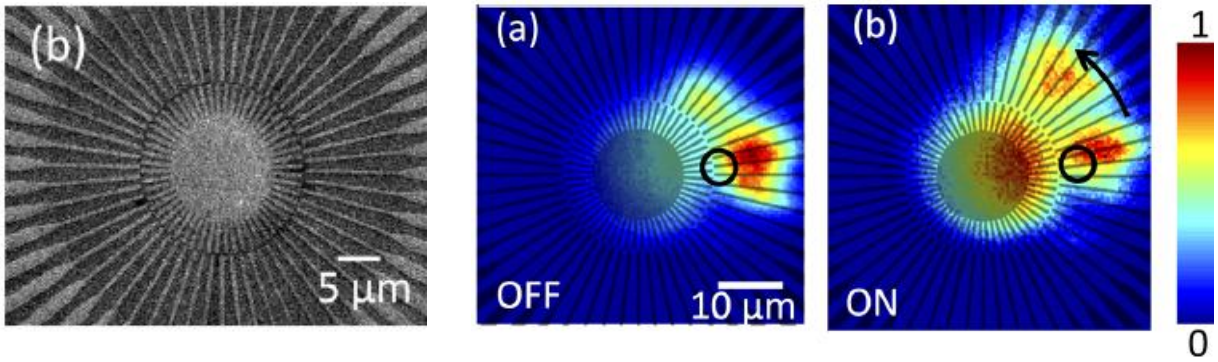

Fig. 2. Stirring potential for IXs. (left) SEM image of the electrode pattern forming the stirring potential for IXs. (right) x–y emission images of IXs with AC voltage off and on. Arrow indicates the rotation of the exciton cloud by stirring potential. Black circles show the excitation spot. From [2].

Nonlinear optical spectroscopy of IXs [3,4].

We proposed [3] and experimentally demonstrated [4] how nonlinear optics can be applied for studies of IXs with vanishing oscillator strength. The performed photoinduced reflectivity and Kerr rotation experiments unraveled spin dynamics of IXs. The experiments showed that spin relaxation time of IXs exceeds one of direct excitons by two orders of magnitude.

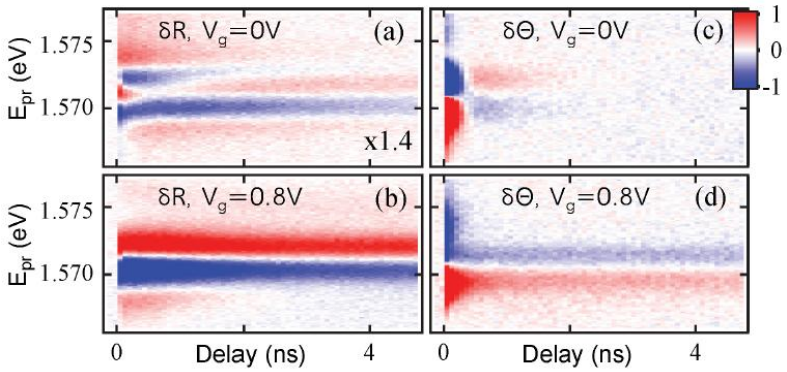

Fig. 3. Nonlinear optical spectroscopy of IXs. Photoinduced reflectivity (a, b) and Kerr rotation (c, d) measured as a function of the pump-probe delay and probe energy in the direct (a, c) and indirect (b, d) regimes. From [4].

Spin currents and spin textures in a coherent IX gas [5,6].

We detected long-range spin currents in a coherent gas of IXs [5]. The observed long-range spin currents originate from a suppression of spin relaxation in a coherent gas of IXs that gives a strong enhancement of electron and hole spin relaxation times. The spin currents result in the appearance of a variety of polarization patterns including helical, four-leaf, spiral, bell-shaped, and periodic patterns. The spin currents are controlled by a magnetic field. Simulations of coherent exciton spin transport describe the measured exciton polarization patterns [5,6].

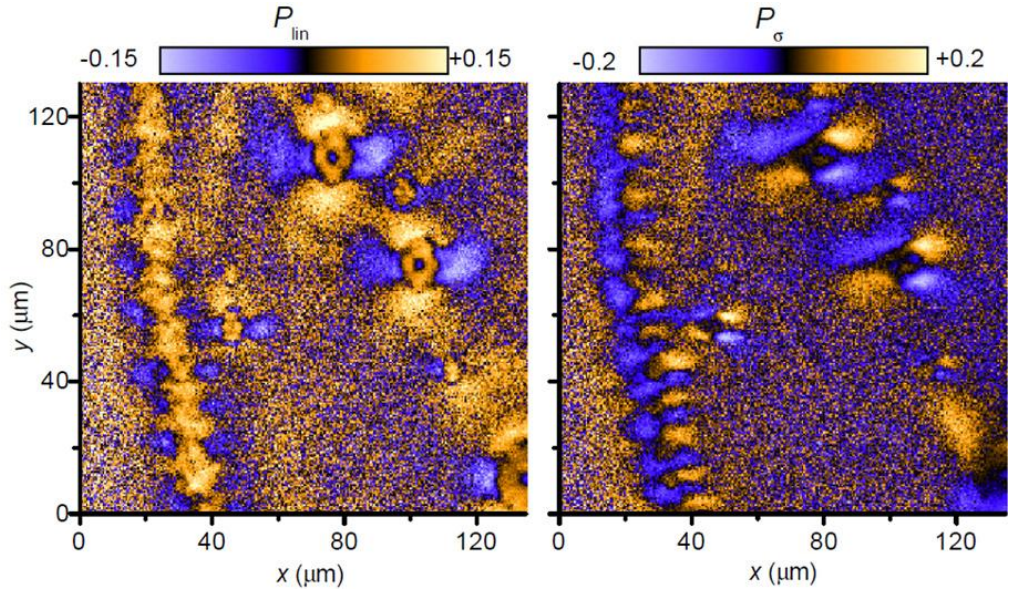

Fig. 4. Spin Currents in a coherent IX gas. Patterns of linear (left) and circular (right) polarization of the emission of IXs. The polarization patterns are associated with spin currents in a coherent IX gas. From [5].

Excitons in van der Waals heterostructures

The binding energies of excitons in van der Waals heterostructures composed of single-atomic-layers of transition metal dichalcogenides are much higher than in GaAs structures. This allows extending the operation of couple quantum well excitonic devices to high temperatures. We

studied excitons in a coupled quantum well van der Waals heterostructure based on single-atomic-layers of MoS2 and hBN. We studied control of the emission of neutral excitons and charged excitons, trions, by voltage, temperature, and helicity and power of optical excitation [work is prepared for publication].

Future Plans

We plan to study spin currents and spin textures in IXs by polarization-resolved imaging experiments. In recent experiments, we detected spin currents and spin polarization textures in optically generated IXs. The textures are observed in linear and circular polarizations and are controlled by magnetic fields. We plan to complete the experiments on spin textures and spin currents both for optically generated IXs and for IXs created from optically generated holes and electrically generated electrons and analyze the results. The long range spin currents appear in a coherent IX gas and we plan to analyze the relation between coherence and spin currents. We also plan to work on the development of control of the spin currents. We also plan to study coherence of IXs in lattices using shift-interferometry imaging and study the effect of the lattice potential on IX coherence.

Publications resulting from work supported by the DOE grant over the previous two years

1. M. Remeika, J.R. Leonard, C.J. Dorow, M.M. Fogler, L.V. Butov, M. Hanson, A.C. Gossard, Measurement of exciton correlations using electrostatic lattices, arXiv:1508.04407

2. M.W. Hasling, Y.Y. Kuznetsova, P. Andreakou, J.R. Leonard, E.V. Calman, C.J. Dorow, L.V. Butov, M. Hanson, A.C. Gossard, Stirring potential for indirect excitons, J. Appl. Phys. 117, 023108 (2015).

3. A.V. Nalitov, M. Vladimirova, A.V. Kavokin, L. V. Butov, N.A. Gippius, Nonlinear optical probe of indirect excitons, Phys. Rev. B 89, 155309 (2014).

4. P. Andreakou, S. Cronenberger, D. Scalbert, A. Nalitov, N.A. Gippius, A.V. Kavokin, M. Nawrocki, J.R. Leonard, L.V. Butov, K.L. Campman, A.C. Gossard, M. Vladimirova, Nonlinear optical spectroscopy of indirect excitons in coupled quantum wells, Phys. Rev. B 91, 125437 (2015).

5. A.A. High, A.T. Hammack, J.R. Leonard, Sen Yang, L.V. Butov, T. Ostatnický, M. Vladimirova, A.V. Kavokin, T.C.H. Liew, K.L. Campman, A.C. Gossard, Spin currents in a coherent exciton gas, Phys. Rev. Lett. 110, 246403 (2013).

6. A.V. Kavokin, M. Vladimirova, B. Jouault, T.C.H. Liew, J.R. Leonard, L.V. Butov, Ballistic spin transport in exciton gases, Phys. Rev. B 88, 195309 (2013).

Session X

Program Title: Digital Synthesis: A Pathway to New Materials at Interfaces of Complex Oxides

Principle Investigator : Anand Bhattacharya
Address: Materials Science Division, Bldg. 223, 9700 S. Cass Ave., Argonne National Laboratory, Argonne, IL 60657.
email: anand@anl.gov

***Program Scope*:**

In our program, we seek to create, characterize and understand superlattices and heterostructures of complex oxides with novel electronic and magnetic states. We synthesize these materials using oxide molecular beam epitaxy (MBE). This allows us to tailor chemically precise interfaces with roughness comparable to or less than the length scales for interfacial charge transfer and exchange interactions.

The complex oxides host a very diverse range of collective states of condensed matter. The richness of observed phenomena in these materials, which have also presented some of the greatest challenges to our understanding, are due to their strongly interacting degrees of freedom. Surfaces and interfaces between complex oxides provide a unique environment where these degrees of freedom may 'reconstruct' and lead to new properties that are qualitatively different from those of their bulk constituents. More specifically, we seek to discover and explore states with novel responses to external electric fields, thermal gradients and magnetic fields. We explore novel magnetic structures that arise as a result of charge transfer, electronic states that arise as a result of strong spin-orbit coupling, multiferroic heterostructures and non-collinear interfacial magnetic structures. We seek to explore materials that are known to have interesting phases where the atoms have been 're-arranged' in simple ways – for example by layering the cations in a manner such that the effects of disorder have been engineered away – to reveal new properties. We create these materials systems using ozone-assisted oxide MBE at Argonne, and characterize them using the major DOE facilities for neutron and photon scattering, and at the DOE Nanoscale Science Research Centers.

***Recent Progress* (since 2013):**

1. Tailoring polarity in a two-dimensional nickelate with single atomic layer control

Many of the 3*d* transition metal oxides share a common structural MO_6 building unit—a central transition metal (TM) cation octahedrally coordinated with oxygen nearest neighbors. The electronic states in these materials can be modified by tailoring the *M*-O bonds, which typically include the application of epitaxial strain in thin films, or pressure and isovalent cation substitution in bulk samples. We have found a new route to tailor the *M*-O bonds without changes to the strain state or stoichiometry in two-dimensional perovskite nickelate (n =1 in the Ruddlesden Popper (RP) series). We do this by tailoring the dipolar electrostatic interactions at the unit cell level in nominally non-polar $LaSrNiO_4$ via single atomic layer-by-layer synthesis using oxide-MBE. We can reconstruct the response of the crystal lattice to the induced polarity using an x-ray phase retrieval technique (COBRA). We find that the response of the O anions to the resulting local electric fields distorts the *M*-O bonds, being largest for the apical oxygens (O_{ap}). It also alters the Ni valence. This structural control strategy has broad implications for tailoring electronic properties in oxides that are sensitive to the *M*-O_{ap} bond geometry (B. B. Nelson-Cheeseman et al., *Adv. Funct. Mater.* 2014).

2. Spin Seebeck Effect in Paramagnets and Antiferromagnets

We have developed a new approach for generating spin currents in *patterned* magnetic heterostructures via the Spin Seebeck effect (SSE). By using a microscale on-chip local heater, we are able to generate a large thermal gradient confined to the chip surface *without* a large increase in the total sample temperature (S. Wu et al., *Appl. Phys. Lett*. 2014; *J. Appl. Phys.* 2015). This approach allows the study of the Spin Seebeck effect at very low temperatures (even less than 1K), as the total heat load from the patterned heater wire can be readily handled by standard cryostats. Using this approach, we discovered a large spin Seebeck effect in paramagnetic oxide insulators $Gd_3Ga_5O_{12}$ (GGG) and $DyScO_3$ (DSO), where the signal grows strongly in magnitude below ~ 20K. (S. Wu et al., *Phys. Rev. Lett.* 2015) and also in antiferromagnetic insulators (S. Wu et al*., arXiv*:1509.00439). GGG is a classical spin liquid at low temperatures (<300 mK), and we have carried out SSE experiments in this regime as well, where we now have a complete picture of how the SSE evolves in high magnetic fields ($\mu_B B >> kT$) in a paramagnetic insulator. The techniques developed here can readily be extended to other geometrically frustrated spin systems.

3. *Tailoring magnetic and electronic states via charge transfer at interfaces*

In conventional semiconductors and metals, a mismatch between the chemical potential for charge carriers at an interface leads to charge transfer, interfacial electric fields and consequences such as band bending and Schottky barriers. In narrow band correlated insulators and metals derived from them, this charge transfer can have profound consequences. We investigated the interface between two very dissimilar perovskites, $LaMnO_3$ and $LaNiO_3$. $LaMnO_3$ is an antiferromagnetic orbital-ordered Mott insulator and $LaNiO_3$ is a paramagnetic metal. In superlattices of $(LaMnO_3)_2/(LaNiO_3)_2$, we demonstrated that charge transfer at the interface leads to a metal-insulator transition and changes in the magnetic properties as n is varied (J. Hoffman et al., *Phys. Rev*. B 2013). The mechanism behind the metal insulator transition, which involves a transfer of spectral weight away from the Drude peak, was further elucidated in measurements of optical conductivity of these superlattices by our collaborators (P. Di Pietro et al., *Phys. Rev. Lett.* 2015). Charge transfer can also have a profound influence on properties of superlattices where both constituents are *metals*, due to the relatively large Thomas Fermi screening length in the 3*d* perovskite oxides. In superlattices of $(La_{2/3}Sr_{1/3}MnO_3)_9/(LaNiO_3)_n$ where both constituent materials are metals, we used neutron scattering and x-ray absorption spectroscopy to show that interfacial charge transfer leads to a *non-collinear* magnetic structure. Our data are consistent with the development of a spin-spiral within the $LaNiO_3$ layers. (J. Hoffman et al., *arXiv*:1411:4344). Measurements of the angular dependence of Nernst effect combined with anisotropic magnetoresistance data confirm the non-collinear magnetic structure measured using neutron scattering on the same samples. We also have ongoing collaboration with Prof. Jian-Min Zuo's group (UIUC) and with Dr. Albina Borisevich (ORNL) to understand how charge transfer might affect local electronic properties near these interfaces using transmission electron microscopy (STEM EELS).

***Future Plans*:**

a) *Tailoring M-O_{ap} bond lengths:* Motivated by our results in the past few years, we have plans to create and explore a number of materials systems using the synthesis approach that has been outlined earlier. In the cuprates, we will tailor the Cu-O_{apical} bond length[1] in a systematic way using dipoles and electrostatics and explore changes in properties including possible changes in

T_c. In insulating single layer RP aluminates, there is a prediction[2] of a very large (>200%) change in the optical bandgap in polar cation ordered analogs where the Al-O_{ap} bond length, which we plan to explore.

b) *Interfacial Charge Transfer in 'Mott' materials:* Fermi-level mismatch and charge transfer should occur for a broad range of oxides, beyond the nickelate/manganite interfaces that we are currently exploring. A general understanding of what happens at such interfaces is lacking because the 3*d* transition metal oxides have narrow bands where the charge carriers are strongly correlated and the ideas of 'band bending' have to be considered in light of the dynamic nature of the bands, i.e. the sensitivity of the band structure to filling. More specific to our recent findings, we are interested in creating nanowires of $LaNiO_3$ and of $La_{2/3}Sr_{1/3}MnO_3/LaNiO_3$ bilayers where the spin-density wave like instabilities might manifest themselves, open gaps and create spatially modulated phases.

c) *Oxide MBE growth of* 4*d* and 5*d transition metal oxides*: We have set up a new oxide MBE system that will enable us to synthesize thin films and heterostructures of oxides incorporating 4*d* and 5*d* transition metals. The materials of interest include perovskite iridates, that have been the focus of much recent activity due to the interplay of spin-orbit coupling and Mott physics.[3] The spin Seebeck effect measurement techniques developed in our program will be extended to the 4*d* and 5*d* transition metal pyrochlores, where a number of novel ground states are found,[4] several of which may give rise to spin currents. Metallic 4*d* and 5*d* transition metal oxides may also be effective detectors of spin currents via the inverse spin Hall effect.

References

[1] "Band-structure trend in hole-doped cuprates and correlation with T_c max." Pavarini, E., et al. *Physical Review Letters* **87,** 047003 (2001).

[2] "Massive band gap variation in layered oxides through cation ordering", P. V. Balachandran and J. M. Rondinelli, *Nature Communications* **6**, 6191 (2015).

[3] "Novel J_{eff}= 1/2 Mott state induced by relativistic spin-orbit coupling in Sr_2IrO_4." B. J. Kim et al. *Phys. Rev. Lett.* **101,** 076402 (2008).

[4] "Magnetic pyrochlore oxides", J. S. Gardner, M. J. Gingras, & J. E. Greedan, *Reviews of Modern Physics* ***82,*** 53 (2010).

Publications **(supported by Department of Energy, Basic Energy Sciences, since 2013):**

P1. "Near-nanoscale-resolved energy band structure of $LaNiO_3/La_{2/3}Sr_{1/3}MnO_3/SrTiO_3$ heterostructures and their interfaces." Thaddeus J. Asel, Hantian Gao, Tyler J. Heinl, Drew Adkins, Patrick M. Woodward, Jason Hoffman, Anand Bhattacharya, and Leonard J. Brillson. *J. Vac. Sci. Tech. B* **33**, 04E103 (2015).

P2. "Spin Seebeck devices using local on-chip heating", S. M. Wu, F. Y. Fradin, J. Hoffman, A. Hoffmann, A. Bhattacharya, *J. Appl. Phys*. **117**, 17C509 (2015).

P3. "Paramagnetic Spin Seebeck Effect", S. M. Wu, JE Pearson, A Bhattacharya, *Phys. Rev. Lett.* **114**, 186602 (2015).

P4. "Spectral Weight Redistribution in $(LaNiO_3)_n/(LaMnO_3)_2$ superlattices from Optical Spectroscopy", P. Di Pietro, J. Hoffman, A. Bhattacharya, S. Lupi, A. Perucchi, *Phys. Rev. Lett.* **114**, 156801 (2015).

P5. "Spin waves in micro-structured yttrium iron garnet nanometer-thick films", M. B. Jungfleisch, Wei Zhang, Wanjun Jiang, Houchen Chang, J. Sklenar, S.M. Wu, J. E. Pearson, A. Bhattacharya, J. B. Ketterson, Mingzhong Wu, A. Hoffmann, *J. Appl. Phys.* **117,** 17D128 (2015).

P6. "Unambiguous separation of the inverse spin Hall and anomalous Nernst Effects within a ferromagnetic metal using the spin Seebeck effect" S.M. Wu, J. Hoffman, J.E. Pearson, A Bhattacharya, *Appl. Phys. Lett.* **105**, 092409 (2014).

P7. "Polar cation ordering: A route to introducing > 10% bond strain into layered oxide films", Brittany B. Nelson-Cheeseman, Hua Zhou, Prasanna V. Balachandran, Gilberto Fabbris, Jason Hoffman, Daniel Haskel, James M. Rondinelli, Anand Bhattacharya, *Advanced Functional Materials* **24** (2014).

P8. "Inductive crystal field control in layered metal oxides with correlated electrons", P. V. Balachandran, A. Cammarata, B. B. Nelson-Cheeseman, A. Bhattacharya and J. M. Rondinelli, *APL Materials* ***2,*** 076110 (2014).

P9. "Dynamic layer rearrangement during growth of layered oxide films by molecular beam epitaxy", June Hyuk Lee, Guangfu Luo, I-Cheng Tung, Seo Chang, Zhenlin Luo, Milind Malshe, Milind Gadre, Anand Bhattacharya, Serge Nakhmanson, Jeffrey Eastman, Hawoong Hong, Julius Jellinek, Dane Morgan, Dillon Fong, and John Freeland, *Nature Materials (*2014).

P10. "Correlating interfacial octahedral rotations with magnetism in $(LaMnO_{3+\delta})_N/(SrTiO3)_N$ superlattices." Xiaofang Zhai, Long Cheng, Yang Liu, Christian M. Schlepütz, Shuai Dong, Hui Li, Xiaoqiang Zhang, Chu Shengqi, Zheng Lirong, Zhang Jing, Zhao Aidi, Hong Hawoong, Anand Bhattacharya, James N. Eckstein, Changgan Zeng, *Nature Communications* **5,** 4283 (2014).

P11. "Oxygen-Vacancy-Induced Polar Behavior in $(LaFeO_3)_2/(SrFeO_3)$ Superlattices", Rohan Mishra, Young-Min Kim, Juan Salafranca, Seong Keun Kim, Seo Hyoung Chang, Anand Bhattacharya, Dillon D. Fong, Stephen J. Pennycook, Sokrates T. Pantelides, and Albina Y. Borisevich, *Nano Letters 14* , 2694-2701 (2014).

P12. "Magnetic Oxide Heterostructures", A. Bhattacharya and S.J. May, *Annual Review of Materials Research* **44**: 5.1 – 5.26 (2014).

P13. "Charge transfer and interfacial magnetism in $(LaNiO_3)_n/(LaMnO_3)_2$ superlattices", J. Hoffman, I. C. Tung, B. Nelson-Cheeseman, M. Liu, J. Freeland, & A. Bhattacharya, *Phys. Rev* B **88**, 144411 (2013).

P14. "Non-volatile ferroelastic switching of the Verwey transition and resistivity of epitaxial Fe_3O_4/PMN-PT (011)", Ming Liu, J. Hoffman, J. Wang, J. Zhang, B. Nelson-Cheeseman, A. Bhattacharya, *Scientific Reports* **3**, Article No. 1876 (2013).

Program Title: Establishing the Consequences of Intertwined Order Parameters in Spatially Modulated Superconductors

Principle Investigator: Gregory MacDougall; **Co-PIs:** Peter Abbamonte (8/1/2014-7/31/2015), Lance Cooper, Eduardo Fradkin, Dale Van Harlingen

Mailing Address: Department of Physics and Frederick Seitz Materials Research Laboratory, University of Illinois at Urbana-Champaign, 104 S. Goodwin Ave. Urbana, IL, 61801

Email: gmacdoug@illinois.edu

Program Scope:

The purpose of this project is to establish the generality and full implications of phase-sensitive coupling between charge and superconducting order parameters in materials exhibiting charge inhomogeneity. Specifically, we are seeking to first confirm experimentally a number of unique phenomena predicted by Berg *et al* [1,2] for the cuprate material $La_{2-x}Ba_xCuO_4$ (LBCO), commonly believed to contain such coupling [3,4], and then extend the work to include several other superconducting families. The long-term goal is to identify symmetry-based unifying principles, which might provide the foundation for a universal phenomenological theory, appropriate to describe to multiple families containing unconventional superconductivity.

To definitively address the question of whether coherent charge-SC coupling exists in superconductors, we are to carrying out a targeted search for these phenomena using a necessary complement of experimental techniques. This includes neutron scattering (**MacDougall**), x-ray scattering (**Abbamonte**), scanning SQUID microscopy (**Van Harlingen**), Raman scattering (**Cooper**), and Josephson interferometry (**Van Harlingen**). Experimental results are being interpreted in the context of the theoretic framework of **Eduardo Fradkin**, and used by him to develop a more general theory.

For maximal impact, we are choosing to focus our efforts on two specific material systems: the 214 - phase cuprates and the transition metal chalcogenides. Initial measurements are being performed on crystals of the prototypical system, LBCO, currently in our possession. To circumvent complications associated with the known `LTT' structural transition in the phase diagram of LBCO [5], we are also undertaking a focused effort to grow large, high-quality crystals of $La_{2-x-y}Eu_ySr_xCuO_4$ (LESCO), which contains similar charge and stripe order [6,7], but removes the obscuring effects of the LTT transition to higher temperatures. To complement these materials and broaden our scope beyond the cuprate superconductors, we are further growing crystals of doped $TiSe_2$, known to contain both charge density wave (CDW) order and superconductivity (SC) [8-10], while investigating crystals of similar systems which we have at our disposal.

Recent Progress

Search for Meissner subharmonics in $La_{2-x}Ba_xCuO_4$ and $NbSe_2$ with x-ray diffraction: One of the major goals of this project is to perform x-ray scattering studies of charge ordered superconductors to determine whether subharmonic charge order reflections, whose wave vector is half that of the primary reflections, appears below the zero-resistance SC transition. The existence of such reflections is allowed by symmetry from cubic terms in the Landau theory of charge ordered superconductors and, if observed, would be a powerful validation of the phase-sensitive coupling scenario of Berg et al. [1,2]. To search for these reflections, PI Abbamonte performed a low-temperature x-ray scattering measurement of the two charge ordered superconductors LBCO and $NbSe_2$ (Fig. 1). These measurements were performed on the A2 wiggler line at CHESS using a Huber diffractometer equipped with a Pilatus area detector, and a 4K closed-cycle cryostat, which is capable of cooling below the zero-resistance transition in both materials.

He successfully identified peaks in both materials associated with CDW order, but unfortunately did not find a subharmonic signal in either material. This allows us to put an upper limit on the strength of SC-CDW coupling. For reasons related to imperfect functioning of the beamline optics, the signal in both of these measurements was much lower than expected. We plan to repeat this measurement again under better conditions at Sector 4 at the Advanced Photon Source, where more signal is expected.

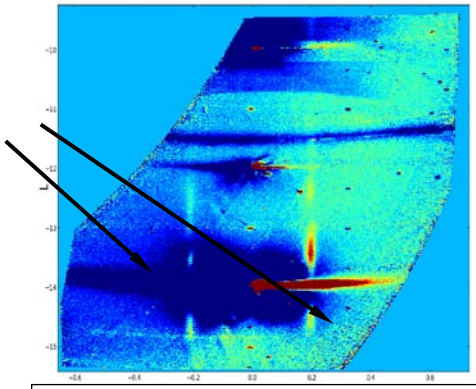

Figure 1: Reciprocal space maps of LBCO from x-ray diffraction measurements at T =6K. Arrows indicate the locations of the normal charge order reflections, which have been observed previously in both materials by many groups.

Raman scattering study of the pressure-tuned CDW-to-SC Transition in $ZrTe_3$: As part of our research into CDW-SC interactions in transition-metal chalcogenides, PI Cooper performed a detailed inelastic light (Raman) scattering study of the electronic and structural phases of $ZrTe_3$ as functions of temperature and pressure [9]. This study uncovered dramatic phonon linewidth changes that allowed for an identification of specific phonon modes that couple strongly to the electronic degrees of freedom and for a determination of electron-phonon coupling strengths through the temperature- and pressure-dependent phase changes in $ZrTe_3$. As a function of pressure, he also found evidence for a breakdown of coherence associated with the Te-Te shear phonon modes, suggesting that the one-dimensional Te-Te chains that support the CDW in $ZrTe_3$ lose their structural integrity with increasing pressure. The different pressure dependences of the "external" and "internal" phonon modes further provided structural evidence for pressure-induced 1D-to-3D dimensional crossover in $ZrTe_3$, revealing a distinct structural mechanism for the suppression of CDW behavior above 20 kbar and providing insights into the nature of pressure induced superconductivity in $ZrTe_3$.

Materials synthesis and initial growths of LESCO and $TiSe_2$ crystals: Our stated goal of establishing generality depends critically on the synthesis of appropriate model systems beyond LBCO, and growing large single crystals for further study. As such, PI MacDougall has spent several months establishing the groundwork for growing members of the two SC families mentioned above: LESCO and Cu_xTiSe_2. For LESCO, small amounts of powders were synthesized to explore the evolution of bulk properties with both Eu and Sr-doping, and multiple thermodynamic probes are being employed to establish modern phase diagrams. Growth of LESCO crystals have been pursued via the travelling solvent float zone technique, and after spending the requisite time determining growth conditions, large single (~1cm) crystals now exist at dopings above, near and below the x=1/8 anomaly. The growth of Cu_xTiSe_2 has been pursued via chemical vapor transport, and several large (~5mm) crystals exist of the parent material, $TiSe_2$. Intercalation with multiple different elements will be attempted in the coming year.

Growth of thin-films and characterization of their transport and noise properties: Although crystals of LBCO exist over a range of doping levels, a reliable process for controlling the doping of thin films has not been developed. This capability would be very helpful to this project, as many of the experiments necessary to characterize charge-SC coupling are more readily achieved on thin film samples, and epitaxy is an alternative method for suppressing unwanted structural transitions. Following up on this idea, PI Van Harlingen is growing thin films of LBCO and LESCO by Pulsed Laser Deposition (PLD), and characterizing them by a variety of spectroscopic probes (x-ray, AFM, SIMS), transport properties, and noise spectroscopy. Resistance noise measurements exhibit a change in the magnitude and spectrum at the charge ordering transition, a signature of stripe formation and dynamics. Further support for this picture comes from the observation that the resistance noise depends on the bias current as expected for alignment and/or pinning of the stripes. Plans are underway to study these films via Josephson

interferometry (Van Harlingen), x-ray scattering (Abbamonte) and neutron scattering (MacDougall) to establish stripe phenomenology and search for indications of a PDW state.

Development of theoretical underpinnings: PI Fradkin has made great progress in the theory of intertwined orders, which has resulted in the publication of a new review paper (coauthored with Prof. Steven Kivelson (Stanford) and Dr. John Tranquada (Brookhaven National Laboratory) [10]. In this paper, they articulate the notion that in a strongly correlated system, phases with intertwined orders are generic and arise for a large local energy scale (usually magnetism). The result is a complex phase diagram in which both uniform and inhomogeneous superconducting states (e.g. pair-density-wave (PDW) order) appear with critical temperatures of comparable scale for a wide range of microscopic parameters. Separately, he has solved explicitly models of strongly correlated systems which harbor such PDW states [8]. This includes a theory of one-dimensional systems (typically ladders) in which he showed not only that these states are present, but also, quite unexpectedly, that the PDW phases are topological SCs with protected Majorana edge modes. Fradkin further developed a quasi-1D theory of PDW superconductors [11]. The main result of this work is that these states, which cannot be derived using controlled approximations as conventional BCS superconductor, appear naturally in the strong correlation regime. A phase diagram was worked out using the dimensional crossover mean field theory.

Future Plans

Expanded crystal and thin film growth**:** Work by PI MacDougall to determined ideal growth conditions will lay the groundwork for production LESCO and Cu_xTiSe_2 crystals in the coming year with a wide range of dopings. Additionally, he is set to grow LESCO crystals enriched with Eu-153, allowing for the first neutron scattering studies of spin stripe order and dynamics in this compound. Likewise, work by PI Van Harlingen has determined best PLD growth conditions for LBCO and LESCO thin films, resulting in a number of samples spanning the 1/8 anomaly, and he has now turned to determining methods for better doping control. He further is developing a combinatorial PLD growth process to prepare a continuous range of Ba concentrations and techniques for probing doping-dependent transport properties-- this should enable us to explore carefully the properties of these samples close to the 1/8-anomaly.

Josephson interferometry experiments: Josephson interferometry is a key, phase sensitive technique which allows for determining both the symmetry of the SC order parameter, and also measuring the current-phase relation (CPR) of single junctions, in search of predicted 4π-periodic $\sin(2\phi)$-component for the PDW-state. PI Van Harlingen is fabricating Josephson junctions between conventional superconductors (e.g. Nb) and crystals/thin films of LBCO near x=1/8. These will then be used to measure the pairing symmetry of the SC order parameter via Josephson interferometry and the CPR of the hybrid junctions. The long-range plan is to characterize the CPR as a function of doping to assess the evidence for a PDW-state and its stability.

Scanning SQUID microscope (SSM): SSM imaging can identify the nucleation of half-quantum vortices at defects and interfaces that would provide a direct test of the 4e-superconductivity in the PDW-state. This is one of the central experiments in the original proposal for this project, and PI Van Harlingen is in the process of outfitting a cryogenic scanning system with a sub-micron scale SQUID detector capable of imaging vortices over a wide temperature range. Once operational, this system will be used to search LBCO and LESCO samples for half-quantum vortices and other magnetic structures at defects and interfaces, and to survey other materials considered PDW candidates.

Raman scattering studies of charge ordered superconductors: PI Cooper has made preliminary measurements of CDW order in $NbSe_2$, and will expand on these results to lower temperatures to observe the superconducting "Higgs" mode is this system. The goal is to study the interplay between superconductivity and CDW formation as he tunes the pressure and magnetic field, which has not been studied before. Cooper will perform similar measurements on LESCO, $TiSe_2$ under pressure and other

PDW candidate systems to compare with predictions for Higgs modes from Fradkin (see below).

Microscopic and phenomenological theories: In collaboration with a new postdoc, Dr. Yuxuan Wang and former post-docs Dr. Rodrigo Soto Garrido (now in Chile) and Dr. Gil Young Cho (KAIST, in Korea), PI Fradkin plans to look for tell-tale signatures of PDW order states, and of states in which PDW order coexists with uniform d-wave SC states. A current ongoing project involves looking for Higgs modes in both phases. This is an attractive direction of inquiry since the PDW state has two complex SC order parameters which when coexisting with the uniform d-wave SC state may increase to three Higgs-type modes, in contrast to conventional SC+CDW states, which have only one. These modes should be detectable in Raman scattering experiments, and will be compared to the results of Cooper.

References

[1] E. Berg, E. Fradkin, and S. A. Kivelson, Theory of the striped superconductor, Phys. Rev. B 79, 064515 (2009)

[2] E. Berg, E. Fradkin, S. A. Kivelson and J. M. Tranquada, Striped superconductors: how spin, charge, and superconducting orders intertwine in the cuprates, New Journal of Physics 11, 115004 (2009)

[3] Q. Li, M. Hücker, G.D. Gu, A.M. Tsvelik, and J.M. Tranquada, Two-dimensional superconducting fluctuations in stripe-ordered $La_{1.875}Ba_{0.125}CuO_4$, *Physical Review Letters* **99**, 067001 (2007).

[4] J.M. Tranquada, G.D. Gu, M. Hücker, Q. Jie, H.-J. Kang, R. Klingeler, Q. Li, N. Tristan, J.S. Wen, G.Y. Xu, Z.J. Xu, J. Zhou, and M.v. Zimmermann, Evidence for unusual superconducting correlations coexisting with stripe order in $La_{1.875}Ba_{0.125}CuO_4$, *Physical Review B* **78**, 174529 (2008)

[5] J. D. Axe, A.H. Moudden, D. Hohlwein, D.E. Cox, K.M. Mohanty, A.R. Moodenbaugh, and Y. Xu, Structural phase transformations and superconductivity in $La_{2-x}Ba_xCuO_4$, *Physical Review Letters* **62**, 2751 (1989)

[6] J. Fink, V. Soltwisch, J. Geck, E. Schierle, E. Weschke, and B. Buchner, Phase diagram of charge order in $La_{1.8-x}Eu_{0.2}Sr_xCuO_4$ from resonant soft x-ray diffraction, *Physical Review B* **83**, 092503 (2011

[7] H.-H. Klauss, W. Wagener, M. Hillberg, W. Kopmann, H. Walf, F. J. Litterst, M. Hücker, and B. Büchner, From antiferromagnetic order to static magnetic stripes: the phase diagram of $(La,Eu)_{2-x}Sr_xCuO_4$, *Physical Review Letters* **85**, 4590 (2000)

[8] E. Morosan, H. W. Zanderberg, B.S. Dennis, J. W. G. Bos, Y. Onose, T. Klimczuk, A. P. Ramirez, N. P. Ong and R. J. Cava, Superconductivity in Cu*x*TiSe2, *Nature Physics* **2**, 544 (2006)

[9] Y. I. Joe, X. M. Chen, P. Ghaemi, K. D. Finkelstein, G. A. de la Peña, Y. Gan, J. C. T. Lee, S. Yuan, J. Geck,, G. J. MacDougall, T. C. Chiang, S. L. Cooper, E. Fradkin and P. Abbamonte, Emergence of charge density wave domain walls above the superconducting dome in *1T*-$TiSe_2$, *Nature Physics,* **10**, 421 (2014)

[10]A. F. Kusmartseva, B. Sipos, H. Berger, L. Forro, and E. Tutis, Pressure Induced Superconductivity in Pristine 1*T*-TiSe2, *Physical Review Letters* **103**, 236401 (2009).

Sponsored Publications

[7] Krishna Kumar, Kai Sun and Eduardo Fradkin, "Chern-Simons theory of the magnetization plateaus of the spin-1/2 quantum XXZ Heisenberg model on Kagome Lattice," Physical Review B **90**, 174409 (2014).

[8] Gil Young Cho, Rodrigo Soto-Garrido and Eduardo Fradkin, "Topological Pair-Density-Wave Superconducting States". Physical Review Letters **113**, 256405 (2014).

[9] S.L. Gleason, Y. Gim, T. Byrum, A. Kogar, P. Abbamonte, E. Fradkin, G.J. MacDougall, D.J. Van Harlingen, C. Petrovic, and S.L. Cooper, "Structural contributions to the pressured-tuned charge-density-wave to superconductor transition in $ZrTe_3$: Raman scattering studies," Physical Review B **91**, 155124 (2015).

[10] Eduardo Fradkin, Steven A. Kivelson and John M. Tranquada. "Colloquium: Theory of Intertwined Orders in High Temperature Superconductors," Reviews of Modern Physics **87**, 457 (2015).

[11] Rodrigo Soto-Garrido, Gil Young Cho and Eduardo Fradkin, "Quasi One Dimensional Pair Density Wave Superconducting State," Physical Review B **91**, 195102 (2015).

[12] X. M. Chen, A. J. Miller, C. Nugroho, G. A. de la Peña, Y. I. Joe, A. Kogar, J. D. Brock, J. Geck, G. J. MacDougall, S. L. Cooper, E. Fradkin, D. J. Van Harlingen and P. Abbamonte, "Influence of Ti doping on the incommensurate charge density wave in 1T-TaS2', Physical Review B **91**, 245113 (2015).

Exploring Photon-Coupled Fundamental Interactions in Colloidal Semiconductor Based Hybrid Nanostructures

Min Ouyang, University of Maryland – College Park

Program Scope

The interplay between photon and matter is the basis of many fundamental processes and various applications. Harnessing light-matter or even more exotic light-matter-spin interactions can allow new underlying physical principles as well as technologies of solid-state information processing. In particular, when the size of matter is reduced to nanoscale, strong quantum confinement effect appears, and their charge, phonon and spin characteristics could respond differently to external stimuli such as photon, leading to tailored photon coupling processes. The overall goal of this program is to gain an improved understanding of emerging fundamental photon-coupled processes involving excitons, plasmons and/or spins at the nanoscale. The main strategy that we have employed to achieve our goals is to combine materials development of precisely tailored colloidal hybrid nanostructures (HNs) with far-field time-resolved optical spectroscopy. A HN is defined as a nanoscale system that can uniquely integrate different functional subunits (e.g. semiconductor, metal and magnetic nanoparticles) in a single entity. Such HNs can offer a way to create and control various fundamental coupling at the nanoscale by engineering their structural parameters, including composition, morphology and arrangement of subunits. Femtosecond lasers are further applied to probe and control dynamics of plasmon, exciton and spin within as-synthesized HNs. To that, this program has involved both chemical synthesis and characterization of HNs and far-field ultrafast optical measurement and control.

Recent Progress

During the grant period from 2013-2015 we have achieved substantial progress in both materials development of HNs possessing tunable *intra*-synergistic coupling and ultrafast optical control and measurement of emerging physical processes enabled by as-synthesized HNs, with a few selected results highlighted below:

- Development of centrosymmertic and non-centrosymmetric HNs with fine control of structural parameters [*Nat.Commun*. **5**, 4792 (2014) and *Science* (submitted, 2015)].

The HNs have become an important class of nanomaterials that can allow integration of distinct subunits with different functionalities and have facilitated unique synergistic coupling effects. Therefore, precise control of each subunit in a HN is crucial. Figure 1A shows schematic model of two simplest HNs, possessing centrosymmetric and non-centrosymmetric arrangement of two distinct subunits, respectively. The main synthetic obstacle of high quality complex HNs originates from intrinsic chemical and structural incompatibility among different subunits. For

example, traditional methods for making such HNs are all based on epitaxial growth principle, which typically requires interfacial lattice match within 1% in order to avoid defects and lattice strains. My research group has pioneered in developing non-epitaxial synthetic methodology for achieving nanoscale core-shell HNs without limitation of lattice mismatch, and has demonstrated new light-matter interactions that can be enabled by synergistic plasmon-exciton coupling in such HNs. In this program, we have further developed different non-epitaxial synthetic strategies to achieve more complex HNs that can possess multiple subunits with controllable structural symmetry and dimension ranging from nm- to μm- scale, with a few examples demonstrated in Figure 1B and 1C. All these exciting development of hybrid nanostructures in the first two fiscal yrs has provided us unique condensed matter model systems for studying various photon-coupled processes at the nanoscale.

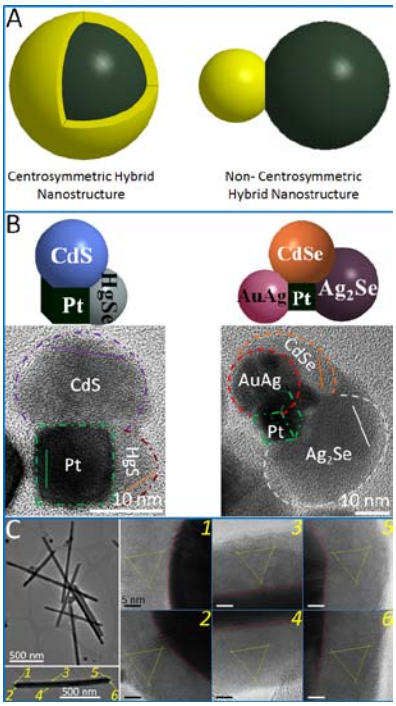

Fig.1 (A) Model of HNs; (B) Non-centrosymmetric HNs with three and four subunits, respectively; (C) Centrosymmetric one-dimensional Au-CdS HNs with perfect monocrystalline CdS shells.

- Nanodiamond based HNs with tailored emission characteristics of nitrogen-vacancy (NV) centers [*Nat.Commun*. (submitted, 2015)].

The NV centers in diamonds have attracted substantial interest over the past years as well-defined two-level quantum emitters. The ability to control the interaction between such quantum emitters and photonic and/or broadband plasmonic nanostructures is crucial for development of solid-state quantum devices with tunable performance, but has yet to materialize as free-standing structures, which is vital for realizing the full potential of NV centers in physical, biological and chemical applications. We have developed a general facile bottom-up strategy for a new type of HNs that consist of NV center in nanodiamonds and other functional nanoparticles (Fig. 2A). Precise control of critical structural parameters of such HNs, including size, composition, coverage, and inter-particle spacing is a pre-requisite for investigating the underlying physics and further engineering related optical properties. Figs. 2B and 2C show examples of nanodiamond-Ag nanoparticles with the control of size and surface coverage, respectively. Figure 2B shows size evolution with the same coverage of 0.016 ± 0.002 particles/nm^2, whereas Figure 2C demonstrates the capability of tuning surface coverage for the same size of Ag nanoparticles (8.6 ± 1.1nm). Coupling NV to other metal and semiconductor nanoparticles has also been achieved in this program. To demonstrate enabled synergistic coupling in as-synthesized HNs, we have investigated the modification of fluorescence lifetime of NV centers when coupled to 5nm sized Ag nanoparticles using a lab-built confocal microscope. Figure 2D shows comparison of NV

emission lifetime with and without Ag nanoparticles, manifesting a 1.8-fold enhancement of Purcell factor due to the plasmon enhancement. Our work opens a rich toolbox to engineer properties of quantum emitters from the bottom-up and to offer a high level control in the structure formation by overcoming the limitations of current attempts.

- Tailoring acoustic phonons and electron-phonon coupling through precisely engineered nanoscale interface [*Nano Lett*. (DOI: 10.1021/acs.nanolett.5b03227, 2015)].

Precise engineering of phonon-phonon and electron-phonon interactions by materials design is essential for an in-depth understanding of thermal, electrical and optical phenomena as well as new technology breakthrough governed by fundamental physical laws. Due to their characteristic length scale, the phonon-phonon and electron-phonon interactions can be dramatically modified by nanoscale spatial confinement, thus opening up opportunity to finely tailor underlying coupling processes through the interplay of confined size and interface. For example, Figure 3A shows one computed lattice stress field distribution of Au-Ag core-shell under excitation of *n*=2 acoustic phonon mode by finite element method. Two local stress minima and maxima along radial direction can be identified for the *n*=2 phonon mode, whose placements are determined by the composition and configuration of a core-shell structure. For example, when the aspect ratio of a core-shell structure is varied, the stress minimum and maximum will evolve through its interface continuously, leading to weak and strong interfacial phonon coupling between the core and shell with manifestation of unique oscillation of normalized phonon frequency (Fig.3B). We have also employed pump-probe ultrafast spectroscopy to explore such interfacial phonon coupling, with one typical time-resolved data shown in Fig.3C and a summary of measured phonon frequencies of different core-shells extracted from the pump-probe measurement in Fig.3B. This result has confirmed for the first time unambiguous evidence of interfacial phonon coupling. By combining with recent materials advances in fine synthetic control of various complex HNs as highlighted

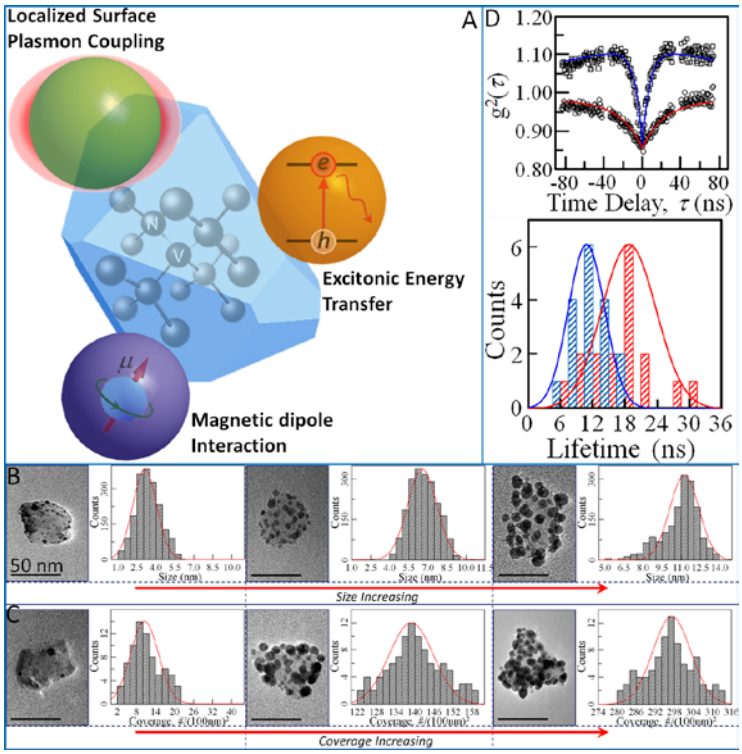

Fig.2 (A) Schematics of NV based HN with different synergistic coupling; (B) and (C) are size and coverage control of Ag nanoparticles on nanodiamond surface, respectively. (D) Auto-correlation measurement (top) of samples with (blue) and without (red) Ag nanoparticles, showing reduction of NV lifetime (bottom).

in Fig.1, nanoscale interface can be tailored in a highly controllable manner through different combination of acoustic characteristics, which might lead to phonon spectrum by design. Additional importantly, our phonon measurement is based on ultrafast spectroscopy with very fine temporal resolution. This should allow combining recent advance in shaped ultrafast optical laser pulses to achieve fully optical control of interfacial quantum states and dynamic process at the nanoscale.

Future Plans

The as-synthesized HNs achieved in the first two grant years have offered unique condensed matter model systems to explore various synergistic coupling effects. We will continue our ultrafast optical measurement, with particular focus on understanding and controlling the coupling among plasmon, exciton, phonon and spin within HNs at the ensemble level. In addition, we will pursue controlled assembly of HNs to create large scale ordered structures with new inter-particle coupling for understanding some collective particle interactions.

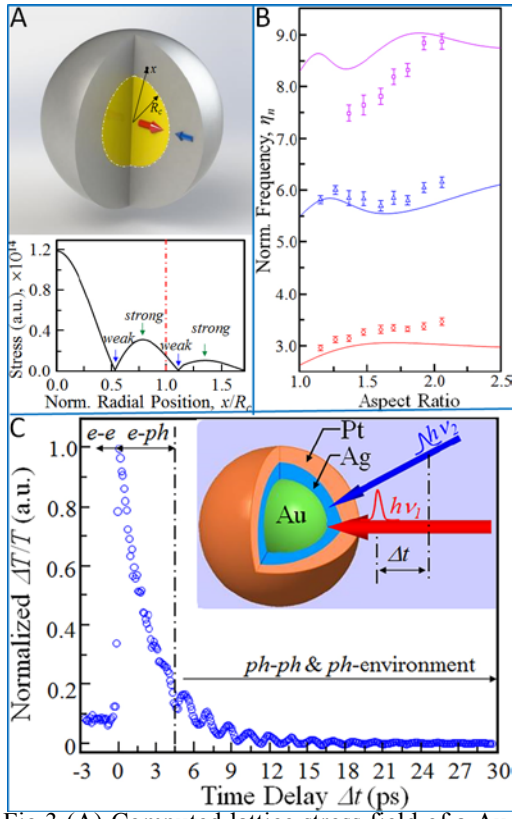

Fig.3 (A) Computed lattice stress field of a Au-Ag core-shell model; (B) Computed (solid lines) and experimental (discrete points) phonon frequencies for different aspect ratio; (C) Time-resolved measurement for determining acoustic phonon frequencies.

Publications (that acknowledged DOE support)

1. L. Weng, H. Zhang, A.O. Govorov & M. Ouyang, Hierarchical synthesis of non-centrosymmetric hybrid nanostructures and enabled plasmon-driven photocatalysis, *Nat. Commun.* **5**, 4792 (2014).

2. S. Yu, J. Zhang, Y. Tang & M. Ouyang, Engineering acoustic phonons and electron-phonon coupling by the nanoscale interface, *Nano Lett.* ASAP (2015) (DOI: 10.1021/acs.nanolett.5b03227).

3. J. Gong, N. Steinsultz & M. Ouyang, Nanodiamond based hybrid nanostructures: coupling nitrogen vacancy centers to metal nanoparticles and semiconductor quantum dots with fine structural tuning, *Nature Communications* (submitted).

4. K. Lee, J. Zhang, N. Ouyang & M. Ouyang, Injective morphology imprinting for anisotropic hybrid nanostructures and enabled single nanowire solar cells with record efficiency, *Science* (submitted).

Poster Sessions

Experimental Condensed Matter Physics Principal Investigators' Meeting

POSTER SESSION I
Monday, September 28, 2015

1. *Spin effects in magnetic and non-magnetic 2d correlated insulators*
   Phil Adams, Louisiana State University

2. *Atomic engineering oxide heterostructures: materials by design*
   Harold Hwang, SLAC National Accelerator Laboratory

3. *Magnetic thin films*
   Axel Hoffmann, Argonne National Laboratory Argonne

4. *Spin-coherent transport under strong spin-orbit interaction*
   Jean Heremans, Virginia Polytechnic Institute and State University

5. *Electronic and photonic phenomena of graphene, boron nitride and graphene/boron nitride heterostructures*
   Dimitri Basov, University of California, San Diego

6. *Quantum coherence and random fields at mesoscopic scales*
   Tom Rosenbaum, University of Chicago

7. *Topological superconductor core-shell nanowires*
   Judy Cha, Yale University

8. *High-bandwidth scanning hall probe imaging of driven vortices in periodic potentials*
   Stuart Field, Colorado State University

9. *Emerging materials*
   John Mitchell, Argonne National Laboratory

10. *Atomic layer controlled growth of artificially engineered pnictide superlattices by design*
    Chang-Beom Eom, University of Wisconsin

11. *Colloidal quantum dot films, transport and magneto-transport*
    Philippe Guyot-Sionnest, University of Chicago

12. *Antiferromagnetism and superconductivity*
    Bill Halperin, Northwestern University

13. *Tuning phase transformations for designed functionality*
    Athena Sefat, Oak Ridge National Laboratory

14. *Thermalization of artificial spin ice and related frustrated magnetic arrays*
    Peter Schiffer, University of Illinois, Champaign

15. *Magneto-transport in GaAs two-dimensional hole systems*
    Mansour Shayegan, Princeton University

16. *Experimental study of quantum critical fluctuations in two-dimensional superconducting cuprate films*
    Tom Lemberger, Ohio State University

17. *Charge and energy transfer in molecular superconductors and molecular machines*
    Saw-Wai Hla, Ohio University

18. *High-speed rotational anisotropy second harmonic generation study of a 112-type iron-based superconductor*
    Dave Hsieh, California Institute of Technology

19. *Electronic complexity of epitaxial rutile heterostructures*
    Hanno Weitering, Oak Ridge National Laboratory

20. *Nonlinear transport in mesoscopic structures in the presence of strong many-body phenomena*
    Jon Bird, University of Buffalo

21. *Correlated electrons in graphene at the quantum limit*
    Philip Kim, Harvard University

22. *Spectroscopic investigations of novel electronic and magnetic materials*
    Jan Musfeldt, University of Tennessee

23. *Transport studies of quantum magnetism: physics and methods*
    Minhyea Lee, University of Colorado

24. *Epitaxial complex oxides*
    Ho Nyung Lee, Oak Ridge National Laboratory

25. *Studies of multiband and topological superconductors*
    Qi Li, Pennsylvania State University

26. *Investigating the magnetic, electronic, and lattice degrees of freedom that determine the emergent properties of complex transition metal compounds*
    Rongying Jin (Louisiana State University) and John DiTusa (Louisiana Consortium for Neutron Scattering)

Experimental Condensed Matter Physics Principal Investigators' Meeting

POSTER SESSION II
Tuesday, September 29, 2015

1. *Charge inhomogeneity in correlated electronic systems*
   Barry Wells, University of Connecticut

2. *Understanding topological pseudospin transport in Van der Waals' materials*
   Kin Fai Mak, Pennsylvania State University

3. *Experimental studies of correlations and topology in two dimensional hybrid structures*
   Jinhai Mao, Rutgers University (Eva Andrei PI)

4. *Fermi gases in bichromatic superlattices*
   John Thomas, North Carolina State University

5. *Spin wave interactions in metallic ferromagnets*
   Kristen Buchanan, Colorado State University

6. *Photonic systems*
   Thomas Koschny, Ames Laboratory (Joe Shinar FWP)

7. *Engineering of mixed pairing and non-Abelian Majorana states of matter in chiral p-wave superconductor Sr_2Ru0_4 and other materials*
   Ying Liu, Pennsylvania State University

8. *Probing nanocrystal electronic structure and dynamics in the limit of single nanocrystals*
   Moungi Bawendi, Massachusetts Institute of Technology

9. *Magneto-optical study of correlated electron materials in high magnetic fields*
   Dmitry Smirnov, Florida State University

10. *Spectroscopy of degenerate one-dimensional electrons in carbon nanotubes*
    Jun Kono, Rice University

11. *The electron response of artificial 2D heterostructures*
    Rick Osgood, Columbia University

12. *Novel behavior of ferromagnet/superconductor hybrid systems*
    Norman Birge, Michigan State University

13. *Probing electron correlations in 1D electronic materials using single quantum channels*
    Jeremy Levy, University of Pittsburgh

14. *Synthesis and observation of emergent phenomena in Heusler compound heterostructures*
    Chris Palmstrøm, University of California, Santa Barbara

15. *Magnetic nanosystems: making, measuring, modeling, and manipulation*
    Ruslan Prozorov, Ames Laboratory

16. *Dynamics of electronic interactions in superconductors and related materials*
    Dan Dessau, University of Colorado

17. *Structured light-matter interactions enabled by novel photonic materials*
Natasha Litchinitser, SUNY Buffalo

18. *Electron spectroscopy*
Tony Valla, Brookhaven National Laboratory (Peter Johnson FWP)

19. *Science of 100 Tesla*
Neil Harrison, Los Alamos National Laboratory

20. *Bose-Einstein condensation of magnons and potential device applications*
John Ketterson, Northwestern University

21. *Engineering topological superconductivity towards braiding Majorana excitations*
Leonid Rokhinson, Purdue University

22. *Nanostructure studies of strongly correlated materials*
Doug Natelson, Rice University

23. *Novel sample structures and probing techniques of exotic states in the 2nd Landau level*
Gabor Csathy and Mike Manfra, Purdue University

24. *Topological materials with complex long-range order*
James Analytis, University of California, Berkeley

25. *Nanoscale magnetic Josephson junctions and superconductor/ferromagnet proximity effects for low-power spintronics*
Ilya Krivorotov, University of California, Irvine, co-PI Oriol Valls, University of Minnesota

26. *Linear and nonlinear optical properties of metal nanocomposite materials*
Richard Haglund, Vanderbilt University

Poster Abstracts

Program Title: **Spin Effects in Magnetic and Non-magnetic 2D Correlated Insulators**

Principle Investigator: **Philip W. Adams**
Mailing Address: **Department of Physics and Astronomy, Louisiana State University, Baton Rouge, LA 70803**
Email: **adams@phys.lsu.edu**

Program Scope

This program focuses on the magneto-transport, non-equilibrium relaxation, and spin-resolved density-of-states properties of disordered two-dimensional paramagnetic, ferromagnetic, and superconducting systems. In addition, we are investigating proximity effects in bilayer hybrids of these systems with the aim of understanding and controlling the interface-induced exchange fields and spin-orbit effects in these structures. Our specific research agenda is organized into two separate but related areas.

The first is a study of disorder and correlation effects in superconducting Al and V films that have been subjected to high Zeeman fields. We are primarily interested in what role local spin-triplet fluctuations play in determining the nature of the superconductor-insulator transition in these systems. We now have good evidence that a disordered Larkin-Ovchinnikov phase emerges near the Zeeman-limited transition and that this phase has a significant influence on the character of the transition. Thus, the spin behavior near the transition is much more complex than expected.

The second class of systems is proximity structures comprised of superconducting/ferromagnetic (SC/FM) and superconducting/heavy metal (SC/HM) bilayers. We have developed spin-resolved tunneling probes that give us a direct measure of the proximity-induced exchange field in the SC/FM structures, as well as the spin-orbit scattering rate in SC/HM structures. Recently we have demonstrated that the magnitude of the exchange field can be modulated with an external gate, thereby producing a magnetoelectric response in the bilayers. We plan to optimize this magneto-electric effect by getting a better understanding of the microscopic mechanism of the interface-induce exchange field, as well as improving the gate barriers and/or the bilayer interface quality. The ultimate goal is to develop a device such as a voltage-controlled superconducting switch or a spin- polarized electron source with a voltage-tunable Zeeman splitting.

Recent Progress

Spin-imbalanced superconductivity is a historically important problem that remains at the forefront of condensed matter physics. By the late 1960's it was known that a Zeeman field could induce a spatially modulated order parameter in a spin singlet superconductor, i.e. the Ferrel-Fulde-Larkin-Ovchinnikov (FFLO) state [1,2]. To date, however, no definitive signature of an FFLO phase has been identified, although extensive circumstantial evidence for the phase has emerged in recent years [3,4,5,6,7]. We find evidence, in the form of non-equilibrium dynamics, for an inhomogeneous superconducting phase near the Zeeman critical field transition in ultra-thin Al and Be

films [8]. These systems exhibit asymmetric avalanche behavior in the tunneling density of states along with slow, non-exponential, relaxations. We believe these effects are a manifestation of a disordered remnant of FFLO correlations, see Fig. 1. The avalanches are not due to quantized vorticity, because the films are in a carefully aligned parallel magnetic field. These unusual dynamics arise from the convolution of low dimensionality, disorder, Zeeman-splitting, and spin-singlet pairing.

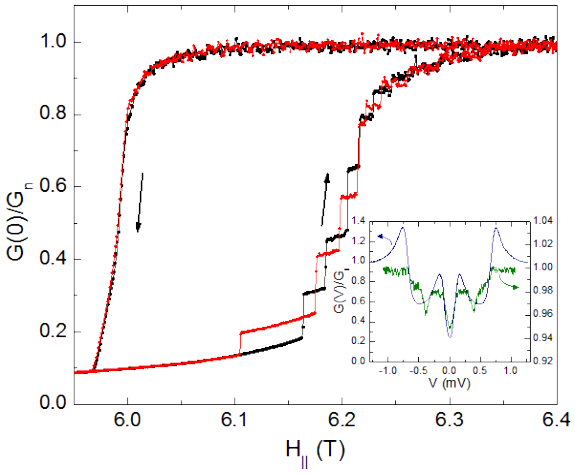

Fig. 1 The zero bias tunneling conductance normalized by its normal state value at 52 mK. The data was taken on a 540 Ohm/sq Al film using a non-superconducting Al counter-electrode. The magnetic field was applied parallel to the film surface. The red and black lines represent two separate sweeps through the hysteresis loop. The arrows depict the field sweep direction. Inset: The tunnel density of states spectrum of a 200 Ohm/sq film in a subcritical (5.4 T, blue) and a supercritical (5.9 T, green) parallel magnetic field at 80 mK.

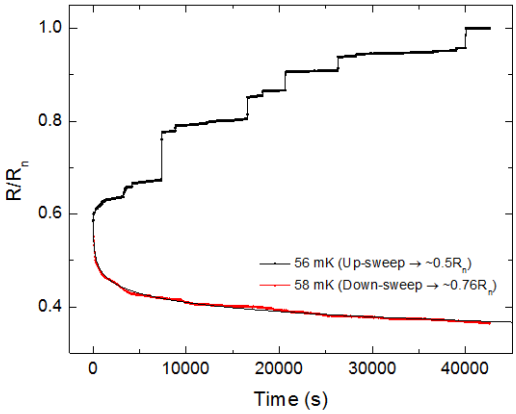

Fig. 2. Time dependence of the sheet resistance of a 320 Ohm/sq film after pausing the magnetic field sweep in the hysteretic region of the transition. These data were taken at 70 mK. The upper curve is a relaxation off of the up-sweep branch, and the lower is off of the down-sweep branch. The solid line through the lower curve is a fit to the stretched exponential form.

Finally, we have just completed collaboration with Jiang Wei's group at Tulane University, studying quantum phonon confinement effects in layered van der Waals material Nb_3SiTe_6. This work resulted in the first definitive observation of a modified *e-ph* interaction due to the phonon dimensionality crossover on 2D atomic crystals of Nb_3SiTe_6. When the thickness of crystals was reduced below a few unit-cells, we observed an unexpected, enhanced anti-localization signature in magneto-transport, which is attributable to the suppression of the *e-ph* interaction that arises from 2D confinement of the relevant phonons. A manuscript reporting these results was published in Nature Physics this summer [9].

Future Plans

Over the past year we have been collaborating with Ken Shih at UT Austin, who is supplying us with ultra-thin epitaxially-grown superconducting metal films. We began with a magneto-transport study of several-monolayer-thick crystalline Pb films. After

devising a way to make electrical contact to the films, we measured their critical field in both perpendicular and parallel field orientations. Our data show a robust superconducting transition, with a $T_c \sim 5.5$ K, in 5 monolayer thick films. The films are only moderately disordered and have a normal state sheet resistance that is about 100 times smaller than the quantum resistance. However, the superfluid density, as measured by Tom Lemberger's group and separately by Karen Moler's group, is anomalously small in the films. Indeed, the superfluid density is somewhat lower that one would expect based on the values of the sheet resistance and the gap. We are currently preparing a manuscript on this work.

The spin-orbit scattering rate in Pb is too high to be useful for studies of Zeeman-limited superconductivity. Indeed, the parallel critical field of the thinnest Pb films is more than 50 T, due to the large spin-orbit coupling! Fortunately, however, Prof. Shih's group has succeeding in growing epitaxial Al films on Si substrates. Our immediate plan is to measure the non-equilibrium dynamics of the epitaxial Al films in the same manner as we did with the highly disordered quenched-condensed Al films. We hope to be able to sort out the role of disorder in the observed avalanche behavior and ultimately gain a better understanding of the Zeeman-limited ground state.

Finally, we are planning to measure the effective penetration depth of spin-obit coupling in thin Al films. Because of its low atomic mass, Al has very little intrinsic spin-orbit scattering and the electron spin states are well defined. Consequently, the Cooper pairs in the superconducting phase are in a true spin-singlet state, with virtually no spin-triplet mixing. However, it is well known that a heavy metal impurity, such as a gold atom, will induce spin-orbit scattering in the film and, in the superconducting phase, the Cooper pairs will pick up a spin-triplet component in the vicinity of a "spin-orbit" impurity. The spin-orbit impurity does not break Cooper pairs, it only mixes their spin states. Our plan is to deposit an Al film onto a matrix of Au islands of varying separation and size. In the absence of spin-orbit scattering, the Zeeman critical field of our films is about 6 T. However, with finite spin-orbit scattering the Zeeman critical field will be much higher, perhaps over 20 T. So we can measure the Zeeman critical field as a function of the island separation in order to determine how far the spin-orbit mixing extends beyond the island edges. In doing so, we can determine the lateral spin-orbit penetration depth. We are currently producing well-formed Au islands by annealing pristine Au films at 550 C in an Argon atmosphere. The details of the island structure, such as the island separation, are a sensitive function of the initial Au film thickness and the annealing protocol. After the islands are formed we simply deposit a thin Al film over the matrix and then measure the parallel critical field of the system. This project is progressing well and we should have our first results in a couple of months.

References

1. P. Fulde and R. A. Ferrell, Phys. Rev. **135**, A550 (1964).
2. A. I. Larkin and Y. N. Ovchinnikov, Zh. Eksp. Teor. Fiz. **47** (1964).
3. H. A. Radovan, N. A. Fortune, T. P. Murphy, S. T. Hannahs, E. C. Palm, S. W. Tozer, and D. Hall, Nature **425**, 51 (2003).
4. G. Koutroulakis, M. D. Stewart, V. F. Mitrovi?, M. Horvati?, C. Berthier, G. Lapertot, and J. Flouquet, Phys. Rev. Lett. **104**, 087001 (2010).
5. H. Mayaffre, S. Kramer, M. Horvatic, C. Berthier, K. Miyagawa, K. Kanoda, and V. F. Mitrovic, Nature Physics **10**, 928 (2014).
6. R. Leo and E. S. Daniel, Rep. Prog. Phys. **73**, 076501 (2010).

7. Y.-a. Liao, A. S. C. Rittner, T. Paprotta, W. Li, G. B. Partridge, R. G. Hulet, S. K. Baur, and E. J. Mueller, Nature **467**, 567 (2010).
8. J.C. Prestigiacomo, T.J. Liu, and P.W. Adams, *Phys. Rev. B* 90, 184519 (2014).
9. J. Hu, X. Liu, C.L. Yue, J.Y. Liu, H.W. Zhu, J.B. He, J. Wei, Z.Q. Mao, L.Y. Antipina, Z.I. Popov, P.B. Sorokin, T.J. Liu, P.W. Adams, S.M.A. Radmanesh, L. Spinu, H. Ji, D. Natelson, *Nature Phys*. 11, 471 (2015).

Publications (2013 - 2015)

1. “Electrostatic Tuning of the Proximity-Induced Exchange Field in EuS/Al Bilayers”, T. J. Liu, J. C. Prestigiacomo, and P. W. Adams, *Phys. Rev. Lett.* 111, 027207 (2013).
2. “Mn1-xFexCoGe: A Strongly Correlated Metal in the Proximity of a Non-collinear Ferromagnetic State”, T. Samanta, I. Dubenko, A. Quetz, J. Prestigiacomo, P.W. Adams, S. Stadler, and N. Ali, *Appl. Phys. Lett.* 103, 042408 (2013).
3. "Field-pulse Memory in a Spin-glass", D.C. Schmitt, J.C. Prestigiacomo, P.W. Adams, D.P. Young, S. Stadler, and J.Y. Chan, *App. Phys. Lett*. 103, 082403 (2013).
4. "Hall Effect and the Magnetotransport Properties of Co2MnSi1-xAlx Heusler Alloys", J.C. Prestigiacomo, D.P. Young, P.W. Adams, S. Stadler, *J. App. Phys*. 115, 043712 (2014).
5. "Magnetic, Thermodynamic, and Electrical Transport Properties of the Noncentrosymmetric B20 Germanides MnGe and CoGe", J.F. Ditusa, S.B. Zhang, K. Yamaura, Y. Xiong, J.C. Prestigiacomo, B.W. Fulfer, P.W. Adams, M.I. Brickson, D.A. Browne, C. Capan, Z. Fisk, and J.Y. Chan, *Phys. Rev. B* 90, 144404 (2014).
6. "Asymmetric Avalanches in the Condensate of a Zeeman-limited Superconductor", J.C. Prestigiacomo, T.J. Liu, and P.W. Adams, *Phys. Rev. B* 90, 184519 (2014).
7. "Hydrostatic Pressure-induced Modifications of Structural Transitions Lead to Large Enhancements of Magnetocaloric Effects in MnNiSi-based Systems", T. Samanta, D.L. Lepkowski, A.U. Saleheen, A. Shankar, J.C. Prestigiacomo, I. Dubenko, A. Quetz, I.W. H. Oswald, G.T. McCandless, J.Y. Chan, P.W. Adams, D.P. Young, N.Ali, and S. Stadler, *Phys. Rev. B* 91, 020401 (2015). (RC) (*Editor's suggestion*)
8. "Competing Magnetic States, Disorder, and the Magnetic Character of Fe3Ga4", J.H. Mendez, C.E. Ekuma, Y. Wu, B. W. Fulfer, J.C. Prestigiacomo, W.A. Shelton, M. Jarrell, J. Moreno, D.P. Young, P. W. Adams, A. Karki, R. Jin, J.Y. Chan, and J.F. DiTusa, *Phys. Rev. B* 91, 144409 (2015).
9. "Effects of Hydrostatic Pressure on Magnetostructural Transitions and Magnetocaloric Properties in (MnNiSi)(1-x)(FeCoGe)(x)", T. Samanta, D.L. Lepkowski, A.U. Saleheen, A. Shankar, J.C. Prestigiacomo, I. Dubenko, A. Quetz, I.W.H. Oswald, G.T. McCandless, J.Y. Chan, P.W. Adams, D.P. Young, N. Ali, and S. Stadler, *J. App. Phys*. 117, 123911 (2015).
10. "Enhanced electron coherence in atomically thin Nb3SiTe6", J. Hu, X. Liu, C.L. Yue, J.Y. Liu, H.W. Zhu, J.B. He, J. Wei, Z.Q. Mao, L.Y. Antipina, Z.I. Popov, P.B. Sorokin, T.J. Liu, P.W. Adams, S.M.A. Radmanesh, L. Spinu, H. Ji, D. Natelson, *Nature Phys*. 11, 471 (2015).

Program Title: Topological materials with complex long-range order.
Principle Investigator: James Analytis.
Mailing Address: Materials Science Division, Lawrence Berkeley National Lab, Berkeley, CA 94720
E-mail: analytis@berkeley.edu

Program Scope

The object of this program is to study exotic metallic and magnetic behavior of frustrated quantum magnets. These materials are closely associated with quantum spin liquids, an exotic state of matter characterized by strong quantum entanglement. Few (possibly none) of the candidate materials manifest the quantum spin liquid state, but instead find complex ordered ground states. This complexity comes in the form of multiple, often coupled broken symmetries so that time reversal, inversion and translational symmetries are simultaneously involved. My central hypothesis is that if metallic states can coexist in this complex magnetic background, the metal attains an exotic topological character that can be manifested as an anomalous Hall effect, a large magneto-transport response, and novel magnetic and thermodynamic properties.

The materials that can manifest this physics have strong magnetic interactions in a complex lat- tice geometry, such that simple co-linear magnetic order cannot form. There is a growing number of materials that satisfy these conditions including triangular, Kagome´ and pyrochlore lattices, but I will focus on just one class: honeycomb networks of octahedrally coordinated transition metals. This builds on my recent success in the field or iridium based quantum magnets, where I discovered a new three-dimensional honeycomb structure [1-5]. These systems have the advantage that many transition metals form similar structures, and this in turn gives us a pathway to chemical control via doping, substitution and chemical pressure. More importantly, my work has already shown that these systems form the right kind of complex magnetic order, namely one that could endow metallic quasiparticles with exotic topologcal properties.

The field of quantum spin liquids is in its infancy and there are many easily identifiable deficiencies in current research. Firstly, it has proven difficult to understand the dominant driving force that lifts the frustration when the ordered state itself breaks several symmetries, some of which will be coupled to one-another. Secondly, the field is limited by the number of materials available to study. We need systems with control 'knobs', that can be tuned in well defined ways.

Recent Progress

We have synthesized the first single crystals of a new structural motif of Li_2IrO_3, shown in Figure 1A.

Background: In the honeycomb iridates A_2IrO_3 (A is an alkali), an exotic kind of anisotropic exchange emerges which maps these structures onto a remarkable theoretical model pioneered by Kitaev [6,7]. This supports a novel state of matter known as the quantum spin liquid (QSL), which is characterized by the emergence of chargeless, spinful fermions with fractional statistics. The layered honeycomb structure is composed of octahedrally coordinated Ir^{4+}, bonded together their O_2 edges. The exchange pathway between spin-1/2 Ir, is across these bonds and is predicted to be highly anisotropic due to the spin-orbit

coupling. The idealized case where these satisfy the Kitaev model, relies on the ideal symmetry of the octahedral environment, and the present focus on Li_2IrO_3, is due to its small octahedral distortion as compared to that of Na_2IrO_3 [1].

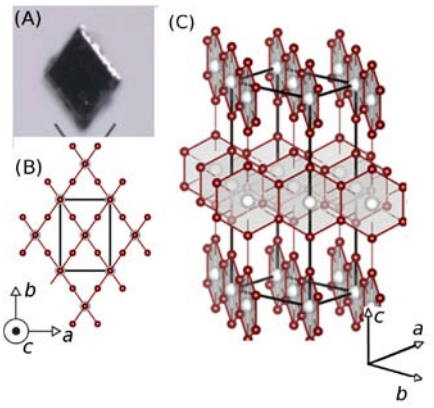

Figure 1: (A) The first single crystals of {1}-HHC. (B) and (C) the crystal structure showing only the Ir positions but for one Li at the center of a honeycomb plaquette [1].

Results and Discussion: There is a generalization of the Kitaev model to three-dimensions, as pointed out by my co-workers and me [2]. The importance of having a three-dimensional system is that the QSL can be stable to thermal fluctuations, whereas in two-dimensions it is not [3]. Remarkably a three-dimensional version of this compound exists in nature, and we discovered it last year. The material is a polytype of the original layered honeycomb α-Li2IrO3 and is commonly referred to as γ-Li2IrO3 (or H□1□-Li2IrO3) [1]. In this work, I also predicted that there could be a family of such compounds known as the 'harmonic honeycomb' iridates, shown in Figure 2. Every member of the harmonic honeycomb series satisfies the 3D Kitaev model and in principle could be Kitaev QSLs.

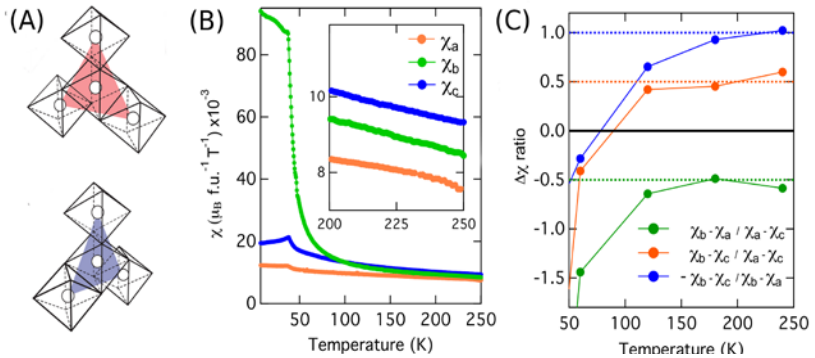

Figure 2: (A) Two HHC planar orientations which determine high T properties. (B) Magnetic susceptibility along three different crystallographic directions. (C) Magnetic anisotropy determined by torque magnetometry [2].

The remarkable structure of our compound is composed of simple building blocks - a repeating pattern along the *c*-axis, one link in the same honeycomb plane, followed by one that rotates to the other honeycomb plane. The extent of the honeycomb prior to rotation tunes the dimensionality of these materials from 3D (N=0) to 2D (N=∞). This provides a new structural family in which to study the interplay of dimensionality and magnetism in a strong spin-orbit environment. Importantly, all members of this family preserve the edge-sharing planar superexchange between Ir, such that the anisotropic Kitaev exchange is equally pertinent. The discovery of this compound, does not end with this material, but rather is the beginning of a connected structural family a kin to the Ruddlesden-Popper or homologous cuprate series.

To understand whether the magnetic exchange pathway is indeed Kitaev-like, we consider the low temperature characteristics (Figure 2B). At T=38K the system undergoes a magnetic phase transition. As this temperature is approached on cooling, the simple geometric relationship between the components of the susceptibility at high T breaks down. χ_b appears to diverge, becoming ten times larger than χ_a before it finds some long-range ordered state. This kind of anisotropy cannot be explained by an isotropic

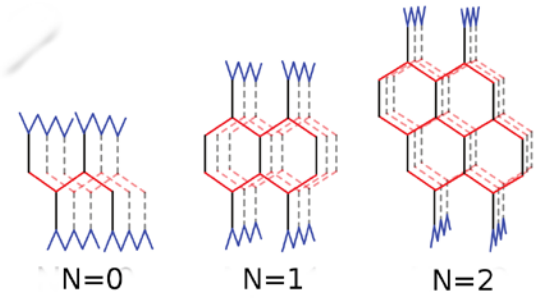

Figure 3: The hyper-honeycomb series is a complete family of compounds, of which he N=1 and N=∞ have been synthesized, for the first time, by the QM program [2].

Heisenberg exchange mechanism. Indeed, comparing this direction with the crystal structure, it is apparent that the *b*-axis is associated with one specific Ir-O_2-Ir bond – just one plane where a Kitaev-like mechanism might be expected. These anisotropies are a smoking-gun for an exotic type of exchange mechanism, driven by correlations in these strongly spin-orbit coupled materials.

Indeed, Resonant Magnetic X-ray scattering experiments have recently shown that the transition at 38K is an incommensurate order composed of two counter-propagating spirals. The order is shown in Figure 4.

Future Directions

Carrier tuned magnetism: With the synthesis of γ-Li_2IrO_3 optimized, the next step is to dope with an appropriate element. To avoid competing phases, I choose transition metal dopants that are known to form the layered honeycomb structure γ-Li_2IrO_3. The include Rh, Ru, Pt and Os. The elements not only dope, they also tune the local bonding structure, which can have addition effects in the magnetism. At present, ab initio calculations of these effects have only been calculated for a few special cases, and so it is difficult to predict what the effect of the bond angles and reduced spin-orbit coupling will be on the exchange mechanism. However, our preliminary studies have shown that hole doping these materials stabilizes ferromagnetism, whereas electron doping stabilizes anti-ferromagnetism. This provides a unique way in which to tune across the 3D Kitaev phase diagram, for the first time.

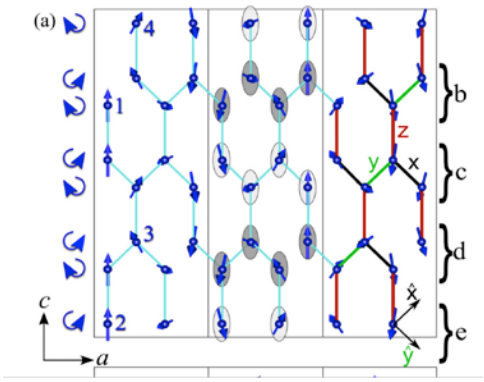

Figure 4: Magnetic structure of the β-Li2IrO3 system, consisting of two counter-propagating incommensurate spirals.

Meta-magnetism in high fields: A big question is the response of these systems to broken time-reversal symmetry. In the presence of a strong magnetic field, the stripy order in the α-Li2IrO3 systems remains robust, and at least up to 14T, cannot be suppressed. However, in the γ-Li_2IrO_3, the incommensurate order can be suppressed by as little as 3T. The questions is whether this is a paramagnetic phase, or an intermediate meta-magnetic phase. We will combine magnetization, heat capacity and scattering measurements to understand the thermodynamic nature of this phase. Our preliminary studies have shown that this phase is indeed anti-ferromagnetic, but *commensurate* with the crystal lattice.

Elastic constant studies: There are few symmetry sensitive *thermodynamic* probes, which makes measurements of elastic constants a rare but powerful technique to understand the presence and symmetry of phase transitions. Our future measurements will investigate the symmetry of the incommensurate phase, and possible crossover phases at higher

temperatures, such as the temperature where the principal components of the magnetization switch order (see Fig. 2B).

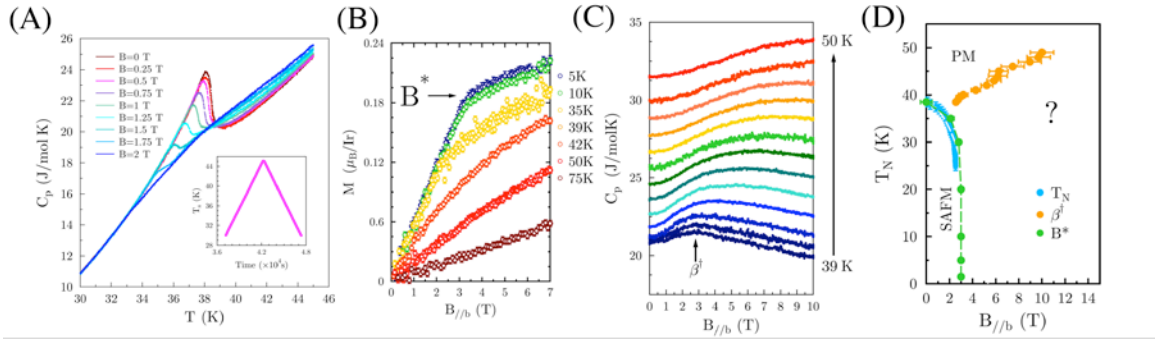

Figure 5: (A) Specific heat as a function of temperature with constant field applied along the crystallo- graphic b-axis of H□1□-Li2IrO3. At zero field the transition is triangular with no evidence of latent heat in the temperature profile as a function of time (inset), suggesting the transition is second order. (B) The magnetization as a function of field pointed along b, showing a kink at H* ∼ 3T as the systems enters a high magnetic field phase. (C) Specific heat as a function of field at fixed temperatures showing a crossover into a high field state. This crossover is not consistent with a Schottky anomaly where the peak position would be constant in B/T. (D) The high field phase has a very steep boundary (blue and green) which is consistent with the transition becoming much broader in the specific heat. The nature of the low temperature/high field phase beyond the crossover field remains unknown.

References with DOE support

[1] Kimberly A Modic, Tess E Smidt, Itamar Kimchi, Nicholas P Breznay, Alun Biffin, Sungkyun Choi, Roger D Johnson, Radu Coldea, Pilanda Watkins-Curry, Gregory T McCandless, Felipe Gandara, Z Islam, Ashvin Vishwanath, Julia Y Chan, Arkady Shekhter, Ross D McDonald, James G Analytis, "Realization of a three-dimensional spin–anisotropic harmonic honeycomb iridate", Nature Communications 5, 4203 (2014).

[2] Itamar Kimchi, James G. Analytis, and Ashvin Vishwanath, "Three-dimensional quantum spin liquids in models of harmonic-honeycomb iridates and phase diagram in an infinite-D approximation", Phys. Rev. B 90, 205126 (2014)

[3] A. Biffin, R. D. Johnson, I. Kimchi, R. Morris, A. Bombardi, J. G. Analytis, A. Vishwanath, and R. Coldea, "Noncoplanar and Counterrotating Incommensurate Magnetic Order Stabilized by Kitaev Interactions in γ−Li2IrO3″ , Phys. Rev. Lett. 113, 197201 (2014)

[4] Observation of Coherent Helimagnons and Gilbert damping in an Itinerant Magnet J. D. Koralek, D. Meier, J. P. Hinton, A. Bauer, S. A. Parameswaran, A. Vishwanath, R. Ramesh, R. W. Schoenlein, C. Pfleiderer, J. Orenstein, Phys. Rev. Lett. 109, 247204 (2012)

[5] J. P. Hinton, S. Patankar, E. Thewalt, J. D. Koralek, A. Ruiz, G. Lopez, N. Breznay, I. Kimchi, A. Vishwanath, J. Analytis, J. Orenstein, Photoexcited states of the harmonic honeycomb iridate γ-Li2IrO3, arXiv:1503.01353

[6] A. Kitaev, Annals of Physics 321, 2 (2006).

[7] Doping a spin-orbit Mott Insulator: Topological Superconductivity from the Kitaev-Heisenberg Model and possible application to (Na2/Li2)IrO3, Yi-Zhuang You, Itamar Kimchi, Ashvin Vishwanath, Phys. Rev. B 86, 085145 (2012).

Program Title: Experimental studies of two dimensional electron systems and hybrid structures

Principal Investigator: Eva Y. Andrei

Mailing Address: Department of Physics, Rutgers University, 136 Frelinghuysen Rd, Piscataway, NJ 08904

1. **Program Scope**

This program aims to explore the emergence of novel electronic properties in 2D electron systems resulting from the interplay between reduced dimensionality, interactions, incomplete screening, defects and boundaries. Insights gained from this work should lead to the development of nanometer scale 2D materials with designer electronic properties that are important for scientific and technological applications. The 2D materials that we study such as graphene, MoS_2, $NbSe_2$ used individually or as hybrid structures, could become building blocks in applications such as ultra-sensitive electronic, biological and chemical sensors; electronic and circuit components; amplifiers, photo-detectors and switches.

Our strategy for achieving the program objectives is to start out by developing a fundamental understanding of the undisturbed 2D material of interest in its pristine form. These materials being only one or few atoms thick are extremely susceptible to external disturbances. As a result, the uncontrolled exposure to the environment such as substrates adsorbents or electrical leads can completely obscure their intrinsic properties. It is therefore critical to develop strategies to ensure minimally invasive experimental conditions. For example in our earlier DOE funded work we have demonstrated that it is possible to effectively isolate graphene from the environment by eliminating the substrate altogether in a suspended sample geometry. This lead to the discovery of ballistic transport on micrometer length scales in graphene [1]. For magneto-transport measurements we developed a technique to isolate these suspended samples from the invasiveness of electrical leads which led our group to the first observation of the fractional quantum Hall effect in graphene [2]. For accessing the intrinsic local electronic properties in STM measurements, where suspending the sample is not practical, we focused our efforts on finding ways to render the substrate minimally invasive. This resulted in the first observation of Landau levels [3] and to the direct observation of edge states in graphene [4]. Armed with techniques to ensure access to the intrinsic electronic properties of 2D materials we are now in the process of exploring the consequences of controllably introducing local defects, various substrates and geometric constraints.

The research in this project utilizes a wide range of expertise and experimental techniques that were developed in our group. These include sample preparation and fabrication techniques and characterization tools [5] that allow us to access and probe the electronic properties of 2D systems and to follow their evolution with parameters such as distance from an edge, with magnetic field, doping, screening and local defects. The primary characterization techniques deployed in this program cover a range of local probes such as low temperature scanning tunneling microscopy, scanning tunneling spectroscopy, Landau level spectroscopy, atomic force microscopy, intermediate range probes such as Raman spectroscopy, and global probes such transport and magneto-transport.

2. Recent Progress

- *Realization of a Tunable Artificial Atom at a Charged Vacancy in Graphene*

Graphene's remarkable electronic properties have fueled the vision of a graphene-based platform for lighter, faster and smarter electronics and computing applications. But progress towards this goal was stalled by the inability to confine its charge carriers with electrostatic potentials. We have invented a technique to stably host and controllably modify a localized charge state by using a single atom vacancy in a gated graphene device. We demonstrated that the charged states at the vacancy site are gate tunable and that the trapping mechanism can be turned on and off, providing a new paradigm to control and guide electrons in graphene.

Background. Supercriticality in atoms occurs when the Coulomb coupling, $\beta = Z\alpha$, exceeds a critical value of order unity, where Z is the atomic number and $\alpha \sim 1/137$ is the fine structure constant. In the supercritical regime the electronic orbitals, starting with the 1S state, sink into the Dirac continuum until Z is reduced to the critical value. This process, known as atomic-collapse (AC), is accompanied by vacuum polarization and the spontaneous generation of positrons. But accessing the new physics expected in the supercritical regime requires ultra-heavy nuclei which do not exist in nature. In graphene, where the effective fine structure constant is much larger the critical coupling can be reached for a relatively modest charge of 0rder ~1. The transition to the supercritical regime in graphene is marked by the emergence at the supercritical charge of a sequence of quasi-bound states which can trap electrons. However, because graphene is a good conductor it is difficult to deposit and maintain a charge on its surface. Attempts to create charge by ionizing ad-atoms or donors with an STM tip showed that the charge decays when the field is removed. Alternatively ions can be deposited directly on graphene but, because the charge transfer is inefficient, attaining the critical Z requires piling them up of many ions which is very challenging.

Discussion of findings. We have demonstrated that a vacancy in graphene can stably host a positive charge and that it is possible to deposit the charge and to build it up gradually by applying voltage pulses with the tip of a scanning tunneling microscope. The charge buildup was monitored with scanning tunneling spectroscopy (STS) and Landau level (LL) spectroscopy (Fig. 1), and compared to numerical simulations. As the charge increases its interaction with the conduction electrons in graphene undergoes a transition into a supercritical regime where the itinerant electrons can be trapped in a sequence of quasi-bound states resembling an artificial atom. We detected the formation of such artificial atoms by the appearance of negative energy quasi-bound electron states at the vacancy site. The quasi-bound electron-states produce a strong enhancement of the density of states within a disc centered on the vacancy site which is surrounded by halo of hole states (Fig. 2). These hole states are the equivalent of spontaneous positrons expected to be produced in the collapse of supercritical atoms.

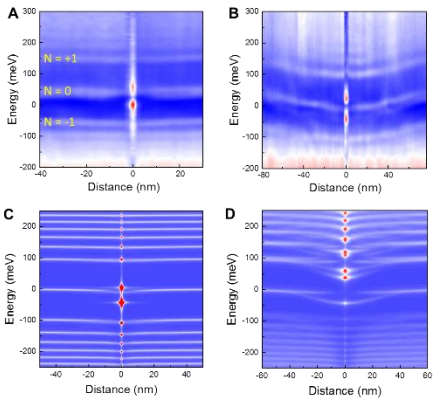

Figure 1. Effect of charged vacancy on the Landau level spectra. Spatial dependence of the LLs across a line-cut traversing the vacancy before (A) and after (B) applying the voltage pulse. The position of the vacancy is marked by the enhanced intensity at its center. The energy shift of the Landau level corresponds to an effective charge of $Z/\kappa \sim 0.2$l. (C), (D) Numerical simulation of the LL spectra across a line-cut reproduces the experimental results in (A) and (B) respectively.

We have found that screening of the vacancy charge is strongly doping dependent and as a result the bound states at the vacancy site are gate tunable. Moreover we have shown that screening of the vacancy charge is surprisingly asymmetric exhibiting relatively weak screening in the p-doped regime but unusually strong screening on the n-doped side. One of the direct experimental consequences of this asymmetry is that the states associated with this artificial atom can be turned on or off with a modest gate voltage, providing a switching mechanism for localized states, and making it possible to electrostatically guide and control electrons in graphene.

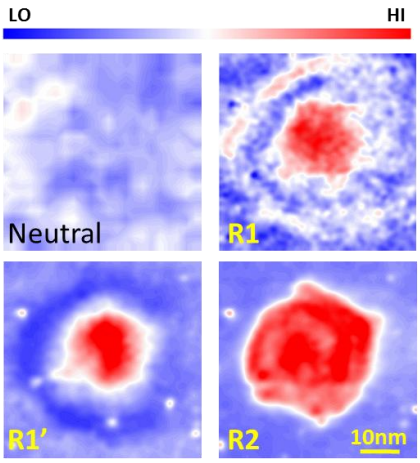

Figure 2. Spatial evolution of the atomic collapse state visualized by constant energy dI/dV maps in the vicinity of the vacancy. Top left: map of neutral vacancy. Top right: corresponds to the DOS map of lowest energy state which is the equivalent of the 1S state in atoms. The halo around the central state corresponds to hole states considered to be the equivalent of positrons produced in atomic collapse. Bottom right is the equivalent of the 2S state in atoms.

- *Screening Charged Impurities and Lifting the Orbital Degeneracy in Graphene by Populating Landau Levels.*

In this part of the project we studied an isolated charged impurity in graphene and the interplay between the local charge and its electronic environment. Using scanning tunneling microscopy and Landau level spectroscopy we demonstrated that in the presence of a magnetic field the effective charge can be tuned and controlled by a gate voltage. This is because the gate voltage determines the Landau level occupancy which in turn controls the screening. We found that when the Fermi energy was tuned to the center of a Landau level the charge was almost completely screened. In contrast, when the Fermi energy was placed in the gap between Landau levels screening was vanishingly small and the charge reached its maximum value. In this regime we observed lifting the local orbital degeneracy seen as splitting of the Landau levels into spatially separated orbital momentum states, shown in Figure 1. The resulting discrete localized sublevels act as a tunable multilevel quantum dot with energy scales comparable to room temperature.

3. Future Plans

The emergence of novel phases and macroscopic properties in the presence of electronic correlations at the atomic level, is one of the central problems in condensed matter physics. An example of this phenomenon is the so called Kondo effect in metals containing magnetic impurities, whereby coupling between the conduction electrons and the local magnetic moments leads to screening of the moment so that an initially paramagnetic material becomes non-magnetic. While the Kondo effect in conventional metals, where the density of states is flat and the conduction electrons are described by a Fermi liquid, has been studied extensively and is by now well understood, much less is known about Kondo screening in un-conventional materials where the density of states exhibits pseudo-gap behavior.

We will explore physical phenomena and possible device applications associated with magnetism and Kondo screening in low dimensional electron systems. We will focus on graphene with local magnetic moments induced by point defects, primarily vacancies. The

pseudo-gap dispersion of electrons in graphene is expected to lead to unusual screening of magnetic moments, which is characterized by a zero temperature quantum critical transition that separates paramagnetic from non-magnetic behavior. One particularly interesting consequence of this transition is the possibility of tuning the presence and strength of Kondo screening by shifting the chemical potential away from charge neutrality with a gate voltage. Consequently it should be possible to switch the magnetic moments in graphene on or off with an electric field. This is important not only as a realization of a new class of quantum critical transitions, but also as a potential building block in spintronics applications.

The research topics that will be addressed in this work include:

- Gate induced Kondo screening and quantum criticality in graphene.
- Effects of local curvature on Kondo criticality.
- Substrate induced Kondo screening by electrons in gated transition metal dichalcogenide crystalline layers.

The experimental probes will include scanning tunneling microcopy and spectroscopy, Landau level spectroscopy, atomic force microscopy and magneto transport. Substrates will include atomically flat hBN as well as exfoliated thin layers of small gap transition metal dichalcogenide crystals.

4. References

[1] X. Du, I. Skachko, A. Barker, E.Y. Andrei, Approaching ballistic transport in suspended graphene, Nature Nanotechnology, 3 (2008) 491-495.

[2] X. Du, I. Skachko, F. Duerr, A. Luican, E.Y. Andrei, Fractional quantum Hall effect and insulating phase of Dirac electrons in graphene, Nature, 462 (2009) 192.

[3] G. Li, A. Luican, E.Y. Andrei, Scanning Tunneling Spectroscopy of Graphene on Graphite, Physical Review Letters, 102 (2009) 176804.

[4] G. Li, A. Luican, D. Abanin, L. Levitov, E.Y. Andrei, Evolution of Landau levels into edge states at an atomically sharp edge in graphene, Nature Communication, 4 (2013) 1744.

[5] G. Li, A. Luican, E.Y. Andrei, Self-navigation of an STM tip toward a micron sized sample, Rev. Sci. Instrum., 82 (2011) 073501.

5. Recent Publications acknowledging DOE support

- Realization of a Tunable Artificial Atom at a Charged Vacancy in Graphene, J. Mao, Y. Jiang, D. Moldovan , G. Li, K. Watanabe, T. Taniguchi, M.R. Masir, F. M. Peeters, E.Y. Andrei, submitted (2015).
- Local and Global Screening Properties of Graphene Revealed through Landau Level Spectroscopy, C.P. Lu, M. Rodriguez-Vega, G. Li, A. Luican, K. Watanabe, T. Taniguchi, E. Rossi, E.Y. Andrei arXiv:1504.07540, submitted.
- MoS_2: Choice Substrate for Studying Graphene by Scanning Tunneling Microscopy and Spectroscopy, Chih-Pin Lu, Guohong Li, K. Watanabe, T. Taniguchi, Eva Y. Andrei , Phys. Rev. Lett. 113, 156804 (2014) Editor's Suggestion
- Probing Dirac Fermions in Graphene by Scanning Tunneling Probes, Adina Luican-Mayer and Eva Y. Andrei, in "The Physics of Graphene", editors H. Aoki and M. Dresselhaus, Springer 2014
- Screening Charged Impurities and Lifting the Orbital Degeneracy in Graphene by Populating Landau Levels, Adina Luican-Mayer, Maxim Kharitonov, Guohong Li, ChihPin Lu, Ivan Skachko, Alem-Mar B. Goncalves, K. Watanabe, T. Taniguchi and Eva Y. Andrei, Physical Review Letters, 112, 036804 (2014).
- Bandgap and doping effects in MoS2 measured by Scanning Tunneling Microscopy and Spectroscopy, Chih-Pin Lu, G. Li, K. Watanabe, T. Taniguchi, E.Y. Andrei, Nano Letters 14, 4628 (2014)

Electronic and photonic phenomen of graphene, boron nitride and graphene/boron nitride heterostructures

D.N. Basov

Department of Physics, University of California San Diego

Program Scope

Graphene and hexagonal boron nitride (hBN) are emerging as prototypical examples of two-dimensional layered van der Waals (vdW) crystals: materials in which atomic layers are weakly coupled by vdW interaction. These systems can harbor superconductivity and ferromagnetism with high transition temperatures, emit light, and exhibit topologically protected surface states, among many other effects. An ambitious practical goal is to exploit atomic planes of vdW crystals as building blocks of more complex artificially stacked structures where each such block will deliver layer-specific attributes for the purpose of their combined functionality. Heterostructures assembled from atomically thin crystalline layers of diverse vdW solids are emerging as a new paradigm in the design of materials with tailored physical properties. Within the proposed program the PI will investigate the simplest vdW heterostructure: hBN-graphene-hBN. The experimental focus will be on the nano-infrared and nano-optical investigations of electronic, plasmonic and phonon-polaritonic effects that are difficult or impossible to access using alternative experimental means.

The proposed program is comprised of three complementary research directions:

i) intrinsic electrodynamics of graphene that has remained elusive for nearly a decade but is now within the experimental reach due to the availability of high mobility graphene/hBN samples;
ii) physics of phonon polaritons in hBN that are relevant to the entire class of vdW crystals;
iii) properties of the graphene/hBN interfaces including controlled modification of the electronic and photonic phenomena by moire superlattice patterns as well as by plasmon-phonon interaction.

Recent Progress

Experiments carried out by the PI have established that hexagonal boron nitride (h-BN) is a natural hyperbolic material, in which the dielectric constants are the same in the basal plane ($\varepsilon t \equiv \varepsilon x = \varepsilon y$) but have opposite signs ($\varepsilon t \varepsilon z < 0$) in the normal plane ($\varepsilon z$). Owing to this property, finite-thickness slabs of h-BN act as multimode waveguides for the propagation of hyperbolic phonon polaritons—collective modes that originate from the coupling between photons and electric dipoles in phonons. However, control of these hyperbolic phonon polaritons modes has remained challenging, mostly because their electrodynamic properties are dictated by the crystal lattice of h-BN. The PI has been able to show, by direct nano-infrared imaging, that these hyperbolic polaritons can be effectively modulated in a van der Waals heterostructure composed of monolayer graphene on h-BN. The physics behind this tunability originates from the hybridization of surface plasmon polaritons in graphene with hyperbolic phonon polaritons in h-

BN, so that the eigenmodes of the graphene/h-BN heterostructure are hyperbolic plasmon–phonon polaritons. The hyperbolic plasmon–phonon polaritons in graphene/h-BN suffer little from ohmic losses, making their propagation length 1.5–2.0 times greater than that of hyperbolic phonon polaritons in h-BN. The hyperbolic plasmon–phonon polaritons possess the combined virtues of surface plasmon polaritons in graphene and hyperbolic phonon polaritons in h-BN. Therefore, graphene/h-BN can be classified as an electromagnetic metamaterial as the resulting properties of these devices are not present in its constituent elements alone..

Future Plans

The PI will carry out systematic nano-infrared studies of moire superlattices at the interface of graphene and hBN. Furthermore, the PI will investigate ultrafast electrodynamics of graphene using a novel pump-probe system suitable nano-scale exploration of sub-ps phenomena in solids.

References

N/A

Publications

S. Dai, Q. Ma, M. K. Liu, T. Andersen, Z. Fei, M. D. Goldflam, M.Wagner, K.Watanabe, T. Taniguchi, M. Thiemens, F. Keilmann, G. C. A. M. Janssen, S-E. Zhu, P. Jarillo-Herrero, M. M. Fogler and D. N. Basov "*Graphene on hexagonal boron nitride as a tunable hyperbolic metamaterial*" Nature Nanotechnology 10, 682 (2015).

K. W. Post, Y. S. Lee, B. C. Chapler, A. A. Schafgans, Mario Novak, A. A. Taskin, Kouji Segawa, M. D. Goldflam, H. T. Stinson, Yoichi Ando, and D. N. Basov "*Infrared probe of the bulk insulating response in $Bi_{2-x}Sb_xTe_{3-y}Se_y$ topological insulator alloys*" Physical Review B 91, 165202 (2015)

I. T. Lucas, A. S. McLeod, J. S. Syzdek, D. S. Middlemiss, C. P. Grey, D. N. Basov, and R. Kostecki, "*IR Near-Field Spectroscopy and Imaging of Single Li_xFePO_4 Microcrystals*" Nanoletter 15, 1 (2015).

D. N. Basov, M. M. Fogler, A. Lanzara, Feng Wang, and Yuanbo Zhang "*Graphene spectroscopy*" Reviews of Modern Physics 86, 959 (2014).

S. Dai, Z. Fei, Q. Ma, A. S. Rodin, M. Wagner, A. S. McLeod, M. K. Liu, W. Gannett, W. Regan, K. Watanabe, T. Taniguchi, M. Thiemens, G. Dominguez, A. H. Castro Neto, A. Zettl, F. Keilmann, P. Jarillo-Herrero, M. M. Fogler, D.N.Basov "*Tunable Phonon Polaritons in Atomically Thin van der Waals Crystals of Boron Nitride*" Science 343, 1125 (2014).

Martin Wagner, Zhe Fei, Alexander S. McLeod, Aleksandr S. Rodin, Wenzhong Bao, Eric G. Iwinski, Zeng Zhao, Michael Goldflam, Mengkun Liu, Gerardo Dominguez, Mark Thiemens, Michael M. Fogler, Antonio H. Castro Neto, Chun Ning Lau, Sergiu Amarie, Fritz Keilmann, and D. N. Basov, "*Ultrafast and Nanoscale Plasmonic Phenomena in Exfoliated Graphene Revealed by Infrared Pump–Probe Nanoscopy*" Nano Lett. 14, 894 (2014).

Program Title: Probing Nanocrystal Electronic Structure and Dynamics in the Limit of Single Nanocrystals

Principle Investigator: Moungi Bawendi
Mailing Address: Dept. of Chemistry, MIT, Rm. 6-221, Cambridge, MA 02139
E-mail: mgb@mit.edu

Program Scope: Nanocrystals (NCs) of semiconductors have been incorporated into hybrid organic/inorganic solar photovoltaic devices for increased light absorption, increased charge separation rates, and enhanced mobilities. NCs have also been incorporated as the functional light emitting material in a variety of solid-state light emitting structures for lighting and displays. The NCs, optimized in this case for high quantum efficiency and a saturated color in emission, serve either as energy efficient color downshifting elements, pumped with a blue diode, or directly electrically pumped as the primary emissive component. The foundation of all this activity is the synthesis and thorough characterization, both structural and optical, of the NCs themselves. Given the potential impact of devices that use NCs as a functional material in the energy field, it is crucial to understand *at a very basic level* the optical physics, both static and dynamic, of NCs of a variety of materials and morphologies.

The program consists of a set of critical studies of nanocrystal electronic structure and dynamics, largely at the level of single NCs, including: (1) utilizing a novel single molecule characterization technique that we have developed, Photon-Correlation Fourier Spectroscopy (PCFS), to reveal the intrinsic single NC spectrum and its dynamics; (2) probing the dynamical and spectral properties of multiexcitons, through the development of solution and nth-order Photon Correlation Spectroscopy (nPCS); (3) applying PCFS and single NC Photon-Correlation Spectroscopies to Shortwave Infrared (SWIR) emitting NCs using superconducting nanowire single photon detectors (SNSPDs). In addition we are also applying the tools that we have developed to elucidate exciton transport in tubular J-aggregate structures that mimic the antennae structures in the photosynthetic systems of green sulfur bacteria.

Recent Progress:

Revealing the Intrinsic Single-Nanocrystal Spectrum using photon-correlation Fourier Spectroscopy

The coupling between excitons and local vibrations is a fundamental physical property of nanocrystals with important consequences for their device applications. In modern samples with high monodispersity and reduced spectral diffusion, it is the primary source of line-broadening in the fluorescence spectrum. Nevertheless, the dependence of the single-nanocrystal linewidth on the synthetic

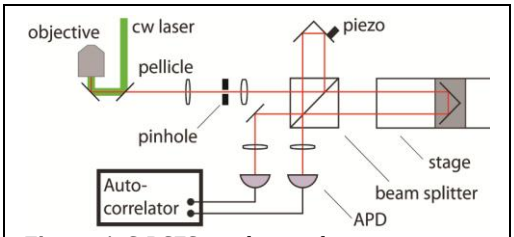

Figure 1. S-PCFS combines photon correlation and interferometry to reveal the average single-nanocrystal fluorescence lineshape.

parameters of nanocrystals remains a topic of controversy due to poor control of sample properties and a variety of experimental artifacts. Our recently-developed technique, solution-phase photon-correlation Fourier spectroscopy (S-PCFS, Fig. 1), can reveal the average single-nanocrystal fluorescence lineshape with large sample statistics, high signal-to-noise ratios, and short exposure times, and without user selection bias and high excitation flux. We have recently focused on using S-PCFS to investigate infrared-emitting nanocrystals.

Nanocrystals made of InAs, PbSe, and PbS are promising short-wave infrared-emitting (SWIR) materials with high quantum yields, tunable emission wavelengths, and narrow fluorescence linewidths compared to other SWIR materials. However, their synthesis is still under-developed and their fluorescence linewidths are still considerably broader than most visible-emitting nanocrystals. Whether these broad linewidths are caused by sample polydispersity or unique exciton-phonon coupling properties has not been determined because of the difficulties of infrared single-photon detection. In our proposal, we outlined our strategy to apply S-PCFS to infrared-emitting materials in order to study the basic physics behind their fluorescence lineshapes.

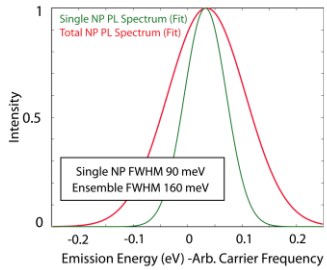

Figure 2. Modeled ensemble and average single-nanocrystal spectra for a sample of PbS nanocrystals. The 90 meV single-nanocrystal linewidth is as broad as the broadest visible-emitting samples of CdSe.

We have finished the construction of an experimental setup capable of performing S-PCFS on near-IR infrared-emitting materials (700-1000nm). This setup still relies on the silicon detectors used to study visible-emitting systems, but will be adapted to study SWIR emission between 1000-1600nm using superconducting nanowire single-photon detectors. Our preliminary results on PbS nanocrystals shown in Figure 2 suggest that, even though their ensemble spectra are broadened considerably by polydispersity, their average single-nanocrystal linewidths are also as broad as the broadest visible-emitting nanocrystals made from CdSe. differences between exciton-phonon coupling

Measuring the Ensemble-Averaged Biexciton Quantum Yield

One of the major findings in our previous work was that there is considerable variability in the quantum yield of biexcitonic states amongst nanocrystals in a given sample, suggesting that current nanocrystal syntheses do not carefully control the structural parameters responsible for promoting or suppressing multiexciton fluorescence. This makes it difficult to understand the effect of synthesis on multiexciton recombination using single-molecule techniques because dozens of particles must be measured to compile adequate sample statistics. We have completed the development of an ensemble-

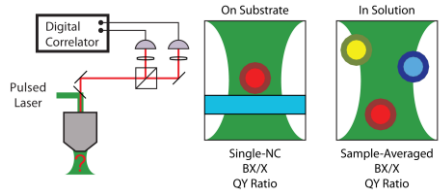

Figure 3. A pulsed-g(2) antibunching experimental setup. Performing the experiment on a substrate reveals the single-nanocrystal biexciton-exciton quantum yield ratio, whereas performing the experiment on a solution-phase sample reveals the ensemble-averaged biexciton-exciton quantum yield ratio.

averaged analogue to the single-nanocrystal $g^{(2)}$ experiment that analyzes a small focal volume of nanocrystals freely diffusing in solution (S-$g^{(2)}$, Fig. 3). Our S-$g^{(2)}$ experiment measures the same observable as the $g^{(2)}$ experiment, but averages over all of the particles that diffuse through the focal volume during the experiment.

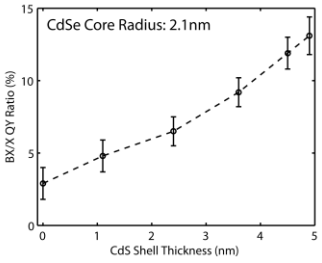

Figure 4. The efficiency of multiexciton fluorescence increases during our new CdS shell growth synthesis.

This experiment allows us to easily characterize the average properties of a sample with high precision. For example, in our recently-published manuscript, we examined the change in biexciton quantum yield as a CdSe sample is overcoated with a CdS shell (Fig. 4). Biexciton quantum yield measurements on other CdS shell growth methodologies suggested that CdS shell growth could promote multiexciton fluorescence, but only if the interface between the core and shell was alloyed either intentionally, via precursor addition, or unintentionally, via a prolonged multi-day shell growth procedure. By using a less reactive precursor, our CdS shell growth procedure appears to promote multiexciton fluorescence without the need for a prolonged alloying period.

Exciton Diffusion in Tubular J-Aggregates

Like nanocrystals, J-aggregates have delocalized excitons, high oscillator strengths and narrow emission profiles, making them ideal excitonic antenna for hybrid materials. Considerable effort has recently been dedicated to understanding the optical properties of C_8S_3 J-Aggregates, a supramolecular dye structure which self-assembles into highly-ordered extended tubular helices. Nevertheless, there have been few studies into the *dynamics* of excitonic motion in these structures. The investigation of the excitonic diffusion in materials like C_8S_3 J-Aggregates, with low dynamic and static disorder, allows us to determine how efficient energy transfer can be controlled in highly organized organic networks.

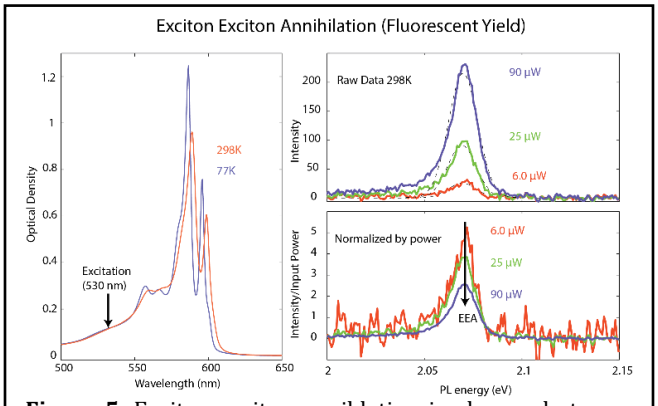

Figure 5. Exciton-exciton annihilation is observed at very low laser fluxes, indicating long-range exciton transport.

To probe this exciton diffusion, we have developed a new sample preparation, which isolates the J-Aggregates in a sugar-based cryoprotectant that dramatically improves their chemical and photostability. We have measured the temperature-dependence of their absorption and fluorescence spectra, and analyzed signatures of exciton-exciton annihilation. We observe that exciton diffusion in this material is very long, upwards 3 microns at 77K, and 1 micron at room temperature (Figure 5). The increased diffusion length with decreased temperature suggests that excitons are undergoing band-like transport in a supramolecular material, and demonstrate high delocalization and transport.

Future Plans:

1. *Revealing the Intrinsic Single-Nanocrystal Spectrum and its Dynamics Using PCFS in the SWIR region (1-2 micron).* We plan to probe the spectrum and dynamics of IR emitting QDs of interest in solar energy applications using newly developed highly sensitive Single Nanowire Superconductive Photodetectors (SNSPD's)

2. *Understanding Multiexciton States in Single Nanocrystals*. We plan to develop a PCFS-based technique for extracting the average biexciton binding energy of single NC's.

3. *Probing Diffusion in Tubular J-Aggregates.* We plan on constructing hybrid QD-J-aggregate structures to harness the long-range exciton transport of the J-aggregates and couple this to QD's as emitting "traps".

Publications with support from this DoE program in the last two years.

1. *Beyler AP, Marshall LF, Cui J, Brokmann X, Bawendi MG. "Direct Observation of Rapid Discrete Spectral Dynamics in Single Colloidal CdSe-CdS Core-Shell Quantum Dots."* **Physical Review Letters.** ***2013,*** *111, 177401.*
2. *Cui J, Beyler AP, Bischof TS, Wilson MWB, Bawendi MG. "Deconstructing the photon stream from single nanocrystals: from binning to correlation."* **Chemical Society Reviews.** ***2014****, 43, 1287-1310.*
3. *Beyler AP, Bischof TS, Cui J, Coropceanu I, Harris DK, Bawendi MG. "Sample-Averaged Biexciton Quantum Yield Measured by Solution-Phase Photon Correlation."* ***Nano Letters. 2014****, 14, 6792-6798.*
4. *Chen O, Riedemann L, Etoc F, Herrmann H, Coppey M, Barch M, Farrar CT, Zhao J, Bruns OT, We H, Guo P, Cui J, Jensen R, Chen Y, Harris DK, Cordero JM, Wang Z, Jasanoff A, Fukumura D, Reimer R, Dahan M, Jain RK, Bawendi MG. "Magneto-fluorescent core-shell supernanoparticles."* **Nature Communications.** ***2014****, 5, 5093.*
5. *Han H-S, Niemeyer E, Huang Y, Kamoun WS, Martin JD, Bhaumik J, Chen Y, Roberge S, Cui J, Martin MR, Fukumura D, Jain RK, Bawendi MG, Duda DG. "Quantum dot/antibody conjugates for in vivo cytometric imaging in mice."* ***Proceedings of the National Academy of Sciences of the United States of America. 2015,*** *112 (5), 1350-1355.*
6. *Cui J, Beyler AP, Coropceanu I, Cleary, L, Avila T, Chen Y, Cordero J, Heathcote SL, Harris DK, Chen O, Cao J, Bawendi MG. "The Evolution of the Single-Nanocrystal Fluorescence Linewidthwith Size and Shell: Implications for Exciton-Phono Coupling and the Optimizatino of Spectral Linewidths" (****under review 2015****).*
7. *Caram JR, Eisele DM, Doria S, Lloyd S, Bawendi MG. "Long-Distance Coherent Exciton Diffusion in Supramolecular Light-Harversting Nanotubes" (****under review 2015****).*

Title: Nonlinear Transport in Mesoscopic Structures in the Presence of Strong Many-Body Phenomena
Principal Investigator: Jonathan Bird, University at Buffalo, jbird@buffalo.edu

PROJECT SCOPE

On approaching the microscopic realm from the classical world one enters an intermediate, "mesoscopic", regime, in which rich quantum-mechanical behavior may be manifested by systems with large numbers of interacting particles. The study of physics on this mesoscopic scale has a long history of informing the development of condensed-matter physics. At the same time, this field remains fertile for fundamental discovery, most notably by addressing issues at the nexus of two distinct fields – nonequilibrium quantum transport and many-body physics. It is the exploration of novel phenomena in these regimes that provides the overarching motivation for this project. Addressing these problems requires the use of novel experimental techniques, most notably transient electrical measurements that probe transport in mesoscopic systems in real-time with sub-nanosecond resolution. In this project we apply such techniques to investigate aspects of nonequilibrium transport in quasi-one-dimensional structures, formed in high mobility two-dimensional electron gas systems, as well as in various graphene devices.

RECENT PROGRESS

1. Protected Subband for Conduction in Quantum Point Contacts Subjected to Extreme Biasing

Managing energy dissipation in nanodevices is critical to the scaling of current microelectronics, and to the development of novel devices that use quantum coherence to achieve enhanced functionality. To this end, strategies are needed to tailor the electron-phonon interaction, which is the dominant mechanism for cooling non-equilibrium ("hot") carriers in semiconductors. In this work we have demonstrated a counterintuitive result, showing that strong electron-phonon scattering may generate a robust mode for electrical conduction in nanodevices, driven into extreme non-equilibrium by nanosecond voltage pulses. When the amplitude of these pulses is much larger than all other relevant energy scales, strong electron-phonon scattering induces an attraction between electrons in the channel of the nanodevice. This leads to the spontaneous formation of a narrow current filament, and to a renormalization of the electronic states responsible for transport. The lowest of these states coalesce to form a subband that is separated from all others by an energy gap larger than the source voltage. Evidence for this renormalization is provided by a suppression of heating-related signatures in the transient conductance, which becomes pinned near $2e^2/h$ for a broad range of source and gate voltages. This collective non-equilibrium mode is observed over a wide range of temperature (4.2 - 300 K), and may provide an effective means to manage electron-phonon scattering in nanoscale devices.

In this work, transient heating of carriers was investigated in quantum point contacts (QPCs) implemented in the high-mobility two-dimensional-electron-gas of a GaAs/AlGaAs heterostructure. Experiments were performed in the extreme nonequilibrium limit, where the bias was very much larger than all other energy scales in the system (i.e. $eV_{sd} \sim 10^2$ mV >> Δ & E_F, where E_F is the Fermi energy). The new behaviour we have revealed in this regime is that transport changes significantly when carriers are driven far from equilibrium, while simultaneously being subjected to strong lateral confinement. Under such conditions, we find that the conductance appears to be dominated by a single "protected" subband that shows unexpected immunity to local heating. To describe this new state, we have calculated the effective inter-subband coupling arising from electron-phonon scattering. A key assumption, driven by the phenomenology of the experiment, is that electron-phonon coupling under extreme nonequilibrium is strongly dependent on the local electron density, a characteristic that we incorporate empirically by imposing a nonlinear correction to this coupling. This correction gives rise to a positive feedback, in which the phonon-mediated attraction induces a local enhancement of the electron density, producing an even stronger attraction yet. As this feedback grows with increase of V_{sd} a self-organized spatial inhomogeneity, consisting of a narrow current filament that flows along the centre line of the QPC, ultimately develops spontaneously. It is the formation of this filament that drives the emergence of the protected subband, which is energetically separated from the higher subbands. Since the energy trans-

fer processes involved in the formation of this subband structure are quite generic to semiconductor devices, our observations provide an important demonstration of how hot-carrier relaxation via strong phonon emission may be managed in nanodevices.

Related Publication:

1. J. Lee, J. E. Han, S. Xiao, J. Song., J. L. Reno, and J. P. Bird, "*Formation of a protected sub-band for conduction in quantum point contacts under extreme biasing*", Nature Nanotechnology **9**, 101 (2014).

2. Tuning the Fano Resonance with an Intruder Continuum

Arising from the coupling of a discrete level to a continuum, the Fano resonance (FR) is ubiquitous to atomic-, molecular-, and condensed-matter systems. As a wave-interference phenomenon, it is also of increasing importance in optics, plasmonics, and metamaterials, where its ability to cause rapid signal modulations under variation of some suitable parameter makes it desirable for a variety of applications. In the field of nanoelectronics, FRs have been widely observed in semiconductor quantum dots, and have attracted interest as a means for electrical- or optical-signal control. A surprising feature of the FR is that its rich variations are obtained from a simple interference geometry, involving an electron that is excited from an initial atomic level to a final state in a continuum via two separate paths. The first of these is direct, while the second involves an intermediate transition through a discrete level.

While the standard two-path Fano interferometer provides a powerful scheme for manipulating wave transmission, in this work we have demonstrated the possibility of achieving even stronger resonant control by making just a simple modification to that interference geometry. The essential element of our approach involves coupling an additional continuum to the original Fano system, thereby forming a three-path interferometer. By varying the strength of the coupling to this continuum, we have found that it is possible to induce significant lineshape distortions, which may even exceed the amplitude of the original FR. For a proof-of-concept demonstration of its influence, we have realized this system in a nanoscale interferometer formed by a pair of coupled quantum point contacts. It must be emphasized, however, that this interference scheme is a completely general one. As such, it should be broadly applicable across a variety of different wave-based systems, including those in both photonics and electronics.

Related Publications:

1. J. Fransson, M.-G. Kang, Y. Yoon, S. Xiao, Y. Ochiai, J. L. Reno, N. Aoki, and J. P. Bird, "*Tuning the Fano resonance with an intruder continuum*", Nano Lett. **14**, 788 (2014).
2. S. Xiao, Y. Yoon, Y.-H. Lee, J. P. Bird, Y. Ochiai, N. Aoki, J. L. Reno, and J. Fransson, "*Detecting weak coupling of quantum systems with a nonequilibrium Fano resonance*", under review (2015).

FUTURE PLANS

Current efforts are strongly focused on the study of nonequilibrium phenomena in 2D semiconductors, most notably MoS_2 and graphene. In the latter material, a strong point of interest concerns the mechanisms for high-field drift-velocity saturation (DVS). Arising from optical-phonon emission by “hot” electrons or holes, this phenomenon has long been studied in conventional semiconductors. With the emergence of graphene as a candidate for use in future nanoelectronics, however, it is vital to understand the origins of DVS in this novel material. Although the large optical-phonon energies of graphene promise high saturation velocities, experiments reveal much lower values that are degraded by Joule heating of the supporting substrate. We are therefore exploring a strategy to overcome this problem, using nanosecond pulsing to drive graphene’s hot carriers on time scales much faster than those on which substrate heating can occur. The rapid pulsing is performed at room temperature in an impedance-matched setup, in which electrical contact to graphene flakes, exfoliated on SiO_2, is provided by on-chip coplanar waveguides (CPWs, see Fig. 1(a)). The carrier density is then varied by making use of an aligned top-gate (TG), isolated from the graphene by 120 nm of hardened PMMA (Fig. 1(b)). Pulses of various amplitude (v_p^{in}) and duration are applied to the input CPW, and the resulting current is measured by connecting the output waveguide to the 50-Ω input of a sampling oscilloscope.

Using structures such as those indicated in Fig. 1, we are able to observe, for the first time, the inherent velocity-saturation characteristics of graphene, independent of the influence of its (SiO_2) substrate. Resultant saturation velocities (approaching 10^8 cm/s near the Dirac point) are found to exceed those reported for suspended graphene and for devices on boron nitride substrates, with corresponding current densities (~10^9 A/cm^2) reaching those found in carbon nanotubes and graphene-on-diamond transistors.

Previous theoretical work has suggested that the role of substrate phonons can mean that enhancements in graphene's low-field properties, achieved through substrate engineering, may not necessarily translate into similarly-improved high-field characteristics. Our work is consistent with these ideas, in the sense that we obtain saturated velocities much higher than those reported previously, in spite of the much lower mobility of our devices when compared to suspended material or to graphene on BN. The essential element here is rather the use of rapid pulsing as a technique to avoid the influence of the substrate completely, providing a strategy that should be useful to manage heat dissipation in graphene and other 2D semiconductors.

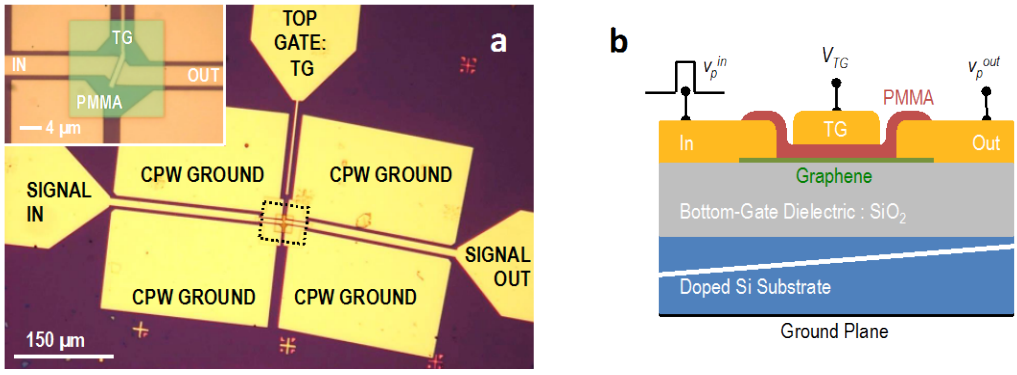

Figure 1. (a) The main panel is an optical micrograph of one of the graphene transistors (Device D5) studied here, showing the CPW structure used to make contact to the graphene flake. The area enclosed by the dotted line is shown in expanded form in the inset, in which the hardened PMMA layer has been colorized to highlight the top-gate geometry. **(b)** Cross-sectional schematic indicating the essential components of our top-gated devices.

Having established the viability of pulsed techniques for studies of DVS, we are planning to extend these measurements to other systems, most notably to graphene on BN substrates, as well as (in the longer term) to MoS_2 on BN.

Related Publications:

1. H. Ramamoorthy, R. Somphonsane, J. Radice, G. He, C.-P. Kwan, and J. P. Bird, "*Freeing graphene from its substrate: Observing intrinsic velocity saturation with rapid electrical pulsing*", to be submitted.

PUBLICATIONS RESULTING FROM DOE SUPPORT: 2012 - 2015

1. I. Rotter and J. P. Bird, "*Recent Progress in the Physics of Open Quantum Systems: Theory and Experiment*", Rep. Prog. Phys., *in press* (2015).
2. G. He, K. Ghosh, U. Singisetti, H. Ramamoorthy, R. Somphonsane, G. Bohra, M. Matsunaga, A. Higuchi, N. Aoki, S. Najmaei, Y. Gong, X. Zhang, R. Vajtai, P. M. Ajayan, and J. P. Bird, "*Conduction mechanisms in CVD-grown monolayer MoS2 transistors: From variable-range hopping to velocity saturation*", Nano Lett. 15, 5052 – 5058 (2015).
3. H. Ramamoorthy, R. Somphonsane, G. He, N. Aoki, Y. Ochiai, D. K. Ferry, and J. P. Bird, "*Reversing hot-carrier energy relaxation in graphene with a magnetic field*", Appl. Phys. Lett. **104**, 193115 (2014).

4. J. Fransson, M.-G. Kang, Y. Yoon, S. Xiao, Y. Ochiai, J. L. Reno, N. Aoki, and J. P. Bird, "*Tuning the Fano resonance with an intruder continuum*", Nano Lett. **14**, 788 – 793 (2014).
5. J. Lee, J. E. Han, S. Xiao, J. Song., J. L. Reno, and J. P. Bird, "*Formation of a protected sub-band for conduction in quantum point contacts under extreme biasing*", Nature Nanotechnol. **9**, 101 – 105 (2014).
6. R. Somphonsane, H. Ramamoorthy, G. Bohra, G. He, D. K. Ferry, Y. Ochiai, N. Aoki, and J. P. Bird, "*Fast energy relaxation of hot carriers near the Dirac point of graphene*", Nano Lett. **13**, 4305 – 4310 (2013).
7. G. Bohra, R. Somphonsane, N. Aoki, Y. Ochiai, R. Akis, D. K. Ferry, and J. P. Bird, "*Nonergodicity and microscopic symmetry breaking of the conductance fluctuations in disordered mesoscopic graphene*", Phys. Rev. B **86,** 161405(R) (2012).
8. Z. Chen, T.-Y. Lin, X. Wei, M. Matsunaga, T. Doi, Y. Ochiai, N. Aoki, and J. P. Bird, "*The magnetic Y-branch nanojunction: Domain-wall structure and magneto-resistance*", Appl. Phys. Lett. **101**, 102403 (2012).
9. G. Bohra, R. Somphonsane, N. Aoki, Y. Ochiai, D. K. Ferry, and J. P. Bird, "*Robust mesoscopic fluctuations in disordered graphene*", Appl. Phys. Lett. **101**, 093110 (2012).
10. Y. Yoon, M.-G. Kang, T. Morimoto, M. Kida, N. Aoki, J. L. Reno, Y. Ochiai, L. Mourokh, J. Fransson, and J. P. Bird, "*Coupling quantum states through a continuum: a mesoscopic multistate Fano resonance*", Phys. Rev. X **2**, 021003 (2012).

Program Title: Novel Behavior of Ferromagnet/Superconductor Hybrid Systems

Principle Investigator: Norman O. Birge; co-PI: William P. Pratt, Jr.
Department of Physics and Astronomy, Michigan State University
E-mail: birge@pa.msu.edu

Program Scope

The interplay between superconductivity and ferromagnetism gives rise to a number of new and fascinating phenomena. The project focuses on the unusual proximity effects that arise when conventional superconducting (S) materials are placed in contact with conventional ferromagnetic (F) materials. Because of the strong exchange field, the electron pair correlations in F oscillate and decay rapidly with increasing distance from the S/F interface [1]. In 2001, however, it was predicted that a new type of pair correlations, with spin-triplet symmetry, could be induced in S/F systems in the presence of certain kinds of magnetic inhomogeneity [2]. Those pair correlations penetrate deeply into ferromagnetic materials; hence they are sometimes called "long-range triplet correlations," or LRTC. We first observed strong evidence for the LRTC in 2010 [3]. Since then, we have been deeply engaged in characterizing, optimizing, and controlling the LRTC. The objectives of this project are: i) to optimize generation of the LRTC in S/F/S Josephson junctions; ii) to fabricate sub-micron samples with single-domain magnetic layers, which will allow us to control the LRTC in a single sample; iii) to find a new signature of the LRTC in the tunneling density of states; and iv) to measure the spatial decay of the LRTC over long distances, in planar samples patterned by e-beam lithography.

Recent Progress

Amplitude control of the spin-triplet Josephson coupling: The Josephson junction samples we used to observe the LRTC have the sandwich geometry shown schematically in Figure 1, with the general structure S/F′/F/F″/S, where F′ and F″ are thin ferromagnetic layers (≈ a few nm), whereas F can be quite thick – up to 50 nm so far. Cu layers (not shown) are inserted between adjacent ferromagnetic layers to suppress exchange coupling. For the F layer, we use a Co/Ru/Co synthetic antiferromagnetic (SAF), in which the magnetizations of the two Co layers are coupled antiparallel to each other. Figure 1 represents the SAF as a single magnetic layer for simplicity. When the magnetizations of adjacent layers in the structure are orthogonal, the spin-triplet supercurrent is optimized [4]. If two adjacent layers are parallel, such as in the cartoon on the far left, there

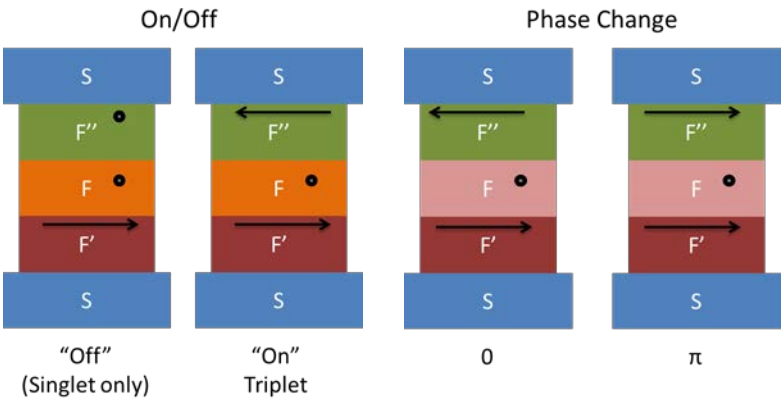

Figure 1: Schematic representation of our S/F′/F/F″/S Josephson junction samples (not to scale). The current flows in the vertical direction. Arrows show magnetization directions for amplitude control (left) or phase control (right) of spin-triplet supercurrent.

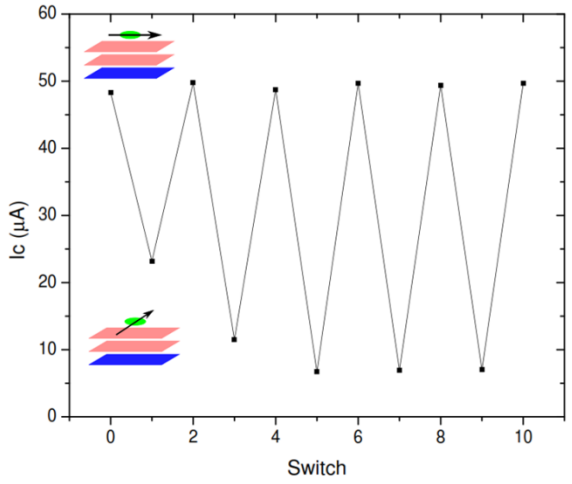

Figure 2: Critical current of an S/F′/F/F″/S Josephson junction during multiple "on-off" switches – i.e. after applying a 20 mT field either along or perpendicular to the F′ layer magnetization.

should be no spin-triplet supercurrent, hence we represent this situation as the "off" state. To demonstrate on-off control, we must construct a system where we can rotate the magnetization direction of one magnetic layer in the stack while keeping the other two fixed. To achieve this goal, we use a soft magnetic material, Permalloy, for F″, while using a hard material, Ni, for F′. We also verified that the magnetizations of the two layers in the SAF do not move much for applied fields smaller than 20 mT. Our procedure is to start by initializing the sample with a large (260 mT) in-plane field. This causes both the F′ and F″ layers to magnetize along the field direction, while the SAF undergoes a "spin-flop" transition and the two layers magnetize along directions perpendicular to the field [5]. We then apply a small (10 – 20 mT) in-plane field in the perpendicular direction to rotate F″ and put the sample in the "off" state. We can recover the on state with a small parallel field. Figure 2 shows results of repeated on-off switching from one of our samples. After a small training period, the amplitudes of the supercurrent in the on and off states obtain an on/off ratio of 7. Two other samples exhibited ratios of 5 and 19. The amplitude of the spin-triplet supercurrent in the on state is quite consistent between the three samples, whereas the off-state amplitude varies slightly, giving rise to large fluctuations in the on-off ratio. These new results confirm an important prediction of the theory [2,4].

Phase control of the spin-triplet Josephson coupling: Theory predicts that one can control the sign of the Josephson coupling by reversing the direction of the F″ magnetization while keeping the F′ and F magnetizations fixed, as shown in the two right-hand pictures of Figure 1. Standard Josephson junctions have positive coupling, meaning that the phases of the superconducting condensates in the superconductors on either side of the junction are the same in equilibrium (in the absence of supercurrent). Such junctions are called "0" junctions. Negative coupling gives rise to "π" junctions, in which the phases of the condensates differ by π in equilibrium. To measure the phase, we use a Superconducting Quantum Interference Device, or SQUID, containing two elliptically-shaped junctions with different eccentricities, hence with different switching fields. A schematic diagram of SQUID is shown in Figure 3. Figure 4 shows the SQUID critical current, I_c, as a function of flux (labeled as I_Squid) and in-plane set field. After initializing the sample, we apply gradually-increasing set fields to reverse the magnetization direction of the F″. After each set field is applied, we measure

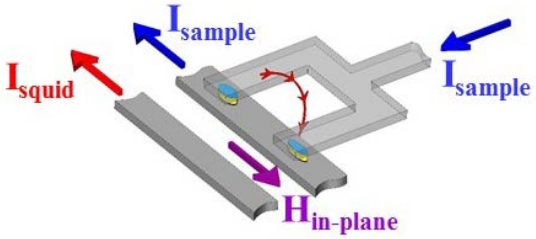

Figure 3: Schematic diagram of SQUID containing two S/F′/F/F″/S Josephson junctions.

a sweep of I_c vs flux. At the set field of 180 Oe, the Ic vs flux curves shift by a half-period, indicating that one of the junctions in the SQUID has acquired a phase shift of π. At the set field of 200 Oe, the curves shift back again, indicating that the second junction switched to the π state. While these data are very exciting, this sample exhibited multiple phase switches in the negative field direction, possibly indicating that the magnetizations of the two "hard" layers, F′ and F, were not completely rigid. These data are in the Ph.D. thesis of Eric Gingrich, but have not been published.

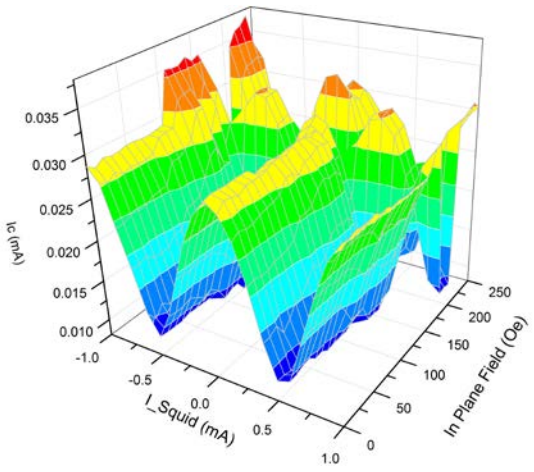

Figure 4: Critical current of a SQUID containing two S/F′/F/F′′/S Josephson junctions as a function of flux current (I_Squid) and in-plane set field. A junction transitions between the 0 and π states at set fields of 180 and 200 Oe.

Future Plans

Our highest priority in the near future is to complete the phase control experiment described above. After that we have several directions to pursue:

1. Measuring spin-triplet supercurrent in Josephson junctions is not the only way to observe the LRTC. Tunneling measurements should provide a spectroscopic signature of the LRTC, which provides complementary information to the Josephson effect. In earlier work on samples of the form S/F/I/N, where I is a thin insulating tunnel barrier and N is a non-magnetic normal metal, we observed a series of oscillations in the proximity-induced features in the tunneling density of states as a function of F layer thickness [6]. Insertion of an additional F′ layer, however, did not reveal the predicted signatures of the LRTC. We are currently trying a new approach, which is to tunnel into the S side, rather than the F side, of an S/F′/F system. The advantage of this new approach is that there is zero background, since the tunneling density of states in a spin-singlet superconductor is zero below the gap.

2. Our sandwich-style Josephson junctions have total ferromagnetic layer thicknesses of a few tens of nanometers at most. When one speaks of a "long-range proximity effect," however, one is usually thinking of hundreds of nanometers. An important goal is to understand the ultimate limits on the decay length of the spin-triplet correlations. Layer thicknesses in excess of 100 nm are not practical in the sandwich geometry (due to variations in growth morphology with increasing film thickness), but they are easily accessible in a planar geometry, using electron-beam lithography fabrication techniques. We have fabricated and measured S/N/S Josephson junctions in a planar geometry and observe supercurrent of the expected magnitude. Surprisingly, however, we have never observed supercurrent in planar S/F/S junctions fabricated using identical techniques. We have not yet resolved this mystery.

3. There are several theoretical proposals in the literature regarding generation of spin-triplet supercurrent using materials with large spin-orbit scattering [7]. A crucial point is that the spin-orbit interaction must have a preferred direction, such as Rashba type; it cannot be the random type of spin-orbit interaction that occurs in disordered metals due to scattering from heavy point

defects. Exploring this potentially rich field will require delving into a totally new area for us, namely semiconductor systems or ultra-thin epitaxial metallic films. This topic is beyond the scope of our current project, but it is a promising topic to be included in a renewal proposal.

References

[1] See, for example, Proximity effects in superconductor-ferromagnet heterostructures, A.I. Buzdin, *Rev. Mod. Phys*. **77**, 935-976 (2005).
[2] Josephson current in superconductor-ferromagnet structures with a nonhomogeneous magnetization, F.S. Bergeret, A.F. Volkov, and K.B. Efetov, *Phys. Rev. B* **64**, 134506 (2001).
[3] Observation of spin-triplet superconductivity in Co-based Josephson junctions, T.S. Khaire, M.A. Khasawneh, W.P. Pratt, Jr., and N.O. Birge, *Phys. Rev. Lett.* **104**, 137002 (2010).
[4] Long range triplet Josephson effect through a ferromagnetic trilayer, M. Houzet and A.I. Buzdin, *Phys. Rev. B* **76**, 060504(R) (2007).
[5] Optimization of spin-triplet supercurrent in ferromagnetic Josephson junctions, C. Klose, T.S. Khaire, Yixing Wang, W.P. Pratt, Jr., N.O. Birge, B.J. McMorran, T.P. Ginley, J.A. Borchers, B.J. Kirby, B.B. Maranville, and J. Unguris, *Phys. Rev. Lett.* **108**, 127002 (2012).
[6] Proximity-induced density-of-states oscillation in a superconductor/strong ferromagnet system, K. Boden, W.P. Pratt, Jr., and N.O. Birge, *Phys. Rev. B* **84**, 020510(R) (2011).
[7] Singlet-triplet conversions and the long-range proximity effect in superconductor-ferromagnet structures with generic spin dependent fields, F.S. Bergeret and I.V Tokatly, Phys. Rev. Lett. **110**, 117003 (2013).

Publications since 2012 acknowledging DOE support:

1. Optimization of spin-triplet supercurrent in ferromagnetic Josephson junctions, C. Klose, T.S. Khaire, Yixing Wang, W.P. Pratt, Jr., N.O. Birge, B.J. McMorran, T.P. Ginley, J.A. Borchers, B.J. Kirby, B.B. Maranville, and J. Unguris, *Phys. Rev. Lett.* **108**, 127002 (2012).
2. Spin-triplet supercurrent in Co/Ni multilayer Josephson junctions with perpendicular anisotropy, E.C. Gingrich, P. Quarterman, Y. Wang, R. Loloee, W.P. Pratt, Jr., and N.O. Birge, *Phys. Rev. B* **86**, 224506 (2012).
3. Area-dependence of spin-triplet supercurrent in ferromagnetic Josephson junctions, Y. Wang, W.P. Pratt, Jr., and N.O. Birge, *Phys. Rev. B* **85**, 214522 (2012).
4. Spin-triplet supercurrents in Josephson junctions containing strong ferromagnetic materials, N.O. Birge, to appear in Phil. Trans. A (2015).
5. Amplitude control of spin-triplet supercurrent in S/F/S Josephson junctions," W. Martinez, W.P. Pratt, Jr., and N.O. Birge, in preparation (2015).

Program Title: Spin wave interactions in metallic ferromagnets
Principle Investigator: Kristen Buchanan
Mailing Address: Department of Physics, Colorado State University, Fort Collins, CO 80523
E-mail: kristen.buchanan@colostate.edu

Program Scope

Spintronics and magnonics are two areas of active research in condensed matter physics and there are important connections between the two. The former refers to a new paradigm for electronic devices that make use of not only the charge but also the spin property of the electron. The latter refers to new ideas for how to utilize spin waves to transmit and process information. Both areas are attracting interest not only because they encompass a range of basic physics topics but also because of their potential to inspire new technologies. One of the broad goals of this project is to study spin waves and how they respond to external stimuli. Towards this goal we have performed micro-Brillouin light scattering experiments (micro-BLS) to map the spin wave distributions in patterned magnetic nanowires. We have explored the effects of the static spin configuration at an intersection on the spin dynamics, where we show that an antivortex spin state can be used to select for a higher wavevector spin waves [1] in a structure where the intersection spin state can be easily reconfigured [2]. We have also conducted measurements of spin waves propagating in saturated magnetic microstrips that demonstrate that it is feasible to directly excite spin waves in the backward volume (BV) configuration using a microstrip antenna, even at remanence [3].

The main technique used for this project is BLS, which is a powerful method for investigating dynamic excitations in magnetic materials and multilayers as well as patterned magnetic structures nanostructures [4]. Photons interact with spin waves or magnons in magnetic materials via inelastic scattering whereby a scattered photon gains or loses energy, which results in a small but measurable shift in the photon frequency that is equal to the magnon frequency. BLS is capable of detecting spin waves at frequencies of ~1-120 GHz with diffraction-limited spatial resolution with a micro-BLS setup (Fig. 1) and it is sensitive enough to measure thermally-generated spin waves.

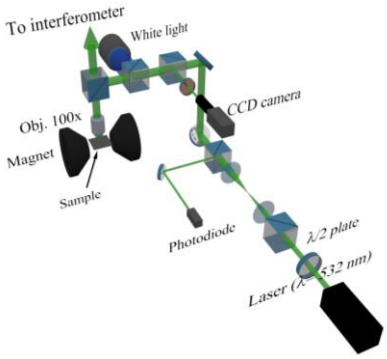

Fig. 1: Diagram of the micro-BLS. The sample position and focus are continuously stabilized using feedback from a camera. An electromagnet provides a DC magnetic field and high frequency probes deliver microwaves to the sample. The scattered light from a focused spot (~300 nm) is directed into a Fabry Perot Interferometer to determine the frequencies of the inelastically scattered photons.

Recent Progress

Spin waves interactions with a magnetic antivortex: Many proposed magnonics devices require high wavenumber excitations, and while the traditional method for exciting spin waves using microwave

antennas works well, the wavelengths that can be efficiently excited are on the order of the antenna width hence it is not practical to drive spin waves with large wavenumbers using this method. To overcome this difficulty, several methods for spin wave generation have been proposed including parametric pumping, spin transfer torque nano-oscillators, and the dynamic response of magnetic textures such as the vortex and antivortex. The antivortex (AV) spin state involves spins that sweep in towards a central core from two opposing directions and away for the other directions. Because of the seamless transition of the magnetization state from the intersection to the legs regions, there is a high potential to generate propagating spin waves by exciting the AV state. In order to make use of this advantage, however, the dynamic excitations of the AV must be understood.

In recent work, we used micro-BLS to measure the dynamic response of a magnetic AV stabilized at the intersection of 37-nm thick Permalloy magnetic microstrips, each 1-μm wide, at frequencies above the gyrotropic mode (>1 GHz). Micro-BSL spectra obtained selected positions within the intersection show a complex dynamic response, where several of the observed modes are close in frequency to azimuthal-like modes that are observed in micromagnetic simulations. Fig. 2 shows a comparison of spatial maps obtained from experimental measurements and numerical simulations for two prominent resonances. At frequencies >3 GHz the simulations show coupling between the AV modes that in some cases influences the dominant wavelength in the microstrips, e.g., for 3.4 GHz. Furthermore, for some modes the spin waves appear to propagate away from the AV region, which suggests the AV excitations may provide a means to not only control the spin waves but also potentially to serve as a source. The AV's studied here are part of a larger pound-key like shape, a geometry that we recently showed will facilitate the formation of the AV spin configuration and that can be easily reconfigured using an external magnetic field [2]. Not only are these the first experimental measurements of high-frequency modes of a magnetic antivortex, but this work also shows that the spin state at the intersection can influence

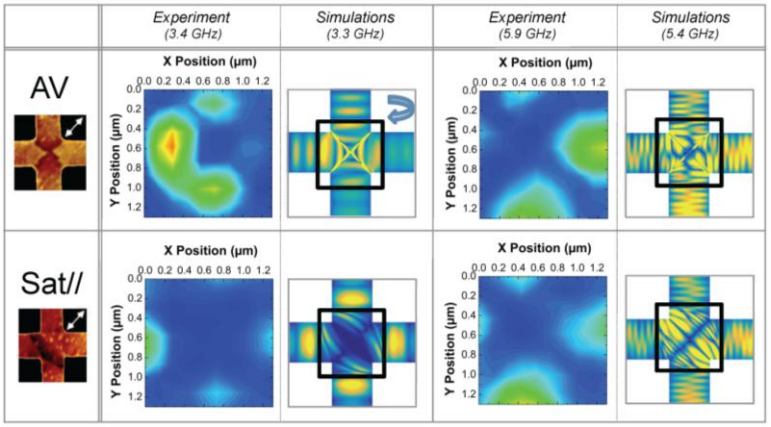

Fig. 2: A comparison of experimental measurements (left images) and mode maps obtained from numerical simulations (right images) for samples with either a magnetic antivortex (AV) or saturated spin state (Sat//) at the intersection of 1-μm wide Permalloy wires. Magnetic force microscopy images show the static spin configurations (left-most column), and the white arrows illustrate the direction of the dynamic magnetic field. The micro-BLS scan regions correspond to the black square on the simulated images. Scans are shown for 3.4 GHz and 5.4 GHz, which correspond to an *n=2* AV azimuthal mode and a higher-frequency mode that involves *m=2* quantization across leg width, respectively. For the former, the mode characteristics are considerably different for the two spin configurations not just in the intersection but also in the legs where the wavelength is smaller when an AV is present.

the dominant mode in attached nanowires where an antivortex spin state selects for a higher wavevector [1].

Backward volume spin waves in patterned ferromagnetic nanowires: In microstrips the propagation characteristics depend on the structure geometry as well as the orientation of the external magnetic field. The majority of the experiments that have been done thus far on microstrips have been performed in the Damon Eshbach (DE) geometry where the static magnetization is in-plane, perpendicular to the direction of the spin wave propagation. Sizable external magnetic fields are required to maintain this configuration due to shape anisotropy and, furthermore, deviations from a straight path, a requirement for most devices, can also be problematic. While the latter can be overcome by sending a current through a conducting layer under the magnetic microstrip [5], this requires additional device complexity and adds unwanted heat. In contrast, little or even no magnetic field is required for the backward volume (BV) geometry since the shape anisotropy maintains the desired magnetic state and, in part for this reason, numerical work on potential devices has focused mainly on the BV configuration [6-8].

Recently we have studied BV spin wave propagation in patterned microstrips. Micro-BLS measurements of spin waves excited using a microwave antenna with a width of d = 2 µm were made in a Permalloy ($Ni_{80}Fe_{20}$) microstrip with a thickness of 30 nm and a width of 2.5 µm (Fig. 3). The frequencies of the peak signals f_{peak} as well as the signal shape can be understood by considering calculations of the dispersion curves (left plots) and the antenna efficiency. Dispersion relations are shown for the two lowest order width modes that have a net non-zero magnetization across the microstrip width and hence can be excited by an antenna. The antenna efficiency, obtained from a Fourier transform of the antenna field, is highest for small k, decreases with increasing k, and has a zero efficiency at $k_{max} = 2\pi/d$. The DE intensities decrease with increasing frequency f for $f > f_{peak}$ and the BV signal diminishes with decreasing f for $f < f_{peak}$, which corresponds to increasing k and hence decreasing antenna efficiency for both configurations. Measurable spin wave intensities were observed in the BV configuration for a range of H and the observed peak frequencies agree well with dispersion calculations at all H, including H = 0 Oe. The excitation efficiency is lower for the BV configuration and the decay lengths are smaller, however, the material and thickness can be adjusted to improve decay lengths and the advantages offered by the BV geometry,

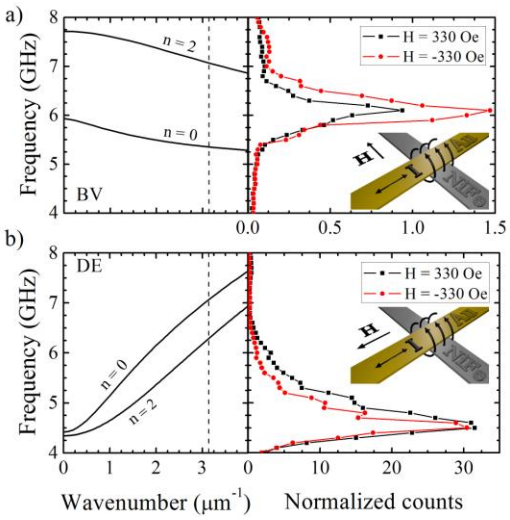

Fig. 3: Calculated dispersion relations for the first two even width-quantized modes and measured BLS signal as a function of the pumping frequency f_p are shown on the left and right, respectively, for 2.5-µm wide Permalloy microstrips magnetized in the (a) BV and (b) DE configurations with H = ±330 Oe, measured 1 µm from the antenna. The dashed lines are at k_{max}, the k where the antenna efficiency drops to zero.

including the flexibility to operate in the absence of a bias field and to handle curves, may outweigh these disadvantages for some applications, especially those that involve spin wave/domain wall interactions that cannot easily be set up in a DE geometry [8]. Our work [3] shows that it is possible to excite propagating spin waves using a conventional microstrip antenna in the BV geometry at remanence and that recently developed theories [9,10] agree well with the experimental results, both of which are important steps towards the development of nanoscale magnonics devices.

Future Plans

Going forward, BLS and BLS microscopy combined with analytical and numerical modeling will be used to explore spin wave propagation in magnetic nanowires and films, including the interplay between spin waves and spin currents in patterned magnetic nanowires and thermal effects on spin wave processes. Further studies of the coupling between antivortex and the backward volume spin waves in the attached nanowires are also underway, including additional measurements with an out-of-plane driving field, with the goal of developing a more complete understanding of how the intersection spin state can be used to control spin waves and potentially to generate high-k spin waves.

References (which acknowledge DOE support)

1. G. A. Riley, H. J. Jason Liu, M. A. Asmat-Uceda, A. Haldar, and K. S. Buchanan, "Observation of the dynamic modes of a magnetic antivortex using Brillouin light scattering", *Phys. Rev. B* **92**, 064423 (2015).
2. M. Asmat-Uceda, L. Li, B. Shaw, A. Haldar, and K. S. Buchanan, "The role of shape anisotropy in the stabilization of magnetic antivortices in pound-key like structures", *J. Appl. Phys.* **117**, 173902 (2015).
3. H.J. Liu, G. A. Riley, and K. S. Buchanan, "Directly-excited backward volume spin waves in Permalloy microstrips", submitted 2015.

Other References

4. B. Hillebrands, in *Modern techniques for characterizing magnetic materials*, edited by Y. Zhu (Kluwer Academic Publishers, Boston, 2005).
5. K. Vogt, H. Schultheiss, S. Jain, J. E. Pearson, A. Hoffmann, S. D. Bader, and B. Hillebrands, *Appl. Phys. Lett.* **101**, 042410 (2012).
6. Y. Au, M. Dvornik, O. Dmytriiev, and V. V. Kruglyak, *Appl. Phys. Lett.* **100**, 172408 (2012).
7. K.-S. Lee and S.-K. Kim, *J. of Appl. Phys.* **104**, 053909 (2008).
8. R. Hertel, W. Wulfhekel, and J. Kirschner, *Phys. Rev. Lett.* **93**, 257202 (2004).
9. M. Kostylev, G. Gubbiotti, J. G. Hu, G. Carlotti, T. Ono, and R. L. Stamps, *Phys. Rev. B* **76**, 054422 (2007).
10. K. Y. Guslienko and A. N. Slavin, *J. Magn. Magn. Mater.* **323**, 2418 (2011).

Program Title: Topological Superconductor Core-Shell Nanowires

Principal Investigator: Judy J. Cha
Department of Mechanical Engineering and Materials Science, Yale University
Mailing Address: 15 Prospect Street, New Haven, CT 06511
Email: judy.cha@yale.edu

Program Scope

The goal of this program is to realize a one-dimensional (1D) topological superconductor that is environmentally tolerant. Particularly, we aim to answer if an In-doped SnTe nanowire is a 1D topological superconductor. Topological superconductors are expected to host Majorana fermions [1,2]. For this purpose, we propose to synthesize two nanowire systems: 1) an In-doped SnTe superconducting nanowire and 2) a SnTe-InTe core-shell nanowire to protect the surface states from environmental degradation and unwanted band bending. We will use narrow In-doped SnTe nanowire interferometers to study the evolution of Aharonov-Bohm (AB) oscillations [3] to Little-Parks (LP) oscillations [4] as temperature reaches the superconducting transition temperature. Features of the AB and LP oscillations will be compared to theoretical predictions for the surface states in the nanowire geometry.

Results from this program are expected to provide a robust material system to test the existence of Majorana fermions and to protect the environmentally sensitive surface states.

Recent Progress

1) Superconducting In-doped SnTe nanoplates

We synthesized SnTe nanoplates via the mixture of vapor-liquid-solid and vapor-solid growth mechanisms using gold nanoparticles as metal catalysts and SiO_2 as growth substrates [5]. We doped SnTe nanoplates with In to induce superconductivity [6]. This was achieved by mixing SnTe and InTe powders as source powder and following the growth conditions of SnTe nanoplates. In dopants were uniformly distributed within the SnTe nanoplates, measured by energy dispersive X-ray spectroscopy in a scanning transmission electron microscope (Figure 1A). Superconductivity was confirmed by the rapid drop in resistance as a function of temperature in the In-doped SnTe nanoplate nanodevices (Figure 1B and 1C).

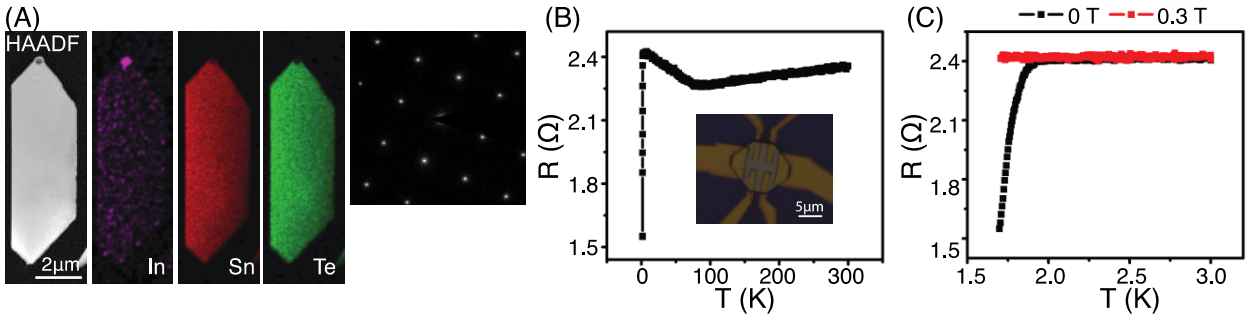

Figure 1. (A) In-doped SnTe nanoplate. (B) The rapid drop in resistance below 2 K indicates a superconducting transition, which is further supported by the field-cool data (C).

2) Surface states revealed via 2D linear magnetoresistance

We show that the surface states of the In-doped SnTe nanoplates are preserved at the In doping concentrations that show superconductivity at ~ 2 K [6]. Angle resolved photoemission

spectroscopy has shown intact surface states in In-doped SnTe bulk samples [7]. However, our results signify the first verification of intact surface states via electrical transport measurements. The surface states were manifested by 2D linear magnetoresistance, confirmed by the angle-dependent transport studies (Figure 2). Theoretical models suggest that Dirac dispersive electrons should exhibit linear magnetoresistance [8,9]. The linear magnetoresistance is insensitive to temperature up to 10 K, further supporting its surface origin.

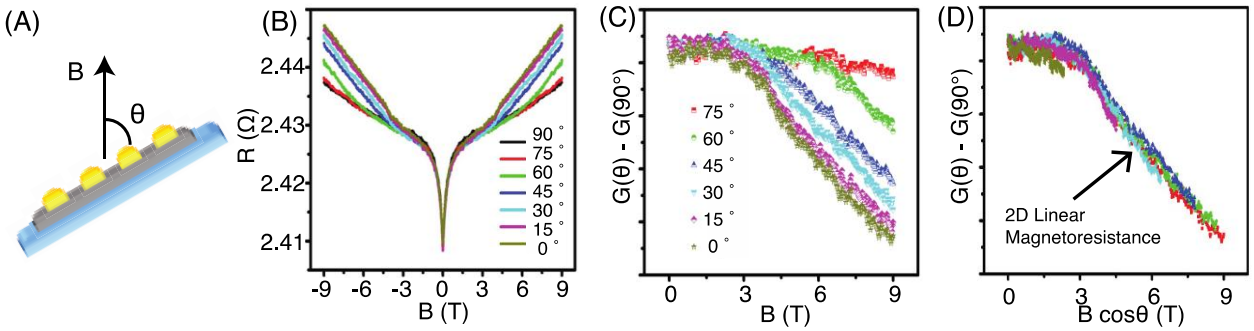

Figure 2. (A, B) Angle-dependent magnetotransport of an In-doped SnTe nanoplate at 1.7 K. A large current was applied to suppress the superconductivity. (C) Magnetoconductances at various angles of the magnetic field, after subtracting the bulk signal. (D) All the conductance traces overlap when they are plotted in *Bcosθ*, the perpendicular B, showing the 2D nature of the linear magnetoresistance.

3) Degradation of the surface states under ambient conditions

The linear magnetoresistance originating from the surface states was used as a probe to monitor how the surface states would degrade over time when the In-doped SnTe nanoplates were left in ambient conditions. The same device that exhibited the linear magnetoresistance was measured one month later. The magnetic field at which the linear magnetoresistance emerged was increased, which indicates the decrease in the mobility of the surface states (Figure 3). The slope of the linear magnetoresistance remained the same to indicate that the surface state carrier density did not change [9]. While the linear magnetoresistance changed with time, the bulk transport properties such as the bulk carrier density and the mobility remained the same, further supporting that the linear magnetoresistance is from the surface state.

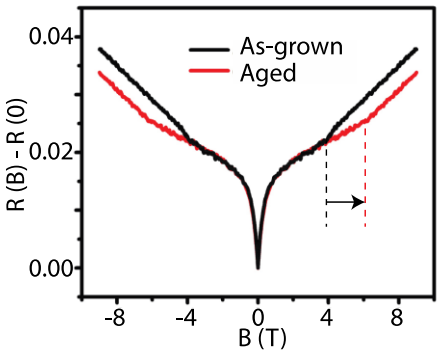

Figure 3. The 2D linear magneto-resistance changed significantly after one month, showing the degradation of the surface state.

Future Plans

1) Synthesis of narrow In-doped SnTe nanowires

We aim to answer if In-doped SnTe is a topological superconductor. We will use narrow In-doped SnTe nanowires as interferometers for the surface states and study how they change as the transport regime approaches the superconducting regime. We expect AB and LP oscillations from the In-doped SnTe nanowires at temperatures above and near the superconducting transition temperature, respectively.

We will first synthesize In-doped SnTe narrow nanowires. We have previously synthesized In-doped SnTe nanoplates. We will vary the growth conditions to achieve the nanowire geometry. First, instead of using a mixture of InTe and SnTe as source powder, we will try a

mixture of In and SnTe powders as source powder. The reason behind this is that when we tried a mixture of Bi and SnTe as source powder to dope SnTe with Bi to reduce the bulk carrier density, the majority growth products were SnTe nanowires, instead of nanoplates. We anticipate similar results with mixing In and SnTe. We will also increase the substrate temperature and reduce the growth time to control the morphology. Safdar *et. al.*, showed SnTe nanowire growth via vapor liquid solid growth mechanism [10]. In their report, the growth temperature and the substrate temperature were higher than conditions we used that produced the nanoplate geometry.

The superconducting transition temperature of synthesized In-doped SnTe narrow nanowires will be correlated with the In doping concentration. The In doping concentration will be measured by energy dispersive X-ray spectroscopy (EDX) inside a transmission electron microscope (TEM). X-ray photoemission spectroscopy will also be used to measure the average In doping concentration and compare the result with the TEM-EDX. Transport measurements will be carried out by fabricating nanodevices and measuring the longitudinal and transverse resistances as a function of temperature and magnetic fields. The Physical Property Measurement System (PPMS) from Quantum Designs will be used. In the first year, we will purchase the ^{3}He insert so that we can reach down to 300 mK. We will characterize the ^{3}He insert. Aharonov-Bohm oscillations will be measured in these nanowires by applying magnetic fields parallel to the long axis of the nanowires. We will measure the oscillations at different temperatures and analyze the amplitude, the period, and the phase of the AB oscillations. More importantly, we will monitor how the AB oscillations change as the temperature reaches near the superconductivity transition temperature. We expect that the AB oscillations will change to LP oscillations. We will simulate LP oscillations expected for normal s-wave superconductors and compare that to the observed LP oscillations. We expect distinct differences. We will develop LP oscillations expected from a 1D topological superconductor, in collaboration with Dr. Liang Fu at MIT.

2) Coat SnTe nanowires with a Te protection layer

The change in the linear magnetoresistance with time (Figure 3) shows the critical need to protect the surface states of SnTe from impurities that could stem from surface oxide formation and Fermi level pinning near the surface that may result in additional low-mobility carriers. Our ultimate goal is to produce epitaxial SnTe-InTe core-shell nanowires in which the InTe shell serves as a protection layer. As a stepping-stone and easier route, we will first coat SnTe nanowires with an amorphous Te layer, *in situ*. This will be carried out by evaporating Te powder inside the tube furnace after the SnTe nanowire growth. The Te vapor will condense onto the SnTe nanowires and form a coating layer because the growth substrates will be in a colder zone. A similar strategy was used to coat successfully Bi_2Se_3 nanoribbons with an amorphous Se layer, which effectively protected the surface states of Bi_2Se_3 [11]. We will measure the linear magnetoresistance as a function of aging time to monitor how robust the surface state remains. We will develop an etching process to etch away the Te layer in the electrode contact region in order to make electrical contacts directly to SnTe. We will explore both plasma etching and wet etching.

References

1 Majorana, E. *Nuovo Cimento* **5**, 171-184 (1937).

2 Qi, X.-L. & Zhang, S.-C. Topological insulators and superconductors. *Reviews of Modern Physics* **83**, 1057-1110 (2011).
3 Aharonov, Y. & Bohm, D. Significance of Electromagnetic Potentials in teh Quantum Theory. *The Physical Review* **115**, 485-491 (1959).
4 Little, W. A. & Parks, R. D. Observation of Quantum Periodicity in the Transition Temperature of a Superconducting Cylinder. *Phys. Rev. Lett.* **9**, 9-12 (1962).
5 Shen, J., Jung, Y., Disa, A. S., Walker, F. J., Ahn, C. H. & Cha, J. J. Synthesis of SnTe Nanoplates with {100} and {111} Surfaces. *Nano Lett.* **14**, 4183-4188, doi:10.1021/nl501953s (2014).
6 Shen, J., Xie, Y. & Cha, J. J. Revealing Surface States in In-Doped SnTe Nanoplates with Low Bulk Mobility. *Nano Letters* **15**, 3827-3832, doi:10.1021/acs.nanolett.5b00576 (2015).
7 Sato, T., Tanaka, Y., Nakayama, K., Souma, S., Takahashi, T., Sasaki, S., Ren, Z., Taskin, A. A., Segawa, K. & Ando, Y. Fermiology of the Strongly Spin-Orbit Coupled Superconductor $Sn_{1-x}In_xTe$: Implications for Topological Superconductivity. *Phys. Rev. Lett.* **110**, 206804 (2013).
8 Abrikosov, A. A. Quantum magnetoresistance. *Physical Review B* **58**, 2788-2794 (1998).
9 Wang, C. M. & Lei, X. L. Linear magnetoresistance on the topological surface. *Physical Review B* **86**, 035442 (2012).
10 Safdar, M., Wang, Q., Mirza, M., Wang, Z., Xu, K. & He, J. Topological Surface Transport Properties of Single-Crystalline SnTe Nanowire. *Nano Lett.* **13**, 5344-5349, doi:10.1021/nl402841x (2013).
11 Hong, S. S., Zhang, Y., Cha, J. J., Qi, X.-L. & Cui, Y. One-Dimensional Helical Transport in Topological Insulator Nanowire Interferometers. *Nano Lett.* **14**, 2815-2821, doi:10.1021/nl500822g (2014).

Publications

The funded program starts from August 2015. Thus there are no publications to report.

Novel sample structures and probing techniques of exotic states in the second Landau level

Principal Investigators: Gabor Csathy and Michael Manfra
Institution: Purdue University
Address: 525 Northwestern Ave., West Lafayette, IN 47907
E-mail of PIs: gcsathy@purdue.edu, mmanfra@purdue.edu

Program Scope

The two-dimensional electron gas hosts a wealth of unusual phases arising from the interplay of reduced dimensionality and strong electron-electron interactions. Recently it was suggested that this system may support unusual ground states which harbor exotic particles with special topological properties. Specifically, the ground states are thought to have Abelian and non-Abelian properties of various kinds [a]. The most interesting states form in the region of the phase space commonly referred to as the second Landau level.

Examples of such unusual ground states in the second Landau level are the fractional quantum Hall states at the quantum numbers 5/2 and 12/5. These ground states are not only of fundamental interest as they may manifest behavior not seen in any other physical system, but also may find technological utility in fault-tolerant schemes for quantum computation [b]. These exotic states are, however, fragile and hence they develop only under special conditions.

Two-dimensional electron gases are realized in a large variety of semiconductor hosts. GaAs/AlGaAs plays an important role among these semiconductors and the low temperature mean free path is the longest. Because of the very long mean free path, conditions are favorable for the development of a large number of exotic ground states, including several states believed to be non-Abelian.

At Purdue University we have developed a synergistic experimental program based on systematic growth and ultra-low temperature measurement of high quality GaAs/AlGaAs crystals tailored to answering outstanding questions concerning the collective behavior of the correlated electronic ground states of the two-dimensional electron gas. Our primary focus is the study of the fractional quantum Hall states and exotic electronic solids of the second Landau level, i.e. corresponding to Landau level filling factors $2 \leq \nu \leq 4$. The goal of our program is to use state-of-the-art growth and incisive experimental measurement techniques to generate new insight into the nature of the exotic correlated states of the second Landau level.

Recent Progress

This project builds on the ongoing collaboration of the PIs and unique experimental capabilities developed at Purdue University. **Manfra** operates state-of-the art MBE growth producing wafers with record high mobility. **Csathy** has an ultra-low temperature instrument capable of producing one of the lowest electron temperatures of 5 mK.

Advances in material growth In the past year we have made several advances in material quality and improved our understanding of the relationship between disorder-induced scattering, ever-present density inhomogeneity, and low temperature transport characteristics in the second Landau level. Improvements made to our MBE system and materials preparation techniques resulted in a dramatic improvement in low temperature mobility. We produced samples with

mobility in excess of $35x10^6cm^2/Vs$ - a 75% improvement over our first growth campaign. Importantly, we discovered that the purity of gallium source material is the primary limiting factor in the achievement of ultra-high mobility. As shown in the Fig. 1 below, in-situ purification of gallium resulted in discrete jumps in mobility.

While mobility is one metric of film quality we have also made progress in our understanding of what parameters control the strength of the fragile states in the second Landau level. In collaborative work with the Folk group at Univ. of British Columbia we demonstrated the careful study of low temperature illumination and thermal annealing can increase the excitation gap at $\nu=5/2$ ($\Delta_{5/2}$) to 0.6K [10]. While $\Delta_{5/2}$ increases by a factor of 3 in these illumination experiments, mobility changes minimally, indicating that the disorder that controls the strength of the gap is not the same that sets mobility. We have initiated experiments to determine what metrics of two-dimensional electron gas quality measured during sample screening at T=0.3K correlate best with low temperature (T=10mK) behavior in the second Landau level. In addition to mobility we also measure quantum scattering time and the resistivity at $\nu=5/2$ at T=0.3K. We find interesting behavior where the resistivity at 5/2 saturates to a minimum value of approximately 40Ω/sq. even as the mobility continues to improve during the growth campaign (see Fig. 2). Our initial data indicate that the value of 5/2 resistivity at T=0.3K correlates inversely with the strength of the $\nu=5/2$ gap and is a better indicator of transport in the second Landau level at low temperatures than mobility.

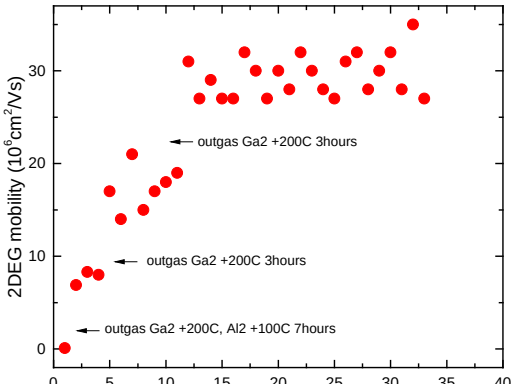

Figure 1: Mobility as a function of growth number and outgassing of gallium source.

Studies of the effects of heterostructure design We have also studied the impact of heterostructure design on the transport properties in the second Landau level in samples with an in-situ back gate [1]. In this work we demonstrated the placement of AlAs/GaAs superlattice between the back gate and the 2DEG has enormous impact on reducing the gate-to-2DEG leakage current. Reduction of gate leakage is extremely important in devices designed to explore states in the second Landau level. In this work we demonstrated that leakage current as low as a few 10s of picoamps can result in heating detrimental to observation of fragile correlated states in the second Landau level. Properly designed heterostructures allowed us to produce devices that could be tuned from full depletion up to an electron density of $3.35x10^{11}cm^{-2}$, where we observed $\Delta_{5/2}$=625mK, the highest value to be reported to date. These devices form a novel platform where the properties of the second Landau can be explored as a function of the electron density.

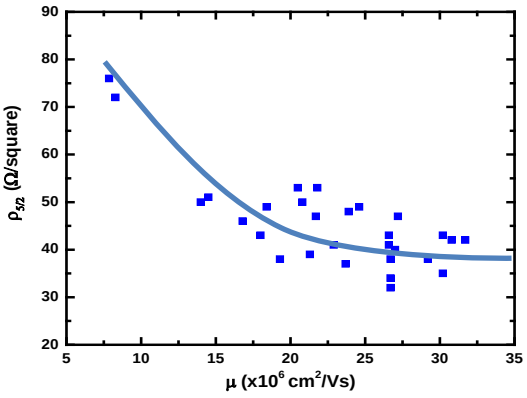

Figure 2: Resistivity at 5/2 filling at T=0.3K as a function of mobility.

Alloy disorder and the even denominator fractional states Unraveling the impact of disorder is an important endeavor in contemporary condensed matter physics. Disorder is well understood in the single particle regime, but remains under scrutiny in novel systems such as topological insulators and atomic condensates. In contrast, understanding disorder in correlated electron

systems, often referred to as many-body localization, continues to pose serious challenges. The Molecular Beam Epitaxy technique allows not only the growth of very low disorder 2DEGs, but also enables controlled introduction of minute amounts of disorder into the 2DEG. Such specially tailor samples with one kind of disorder, called alloy disorder, were recently grown by Manfra [3] and studied at low temperatures in Csathy's laboratory [2]. As reported in a recent Physical Review Letters, a very surprising lowering of the mobility threshold for the even denominator 5/2 fractional state has been observed. Indeed, in high quality samples the 5/2 state has not been observed below the mobility of $7x10^6 cm^2/Vs$. In contrast, Csathy and his students found a mobility threshold in alloy samples of only $1.8x10^6 cm^2/Vs$. The lowering of the mobility threshold is currently not yet understood. However, these results are expected to stimulate theoretical research on disorder effects and provide input for the design of future, improved sample structures.

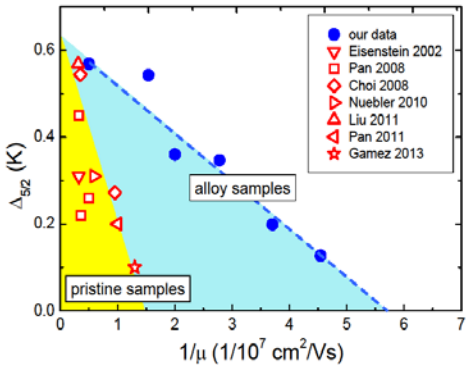

Figure 3: The gap at 5/2 filling as a function of mobility for pristine and alloy samples.

Tuning the exotic states with hydrostatic pressure One current focus of Csathy's research is the development of novel, incisive techniques probing the two-dimensional electron gas. Historically the most popular measurement technique used in investigations of this system is electronic transport. However, over the last decade or so it became increasingly clear that the probing of the new topologically ordered states requires more sophisticated techniques. Measurement of these systems at high hydrostatic pressures is one such technique currently being implemented by Csathy. The commercial pressure cell used is seen in the figure in the right. At pressures of the order of 10,000 atmospheres one can tune many relevant quantities which are expected to impact numerous ground states. We have recently discovered a novel transition from a fractional quantum Hall state to an electronic stripe phase.

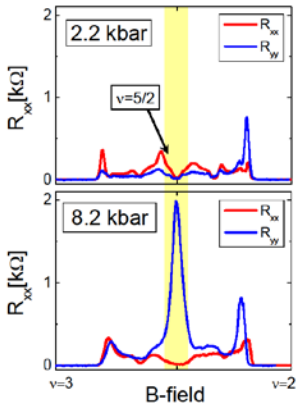

Figure 4: The application of hydrostatic pressure induces an unexpected phase transition.

Collaborative efforts Under this program, **Manfra** has grown high quality materials used by several researchers, many of whom are DOE supported: Piczuk at Columbia, Zudov at Univ. Minnesota, Kono at Rice, and Engel at the Nationa High Magnetic Field Lab in Tallahassee [4-12]. **Csathy** is using the ultra-low temperature capability in his lab to work with two other DOE supported colleagues: Du at Rice [13] and Rokhinson at Purdue.

Future Plans We will continue our effort in studying disorder effects by expanding the energy gap measurements for other types of well-controlled disorder, such as charged disorder. We expect that disorder-specific information will guide us in further improvements of the growth process and may lead to new insight of the behavior of these systems. Encouraged by our recent results, we will continue to study pressure effects in the GaAs system. Specifically, we will investigate the spin polarization effects in the exotic ground states. We have recently started an effort to study the evolution of the interesting ground state with the width of the quantum well they reside in. Such investigations involve a coordinated effort between growth and ultra-low temperature measurement and are part of our long term effort aimed at exploring unconventional collective behavior in low-dimensional systems.

References

a) A. Stern, "Non-Abelian States of Matter", Nature (London) **464**, 187 (2010).
b) C. Nayak, S. Simon, A. Stern, M. Freedman, and S. Das Sarma, "Non-Abelian Anyons and Topological Quantum Computing", Review of Modern Physics. **80**, 1083 (2008)

Publications acknowledging DOE BES support since 2013

1. J.D. Watson, G.A. Csathy, and M.J. Manfra, "Impact of heterostructure design on transport properties in the second Landau level in in-situ back-gated two-dimensional electron gases", Physical Review Applied **3**, 064004 (2015)
2. N. Deng, G.C. Gardner, S. Mondal, E. Kleinbaum, M.J. Manfra, and G.A. Csathy, "Anomalous Robustness of the ν=5/2 Fractional Quantum Hall state in the Presence of Alloy Disorder", Physical Review Letters **112**, 116804 (2014)
3. G.C. Gardner, J.D. Watson, S. Mondal, N. Deng, G.A. Csathy, and M.J. Manfra, "Growth and electrical characterization of $Al_{0.24}Ga_{0.76}As/Al_xGa_{1-x}As/Al_{0.24}Ga_{0.76}As$ modulation-doped quantum wells with extremely low x", Applied Physics Letters **102**, 252103 (2013)
4. Q. Shi, P.D. Martin, A.T. Hatke, M.A. Zudov, J.D. Watson, G.C. Gardner, M.J. Manfra, L.N. Pfeiffer, and K.W. West, "Shubnikov–de Haas oscillations in a two-dimensional electron gas under subterahertz radiation", Physical Review B **92**, 081405 (2015)
5. Z. Wan, A. Kazakov, M.J. Manfra, L.N. Pfeiffer, K.W. West, and L.P. Rokhinson, "Induced superconductivity in high-mobility two-dimensional electron gas in gallium arsenide heterostructures", Nature Communications **6**, 7426 (2015)
6. M.J. Manfra, "Molecular Beam Epitaxy of Ultra-High-Quality AlGaAs/ GaAs Heterostructures: Enabling Physics in Low-Dimensional Electronic Systems", Annu. Rev. Condens. Matter Phys. **5**, 347 (2014)
7. Q. Zhang, T. Arikawa, E. Kato, J.L. Reno, W. Pan, J.D. Watson, M.J. Manfra, M.A. Zudov, M. Tokman, M. Erukhimova, A. Belyanin, and J. Kono, "Superradiant Decay of Cyclotron Resonance of Two-Dimensional Electron Gases", Physical Review Letters **113**, 047601 (2014)
8. N.J. Goble, J.D. Watson, M.J. Manfra, and X.P.A. Gao, "Impact of short-range scattering on the metallic transport of strongly correlated two-dimensional holes in GaAs quantum wells", Physical Review B **90**, 035310 (2014)
9. S. Chakraborty,1 A. T. Hatke,1 L. W. Engel,1 J. D. Watson,2,3 and M. J. Manfra, "Multiphoton processes at cyclotron resonance subharmonics in a two-dimensional electron system under dc and microwave excitation", Physical Review B **90**, 195437 (2014)
10. M. Samani, A.V. Rossokhaty, E. Sajadi,S. Luscher, J. A. Folk, J. D. Watson, G.C. Gardner, and M.J. Manfra, "Low-temperature illumination and annealing of ultrahigh quality quantum wells", Physical Review B **90**, 121405 (2014)
11. A.T. Hatke, M. A. Zudov, J. D. Watson, M. J. Manfra, L. N. Pfeiffer, and K. W. West, "Effective mass from microwave photoresistance measurements in GaAs/AlGaAs quantum wells", Journal of Physics: Conference Series **456,** 012040 (2013)
12. A.T. Hatke, M.A. Zudov, J.D. Watson, and M.J. Manfra, L.N. Pfeiffer, and K.W. West, "Evidence of Effective Mass Reduction in GaAs/AlGaAs Quantum Wells", Physical Review Letters **B** 87, 161307 (2013)
13. Tingxin Li, Pengjie Wang, Hailong Fu, Lingjie Du, Kate Schreiber, Xiaoyang Mu, Xiaoxue Liu, Gerard Sullivan, G.A Csathy, Xi Lin, and Rui-Rui Du, "Observation of Helical Luttinger-Liquid in InAs-GaSb Quantum Spin Hall Edges", in press with Physical Review Letters

Dynamics of electronic interactions in superconductors and related materials.

Dan Dessau, Department of Physics, University of Colorado, Boulder

Dessau@Colorado.edu or 303-492-1607

Project Scope:

Our project centers on experimental studies of the dynamics of electronic interactions in high temperature cuprate superconductors and related materials. We primarily utilize high-resolution angle-resolved photoemission (ARPES) and we have been focusing on extracting the self-energies or electronic interactions in a much more quantitative manner than what has been previously carried out. This is possible due to the significantly improved quantitative accuracy in both the measurements as well as in the data analysis, coming out of our work from within this program. We argue that these self-energies are likely to be especially important in materials like the cuprate superconductors, and that our methods are particularly well-suited to extract this information. For other materials of interest, such as iridates, nickelates, or topological insulators, much new information may be obtained through a simpler analysis solely relying on band dispersions and Fermi surfaces, and we carry out such experiments as well.

Recent Progress:

Here we focus on our work on cuprate superconductors, though as shown by the publications listed below we have made good progress on many other materials as well. We begin discussion with the two methods papers, which were critical for enabling the progress we made here. First, there is paper M1, in which we developed a rapid and robust method for recognizing and removing ARPES detector nonlinearities, which have negative impacted the quantitative accuracy of count rates in almost all modern ARPES experiments. This improved quantitative accuracy was critical for the next level of advancements in the technique, which was first discussed in paper O1. This paper introduced the new TDoS or Tomographic Density of States technique for ARPES analysis, which allows a uniquely powerful determination of the superconducting pairing gap Δ and the pair-breaking self energy Γ. This technique was subsequently used in papers C1, C3, C6, and C7, which each explored new aspects of cuprate physics that could be uncovered from this new method, including the evolution of the "Fermi arcs" with temperature (C8), the filling of the gap with temperature (C7), and the effect of impurities on the pairing and pair-breaking terms (C6). Our paper C1 compiles a great amount of data and new understanding, as shown in figures 1 and 2. In general we see that the superconducting gap in the cuprates "fills in" with increasing temperature, which is due to a rapidly increasing pair-breaking term Γ with temperature. This contrasts with the BCS case in which the gap closes with temperature, i.e. the gap gets smaller and smaller rather than it filling.

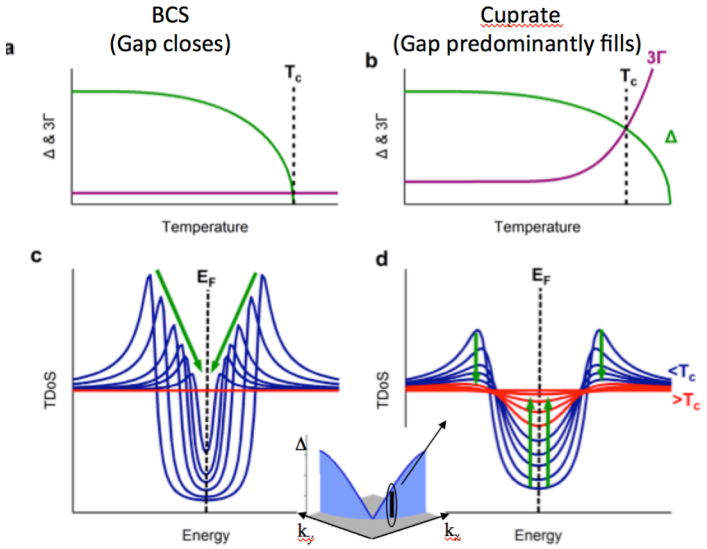

Fig 1. (from paper C1). Our TDoS analysis method allows a uniquely quantitative determination of the superconducting pairing gap Δ and the pair-breaking self energy Γ. We find that Γ is strongly temperature dependent in the cuprates (right side), which fills in the superconducting gap with increasing temperature, in contrast to the BCS gap in which the gap closes with temperature. The gap in the cuprates still exists above T_c (red curves). We empirically determined that T_c is determined by a crossover between Δ and 3Γ (schematic, top curves), in contrast to the BCS case in which Γ is mostly ignored and Tc is determined by Δ going to zero.

Experimentally we find that the gap in the cuprates still exists above T_c (red curves of fig 1d), with it closing at a temperature 20-30K above Tc that we call T_{pair}. A key result is that we empirically determined that T_c is determined by a crossover between Δ and 3Γ (8 different samples shown in fig 2), in contrast to the BCS case in which Γ is mostly ignored and Tc is determined by Δ going to zero (panel a of fig 1). Thus we show the tremendous importance of the self-energy term Γ in the cuprates – it effectively sets the Tc, lowering it from the pairing onset temperature that is expected from any BCS-like theory.

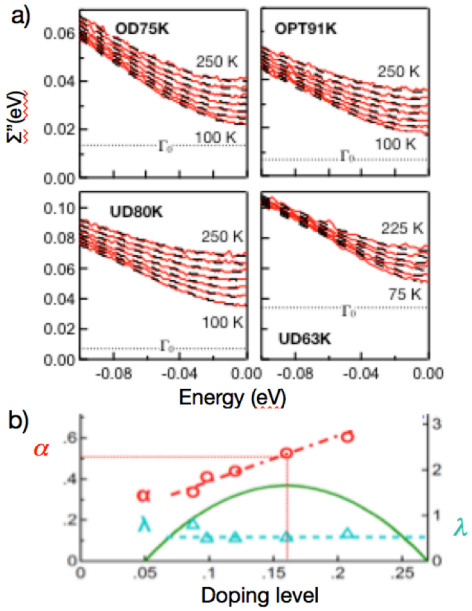

Fig 3. (From paper C2). (a) Normal state nodal electronic scattering rates are measured as a function of both temperature and energy for 4 cuprate samples of widely different doping levels. Data are red curves and simultaneously fitted temperature and energy data are black dashed lines. (b) We ansatz a "power law liquid" state for the scattering rates with key parameter the power law exponent α and coupling parameter λ (found not to vary with doping). With this single effective parameter α a huge range of spectroscopic and transport results as a function of energy, temperature and doping can be understood, potentially implying a deep scaling law.

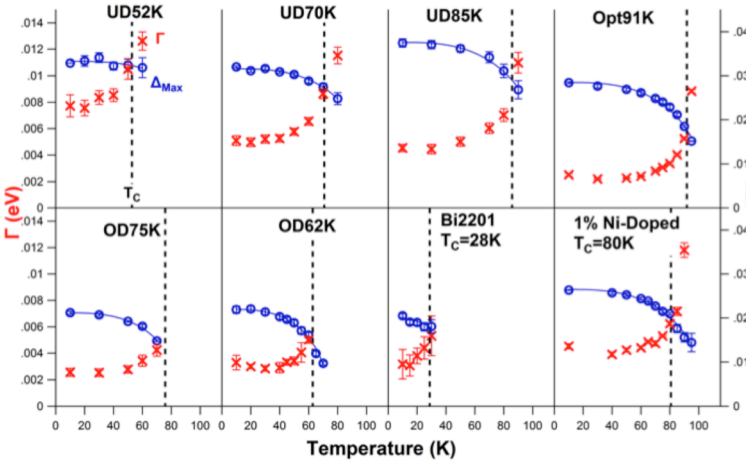

Fig 2. (From paper C1) Experimentally measured superconducting pairing gap Δ (blue) and pair breaking self energy Γ (red) vs. temperature, for many different samples. Tc's range from 30K to 91K and are marked by the black dashed lines. Δ and 3Γ cross at Tc for all samples.

We also made significant recent progress in understanding the self-energies in the normal state of the cuprates, which has been known to be a critical mystery since the first year of study of the cuprates. In particular, the normal state scattering rate (imaginary part of the self-energy Σ", which could also be called simply Γ) is expected by Fermi Liquid theory to be quadratic (power law 2) in energy and temperature, but has been known to be closer to linear (power law 1) for the cuprates. In paper C2 we measured the normal state nodal self-energies of a range of doping levels of cuprates and fit these simultaneously with an ansatz for the self-energies as a function of temperature and energy, giving serious extra constraints over previous attempts (panel a of fig 3). We found that our ansatz self-energy effectively only has one parameter that varies with doping, the power law exponent α (red in panel b). With this ansatz and the one-parameter α, we are able to reproduce transport and optics data as a function of energy, temperature and doping nearly quantitatively. String theorists and others are showing great interest, as the unified power laws on the electronic interactions appear to put especially strong constraints on any theory of correlated matter.

Future Plans:

Our past work has made strong progress in uncovering the electronic self energies in both the normal and superconducting states, though we still do not have an adequate understanding of the origin of the self-energy effects or how these connect between the different states, or possibly

even drive the transition between these states. In preliminary work we are making good progress in making these connections, and we are also making strong connections to thermodynamics and other probes of the superconducting and normal states of the cuprates. We also are starting to make good progress on understanding the pseudogap state from a new perspective based upon our work on self-energy effects, and we plan to continue this as well. These studies will be carried out on our ultra-resolution laser-ARPES system as well as with synchrotron beamlines and discharge lamps so that we can access the entire Brillouin zone.

We have been working hard on ARPES experiments on iridate single crystals with a wide variety of doping, through a collaboration with Gang Cao (Kentucky). We (paper I1) and others have found that these have many similarities to the cuprates, including pseudogaps, non-Fermi Liquid scattering rates (self energies), etc. They give a new window to measure and understand the evolution of the Fermi surface, Mott gaps, scattering rates, etc. with doping and temperature, and we will continue to study these and related materials. We also have a collaboration with John Mitchell (Argonne) to study a new class of nickelate single crystal samples that just became available as they require a special high pressure growth furnace. These materials appear to be a close analogue of the cuprates in their electronic structure and charge states, and we have shown that we can get excellent quality ARPES spectra. As these are brand new materials with a variety of stoichiometries, possible doping levels, etc., a great many opportunities are available.

Publications acknowledging DOE support, 2013-1015:

Cuprate superconductors:

C1 T. J. Reber, S. Parham, N. C. Plumb, Y. Cao, H. Li, Z. Sun, Q. Wang, H. Iwasawa, M. Arita, J. S. Wen, Z. J. Xu, G.D. Gu, Y. Yoshida, H. Eisaki, G.B. Arnold, D. S. Dessau "Pairing, pair-breaking self energies, and their roles in setting the Tc of cuprate high temperature superconductors" arXiv:1508.06252 (submitted to Nature Physics)

C2 T.J. Reber, J.A. Waugh, N.C. Plumb, S. Parham, Y. Cao, Z. Sun, Q. Wang, J.S. Wen, Z.J. Xu, G. Gu, Y. Yoshida, H. Eisaki, Y. Aiura, G.B. Arnold, D. S. Dessau. "Power Law Liquid – A Unified Form of Low-Energy Nodal Electronic Interactions in Hole Doped Cuprate Superconductors" arXiv:1509.01611 (Under peer review at Nature Physics)

C3 T. J. Reber, S. Parham, N. C. Plumb, Y. Cao, H. Li, Z. Sun, Q. Wang, H. Iwasawa, J. S. Wen, Z. J. Xu, G. Gu, S. Ono, H. Berger, Y. Yoshida, H. Eisaki, Y. Aiura, G. B. Arnold, and D. S. Dessau "Coordination of the energy and temperature scales of pairing across the doping phase diagram of $Bi_2Sr_2CaCu_2O_{8+\delta}$" arXiv:1509.01556 (Under peer review at Phys. Rev. Lett.)

C4 S.R. Park, Y. Cao, Q. Wang, M. Fujita, K. Yamada, S.-K. Mo, D. S. Dessau, D. Reznik "Broken relationship between superconducting pairing interaction and electronic dispersion kinks in $La_{2-x}Sr_xCuO_4$ measured by angle-resolved photoemission" Phys. Rev. B 88,220503(R) (2013)

C5 N.C. Plumb, T. J. Reber, H. Iwasawa, Y. Cao, Y. Yoshida, H. Eisaki, Y. Aiura, D. S. Dessau, "Large momentum-dependence of the main dispersion "kink" in the high-Tc superconductor $Bi_2Sr_2CaCu_2O_{8+\delta}$ New J. Phys. **15** 113004 (2013)

C6 S. Parham, T.J. Reber, Y.Cao, J.A. Waugh, G. Gu, D.S. Dessau Effects of Fe Impurities on the Gap and Electronic Scattering Rates in the High-Tc Superconductor $Bi_{2.1}Sr_{1.9}Ca(Cu_{1-y}Fe_y)_2O_x$ PRB 87, 104501 (2013)

C7 T. J. Reber, N. C. Plumb, Y. Cao, Z. Sun, Q. Wang, K.E. McElroy, H. Iwasawa, M. Arita, J.S. Wen, Z.J. Xu, G. Gu, Y. Yoshida, H. Eisaki, Y. Aiura, and D. S. Dessau Prepairing and the "filling" gap in the cuprates from the tomographic density of states Phys. Rev. B **87**, 060506

(2013).

Fe pnictide superconductors:

F1 Q. Wang, Z. Sun, E. Rotenberg, F. Ronning, E. D. Bauer, H. Lin, R. S. Markiewicz, M. Lindroos, B. Barbiellini, A. Bansil, and D. S. Dessau "Symmetry-Broken Electronic Structure and Uniaxial Fermi Surface Nesting of Untwinned $CaFe_2As_2$" Phys. Rev. B **88**, 235125 (2013)

F2 M. P. Allan, T.-M. Chuang, Yang Xie, Jinho Lee, Ni Ni, S. L. Bud'ko, G. S. Boebinger, Q. Wang, D. Dessau, P. C. Canfield and J. C. Davis, "Anisotropic Impurity-States, Quasiparticle Scattering and Nematic Transport in Underdoped $Ca(Fe_{1-x}Co_x)_2As_2$" Nature Physics **9**, 220 (2013)

Iridates:

I1 Yue Cao, Qiang Wang, Justin A. Waugh, Theodore J. Reber, Haoxiang Li, Xiaoqing Zhou, Stephen Parham, Nicholas C. Plumb, Eli Rotenberg, Aaron Bostwick, Jonathan D. Denlinger, Tongfei Qi, Michael A. Hermele, Gang Cao, Daniel S. Dessau "Hallmarks of the Mott-Metal Crossover in the Hole Doped J=1/2 Mott insulator Sr2IrO4" arXiv:1406.4978 (under review at Nature Materials).

I2 Q. Wang, Y. Cao, X.G. Wan, J. D. Denlinger, T. F. Qi, O. B. Korneta, G. Cao, and D. S. Dessau "Experimental Electronic Structure of the Metallic Pyrochlore Iridate Bi2Ir2O7" Journal of Physics: Condensed Matter 27, 015502 (2015)

Manganites:

M1 Millard Baublitz, Christopher Lane, Hsin Lin, Hasnain Hafiz, Robert Markiewicz, Bernardo Barbiellini, Zhe Sun, Dan Dessau, and Arun Bansil "A Minimal tight-binding model for ferromagnetic canted bilayer manganites" Scientific Reports 4, 7512 (2014).

Topological Insulators:

T1 Yue Cao, J. A. Waugh, X.-W. Zhang, J.-W. Luo, Q. Wang, T. J. Reber, S. K. Mo, Z. Xu, G. Gu, M. Brahlek, N. Bansal, S. Oh, A. Zunger, D.S. Dessau "Mapping the Orbital Wavefunction of the Surface States in 3D Topological Insulators" Nature Physics **9**, 499–504 (2013)

Graphene

G1 P. Matyba, A. V. Carr, C. Chen, D. L. Miller, G. Peng, S. Mathias, M. Mavrikakis, D. S. Dessau, M. W. Keller, H. C. Kapteyn, and M. M. Murnane, "Controlling the electronic structure of graphene using surface-adsorbate interactions," Phys. Rev. B 92, 041407(R) (2015)

Methods:

M1 T.J. Reber, N.C. Plumb, D.S. Dessau, "Effects, determination, and correction of count rate nonlinearity in multi-channel analog electron detectors." Rev. Sci. Instrum. **85**, 043907 (2014).

Older Reference (with DOE support):

O1: T. J. Reber, N. C. Plumb, Z. Sun, Y. Cao, Q. Wang, K. McElroy, H. Iwasawa, M. Arita, J. S. Wen, Z. J. Xu, G. Gu, Y. Yoshida, H. Eisaki, Y. Aiura, and D. S. Dessau The Non-Quasiparticle Nature of Fermi Arcs in Cuprate High-T_C Superconductors Nature Physics **8**, 606–610 (2012)

Investigating the magnetic, electronic and lattice degrees of freedom that determine the emergent properties of complex transition metal compounds.

J. F. DiTusa[1] (ditusa@phys.lsu.edu), R. Jin[1], Z. Mao[2], J.D. Zhang[1], W. A. Shelton[3], E. W. Plummer[1], and D. P. Young[1]

[1]Department of Physics & Astronomy, Louisiana State University, Baton Rouge, LA 70803
[2]Department of Physics & Engineering Physics, Tulane University, New Orleans, LA 70118
[3]Department of Chemical Engineering, Louisiana State University, Baton Rouge, LA 70803

Program Scope

LaCNS, a DOE EPSCoR / Louisiana Board of Regents program, aims to build a major neutron scattering infrastructure capable of treating both soft and hard materials. The objectives of this initiative include the discovery of the role of coupling of degrees of freedom that determine the emergent properties of complex materials, the training of students and postdocs in synthesis and neutron scattering techniques and the building of new scientific communities who will become the next generation of neutron users with a specific target of increasing the base of users of the Spallation Neutron Source and the High Flux Isotope Reactor in the USA.

The main scientific focus of this program is to understand the role of coupling between the important degrees of freedom in complex materials and its impact on the structure/property relationship, and to explore how this information can be utilized or applied in the guided-design of materials with desired properties. For hard materials, our goal is to tune dominant couplings that impact the magnetic, electronic, and phonon properties of complex transition metal compounds to enhance a critical property in order to derive new functionality. In particular, many of the most interesting materials display coupling both in their static and dynamical behavior, making neutron scattering the ideal tool to elucidate these fundamental relationships.

Recent Progress

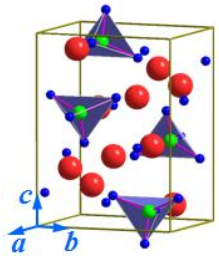

Fig 1. Lattice structure of Ba_2CoO_4.

The materials systems under investigation in the LaCNS hard matter program include transition metal oxides such as Sr_2RuO_4 (Sr214) and $Sr_3Ru_2O_7$ (Sr327) which have been of continuing interest because of the competing magnetic states and their connection to *p*-wave superconductivity. Here we focus on Ru-site substitutions which tend to modify the lattice and nucleate magnetic ordered phases. The evolution of the magnetic and lattice coupling with chemical substitution is investigated using various techniques including neutron scattering. Recently we have discovered that Fe substitution for Ru in Sr214 leads to a commensurate antiferromagnetic (AFM) ordering which is distinct from Mn or Ti substitutions which lead to an incommensurate AFM state or from Co doping resulting in a ferromagnetic (FM) ground state[1]. This magnetic order is

accompanied by charge localization suggesting a strong coupling between the charge and magnetic degrees of freedom. Similarly, we have synthesized large single crystals of $Sr_3(Ru_{1-x}Mn_x)_2O_7$ for exploring charge-spin-lattice couplings. Mn doping tends to reduce the structural distortion and at the same time enhances AFM interactions such that an unusual quasi-2D AFM ordered system is formed[2]. Neutron scattering experiments investigate the relationship between the subtle changes in the crystal structure and the unusual AFM ordering, including competitive magnetic interactions and cooperative spin-lattice interactions. Of particular interest is the non-standard temperature dependence of the AFM order parameter and the spin dynamics. Using neutron scattering, we find, for the first time in the Sr327 system, an energy gap of about 2.7 meV for spin wave excitations in $Sr_3(Ru_{0.84}Mn_{0.16})_2O_7$ demonstrating a Mn induced anisotropy. Ba_2CoO_4 is another transition metal oxide system we are exploring which, despite the separation between Co atoms in its lattice structure (Fig. 1), is AFM below 25 K. Using neutron scattering, we identify a spin gap with large anisotropy due to the single-ion anisotropy of Co^{4+}[3]. Moreover, there is clear dispersion along the a-axis but less so along the c-axis indicating low-dimensional magnetism.

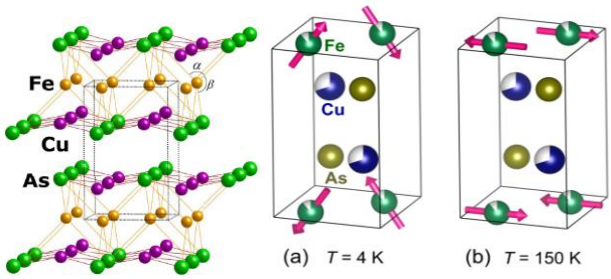

Fig 2. Crystal and magnetic structure of Cu_xFeAs.

These systems contain a range of correlation and coupling so that modeling and simulation will play a crucial role in understanding these phenomena and their associated mechanisms. This information will be used with the experimental groups to devise strategies for either improving or developing new materials with advanced properties. We have developed a process for simulating these materials using a single hybrid DFT approach that accurately captures the range of correlation in these systems. In collaboration with experimental groups, we have successfully applied our approach to $La_{1-x}Sr_xMnO_3$ where we are investigating effects of uniaxial pressure. We are currently applying this technique to the aforementioned ruthenates and SrTiO3/ $La_{1-x}Sr_xMnO_3$ heterostructures. In addition, we are developing new software tools for simulating phonons for disorder systems including defects (antisite, vacancies).

In addition, we have strong synthesis effort that is currently designing materials with unconventional but highly desirable properties. Currently, we are investigating several materials that are relatives to the Fe-based superconducting systems, where our efforts have been focused on the $FeTe_{1-x}Se_x$ series of compounds, as it represents the simplest of the various families of iron pnictide and chalcogenide superconductors. Here we found that uniaxial pressure does not induce magnetic correlations as expected. Although Cu_xFeAs is isostructural to superconducting LiFeAs (Fig. 3)[4], it did not prove to be superconducting. Instead our neutron scattering experiments discovered collinear G-type AFM order below 220 K. This state evolves into a canted AFM state below 142 K explaining the weak FM behavior observed below 60 K. The G-

type AFM order of Cu_xFeAs bears striking similarity to the high-T_c cuprates, thus directly bridging the Fe-based and Cu-based unconventional super-conducting systems. Other related materials that we are exploring include newly discovered $BaMn_2Sb_2$ which is isostructural to $BaFe_2As_2$, a member of the 122 family of superconductors[5]. Large single crystals of $BaFe_2As_2$ and $Ba(Mn_{1-x}Fe_x)_2Sb_2$ were grown to explore the magnetic, charge carrier, thermodynamic, and structural properties. Recently, Liu et al. have synthesized a new topological semimetal, $Sr_{1-x}MnSb_2$ that is likely the first FM Weyl semimetal[6]. The Weyl semimetal state refers to a Dirac semimetal that lacks either time-reversal or space inversion symmetry so that each Dirac point with chiral symmetry splits into two Weyl points. This discovery offers the opportunity to explore the time reversal breaking Weyl state. Here we have characterized the magnetic ordering of this interesting system finding two magnetically ordered structures at high and low temperatures (Fig. 3). We have discovered via neutron scattering that Fe_3Ga_4[7] displays incommensurate spin density wave (SDW) ordering that competes with a FM ground state. In addition, we synthesized large single crystals to explore the sensitivity of the SDW ordering to pressure (Fig. 4).

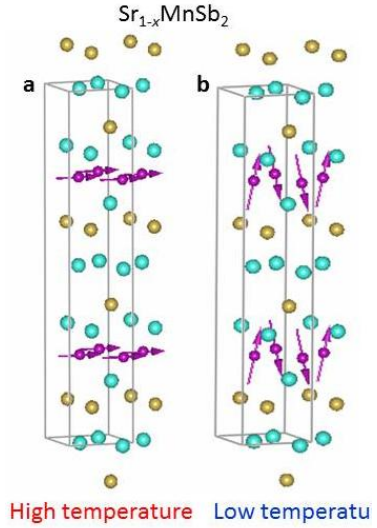

Fig. 3: Magnetic structure of $Sr_{1-x}MnSb_2$ for a) 304<*T*<565 K and for b) *T*<304 K.

The simple cubic *B*20 crystal structure is interesting because it is chiral, allowing spin-orbit coupling to play a key role in electronic and magnetic properties. A large number of binary silicides and germanides form in this crystal structure which is responsible for both the long period helimagnetism and the formation of Skyrmion lattice phases that are ubiquitous in this family of materials[8]. We have discovered that the chemical substitution series between the nonmagnetic small gap insulator RuGe (*B*20) and the diamagnetic metal CoGe, $Ru_{1-x}Co_xGe$, yields magnetic metals for a wide range of *x*. Polycrystalline and single crystalline samples of these materials have been grown which will allow us to map out the magnetic phase diagram.

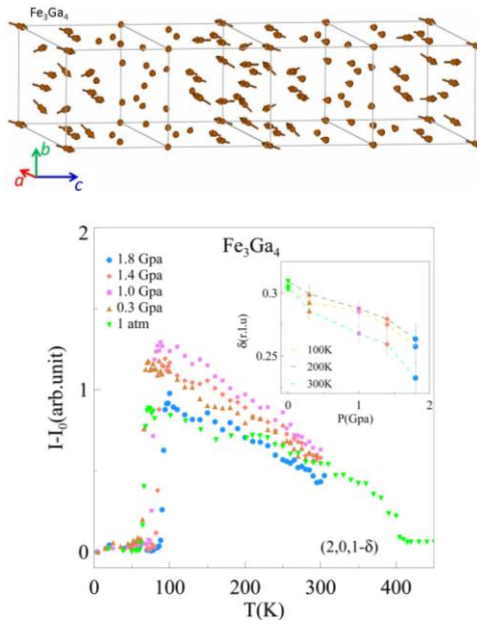

Fig 4. a) Magnetic structure of Fe_3Ga_4. b) Pressure dependence of the SDW state and SDW wavevector (inset) (unpublished).

Future Plans

Our future plans involve both the continued study of these materials, as well as to identify new materials for investigation, with a focus on the use of neutrons to probe the elastic and

inelastic properties. The goal is to connect the results of neutron scattering experiments to their novel emergent properties.

References

[1]M. Braden *et al*. *Phys. Rev. Lett.* **88**, 197002 (2002); J. E. Ortmann *et al*. *Nat. Sci. Rep.* **3**, 2950 (2013).
[2]D. Mesa *et al*., *Phys. Rev. B* **85**, 180410 (2012).
[3]R. Jin *et al*. *Phys. Rev. B* **73**, 174404 (2006).
[4]B. Qian *et al. Phys. Rev. B* **91**, 014504 (2015).
[5]B. Saparov and A. S. Sefat, *J. Sol. St. Chem*. **204**, 32-39 (2013).
[6]J. Liu *et al*. *arxiv.org*/pdf/1507.07978 (2015).
[7]J. H. Mendez *et al*. *Phys. Rev. B* **91**, 144409 (2015).
[8]S. Muhlbauer *et al*. *Science* **323**, 915-919 (2009).

Publications

Qian, B., Hu, J., Liu, J., Han, Z., Zhang, P., Guo, L., Jiang, X., Zou, T., Zhu, M., Dela Cruz, C. R., Ke, X. and Z.Q. Mao. "Weak ferromagnetism of $Cu_xFe_{1+y}As$ and its evolution with Co doping." *Phys. Rev. B* **91**, 014504 (2015).

Wang, H., Lou, W., Luo, J., Wei, J., Liu, Y., Ortmann, J. E. and Z. Q. Mao, "Enhanced superconductivity at the interface of W/Sr_2RuO_4 point contact." *Phys. Rev. B* **91**, 184514 (2015).

Dzamukova, M.R., Lvov, Y.M., Fakhrullin, R.F., "Enzyme-activated intracellular drug delivery with tubule clay nanoformulation." *Scientific Reports (Nature Publ)* **5**, 10560 (2015).

Y. Lvov, R. Fakhrullin, L. Zhang, , "Halloysite Clay Nanotubes for Loading and Sustained Release of Functional Compounds", *Adv. Mater.* accepted (2015).

Xuan, S.; Lee, C. -H.; Chen, C.; Doyle, A. B.; Zhang, Y.; Li, G.; John, V. T.; Hayes, D.; Zhang, D.* Design, Synthesis and Characterization of Polypeptoid Thermogels and Investigation of Stem Cell and Protein Encapsulation. *J. Am. Chem. Soc.*, submitted (2015).

Bhaskaran-Nair, K., Kowalski, K., Moreno, J., Jarrell, M. and Shelton, W.A., "Equation of motion coupled cluster methods for electron attachment and ionization potential in polyacenes," *Journal of Physical Chemistry A*, submitted (2015).

Bhaskaran-Nair, K., Kowalski,K., Valiev, M., Wang, X. and Shelton, W.A., "Coupled cluster characterization of the ionization potentials and electron affinities of GFP chromophores," *Physical Chemistry Chemical Physics*, submitted (2015).

Nesterov: Youm, S. G., Hwang, E., Chavez, C. A., Li, X., Chatterjee, S., Lusker, K. L., Lu L., Strzalka, J., Ankner, J. F., Losovyj, Y., Garno, J. C. and Nesterov, E. E. "Polythiophene Thin Films by Surface-Confined Polymerization," *Journal of the American Chemical Society*, submitted (2015).

Program Title: Artificially Layered Superlattice of Pnictide by Design

Principle Investigator: Chang-Beom Eom
Mailing Address: Room 2166 ECB, 1550 Engineering Drive, University of Wisconsin-Madison, Madison, WI 53706
E-mail: eom@engr.wisc.edu

Program Scope

The goals of the program are to grow artificially engineered superlattices of pnictide materials by atomic layer-controlled growth, and to understand how structure property-relationships interact with the novel superconductivity in the pnictides so as to develop new understanding, applications, and devices. The critical scientific issues we will address include growth mechanisms, interaction between superconductivity and magnetism, interfacial superconductivity and physics of flux pinning in pnictide thin film heterostructures. We expect that this goal will also enable an understanding of the fundamental heteroepitaxial growth of intermetallic systems on oxide surfaces and role of interfacial layers in a sufficiently general way that can be applied broadly to many different material systems.

The discovery of superconductivity with transition temperatures of 20K-50K in iron-based materials has initiated a flurry of activity to understand and apply these novel materials. The superconducting mechanism, the structural transitions, the magnetic behavior above and below T_c, the doping dependence, and the critical current and flux-pinning behavior have all been recognized as critical to progress toward understanding the pnictides. A fundamental key to both basic understanding and applications is the growth and control of high-quality epitaxial thin films and superlattices with atomic layer control. The ability to control the orientation, the strain state, defect and pinning site incorporation, the surface and interfaces, and the layering at the atomic scale, are crucial in the study and manipulation of superconducting properties.

An important characteristic of the Co-doped $BaFe_2As_2$ (Ba-122) material is the relatively low values of doping required to produce superconductivity. This leads to homogeneous films, and similar lattice constants between differently doped films, and great potential for epitaxial superlattices. The 122 materials share the fundamental iron-containing planes that are believed to be responsible for superconductivity, and they potentially all share the same basic mechanism of superconductivity, with a leading candidate being s^{+-} pairing between electron and hole pockets at the zone center and boundary. All share the five Fe 3*d*-orbitals important in the electronic structure, leading to a richness that has great potential for manipulation. In addition, the likely coexistence of magnetism and superconductivity for low-doping, and the nearby structural transitions in the intermediate-doping region, offer great flexibility in the design of new superlattices of, for instance, doped 122 and perovskite oxides, 122 layers of different doping levels, and doped 122 layers with the semi-metallic undoped parent compound.

We are guided to the main goals by our understanding developed over the last three years in relating pnictide structural and superconducting properties. The new film growth methods used in this project enables us to not only resolve these uncertainties, but also to design and synthesize new pnictide atomic layered structures that explore the limits of this material's superconducting properties. The **thrusts** of our project are:

(1) *Atomic-layer-controlled growth of artificially engineered superlattice synthesis*
(2) *Designing interfacial superconductivity at pnictide and FeSe interfaces.*
(3) *Investigation of interaction between superconductivity and magnetism by proximity effect*
(4) *Understanding and control of flux-pinning mechanisms*
(5) Study of growth mechanisms of heteroepitaxial superlattices and artificial pinning centers

Recent Progress

1. Atomic-layer-controlled growth of $Ba(Fe_{1-x}Co_x)_2As_2$ films

BACKGROUND

The discovery of superconductivity with transition temperatures of 20K-50K in iron-based materials has initiated a flurry of activity to understand and apply these novel materials. The superconducting mechanism, the structural transitions, the magnetic behavior above and below T_c, the doping dependence, and the critical current and flux-pinning behavior have all been recognized as critical to progress toward understanding the pnictides. A fundamental key to both basic understanding and applications is the growth and control of high-quality epitaxial thin films and superlattices with atomic layer control. The ability to control the orientation, the strain state, defect and pinning site incorporation, the surface and interfaces, and the layering at the atomic scale, are crucial in the study and manipulation of superconducting properties.

DISCUSSION and FINDINGS

We have studied the influence of perovskite substrate surface termination on the properties of superconducting pnictide thin films to understand the thermodynamic equilibrium between at pnictide thin film/oxide interfaces. To explain the dependence on substrate surface termination, we proposed the schematic growth model of Co-doped $BaFe_2As_2$ described in Fig. 1. Due to the different crystal structures, the interface with SrO terminated substrate will have high interfacial energy with the film, and need additional stabilization through surface reconstruction. However, Ba layer as the 1st layer on top of TiO_2 surface maintains the perovskite stacking of $SrTiO_3$. We find in this case that the unit cell of $BaFe_2As_2$ grows epitaxially after reaching interfacial equilibrium. In contrast, it is relatively hard to reach phase stability at the interface between Ba122 and SrO surface because arsenic is volatile as a starting layer. Fe and Co elements may interdiffuse/intermix with Ti at the surface of $SrTiO_3$ to move toward thermodynamic stability. We have grown Co-doped pnictide thin films on $SrTiO_3$ (001) substrates with the controlled termination states. As-received $SrTiO_3$ substrates have the mixed termination states of both TiO_2 and SrO, whereas the single TiO_2 termination can be attained by chemical etching treatments using buffered hydrofluoric (BHF) acid etchant.

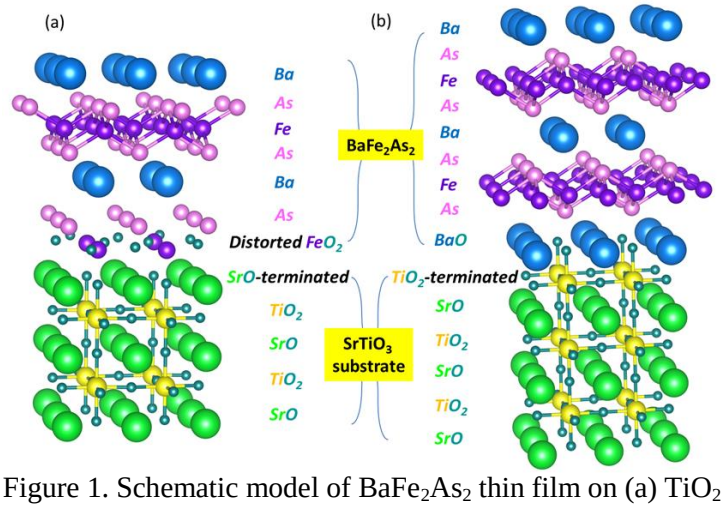

Figure 1. Schematic model of $BaFe_2As_2$ thin film on (a) TiO_2 and (b) SrO-terminated $SrTiO_3$.

Scanning transmission electron microscopy (STEM) measurements show that the interfacial layer depends on the surface termination of $SrTiO_3$ substrates. In TiO_2-terminated regions, a Ba layer was imaged as the first interfacial layer, whereas a FeAs layer was shown on SrO-terminated regions as shown in Fig. 2. Note that one unit-cell of $BaFe_2As_2$ is consisted of the stacking structures of Ba-AsFeAs-Ba-AsFeAs-Ba. Therefore, clear and abrupt interface for epitaxial $BaFe_2As_2$ film growth can be apparently found on TiO_2-terminated $SrTiO_3$ with less diffusion. On the other hand, there is more diffusion with broader interface on SrO surface termination. We have also found that superconducting transition temperature (T_c) for Ba122 on TiO_2-terminated $SrTiO_3$ is significant higher than mixed surface terminated $SrTiO_3$. In particular, the difference in T_c is much more pronounced in ultrathin films because atomically sharp interface can be formed and chemical diffusion is also suppressed with less reaction layer.

Importance of findings both from experimental and theoretical perspectives:

Based on theoretical calculations and STEM imaging at the Ba122/$SrTiO_3$ interfaces with the surfaces termination control, we have confirmed that non-perovskite Ba-122 films shows atomically sharp and well-defined interfaces with TiO_2-terminated STO perovskites. This interface engineering is not only limited to STO substrates, but can also be used to explore the STO buffer layer on various perovskite substrates with different lattice parameters and artificially layered superlattices. We believe that deliberately strained STO template layer with TiO_2 surface termination can also open many possibilities for fundamental research for strain engineering in monolayer FeSe. It can be tailored to improve performance and new functionalities of Fe-based superconducting thin films with engineered interface of various perovskite oxide substrates.

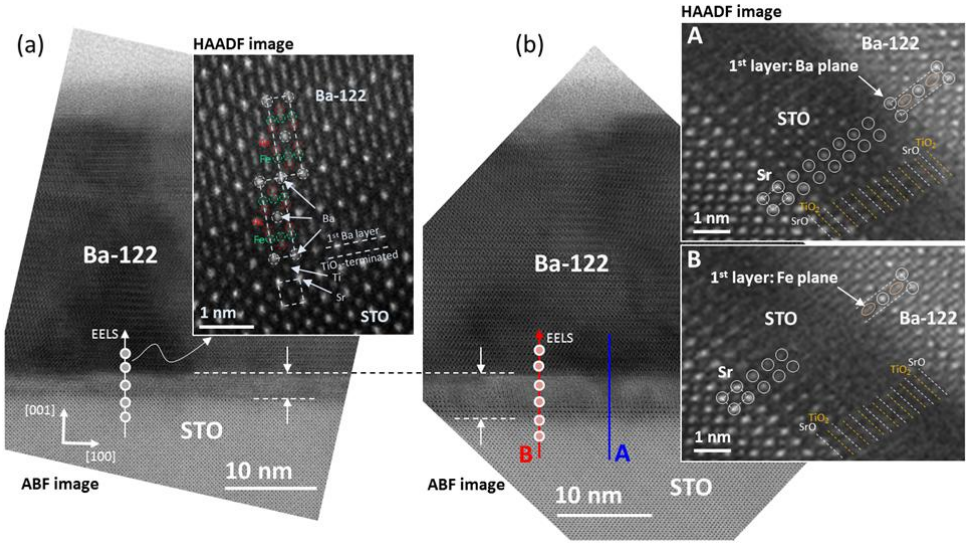

FIG. 2. High resolution STEM ABF and HAADF images for 24 nm thick Ba-122 films on (a) TiO_2-terminated STO by BHF etching and (b) mixed surface termination of as-received STO. There is a clear interface with Ba layer as a 1st layer on top of TiO_2 terminated STO, whereas SrO surface termination has blurred interface with more diffusion.

Future Plans

(1) Superconductivity and magnetism at atomically abrupt Pnictide interfaces

The interaction between magnetism and superconductivity is central to the physics of pnictide superconductors, as well as other modern superconductors with potential applications. We have demonstrated that epitaxial heterostructures with sharp interfaces can be made between the optimally-doped material $Ba(Fe,Co)_2As_2$ and other doping levels, as well as insulators such as $SrTiO_3$, and metallic ferromagnets such as Ni, Co, and Fe. We will compare two different Normal Metal (N) / Superconductor (S) configurations, using the same superconducting layer and changing the N layer properties to determine the interfacial interaction of superconductivity and magnetism. The SC material will be fixed at optimal doping $Ba(Fe_{0.92}Co_{0.08})_2As_2$ (x=0.08), with maximum T_c (see Fig. 3, the phase diagram for Ba-122 with Co doping). In the first N_u (undoped normal metal) /S (superconductor) interface, the normal metal (N_u) will be undoped $BaFe_2As_2$ in which the AFM-SDW correlations dominate. In the second N_o (overdoped normal metal) /S (superconductor) interface, the normal metal (N_o) will be heavily doped Ba122 (x=0.20), a paramagnetic metal with no AFM ordering and no SC transition. In Fig. 3 the blue, purple and red arrows represent, respectively, the low doping, optimally doping and over-doping Ba-122 compounds, whose relative interaction we propose to study. Any weakening or enhancement of superconductivity in these systems (i.e., seen as a decrease or increase of T_c) will provide a straightforward demonstration of the competitive nature or coexistence of the two long-range orders. The comparison between the two heterostructures will also determine if magnetism has an important role as mediator in the interaction that drives superconductivity in pnictides.

(2) Designing interfacial superconductivity at FeSe interfaces

We plan to grow FeSe monolayers on different ferroelectric surfaces in collaboration with Lian Li's group at UW-Milwaukee, exploiting our group's long history in the preparation of strained ferroelectric films. The motivation here is the suggestion that screening by ferroelectric (FE) phonons may be responsible for the greatly enhanced T_c in monolayer FeSe grown on $SrTiO_3$ (STO). Such FE phonons in STO are relevant at temperatures below ~100K when the dielectric constant becomes quite large, but are present already at higher temperatures in other FE materials such as $BaTiO_3$.

Alternative ferroelectric surfaces will be explored starting with biaxially strained epitaxial thin films of Ti- surface terminated $BaTiO_3$ on rare-earth scandate ($RE ScO_3$) substrates with different lattice parameters. These new substrates include seven different $RE ScO_3$ compositions with lattice constants that vary in 0.01 Å increments. High quality single crystal $BaTiO_3$ thin films are necessary, as bulk single-crystal substrates of BTO crack easily under thermal cycling due to the phase transitions. The strain state and remnant polarization of the strained $BaTiO_3$ thin film prior to FeSe monolayer deposition can be controlled by using substrates with different lattice mismatch, keeping the FE film thickness less than the critical one for relaxation. Such film strain will change the frequency of the zero-point FE phonon mode, the mode suggested as responsible for the dielectric screening, offering a new parameter to control the dielectric screening of the FeSe film. In addition, the final surface termination of these FE films (i.e., AO or BO_2, or mixed) can be controlled by *in situ* RHEED before the FeSe monolayer films are grown, offering an additional degree of freedom as compared to single-crystal substrates. We also plan to study the electronic band structures of monolayer FeSe on strained $SrTiO_3$ template using our ARPES system. We are currently setting up an ARPES system integrated with *in situ* laser MBE thin film growth system.

References (which acknowledge DOE support)

1. "Gate-tunable superconducting weak link behavior in top-gated $LaAlO_3$-$SrTiO_3$", V.V. Bal, M.M. Mehta. S. Ryu. H. Lee. C.M. Folkman, C.B. Eom, V. Chandrasekhar, *Appl. Phys. Letts.*, **106**, 212601, (2015)
2. "Epitaxial CrN Thin Films with High Thermoelectric Figure of Merit", C.X. Quintela, J.P. Podkaminer, M.N. Luckyanova, T.R. Paudel, E.L. Thies, D.A. Hillsberry, D.A. Tenne, E.Y. Tsymbal, G. Chen, C.B. Eom, and F. Rivadulla, *Adv. Mat.*, **27**, 3032, (2015)
3. "Atomic and electronic structures of superconducting $BaFe_2As_2$/$SrTiO_3$ superlattices" P. Gao, Y. Zhang, S. Y. Zhang, S. Lee, J. Weiss, J. R. Jokisaari, E. E. Hellstrom, D. C. Larbalestier, C. B. Eom, and X. Q. Pan, *Phys. Rev B.*, **B91**, 104525 (2015)
4. "Development of very high Jc in $Ba(Fe_{1-x}Co_x)_2As_2$ thin films grown on CaF_2", C. Tarantini, F. Kametani, S. Lee, J. Jiang, J. D. Weiss, J. Jaroszynski, E. E. Hellstrom, C. B. Eom and D. C. Larbalestier, *Scientific Report*, **4** : 7305 (2014)
5. "Electrodynamics of superconducting pnictide superlattices", A. Perucchi, F. Capitani, P. Di Pietro, S. Lupi, S. Lee, J.H. Kang, J. Jiang, J.D. Weiss, E.E. Hellstrom, C.B. Eom, P. Dore, *Appl. Phys. Letts.*, **104**, 222601 (2014)
6. "Epitaxial Al_2O_3 capacitors for low microwave loss superconducting quantum circuits" K.-H. Cho, U. Patel, J. Podkaminer, Y. Gao, C. M. Folkman, C. W. Bark, S. Lee, Y. Zhang, X. Q. Pan, R. McDermott and C. B. Eom, *APL Materials*. **1**, 042115 (2013)
7. "Transmittance and reflectance measurements at terahertz frequencies on a superconducting $BaFe_{1.84}Co_{0.16}As_2$ ultrathin film: an analysis of the optical gaps in the Co-doped $BaFe_2As_2$ pnictide" A. Perucchi, L. Baldassarre, B. Joseph, S. Lupi, S. Lee, C.B. Eom, J. Jiang, J.D. Weiss, E.E. Hellstrom, P. Dore, *European Physical Journal B*, **86**, 274 (2013)

Other References

8. "Electron Pairing Without Superconductivity", Guanglei Cheng, Michelle Tomczyk, Shicheng Lu, Josh Veazey, Mengchen Huang, Patrick Irvin, Sangwoo Ryu, Hyungwoo Lee, Chang-Beom Eom, C. Stephen Hellberg, Jeremy Levy, *Nature*, **521**, 196, (2015)

Program Title: High-Bandwidth Scanning Hall Probe Imaging of Driven Vortices in Periodic Potentials

Principle Investigator: Stuart Field

Mailing Address: Department of Physics, Colorado State University, Fort Collins, CO 80523

E-mail: stuart.field@colostate.edu

Program Scope

The goal of this project is to use a novel technique, *high-bandwidth scanning Hall probe microscopy*, to study the local, real-time dynamical states of current-driven vortices in artificially structured periodic potentials. This technique extends the frequency response of Hall probe microscopy from the usual 10–100 Hz used for imaging into the MHz range. Using this technique, the dynamics of driven vortices can be probed with an unprecedented combination of temporal and spatial resolutions, allowing a wealth of new physics, inaccessible to standard transport and magnetization measurements, to be uncovered.

Recent lithographic advances have made it possible to fabricate superconducting films that present a variety of *periodic* potentials to vortices in the film. Interesting effects of commensurability arise when the vortex spacing, easily adjusted by varying the magnetic field, matches the period of the underlying potential. These effects include strong increases in the critical current and dips in the resistance, indicating that vortices become particularly strongly pinned at these special matching fields. More recently, attention has turned to the *dynamics* of vortices driven across the film by the imposition of an external current. Again, commensurability has a profound effect on the depinning of vortices from their static configurations, and on the detailed nature of their dynamical trajectories.

In order to understand the nature of these states, this project makes use of high-bandwidth scanning Hall probe microscopy to image the trajectories of vortices moving in a periodic potential. The technique uses a powerful combination of standard low-bandwidth imaging with several high bandwidth (~5 MHz) imaging modes, including a method of making high-speed movies for vortices driven by an ac current in a periodic potential. Using these advanced imaging techniques, many of the outstanding questions concerning vortex dynamics in these systems can be directly addressed.

A number of specific experimental systems are being explored. Vortices in two-dimensional potentials have unique depinning signatures that can best be addressed by real-space imaging. Once vortices are moving, a variety of dynamical states are predicted, including simple channeled flow and several more complex disordered flows. There are also remarkable effects observed when vortices are driven, in addition to a dc current, a high-frequency ac current. The real-space, dynamical nature of these systems is best explored by a high-bandwidth imaging technique.

Recent Progress

The superconducting samples required for this experiment are highly specialized. Ideally, the vortices will move in a potential that is not only periodic but is also *smooth*, that is, fairly sinusoidal and without rapid changes in its value. We expect in such potentials that the vortex motion will also proceed smoothly through the pinning transition to a

multiplicity of interesting dynamical regimes, making imaging experiments simpler to interpret. Further, potentials of this kind can be made with built-in asymmetries, leading to interesting "ratchet" effects in which symmetric ac driving currents lead to a net directed vortex flow.

We have invested a considerable effort into fabricating and characterizing samples that present smooth, controlled periodic potentials to moving vortices. To do so, we introduce a corresponding periodic modulation into the *thickness* of our superconducting films. This modulation leads to a corresponding modulation of the vortex potential. We have developed a novel method for fabricating smooth and reproducible thickness modulations by angle-evaporating the superconducting film onto a substrate which itself has a modulation in its surface profile.

To fabricate these substrates, we use electron-beam lithography to create a grating pattern in chrome-on-glass wafers. The chrome serves as a mask for a subsequent HF wet etch. When the chrome is removed, we are left with a glass substrate with a square-wave profile. Subsequent thermal annealing near the glass transition temperature then smooths this square wave into the required sinusoidal profile.

Next, extremely low-pinning granular aluminum is sputtered at an angle onto the modulated substrate. The film thickness is greater on those slopes of the substrate that more directly face the incident flux, and thinner on those slopes that face the flux less directly. In this way the substrate modulation is transferred to the film.

A sample fabricated using this technique is shown in Fig. 1. Figure 1a shows an overview of the 150 μm wide sample. In Fig. 1b, we show a closeup of the sample taken using a Zygo optical surface profiler. This instrument uses white-light interference to construct a 3D image of a surface, much like AFM but in a noncontact mode and with rapid operation. Here, the superconducting film appears red and the underlying surface-modulated glass substrate appears blue.

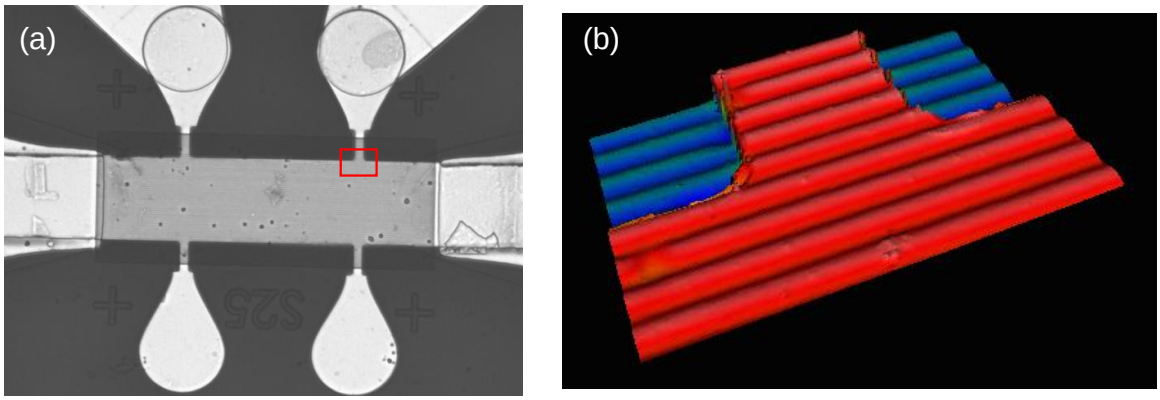

Figure 1. (a) A thickness-modulated granular aluminum superconducting sample. (b) Closeup of an area of the sample (red box in (a)) near a voltage lead. The 500-nm-thick film appears red in this image taken with a Zygo optical surface profiler. The film is grown on a glass substrate (blue) that has a periodic surface modulation. The modulation period is 3.0 μm.

It is important to note that the overall film thickness is actually the *difference* between the surface profile of the film and that of the substrate. Thus images like those in Fig. 1b (and their higher-resolution AFM versions) are critical because both surfaces are visible at once, allowing the modulated film thickness to be calculated.

We have performed extensive transport measurements on film of this kind. Typical results are shown in Fig. 2. In Fig. 2a we measure the voltage V generated by moving vortices, at many values of the driving current, as the magnetic field B is swept from 0 to about 24 G. The vortex velocity is proportional to V/B. Matching fields are indicated by smooth kinks and dips in the voltage. These features are weak because the vortex potential is smooth and relatively weak itself. Figure 2b shows the critical current as a function of magnetic field for currents in each direction through the sample. Here, we are searching for asymmetries in the critical current due to asymmetries intentionally fabricated into the vortex potential.

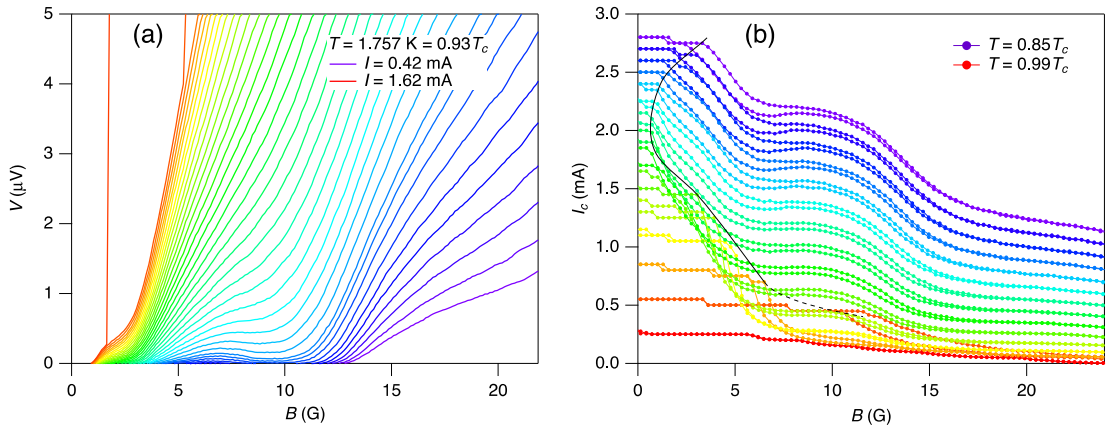

Figure 2. (a) Voltage vs. magnetic field at different driving currents, ranging from 0.42 mA to 1.62 mA. A weak feature at around 2.5 G indicates the first matching field; a stronger dip near 10 G indicates the second matching field. At the highest currents, the system suddenly jumps to the normal state due to a well-known instability in weak-pinning superconductors. (b) The critical current (0.2 μV criterion) for temperatures in the range from 85% to 99% of T_c. At each temperature, the critical current was determined for currents flowing in each direction throught the sample. The black line roughly indicates the field regime below which instabilities of the kind observed in (a) occur.

Several issues remain to be resolved. First, in our technique we need to sputter the films at fairly steep angles. Under these conditions the film surface tends to roughen. We have made progress in subsequently smoothing the films using argon ion bombardment. Second, the pinning by the film edges plays an important role in films with weak bulk pinning. We are developing techniques to yield tapered film edges that should significantly reduce this edge pinning.

We have also fabricated more conventional samples in which the periodic potential is provided by a periodic array of holes through the sample. For samples of this kind the potential is very strong. An example of transport measurements carried out on such a sample is shown in Fig. 3. Here, the strong periodic potential leads to a wide array of very conspicuous matching features. In these kinds of samples, vortex motion is expected proceed via the hopping of vortices from one well to the next, a very different process than the regular motion sinusoidal potential of our smooth samples.

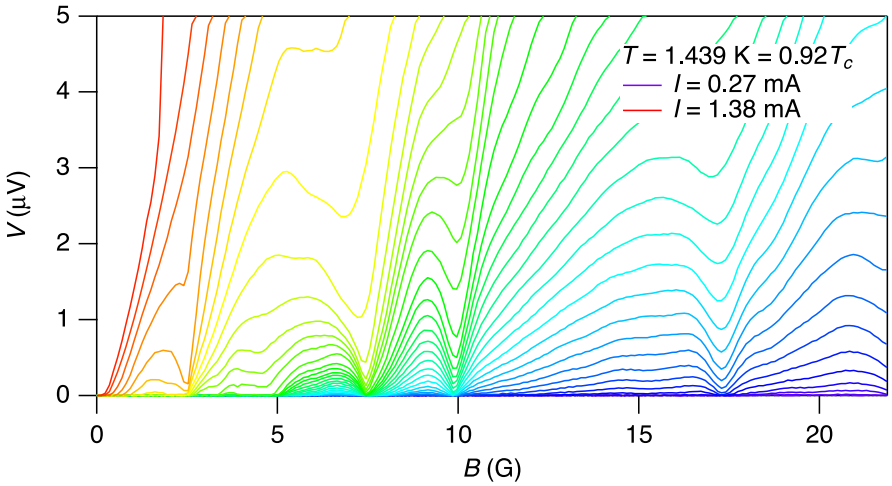

Figure 3. Voltage vs. magnetic field runs at many of the driving current I for a sample with small holes in a triangular pattern. The distance between holes is 3.0 μm. The dips indicate strong matching effects at magnetic fields for which the vortex lattice is commensurate with the underlying potential.

Future Plans

The overall goal of the project is high-bandwidth imaging studies of dynamical vortex states using scanning Hall probe microscopy. We have now constructed and tested the necessary instrumentation for this phase to begin. To cool the samples we have constructed a closed-cycle cryocooler with a pumped pot capable of reaching 1.2 K. We have also installed and characterized an anti-vibration stage for the microscope. Recent tests have yielded our first images of vortices, and we will begin imaging moving vortices in the very near future.

Publications which reference DOE support

1 K cryostat with sub-millikelvin stability based on a pulse-tube cryocooler, S. B. Field, A. DeMann, and Sara Mueller, *Cryogenics* (submitted).

Program Title: "Colloidal quantum dot films, transport and magneto-transport"
Principal Investigator: Philippe Guyot-Sionnest
Mailing Address: James Franck Institute, 929 E. 57th Street, The University of Chicago, Chicago, IL 60637

E-mail: pgs@uchicago.edu

Program Scope

The two goals of the program are to understand and optimize charge transport in Colloidal Quantum Dot (CQDs) solids and to develop magneto electrical properties. Our group developed fruitful topics in this direction. In 2009, we patented the use of Atomic Layer Deposition in multilayer films of quantum dots to tune the coupling between nanoparticles and strengthen the films. In a different project aiming for an alternative approach to tuning superconducting properties, we made a nanostructured inorganic films of Pb/PbSe nanocrystals. We observed the insulator to superconducting transition, with the same T_c as bulk Pb and about 50 times higher critical fields. We developed HgTe quantum dots for mid-infrared detection. Using the inorganic matrix As_2S_3, we obtained photoconductive devices with about 1/10 the detectivity of epitaxial materials at 3.5 microns and at higher operating temperature. We performed a fundamental study of the 1/f noise and found a rather universal magnitude largely proportional to the number of nanocrystals in the devices. As a result, we recently turned our attention to PV detection and observed that films of HgTe colloidal quantum dots exhibited photovoltaic response with thermal background limit, meaning that the noise originates from the photoresponse to the fluctuation of the photon flux at 295K background scene, a milestone in the development of optoelectronic infrared devices based on colloidal quantum dots. We also achieved the first instance of stable doping and observed intraband photoconductivity in the mid-infrared with HgSe and HgS CQDs.

On the magnetic properties front, we investigated the magnetoresistance of colloidal quantum dots solids with controlled Fermi level but without and with magnetic dopants. Bulk semiconductors doped with magnetic impurities (DMS) have been an active field of research for decades. The interest is motivated by the possibility of controlling the magnetization by the carrier density. In bulk DMS, the exchange interaction of magnetic impurities and delocalized carriers gives rise to various effects, including giant Zeeman splitting and exciton magnetic polarons. Such effects are expected to be stronger in nanostructures because quantum confinement increases the wave function overlap between the carriers and the magnetic impurities and increases the exchange interaction. Therefore, confined nanostructures are of much interest as well. In our most recent studies on Mn doped CdSe and HgS CQDs, we observe MR that is attributed to the electron-magnetic polarons.

Progress of past grant

Urbach Tail in CdSe quantum dot films: The redshift seen upon a coupling procedure is often taken as a quantitative measure of the interaction between the quantum states of the quantum dots, without further inquiry. The chemical processing and annealing may however strongly alter the surface of the dots creating other possibilities. We conducted an investigation of the band edge of the CdSe quantum dots upon coupling with ammonium sulfide, a strong coupling

procedure. We observed that the large redshift reported were also accompanied by extended Urbach tail, reaching well beyond the bandgap of bulk CdSe. It was concluded that the redshift, the broadening and the absorption tails of interband absorption could not be solely attributed to a strong electronic coupling between the dots. Instead, mixing of surface and core hole states was proposed to dominate the changes of the interband spectra at the absorption edge.

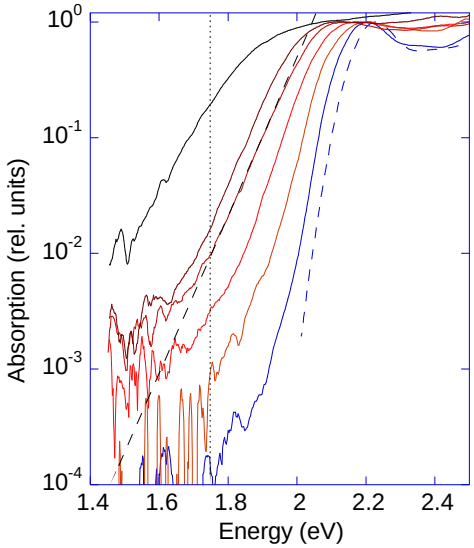

Figure 1: Absorption spectra of CdSe films processed with Ammonium sulfide and annealed at several temperatures. The dashed line is the absorption for a hexane solution. The solid lines are the absorption measured for thin films by Thermal Deflection Spectroscopy with, from right to left Heptanediamine (weak coupling), and the sulfide ions 20°C, 50°C, 100°C, 150°C, and 200°C. The dashed vertical line is at 1.75 eV, which is the bulk bandgap of CdSe. The dashed line superimposed on the 100°C spectrum is its steepest slope at 60 meV.

1/f electrical noise in Nanocrystals solids: In the weak coupling limit, nanocrystal solids are actively researched for sensors, such as chemically sensitive resistors and photoconductive detectors. In these systems, electrical noise limits the performances. In particular, the nanocrystal systems can exhibit large excess 1/f noise. For our HgTe infrared detectors, the 1/f noise limits the Detectivity below 1 kHz. 1/f noise is often attributed to charges moving into different states with a wide range of tunneling distance or activation energies, and these charges affect the transport by either contributing to the number of mobile charges or modulating the mobility. We therefore initiated a study to determine if the 1/f noise could be reduced by film processing, by the choice of the materials comprising the nanocrystals, and by the choice of the matrix. It seemed to us obvious that, just as for bulk materials, we would be able to strongly affect the noise level by using different materials. We did find that diminishing the prevalence of cracks in the films was effective in lowering the 1/f noise, and this was expected. However, our results show also some universal 1/f noise floor with all the materials studied, with a noise scaling as the number of nanocrystals in the system, i.e. extensive as for bulk systems, and approximately proportional to the interdot conductance, irrespective of the materials. We qualitatively conclude that the noise is an intrinsic effect of the disorder of the granularity in conduction, where charges moving in part of the network act to modify transport in the higher conductivity, and better connected part of the network, yielding effectively a noise mechanism that only depends on the interdot conductance and not on the nature of the material.

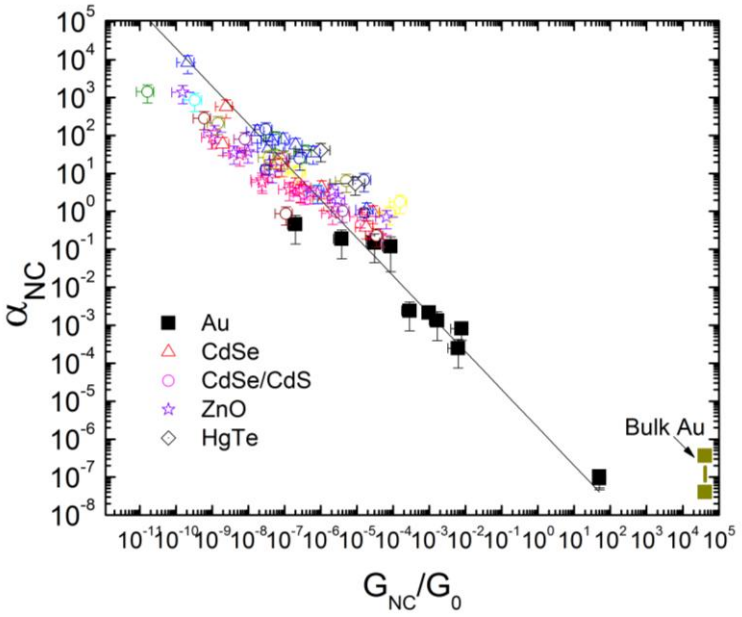

Fig. 2: Comparison between gold nanoparticle (black squares) and the semiconductor nanocrystal films. They both show universal scaling of the noise per nanocrystal, with interdot conductance. All the data in hopping regime were taken under 1V bias , corresponding to ~0.3-0.6 mV/nanocrystal.

Magnetotransport The role of magnetic polarons in the transport between heavily Mn-doped II-VI colloidal quantum dots was investigated in a first study of the MR of such systems. Mn doping of CdSe, ZnO, ZnTe and HgS CQDs was confirmed. N-type and Mn doped CdSe, ZnO and HgS exhibited similar MR of ~ 50-200% at low temperatures. However, there was a clear distinction observed between lightly doped Mn:QDS, and heavily doped systems.

With lightly doped systems of less than ~ 1% dopant, the MR shows no effects of magnetic polarons. The MR is always positive and, as a function of magnetic field, it shows a crossover from quadratic at low charging to linear at high charging levels. The low charging quadratic positive MR is attributed to a wavefunction squeezing effect under the magnetic field and the experimental MR shows a good agreement with the VRH model, with no specific role played by the magnetic impurities. A saturation of the MR at high field at the 100-200% level is also explained by a model due to Shklovskii. With CQDs that are highly charged such as Mn:CdSe and Mn:ZnO, and weakly doped, it was found that the MR becomes linear up to 6T and this is not yet understood.

In contrast, with heavily doped Mn:CQDs with $\gtrsim$ 5% dopant, the MR shows a clear effect of the magnetic impurities with a 10-30 times larger quadratic positive MR at low magnetic field, compared to lightly doped Mn:QDS. However, the MR also saturates at the ~ 100% level at high field. For high charging level, there is also a negative MR. The MR with the heavily doped CQDs is attributed to the formation of magnetic polarons between the manganese ions and the injected electrons.

The effective g-factors extracted from the parabolic low field regime are small, ~10, and therefore the magnetic polarons have a weak magnetization. This is attributed to the use of n-type quantum dots and this limits the range of temperature where significant effects are observed to below 10K in this work. This initial study points to the need to develop p-type quantum dots with large Mn concentrations for observing the MR of magnetic polarons at higher temperatures.

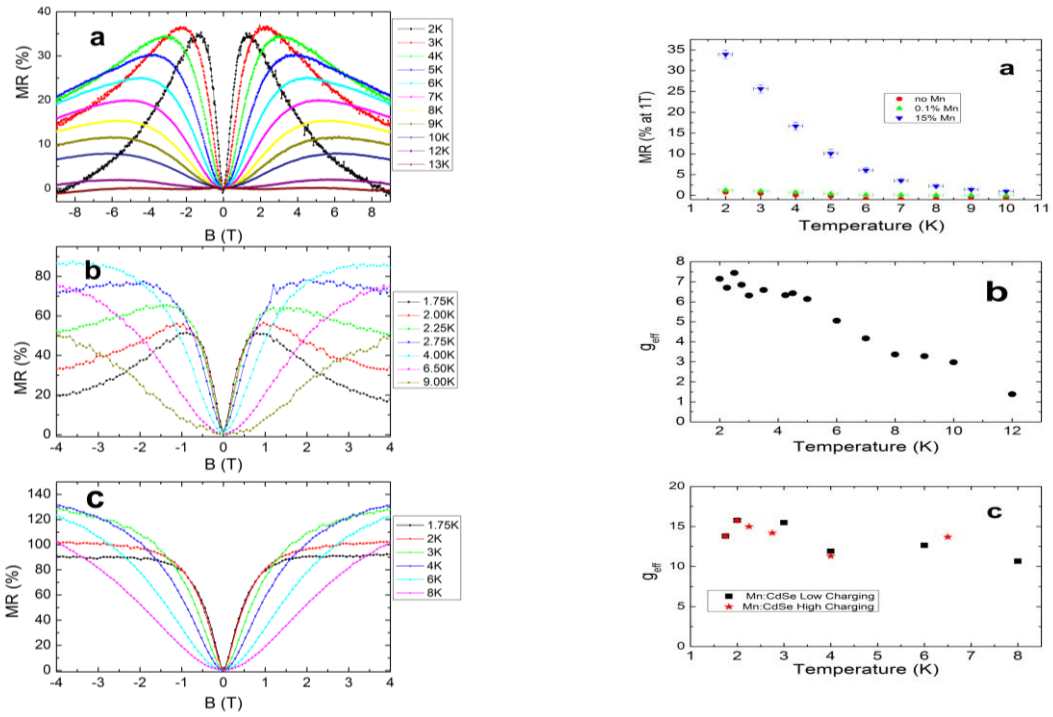

Figure3: Left: a) Heavily Mn doped HgS (15%) with particle diameter of 10nm shows a strong positive MR at low field and a negative MR components at high magnetic fields. b) Heavily doped CdSe (20%) at a high charging level c) Same but at lower charging level. Right: a) The low magnetic field (1T) MR increases sharply below 10K, much faster than lightly Mn doped HgS (green) and pristine HgS (red). b) geff of heavily Mn doped HgS as a function of temperature obtained by fitting the low field MR of left(a) to a quadratic response as described in the text. c) geff of heavily Mn doped CdSe as a function of temperature obtained by fitting the low field quadratic response of left (b)(c).

References (which acknowledge DOE support)

Mott and Efros-Shklovskii Variable Range Hopping in CdSe Quantum Dots Films, Liu H, Pourret A, Guyot-Sionnest P**, ACS Nano 4, 5211-5216 (2010)**

n- and p-Type HgTe Quantum Dot Films, Liu Heng; Keuleyan Sean; Guyot-Sionnest P **J. Phys. Chem. C 116, 1344-1349 (2012)**

Electrical Transport in Colloidal Quantum Dot Films, Guyot-Sionnest P, **J. Phys. Chem. Lett. 3, 1169-1175 (2012)**

A"mirage" study of CdSe colloidal quantum dot films, Urbach tail and surface states, Guyot-Sionnest P, Lhuillier E., Liu H., **J. Chem. Phys. 137, 154704 (2012)**

Electrical Transport in Colloidal Quantum Dot Films, by Guyot-Sionnest P. **J. Phys. Chem. Lett. 3, 1169-1175 (2012)**

1/f noise in semiconductor and metal nanocrystal solids, H Liu, E Lhuillier, P Guyot-Sionnest, **Journal of Applied Physics 115 (15), 154309 (2014)**

Magnetoresistance of Manganese Doped Colloidal Quantum Dot Films, H Liu, P Guyot-Sionnest, **J. Phys. Chem. C 119, 14797-14804 (2015)**

Program Title: Linear and Nonlinear Optics in Metal-Nanoparticle Composites

Principal Investigator: Richard F. Haglund, Jr.
Mailing Address: Department of Physics and Astronomy, Vanderbilt University, Nashville, TN 37235-1807
E-mail: *richard.haglund@vanderbilt.edu*

Program Scope

Background. Long before the word "plasmonics" was coined, Michael Faraday had already proposed that "finely divided metal particles" lent the beautiful colors to the stained glass of cathedrals and Gustav Mie had developed analytic descriptions of light scattering from nanoparticles based on Maxwell's equations. Yet the ramifications of that intuitive and theoretical understanding only blossomed in the last quarter century, with the development of robust nanofabrication techniques, nanometer-resolution microscopies, optical spectroscopies with unprecedented wavelength and temporal resolution, and a full complement of computational tools.

Approach. We have employed many of these new tools to characterize the linear and nonlinear responses of "designer" nanostructures comprising metals and phase-changing (VO_2) or optically active (ZnO) metal oxides. This has made it possible, for example, to: deploy Au plasmons as nanoantennas to probe the metal-insulator transition in VO_2; enhance the yield of ultraviolet band-edge luminescence a hundred-fold even in highly defective ZnO by exciton-plasmon coupling; demonstrate localization of defects in ZnO thin films at interfaces using femtosecond laser spectroscopy; and use Al nanoparticles coupled to ZnO quantum wells to map the transition from weak to strong exciton-plasmon coupling.

Aided by finite-difference time-domain and finite-element calculations, we design and fabricate heterostructures in our group in which we can excite electrons and quasiparticles (e.g., excitons, phonons, plasmons) and map the material response at femtosecond time and nanometer length scales. We employ nanofabrication tools (including dual-layer e-beam lithography and etching techniques, exfoliation of metal dichalcogenides, focused ion-beam nanomachining) and materials synthesis techniques (e-beam evaporation, pulsed laser deposition, sputtering and vapor-solid nanowire/nanocrystal synthesis) to create novel heterostructures designed to elicit specific kinetic and dynamical responses. The complex optical phenomenology of these structures is studied using coherent, time-resolved second- and third-order optical spectroscopies (ultrafast white-light pump-probe spectroscopy and femtosecond harmonic generation, pulse shaping) along with confocal and scanning-probe optical and electron microscopies (confocal Raman microscopy with single-nanoparticle resolution, surface-enhanced Raman scattering in nanoparticle arrays, variable-temperature spectral ellipsometry and scanning and trnsmissioin electron microscopies).

Overall objective. The focus in our program is currently on nonlinear and ultrafast optics in metamaterials, exciton-plasmon coupling and plasmonic effects in metal-insulator transitions. Our goal is for the research to have significant impact at the intersection of condensed-matter and optical physics, including: (1) optical physics in active and nonlinear metamaterials; and (2) ultrafast dynamics in heterostructures designed to elucidate the interactions of plasmons with material degrees of freedom. The use of coherent spectroscopies — such as interferometric second-order autocorrelation and spatial light modulation — accesses to the full panoply of coupling dynamics of interest: plasmons to photons, phonons and excitons, and to plasmonic and dielectric structures within the optical near field.

The narratives on *Recent Progress* and *Future Plans* on the following pages are intended to be illustrative, rather than comprehensive, examples of the products of our research program.

Recent Progress

Ultrafast electron dynamics in metamaterials. Our recent work in this thematic grouping includes plasmon-driven electron injection to promote phase transitions in VO_2 [2, 4] and second-harmonic generation (SHG) in planar metamaterials designed to have no inversion symmetry. The Archimedean nanospiral is one such potential SHG material that we have explored in this program.[9] In just-published experiments [5], we have shown that arrays of sub-wavelength-dimension nanospirals have an effective second-order susceptibility roughly equal to that of beta-barium borate, and thus are an effective planar or metasurface nonlinear optical element.

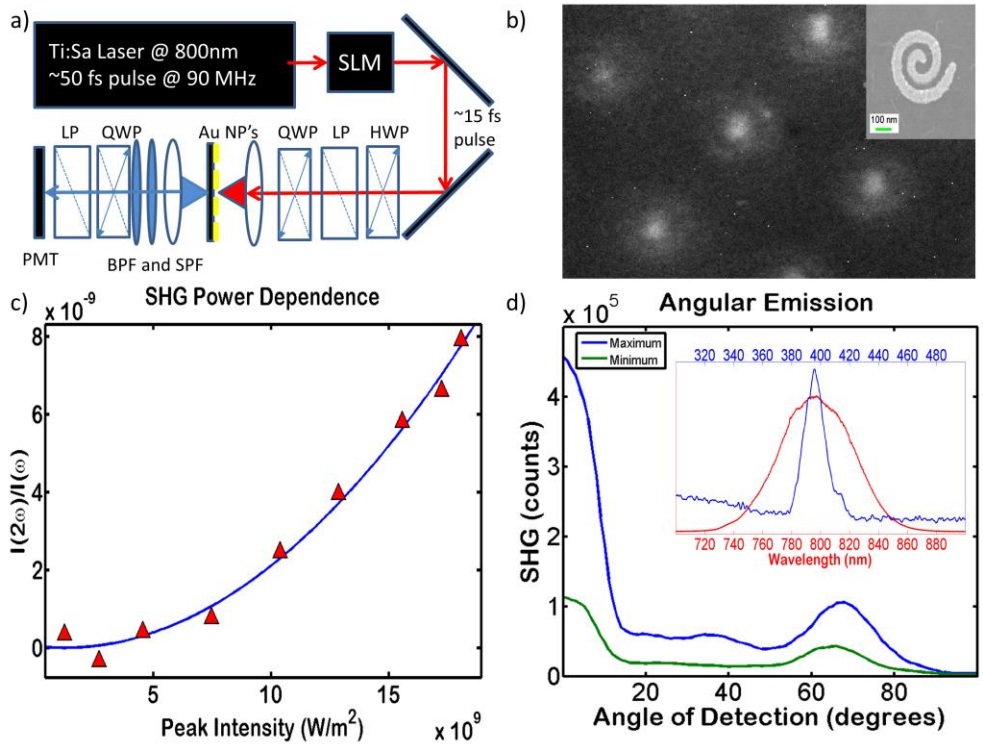

Figure 1. (a) Laser arrangement for second-harmonic generation in Archimedean nanospirals. (b) Ultrafast PEEM micrograph showing a section of the nanospiral array with selective excitation at the center of the spirals as predicted by simulations. (c) Second-harmonic yield as a function of peak intensity showing the expected quadratic dependence on laser intensity. (d) Angular dependence of the second-harmonic output of the array, showing strong forward direction and a diffraction peak at 70˚ due to the array structure. The inset shows the narrowed bandwidth (and thus longer temporal duration) of the second harmonic pulse.

Dimensional and structural effects in plasmonic coupling. Exciton-plasmon coupling - in ZnO quantum wells [10], nanowires [3] and in structures incorporating two-dimensional atomic crystals – and tunable plasmon-induced transparency in heterostructures incorporating phase-changing VO_2 have been a significant part of recent work. The ZnO nanowires [3] in particular have shown unusual optical-cavity effects that have led us to develop a collaboration based at Oak Ridge National Laboratory in which we have used scanning-transmissioin electron microscopy (STEM) in conjunction with electron energy loss spectroscopy (EELS) and cathodoluminescence (CL) to better understand the microscopic details of the exciton-plasmon coupling in ZnO nanowires decorated with silver nanoparticles. The first experiments have been completed and a first publication is being prepared [12].

Future Plans

Nonlinear optics driven by plasmon fields. The nanospiral geometry used to generate efficient second harmonic light [Figure 1] is only one of many possible ways of generating nonlinear optical signals from plasmonic interactions with materials. We have developed a serrated nanogap (SNG) geometry in which we can deposit nonlinear materials in order to generate nonlinear signals or, alternatively, to probe the nonlinear response of a material. In order to generate second-harmonic light on a femtosecond time scale, we employ a spatial light modulator (SLM) as shown in Fig. 2a to generate a collinear orthogonally polarized pulse pair to simultaneously excite and probe the plasmonic system.[11] As shown in Fig. 2b, the pump (control) pulse polarized perpendicular to the nanogap excites the plasmon field, while the second pulse probes the state of the polarized dielectric. The orthogonally polarized pulses generate an interference pattern that is distinctive for structures with and without PMMA, at time resolutions as short as 900 as. Moreover, the high aspect ratio (4:1) of the SNG structure forces the femtosecond plasmon field to polarize the dielectric in the gap and enhance the second-harmonic signal. Therefore this interference signature is the direct result of the plasmon-induced optical nonlinearity in the PMMA. Aside from the extraordinary time resolution enabled by the spatial light modulator, this metasurface nanostructure lends itself to a variety of second- and third-order nonlinear optical studies, including parametric amplification, optical rectification and four-wave mixing.

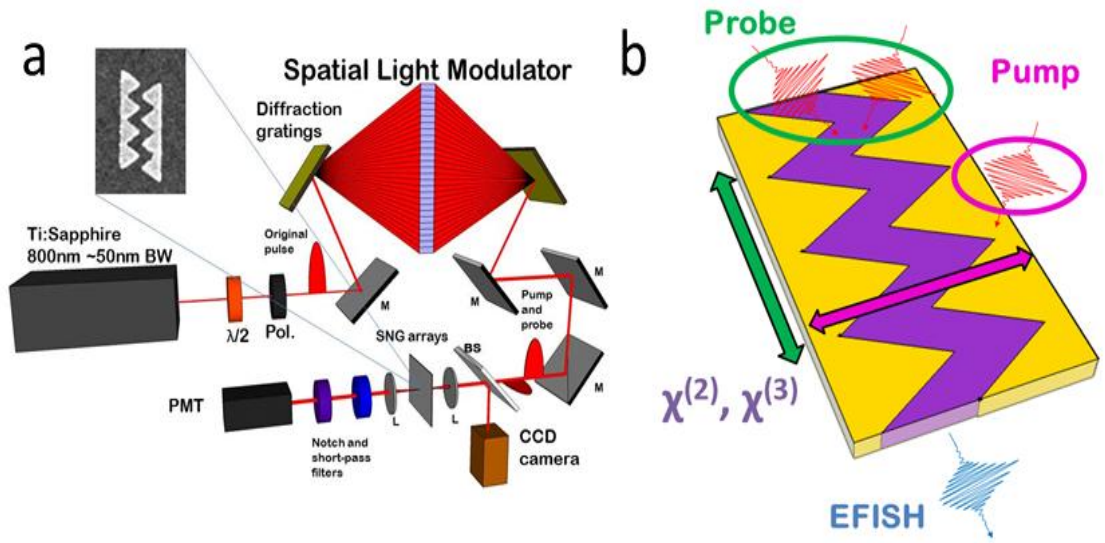

Figure 2 | Experimental configuration for all-optical second-harmonic generation. a - A Ti:Sapphire mode-locked laser is coupled with a spatial light modulator for temporal pulse shaping and polarization control; the optical train is as shown and the nanogap structure is at the focus of the pump and probe laser pulses. The width of the nanogap structure is 75 nm. The SLM generates transform limited control and probe pulses with orthogonal polarization and variable optical power and temporal delay from each 30 fs 800 nm pulse. **b-**Nanogap structures are excited by a horizontally polarized pump pulse (magenta) and probed with a vertically polarized probe pulse (green).

Plasmonic probes of single-crystal VO_2. We have recently shown [8] that gold nanorod antennas lithographically fabricated on VO_2 thin films display a switchable response during the insulator-to-metal transition of the VO_2. Depending on whether neither, one or both ends of the nanorod are resting on metallic nanograins of the VO_2, the antenna-like response of the nanorods has dipole, monopole or fully quenched characteristics. We are now pursuing such experiments on

single-crystal VO_2 nanobeams to test the sensitivity of the nanoantennas to crystal orientations and test for the long-conjectured growth of metallic "nanopuddles" within single crystal grains.

References acknowledging DOE support last two years

1. "Electron-beam deposition of VO_2 thin films for optical applications," R. E. Marvel, K. Appavoo, J. Nag, B. K. Choi and R. F. Haglund, Jr., *Applied Physics A*: *Materials and Processing* **111**, 975-981 (2013). DOI 10.1007/s00339-012-7324-5.

2. "Plasmonic Probe of the Semiconductor to Metal Phase Transition in Vanadium Dioxide," D. W. Ferrara, J. Nag, E. R. MacQuarrie, A. B. Kaye and R. F. Haglund, Jr., *Nano Letters* **13**(9), 4169-4175 (2013). DOI: 10.1021/nl401823r.

3. "Surface-plasmon-mediated photoluminescence from Ag-coated ZnO-MgO core-shell nanowires," D. C Mayo, C. Marvinney, E. Bililign, R. Mu and R. F. Haglund, Jr., *Thin Solid Films* **553**, 132-137 (2014). DOI: 10.1016/j.tsf.2013.11.131.

4. "Ultrafast Phase Transition via Catastrophic Phonon Collapse Driven by Plasmonic Hot-Electron Injection," K. Appavoo, N. F. Brady, B. Wang, M. Seo, J. Nag, R. P. Prasankumar, S. T. Pantelides, D. J. Hilton and R. F. Haglund, Jr., *Nano Letters* **14**, 1127-1133 (2014). DOI: 10.1021/nl4044828

5. "Efficient Forward Second-Harmonic Generation from Archimedean Nanospirals," R. B. Davidson, J. I. Ziegler, G. Vargas, S. M. Avanesyan, R. F. Haglund, Jr., Y. Gong and W. P. Hess. *Nanophotonics* **4**, 108-115 (2015). DOI 10.1007/s00339-014-8566-1.

6. "Effects of Ti charge state, ion size and beam-induced compaction on the formation of Ag metal nanoparticles in fused silica," R. H. Magruder III, A. Meldrum and R. F. Haglund, Jr., *invited paper*, *Applied Physics A – Materials and Processing* **119**(1), 19-31 (2014). DOI 10.1007/s00339-014-8953-7.

7. "Hybrid SiO_2/VO_2/Au Optical Modulator Based on Near-Field Plasmonic Coupling," Petr Markov, K. Appavoo, R. F. Haglund, Jr. and S. M. Weiss. *Optics Express* **23**(5), 6878-6887 (2014). DOI 10.1364/OE.23.0006878.

8. "Control of plasmonic nanoantennas by reversible metal-insulator transition," Y. Abate, R. E. Marvel, J. I. Ziegler, S. Gamage, M. H. Javani, M. I. Stockman, R. F. Haglund, Jr., accepted in *Nature Scientific Reports*, July 23, 2015. http://arxiv.org/abs/1504.02286.

Other references acknowledging DOE support

9. "Plasmonic response of nanoscale spirals," J. I. Ziegler and R. F. Haglund, Jr., *Nano Letters* **10**, 3010-3015 (2010).

10. "Plasmon-exciton hybridization in ZnO-quantum well-Al nanodisc heterostructures," B. J. Lawrie, K.-W. Kim, D. P. Norton and R. F. Haglund, Jr., *Nano Letters* **12**, 6125-6157 (2012).

11. "All-Optical Field-Induced Second-Harmonic Generation," Roderick B. Davidson, II, Anna Yanchenko, Jed I. Ziegler, Sergey M. Avanesyan, Ben J. Lawrie and Richard F. Haglund, Jr., ready for re-submission to *ACS Photonics*, May 2015.

12. "Nanoscale probing of surface plasmons in three dimensions in random-morphology nanostructures," J. Hachtel, A. Mouti, D. Mayo, C. Marvinney, R. Mu, S. J. Pennycook, A. Rupini, M. F. Chisholm, R. F. Haglund and S. T. Pantelides, in preparation.

Program Title: Antiferromagnetism and Superconductivity
Principal Investigator: W.P. Halperin
Mailing Address: Department of Physics, Northwestern University, Evanston, IL 60208
E-mail: w-halperin@northwestern.edu

Program Scope

This report is based on a portion of the work in the program scope of the grant DE-FG02-05ER46248, entitled Antiferromagnetism and Superconductivity for which there are publications from the past two years listed in the references that acknowledge DOE support.[1-8] A wide class of compounds including heavy fermions, cuprates, and pnictides exhibit superconductivity in concert with magnetism, in some cases in the form of a spin-density wave, antiferromagnetism, or even ferromagnetism.[i] Many of these have been the subject of investigations within the scope of my program. Some of them are unconventional superconductors, *i.e* having lower symmetry than the normal state in addition to the obvious requirement for broken gauge symmetry. A few of these compounds are suggested to have topologically complex order parameters, a topic I will focus upon here, notably with UPt_3 which can be compared with ^3He in Fig. 1. A grand challenge in the field is to identify the relationship between magnetism and superconductivity. It is especially interesting to understand this relation for superconductors with chiral order parameters which necessarily have important topological properties relevant to basic ideas for protection of quantum information.[ii,iii] In my program a broad suite of experimental tools have been used including: NMR at Northwestern University and at the National High Magnetic Field Laboratory, neutron scattering at the Paul Scherrer Insitute and the Institut Laue Langevin, tunneling at the University of Illinois, Urbana-Champaign, Polar Kerr effect at Stanford University, and thermodynamic measurements such as specific heat at Northwestern University and the University of Waterloo and Los Alamos National Laboratory.

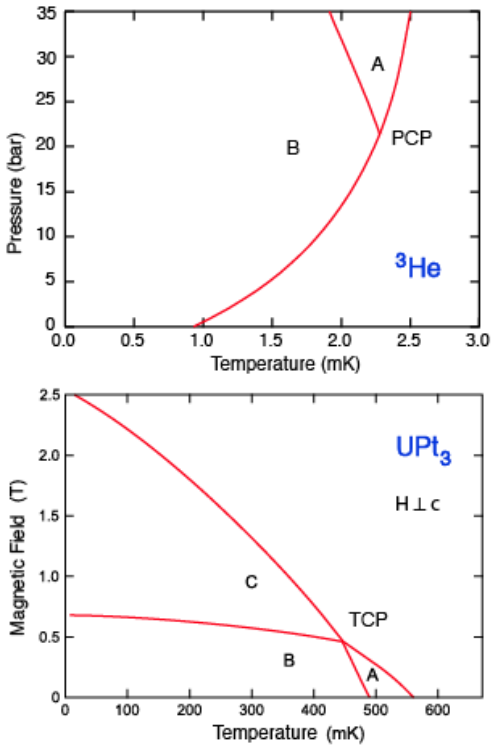

Figure 1. Phase diagrams for two unconventional pairing systems for comparison, He^3 and UPt_3. Multiple phases are a key signature of unconventional pairing. For He^3 the A-phase is chiral and for UPt_3 it is the B-phase which is thought to be chiral.[1]

An important component of our work is crystal growth and characterization using float-zone techniques that have been developed at Northwestern University and now are being extended to a new hybrid growth scheme specifically designed for crystals with volatile components that require growth at high pressure. In this report we focus on one aspect of the program, the heavy fermion compound UPt_3, where we have grown crystals using electron beam

UHV float-zone techniques, known to be the best ever produced, and can be as large as 20 g. High quality starting materials is an essential requirement for establishing the physical behavior of any system. Consequently, UPt_3 may be one of the better choices for understanding spontaneously broken symmetry in superconductors in the presence of competing interactions, and in this case antiferromagnetism.

The existence of cryogenic platforms for research on superconductivity and for many of my colleagues in condensed matter physics depends critically on availability of liquid helium which I am committed to understanding and evaluating, through survey and analysis to determine prospects for availability of liquid helium and alternate technology.[2]

Recent Progress

Crystal growth of UPt_3 has been further developed at Northwestern University with emphasis on improvements in purity and crystal facet presentations for surface sensitive experiments, characterization, and collaborations with colleagues at other institutions performing, elastic and inelastic neutron scattering (University of Notre Dame, Rice University), scanning tunneling microscopy (Cornell University), directional thermal conductivity and heat capacity (Los Alamos National Laboratory, University of Waterloo), directional tunneling and Josephson tunneling (University of Illinois-Urbana Champaign), and polar Kerr effect measurements (Stanford University).

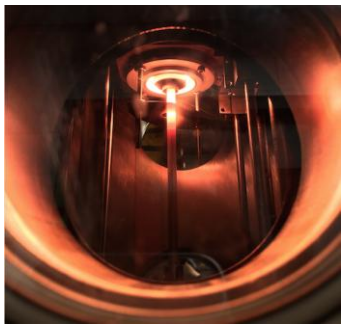

Figure 2. Crystal growth and zone refining in a hybrid scheme.

Directional tunneling into UPt_3 performed by Dale van Harlingen's group at the University of Illinois, Urbana-Champaign makes use of crystals that display both *c*- and *b*-axis facets with high quality as-grown surfaces. These ultra-clean crystals have been investigated to directly identify the nodal structure in the A-phase[iv] and further constrain the theoretical models for the symmetry of the superconducting state. Currently we are searching for the predicted nodes of the order parameter in the B-phase. Aharon Kapitulnik's group at Stanford University has performed polar Kerr effect measurements[1] on crystals with an as-grown surface facet having *c*-axis normal to the facet that identified onset of time reversal symmetry breaking in the B-phase which was clearly absent in the A-phase. These measurements in small magnetic fields are consistent with several possible group representations of the order parameter (E_{2u} and E_{1g}). This investigation continues with crystals having a *b*-axis facet which should be orthogonal to the chiral axis and therefore should not exhibit a polar Kerr effect.

The temperature dependence of the penetration depth can yield valuable information about the dispersion of the energy gap near its nodes and its nodal structure. In our work using small angle neutron scattering at ILL we have found that the temperature dependence of the penetration depth is linear at low temperatures, $T << T_c$, for all directions of induced currents in the vortex state. This is expected only for the E_{2u} theoretical model originally proposed by Jim Sauls. In our collaboration with Anton Vorontsov at Montana State University we could account for the temperature dependence over a wide range of temperature with this theoretical model. Moreover

the results were found inconsistent with competing models of the order parameter symmetry.[4] One of the questions being addressed is the role of anisotropic impurity in unconventional superconductors with anisotropic order parameters and in particular for the superconductor UPt_3. I make the proposition that the symmetry-breaking field that has been proposed to explain the field-temperature phase diagram, Fig. 1, is not antiferromagnetism *per se*, but rather is anisotropic quasiparticle scattering from materials defects. With colleague David Seidman at Northwestern University using TEM some years ago we have measured the density of prism plane stacking faults in UPt_3 which dominate the resistivity. To test this hypothesis we have studied the effects of anisotropic scattering in the best known chiral quantum system, ^3He.[v] Consequently, we were led to use NMR to characterize the anisotropy of the silica aerogel framework that favors the chiral A-phase over the B-phase for superfluid ^3He imbibed within the aerogel. This is an important (possibly crucial) step for understanding that the phase diagram of UPt_3 depends on anisotropic impurity scattering. The anisotropy in silica aerogel can best be characterized with measurements of the gas diffusion coefficient using NMR.[3]

Future Plans

We will be developing crystal growth techniques suitable for high volatility elements applicable for superconducting materials, including URhGe, UGe_2, and Hg1201. Our program is to grow these crystals using a unique hybrid scheme combining encapsulation for high pressure growth and electron-beam zone-refining, and crystal growth. The crystal growth development is performed by Northwestern graduate students, Keenan Avers and Jeongseop Lee, fully supported by the DOE. In Fig. 2, this approach has been implemented following a similar procedure which we have used before, ultra-high vacuum float-zone refining, crystal growth, that has produced the highest quality of single crystal heavy fermion compounds to date in the instance of UPt_3. In Fig. 2, a UPt_3 polycrystal sample was enclosed in a ceramic crucible and then encapsulated in a welded Ta tube heated to 1800 °C by an electron beam focused by optics to a narrow zone which was transported slowly across the sample region. This is a demonstration of a new technique in a known system. However, many interesting compounds have volatile elements or are unstable in an open environment and crystal growth is challenging requiring encapsulation. We have tested this procedure to pressures ~ 100 bar at high temperature.

Future research will include the study of the superconducting vortex structures in UPt_3 using small angle neutron scattering. Preliminary results indicate a field-induced bifurcation of the usual six-fold diffraction pattern for H||c, into a twelve-fold pattern where the splitting appears to be a linear function of magnetic field. With collaborator Morten Eskildsen and my student Keenan Avers, together with my former student William Gannon, this work will be pursued at PSI and at ILL where we have beam time assigned in the near future. Additional work to define the symmetry of the superconducting order parameter in this paradigm heavy fermion compound will be conducted with Aharon Kapitulnik's group at Stanford University performing polar Kerr effect measurements on the *b*-axis facets which we have provided to them. This should be a direction perpendicular to the chiral axis according to the theory and will be an excellent test of experiment compared with prediction. Additionally, Dale Van Harlingen's group at the University of Illinois has crystals from us recently provided, which have high quality as-grown surfaces in order to explore the nodal structure in the B-phase of this unconventional superconductor. Recent heat capacity measurements have been performed on our single crystals

by Jan Kycia's group at the University of Waterloo which, combined with results from measurements at Northwestern and Los Alamos, indicate that the chiral B-phase in zero field can be enhanced, increasing T_{BA} with improved crystal quality, potentially to include the entire H-T phase diagram. A new collaboration has started with Séamus Davis' group at Cornell University performing STM spectroscopy on these UPt_3 crystals.

References (which acknowledge DOE support)

1. E. R. Schemm, W. J. Gannon, C. Wishne, W. P. Halperin, A. Kapitulnik, *Observation of Broken Time-reversal Symmetry in the B-phase of the Heavy Fermion Superconductor UPt_3*, Science **345**, 190 (2014).
2. W.P. Halperin, *The Impact of Helium Shortages on Basic Research*, Nature Physics **10**, 467 (2014).
3. J.A. Lee, A.M. Mounce, S. Oh, A.M. Zimmerman, W.P. Halperin, *Enhanced Self-diffusion of Adsorbed Methanol in Silica Aerogel*, Phys. Rev. B **90**, 174501 (2014).
4. W.J. Gannon, W.P. Halperin, C. Rastovski, K.J. Schlesinger, J. Hlevyack, C. Steiner, M.R. Eskildsen, A.B. Vorontsov, J. Gavilano, U. Gasser, G. Nagy, *Nodal Gap Structure and Order Parameter Symmetry of the Unconventional Superconductor UPt_3*, New J. Phys. **17**, 023041 (2015).
5. A.M. Mounce, Sangwon Oh, Jeongseop A. Lee, W.P. Halperin, A.P. Reyes, P.L. Kuhns, M.K. Chan, C. Dorow, L. Ji, D. Xia, X. Zhao, M. Greven, *Absence of Static Orbital Current Magnetism at the Apical Oxygen Site in $HgBa_2CuO_{4+\delta}$ from NMR*, Phys. Rev. Lett. **111**, 187003 (2013).
6. L. Bossoni, P. Carretta, W.P. Halperin, S. Oh, A. Reyes, P. Kuhns, P.C. Canfield, *Evidence of Unconventional Low-frequency Dynamics in the Normal Phase of $Ba(Fe_{1-x}Rh_x)_2As_2$ Iron-based Superconductors*, Phys. Rev. B **88**, 100503 (2013).
7. S. Oh, A.M. Mounce, J.A. Lee, W.P. Halperin, C.L. Zhang, S. Carr, P. Dai, A.P. Reyes, P.L. Kuhns, *Microscopic Coexistence of a Two-component Incommensurate Spin-density Wave with Superconductivity in Underdoped $NaFe_{0.983}Co_{0.017}As$*, Phys. Rev. B **88**, 134518 (2013).
8. S. Oh, A.M. Mounce, J.A. Lee, W.P. Halperin, C.L. Zhang, S. Carr, P. Dai, *Spin-Pairing and Penetration Depth measurements from Nuclear Magnetic Resonance in $NaFe_{0.975}Co_{0.025}As$*, Phys. Rev. B **87**, 174517 (2013).

Other References

i. M.R. Norman, *Unconventional Superconductivity*, arXiv:1302.3176v2 (2014).
ii. D.A. Ivanov, *Non-Abelian Statistics of Half-Quantum Vortices in p-Wave Superconductors*, Phys. Rev. Lett. **86**, 268 (2001).
iii. G. E. Volovik, *Fermion Zero Modes on Vortices in Chiral Superconductors*, Pis'ma Zh. Eksp. Teor. Fiz. **70**, 601 [JETP Lett. 70, 609 (1999)]; G. E. Volovik, *Quantum phase transitions from topology in momentum space: Lect. Notes*, Phys. **718**, 31 (2007).
iv. J.D. Strand, D.J. Bahr, D.J. Van Harlingen, J.P. Davis, W.J. Gannon, W.P. Halperin, *The Transition Between Real and Complex Superconducting Order Parameter Phases in UPt_3*, Science **328** , 1368 (2010).
v. J. Pollanen, J.I.A. Li, C.A. Collett, W.J. Gannon, W.P. Halperin and J.A. Sauls, *New Chiral Phases of Superfluid ^{3}He Stabilized by Anisotropic Silica Aerogel*, Nature Physics **8**, 317-320 (2012).

Project title: Science of 100 tesla

Principle investigator: Neil Harrison; co-PI's: M. Chan, M. Jaime, R.D. McDonald, B.J. Ramshaw, J. Singleton, V. Zapf

Mailing address: Los Alamos National Labs., Mail stop E536, Los Alamos, NM 87545

Program Scope

This program consists of a coordinated research plan at the extremes of non-destructive high magnetic field, tackling pressing questions in condensed matter physics that only magnetic fields approaching 100 tesla can answer. Magnetic fields manipulate matter either through tunable nanometer length scales or tunable magnetic energy scales (or sometimes both), enabling a great variety of different physical effects to be studied. The magnetic lengthscale, for example, is important for pairing and cyclotron motion in unconventional superconducting materials, which constitutes one of our primary focus areas in 100 tesla magnetic fields. The magnetic energy scale, by contrast, is most relevant for tuning competing interactions or phase transitions in magnetic materials — multifunctional magnetic materials being a second focus area. The magnetic lengthscale can further be used for tuning commensurability phenomena in low dimensional materials.

Recent Progress

During the past two years, we have made progress in a number of areas, most notably in the area of high T_c superconductivity by way of magnetic quantum oscillation studies. By using high magnetic fields, the resolution of quantum oscillations increases, which provides more detailed information about the various frequencies originating from the normal state Fermi surface. High magnetic fields also enable a much wider range of parameter space to be mapped. For example, by going to higher magnetic fields, we can tilt the orientation of the magnetic field further from the c-axis, enabling a more complete angle resolved mapping of the Fermi surface geometry. This has thus far been achieved in $YBa_2Cu_3O_{6.56}$ (with a nominal hole doping around 11%) [15] and $YBa_2Cu_4O_8$ (which has a nominal hole doping between 12 and 14%) [1]. The more detailed study was possible for $YBa_2Cu_3O_{6.56}$, enabling a determination of the broken lattice translational symmetry consistent with x-ray scattering results [15]. Going to high magnetic fields also enables us to measure samples with higher upper critical magnetic fields, which in turn enables a broader range of dopings to be accessed. In $YBa_2Cu_3O_{6.+x}$, this has enabled the effective mass of the carriers to be measured over a broad range of hole dopings spanning from 9% to 15% (see Fig.1) [8]. The inverse effective mass shows a strong downturn near optimal doping in the recent measurements, which provides strong thermodynamic evidence for a quantum critical point.

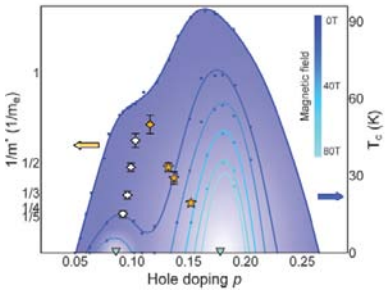

Fig. 1. Inverse effective mass versus doping in $YBa_2Cu_3O_{6+x}$. Light regions indicates robust superconductivity magnetic field.

In the pressure-induced heavy fermion superconductor $CeRhIn_5$, high magnetic field experiments extending to 90 T were performed for the first time [9,11]. In one of these studies [9], magnetotransport measurements were performed on samples that

had been cut into zigzag meandering devices by focused ion beam lithography. The measurements yielded several magnetic field-induced resistive transitions consistent with a high magnetic field charge density-wave phase.

Several high magnetic fields studies were completed on topological insulating compounds Bi_2Te_3 doped with sulphur, which are expected to have a topologically protected surface layer. These studies revealed nascent quantum Hall plateau and changes in the Berry phase at high magnetic fields. However, by far the more interesting experimental results were obtained in the topological Kondo insulator SmB_6. Here, an earlier study had reported to see quantum oscillation evidence for surface states in torque measurements. On performing similar measurements on high purity image furnace-grown samples, however, large three-dimensional sections of Fermi surface were unexpectedly found [2]. This result is surprising in view of the bulk insulating behavior of SmB_6.

In the frustrated quantum magnet $SrCu_2(BO_3)_2$, more than half dozen theoretical models have attempted to explain the presence of multiple plateau, all having limited success. These models largely ignore lattice effects. Our high resolution experimental lattice strain data obtained to 100T combined with DMRG and DFT modeling of the system have recently shown that an intriguing lattice 'pantograph effect' is behind relatively large changes in the Cu-O-Cu superexchange angles, which optimizes the magnetic superstructures [10].

Future Plans

In unconventional superconductivity, we have recently began investigating the mercury cuprates following our recent hire of a postdoc with access to these materials. In the yttrium barium cuprates, a significant breakthrough has been made in their growth at Cambridge, yielding samples superior in quality to those previously studied. In both these systems we plan to study the effect of quantum criticality on the magnetotransport, which requires usage of the highest available magnetic fields. Our ability to perform such measurememts will be greatly improved with the acquisition of an advanced sample prepration capability.

We have also recently began an expanded series of measurements on low carrier density materials with Dirac-like dispersions. We already have preliminary data on graphite and on several Weyl metal materials. Weyl metals have the potential to yield phase transitions into novel ordered phase at high magnetic fields. The sample quality is also significantly better than that of the topological insulators.

In order to promote a greater degree of overlap between our program and the Los Alamos lab mission, we are in the process of developing a capability for performing measurements on plutonium and its compounds in high magnetic fields extending to 100 tesla. We have already designed and constructed a prototype for sample encapsulation, which will enable contactless conductivity, magnetic susceptibility and strain measurements to be made in pulsed magnetic fields.

Publications

1. Tan, B. S., Harrison, N., Zhu, Z., Balakirev, F. F., Ramshaw, B. J., Srivastava, A., Sabok, S. A., Dabrowski, B., Lonzarich, G. G., Sebastian, S. E. Fragile charge order in the

nonsuperconducting ground state of the underdoped high-temperature superconductors. *Proc. Nat. Acad. Sci. USA*. **112**, 9568-9572 (2015).

2. Tan, B. S., Hsu, Y.-T., Zeng, B., Hatnean, M. C., Harrison, N., Zhu, Z., Hartstein, M., Kiourlappou, M., Srivastava, A., Johannes, M. D., Murphy, T. P., Park, J.-H., Balicas, L, Lonzarich, G. G., Balakrishnan, G., Sebastian, S. E. Unconventional Fermi surface in an insulating state. *Science* **349**, 287-290 (2015).
3. Aczel, A. A., Li, L., Garlea, V. O., Yan, J.-Q., Weickert, F., Zapf, V. S., Movshovich, R., Jaime, M., Baker, P. J., Keppens, V., Mandrus, D. Spin-liquid ground state in the frustrated J_1-J_2 zigzag chain system $BaTb_2O_4$. *Phys. Rev. B* **92**, 041110 (2015).
4. Balakirev, F. F., Kong, T., Jaime, M., McDonald, R. D., Mielke, C. H. Gurevich, A., Canfield, P. C., Bud'ko, S. L. Anisotropy reversal of the upper critical field at low temperatures and spin-locked superconductivity in $K_2Cr_3As_3$. *Phys. Rev. B* **91**, 220505 (2015).
5. Harrison, N.; Ramshaw, B. J.; Shekhter, A. Nodal bilayer-splitting controlled by spin-orbit interactions in underdoped high-T_c cuprates. *Scientific Reports* **5**, 10914 (2015).
6. Rodriguez, G., Jaime, M., Balakirev, F., Mielke, C. H., Azad, A., Marshall, B., La Lone, B. M., Henson, B., Smilowitz, L. Coherent pulse interrogation system for fiber Bragg grating sensing of strain and pressure in dynamic extremes of materials. *Optics Express* **23**, 14219-14233 (2015).
7. Parker, D. S., Ghimire, N., Singleton, J., Thompson, J. D., Bauer, E. D., Baumbach, R., Mandrus, D., Li, L., Singh, D. J. Magnetocrystalline anisotropy in UMn_2Ge_2 and related Mn-based actinide ferromagnets. *Phys. Rev. B.* **91**, 174401 (2015).
8. Ramshaw, B. J., Sebastian, S. E. McDonald, R. D., Day, J., Tan, B. S., Zhu, Z., Betts, J. B., Liang, R. X., Bonn, D. A., Hardy, W. N., Harrison, N. Quasiparticle mass enhancement approaching optimal doping in a high-T_c superconductor. *Science* **348**, 317-320 (2015).
9. Moll, P. J. W., Zeng, B., Balicas, L., Galeski, S., Balakirev, F. F., Bauer, E. D., Ronning, F. Field-induced density wave in the heavy-fermion compound $CeRhIn_5$. *Nature Commun.* **6**, 6663 (2015).
10. Radtke, G., Saul, A., Dabkowska, H. A., Salamon, M. B., Jaime, M. Magnetic nanopantograph in the $SrCu_2(BO_3)_2$ Shastry-Sutherland lattice. *Proc. Nat. Acad. Sci. USA*. **112**, 1971-1976 (2015).
11. Jiao, L., Chen, Y., Kohama, Y., Graf, D., Bauer, E. D., Singleton, J., Zhu, J.-X., Weng, Z. F., Pang, G. M., Shang, T., Zhang, J. L., Lee, H.-O., Park, T., Jaime, M., Thompson, J. D., Steglich, F., Si, Q. M., Yuan, H. Q. Fermi surface reconstruction and multiple quantum phase transitions in the antiferromagnet $CeRhIn_5$. *Proc. Nat. Acad. Sci. USA*. **112**, 673-678 (2015).
12. Rodriguez, G., Jaime, M., Mielke, C. H., Balakirev, F. F., Azad, A., Sandberg, R. L., Marshall, B., La Lone, B. M., Henson, B. F., Smilowitz, L., Marr-Lyon, M., Sandoval, T. Insight into fiber Bragg sensor response at 100 MHz interrogation rates under various dynamic loading conditions. *Fiber Optic Sensors and Applications XII Book Series: Proceedings of SPIE* **9480**, 948004 (2015).

13. Han, T.-H., Singleton, J., Schlueter, J. A. Barlowite: A Spin-1/2 Antiferromagnet with a Geometrically Perfect Kagome Motif. *Phys. Rev. Lett*. **113**, 227203 (2014).
14. Aczel, A. A., Li, L., Garlea, V. O., Yan, J. Q., Weickert, F., Jaime, M., Maiorov, B., Movshovich, R., Civale, L., Keppens, V., Mandrus, D. Magnetic ordering in the frustrated J_1-J_2 Ising chain candidate $BaNd_2O_4$. *Phys. Rev. B* **90**, 134403 (2014).
15. Sebastian, S. E., Harrison, N., Balakirev, F. F., Altarawneh, M. M., Goddard, P. A., Liang, R. X., Bonn, D. A., Hardy, W. N., Lonzarich, G. G. Normal-state nodal electronic structure in underdoped high-T-c copper oxides. *Nature* **511**, 61-64 (2014).
16. Kim, J. W., Khim, S., Chun, S. H., Jo, Y., Balicas, L., Yi, H. T., Cheong, S.-W., Harrison, N., Batista, C. D., Han, J. H., Kim, K. H. Manifestation of magnetic quantum fluctuations in the dielectric properties of a multiferroic. *Nature Commun*. **5**, 4419 (2014).
17. Lin, S.-Z., Barros, K., Mun, E., Kim, J.-W., Frontzek, M., Barilo, S., Shiryaev, S. V., Zapf, V. S., Batista, C. D., Kim, K.-H. Magnetic-field-induced phases in anisotropic triangular antiferromagnets: Application to $CuCrO_2$. *Phys. Rev. B* **89**, 220405 (2014).
18. Harrison, N.; Sebastian, S. E. On the relationship between charge ordering and the Fermi arcs observed in underdoped high T_c superconductors. *New J. Phys*. **16**, 063025 (2014).
19. Lancaster, T., Goddard, P. A., Blundell, S. J., Foronda, F. R., Ghannadzadeh, S., Moller, J. S., Baker, P. J., Pratt, F. L. Baines, C., Huang, L., Wosnitza, J., McDonald, R. D., Modic, K. A., Singleton, J., Topping, C. V., Beale, T. A. W., Xiao, F., Schlueter, J. A., Barton, A. M., Cabrera, R. D., Carreiro, K. E., Tran, H. E., Manson, J. L. Controlling Magnetic order and quantum disorder in molecule-based magnets. *Phys. Rev. Lett*. **112**, 207201 (2014).
20. Zapf, V., Jaime, M., Batista, C. D. Bose-Einstein condensation in quantum magnets. *Rev. Mod. Phys.* **86**, 563-614 (2014).
21. Maiorov, B., Mele, P., Baily, S. A., Weigand, M., Lin, S.-Z., Balakirev, F. F., Matsumoto, K., Nagayoshi, H., Fujita, S., Yoshida, Y., Ichino, Y., Kiss, T., Ichinose, A., Mukaida, M., Civale, L. Inversion of the upper critical field anisotropy in FeTeS films. *Supercon. Sci. Techno*. **27**, 044005 (2014).
22. Kim, J. W., Kamiya, Y., Mun, E. D., Jaime, M., Harrison, N., Thompson, J. D., Kiryukhin, V., Yi, H. T., Oh, Y. S., Cheong, S.-W., Batista, C. D., Zapf, V. S. Multiferroicity with coexisting isotropic and anisotropic spins in $Ca_3Co_{2-x}Mn_xO_6$. *Phys. Rev. B* **89**, 060404 (2014).
23. Mun, E., Frontzek, M., Podlesnyak, A., Ehlers, G., Barilo, S., Shiryaev, S. V., Zapf, V. S. High magnetic field evolution of ferroelectricity in $CuCrO_2$. *Phys. Rev. B* **89**, 054411 (2014).
24. Oh, Y. S., Artyukhin, S., Yang, J. J., Zapf, V., Kim, J. W., Vanderbilt, D., Cheong, S. W. Non-hysteretic colossal magnetoelectricity in a collinear antiferromagnet. *Nature Commun*. **5**, 3201 (2014).
25. Harrison, N., Moll, P. J. W., Sebastian, S. E., Balicas, L., Altarawneh, M. M., Zhu, J.-X., Tobash, P. H., Ronning, F., Bauer, E. D., Batlogg, B. Magnetic field-tuned localization of the 5*f*-electrons in URu_2Si_2. *Phys. Rev. B* **88**, 241108 (2013).

Program Title: Spin-Coherent Transport under Strong Spin-Orbit Interaction
Principal Investigator: Jean J. Heremans
Mailing Address: Department of Physics, Virginia Tech, Blacksburg, VA 24061
Email: heremans@vt.edu

Program Scope

The project seeks fundamental insight in spin-dependent quantum coherent phenomena arising from spin-orbit interaction, via experiments using low-temperature electronic magnetotransport in mesoscopic and nanoscale structures of length scales similar to the quantum phase- and spin-coherence lengths and the carrier mean free path of the materials used. Materials with substantial spin-orbit interaction used in the project include narrow-bandgap InAs and InGaAs heterostructures and thin film semimetallic Bi, patterned into mesoscopic and nanoscale geometries. In two-dimensional electron systems in InAs and InGaAs the objectives include the characterization of quantum states arising from the Aharonov-Casher quantum-mechanical phase and its associated effective field, particularly a dual to the integer quantum Hall effect. The Aharonov-Casher phase is the electromagnetic dual of the Aharonov-Bohm phase, obtained by exchanging the magnetic fields and electric charges in the Aharonov-Bohm phase by electric fields and magnetic moments (spin). These experiments are enabled by the quasi-relativistic dispersions and substantial spin-orbit interaction in InAs and InGaAs. The experiments necessitate a thorough understanding of spin-orbit interaction in mesoscopic structures, obtained here by quantum transport experiments. Objectives also include quantum electronic transport on Bi thin films, particularly to study the strongly spin-orbit coupled surface states. Using Bi mesoscopic structures on the scale of the quantum phase- and spin-coherence lengths, the effects of the strong spin-orbit interaction on electronic properties and quantum states are elucidated. While spin-orbit interaction in the solid-state can provide an avenue for the creation of new quantum states of matter, the project also affords a deeper understanding of spin phenomena and quantum-coherent transport phenomena.

Recent Progress

<u>Measurement of time-reversal symmetry breaking length, and duality between magnetic length and spin-orbit coherence length:</u>

The symmetries underlying quantum states of matter are fundamental to their properties. We explored foundational geometrical aspects of time-reversal symmetry breaking by magnetic fields. The experiments [P1] used a mesoscopic interferometer array fabricated on an InGaAs/InAlAs heterostructure. The h/2e oscillations were used to quantify time-reversal symmetry breaking as a mesoscopic dephasing length or an effective magnetic length. Time-reversal symmetry breaking manifests itself as a reduction of the quantum phase coherence length due to an Aharonov-Bohm phase [R1]. The data (FIG. 1) was found to agree with expressions for ballistic confined systems [R2] and is consistent with a gradual and geometrical origin, a new insight. Similarly, the lengthening of spin coherence lengths in confined geometries with spin-orbit interaction [P3,P4,P7] seems related to geometrical constraints on the accumulation of an Aharonov-Casher

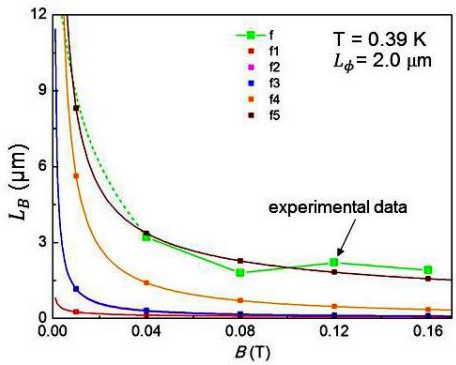

FIG. 1: Experimental data, together with model data, on a time-reversal symmetry breaking length or magnetic length, at 0.39 K in an InGaAs/InAlAs interferometer. Traces f1 to f5 are models. Model f5 for ballistic confined systems, fits best.

phase [R3-R5], the magnetoelectric dual to the Aharonov-Bohm phase. We compared experimental spin coherence lengths in several materials to outline this duality [P3,P4]. The insight leads to the possibility that other Berry's phases may observably reduce quantum phase coherence lengths, and thus be measurable by this avenue. Berry's phases are important for formation of new quantum states of matter but sometimes elusive in measurements.

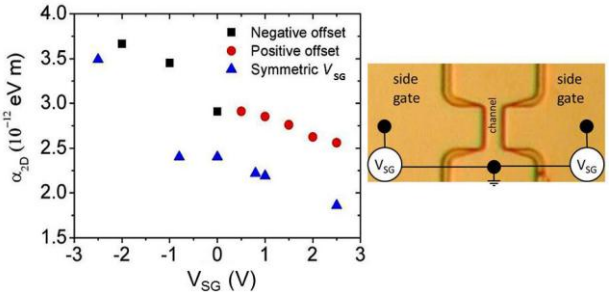

FIG. 2: Left: Rashba parameters obtained by antilocalization at 0.39 K on a side-gated channel on InGaAs/InAlAs, showing a systematic dependence on the side-gate voltage V_{SG} (symmetric: both gates equal bias; pos. offset: one gate +1.5 V, other gate with positive offset indicated; neg. offset: one gate -1.5 V, other gate with negative offset indicated). Right: Channel, 2 μm wide, 4 μm long, between side gates.

Magnitude and origin of spin-orbit interaction in InGaAs channels:

The duality between the magnetic vector potential and the Aharonov-Casher vector potential (equivalent to spin-orbit interaction linear in momentum), suggests the use of emergent electromagnetic fields to generate new quantum states of matter characterized by edge states potentially robust against decoherence [R5]. In side-gated mesoscopic channels on InGaAs/InAlAs heterostructures, we have used the antilocalization magnetoresistance to quantify the effective Rashba parameter as function of side-gate voltage (FIG. 2). The recent analysis is supported by estimates of local electric fields obtained by modeling. The results are consistent with expectations, yet presently also raise deeper points related to Ehrenfest's theorem [R6], and to the exact interpretation of antilocalization data if edge states contribute to the signal.

Measurement of spin interactions between hemin and InAs surface electrons:

To demonstrate that spin-dependent quantum interference measured by antilocalization is a very sensitive probe of spin interactions between surface species and surface carriers, we studied the interactions between the iron center in the biomolecule hemin and a two-dimensional electron system at the surface of (001) InAs, integrated in a bio-organic/semiconductor device structure [P2]. Hemin is an iron porphyrin similar to a group in hemoglobin, where the iron center impacts biological functions. The spin coherence times of the electrons were measured by antilocalization [P9], and spin-flip scattering was found to increase with temperature due to hemin, indicating a spin exchange between the iron center and the electrons. The biomolecule was chosen to emphasize the similarity to the use of spin coherence times in magnetic resonance. The approach demonstrated in this work is indeed in principle similar to magnetic resonance techniques in its use of coherence times, but is implemented electronically.

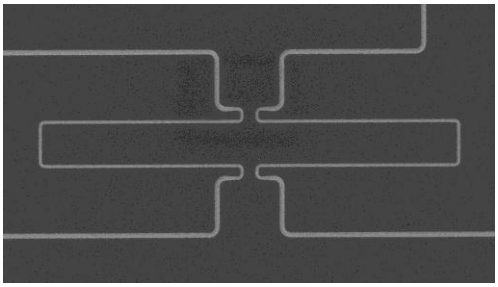

FIG. 3: SEM micrograph of a wide and short Hall bar (geometrical magnetoresistor) as a conformally-mapped approximation to a Corbino geometry, on InGaAs/InAlAs (10 μm wide and 100 μm long).

Mesoscopic Corbino geometries for Aharonov-Casher edge state detection:

To detect and study the edge states induced by the effective Aharonov-Casher vector potential, we study Corbino-type geometries (FIG. 3), some at

mesoscopic length scales comparable to the spin coherence length. In these geometries the isolation between edge states is expected to give rise to clear magnetoresistance signals. This work is in progress.

Future Plans

Detection of edge states induced by the effective Aharonov-Casher vector potential

The electromagnetic duality between the Aharonov-Bohm and the Aharonov-Casher phases can lead us to new quantum states of matter. In particular edge states can be induced by the Aharonov-Casher effective field (in analogy to their magnetic counterparts in the integer quantum Hall effect). The states need to be constructed in mesoscopic channels, on length scales shorter than the spin coherence length, and they rely on tunable electric fields.

1) In that context understanding of spin-orbit interaction in mesoscopic channels is desirable. The data we acquired by antilocalization is consistent with the expected magnitudes of the electric fields, but has given rise to several deeper questions, which need answering. Ehrenfest's theorem precludes spin-orbit interaction from electric field components solely responsible for electrostatic confinement, which gives rise to the question which component of the electric field lies at the origin of the data. Further, edge state confinement is not solely electrostatic, and the implications of Ehrenfest's theorem may need to be revisited in this particular case. Also, it is still unclear which information antilocalization can furnish about the spin-orbit interaction driving edge states since these are protected from backscattering. Further, side-gated channels with a central quantum antidot will be used to perform high-resolution backscattering spectroscopy on the edge states. Particularly the use of materials with different *g*-factors (InAs *vs* InGaAs), and the use of tilted magnetic fields are emphasized because they allow a differentiation between edge state phenomena and other phenomena occurring in mesoscopic channels. Also parallel arrays of wires, rather than single wires, are planned as arrays of wires minimize the signature of universal conductance fluctuations in transport.

2) Corbino disk geometries, or geometries approximating Corbino disks obtained by conformal mapping, will be used to quantify the reduced backscattering of Aharonov-Casher edge states. The measurement of mesoscopic Corbino disks in the regime where edge states appear, will show the appearance of a more insulating bulk, and show characteristic magnetotransport features. The present experiments point to the need of taking into account the spin coherence lengths, as effective persistence lengths for the edge states.

Mesoscopic and magnetoelectronic devices on bismuth and its surface states:

1) We have observed a lengthening of the spin coherence length in Bi wires with narrowing wire widths [R7], pointing to predicted Bi surface states with strong spin-orbit interaction [R8]. On mesoscopic wires and interferometers fabricated on high-quality Bi thin films grown in our laboratory, we plan to perform quantum transport experiments including the use of in-plane (tilted) magnetic fields. The resulting interplay between the effective width of the surface state layer and the magnetic length allows a mapping of the magnitude of the anisotropic spin-orbit interaction.

2) The Bi films are polycrystalline, but with large grains, with the trigonal axis perpendicular to the substrate. The large grain size allows us to pattern and measure ring interferometers fitting on a single grain, using carefully aligned electron-beam lithography. The single-grain mesoscopic structures will lead to a study of spin-dependent quantum interference on Bi and its surface states.

References

R1) C. Texier, P. Delplace, and G. Montambaux, "Quantum oscillations and decoherence due to electron-electron interaction in metallic networks and hollow cylinders", Phys. Rev. B **80**, 205413 (2009).

R2) S. Kettemann, "Dimensional control of antilocalization and spin relaxation in quantum wires", Phys. Rev. Lett. **98**, 176808 (2007); C. W. J. Beenakker, and H. van Houten, "Boundary scattering and weak localization of electrons in a magnetic field", Phys. Rev. B **38**, 3232 (1988).

R3) Y. Aharonov, and A. Casher, "Topological quantum effects for neutral particles", Phys. Rev. Lett. **53**, 319 (1984).

R4) H. Mathur, and D. A. Stone, "Quantum transport and the electronic Aharonov-Casher effect", Phys. Rev. Lett. **68**, 2964 (1992).

R5) L. L. Xu, Shaola Ren, and J. J. Heremans, "Magnetoelectronics at edges in semiconductor structures: helical Aharonov-Casher edge states", Integrated Ferroelectrics **131**, 36 (2011).

R6) R. Winkler, "Rashba spin splitting and Ehrenfest's theorem", Physica E **22**, 450 (2004).

R7) M. Rudolph, and J. J. Heremans, "Spin-orbit interaction and phase coherence in lithographically defined bismuth wires", Physical Review B **83**, 205410 (2011).

R8) Ph. Hofmann, "The surfaces of bismuth: Structural and electronic properties", Prog. Surf. Sci. **81**, 191 (2006).

Publications which acknowledge DOE support

P1) S. L. Ren, J. J. Heremans, C. K. Gaspe, S. Vijeyaragunathan, T. D. Mishima, and M. B. Santos, "Determination of time-reversal symmetry breaking lengths in an InGaAs Sagnac interferometer array", Journal of Physics: Condensed Matter **27**, 185801 (2015).

P2) Vincent Deo, Yao Zhang, V. Soghomonian, and J. J. Heremans, "Quantum interference measurement of spin interactions in a bio-organic/semiconductor device structure", Scientific Reports **5**, 9487; DOI:10.1038/srep09487 (2015).

P3) J. J. Heremans, R. L. Kallaher, M. Rudolph, and M. B. Santos, "Magnetoelectric mapping as observed in quantum coherence phenomena under strong spin-orbit interaction". **Accepted** in Integrated Ferroelectrics.

P4) J. J. Heremans, R. L. Kallaher, M. Rudolph, M. B. Santos, W. Van Roy, and G. Borghs "Spin-orbit interaction and spin coherence in narrow-gap semiconductor and semimetal wires", Proceedings of the SPIE **9167**, 91670-D1 (2014).

P5) Yao Zhang, and J. J. Heremans, "Effects of ferromagnetic nanopillars on spin coherence in an InGaAs quantum well", Solid State Communications **177**, 36 (2014).

P6) Yao Zhang, V. Soghomonian, R. L. Kallaher, and J. J. Heremans, "Antilocalization sensing of interactions between two-dimensional electrons and surface species", Chinese Science Bulletin **59**(2), 133 (2014).

P7) R. L. Kallaher, J. J. Heremans, W. Van Roy, and G. Borghs, "Spin and phase coherence lengths in InAs wires with diffusive boundary scattering", Physical Review B **88**, 205407 (2013).

P8) S. L. Ren, J. J. Heremans, C. K. Gaspe, S. Vijeyaragunathan, T. D. Mishima, and M. B. Santos, "Aharonov–Bohm oscillations, quantum decoherence and amplitude modulation in mesoscopic InGaAs/InAlAs rings", Journal of Physics: Condensed Matter **25**, 435301 (2013).

P9) Yao Zhang, R. L. Kallaher, V. Soghomonian, and J. J. Heremans, "Measurement by antilocalization of interactions between InAs surface electrons and local moments", Physical Review B **87**, 054430 (2013).

Program Title: Charge and Energy Transfer in Molecular Superconductors and Molecular Machines

Principal Investigator: Saw Wai Hla
Mailing Address: 251B Clippinger Lab, Physics & Astronomy Department, Ohio University, Athens, OH 45701.
Email: hla@ohio.edu

Program Scope

This project focuses on how charge and energy transfer taken place at the atomic and nanometer scale in exotic molecular materials and molecular machines exhibiting ferroelectric, superconductivity, and charge density waves behaviors. In donor-acceptor type charge transfer materials, we are investigating the charge density waves and superconducting behaviors in self-assembled molecular islands and the interactions of nearly free two dimensional surface-state electrons with the molecular clusters. We also investigate how a controlled energy transfer in individual molecular motors can achieved directional rotations, and how charge and energy are transferred in the coupled molecular motor networks. Our project includes both conventional and innovative components, and the achievements of these projects will impact on fundamental understanding of charge and energy transfer processes in exotic molecular materials for potential applications in energy sciences.

Recent Progress

One of the goals of nanotechnology is to assemble billions of nanomachines packed in a tiny area that can be operated in a synchronized manner and information can be coherently transferred to multiple destinations within nanometer range. Using dipolar interaction as a mean to communicate among the molecular rotors, we have shown that rotational switching of entire rotor networks can be realized by supplying an electric field from a scanning tunneling microscope tip. Strikingly, over 500 rotors can be simultaneously rotated in the hexagonal rotor network on Cu(111) surface using the biases above ±1 V at 80 K. This phenomenon is observed only in the hexagonal rotor network due to the degeneracy of the ground state dipole rotational energy barrier. A part of this study is described in section I.

Many unconventional superconducting materials show charge density wave behavior above critical temperature. We have studied small self-assembled clusters of a donor-acceptor charge transfer based molecular material, α-(BEDT-TTF)$_2$-I$_3$. This molecular system exhibits superconductivity in bulk molecular crystal below a critical temperature of ~ 1.8 K. In our study conducted at ~6 K on 2-D nanoscale molecular clusters formed on Ag(111) surface, a cogent charge density wave (CDW) is observed. In addition, we are able to manipulate the CDW by using electric field from the scanning tunneling microscope tip in a controlled fashion. A part of this study is described in section II.

I. Simultaneous and coordinated rotational switching of all molecular rotors in a network

Molecular machines are ubiquitous in nature however most of them are sensitive to their environment and lack adaptability to new media and functions. In contrast, artificial nanomachines can be engineered to suit more specific environments than their natural counterparts, and thus they are advantageous to operate in solid state devices. Molecular motors

and rotors can be considered as parts of molecular machines. We have shown that a controlled directional rotation can be achieved in standalone molecular motors using inelastic tunneling electrons as an energy source. An image of this work has been featured in the recent BESAC report, "Challenges at the frontier of matter and energy: Transformative opportunity for discovery science". Following this, we have developed a double-decker class molecular rotor with dipole active rotator arms (Fig. 1). Our goal is to achieve communication among the molecular rotors via dipolar interactions. The double-decker class molecular rotor studied here are the porphyrinate naphthalocyaninate europium complexes (Fig. 1a). In this rotor, the upper deck is a functionalized 5,15-diarylporphyrin, which is designed to act as a rotator. Due to an internal charge transfer between an electron donating and an electron accepting group (butoxy and cyano groups, respectively) located at the opposite positions on the porphyrin macrocycle, it has a permanent electric dipole moment of 8 Debye (Fig. 1a). The lower deck, stator, is a naphthalocyanine designed to anchor on metallic surfaces via 8 sulfur atoms at the end of the macrocycle (Fig. 1a, and 1b). The upper and lower decks are linked via a europium(III) ion, which acts as an atomic ball bearing and allow free rotations of the rotator arm while the stator unit is in fixed position on the surface.

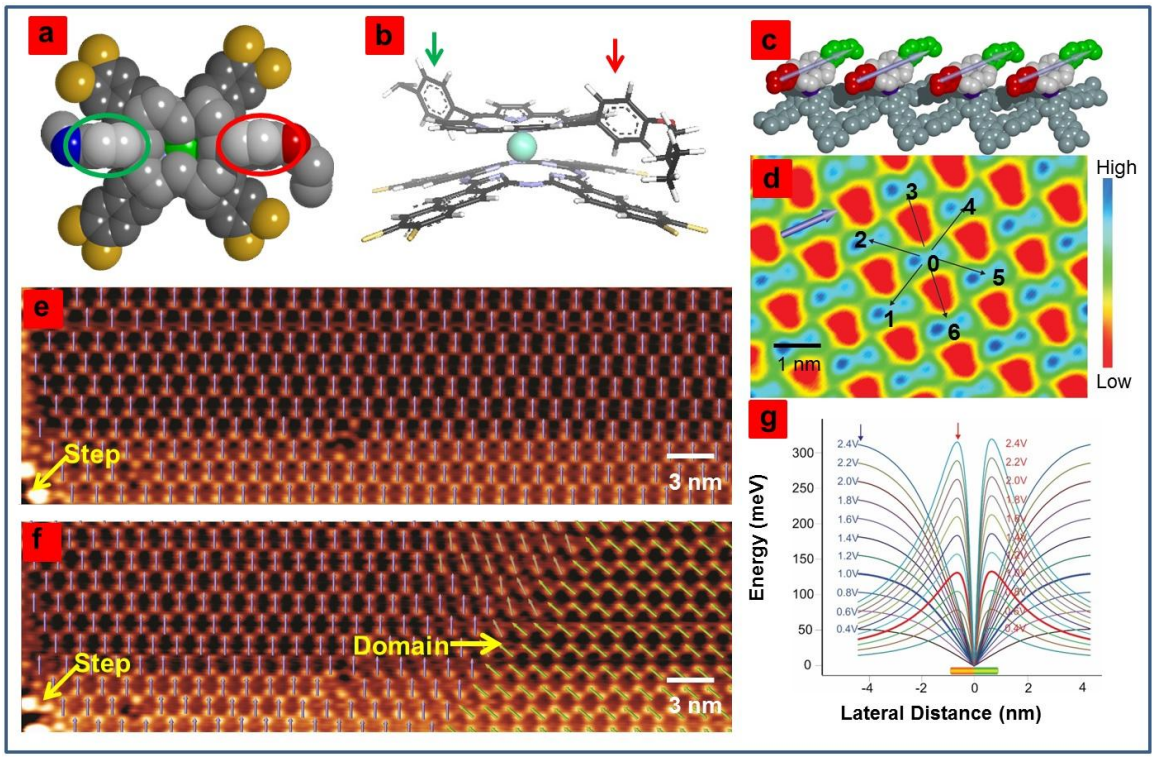

Fig. 1. *Molecular rotor model top view (a) and side view (b). Red and green color ovals and arrows indicate donor and acceptor, respectively. (c) A model displays assembly of dipole active rotors. (d) An STM image of dipolar rotors forming a hexagonal symmetry on Cu(111). 1 to 6 labels near-neighbor dipole of '0' and the arrow indicates the dipole direction. (e) An STM image showing a large area of assembled dipolar rotor. (f) In subsequent scan, the right area has switched to a different orientation. (g) Electric field energy as a function of distance plots.*

These double-decker rotors self-assembled to form a hexagonal dipole network on a Cu(111) surface (Fig. 1c, and 1d). Analyses from the STM images reveal that all the dipoles of the

double-decker rotors in the network are pointing to the same direction and therefore we have a ferroelectric molecular rotor network. Remarkably, we are able to switch a large number of dipole active rotator arms simultaneously by scanning with the STM tip using biases higher than ± 1V. Similar switching of an entire network of dipolar rotors can also be realized by an electric field induced STM manipulation process. Statistical analysis on the rotational switching of 5176 rotors gives an equal probability for the clockwise and anticlockwise switchings within the measurement uncertainty of ±5%. Theoretical analyses further reveal that synchronized rotation is the most favorable condition for the observed simultaneous switching due to the degeneracy of the ground state dipole energy barrier. More interestingly, we find that such simultaneous switching of rotors occurs only if there are defects nearby. This work highlights the essential role of the defects to have an excess energy that is used to drive the rotation. Our findings represent the first direct visualization of dipole interactions in a hexagonal network manifesting mesoscale behaviors collectively achieved by individual rotors. This work opens up possibility to realize communication in more complex molecular-machine networks for potential applications in solid state devices, quantum computation, energy transfer, and information transport at the nanoscale.

II. Molecular charge density waves

It is known that some bulk molecular crystals exhibit charge density waves. But to our knowledge, charge density waves in a two dimensional molecular layer have not been studied in detail. In this part of the project, we have investigated nanoscale clusters formed by α-(BEDT-TTF)$_2$-I$_3$ on Ag(111) surface at low temperatures (Fig. 2). α-(BEDT-TTF)$_2$-I$_3$ is a layered type donor-acceptor charge transfer compound and the BEDT-TTF molecular layer is sandwiched by I_3 layers. By donating ~0.25e charge to I_3, the HOMO level of BEDT-TTF becomes partially filled resulting in a metallic character. When deposited on a Ag(111) surface, these molecular system retains its layered structure and exhibit incommensurate charge density waves (CDW) with a periodicity of 2.75 nm at liquid helium temperatures (Fig. 2c).

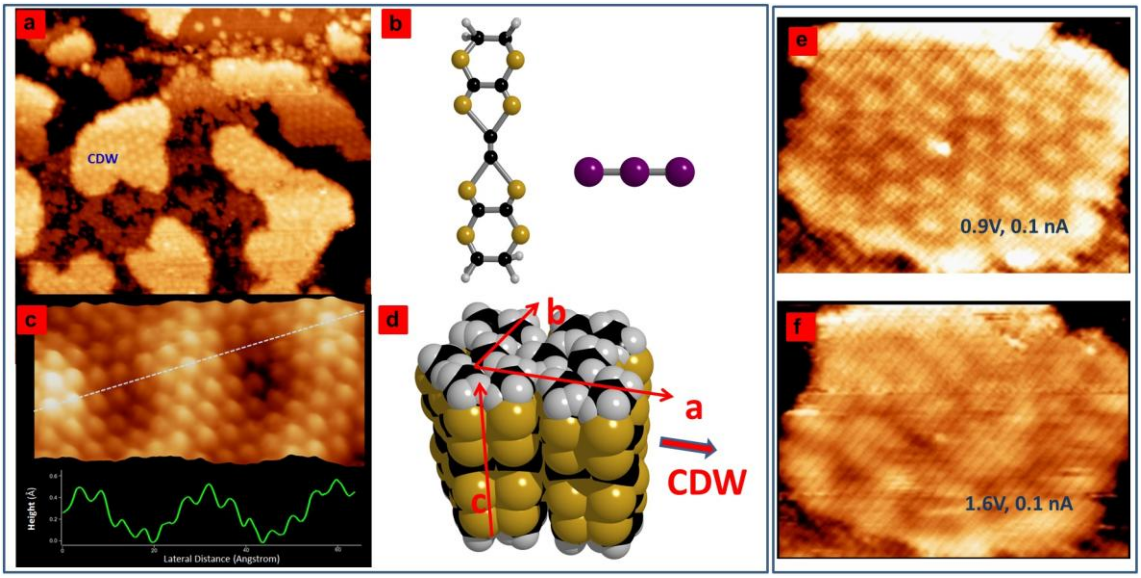

Fig. 2. *(a)CDW in 2-D molecular islands on Ag(111). (b)Models of BEDT-TTF and I_3. (c)A zoom in STM image showing the CDW periodicity. (d) The BEDT-TTF assembly and the CDW direction. (e) CDW observed in a molecular island at 0.9 V can be destroyed at 1.6V (f).*

The CDW in this 2-D molecular system is observed down to the second molecular layer and remarkably, the CDW phase is preserved in small molecular islands having less than 10 nm diameters. Moreover, by using electric field from the STM tip, we are able to manipulate the observed CDW in these nanoscale molecular clusters. In general, CDW phases are routinely observed in many 2-D inorganic material systems such as in $NbSe_2$, and other transition metal dichalcogenides. The finding of CDW in 2-D molecular system that is also known to exhibit superconductivity opens exciting opportunity to explore the correlation between the CDW and superconductivity in complementary materials composed of molecules.

Future Plans

Following the investigations of the double-decker rotor network, which reveals that the defects are necessary for the rotational switching, we plan to investigate the role of defects in more detail. In particular, the rotor domain formation will be studied as a function of defects. For this we plan to induce the defects locally by using high voltage pulses from the STM tip. Moreover, by creating spin active components, we plan to investigate the effect of spin in individual molecular motors and their networks. We are also extending the study using other polar molecular assemblies on surfaces. In the case of charge transfer molecular systems, we are currently investigating the β phase of $(BEDT\text{-}TTF)_2\text{-}I_3$ on Ag(111) surface. In bulk, the β structure exhibit superconductivity at ~ 6 K. Our goal is to investigate the correlation between the superconductivity and CDW phases in molecular materials. In addition we have started the experiments using a recently developed instrument, synchrotron X-ray scanning tunneling microscopy (SXSTM), in Advanced Photon Source. The SX-STM enables simultaneous characterization of elemental, chemical, and magnetic contrast at the atomic limits, and therefore the studies of these exotic molecular systems with SX-STM will provide valuable information that cannot be attained by other experimental means.

List of Publications Acknowledging Current DOE Grant

Published:

1). S.-W. Hla. *Trapping a Charged Atom*. **ACS Nano.** DOI: 10.1021/acsnano.5b04985 (2015).

2). N. Shirato, M. Cummings, H. Kersell, Y. Li, B. Stripe, D. Rosenmann, S.-W. Hla, & V. Rose. *Elemental Fingerprinting of Materials with Sensitivity at the Atomic Limit*. **Nano Lett. 14**, 6499-6504 (2014).

3). S.-W. Hla. *Atomic Level Assembly*. **Rep. Prog. Phys. 77**, 056502 (2014).

4). U.G.E. Perera, F. Ample, H. Kersell, Y. Zhang, G. Vives, J. Echeverria, M. Grisolia, G. Rapenne, C. Joachim, & S.-W. Hla. *Controlled Clockwise and Anticlockwise Rotation of a Molecular Motor***. Nature Nanotechnology 8**, 46-51 (2013).

Submitted:

5). Y. Zhang, H. Kersell, R. Stefak, J. Echeverria, V. Iancu, U. G. E. Perera, Y. Li, A. Deshpande, K.-F. Braun, C. Joachim, G. Rapenne, & S.-W. Hla. Simultaneous and Coordinated Rotational Switching of All Molecular Rotors in a Network.

Program Title: Magnetic Thin Films*
Principle Investigator: A. Hoffmann; Co-PIs: J. S. Jiang and V. Novosad
Mailing Address: Materials Science Div., Argonne National Lab., Argonne, IL 60439
Email: hoffmann@anl.gov

Program Scope

The issues our group addresses in nanomagnetism encompass (1) spin dynamics, (2) spin transport, and (3) the creation of new multilayer materials, based on metallic heterostructures. Our program in spin dynamics provides insights into artificial magnonic materials. The work advances our fundamental understanding of linear and nonlinear excitations in magnetic nanostructures. Our program in spin transport focuses on the physics of pure spin currents. Recently spin currents have been recognized as a way to communicate without charge currents, potentially eliminating wasted heat that impedes further transistor miniaturization. Due to this heat, information technology is an energy technology issue, as well as a U.S. economic competitiveness issue [1]. Finally, the quest for new functional materials via nanoscale multilayering enables us to create systems that possess unusual synergistic properties that may otherwise be mutually exclusive [2]. Such systems include exchange spring composites with low or no rare-earth content than can exceed today's commercial capabilities as used in electric motors and generators, or ferromagnetic-superconducting multilayers that support an exotic interfacial pairing even though the individual components can be as simple as elemental layers. Such multilayering also enables us to explore the energetics and transport mechanisms underlying organic spintronic heterostructures. These concepts and the materials explored within this proposal also provide samples worthy of advanced characterization at BES major characterization facilities.

Recent Progress:

For this presentation we will focus on our recent work related to spin Hall effects [36]. Spin Hall effects intermix spin and charge currents in any, even non-magnetic, materials and, therefore, offer the possibility to generate and detect spin currents without using ferromagnets. Furthermore it has recently been realized that the spin-orbit interactions underlying spin Hall effects provide a very efficient alternative pathway to electrical injection for generating spin currents from charge currents. Unlike for electrical injection the generated spin currents can exceed the initial charge current even for nanoscale devices, since the same electron used for the charge transport can transfer its spin multiple times due to the transverse transport nature of spin Hall effects. Our early experiments had focused on Pt, which is known to have some of the most pronounced spin Hall effects and has become ubiquitous for exploiting them. However, since Pt is also known to be highly polarizable and therefore very susceptible to magnetic proximity effects, questions remained about whether any induced order may be important for understanding the spin transport in this material. In order to clarify this issue, we investigated spin Hall effects in very thin Pt and Pd (another material well known for magnetic proximity effects) in direct contact with permalloy ($Ni_{80}Fe_{20}$) and discovered that the spin Hall effect in both materials is strongly reduced at low temperatures [6]. Interestingly this reduction vanished, when the Pt and Pd was separated from the permalloy by a thin layer of Cu indicating that it is directly related to magnetic proximity. Ab-initio calculations of the spin Hall conductivities for these systems

* Work supported by the U.S. Department of Energy, Office of Science, Basic Energy Sciences, under contract No. DE-AC02-06CH11357.

suggest that the observed reduction is consistent with an induced moment of 0.5 μ_B in Pt. We furthermore extended our investigation of spin Hall effects in magnetically ordered system to metallic antiferromagnets. CuAu-I-type antiferromagnets based on Mn-alloys revealed that the spin Hall conductivity systematically increases with the spin-orbit coupling of the alloying element (Fe, Pd, Ir, or Pt) [16]. Again this experimental observation agrees well with the intrinsic spin Hall conductivities determined from the Berry curvature of the band structure as calculated from first principles. We have also shown that the spin Hall conductivities of these antiferromagnets is high enough to enable electrically driven magnetization dynamics in bilayers with permalloy. This indicates that metallic antiferromagnets can provide functionality in spintronics devices beyond just the well-established exchange bias phenomenon.

Future Plans

As mentioned above the transverse nature of generating spin currents from charge currents via spin-orbit interactions allows for superior scaling the enables highly efficient spin current generation [12]. This idea will be maximized if the charge current is confined to a purely two-dimensional layer. With this in mind we will explore spin-orbit torques that are generated from interfacial Rashba coupling [10]. In this respect, monolayer films of dichalcagonides, such as MoS_2 and WS_2 are especially appealing, since they incorporate heavy elements with strong spin-orbit coupling. Preliminary measurements already demonstrate unexpectedly large spin-orbit torques in bilayers of metallic ferromagnets and MoS_2. Besides, exploring approaches for maximizing spin-orbit torques, we will also utilize them for studying current driven dynamics in insulating magnetic systems, such as yttrium iron garnet (YIG) films. First measurements show that spin Hall effects can be used to generate and detect spin dynamics even in relatively small YIG structures, which will enable us to clarify the role that geometric confinement plays [9] in modifying non-linear dynamics, such as auto-oscillations. Furthermore, direct electric excitation will enable very local excitation of the magnetization dynamics and thus may allow studying short wavelength spin waves that are typically inaccessible for direct magnetic field excitation.

List of Publications resulting from DOE sponsored research in FY14 and FY15

1. New Opportunities at the Frontiers of Spintronics, A. Hoffmann and S. D. Bader, Phys. Rev. Appl. (in press).
2. Mesoscale Magnetism, A. Hoffmann and H. Schultheiß, Curr. Opin. Solid State Mater. Sci. **19**, 253 (2015).
3. Blowing Magnetic Skyrmion Bubbles, W. Jiang, P. Upadhyaya, W. Zhang, G. Yu, M. B. Jungfleisch, F. Y. Fradin, J. E. Pearson, Y. Tserkovnyak, K. L. Wang, O. Heinonen, S. G. E. te Velthuis, and A. Hoffmann, Science **349**, 283 (2015).
4. A Small Signal Amplifier Based on Ionic Liquid Gated Black Phosphourous Field Effect Transistor, S. Das, W. Zhang, L. R. Thoutam, Z. Xiao, A. Hoffmann, M. Demarteau, and A. Roelofs, IEEE Elec. Dev. Lett. **36**, 621 (2015).
5. A new reversal mode in exchange coupled antiferromagnetic/ferromagnetic disks: distorted viscous vortex, D. A. Gilbert, L. Ye, A. Varea, S. Agramunt-Puig, N. del Valle, C. Navau, J. F. López-Barbera, K S. Buchanan, A. Hoffmann, A. Sánchez, J. Sort, K. Liu, and J. Nogués, Nanoscale **7**, 9878 (2015).
6. Reduced spin-Hall effects from magnetic proximity, W. Zhang, Y. Liu, J. E. Pearson, S. G. E. te Velthuis, A. Hoffmann, F. Freimuth, and Y. Mokrousov, Phys. Rev. B **91**, 115316 (2015).

7. Dynamic control of metastable remanent states in mesoscale magnetic elements, J. Ding, S. Jain, J. E. Pearson, S. Lendinez, V. Khovaylo, and V. Novosad, J. Appl. Phys. **117**, 17A707 (2015).
8. Spin Seebeck devices using local on-chip heating, S. M. Wu, F. Y. Fradin, J. Hoffman, A. Hoffmann, and A. Bhattacharya, J. Appl. Phys. **117**, 17C509 (2015).
9. Spin waves in micro-structured yttrium iron garnet nanometer-thick films, M. B. Jungfleisch, W. Zhang, W. Jiang, H. Chang, J. Sklenar, S. M. Wu, J. E. Pearson, A. Bhattacharya, J. B. Ketterson, M. Wu, and A. Hoffmann, J. Appl. Phys. **117**, 17D128 (2015).
10. Spin pumping and inverse Rashba-Edelstein effect in NiFe/Ag/Bi and NiFe/Ag/Sb, W. Zhang, M. B. Jungfleisch, W. Jiang, J. E. Pearson, and A. Hoffmann, J. Appl. Phys. **117**, 17C727 (2015).
11. Magnetization processes in core/shell exchange-spring structures, J. S. Jiang, J. Appl. Phys. **117**, 17A734 (2015).
12. Spin pumping and inverse spin Hall effects – Insights for future spin-orbitronics (invited), W. Zhang, M. B. Jungfleisch, W. Jiang, J. Sklenar, F. Y. Fradin, J. E. Pearson, J. B. Ketterson, and A. Hoffmann, J. Appl. Phys. **117**, 172610 (2015).
13. Self-healing patterns in ferromagnetic-superconducting hybrids, V. K. Vlasko-Vlasov, E. Palacious, D. Rosenmann, J. E. Pearson, Y. Jia, Y. L. Wang, U. Welp, and W. K. Kwok, Supercond. Sci. Techn. **28**, 035006 (2015).
14. Influence of Domain Width on Vortex Nucleation in Superconductor/Ferromagnet Hybrid Structures, M. Iavarone, S. A. Moore, J. Fedor, V. Novosad, J. E. Pearson, and G. Karapetrov, J. Supercond. Novel Magn. **28**, 1107 (2015).
15. Magnetic pinning in a superconducting film by a ferromagnetic layer with stripe domains, D. Mancusi, C. Di Giorgio, F. Bobba, A. Scarfato, A. M. Cucolo, M. Iavarone, S. A. Moore, G. Karapetrov, V. Novosad, V. Yefremenko, S. Pace, and M. Polichetti, Supercond. Sci. Techn. **27**, 125002 (2014).
16. Spin Hall Effects in Metallic Antiferromagnets, W. Zhang, M. B. Jungfleisch, W. Jiang, J. E. Pearson, A. Hoffmann, F. Freimuth, and Y. Mokrousov, Phys. Rev. Lett. **113**, 196602 (2014).
17. Engineering the Transport Gap in Phosphorene, S. Das, W. Zhang, M. Demarteau, A. Hoffmann, M. Dubey, and A. Roelofs, Nano Lett. **14**, 5733 (2014).
18. Study of critical exponents in doped $La_{2/3}Ca_{1/3}Mn_{1-y}Fe_yO_3$ (y = 0, 0.03) manganite films, O. Arnarche, G. Campillo, and A. Hoffmann, Appl. Phys. A **117**, 937 (2014).
19. Efficient Cisplatin Pro-Drug Delivery Visualized with Sub-100 nm Resolution: Interfacing Engineered Thermosensitive Magnetomicelles with a Living System, E. A. Vitol, E. A. Rozhkova, V. Rose, B. D. Stripe, N. R. Young, E. E. W. Cohen, L. Leoni, and V. Novosad, Adv. Mater. Interf. **1**, 1400182 (2014).
20. Magnetocaloric effect in "reduced" dimensions: Thin films, ribbons, and microwires of Heusler alloys and related compounds, V. V. Khovaylo, V. V. Rodionova, S. N. Shevyrtalov, and V. Novosad, Phys. Stat. Solidi B **251**, 2104 (2014).
21. Visualizing domain wall and reverse domain superconductivity, M. Iavarone, S. A. Moore, J. Fedor, S. T. Ciocys, G. Karapetrov, J. Pearson, V. Novosad, and S. D. Bader, Nature Commun. **5**, 4766 (2014).
22. Microwave absorption properties of permalloy nanodots in the vortex and quasi-uniform magnetization states, K. Y. Guslienko, G. N. Kakazei, Y. V. Kobljanskyi, G. A. Melkov,

V. Novosad, and A. N. Slavin, New J. Phys. **16**, 063044 (2014).
23. Vortex-antivortex coexistence in Nb-based superconductor/ferromagnet heterostructures, F. Bobba, C. Di Giorgio, A. Scarfato, M. Longobardi, M. Iavarone, S. A. Moore, G. Karapetrov, V. Novosad, V. Yefremenko, and A. M. Cucolo, Phys. Rev. B **89**, 214502 (2014).
24. Nanometer-Thick Yttrium Iron Garnet Films With Extremely Low Damping, H. Chang, P. Li, W. Zhang, T. Liu, A. Hoffmann, L. Deng, and M. Wu, IEEE Magn. Lett. **5**, 6700104 (2014).
25. Realization of a spin-wave multiplexer, K. Vogt, F. Y. Fradin, J. E. Pearson, S. D. Bader, T. Sebastian, B. Hillebrands, A. Hoffmann, and H. Schultheiss, Nature Commun. **5**, 3727 (2014).
26. Preface to Special Topic: Invited Papers of the 58th Annual Conference on Magnetism and Magnetic Materials, Denver, Colorado, USA, Novmber 2013, A. Hoffmann, J. Appl. Phys. **115**, 172501 (2014).
27. Preface: Proceedings of the 58th Annual Conference on Magnetism and Magnetic Materials, Denver, Colorado, USA, November 2013, A. Hoffmann, J. Appl. Phys. **115**, 17A101 (2014).
28. Dynamic decay of a single vortex into vortex-antivortex pairs, S. Lendinez, S. Jain, V. Novosad, F. Y. Fradin, J. E. Pearson, J. Tejada, and S. D. Bader, J. Appl. Phys. **115**, 17D121 (2014).
29. Ferromagnetic resonance of sputtered yttrium iron garnet films, T. Liu, H. Chang, V. Vlaminck, Y. Sun, M. Kabatek, A. Hoffmann, L. Deng, and M. Wu, J. Appl. Phys. **115**, 17A501 (2014).
30. The Effect of Ligands on FePt-Fe_3O_4 Core-Shell Magnetic Nanoparticles, D. H. Kim, Y. Tamada, T. Ono, S. D. Bader, E. A. Rozhkova, and V. Novosad, J. Nanosci. Nanotechn. **14**, 2648 (2014).
31. Dynamics of coupled vortices in perpendicular fields, S. Jain, V. Novosad, F. Y. Fradin, J. E. Pearson, and S. D. Bader, Appl. Phys. Lett. **104**, 082409 (2014).
32. Rational design of the exchange-spring permanent magnet, J. S. Jiang and S. D. Bader, J. Phys. Conden. Matter **26**, 064214 (2014).
33. Probing the energy barriers in nonuniform magnetization states of circular dots by broadband ferromagnetic resonance, G. A. Melkov, Y. Kobljanskyi, V. Novosad, A. N. Slavin, and K. Y. Guslienko, Phys. Rev. B **88**, 220407 (2013).
34. Determination of the Pt spin diffusion length by spin-pumping and spin Hall effect, W. Zhang, V. Vlaminck, J. E. Pearson, R. Divan, S. D. Bader, and A. Hoffmann, Appl. Phys. Lett. **103**, 242414 (2013).
35. Universal Method for Separating Spin Pumping from Spin Rectification Voltage of Ferromagnetic Resonance, L. Bai, P. Hyde, Y. S. Gui, C.-M. Hu, V. Vlaminck, J. E. Pearson, S. D. Bader, and A. Hoffmann, Phys. Rev. Lett. **111**, 217602 (2013).
36. Spin Hall Effects in Metals, A. Hoffmann, IEEE Trans. Magn. **49**, 5172 (2013).
37. Study of functional infrared imaging for early detection of mucositis in locally advanced head and neck cancer treated with chemoradiotherapy, E. E. W. Cohen, O. Ahmed, M. Kocherginsky, G. Shustakova, E. Kistner-Griffin, J. K. Salama, V. Yefremenko, and V. Novosad, Oral Oncol. **49**, 1025 (2013).
38. Recent Advances in Magnetic Insulators – From Spintronics to Microwave Applications, M. Wu and A. Hoffmann, Solid State Phys. **64** (2013).

Search for Novel Topological Phases in Superconductors using Laser-Based Spectroscopy

Principal Investigator: David Hsieh
Mailing Address: 1200 E. California Blvd., MC 149-33, California Institute of Technology, Pasadena, CA 91125
E-mail: dhsieh@caltech.edu

(i) Program Scope

The goal of this research program is to investigate the possibility of realizing intrinsically topological superconducting phases in unconventional three-dimensional (3D) superconducting compounds through the development and use of novel laser-based spectroscopic techniques. Topological superconductors are predicted to host Majorana excitations at their boundaries[1,2], which exhibit the non-Abelian exchange statistics necessary for realizing fault-tolerant quantum computation[3]. Considerable progress has recently been made towards artificially engineering 1D and 2D topological superconductors by inducing *s*-wave superconductivity in strongly spin-orbit coupled semiconducting nanowires[4–6] and thin films[7,8]. In contrast, no method currently exists for artificially engineering 3D topological superconductors and therefore searches for such phases are constrained to compounds in their native state. The experimental realization of a 3D topological superconducting phase would create a platform for manipulating 2D gases of mobile Majorana excitations at their surfaces and for exploring anomalous thermal Hall effects. Moreover, it may generate insight into methods to realize intrinsically topological 1D and 2D superconducting compounds of different classes, which can circumvent the engineering challenges associated with hybrid superconductor-semiconductor device architectures.

(ii) Recent Progress

Our technical approach to identifying and classifying the intrinsic topological properties of a superconducting compound is to use a combination of angle-resolved photoemission spectroscopy (ARPES) to probe its surface electronic structure and nonlinear optical spectroscopy to probe its bulk symmetry properties.

(a) Ultra-low temperature and ultra-high resolution ARPES

In principle, ARPES can directly measure the dispersion of surface Majorana excitations and thereby ascertain whether or not a 3D superconductor is topologically non-trivial[9]. However, 3D topological superconducting candidate compounds typically have superconducting gaps of order 1 meV and superconducting transition temperatures of order 1 K, which are near or beyond the energy resolution and temperature limits of current ARPES facilities. To overcome this limitation, we are developing a high-resolution ARPES system with sub-Kelvin capability. Our system utilizes a custom ^{3}He cryostat (Fig. 1a) that reaches a base temperature of ~ 0.8 K, the lowest of any currently existing ARPES system. The sample manipulator has three translational and two angular mechanical degrees of freedom (Fig. 1b) that can be operated at base temperature, which allows large areas of the crystal Brillouin zone to be accessed during measurements. High energy resolution is being targeted through the use of a narrow bandwidth continuous-wave UV laser, a state-of-the-art electron energy analyzer and effective magnetic field shielding of the measurement chamber. Preliminary ARPES measurements on the 3D

topological band insulator Bi_2Se_3 show the expected linearly dispersing topological surface state and projected bulk bands[10] (Fig. 1c).

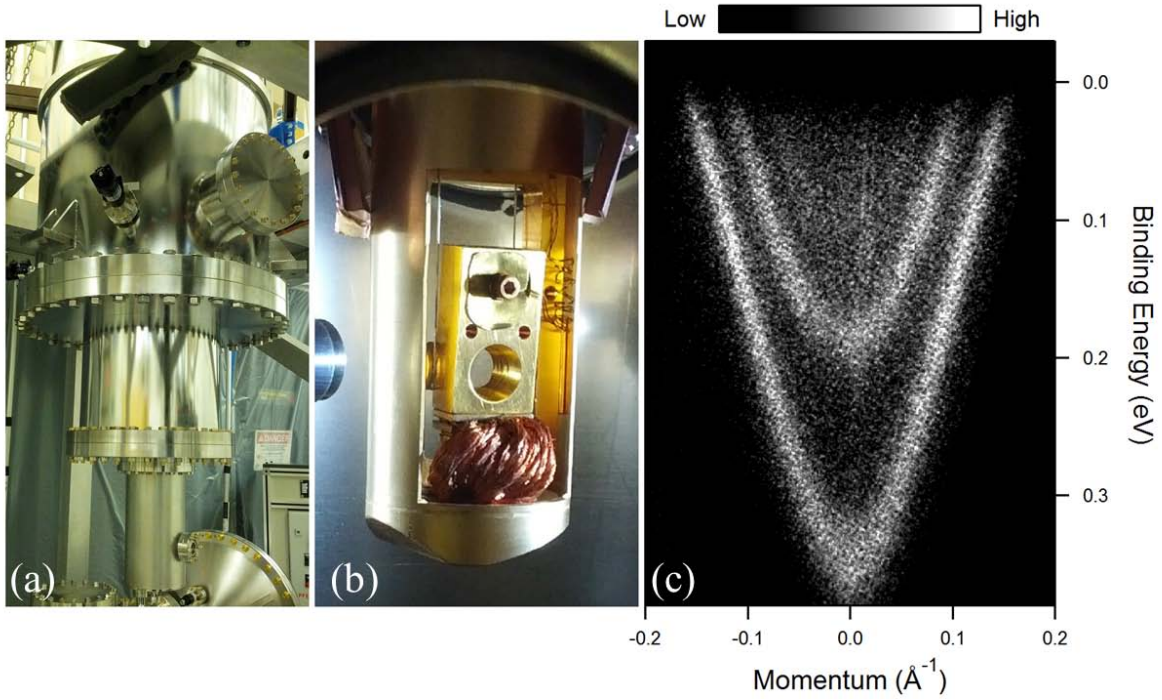

Fig. 1 (a) Picture of the ^{3}He cryostat and (b) sample manipulator. (c) ARPES spectrum of the (001) surface of Bi_2Se_3. Outer conical band is the topological surface state and the inner parabolic band is the projected bulk state.

(b) High-speed measurement of nonlinear optical harmonic generation rotational anisotropy using position sensitive detection

To simultaneously characterize the symmetry properties of the superconducting phase, which is necessary for a detailed topological classification, we are also developing a nonlinear optical probe to measure subtle symmetry changes across the superconducting transition temperature. Nonlinear optical harmonic generation rotational anisotropy (NHG-RA) is a well-established technique for determining the crystallographic, electric and magnetic symmetries of solids[11]. It has been applied across different fields to study a variety of phenomena ranging from lattice reconstruction on semiconductor surfaces and heterostructure interfaces, to charging of metal/electrolyte interfaces, to magnetic ordering in bulk semiconductors and multiferroics. Owing to the need to rotate the crystal with respect to the light scattering plane during such measurements (Fig. 2a), a single rotational anisotropy data set typically requires several minutes to an hour to acquire. This greatly limits the precision of the technique due to ubiquitous low frequency laser noise in the form of power, pointing and/or pulse width fluctuations. In order for NHG-RA to become a high precision technique capable of measuring subtle changes in symmetry, it is imperative that the data collection frequency be significantly increased.

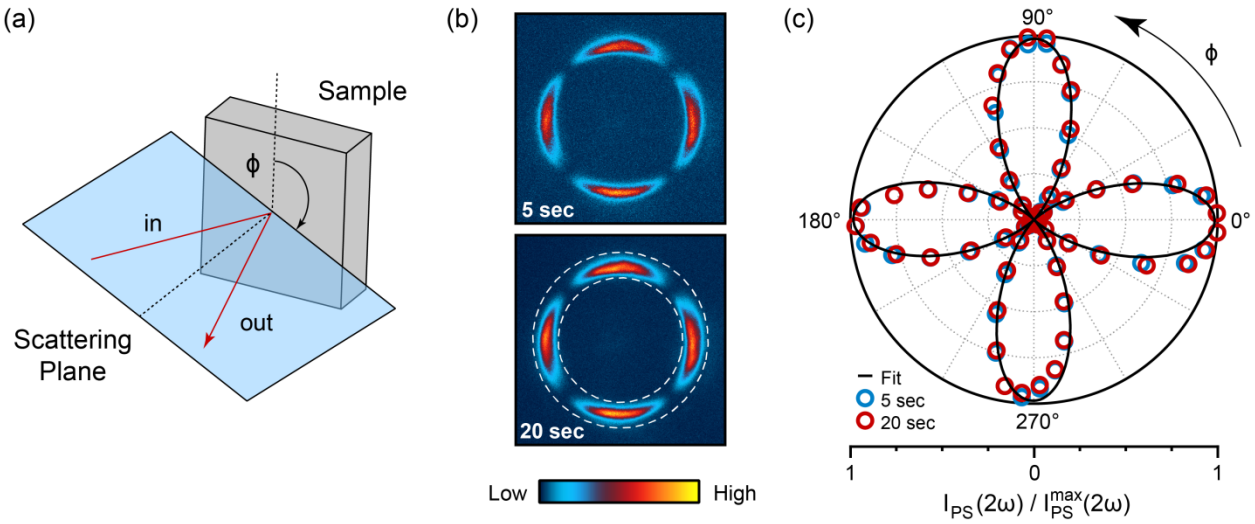

Fig. 2 (a) Schematic layout of our NHG-RA setup. High harmonic light reflected obliquely from a crystal is imaged onto a CCD camera, tracing a circular trajectory on the CCD active area as the scattering plane rotates at several Hz. (b) SHG-RA CCD images of GaAs (001) with 5 and 20 sec exposure times. (c) Polar plot of the SHG intensity obtained by radially integrating the data in panel (b).

We have developed a novel approach to performing NHG-RA measurements using a setup based on position sensitive detection with a CCD camera. Our setup allows rotational anisotropy data to be acquired at least 10^3 to 10^4 times faster than any existing method, which in turn allows unprecedented symmetry refinement precision while easily accommodating low temperature, magnetic or strain field environments. To characterize the performance of our NHG-RA setup, we measured the rotational anisotropy of second harmonic generation (SHG) from the (001) crystal surface of GaAs. Raw CCD images of the SHG-RA data are shown in Fig. 2b for short continuous camera exposure times, which reveals an anisotropic SHG response with four-fold rotational symmetry consistent with theoretical expectations and previous experiments[12]. Rotational anisotropy curves displayed as a polar plot (Fig. 2c), which are obtained by radially integrating the CCD images, reveals a high degree of overlap between data points taken at different exposure times, which demonstrates the high level of precision achievable using our technique and robustness against statistical sources of error such as laser fluctuations.

(iii) Future Plans

ARPES

We will optimize the energy resolution of our ARPES setup with a target of ≤ 1 meV through a careful electrical grounding of the cryostat manipulator. We will then proceed to map the low energy surface electronic structure of candidate 3D topological superconductors including members of the bismuth chalcogenide (e.g. $Cu_xBi_2Se_3$, $T_c \sim 3.8$ K) and ternary half-Heusler (e.g. LuPtBi, $T_c \sim 1$ K) families.

Nonlinear Optical Spectroscopy

We will apply our high-speed NHG-RA technique to study the inversion, mirror and rotational symmetry properties of candidate 3D topological insulators and correlate their spatial dependence in a material with the local surface electronic structure by incorporating NHG-RA into the ARPES measurement chamber. We will also explore the use of NHG-RA as a probe of time-reversal symmetry broken superconducting phases in compounds such as Sr_2RuO_4 ($T_c \sim 1.5$ K) and URu_2Si_2 ($T_c \sim 1.5$ K).

(iv) References

1. Hasan, M. Z. & Kane, C. L. Colloquium : Topological insulators. *Rev. Mod. Phys.* **82,** 3045–3067 (2010).
2. Qi, X.-L. & Zhang, S.-C. Topological insulators and superconductors. *Rev. Mod. Phys.* **83,** 1057–1110 (2011).
3. Nayak, C., Simon, S. H., Stern, A., Freedman, M. & Sarma, S. Das. Non-Abelian anyons and topological quantum computation. *Rev. Mod. Phys.* **80,** 1083–1159 (2008).
4. Mourik, V. *et al.* Signatures of Majorana Fermions in Hybrid Superconductor-Semiconductor Nanowire Devices. *Science* **336,** 1003–1007 (2012).
5. Das, A. *et al.* Zero-bias peaks and splitting in an Al-InAs nanowire topological superconductor as a signature of Majorana fermions. *Nat. Phys.* **8,** 887–895 (2012).
6. Deng, M. T. *et al.* Anomalous Zero-Bias Conductance Peak in a Nb–InSb Nanowire–Nb Hybrid Device. *Nano Lett.* **12,** 6414–6419 (2012).
7. Wang, M.-X. *et al.* The Coexistence of Superconductivity and Topological Order in the Bi_2Se_3 Thin Films. *Science* **336,** 52–55 (2012).
8. Xu, S.-Y. *et al.* Momentum-space imaging of Cooper pairing in a half-Dirac-gas topological superconductor. *Nat. Phys.* **10,** 943–950 (2014).
9. Hao, L. & Lee, T. K. Surface spectral function in the superconducting state of a topological insulator. *Phys. Rev. B* **83,** 134516 (2011).
10. Xia, Y. *et al.* Observation of a large-gap topological-insulator class with a single Dirac cone on the surface. *Nat. Phys.* **5,** 398–402 (2009).
11. Torchinsky, D. H., Chu, H., Qi, T., Cao, G. & Hsieh, D. A low temperature nonlinear optical rotational anisotropy spectrometer for the determination of crystallographic and electronic symmetries. *Rev. Sci. Instrum.* **85,** 083102 (2014).
12. Yamada, C. & Kimura, T. Anisotropy in second-harmonic generation from reconstructed surfaces of GaAs. *Phys. Rev. Lett.* **70,** 2344–2347 (1993).

(v) Publications Acknowledging DOE Support

1. High-speed measurement of rotational anisotropy nonlinear optical harmonic generation using position sensitive detection. J. W. Harter, L. Niu, A. J. Woss & D. Hsieh. In review at *Optics Letters* (2015).

Program Title: Atomic Engineering Oxide Heterostructures: Materials by Design

Principle Investigator: H. Y. Hwang[1,2*]; Co-PIs: Y. Hikita[1], J.-S. Lee[3], and S. Raghu[1,4]

[1]Stanford Institute for Materials & Energy Sciences, SLAC National Accelerator Laboratory, Menlo Park, CA 94025

[2]Department of Applied Physics, Stanford University, Stanford, CA 94305

[3]Stanford Synchrotron Radiation Lightsource, SLAC National Accelerator Laboratory, Menlo Park, CA 94025

[4]Department of Physics, Stanford University, Stanford, CA 94305

****hyhwang@slac.stanford.edu***

Program Scope

A central aim of modern materials research is the control of materials and their interfaces to atomic dimensions. In the search for emergent phenomena and ever-greater functionality in devices, transition metal oxides have enormous potential. They host a vast array of properties, such as orbital ordering, unconventional superconductivity, magnetism, and ferroelectricity, as well as quantum phase transitions and couplings between these states. Our broad objective is to develop the science and technology arising in heterostructures of these novel materials. Using atomic scale growth techniques we explore the synthesis and properties of novel interface phases. Magnetotransport, x-ray, and optical probes are used to determine the static and dynamic electronic and magnetic structure. The experimental efforts are guided and analyzed theoretically, particularly with respect to superconductivity and new states of emergent order. A wide set of tools, ranging from analytic field theory methods to exact computational treatments, are applied towards the understanding and design of heterostructures.

Recent Progress

Understanding and control of the degrees of freedom at the $LaAlO_3/SrTiO_3$ heterointerface: The $LaAlO_3/SrTiO_3$ interface has been a model for emergent phenomena in heterostructures, exhibiting a superconducting 2D electron gas and magnetic instabilities. We have recently focussed on developing the tools to control the density and disorder of the electron gas at this interface. Using polar adsorbates on the surface of the $LaAlO_3$ as well as surface 'charge writing', we can tune the interface electrons over a very wide range of density and mobility, developing a global picture of evolution of the interface electronic structure. At low density and high mobility, we have a semiconductor-like 2DEG, where we observe large amplitude Shubnikov-de Haas oscillations and Hall plateaus reflecting quantum transport in two occupied subbands [16]. At higher density (and lower mobility), increasingly correlated states (superconductivity, ferromagnetism) emerge. While these surface effects are fascinating, they are difficult to precisely control and stabilize. Thus we have developed gate device structures. Most previous gating studies of in $LaAlO_3/SrTiO_3$ were performed using back-gating; as we demonstrated, in this case the electron distribution is compressed to the interface upon depletion, driving a transition to strong disorder. However, by top-gate depletion, we can go to low density with *decreasing* disorder (increasing mobility), accessing an exciting new phase space experimentally [5 & unpublished]. While this contrast between top/back gating is known in semiconductors, we find that it is greatly enhanced by the extremely nonlinear dielectric response in $SrTiO_3$. Combining both gates in one device allows separate tuning of the interface carrier density and disorder over a wide range, which will be used in future work.

New polar discontinuity interfaces with binary oxides: Our motivation for studying $LaAlO_3/SrTiO_3$ was to try and force electronic reconstructions at the interface, using the electrostatic boundary conditions between polar/non-polar perovskites. This was enabled by the ability to control the interface on the atomic scale. While many other perovskite examples have been subsequently demonstrated, it was unclear whether such effects could be induced in heterostructures with binary oxides, since they do not have this internal polar/non-polar degree of freedom. Here we demonstrated this [17] by controlling the interface between (001) $LaAlO_3$ and anatase TiO_2 stabilized on this substrate. We induce a metal-insulator transition in the TiO_2 films by switching the $LaAlO_3$ termination from AlO_2 to LaO. At the same time the optical transparency was unaffected, with mobilities exceeding the best doped TiO_2 films. This opens a general approach to interface reconstructions with the rich family of binary oxides.

Elastoconductivity as a probe of broken point group symmetries: We demonstrated [28] that by measuring the electrical resistance of crystals in the presence of externally applied strains, we can determine whether mirror symmetries are broken. This is possible because the coefficient relating resistance to strain is necessarily a fourth rank tensor, with off diagonal components typically constrained to vanish by point group symmetries. We showed the change of the longitudinal resistivity ρ_{xx}, to shear strains ϵ_{xy} (which we denote the shear-resistivity) can only be non-zero when mirror symmetries are broken. Such measurement may be highly pertinent in the pseudogap phase of cuprate superconductors. This can also be employed in heterostructures, where substrates can enforce a different symmetry than bulk via epitaxy.

Designing interface dipoles: We have developed a new technique for broadly engineering band alignments in oxide heterostructures by designing interface dipoles, which are inserted at the interface. We demonstrate this concept by employing two different approaches in a non-polar $SrRuO_3/Nb:SrTiO_3$ Schottky junction. The first was to insert a *charged* layer at the interface for which the counter charge is supplied by the screening electrons in the metal ($SrRuO_3$) to complete the dipole [26]. This was achieved by inserting a LaO^+ (AlO_2^-) layer via deposition of $LaTiO_3$ ($SrAlO_x$), which shares a common cation with the structure. The second approach was to insert a complete *dipole* layer (ultrathin $LaAlO_3$) which naturally accommodates the $(AlO_2)^-/(LaO)^+$ dipole stacks on the TiO_2-terminated $Nb:SrTiO_3$ substrate [25]. In both cases, the variation in the potential (as probed by electrical, x-ray, and optical measurements) was extremely large, exceeding 1 eV. This is a highly promising approach for tuning band alignments in a wide variety of oxide interface structures and devices.

Future Plans

Towards our long-term agenda to create and control emergent phenomena and functionality in oxide heterostructures, our specific aims for the proposal period FY2016-2018 address the following research topics:

- Investigation of the evolution of long-range crystalline order in two dimensions in free-standing oxide ultrathin films.
- The phase diagram of superconductivity, metallic and insulating behavior in two-dimensional electronic systems.
- Manipulation and interrogation of materials and order parameters in one dimension, using ordered atomic-scale steps in oxide heterostructures.
- Superconducting domes in the vicinity of quantum criticality and at low electron density.
- Development of new synthetic approaches to Ruddlesden-Popper phases.

Publications

1. R. Mahajan, D. Ramirez, S. Kachru, and S. Raghu, "Quantum Critical Metals in d=3+1 Dimensions," *Physical Review B* **88**, 115116 (2013).
2. A. Maharaj, R. Thomale, and S. Raghu, "Particle-Hole Condensates of Higher Angular Momentum in Hexagonal Systems," *Physical Review B* **88**, 205121 (2013).
3. A. L. Fitzpatrick, S. Kachru, J. Kaplan, and S. Raghu, "Non-Fermi-Liquid Fixed Point in a Wilsonian Theory of Quantum Critical Metals," *Physical Review B* **88**, 125116 (2013).
4. H. Inoue, M. Kim, C. Bell, Y. Hikita, S. Raghu, and H. Y. Hwang, "Tunable Coupling of Two-Dimensional Superconductors in Bilayer $SrTiO_3$ Heterostructures," *Physical Review B (Rapid Communications)* **88**, 241104 (2013).
5. M. Hosoda, Y. Hikita, H. Y. Hwang, and C. Bell, "Transistor Operation and Mobility Enhancement in Top-Gated $LaAlO_3/SrTiO_3$ Heterostructures," *Applied Physics Letters* **103**, 103507 (2013).
6. Y. W. Xie and H. Y. Hwang, "Tuning the Electrons at the $LaAlO_3/SrTiO_3$ Interface: From Growth to Beyond Growth," *Chinese Physics B* **22**, 127301 (2013).
7. H. Murakawa, M. S. Bahramy, M. Tokunaga, Y. Kohama, C. Bell, Y. Kaneko, N. Nagaosa, H. Y. Hwang, and Y. Tokura, "Detection of Berry's Phase in a Bulk Rashba Semiconductor," *Science* **342**, 1490 (2013).
8. B. Kalisky, E. M. Spanton, H. Noad, J. R. Kirtley, K. C. Nowack, C. Bell, H. K. Sato, Y. W. Xie, Y. Hikita, C. Woltmann, G. Pfanzelt, R. Jany, H. Y. Hwang, J. Mannhart, and K. A. Moler, "Locally Enhanced Conductivity Due to the Tetragonal Domain Structure in $LaAlO_3/SrTiO_3$ Heterointerfaces," *Nature Materials* **12**, 1091 (2013).
9. S. Chakraverty, T. Matsuda, N. Ogawa, H. Wadati, E. Ikenaga, M. Kawasaki, Y. Tokura, and H. Y. Hwang, "$BaFeO_3$ Cubic Single Crystalline Thin Film: A Ferromagnetic Insulator," *Applied Physics Letters* **103**, 142416 (2013).
10. S. Bordacs, J. G. Checkelsky, H. Murakawa, H. Y. Hwang, and Y. Tokura, "Landau Level Spectroscopy of Dirac Electrons in a Polar Semiconductor with Giant Rashba Spin Splitting," *Physical Review Letters* **111**, 166403 (2013).
11. S. Chakraverty, T. Matsuda, H. Wadati, J. Okamoto, Y. Yamasaki, H. Nakao, Y. Murakami, S. Ishiwata, M. Kawasaki, Y. Taguchi, Y. Tokura, and H. Y. Hwang, "Multiple Helimagnetic Phases and Topological Hall Effect in Epitaxial Thin Films of Pristine and Co-Doped $SrFeO_3$," *Physical Review B (Rapid Communications)* **88**, 220405 (2013).
12. J. A. Mundy, Y. Hikita, T. Hidaka, T. Yajima, T. Higuchi, H. Y. Hwang, D. A. Muller, and L. F. Kourkoutis, "Visualizing the Interfacial Evolution from Charge Compensation to Metallic Screening across the Manganite Metal-Insulator Transition," *Nature Communications* **5**, 3464 (2014).
13. A. L. Fitzpatrick, S. Kachru, J. Kaplan, and S. Raghu, "Non-Fermi Liquid Behavior of Large-N_B Quantum Critical Metals," *Physical Review B* **89**, 165114 (2014).
14. S. Lederer, W. Huang, E. Taylor, S. Raghu, and C. Kallin, "Suppression of Spontaneous Currents in Sr_2RuO_4 by Surface Disorder," *Physical Review B* **90**, 134521 (2014).
15. H. Watanabe, S. Parameswaran, S. Raghu, and A. Vishwanath, "Anomalous Fermi-Liquid Phase in Metallic Skyrmion Crystals," *Physical Review B* **90**, 045145 (2014).
16. Y. W. Xie, C. Bell, M. Kim, H. Inoue, Y. Hikita, and H. Y. Hwang, "Quantum Longitudinal and Hall Transport at the $LaAlO_3/SrTiO_3$ Interface at Low Electron Densities," *Solid State Communications* **197**, 25 (2014).
17. M. Minohara, T. Tachikawa, Y. Nakanishi, Y. Hikita, L. Fitting Kourkoutis, J.-S. Lee, C.-C. Kao, M. Yoshita, H. Akiyama, C. Bell, and H. Y. Hwang, "Atomically Engineered Metal-Insulator Transition at the $TiO_2/LaAlO_3$ Heterointerface," *Nano Letters* **14**, 6743 (2014).
18. A. V. Maharaj, P. Hosur, and S. Raghu, "Crisscrossed Stripe Order from Interlayer

Tunneling in Hole-doped Cuprates," *Physical Review B* **90**, 125108 (2014).
19. Y. Yamada, H. K. Sato, Y. Hikita, H. Y. Hwang, and Y. Kanemitsu, "Photocarrier Recombination and Localization Dynamics of $LaAlO_3/SrTiO_3$ Heterostructures," *Proceedings of the SPIE* **8987**, 898710 (2014).
20. Y. Takahashi, S. Chakraverty, M. Kawasaki, H. Y. Hwang, and Y. Tokura, "In-plane Terahertz Response of Thin Film Sr_2RuO_4," *Physical Review B* **89**, 165116 (2014).
21. Y. Yamada, H. K. Sato, Y. Hikita, H. Y. Hwang, and Y. Kanemitsu, "Spatial Density Profile of Electrons Near the $LaAlO_3/SrTiO_3$ Heterointerface Revealed by Time-Resolved Photoluminescence Spectroscopy," *Applied Physics Letters* **104**, 151907 (2014).
22. A. G. Swartz, S. Harashima, Y. W. Xie, D. Lu, B. J. Kim, C. Bell, Y. Hikita, and H. Y. Hwang, "Spin-Dependent Transport Across $Co/LaAlO_3/SrTiO_3$ Heterojunctions," *Applied Physics Letters* **105**, 032406 (2014).
23. Y. Lei, Y. Z. Chen, Y. W. Xie, S. H. Wang, Y. Li, J. Wang, B. G. Shen, N. Pryds, H. Y. Hwang, and J. R. Sun, "Visible-Light-Enhanced Gating Effect at the $LaAlO_3/SrTiO_3$ Interface," *Nature Communications* **5**, 5554 (2014).
24. X. Liu, J.-H. Park, J.-H. Kang, H. T. Yuan, Y. Cui, H. Y. Hwang, and Mark L. Brongersma, "Quantification and Impact of Nonparabolicity of the Conduction Band of Indium Tin Oxide on its Plasmonic Properties," *Applied Physics Letters* **105**, 181117 (2014).
25. T. Yajima, M. Minohara, C. Bell, H. Kumigashira, M. Oshima, H. Y. Hwang, and Y. Hikita, "Enhanced Electrical Transparency by Ultrathin $LaAlO_3$ Insertion at Oxide Metal/Semiconductor Heterointerfaces," *Nano Letters* **15**, 1622 (2015).
26. T. Yajima, Y. Hikita, M. Minohara, C. Bell, J. A. Mundy, L. F. Kourkoutis, D. A. Muller, H. Kumigashira, M. Oshima, and H. Y. Hwang, "Controlling Band Alignments by Artificial Interface Dipoles at Perovskite Heterointerfaces," *Nature Communications* **6**, 6759 (2015).
27. A. L. Fitzpatrick, S. Kachru, J. Kaplan, S. Raghu, G. Torroba, and H. Wang "Enhanced Pairing of Quantum Critical Metals Near d=3+1," *Physical Review B* **92**, 045118 (2015).
28. P. Hlobil, A. V. Maharaj, P. Hosur, M. C. Shapiro, I. R. Fisher, and S. Raghu, "Elastoconductivity as a Probe of Broken Mirror Symmetries," *Physical Review B* **92**, 035148 (2015).
29. Z. Erlich, Y. Frenkel, J. Drori, Y. Shperber, C. Bell, H. K. Sato, M. Hosoda, Y. W. Xie, Y. Hikita, H. Y. Hwang, and B. Kalisky, "Optical Study of Tetragonal Domains in $LaAlO_3/SrTiO_3$," *Journal of Superconductivity and Novel Magnetism* **28**, 1017 (2015).
30. T. Tsuyama, T. Matsuda, S. Chakraverty, J. Okamoto, E. Ikenaga, A. Tanaka, T. Mizokawa, H. Y. Hwang, Y. Tokura, and H. Wadati, "X-Ray Spectroscopic Study of $BaFeO_3$ Thin Films: An Fe^{4+} Ferromagnetic Insulator," *Physical Review B* **91**, 115101 (2015).
31. S. C. Riggs, M. C. Shapiro, A. V. Maharaj, S. Raghu, E. D. Bauer, R. E. Baumbach, P. Giraldo-Gallo, M. Wartenbe, and I. R. Fisher, "Evidence for a Nematic Component to the Hidden-Order Parameter in URu_2Si_2 from Differential Elastoresistance Measurements," *Nature Communications* **6**, 6425 (2015).
32. P. Munkhbaatar, Z. Marton, B. Tsermaa, W. S. Choi, S. S. A. Seo, J. S. Kim, N. Nakagawa, H. Y. Hwang, H. N. Lee, and K. Myung-Whun, "Room Temperature Optical Anisotropy of a $LaMnO_3$ Thin-film Induced by Ultra-short Pulse Laser," *Applied Physics Letters* **106**, 092907 (2015).
33. K. O. Ruotsalainen, C. J. Sahle, T. Ritschel, J. Geck, M. Hosoda, C. Bell, Y. Hikita, H. Y. Hwang, T. T. Fister, R. A. Gordon, K. Hamalainen, M. Hakala, and S. Huotari, "Inelastic X-ray Scattering in Heterostructures: Electronic Excitations in $LaAlO_3/SrTiO_3$," *Journal of Physics: Condensed Matter* **27**, 335501 (2015).

Program Title: **Bose-Einstein Condensation of Magnons**
Principle Investigator: J. B. Ketterson
Mailing Address: Department of Physics
Northwestern University, Evanston IL, 60208,
E-mail: j-ketterson@northwestern.edu

Program Scope

The major objective of the proposed program is to confirm and then extend astonishing reports that Bose-Einstein Condensation (BEC) can occur *at room temperature* in a dynamically pumped magnon gas, specifically the ferrimagnet yttrium iron garnet (YIG).[1,2] These reports have stimulated much theoretical activity,[3-9] although we are not aware of work from independent experimental groups.[10] If BEC is confirmed, it will not only extend the range of systems in which the phenomenon occurs, but could lead to new classes of magnetic devices since: 1) applications far easier to implement because the phenomena occurs at room-temperature and 2) engineered structures, a focus of the proposed work, allowing the controlled coupling to and among condensates can follow.

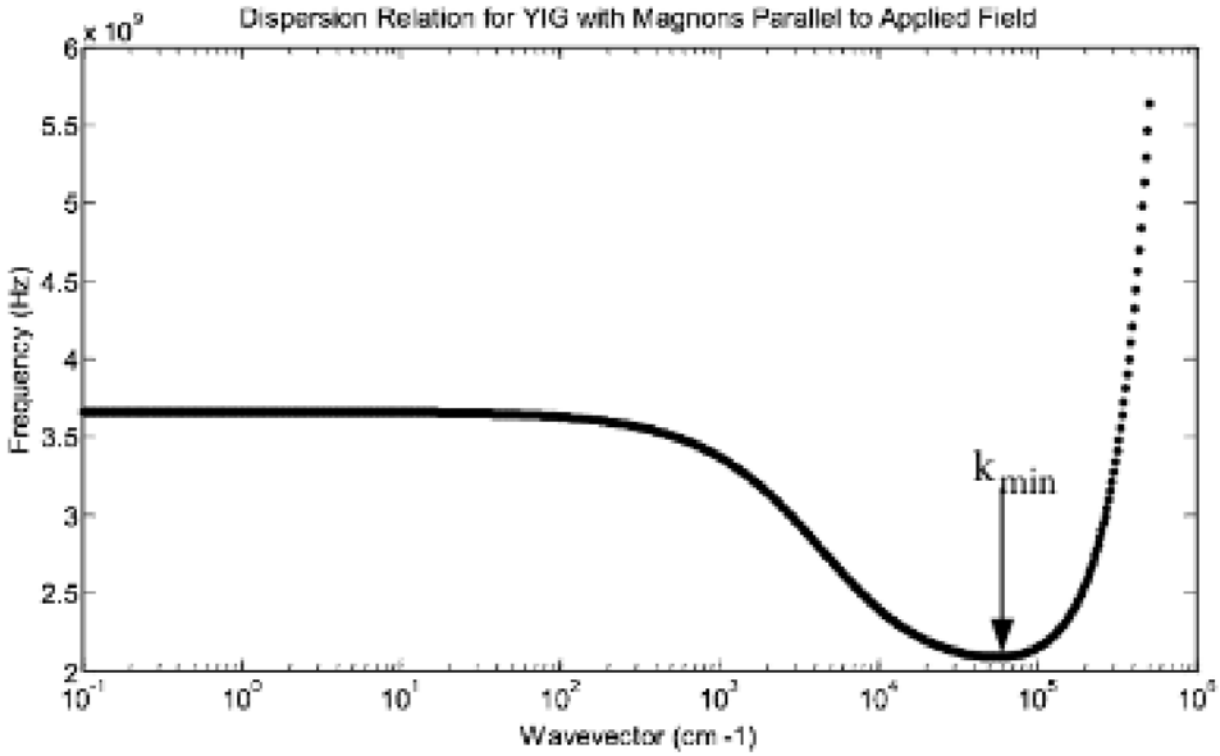

Figure 1. The dispersion of the lowest lying backward volume mode in YIG including the effects of exchange. Note the presence of a minimum at a frequency $f(k_{min})$.

In addition to the excitation and detection of the condensate itself we will attempt to observe collective excitations of the condensate. Here we expect to encounter low frequency modes involving oscillations of the overall or relative phases of the (two) condensates as well as two possible higher frequency "Higgs like" modes involving the amplitudes of the condensates.

Recent Progress

The excitations that form the condensate lie on the lowest lying branch of the spatially quantized backward volume modes. This class of modes has negative dispersion and was first studied by Damon and Eshbach;[11] when the exchange is added this produces a minimum in wave-vector space at some field magnetic dependent k_{min} in a direction lying along the field, as shown in figure 1. Note there is also a minimum $-k_{min}$; one of the unique properties of the system is the possible presence of two condensates and collective modes that involve oscillations of various combinations of their amplitudes and phases, as noted above.

The Domokritov group employed a parametric down conversion process to prepare the initial magnon population which then thermalizes, subsequently forming condensates at $\pm k_{min}$. Our approach will be to pattern a multi-element antenna which allows direct coupling to magnons of a specific wavevector; such an antenna is shown schematically in figure 2. Once patterned the wave vector is fixed by the element spacing at some value k_0, and the spacing would be chosen to correspond to $f(k_{min})$. (Through a combination of the magnetic field and the frequency some flexibility is then available to match the chosen electrode spacing such that $k_0 = k_{min}$.) The antenna should also couple efficiently at the third spatial harmonic, $3k_0$, and we will initially experiment with pumping at a frequency of $f(3k_0)$. Following pumping and thermalization a coherent signal at $f(k_{min})$ should appear if a condensate forms.

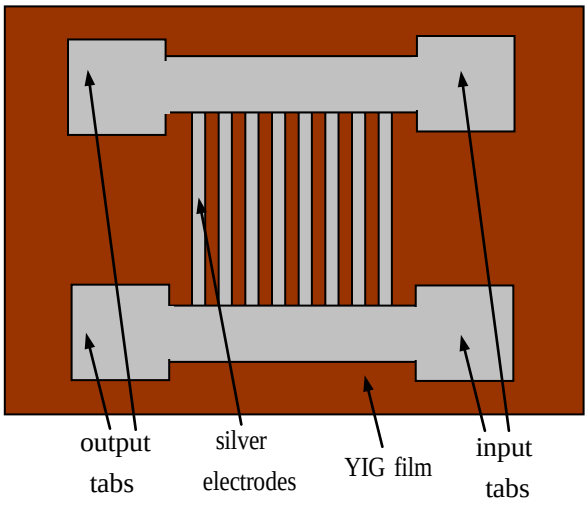

Figure 2. A schematic representation of a patterned silver antenna consisting of an array of sub micron strips on a YIG film. A microwave current (applied via wire-bonds not shown) then produces periodic sub micron scale magnetic fields. For clarity, the device size depicted here is greatly exaggerated relative to the size of the substrate on which it is patterned. The inclusion of both input and output tabs allows the device to function in a transmission mode thereby affording better isolation between transmitter and receiver. Pairs of such devices permit the generation and *remote detection* of spin waves.

Future Plans

Apart from e-beam patterning of the antennas, an early task will be to perform electromagnetic modeling of the coupling efficiency of the antennas.

References

1. *Bose–Einstein condensation of quasi-equilibrium magnons at room temperature under pumping,* S. O. Demokritov, V. E. Demidov, O. Dzyapko, G. A. Melkov, A. A. Serga, B. Hillebrands, and A. N. Slavin, Nature Letters 443, 430 (2006).

2. *Bose-Einstein condensation of spin wave quanta at room temperature,* O. Dzyapko, V. E. Demidov, G. A. Melkov, and S. O. Demokritov, Philosophical Transactions Royal Society A: Mathematical Physical and Engineering Sciences 369, 3575 (2011).

3. *On the theory of spatially inhomogeneous Bose-Einstein condensation of magnons in yttrium iron garnet,* A. I. Bugrij and V. M. Loktev, Low Temperature Physics, 39, 1037 (2013)

4. *Kinetics of pulse-induced magnon Bose-Einstein condensate,* Sergey N. Andrianov, Vladimir V. Bochkarev, and Sergey Moiseev, Eur. Phys. J. B 87, 128 (2014).

5. *Dynamic phase diagram of dc-pumped magnon condensates,* Scott A. Bender, Rembert A. Duine, Arne Brataas, and Yaroslav Tserkovnyak Physical Review B 90, 094409 (2014)

6. *Superfluid Spin Transport Through Easy-Plane Ferromagnetic Insulators,* So Takei and Yaroslav Tserkovnyak, Phys. Rev. Letters 112, 227201 (2014).

7. *Strongly Coupled Magnons and Cavity Microwave Photons,* Xufeng Zhang, Chang-Ling Zou, Liang Jiang, and Hong X. Tang, Phys. Rev. Lett. 113, 156401 (2014).

8. *Magnon qubit and quantum computing on magnon Bose-Einstein condensates,* S. N. Andrianov and S. A. Moiseev, Phys. Rev. A 90, 042303 (2014).

9. *Bose-Einstein condensation in quantum magnets,* Vivien Zapf, Marcelo Jaime, and C. D. Batista Rev. Mod. Phys. 86, (2014).

10. Work from a historically related group has appeared: Bose–Einstein condensation in an ultra-hot gas of pumped magnons, A. A. Serga, V. S. Tiberkevich, C. W. Sandweg, V. I. Vasyuchka, D. A. Bozhko, A.V. Chumak, T. Neumann, B. Obry, G. A. Melkov, A. N. Slavin and B. Hillebrands, Nature Communications 5, 3452 (2014).

11. *Magnetostatic modes in a ferromagnetic slab,* R. W. Daman and J. R. Eshbach, J. Chem. Phys. Sol. **19**, 308 (1961).

Publications:

There are no publications as the work has just started.

Project Title:
DE-SC0012260: Correlated Electrons in Graphene at the Quantum Limit

Principal Investigator: **Philip Kim**
Institution: Department of Physics, Harvard University
Email: pkim@physics.harvard.edu

Project Scope

Interacting systems with internal symmetries will tend to break those symmetries in order to lower their energy. Quantum Hall ferromagnetisms (QHFM) and fractional quantum Hall effect (FQHE) are two good examples of such correlated electronic states where a quantum description of the collective motion of many electrons should be carefully considered. In this project, we will perform our experiment mostly on bilayer graphene (BLG), two monoatomic graphene layers stacked in a half atomic period shifted to each other. We will explore the electron interaction driven spontaneous broken symmetry in the BLG in the extremely high magnetic fields and very low temperatures, where the quantum effect becomes maximized. We particularly focus on BLG, because its multi-component spin is fully experimentally controllable through electric and magnetic fields. In particular, we plan to investigate novel physical phenomena in graphene, stemming from correlated electron physics. Our major proposed tasks are: (i) engineering BLG heterostructures for high mobility and high functionality; (ii) investigating phase transitions of BLG's multi-component spin in integer and FQH states; (iii) exploring the nature of spin/valley-polarized quantum Hall edge states employing quantum point contacts and quantum Hall interferometry; (iv) studying competition between strongly correlated QHF and FQH effects in engineered and adjustable graphene superlattices; (v) realization of symmetry-protected 1-dimensional topological propagation modes in bilayer graphene; (vi) injection of cooper pairs in graphene quantum Hall edge states and investigation of the competition between proximity-induced superconducting states and Landau gap formation.

Recent Progress

Tunable Fractional Quantum Hall Phases in Bilayer Graphene: Symmetry-breaking in a quantum system often leads to complex emergent behavior. In bilayer graphene (BLG), an electric field applied perpendicular to the basal plane breaks the inversion symmetry of the lattice, opening a band gap at the charge neutrality point. In a quantizing magnetic field, electron interactions can cause spontaneous symmetry-breaking within the spin and valley degrees of freedom, resulting in quantum Hall effect (QHE) states with complex order. In this period of work, we report fractional QHE states in BLG that show phase transitions that can be tuned by a transverse electric field [1]. This result provides a model platform with which to study the role of symmetry-breaking in emergent states with topological order. As shown in Fig. 1, we found that the electric-field–driven phase transitions observed in BLG's FQHE indicate that ordering in the SU(4) degeneracy space is critical to the stability of the FQHE. In particular, quantitative agreement between transitions in FQHE states and those in parent integer QHE states suggests that generally, the composite fermions in BLG inherit the SU(4) polarization of the integer state and couple to symmetry-breaking terms with the same strength. However, an apparent disagreement in the transition structure at $\nu = 5/3$ and $\nu = 2$ indicates that there may be subtle differences in the ground-state ordering for the integer and fractional quantum Hall states.

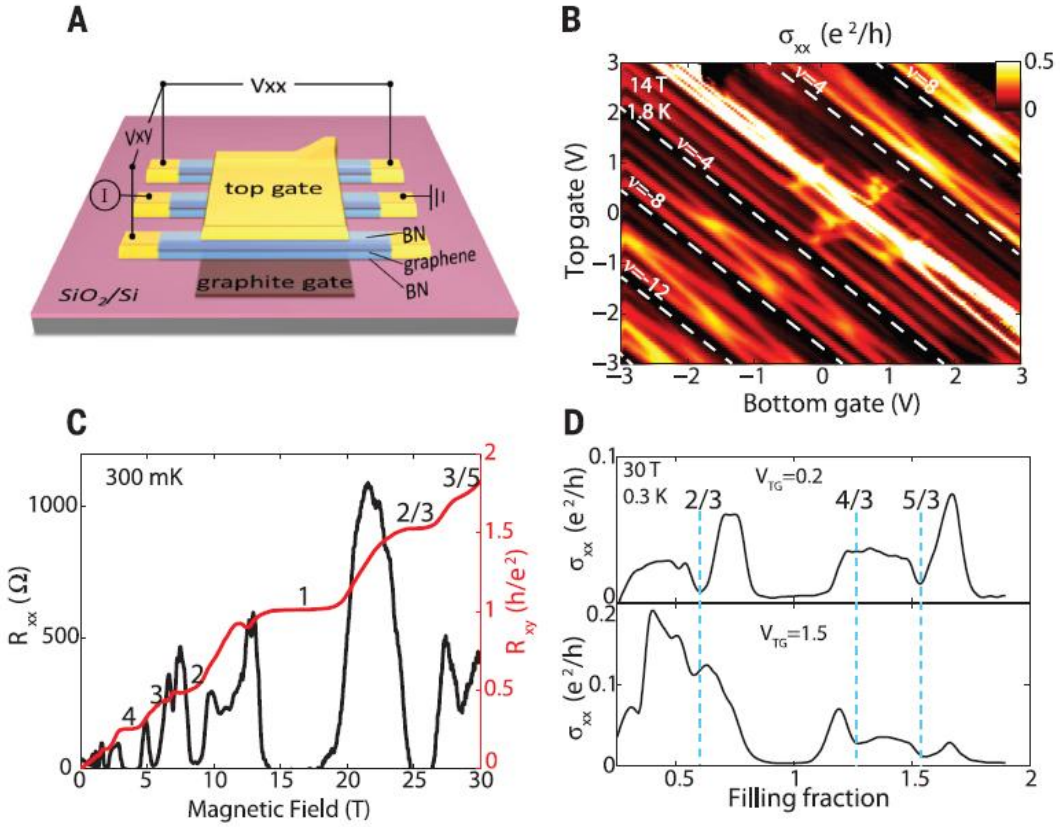

FIG. 1 (a) Diagram of the dual-gate device architecture. (B) magneto-conductivity σ_{xx} as a function of top and bottom gate voltages at $B = 14$ T and $T = 1.8$ K. All broken-symmetry integer states are visible (multiple of 4 filling factors are marked with white dashed lines). (C) R_{xx} and R_{xy} as a function of magnetic field at a fixed carrier density ($n = 4.2 \times 10^{11}$ cm^{-2}). A fully developed $\nu = 2/3$ state appears at ~25 T, with a 3/5 state developing at higher field. (D) σ_{xx} versus filling fraction at 30 T and 300 mK acquired by sweeping the bottom gate for two different top gate voltages.

Specular Interband Andreev Reflection in Graphene: Electrons incident from a normal metal onto a superconductor are reflected back as holes – a process called Andreev reflection. In a normal metal where the Fermi energy is much larger than a typical superconducting gap, the reflected hole retraces the path taken by the incident electron. In graphene with ultra-low disorder, however, the Fermi energy can be tuned to be smaller than the superconducting gap. In this unusual limit, the holes are expected to be reflected specularly at the superconductor-graphene interface due to the onset of interband Andreev processes, where the effective mass of the reflected holes change sign. In this period time, we present measurements of gate modulated Andreev reflections across the low disorder van der Waals interface formed between graphene and the superconducting $NbSe_2$ [2]. As shown in Fig. 2, we find that the conductance across the graphene-superconductor interface exhibits a characteristic suppression when the Fermi energy is tuned to values smaller than the superconducting gap, a hallmark for the transition between intraband retro-and interband specular- Andreev reflections. Our observation of gate tunable transitions between retro intraband and specular interband Andreev reflections opens a new route for future experiments that could employ the gate control of the reflection angles, which can be

continently and independently altered with gate and bias voltages. Most importantly our finding help to draw a general picture of the exact physical processes underlying Andreev reflection.

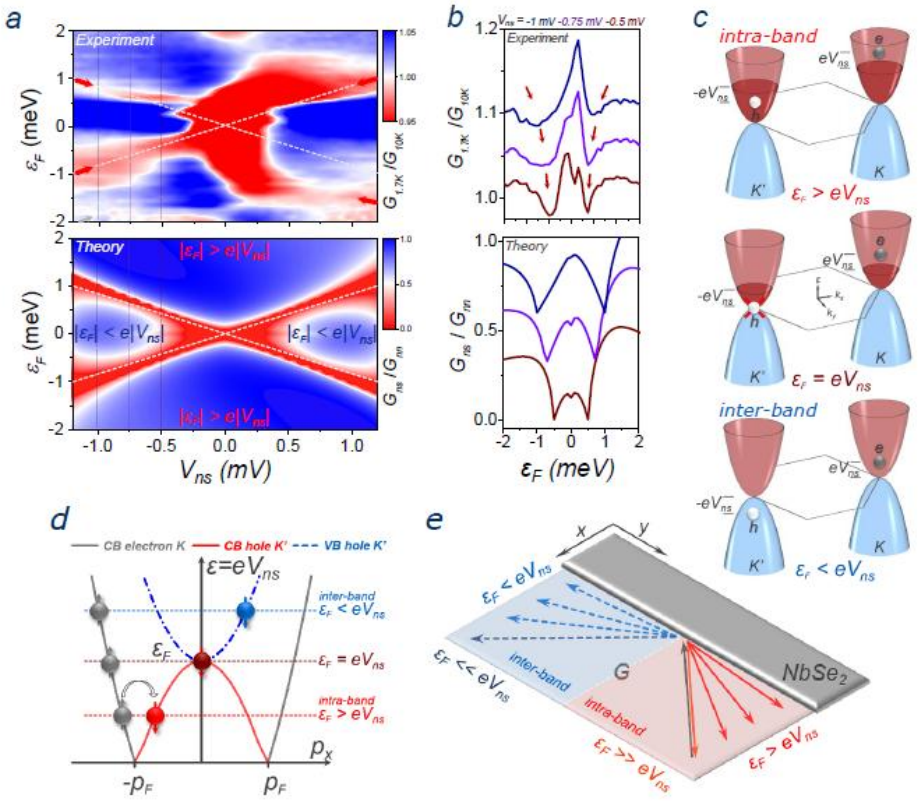

FIG. 2 (a) Experimental and theoretical normalized differential conductance presented in color maps as a function of bias voltage V_{ns} and Fermi energy E_F tuned by gate voltage. A continuous region of lower conductance (red) that is defined for intra and inter band Andreev reflection (AR) transition regime (white dashed lines) subdivides the map into four disconnected regions of comparatively high conductances (blue). (b) Experimental and theoretical normalized differential conductance line-traces demonstrate the evolution of the conductance dips (red arrows) with varying V_{ns}. (c) Schematics of the AR process for BLG at the cross-over from intraband to interband ARs. With decreasing E_F at a fixed V_{ns} the AR hole moves from the CB to the VB. The cross-over point where the hole is re ected onto the CNP is defined by $E_F = eV_{ns}$. (d) Excitation spectrum for a quasiparticle. With an increasing excitation voltage V_{ns}, the momentum p_x of the reflected hole continuously increases from negative to positive values. (e) Schematics of the reflection angles of AR holes in the various energy limits. Starting from perfect intraband retro-reflections in the high E_F limit.

Development of High Frequency and Wide Bandwidth Johnson Noise Thermometry:
Understanding thermal transport in these complex devices requires new thermometry techniques capable of dealing with the challenges unique to nanoscale systems. Diminishing system sizes call for measurements to be non-invasive to avoid thermal agitation of minute heat capacities. As weak electron-phonon coupling can result in different electronic and lattice temperatures, separate probes must be used to measure each temperature independently. In this period of time, we develop a high frequency, wide bandwidth radiometer operating at room temperature, which augments the traditional technique of Johnson noise thermometry for nanoscale thermal transports studies. Employing low noise amplifiers and an analog multiplier operating at 2 GHz, auto- and cross-correlated Johnson noise measurements are performed in the temperature range

of 3 to 300 K, achieving a sensitivity of 5.5mK (110 ppm) in 1 sec of integration time. This setup allows us to measure the thermal conductance of a boron nitride encapsulated monolayer graphene device over a wide temperature range [3]. Our data show a high power law (T^4) deviation from the Wiedemann-Franz (WF) law above T~100 K. Further studies are being carried out to demonstrate to clarify the violation of WF law at the charge neutrality of graphene due to hydrodynamic transport with strongly interacting thermally populated electrons and holes.

Future Plan

Building on the successful progress described in the previous section, we plan to focus our interest on *investigation of the role of electron interactions in graphene* as described below:

SU(4) Spin Control of quantum Hall ferromagnet in bilayer: We now plan to explore complete phase diagram of SU(4) quantum Hall ferromagnet utilizing both electric field and in plan-magnetic fields. Devices with top and bottom gate combined with tilting magnetic fields allow us to tune topological phase transitions in multicomponent integer and fractional quantum Hall states, exploring the nature of spin/valley polarized quantum Hall edge states.

Combining quantum Hall effect in graphene with superconducting electrodes: We have developed device fabrication process to allow us to contact quantum Hall states with superconducting electrodes. Employing this device geometry, we plan to injection of cooper pairs in graphene quantum Hall edge states and investigate the Andreev conversion process across the superconducting electrodes.

Investigation of relativistic hydrodynamic transport at the charge neutrality: Utilizing the sensitive Johnson noise thermometry developed in the previous year, we now plan to investigate quasi relativistic hydrodynamic transport phenomena in the non-degenerate electron/hole gases near the charge neutrality of graphene.

Publications acknowledged the current DOE grant

[1] P. Maher, L. Wang, Y. Gao, C. Forsythe, T. Taniguchi, K. Watanabe, D. Abanin, Z. Papic, P. Cadden-Zimansky, J. Hone, P. Kim, Cory R. Dean, "Tunable Fractional Quantum Hall Phases in Bilayer Graphene," Science 345, 61-64 (2014)

[2] D. K. Efetov, L. Wang, C. Handschin, K. B. Efetov, J. Shuang, R. Cava, T. Taniguchi, K. Watanabe, J. Hone, C. R. Dean, and P. Kim, "Specular Interband Andreev Reflections in Graphene," *submitted to Nature Physics*

[3] J. Crossno, X. Liu, T. Ohki, P. Kim, and K. C. Fong, "Development of high frequency and wide bandwidth Johnson noise thermometry," Appl. Phys. Lett. 106, 023121 (2015)

Project Title: Spectroscopy of Degenerate One-Dimensional Electrons in Carbon Nanotubes

Principal Investigator: Junichiro Kono
Mailing Address: Department of Electrical and Computer Engineering, Rice University, Houston, Texas 77005, U.S.A.
Email Address: kono@rice.edu

Program Scope

The goal of this research program is to understand the fundamental properties of degenerate one-dimensional (1-D) electrons in single-wall carbon nanotubes (SWCNTs). SWCNTs provide an ideal 1-D environment in which to study many-body physics. Semiconducting SWCNTs exhibit rich optical spectra dominated by extremely stable 1-D excitons, whereas metallic SWCNTs contain massless 1-D carriers with ultralong mean-free paths. Despite the large number of electrical, optical, and magnetic studies of SWCNTs during the last two decades, most of the predicted exotic properties of interacting 1-D electrons have yet to be observed, and some of the reported experimental results remain highly controversial.

Here, using an arsenal of spectroscopic methods from the terahertz to the visible spectral range, including ultrafast optical spectroscopy and ultrahigh magnetic fields, we aim to probe correlations and many-body effects in this prototypical 1-D nanostructure. These studies can provide a wealth of new insights into the nature of strongly correlated carriers in the ultimate 1-D limit that will lead to novel nanodevice concepts and implementations.

Specifically, the primary objective of this research program is to address the following key questions and issues, which are of critical importance in many-body physics:

- 'Spinons' and 'holons' in high magnetic field: What will be the signatures of spin-charge separation in electron spin resonance? Will a magnetic field split spinon and holon peaks differently, as predicted?
- Optical conductivity of Tomonaga-Luttinger liquids: How will many-body effects modify the frequency, temperature, and magnetic field dependences of dynamic conductivity of metallic SWCNTs? Will there be any scaling laws indicative of quantum criticality?
- Light emission from high-density 1-D excitons: How will excitons in SWCNTs behave at quantum degenerate densities? How will the bosonic characters of 1-D excitons manifest themselves in emission spectra? Will they cooperate to emit superradiantly?

The overall theme of this research is based on one of the emergent concepts in condensed matter physics today. Namely, dynamical, non-equilibrium, and nonlinear aspects of many-body effects in quantum-confined systems have been poorly addressed to date despite the fact that one can expect a wide range of extraordinary phenomena that are not expected in bulk solids or atoms/molecules. In addition, they will undoubtedly become important when one wants to operate any electrical or photonic nanodevices. Particular emphasis is placed on the dynamical 1-D phenomena in the terahertz, infrared, and optical frequency ranges, which is a widely open research field that deserves more exploration both from basic and applied points of view. Because they are direct band gap materials, SWCNTs are one of the leading candidates to unify electronic and optical functions in nanoscale circuits and elucidate how electron correlations can affect and control finite-frequency phenomena in 1-D systems.

Recent Progress

Although the one-dimensional character of electrons, holes, and excitons in *individual* SWCNTs has stimulated much interest [1], its macroscopic manifestation has been difficult to observe. We have developed a simple but robust method for preparing large-area films of aligned SWCNTs by utilizing spontaneous alignment that occurs during vacuum filtration. The produced films (see, e.g., Fig. 1) are globally aligned and are highly packed, and the film thickness is controllable in a wide range, from a few nm to ~100 nm. This method is applicable to any SWCNTs suspended in aqueous solution. By combining this method with recently developed chirality- and type-sorting techniques, we were able to fabricate aligned and chirality-enriched SWCNT films. Semiconductor films exhibited polarized photoluminescence, polarization-dependent photocurrent, and strong conductivity anisotropy.

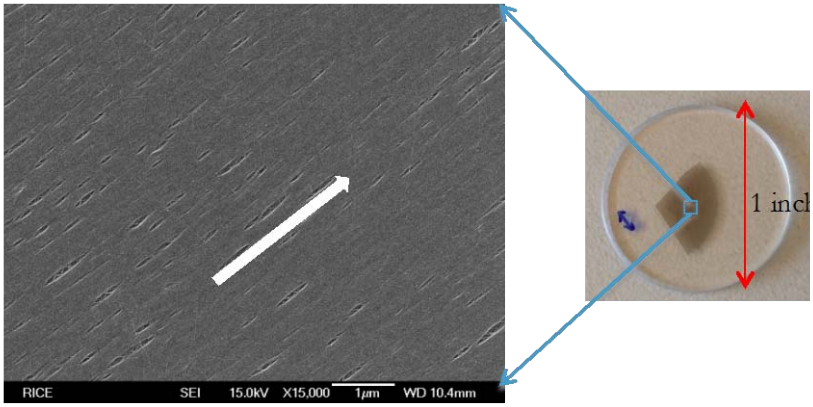

Figure 1: Large-area thin film of highly aligned single-wall carbon nanotubes.

Figure 2 shows polarization-dependent Raman spectra taken for an aligned SWCNT film with an excitation wavelength of 514 nm. We analyzed the data using standard equations for the angular dependence of SWCNT Raman spectra to determine the value of the nematic order parameter, *S*, to be 0.96 for this particular film. We also measured polarization-dependent transmission spectra of this film in a wide spectral range, from the terahertz to the visible. There was essentially no detectable attenuation within experimental errors for the perpendicular polarization in the entire range whereas there was a prominent, broad peak at ~0.02 eV in the parallel case due to the plasmon resonance, similar to our previous studies [1-3]. In the near-infrared and visible ranges, we clearly observed the first two interband transitions for semiconducting nanotubes and the first interband transition in metallic nanotubes in the parallel polarization case. These peaks were absent for the perpendicular polarization, for which we instead observed a broad absorption feature in an intermediate energy region, which we attributed to the cross-polarized E_{12}/E_{21} peak. Such a transition, theoretically predicted more than 20 years ago, has been previously observed in polarized photoluminescence excitation spectroscopy experiments in individualized SWCNTs. We observed this transition in our best-aligned films of large-diameter, arc-discharge SWCNTs only when *S* is nearly 1 and only when the tube density and thickness are high enough.

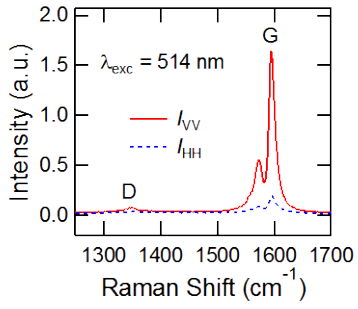

Figure 2: Polarization-dependent Raman spectra showing strong anisotropy.

Future Plans

We will perform gigahertz, terahertz, and infrared spectroscopy experiments on these aligned large-scale carbon nanotubes films to understand their 1-D nature on a macroscopic scale. We will use modern nonlinear and ultrafast optical methods, combined with our unique capabilities of studying materials in ultrahigh magnetic fields using a 30 T table-top magnet [4]. Furthermore, using the developed method, we will be trying to fabricate single crystals of single-chirality single-wall carbon nanotubes (see Fig. 3). Such crystals are expected to exhibit new phenomena arising from the intrinsically one-dimensional nature of the interacting electrons in these systems in a chirality-specific manner.

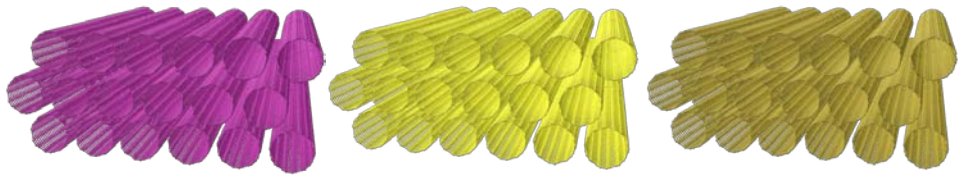

Figure 3: Single crystals of single-chirality single-wall carbon nanotubes with distinct optical, electronic, and magnetic properties.

References

1. See, e.g., S. Nanot, E. H. Hároz, J.-H. Kim, R. H. Hauge, and J. Kono, "Optoelectronic Properties of Single-Wall Carbon Nanotubes," *Adv. Mater.* **24**, 4977 (2012).
2. L. Ren, C. L. Pint, L. G. Booshehri, W. D. Rice, X. Wang, D. J. Hilton, K. Takeya, I. Kawayama, M. Tonouchi, R. H. Hauge, and J. Kono, "Carbon Nanotube Terahertz Polarizer," *Nano Lett.* **9**, 2610 (2009).
3. Q. Zhang, E. H. Hároz, Z. Jin, L. Ren, X. Wang, R. Arvidson, A. Lüttge, and J. Kono, "Plasmonic Nature of the Terahertz Conductivity Peak in Single-Wall Carbon Nanotubes," *Nano Lett.* **13**, 5991 (2013).
4. L. Ren, Q. Zhang, C. L. Pint, A. K. Wójcik, M. Bunney, T. Arikawa, I. Kawayama, M. Tonouchi, R. H. Hauge, A. A. Belyanin, and J. Kono, "Collective Antenna Effects in the Terahertz and Infrared Response of Highly Aligned Carbon Nanotube Arrays," *Phys. Rev. B* **87**, 161401(R) (2013).
5. G. T. Noe, H. Nojiri, J. Lee, G. L. Woods, J. Léotin, and J. Kono, "A Table-Top, Repetitive Pulsed Magnet for Nonlinear and Ultrafast Spectroscopy in High Magnetic Fields Up to 30 T," *Rev. Sci. Instr.* **84**, 123906 (2013).

Publications

1. X. He, W. Gao, Q. Zhang, L. Ren, and J. Kono, "Carbon-Based Terahertz Devices," in: *Proc. of SPIE* **9476**, 947612 (2015).
2. X. He, F. Léonard, and J. Kono, "Uncooled Carbon Nanotube Photodetectors," *Adv. Opt. Mater.* **3**, 989 (2015).
3. E. H. Hároz, J. G. Duque, E. B. Barros, H. Telg, J. R. Simpson, A. R. Hight Walker, C. Y. Khripin, J. A. Fagan, X. Tu, M. Zheng, J. Kono, and S. K. Doorn, "Asymmetric Excitation Profiles in the Resonance Raman Response of Armchair Carbon Nanotubes," *Phys. Rev. B* **91**, 205446 (2015).

4. L. V. Titova, C. L. Pint, Q. Zhang, R. H. Hauge, J. Kono, and F. A. Hegmann, "Generation of Terahertz Radiation by Optical Excitation of Aligned Carbon Nanotubes," *Nano Lett*. **15**, 3267 (2015).
5. H. Telg, E. H. Hároz, J. G. Duque, X. Tu, C. Y. Khripin, J. A. Fagan, M. Zheng, J. Kono, and S. K. Doorn, "Diameter Dependence of TO Phonon Frequencies and the Kohn Anomaly in Armchair Single-Wall Carbon Nanotubes," *Phys. Rev. B* **90**, 245422 (2014).
6. X. He, N. Fujimura, J. M. Lloyd, K. J. Erickson, A. A. Talin, Q. Zhang, W. Gao, Q. Jiang, Y. Kawano, R. H. Hauge, F. Léonard, and J. Kono, "Carbon Nanotube Terahertz Detector," *Nano Lett.* **14**, 3953 (2014).
7. Y.-S. Lim, A. R. T. Nugraha, S.-J. Cho, M.-Y. Noh, E.-J. Yoon, H. Liu, J.-H. Kim, H. Telg, E. H. Hároz, G. D. Sanders, S.-H. Baik, H. Kataura, S. K. Doorn, C. J. Stanton, R. Saito, J. Kono, and T. Joo, "Ultrafast Generation of Fundamental and Multiple-order Phonon Excitations in Highly Enriched (6,5) Single-Wall Carbon Nanotubes," *Nano Lett.* **14**, 1426 (2014).
8. X. Wang, N. Behabtu, C. C. Young, D. E. Tsentalovich, M. Pasquali, and J. Kono, "High-Ampacity Power Cables of Tightly-Packed and Aligned Carbon Nanotubes," *Adv. Func. Mat.* **24**, 3241 (2014).
9. Q. Zhang, E. H. Hároz, Z. Jin, L. Ren, X. Wang, R. S. Arvidson, A. Lüttge, and J. Kono, "Plasmonic Nature of the Terahertz Conductivity Peak in Single-Wall Carbon Nanotubes," *Nano Lett.* **13**, 5991 (2013).
10. X. He, S. Nanot, X. Wang, R. H. Hauge, A. A. Kane, J. E. M. Goldsmith, F. Léonard, and J. Kono, "Photothermoelectric p-n Junction Photodetectors with Intrinsic Polarimetry Based on Macroscopic Carbon Nanotube Films," *ACS Nano* **7**, 7271 (2013).
11. W. D. Rice, R. T. Weber, P. Nikolaev, S. Arepalli, V. Berka, A.-L. Tsai, and J. Kono, "Spin Relaxation Times of Single-Wall Carbon Nanotubes," *Phys. Rev. B* **88**, 041401(R) (2013).
12. D. T. Morris, C. L. Pint, R. S. Arvidson, A. Lüttge, R. H. Hauge, A. A. Belyanin, G. L. Woods, and J. Kono, "Midinfrared Third-Harmonic Generation from Macroscopically Aligned Ultralong Single-Wall Carbon Nanotubes," *Phys. Rev. B* **87**, 161405(R) (2013).
13. L. Ren, Q. Zhang, C. L. Pint, A. K. Wójcik, M. Bunney, Jr., T. Arikawa, I. Kawayama, M. Tonouchi, R. H. Hauge, A. A. Belyanin, and J. Kono, "Collective Antenna Effects in the Terahertz and Infrared Response of Highly Aligned Carbon Nanotube Arrays," *Phys. Rev. B* **87**, 161401(R) (2013).
14. S. Nanot, A. W. Cummings, C. L. Pint, A. Ikeuchi, T. Akiho, K. Sueoka, R. H. Hauge, F. Léonard, and J. Kono, "Broadband, Polarization-Sensitive Photodetector Based on Optically-Thick Films of Macroscopically Long, Dense, and Aligned Carbon Nanotubes," *Sci. Rep.* **3**, 1335 (2013).

Nanoscale magnetic Josephson junctions and superconductor/ferromagnet proximity effects for low-power spintronics

Principal Investigators: I. N. Krivorotov (UC Irvine); Co-PI: O. T. Valls (Minnesota)
Mailing Address (INK): Department of Physics and Astronomy, University of California at Irvine, 4129 Frederick Reines Hall, Irvine, CA 92697-4575, E-mail: ikrivoro@uci.edu
Mailing Address (OTV): School of Physics and Astronomy, University of Minnesota, Minneapolis, MN 55455, E-mail: otvalls@umn.edu

Program Scope

The past two decades have seen rapid advances in two relatively disjoint fields: (i) proximity effects in ferromagnet/superconductor (F/S) hybrid systems and (ii) spin dependent transport in magnetic heterostructures. Notable discoveries in the former field include Josephson π-junctions with ferromagnetic barriers [1], spin switch effects in superconducting spin valves [2] and long-range odd triplet superconductivity in F/S multilayers [3,4]. Important discoveries in the latter field include giant magneto-resistance [5], tunneling magneto-resistance [6] and the spin transfer torque effect [7]. The present research proposal is dedicated to studies of new physics arising from coupling between the F/S proximity and spin-dependent transport in several types of F/S nanostructures. We envision eventual applications to low-power cryogenic computing. In particular, we plan to study current-perpendicular-to-plane magneto-transport and spin torque magnetization dynamics in three types of metallic multilayer nanostructures:

- F/F/S nanopillars (spin valve/superconductor hybrids)
- S/F/F/S nanopillars (spin valve Josephson junctions)
- F/N/S nanopillars (where N is a nonmagnetic metal with strong spin orbit interaction)

The proposed studies will be carried out as a function of magnetic configuration (e.g. the angle between the magnetic moments of the two F layers) and of voltage bias applied perpendicular to the plane of the layers. Ours is an experiment/theory collaboration, and we expect that it will shed light on the intricate interplay between the singlet/triplet condensate induced by the F/S proximity effect and its influence on magneto-resistance and spin torque in these nanostructures. Apart from their importance for understanding of the fundamental physics of coupling between the F/S proximity and spin-dependent transport, these studies are of significant practical importance because these types of nanostructures are candidates for the next generation of ultra-low-power non-volatile memory for cryogenic computing [8].

Recent Progress

This research project started very recently (August of 2015). For this reason we describe here (except for the last paragraph) the research progress of this collaborative team prior to the start date of this project. The two PI's have a history of successfully working together in the field of F/S hybrid structures. Joint publications of their groups include Refs. [9,10]. The PI's

recently demonstrated proof of principle that spin-valve superconducting structures (Nb/Co/Cu/Co/CoO, Fig. 1) could be fabricated by the experimental group (Krivorotov, UCI) while the theoretical work could explain quantitatively the observed behavior (Valls, Minnesota). In these experiments, the magnetization orientation of the bottom Co layer (the "pinned" layer of thickness d_p) was kept fixed, while that of the top "free" layer, of thickness d_f, was rotated by an angle $\alpha$and the valve effects were investigated as α varied. A Cu layer of thickness d_n separated the two magnetic layers. The combined experimental and theoretical work led to the determination of the optimal thicknesses and compositions of the superconducting spin valve layers that maximize control of the superconducting transition temperature Tc via the valve's magnetic configuration [9].

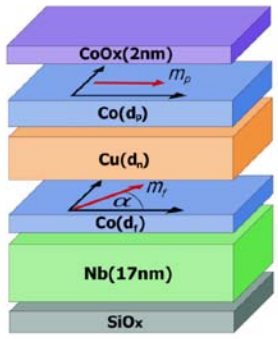

Fig. 1. F/F/S samples used for measurements of angular dependence of T_c in Ref. [9].

An example of these recent results, among the many found in Ref. [9], is shown in Fig. 2. There, the theoretical and experimental results for the change in the transition temperature of the F/F/S spin valve as a function of the angle αbetween magnetic orientations are shown for nine different combinations of the thicknesses of the magnetic and nonmagnetic layers. The agreement between theoretical and experimental values is truly remarkable, particularly as one recalls that transition temperatures are notoriously difficult quantities to compute: for instance, in ordinary superconductors T_c depends exponentially on the coupling constant. Indeed, until very recently it was still impossible to predict the quantity plotted in this figure, even for the simpler case [10] of a trilayer: the typical error was one or two orders of magnitude. In Ref. [9], however, the agreement is not only excellent but predictive: the behavior of the position of the maxima and minima in T_c (α) was computed in advance.

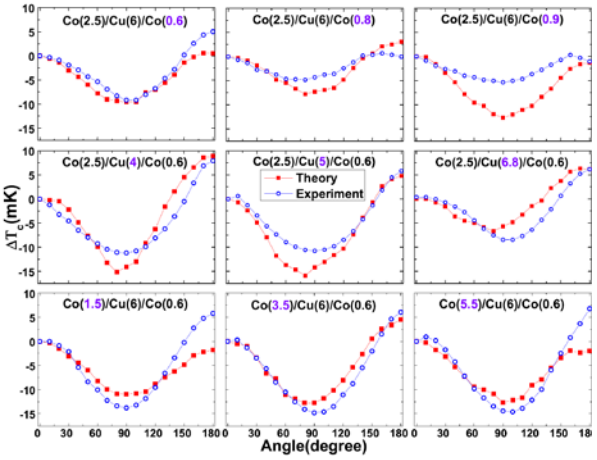

Fig. 2. Comparison between measured and calculated angular dependence of T_c in a F/F/S multilayer from our recent collaborative work [9].

Another important example from the same work [9] is shown in Figure 3: we were able to demonstrate quantitatively for the first time the correlation between the penetration of triplet amplitudes in the spin valve geometry, and the transition temperature. This penetration is seen in the figure to be maximal when the magnetizations are most non-collinear (that is, α near $\pi/2$). In the panels of Fig. 3 we plot two quantities: the red squares and left scale correspond to the theoretically calculated average value of the triplet amplitudes in the outer (pinned) F layer,

while the blue circles (right scale) represent the experimental change in the transition temperature (left scale). The left scale is inverted since T_c is correlated with triplet penetration, and the triplets are formed from the s-wave singlets, hence lowering T_c. Both are plotted against the same quantity, namely the angle α of F-F magnetization misalignment. Results are shown in the three panels for different values of the thicknesses studied. One can see that two plots behave in the same way. This is the first ever proof that the long range proximity effect is quantitatively related to the formation of triplet pairs. Our ability to study and understand triplet correlations as they relate to valve effects will be very useful throughout our proposed studies, enabling us in many cases to refine our predictions before experiments are conducted.

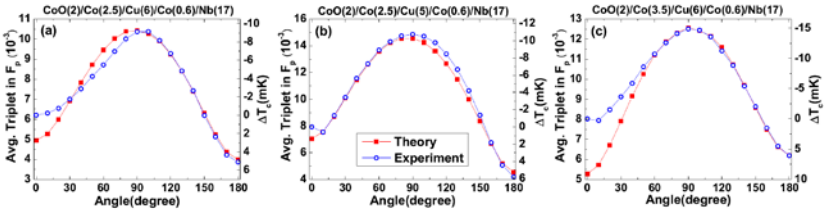

Fig. 3. Anti-correlation of the predicted angular dependence of the triplet amplitude and the transition temperature in the F/F/S spin valve [9].

During the brief time the grant has been in force, he training of a theoretical graduate student at Minnesota has begun. This student has become familiar with the necessary theoretical background, the computational techniques and computer programs that have to be modified from previous work or rewritten. At UCI, the experimental student has begun sample fabrication.

Future Plans

In the course of the project, we will continue to use the same highly collaborative approach that resulted in our previous successful joint work. We will exchange experimental data and theoretical calculations essentially in real time. It is this rapid exchange of data and ideas between our teams that resulted in rapid progress from ideas to published results in our past collaborative projects [9].

In Year 1 of the project, we will deposit Co/Cu/Co/Nb (F/F/S) magnetic multilayers and make nanopillar spin valves based on these multilayers (UCI). We will perform measurements of the angular and bias dependence of magneto-resistance and spin torque in these nanopillar structures above and below the superconducting transition temperature of the Nb layer. Changes in the magnitude and symmetry of the angular dependences of these quantities across the superconducting transition will be fully characterized as functions of the voltage bias and thickness of the magnetic layers (UCI). At the same time, the theory team (Minnesota) will calculate these angular dependences using the exact material and device parameter employed in the experiment. Detailed comparison to the experimental values will be performed and important novel phenomena such as anomalous Andreev reflection will be quantified for the materials employed in the experiment (Minnesota and UCI).

In Year 2 of the project, Nb/Co/Cu/Co/Nb (S/F/F/S) nanoscale magnetic Josephson junctions will be fabricated and tested (UCI). Measurements of the angular and bias dependences

of the Josephson critical current will be carried out for these devices (UCI). We hope to be able to experimentally demonstrate very strong dependence of the Josephson critical current by turning on and off the triplet Josephson current channel via control of the magnetic configuration of the barrier. The theory team (Minnesota) will also compute the angular dependence of the Josephson critical current in this Josephson junction device. These theoretical results will be compared to the experimental observations (Minnesota and UCI).

In Year 3 of the project, we will make and study S/F/Nso/S and S/Nso/F/Nso/S Josephson junctions, where S = Nb, F = Co and Nso = Pt (UCI). We will vary the thickness of the Pt layer and study the effect of spin-orbit interaction on the long-range Josephson current in these structures. The measured dependences of the critical current on the Pt layer thickness will be compared to theoretical calculations (Minnesota). We will also make time-resolved measurements of ultrafast switching of magnetization by spin torque in the Nb/Co/Cu/Co/Nb nanopillar Josephson junctions (UCI). The values of the switching current and switching time are of great importance for cryogenic memory applications of these nanostructures.

References

[1] V. V. Ryazanov et al., Phys. Rev. Lett. 86, 2427 (2001); T. Kontos et al., Phys. Rev. Lett. 89, 137007 (2002).
[2] J. Y. Gu et al., Phys. Rev. Lett. 89, 267001 (2002).
[3] J. W. A. Robinson et al., Science 329, 59 (2010); T. S. Khaire et al., Phys. Rev. Lett. 104, 137002 (2010).
[4] K. Halterman, P.H. Barsic and O.T. Valls, Phys.Rev. Lett. 99, 127002 (2007); K. Halterman, O.T. Valls, and P.H. Barsic, Phys. Rev B 77, 174511 (2008).
[5] M. N. Baibich et al., Phys. Rev. Lett. 61, 2472 (1988); G. Binasch et al., Phys. Rev. B 39, 4828 (1989).
[6] T. Miyazaki, N. Tezuka, J. Magn. Magn. Mater. 139, L231 (1995); J. S. Moodera et al., Phys. Rev. Lett. 74 3273 (1995).
[7] J. C. Slonczewski, J. Magn. Magn. Mater. 159, L1 (1996); L. Berger, Phys. Rev. B 54, 9353 (1996).
[8] D. S. Holmes et al., IEEE Trans. Appl. Supercond. 23, 1701610 (2013).
[9] A. A. Jara, C. Safranski, I. N. Krivorotov, C.-T. Wu, A. N. Malmi-Kakkada, O. T. Valls, K. Halterman, Phys. Rev. B 89, 184502 (2014).
[10] J. Zhu, I. N. Krivorotov, K. Halterman, O. T. Valls, Phys. Rev. Lett. 105, 207002 (2010).

Publications

The project started one month before the Abstract submission deadline, so there are no publications yet. The following manuscript, the very latest stages of which were finished during the grant period, has been submitted for publication. “Charge and Spin Currents in Ferromagnetic Josephson Junctions”, arXiv:1506.05489.

Epitaxial Complex Oxides

Ho Nyung Lee (hnlee@ornl.gov), G. Eres, T. Z. Ward, C. M. Rouleau, and H. M. Christen

Oak Ridge National Laboratory, Oak Ridge, TN 37831

Project Scope

The overarching goal of this project is on understanding, controlling, and ultimately designing epitaxial complex oxide thin films and heterostructures to obtain novel functionalities. Our specific objectives are to create such functionalities in complex oxides by epitaxial stabilization, to control order parameters, e.g. spin, electron, charge, and lattice, in interfacial oxides to achieve novel functionalities, and to probe the growth and functionality dynamically to provide foundational insight required for the design of new functional materials. A variety of *in situ* and *ex situ* characterization techniques are employed to unveil detailed information on crystallographic orientation and structure, electronic and ionic transport, and various functionalities, such as magnetism, ferroelectricity, and superconductivity. In addition, a combination of microstructural imaging and local spectroscopy, neutron scattering, optical and soft x-ray spectroscopy, and theory play key roles in all aspects of this work. Thus, the outcome of this work will result in enhanced understanding of interfacial behaviors and properties of complex oxides, providing unprecedented guidance in the design of technologically relevant materials for energy conversion and storage.

Recent Progress

The research has been focused on the discovery of new materials and phenomena arising from well-controlled, functionally cross-coupled interfaces. In particular, we have focused closely on the development of interfacial heterostructures and their emerging electronic, ionic, magnetic, and structural properties. Selected research highlights are listed as follows:

Fractionally delta doped oxide heterostructures for enhanced transport and thermoelectric properties. "Fractional δ-doping," i.e. the use of single-unit-cell thick layers of a solid-solution complex oxide (see Fig. 1), is found to effectively change the electron effective mass in the $La_xSr_{1-x}TiO_3/SrTiO_3$ (LSTO/STO) superlattice system [Choi 2012]. In this approach, a *d*-band electron filling effect was observed, in which the electron effective mass and the density of the charge carriers are sensitive to compositional changes within layers just one unit cell thick and stacked in various $La_xSr_{1-x}TiO_3/SrTiO_3$ superlattices. Moreover, it turned out that this approach could improve the thermopower of oxide thermoelectrics by 300% compared to that of bulk counterparts [Choi 2014]. Thus, these results add another degree of freedom in tuning the physical properties of complex oxides, particularly those related to two-dimensional electron gases (2DEGs), and will aid in the development of new materials needed for next generation high-speed

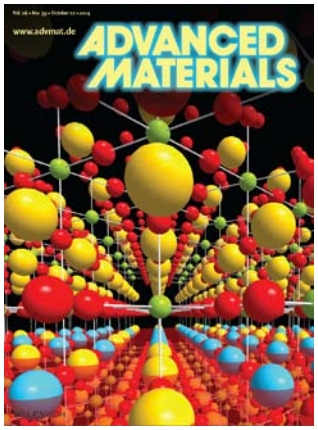

Fig. 1 A precise tuning of the 2D carrier density by using fractional *δ*-doping of 3*d* electrons at the interface of $SrTiO_3/LaTiO_3$ superlattices is found to greatly improve the thermoelectric properties of oxide heterostructures.

microprocessors with low power consumption, displays, and portable electronic devices.

Room temperature multiferroics $LuFeO_3$. Hexagonal $LuFeO_3$ is discovered to be the second example of a room temperature multiferroic [Wang 2013]. This behavior was not previously observed due to the fact that the multiferroic hexagonal phase is only achievable through interfacial strain stabilization in thin films. The polar structure of the films and switchable piezo-response indicated ferroelectricity. Weak ferromagnetism of the films at room temperature was observed followed by a spin reorientation at 130 K, which may be related to observed subtle structural distortion. It is shown that the physical mechanisms driving this phenomenon in $LuFeO_3$ are fundamentally different than those observed in $BiFeO_3$, which should help direct researchers in identifying new directions for the discovery and manipulation of other room temperature multiferroics.

Reversible valence state in epitaxial $SrCoO_x$ ($2.5 \leq x \leq 3.0$). Fast and reversible redox reactions at considerably reduced temperatures are achieved by epitaxial stabilization of multivalent transition metal oxides [Jeen 2013, Choi 2013a]. In general, thermomechanical degradation reduces the overall performance and lifetime of many perovskite oxides undergoing reversible redox reactions. To mitigate this degradation, these reactions must occur at lower temperatures. However, high temperatures (>700 °C) are often required in conventional perovskites for fast ionic conduction. The epitaxial stabilization of strontium cobaltite ($SrCoO_x$) is shown to lower the redox temperature to ~ 200°C (Fig. 2). Switching between two distinct topotactic crystalline phases − either the perovskite $SrCoO_{3-\delta}$ or the brownmillerite $SrCoO_{2.5}$ − occurred rapidly and reversibly, forming a low temperature oxygen sponge. Theory and optical spectroscopy indicated that this transformation corresponds to a metal-insulator transition. Therefore, the oxygen sponge developed in this work illustrates the unprecedented potential of complex oxides for oxide-ionics, where oxidation state changes are used for energy generation, storage and electrochemical sensing.

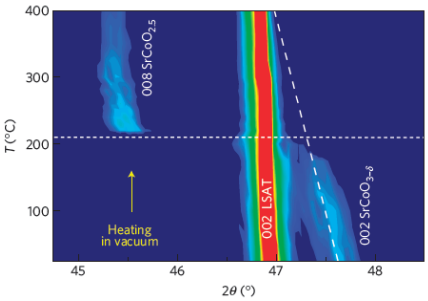

Fig. 2 Direct probing of a reversible valence change at ~200 °C in a $SrCoO_x$ film by real-time x-ray diffraction.

Noble ion implantation for local strain doping. Crystal lattice structure is of central importance to understanding and controlling complex materials that offer untapped potential functionality, such as high-temperature superconductivity, multiferroicity, and colossal magnetoresistivity. However, current methods of controlling lattice structure are limited. We have overcome these restrictions by implanting helium atoms into a crystal, providing a means to finely control electron orbits, active temperature range, and electronic and magnetic behaviors [Guo 2015]. This approach can be applied to any epitaxially locked thin film across a wide spectrum of materials. This new ability is critical to fundamental studies and promises to accelerate commercial deployment of complex materials by providing a way to tune material properties using wafer-scale processing that can be implemented using existing ion-implantation infrastructure.

Future Plans

Controlling order parameters in interfacial oxides to discover novel functionalities: The highly correlated order parameters of spin, charge, orbital, and lattice in complex oxides are at the heart of what makes these materials so promising for technological upheavals in applications

dependent on controlling energy quanta, such as electrons, phonons, photons, and ions. Therefore, by taking advantage of the inherent sensitivity of correlated electron oxides to external stimuli, including strain, chemical doping, etc., we will investigate various heterostructures designed to control the order parameters to disentangle the underlying complexity toward realization of better control over the electronic and magnetic ground states.

Creating functionalities in epitaxially stabilized complex oxides: We also plan to study the functionality of novel phases that result from a systematic tuning of several key parameters that control interface stability, including lattice strain, metal oxidation state, oxygen stoichiometry, chemical composition, and dimensional confinement. Controlling the metal oxidation state by epitaxial stabilization will be used to study novel functionalities arising from oxygen non-stoichiometry or chemical valence variation. Strain control of physical properties is known as a powerful way to improve electronic and magnetic properties and to discover new phases in epitaxial oxides. Thus, we will use epitaxial strain to control the phase of strongly correlated oxides and, thereby, to improve the performance of complex oxide materials. The use of strain doping for controlling orbital populations and crystal symmetry to produce novel functionalities in the manganites, iridates, and cuprates will also be explored.

Understanding the role of oxygen vacancies in complex oxides: The formation of oxygen defects, such as vacancies, in crystalline materials subsequently modifies the overall physical properties and behaviors due to extra charges created around the defects to compensate the charge difference. Thus, we plan to exploit such functional defects in multivalent oxides as they can provide opportunities to discover novel functionalities and phenomena useful for energy applications. In particular, we will focus on controlling oxygen stoichiometry in oxide films by various means. As the valence state of a transition metal can be reversibly changed depending on the reactive oxygen background, providing a means to reversibly switch the electronic and magnetic ground states.

Dynamic probing of the formation and evolution of functionality in epitaxial oxides: The functionality of materials is governed by the structure-property correlations. Epitaxial oxides are particularly attractive because their compositional and structural complexity spans a large parameter space for tuning functionality. Our previous work has already demonstrated the great importance of real-time measurements in the understanding of atomic structure formation in complex oxide film growth mechanisms. Thus, we plan to explore dynamic features of functional properties and the formation and evolution of functionality by using *in situ* time-resolved measurements of the atomic and electronic structure changes. Specifically, this work will advance understanding of the novel functionalities that are related to the chemical valence changes and electronic structure evolution not only during growth, but also in the utilization of these functionalities.

Publications (FY12-FY15): (selected from publications led by this program)

1. W. S. Choi, C. M. Rouleau, S. S. A. Seo, Z. Luo, H. Zhou, T. T. Fister, J. A. Eastman, P. H. Fuoss, D. D. Fong, J. Z. Tischler, G. Eres, M. F. Chisholm, and H. N. Lee, "Atomic layer engineering of perovskite oxides for chemically sharp heterointerfaces," *Adv. Mater.* **24**, 6423 (2012).
2. W. S. Choi, M. F. Chisholm, D. J. Singh, T. Choi, G. E. Jellison, and H. N. Lee, "Wide band gap tunability in complex transition metal oxides by site-specific substitution," *Nat. Comm.* **3**, 689 (2012).
3. W. Wang, Z. Gai, M. Chi, J. D. Fowlkes, J. Yi, L. Zhu, X. Cheng, D. Keavney, P. C. Snijders, T. Z. Ward, J. Shen, and X. Xu, "Growth diagram and magnetic properties of hexagonal $LuFe_2O_4$ thin films," *Phys. Rev. B* **85**, 155411 (2012).

4. W. S. Choi, J.-H. Kwon, H. Jeen, J. E. Hamann-Borrero, A. Radi, S. Macke, R. Sutarto, F. He, G. A. Sawatzky, V. Hinkov, M. Kim, and H. N. Lee, "Strain-induced spin states in atomically ordered cobaltites," *Nano Lett.* **12**, 4966 (2012).
5. W. S. Choi, S. Lee, V. Cooper, and H. N. Lee, "Fractionally δ-doped oxide superlattices for higher carrier mobilities," *Nano Lett.* **12**, 4590 (2012).
6. W. Siemons, M. A. McGuire, V. R. Cooper, M. D. Biegalski, I. N. Ivanov, G. E. Jellison, L. A. Boatner, B. C. Sales, and H. M. Christen, "Dielectric-constant-enhanced Hall mobility in complex oxides," *Adv. Mater.* **24**, 3965 (2012).
7. L. Jiang, W. S. Choi, H. Jeen, T. Egami, and H. N. Lee, "Strongly coupled phase transition in ferroelectric/correlated electron oxide heterostructures," *Appl. Phys. Lett.* **101**, 042902 (2012).
8. W. S. Choi, H. Jeen, J. H. Lee, S. S. A. Seo, V. R. Cooper, K. M. Rabe, and H. N. Lee, "Reversal of the lattice structure in $SrCoO_x$ epitaxial thin films studied by real-time optical spectroscopy and first-principles calculations," *Phys. Rev. Lett.* **111**, 097401 (2013).
9. H. W. Guo, J. H. Noh, S. Dong, P. D. Rack, Z. Gai, X. Xu, E. Dagotto, J. Shen, and T. Z. Ward, "Electrophoretic-like gating used to control metal-insulator transitions in electronically phase separated manganite wires," *Nano Lett.* **13**, 3749 (2013).
10. H. Jeen, W. S. Choi, J. W. Freeland, H. Ohta, C. U. Jung, and H. N. Lee, "Topotactic phase transformation of the brownmillerite $SrCoO_{2.5}$ to the perovskite $SrCoO_{3-\delta}$," *Adv. Mater.* **25**, 3651 (2013).
11. J. Park, B.-G. Cho, K. D. Kim, J. Koo, H. Jang, K.-T. Ko, J.-H. Park, K.-B. Lee, J.-Y. Kim, D. R. Lee, C. A. Burns, S. S. A. Seo, and H. N. Lee, "Oxygen vacancy-induced orbital reconstruction of Ti ions at the interface of $LaAlO_3/SrTiO_3$ heterostructures: a resonant soft x-ray scattering study," *Phys. Rev. Lett.* **110**, 017401 (2013).
12. W. Wang, J. Zhao, W. Wang, Z. Gai, N. Balke, M. Chi, H. N. Lee, W. Tian, L. Zhu, X. Cheng, D. J. Keavney, J. Yi, T. Z. Ward, P. C. Snijders, H. M. Christen, W. Wu, J. Shen, and X. Xu, "Room-temperature multiferroic hexagonal $LuFeO_3$ films," *Phys. Rev. Lett.* **110**, 237601 (2013).
13. H. Jeen, W. S. Choi, M. D. Biegalski, I. C. Tung, J. W. Freeland, D. Shin, H. Ohta, M. F. Chisholm, and H. N. Lee, "Reversible redox reactions in an epitaxially stabilized $SrCoO_x$ oxygen sponge," *Nature Mater.* **12**, 1057 (2013).
14. H. Jeen, Z. Bi, W. S. Choi, M. F. Chisholm, C. A. Bridges, M. P. Paranthaman, and H. N. Lee, "Orienting oxygen vacancies for fast catalytic reaction," *Adv. Mater.* **25**, 6459 (2013).
15. L. Jiang, W. S. Choi, H. Jeen, S. Dong, Y. S. Kim, M. G. Han, Y. Zhu, S. V. Kalinin, E. Dagotto, T. Egami, and H. N. Lee, "Tunneling electroresistance induced by interfacial phase transitions in ultrathin oxide heterostructures," *Nano Lett.* **13**, 5837 (2013).
16. V. R. Cooper, S. S. A. Seo, S. Lee, J. S. Kim, W. S. Choi, S. Okamoto, and H. N. Lee, "Transparent conducting oxides: A delta-doped superlattice approach," *Sci. Rep.* **4**, 6021 (2014).
17. C. Beekman, W. Siemons, T. Z. Ward, M. Chi, J. Howe, M. D. Biegalski, N. Balke, P. Maksymovych, A. K. Farrar, J. B. Romero, P. Gao, X. Q. Pan, D. A. Tenne, and H. M. Christen, "Phase transitions, phase coexistence, and piezoelectric switching behavior in highly strained $BiFeO_3$ films," *Adv. Mater.* **25**, 5561 (2013).
18. W. Siemons, C. Beekman, J. D. Fowlkes, N. Balke, J. Z. Tischler, R. Xu, W. Liu, C. M. Gonzales, J. D. Budai, and H. M. Christen, "Focused-ion-beam induced damage in thin films of complex oxide $BiFeO_3$," *APL Mat.* **2**, 022109 (2014).
19. W. Choi, H. Ohta, and H. N. Lee, "Thermopower enhancement by fractional layer control in 2D oxide superlattices," *Adv. Mater.* **26**, 6701 (2014).
20. S. Lee, T. Meyer, S. Park, T. Egami, and H. N. Lee, "Growth control of the oxidation state in vanadium oxide thin films," *Appl. Phys. Lett.* **105**, 22515 (2014).
21. D. W. Jeong, W. S. Choi, S. Okamoto, J.-Y. Kim, K. W. Kim, S. J. Moon, D.-Y. Cho, H. N. Lee, and T. W. Noh, "Dimensionality control of *d*-orbital occupation in oxide superlattices," *Sci. Rep.* **4**, 6124 (2014).
22. K. Seal, A. Sharoni, J. M. Messman, B. S. Lokitz, R. W. Shaw, I. K. Schuller, P. C. Snijders, and T. Z. Ward, "Resolving transitions in the mesoscale domain configuration in VO_2 using laser speckle pattern analysis," *Sci. Rep.* **4**, 6259 (2014).
23. W. S. Choi, S. A. Lee, I. R. Hwang, S. Lee, and H. N. Lee, Resonant tunneling in a quantum oxide superlattice, *Nature Commun.* **6**, 7424 (2015).
24. H.W. Guo, S. Dong, P.D. Rack, J.D. Budai, C. Beekman, Z. Gai, W. Siemons, C.M. Gonzalez, R. Timilsina, A.T. Wong, A. Herklotz, P.C. Snijders, E. Dagotto, and T.Z. Ward, Strain Doping: Reversible Single-Axis Control of a Complex Oxide Lattice via Helium Implantation, *Phys. Rev. Lett.* **114**, 256801 (2015).

Program Title: Transport Studies of Quantum Magnetism: Physics and Methods

Principal Investigator: Minhyea Lee
Affiliation: Department of Physics, University of Colorado Boulder, Boulder CO 80309
E-mail : minhyea.lee@colorado.edu

Program Scope

The goals of the program are to understand and manipulate the properties of exotic magnetic systems, especially those with multiple broken symmetries, such as time-reversal and inversion symmetry. For metallic such magnets, we focus on systems with helical magnetic ordering where non-collinear and non-coplanar magnetic textures generate unusual electrical transport phenomena. We seek to understand the role of magnetic anisotropy and the contributions of spin-orbit coupling to complex spin textures and the resulting electrical transport properties.
Another focus of the program is exploration of insulating magnets, where frustration leads to unusual states of matter characterized by strong quantum fluctuation and entanglement. This work seeks to identify and establish experimental characteristics of such exotic states, by probing low–energy excitations via thermal transport properties, under the magnetic field as well as using samples with different atomic constituents, which can effectively control the strength of magnetic interaction.

Recent Progress

(1) Metallic helimagnet with the strong magnetic anisotropy

Well-known metallic MnSi and other B20 crystals have demonstrated that unusual electrical transport properties associated with complex magnetic textures, such as topological Hall effect (THE), provide unique possibilities to control the electrical behavior via manipulation of the underlying spin structure. It should be noted that, so far, all materials shown to form spontaneous such spin textures were found exclusively in B20-structured single crystals. Its low crystalline anisotropy allows the formation of continuous and smoothly varying spin textures that directly leads to fascinating electrical properties [1].
In contrast to isotropic B20 helimagnets, $Cr_{1/3}NbS_2$ exhibits large magnetic anisotropy, originating from its highly anisotropic layered crystal structure. Our investigation revealed an intriguing role of spin-orbit coupling in determining the magnetic anisotropy and in altering electrical transport properties. Unlike in B20 helimagnets, we found that the spin structure of Cr1/3NbS2 in a magnetic field B is well described by a 1-dimensional (1D) Heisenberg spin model with Dyzaloshinskii-Moriya (DM) interaction, Zeeman interaction, and strong magnetocrystalline

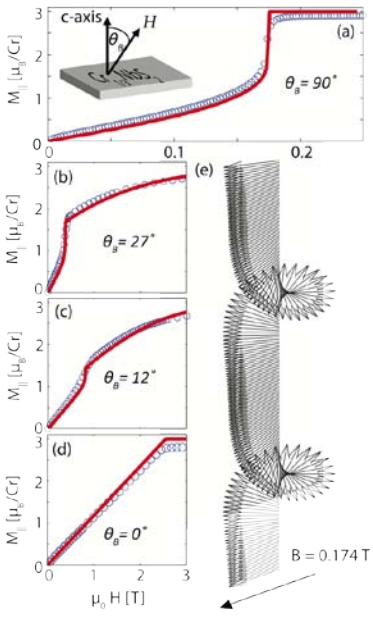

Figure 1 (a-d) Calculated (lines) and experimental (circles) plotted as a function of applied field H. (e) shows the spin structure as B➔B_c.

anisotropy. Fig. 1 shows the result of our simulation and the magnetization measurement (M) with an applied field at different angles measured from the c-axis [2].

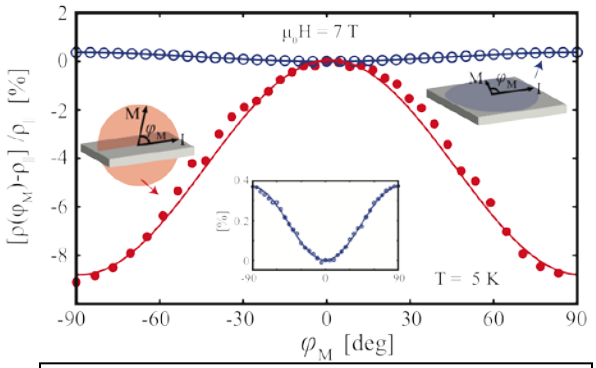

Figure 2 In-plane MR at 7 T for both spin orientations, normalized by with the resistivity at angle φ_M = 0°, Inset: in-plane AMR with magnified y –axis.

We have also discovered that the anisotropy greatly impacts the in-plane electrical conductivity, and is responsible for the unusual field dependence of Hall effect in $Cr_{1/3}NbS_2$ [3]. The spin-orientation dependent in-plane magnetoresistnace (MR) in $Cr_{1/3}NbS_2$ is highlighted in Fig.3, where we plotted angular dependence of MR as a function of in both in-plane and out-of-plane rotation of applied field. Here the applied field is large enough (B = 7 T) to ensure the saturation of the magnetization along the direction of field. The main panel shows both in-plane and out-of-plane angular dependence of the in-plane resistivity normalized with the resistivity at angle $\varphi_M = 0°$, where φ_M denotes the angle between the directions of magnetization and the current. In both cases, the magnetization rotation gives rise to a $\cos^2\varphi_M$ angular dependence, shown in solid lines of Fig. 2. However, the normalized AMR oscillation amplitude for the out-of- plane MR varies up to -9 %, which is usually large. It is also larger by 23 times than the in-plane variation, which corresponds to +0.4%. This out-of-plane AMR effect should also be distinguished from giant magnetoresistance of magnetic multilayers, in which the saturated MR remain the same for both orientations [4]. In order to obtain a better understanding, we performed first principles calculations and found that the Fermi level density of states (DOS) was found to be 3.2 % greater when the moments orient along the c-axis instead of perpendicular to it, while the in-plane plasma frequencies are essentially unaffected by magnetization orientation. Thus, neglecting spin-orientation dependent scattering processes, the increase in DOS is largely responsible for the reduction of the in-plane resistivity when the magnetization lies parallel to the c-axis instead of the ab-plane. It was found that the bands near the Fermi energy have an offset of 1.7 meV ~ 20 K on average when the spins are polarized out of plane. This is a direct result of spin-orbit coupling and the temperature scale is consistent with one at which the spin-orientation dependent MR begins to wash out. The temperature below which the unusual field dependence of Hall voltage appears also coincides with this energy scale. This common temperature scale appears throughout the magnetotransport measurements, and points toward the crucial role played by SOC in this anisotropic helimagnet.

(2) Thermal conductivity of Honeycomb lattice 2D insulating magnet $RuCl_3$

Transition metal compounds with d-orbitals have provided a major playground to realize many fascinating phenomena in modern condensed matter physics. Particularly, spin-orbit coupling in 4d- and 5d- compounds may be responsible for many new ground states, including exotic magnetic ordering, via anisotropic exchange interactions. The exactly solvable Kitaev spin model in the honeycomb lattice [5] describes such competing bond dependent magnetic

exchange interactions. In searching for new 4d- and 5d- honeycomb lattice systems to realize the Heisenberg-Kitaev model, α-$RuCl_3$ turns out to be an excellent candidate, thanks to the ideal 2D honeycomb structure and the low-spin 3+ state of Ru ($4d^5$) that is equivalent to $j_{eff} = ½$. Recent zero-field NMR and specific heat measurements reported by Majumer et al [6] found that below the known "magnetic ordering" temperature, the average hyperfine field is much lower than expected, and the line exhibits a pronounced broadening, which indicates a complex type of magnetic ordering in this system.

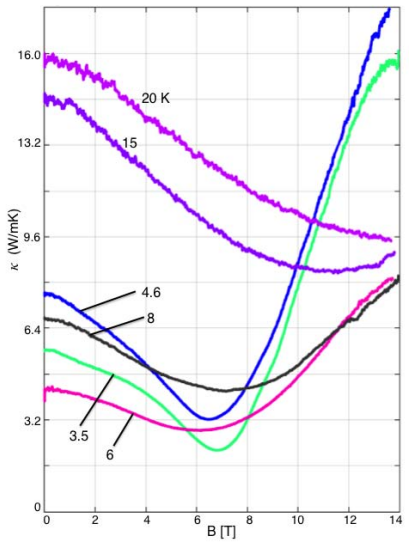

Figure 3 Thermal conductivity at different T's as a function of applied field up to 14 T. In-plane field was applied parallel to the ΔT.

We have measured the thermal conductivity (κ) at low temperature below 20 K. First, we found that just below the second magnetic ordering temperature ($T_2 \approx 7.5$ K), the thermal conductivity is enhanced greatly under applied fields lying in the ab-plane, parallel to the temperature gradient (ΔT). At 14T, as T is lowered, κ (T) decreases until just below T_2 and then increases to a maximum around 4.6 K before decreasing again. Fig. 3 shows κ as a function of applied field, in the same configuration of $\Delta T||B||ab$. Below the ordering temperature T_2, κ (B) exhibits a clear minimum at B ≈ 7 T, while the bulk magnetization with in-plane fields shows only a monotonic increase through this field range. This non-monotonic behavior at low T contrasts with that at higher temperatures (e.g. 15 and 20 K), where a large field reduces κ significantly. In fact, non-monotonic field dependence also appears in the specific heat measurement, where a broad maximum occurs in the same B field range. It possibly implies the field-induced phase transition of this system at around B = 7 T, above which the system enters spin-liquid-like regime [6]. In that case, we speculate the minimum thermal conductivity at this field may be a result of the short-range fluctuation near the phase transition. Further analysis including the phonon contribution is under progress.

Future Plans

Thickness-dependence of magnetic transport properties

Thanks to the layered structure of $Cr_{1/3}NbS_2$, it is possible to study the magnetotransport properties as a function of sample thickness along the c-axis. A single helical pitch length is 50-70nm. We focus on fabricating a device made of $Cr_{1/3}NbS_2$ single crystals, where the thickness is varied from 50 – 500nm. When the helical pitch cannot be completed due to the physical size of sample, the energy gain due to DM interaction is likely to be overwhelmed by boundary effects. Thus, as the thickness is reduced, significant changes in magnetic and transport properties can be expected.

Angular dependence of Topological Hall effect of $Mn_{1-x}Fe_xSi$

Expanding our efforts on the role of magnetic anisotropy, we have been measuring angular dependence of Topological Hall effect (THE) in $Mn_{1-x}Fe_xSi$. THE is generated by the fictitious magnetic field that is felt by conduction electrons travelling through the 2-dimensional Skyrmion lattice (SL) [6], which is formed in the narrow region of the B-T phase diagram. Due to almost

isotropic structure, the 2D SL is formed on the plane perpendicular to the applied field. We will measure the THE as a function of the applied field angle, using $Mn_{0.9}Fe_{0.1}Si$, which has a larger THE signal [2] and larger area observable THE in the B-T phase diagram than pure MnSi. Based on the deviation of THE signal from $B\cos\theta$, where θ is the polar angle of the field, we will be able to test the 2D nature of SL as well as the pinning of skyrmions on Fe impurities.

Angular dependence of magnetization in 2D honeycomb magnet $RuCl_3$

In order to achieve a better understanding of spin anisotropy and its effect on magnetic structure, we are planning to perform torque-magnetometry of $RuCl_3$ using a piezo resistive micro-cantilever as a function of in-plane magnetic field rotation. We have already obtained the magnetization as a function of strength and the direction of the applied field, using a commercial SQUID magnetometer up to 7 T. However, as seen in Figure 3, the interesting field scale begins at around 7 T and the spin anisotropy is expected to play a crucial role to determine the magnetic structure. Thus, in order to fully explore its magnetic behaviors H > 15T and rotation of field within the ab plane is required. Torque magnetometry is an extremely sensitive technique and is well suited for measuring very small single crystals.

References (that acknowledge the support from DOE)

[1] B. J. Chapman, M. G. Grossnickle, T. Wolf and Minhyea Lee. Large enhancement of emergent magnetic fields in MnSi with impurities and pressure. Phys. Rev. B 88, 214406 (2013).

[2] B. J. Chapman, A. C. Bornstein, N. J. Ghimire, D. G. Mandrus, and Minhyea Lee. Spin structure of the anisotropic helimagnet Cr1/3NbS2 in a magnetic field. App. Phys. Lett. 105, 072405 (2014).

[3] A. C. Bornstein, B. J. Chapman, N. Ghimire, D. G. Mandrus, D. S. Parker and Minhyea Lee. Out-of-Plane Spin-Orientation Dependent Magnetotransport Properties in the Anisotropic Helimagnet Cr1/3NbS2. Phys. Rev. B 91, 184401 (2015).

Other References

[4] M. N. Baibich, J. M. Broto, A. Fert, F. Nguyen Van Dau, F. Petroff, P. Etienne, G. Creuzet, A. Friederich, and J. Chazelas. Giant Magnetoresistance of (001)Fe/(001)Cr Magnetic Superlattices. Phys. Rev. Lett. 61, 2472 (1988).

[5] A. Kitaev. Anyons in an exactly solved model and beyond. Annals of Physics 321, 2 (2006).

[6] M. Majumder, M. Schmidt, H. Rosner, A. A. Tsirlin, H. Yasuoka, and M. Baenitz, Anisotropic Ru^{3+} $4d^5$ magnetism in the α-$RuCl_3$ honeycomb system: Susceptibility, specific heat, and zero-field NMR Phys. Rev. B 91, 180401 (2015).

[7] S. Muhlbauer, B. Binz, F. Jonietz, C. Pfleiderer, A. Rosch, A. Neubauer, R. Georgii, P. Boni, Skyrmion Lattice in a Chiral Magnet, Science 323, 915-919 (2009)

Program Title: Experimental study of quantum critical fluctuations in two-dimensional superconducting cuprate films

Principle Investigator: Thomas R. Lemberger
Mailing Address: Dept. of Physics, The Ohio State University, Columbus, OH 43210
e-mail: trl@physics.osu.edu

Program Scope

The main goal of this research program is to explore the physics of superconductivity in cuprate superconductors at compositions close to the quantum critical point at low hole doping, where superconductivity gives way to an insulating state with further underdoping. Earlier work in this project has provided strong evidence that this regime is dominated by critical quantum fluctuations, which makes it particularly interesting to study.

Samples are thin films of cuprates $Y_{1-x}Ca_xBa_2Cu_3O_{7-\delta}$ and $Bi_2Sr_2CaCu_2O_{8+x}$ that we grow by pulsed laser deposition onto appropriate substrates. Our thinnest YBCO films are two unit cells thick, about 2.3 nm. Measurements include low-frequency electron transport done in the PI's lab, and THz conductivity in colleague Rolando Valdes Aguilar's lab at OSU and THz Hall effect in Dennis Drew's lab at U. Maryland.

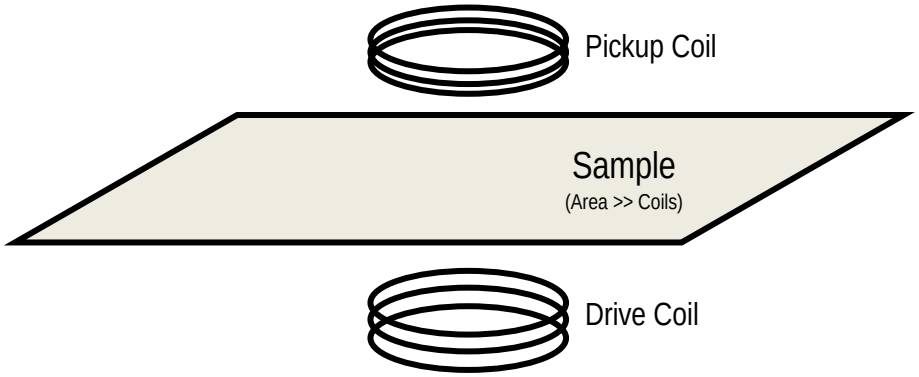

With a low-frequency two-coil mutual inductance system (above) that we've used for many years, we measure the density of superconducting charge carriers (holes) in sample films as a function of temperature, which provides unique insight into both quantum and thermal fluctuation effects. More recently, we adapted the system to enable application of higher magnetic fields from the drive coil, (up from milligauss to tens of gauss), so that we can measure another fundamental superconducting property, the "coherence length", ξ.

THz conductivity measurements enable study of fluctuations from below the superconducting transition to well above it, where fluctuations are short-lived. The THz Hall

effect measurements are sensitive to changes in the Fermi surface, especially transitions from hole-like to electron-like Fermi pockets.

Recent Progress

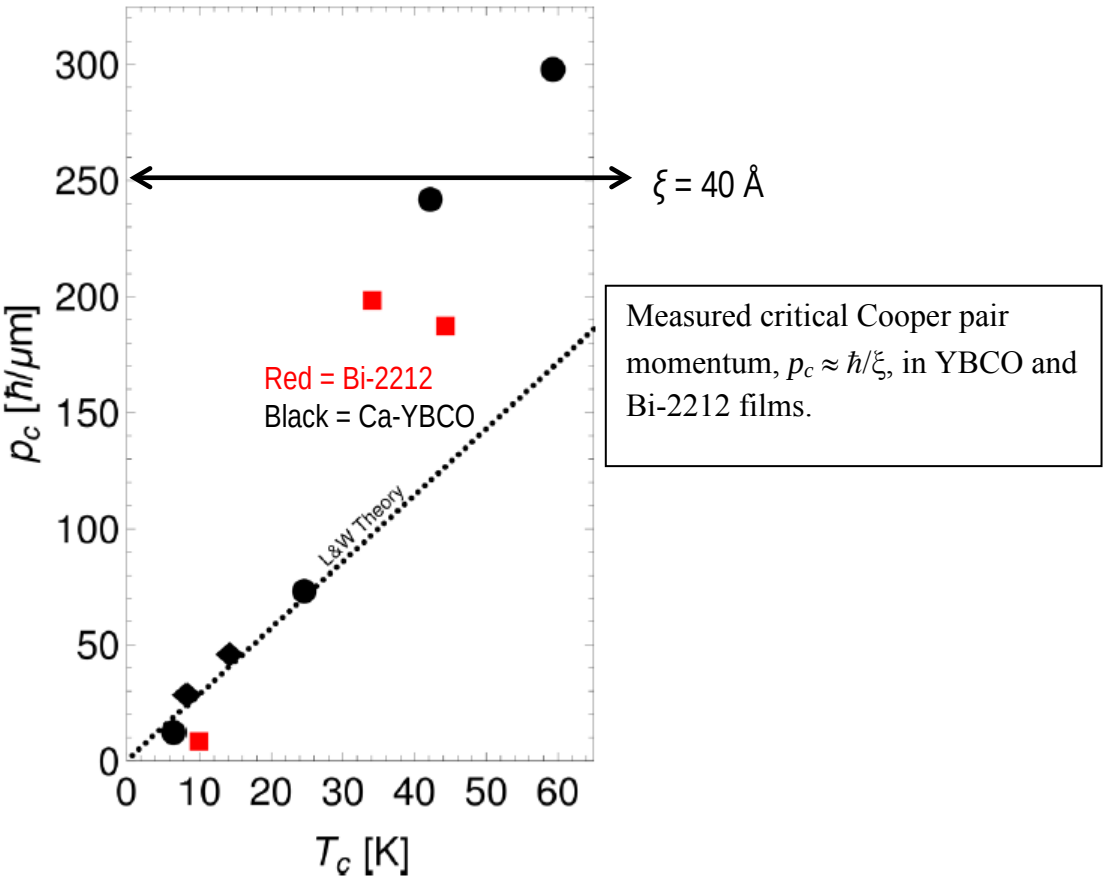

We adapted a two-coil apparatus to enable measurement of the superconducting coherence length, ξ, and used it to show that 1/ξ is linearly proportional to Tc as Tc increases from zero at the critical hole doping concentration of about 0.05 hole/planar-Cu in cuprate superconductors. ξ is expected to be inversely proportional to the characteristic energy in the superconductor; in conventional superconductors it is inversely proportional to the energy gap in the electron density of states. In underdoped cuprates there are at least three possible energy scales – Tc, the pseudogap, and the "nodal" gap from ARPES that could dominate. From the figure above, $p_c \approx \hbar/\xi$ is proportional to Tc so this is the characteristic energy scale, at least for vortex physics.

This new technique is an important advance for the following reason. The conventional determination of coherence length comes from the upper critical magnetic field where vortex

cores overlap so strongly that superconductivity is squeezed out. This measurement typically requires such high fields in cuprates, tens of teslas, that the band structure of the compound is affected. Our measurement determines ξ from the applied field at which vortices first appear. Because the field is applied at the middle of a film, not near the edges, the critical field is well above the nominal lower critical field due to a strong free-energy barrier to appearance of vortices, but still only tens of gauss, a field that has no effect on the background properties of the superconductor.

In an unexpected development, we found that in very thin underdoped YBCO films there is a temperature gap between the Tc where resistivity goes to zero (apparently) and the lower Tc where superfluid density appears. The difference can be as much as 20 K. This behavior points to some sort of filamentary superconducting state, but whether it is trivial or fundamental, due to spontaneous ordering such as formation of "stripes", for example, remains to be determined.

Plans

We had to move our film-growing lab recently, and our immediate efforts are on getting it back to growing high-quality films. The protocol requires some tweaking. We want to grow very thin underdoped Bi-2212 films and measure their coherence lengths to see whether they are also inversely proportional to Tc as in YBCO. It may very well be that the ab vs c-axis anisotropy in Bi-2212 is so high (about 10^4) that two-dimensional physics appears even when films are many unit cells thick.

We want to look for the "gap" between resistive and superfluid Tc's in thin Bi-2212 films to confirm results in YBCO. We want to explore the effect deeper by measuring critical currents in the gap region.

We want to make modestly thin, strongly underdoped YBCO films for THz measurements mentioned above. These samples require special construction. In order to pass THz radiation through them, the substrate should be MgO. In order that the films grow well, the substrate should be $SrTiO_3$. So, a colleague at OSU, Roland Kawakami, will use his MBE machine to grow thin STO layers on MgO substrates for us. We'll use these modified substrates for YBCO films.

References that acknowledge DoE support

1. "*Theory of the lower critical magnetic field for a two-dimensional superconducting film in a non-uniform field*", T. R. Lemberger and John Draskovic, Phys. Rev. B. **87**, 064503 (2013).

2. "*Upper limit of metastability of the vortex-free state of a two-dimensional superconductor in a nonuniform magnetic field*", T.R. Lemberger and A. Ahmed, Phys. Rev. B **87**, 214505 (2013).

3. "*Measuring the superconducting coherence length in thin films using a two-coil experiment*", John Draskovic, T. R. Lemberger, Brian Peters, Fengyuan Yang, Jaseung Ku, Alexey Bezryadin, and Song Wang, Phys. Rev. B **88**, 134516 (2013).

4. "*Comparison of 2-D Quantum and Thermal Critical Fluctuations of Underdoped $Bi_2Sr_2CaCu_2O_{8+\delta}$ with Ultrathin $YBa_2Cu_3O_{7-\delta}$ films*", Michael J. Hinton , Jie Yong , Stanley Steers, T.R. Lemberger, J Supercond Nov Magn **26**, 2617–2620 (2013).

5. "*Cation Non- stoichiometry in Pulsed Laser Deposited $Sr_{2+y}Fe_{1+x}Mo_{1-x}O_6$ Epitaxial Films*", T. L. Meyer, M. Dixit, R. E. A. Williams, M. A. Susner, H. L. Fraser, D. McComb, M. D. Sumption, T. R. Lemberger, P. M. Woodward, J. Applied Physics **116**, 013905 (2014).

6. "*Doping-dependent critical Cooper-pair momentum in thin, underdoped cuprate films*", John Draskovic, Stanley Steers, Thomas McJunkin, Adam Ahmed, and TRL, Phys. Rev. B **91**, 104524 (2015).

Probing electron correlations in 1D electronic materials using single quantum channels

Jeremy Levy, Department of Physics and Astronomy, University of Pittsburgh

Program Scope

This research program focuses on the investigation of strong electron correlations in quasi-one-dimensional oxide nanostructures. The archetypical system consisting of heterostructures formed from an ultrathin layer of $LaAlO_3$ and TiO_2-terminated SrTiO3 offers a unique laboratory for probing strong correlations due to intrinsic richness of the physical system and its ability to be modulated at extreme nanoscale dimensions. Under suitable conditions, $SrTiO_3$ is known to exhibit a variety of important properties associated with strong electronic correlations, especially superconductivity and magnetism. Understanding the nature of these electronic correlations at fundamental scales, and in reduced spatial dimensions, will provide the scientific basis for new energy technologies, information technologies, and materials.

The proposed work is motivated by recent discoveries and technical advances in Levy's lab, specifically, (1) pioneering work to create conductive nanostructures to be created in $LaAlO_3/SrTiO_3$ heterointerfaces with 2 nm spatial resolution, (2) the discovery of a novel correlated electronic phases in which electrons pair without forming a superconductor, and (3) the demonstrated ability to form high-quality quantum point contacts (QPCs) and achieve ballistic electron transport over micrometer-scales in $LaAlO_3/SrTiO_3$ nanowires.

Three main projects are proposed. First, we will press forward to develop a full microscopic understanding of the mechanism for electron pairing in $LaAlO_3/SrTiO_3$ nanostructures. Understanding the "glue" that leads to pairing and superconductivity in a doped semiconductor will help to form a scientific basis for the correlated oxide nanoelectronics platform being developed. Second, we will use our ability to create well-defined quantum channels in nanowires allows to allow novel "scattering" experiments to be performed that probe fundamentally new quasiparticle excitations using an unprecedented combination of experimental methodologies. Experiments already underway with artificially defined superlattices (5 nm period) demonstrate the feasibility of this approach. Third, we will investigate 1D correlations in proximally coupled nanowires, which are predicted exhibit Majorana-like zero modes in the absence of superconductivity or spin-orbit coupling. All of these projects will benefit from a newly available multipurpose scanning probe microscope that operates at millikelvin temperatures, and can be used to image electronic properties and dynamically perturb the electronic nanostructures.

The implications for these studies will be far-ranging, with possible insights into new and emergent phenomena in the rich class of complex oxides, but also fundamental mechanisms of superconductivity and magnetism. Thematically, the proposed research falls under a grander

vision to combine some of the most important and interesting challenges in the physics of semiconductor nanostructures and correlated electronic materials. The proposed investigations will reveal fundamental properties and mechanisms and open new opportunities for scientific discovery and technological application. The increased understanding of electron correlations can pave the way to the development of new materials with outstanding or novel properties, which could be relevant for energy-related technologies such as low-power high performance computing, quantum computation, or the development of novel materials.

The work is extremely important for understanding a wide class of technologically relevant materials that have relevance to basic energy science..

Future Plans

We are currently developing a class of coupled nanowire devices to investigate Coulomb drag between two nanowires.

Program Title: Study of Topological Superconductivity in Nanoscale Structures

Principle Investigator: Qi Li

Mailing Address: Department of Physics, Pennsylvania State University, University Park, PA 16802

e-mail: qil1@psu.edu

Project scope

The goal of the program is to induce and characterize topological superconductivity in topological insulator thin films and nanotubes using proximity effect with relatively high T_c s-wave superconductors. Topological insulators are a new type of state of matter which are insulating in bulk, but conducting on surfaces with many exotic physical properties. For example, fully spin polarization with no back scattering and following time reversal symmetry are very unique phenomena. When a superconductor is in contact with a topological insulator, the bulk will develop a superconducting gap and the surface states will become a topological superconductor due to proximity effect. Since the topological surface states are gapless with spin-momentum locking, the superconducting surface states will have helical-Cooper pairs. This unique feature gives rise to a wide range of exotic physics, including the possibility of hosting Majorana Fermions.

Previous experiments on induced topological superconductivity were using low T_c superconductors. Although there were anomalies reported in the electron tunneling spectra, all were observed at very low temperatures and undistinguishable between the conventional proximity induced superconductivity through the bulk, gaped surface states (trivial) due to top and bottom surface hybridization, and the gapless (nontrivial) surface states. This project aims to use higher T_c s-wave superconductor, like MgB_2 (T_c ~ 40 K), to induce superconductivity in topological insulator thin films and nanotubes. Nanoscale structures can suppress bulk transport by increasing surface to volume ratio. There are also more unique exotic properties in nanoscale structures beyond the simple geometrical effect. For example, quasi-one dimensional nanotubes are also ideal systems to study Majorana fermions. The two sample structures have been developed recently in the PI's group and the main measurement approaches are using electron tunneling and Josephson effects [1-6].

Recent Progress

Resistance quantum oscillation in Bi_2Te_3 nanotubes. Three dimensional topological insulators are characterized by Dirac-like conducting surface states, the existence of which has been confirmed in relatively clean metallic samples by angle-resolved photoemission spectroscopy, as well as by anomalous Aharonov-Bohm oscillations in the magnetoresistance of nanoribbons [7-9].

However, a fundamental aspect of these surface states, i.e. their robustness to time-reversal invariant disorder, has remained relatively untested [10]. In this work, we have synthesized nanotubes of Bi_2Te_3 with extremely insulating bulk at low temperatures due to disorder. Nonetheless, the magnetoresistance exhibits quantum oscillations as a function of the magnetic field along the axis of the nanotubes, with a period determined by the cross-sectional area of the outer surface. Detailed numerical simulations support that the resistance oscillations are arising from the topological surface states which have substantially longer localization length than that of other non-topological states. This observation demonstrates coherent transport at the surface even for highly disordered samples, thus providing a direct confirmation of the inherently topological character of surface states. The result also demonstrates a viable route for revealing the properties of topological states by suppressing the bulk conduction using disorder.

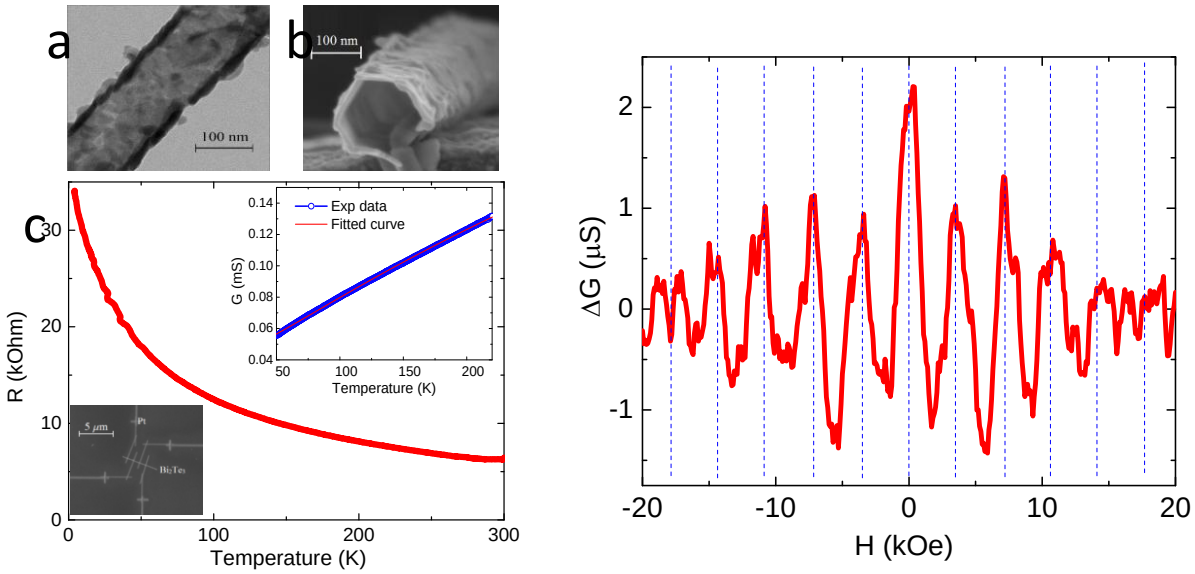

Fig. 1 shows the TEM and SEM images of a Bi_2Te_3 nanotube sample (a and b) and the temperature dependence of resistance (c). The nanotubes are grown using a solution phase method and the sample shown in the figure has an outer diameter of 120 nm and the wall thickness of 10 nm with a length of about 10 μm. The resistance of the nanotube shows a monotonic increase with decreasing temperature, indicating an insulating behavior. The temperature dependence of conductance can be fitted using Mott variable range hopping model plus a constant in a wide temperature range above 50 K, indicating that the bulk is in a strong disorder regime. At low temperatures, the surface conduction dominates the transport. We have observed resistance oscillations as shown on the right. In topological insulator nanostructures, at zero magnetic field, the surface states will open up an energy gap due to quantum confinement. The conductance oscillations are predicted to arise from the appearance of a gapless surface

mode when half integer fluxes are enclosed by the surface of the system. Since these oscillations have a period of *h/e*, the same as AB effect, they are referred to as "anomalous AB oscillations".

Point contact spectroscopy in $NbSe_2/Bi_2Se_3$ bi-layers. We studied the proximity-effect induced superconductivity in epitaxial topological insulator Bi_2Se_3 thin films grown on $NbSe_2$ using a point contact spectroscopy (PCS) method at low temperatures down to 40 mK. We used the so-called "soft" point contact technique with silver planar contacts. We observed a finite superconducting energy gap corresponding to the proximity effect induced superconductivity in the bulk Bi_2Se_3 from the $NbSe_2$ substrate, which is consistent with the gap values reported by the ARPES measurements on similar samples. The induced gap value is ~159 μeV at 1 K for a 16 quadruple layer Bi_2Se_3 on $NbSe_2$. Below 0.45 K, a second peak feature ~120 μeV appeared in the spectrum, which was suppressed by temperatures above ~1 K or in a magnetic field of ~0.03 T. Several possible origins of two induced gap values were discussed. It is plausible that the second induced gap values ~120 μeV is due to the induced superconductivity in the topological surface states. The induced superconducting gap in the spectra is consistent with the gap values observed by the Angle-resolved photoemission Spectroscopy (ARPES) on similar samples [1].

Future Plans

Topological superconductivity has gained tremendous attention recently owing to the unconventional nature and the possibility of observing Majorana fermions. We will study the induced superconducting states, particular those features which may be from the surface superconducting states, using two different systems. First, we will use MgB_2 as the s-wave superconductor using HPCVD grown MgB_2/Bi_2Se_3 bilayers which provide much higher T_c and wider range of temperature for the study. Second, we will study the induced superconductivity in Bi_2Te_3 nanotubes using superconducting contact leads made by using electron beam lithography. Magnetotransport measurements will be conducted at low temperatures and high magnetic fields.

References (acknowledge DOE support)

1. Su-Yang Xu, Nasser Alidoust, Ilya Belopolski, Anthony Richardella, Chang Liu, Madhab Neupane, Guang Bian, Song-Hsun Huang, Raman Sankar, Chen Fang, Brian Dellabetta, Wenqing Dai, Qi Li, Matthew J. Gilbert, Fangcheng Chou, Nitin Samarth, M. Zahid Hasan, "Momentum-space imaging of Cooper pairing in a half-Dirac-gas topological superconductor", **Nature Physics,** 10, 943-950 (2014)
2. Y. Gong, Z. Zhang, D. Ascienzo, A. Abranyos, H. B. Zhao, G. Lüpke, Qi Li, and Y. H. Ren, "Ultrafast optical detection of magnetic inhomogeneity in ferromagnetic La0.67Ca0.33MnO3", **Euro. Phys. Lett,** 108, 17010 (2014).
3. Y. W. Yin, M. Raju, W. J. Hu, J. D. Burton, Y.-M. Kim, A. Y. Borisevich, S. J. Pennycook, S. M. Yang, T. W. Noh, A. Gruverman, X. G. Li, Z. D. Zhang, E. Y. Tsymbal, and Qi Li, "Multiferroic tunnel junctions and ferroelectric control of magnetic state at interface (invited)", **J. Appl. Phys**., 117, 172601 (2015).

4. Steven Carabello, Joseph G Lambert, Jerome Mlack, Wenqing Dai, Qi Li, Ke Chen, Daniel Cunnane, C G Zhuang, X X Xi, and Roberto Ramos "Energy gap substructures in conductance measurements of MgB2-based Josephson junctions: beyond the two-gap model", **Supercond. Sci. and Technol**., 28, 055015 (2015).
5. Renzhong Du, Hsiu-Chuan Hsu, Ajit C. Balram, Yuewei Yin, Sining Dong, Wenqing Dai, Weiwei Zhao, DukSoo Kim, Shih-Ying Yu, Jian Wang, Xiaoguang Li, Suzanne E. Mohney, Srinivas Tadigadapa, Nitin Samarth, Moses H.W. Chan, Jainendra. K. Jain, Chao-Xing Liu, and Qi Li, "Robustness of topological surface states against strong disorder observed in Bi_2Te_3 nanotubes", submittted to Phys. Rev. X (2015).
6. Wenqing Dai, Anthony Richardella, Renzhong Du, Weiwei Zhao, Xin Liu, Moses. H. W. Chan, Jainendra K Jain, C.X. Liu, Nitin Samarth, and Qi Li "Point Contact Spectroscopy Study of Topological Superconductor $NbSe_2/Bi_2Se_3$ Heterostructures", unpublished (2015).

Other References

7. L. Fu, C. Kane, and E. Mele, *Topological Insulators in Three Dimensions*, Phys. Rev. Lett.**98**, 106803 (2007).
8. Y. Xia, D. Qian, D. Hsieh, L. Wray, A. Pal, H. Lin, A. Bansil, D. Grauer, Y. S. Hor, R. J. Cava, and M. Z. Hasan, *Observation of a large-gap topological-insulator class with a single Dirac cone on the surface*, Nature Phys. **5**, 398 (2009).
9. H. Peng, K. Lai, D. Kong, S. Meister, Y. Chen, X. L. Qi, S. C. Zhang, Z. X. Shen, and Y. Cui, *Aharonov-Bohm interference in topological insulator nanoribbons*, Nature Mat. **9**, 225 (2010).
10. J. H. Bardarson, P. W. Brouwer, and J. E. Moore, *Aharonov-Bohm Oscillations in Disordered Topological Insulator Nanowires*, Phys. Rev. Lett. **105**, 156803 (2010).

Program Title: Structured Light-Matter Interactions Enabled by Novel Photonic Materials
Principle Investigator: N. M. Litchinitser; Co-PI: L. Feng
Mailing Address: Department of Electrical Engineering , University at Buffalo, The State University of New York, Buffalo, NY 14260, USA
E-mail: natashal@buffalo.edu

Program Scope

The synergy of complex materials and complex light is expected to add a new dimension to the science of light and its applications [1]. The goal of this program is to investigate novel phenomena emerging at the interface of these two branches of modern optics.

While metamaterials research was largely focused on relatively "simple" linearly or circularly polarized light propagation in "complex" nanostructured, carefully designed materials with properties not found in nature, many singular optics studies addressed "complex" structured light transmission in "simple" homogeneous, isotropic, nondispersive transparent media, where both spin and orbital angular momentum are independently conserved.

However, if both light and medium are complex so that structured light interacts with a metamaterial whose optical materials properties can be designed at will, the spin or angular momentum can change, which leads to spin-orbit interaction and many novel optical phenomena that will be studied in the proposed project. Indeed, metamaterials enable unprecedented control over light propagation, opening new avenues for using spin and quantum optical phenomena, and design flexibility facilitating new linear and nonlinear optical properties and functionalities, including negative index of refraction, magnetism at optical frequencies, giant optical activity, subwavelength imaging, cloaking, dispersion engineering, and unique phase-matching conditions for nonlinear optical interactions.

In this research program we focus on structured light-matter interactions in complex media with three particularly remarkable properties that were enabled only with the emergence of metamaterials: extreme anisotropy, extreme material parameters, and magneto-electric coupling–bi-anisotropy and chirality.

Our proposed project will focus on the following research thrusts:

Thrust 1. Structured light interactions with biaxial hyperbolic metamaterials: Develop comprehensive theory of light interactions in a homogeneous, strongly anisotropic nonmagnetic medium characterized by a diagonal dielectric tensor, with all three diagonal elements different in magnitude and sign. Experimentally demonstrate structured light transformation and de-magnification in such media. Experimentally study conical refraction revealing topological and quantitative differences as compared to those in conventional biaxial media.

Thrust 2. Novel structured light phenomena in magnetic and inhomogeneous metamaterials: Experimentally study structured light propagation in inhomogeneous metamaterials. Exploit the synergy between unique electric and magnetic properties of all-dielectric metamaterials for the realization of low-loss, compact, and broadband platform for structured light manipulation and novel spin-orbit interactions in all-dielectric inhomogeneous metamaterials.

Recent Progress

Experimental demonstration of structured light transformation and de-magnification in strongly anisotropic media: In this sub-project we focus on the unique property of hyperbolic media—the sub-wavelength light confinement enabled by the excitation of electromagnetic states with high momentum (high-k modes). It was previously shown that diffraction patterns in the anisotropic media are different from those in the far zone in air. For example, when nanoslits are combined with hyperbolic media, their diffractive nature becomes drastically different from diffraction in free space. Inside a hyperbolic medium, the propagation of diffracted light from a nanoslit is directional [2]. Since hyperbolic media can

support high-k waves, diffraction patterns can go beyond the diffraction limit [3, 4]. As a result, one of the most promising approaches to high-resolution applications (as discussed in the introduction) is a so-called hyperlens [5-8]. Hyperlenses overcome the diffraction limit by transforming evanescent waves responsible for imaging subwavelength features of an object into propagating waves. Once converted, those formerly decaying (evanescent) components commonly lost in conventional optical imaging can be collected and transmitted using standard optical components.

A hyperlens is a curved (cylindrically or spherically shaped) hyperbolic metamaterial with negative dielectric permittivity along the radial direction and a positive permittivity along the tangential direction. **Until now, a majority of the studies of subwavelength imaging and light confinement in hyperbolic metamaterials and hyperlenses focused on plane wave or Gaussian beams. Here, we investigate the interactions of a wide class of vector beams carrying an OAM in materials with extreme anisotropy.**

Figure 1 shows the numerical simulations of the vortex beam de-magnified using the structure consisting of an Ag-Ti_3O_5 multilayer, where the dielectric permittivity of Ag was taken to be –4.99-0.22*i* and that of Ti_3O_5 was 5.83 at 410nm wavelength. The intensity, field and phase distributions shown in Fig. 1 are

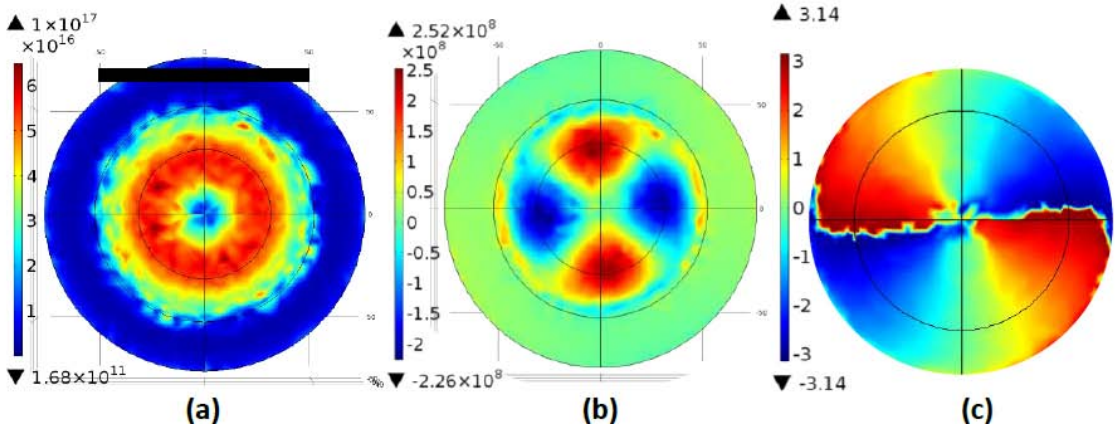

Figure 1. (a) Intensity profile of charge 2 optical vortex, (b) Electric field profile of charge 2 optical vortex, (c) Phase distribution of charge 2 optical vortex.

taken 50nm away from bottom surface of the hyperlens. The scale bar is 100nm long. The full-width at half-maximum (FWHM) of the de-magnified vortex beam is about 50nm. The intensity of the normalized electric field is about 28 times higher than the input one.

In order to fabricate spherical hyperlens sample, a 100 nm thickness Cr layer was first deposited onto a glass substrate. Then, a 50nm wide opening window was made using Focus Ion Beam (FIB). Next, HF etching was used to make hemispherical geometry. Following the first etching, the second 1-minute long HF etching was performed again aiming at elimination of the sharp edges between the hemisphere and the flat surface. Finally, multiple meta-dielectric pairs of layers were deposited onto the substrate using the E-beam evaporator. These steps are summarized in Fig. 2.

If successful, the subwavelength de-magnification of structured light beams will be particularly important for nanoscale trapping, manipulation, and fundamental spectroscopic studies of such nanoscale objects as quantum dots and molecules.

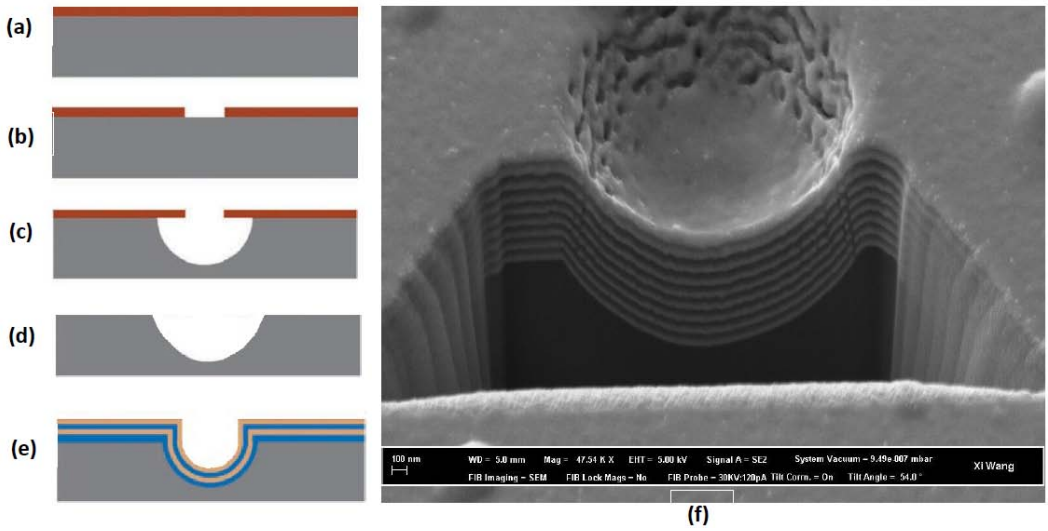

Figure 2. (a) 100nm Cr deposited on a substrate, (b) 50nm opening made by FIB, (c) First HF etching for spherical geometry, (d) Second HF etching to eliminate sharp edges, (e) Multilayer deposition, (f) SEM image of a spherical hyperlens sample with 18-layer deposition.

Future Plans

To date we made progress in fabrication and materials characterization of the hyperlens for vortex de-magnification. However, due to the fact that the size of de-magnified vortex is subwavelength, the de-magnified vortex cannot be imaged by conventional CCD camera since its size beyond the diffraction limit. Therefore, next steps will include advanced optical characterization of the hyperlens. Finally, the lens will be used to probe the dark transitions of a particular object, such as a quantum dot. Currently, the research focused on several potential candidate systems for the proof-of-principle probing experiments is underway.

Another direction of the future research is related to the unique properties of biaxial hyperbolic metamaterials that have not received much attention to date, but may reveal the novel topological and quantitative properties of such phenomena as conical refraction, which attracted significant attention in the linear and nonlinear optics of conventional biaxial crystals. it was also predicted that in the case of biaxial hyperbolic metamaterials the two sheets of the iso-frequency surface intersect forming conical singularities [9]. Conical singularities are somewhat similar to the Dirac points [10] that are of great interest in both condensed-matter physics and optics. These points, where bands cross linearly at a particular frequency and wavevector, were best studied in graphene [11, 12]. Dirac points in optical systems have been found in photonic crystals [13-18], or in materials with a frequency dependent permittivity, which may pass through zero at a particular frequency [19-21]. In these cases degeneracy occurs at a particular frequency matching either the sublattice periodicity or zero-point of the frequency dependent dielectric constant. At other nearby frequencies, there is generally no singularity. In contrast, biaxial materials have conical singularities in the iso-frequency surface in k-space, which is directly comparable to a Fermi surface. Moreover, the new form of refraction in biaxial hyperbolic structures was predicted which does not appear in the uniaxial hyperbolic metamaterials and is topologically and quantitatively different from conical refraction in ordinary biaxial materials.

Finally, we will develop meta-crystals based on meta-atoms with strong magneto-electric coupling. Artificial magnetism is one of the most remarkable properties enabled by metamaterials. Indeed, magnetic response can be engineered at any frequency (including optical range) even if the constitutive component materials are nonmagnetic. A particularly important property enabled by the metamaterials originates from the cross-terms, i.e. magnetic dipoles can be excited by the magnetic field as well as by the electric

field, while electric dipoles can be excited by the electric field as well as by the magnetic field. The effective bi-anisotropic constitutive relation in each unit cell can be described as

$$\begin{aligned} D &= \hat{\varepsilon}E + \hat{\xi}H \\ B &= \hat{\varsigma}E + \hat{\mu}H \end{aligned} \quad (1)$$

This coupling between electric and magnetic fields can be achieved through enhanced optical chirality using metamaterials.

1. N. M. Litchinitser, Structured light meets structured matter, Science 337, 1054-1055 (2012).
2. B. Wood, J. B. Pendry, and D. P. Tsai, Directed subwavelength imaging using a layered metal-dielectric system, Phys. Rev. B 74, 115116(8) (2006).
3. S. Thongrattanasiri and V. A. Podolskiy, Hypergratings: nanophotonics in planar anisotropic metamaterials, Opt. Lett. 34, 890-892 (2009).
4. S. Ishii, A. V. Kildishev, E. Narimanov, V. M. Shalaev, and V. P. Drachev, Sub-wavelength interference pattern from volume plasmon polaritons in a hyperbolic medium, Laser & Photonics Reviews 7, 265–271 (2013).
5. Z. Liu, H. Lee, Y. Xiong, C. Sun, and X. Zhang, Far-field optical hyperlens magnifying sub-diffraction-limited objects, Science 315, 1686-1686 (2007).
6. H. Lee, Z. Liu, Y. Xiong, C. Sun, and X. Zhang, Development of optical hyperlens for imaging below the diffraction limit, Opt. Express, 2007, 15, 15886-15891 (2007).
7. Z. Jacob, L. V. Alekseyev, and E. Narimanov, Optical hyperlens: Far-field imaging beyond the diffraction limit, Opt. Express 14, 8247-8256 (2006).
8. A. Salandrino and N. Engheta, Far-field subdiffraction optical microscopy using metamaterial crystals: Theory and simulations, Phys. Rev. B 74, 075103(5) (2006).
9. K. E. Ballantine, J. F. Donegan, and P. R. Eastham, Conical diffraction and the dispersion surface of hyperbolic metamaterials, Phys. Rev. A 90, 013803 (2014).
10. P. R. Wallace, The band theory of graphite, Phys. Rev. 71, 622-634 (1947).
11. K. S. Novoselov, A. K. Geim, S.V. Morozov, D. Jiang, Y. Zhang, S. V. Dubonos, I. V. Grigorieva, and A. A. Firsov, Electric field effect in atomically thin carbon films, Science 306, 666-669 (2004).
12. A. H. Castro Neto, F. Guinea, N. M. R. Peres, K. S. Novoselov, and A. K. Geim, The electronic properties of graphene, Rev. Mod. Phys. 81, 109-162 (2009).
13. M. Plihal and A. A. Maradudin, Photonic band structure of two-dimensional systems: The triangular lattice, Phys. Rev. B 44, 8565-8571 (1991).
14. O. Peleg, G. Bartal, B. Freedman, O. Manela, M. Segev, and D. N. Christodoulides, Conical diffraction and gap solitons in honeycomb photonic lattices, Phys. Rev. Lett. 98, 103901(4) (2007).
15. N. Mattiucci, M. J. Bloemer, and G. D'Aguanno, Phase-matched second harmonic generation at the Dirac point of a 2-D photonic crystal, Opt. Express 22, 6381-6390 (2014).
16. K. Sakoda, Double Dirac cones in triangular-lattice metamaterials, Opt. Express 20, 9925–9939 (2012).
17. G. D'Aguanno, N. Mattiucci, C. Conti, and M. J. Bloemer, Field localization and enhancement near the Dirac point of a finite defectless photonic crystal, Phys. Rev. B 87, 085135(6) (2013).
18. N. Mattiucci, M. J. Bloemer, and G. D'Aguanno, All-optical bistability and switching near the Dirac point of a 2-D photonic crystal, Opt. Express 21, 11862–11868 (2013).
19. L.-G.Wang, Z.-G.Wang, J.-X. Zhang, and S.-Y. Zhu, Realization of Dirac point with double cones in optics, Opt. Lett. 34, 1510-1512 (2009).
20. X. Huang, Y. Lai, Z. H. Hang, H. Zheng, and C. T. Chan, Dirac cones induced by accidental degeneracy in photonic crystals and zero-refractive-index materials, Nat. Mater. 10, 582–586 (2011).
21. L. Sun, J. Gao, and X. Yang, Giant optical nonlocality near the Dirac point in metal-dielectric multilayer metamaterials, Opt. Express 21, 21542-21555 (2013).

Project Title: Engineering of mixed pairing and non-Abelian Majorana states in chiral *p*-wave superconductor Sr_2RuO_4 and other materials

Principal Investigator: Ying Liu

Institution: Department of Physics, Pennsylvania State University, 104 Davey Lab, University Park, PA 16802

Email: yxl15@psu.edu

1. Project Scope

This project deals with odd-parity superconductor Sr_2RuO_4 and related material systems, aiming at understanding the unconventional nature of superconductivity in this material. An odd-parity superconductor is expected to feature a novel topological object, the half-flux-quantum vortex that hosts a Majorana anyons. Majorana anyons carry a non-Abelian statistics that can be used are the building block for constructing a fault-tolerated topological quantum computer. Half-flux-quantum vortices form in an odd-parity superconductor because of the availability of charge neutral spin supercurrent in addition to the normal supercurrent. Half-height magnetization steps were found in a cantilever magnetometry measurement of doubly connected mesoscopic samples of Sr_2RuO_4 in the presence of an in-plane magnetic field (J. Jang, D. G. Ferguson, V. Vakaryuk, R. Budakian, S. B. Chung, P. M. Goldbart, and Y. Maeno, Science 331, 186 (2011)), which suggests the presence of a half-flux-quantum ($\Phi_0/2 = h/4e$) state. Evidence for half flux quantum states, which can be viewed as coreless half vortices, was obtained in mesoscopic samples of Sr_2RuO_4 in the torque magnetomitry measurements. However, the existence of such an important properties has not been confirmed by any other independent measurement.

While it is widely accepted that Sr_2RuO_4 is an odd-parity superconductor based on results from a large array of experimental studies of this material, whether it is a chiral superconductor is not resolved. In this regard, both the muon spin rotation and Kerr rotation experiments suggest that there exists a spontaneous magnetic field in the bulk Sr_2RuO_4, making it a superconductor with a broken time-reversal symmetry. Within the group theory classification, among all pairing states allowed by the crystalline symmetry of Sr_2RuO_4, D_{4h}, suitable for a tetragonal crystal structure, the only pairing state that possesses a broken time-reversal symmetry is the chiral *p*-wave state. On the other hand, the chiral edge currents expected from a chiral *p*-wave superconductor have not been observed experimentally, causing considerable confusion.

The mechanism for the occurrence of odd-parity superconductor in Sr_2RuO_4 has not been resolved. The eutectic phase of Ru-Sr_2RuO_4 featuring microdomains of pure Ru embedded in the bulk single crystal of Sr_2RuO_4, an enhancement of superconducting transition temperature (T_c) has been observed and associated, unexpectedly, with the presence of dislocation. A mixed pairing state consisting of both odd- and even-parity is expected in this system because of the loss of inversion symmetry, which has not been established experimentally. In addition, the enhancement of T_c to nearly twice of that of bulk Sr_2RuO_4 makes the eutectic phase of Ru-Sr_2RuO_4 a useful system to obtain insight into the mechanism of superconductivity as well. Other materials system closely related to Sr_2RuO_4, such as $Sr_3Ru_2O_7$, may also be relevant to understanding this problem.

With the DOE support we have been working on performing sensitive measurements on the chiral edge currents, providing independent evidence for the presence of the half-flux-quantum vortex, and studying materials system closely related to Sr_2RuO_4 to provide insight into the mechanism of the unconventional superconductivity in this material.

2. Recent Progress

In the past few of years we have developed and refined a process to fabricate and measure various Sr_2RuO_4 microstructures. Because superconducting films of Sr_2RuO_4 are not yet available, all samples are prepared on thin crystals of pure Sr_2RuO_4 that are in turn prepared by mechanical exfoliation. These thin crystals are characterized by Raman spectroscopy, scanning transmission electron microscope (STEM) and electron energy loss spectroscopy (EELS). Photo or e-beam lithography was used to prepare electrical leads needed for the transport measurements. Focused ion beam (FIB) of Ga are used for cutting the microstructures including a ramp, wire, or ring. Magnetic fields can be applied perpendicular and parallel to the plane of the structure such as a ring simultaneously.

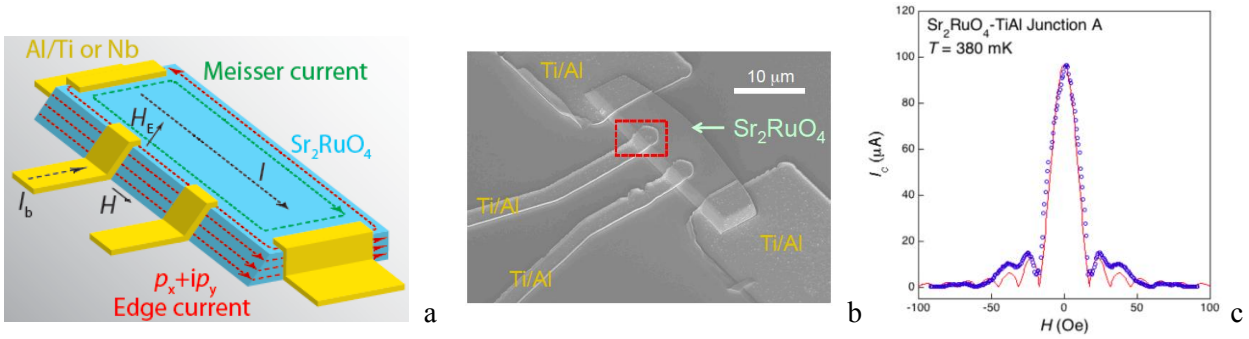

Fig. 1. a-b) Schematic 3D and cross-sectional views of a ramp-type of Josephson junction used to measure the charged chiral edge current in Sr_2RuO_4; b) SEM images of a ramp-type Sr_2 RuO_4-TiAl Josephson junction (A junction is indicated by a red dashed box); c) critical current as a function of applied in-plane magnetic field parallel to the junction taken at 0.38 K. The red curve is Airy-fit to the data.

A device of Sr_2RuO_4 consisting of four electrical leads, was shown schematically in Fig. 1a with SEM image shown in Fig. 1b. Two current leads are used to apply a current ($I_{crystal}$) to generate a magnetic field in the same direction of that of the chiral edge currents. Two as Josephson junctions prepared on the ramp will also be used to measure the crystal plate. The bias current $I_{junction}$ goes into the ground through one of the large leads. The voltage response (V) is measured from the junction to the other junction that has no current. An in-plane magnetic field (H) generated by a superconducting magnet is used to modulate the junction. Assuming that the crystal contains a single chiral domain as depicted in Fig. 1a, the combination of the chiral edge and the Meissner currents tends to create an edge magnetic field (H_E) that is parallel to the ramp, yet perpendicular to the applied magnetic field. Therefore, the Josephson junction will respond to the edge field. The chiral surface current would show up as an asymmetric response when we measure the bias current response of the junction. Josephson coupling was achieved in the device as shown in Fig. 1c. The critical current of the junction I_c as a function of the in-plane magnetic field H, shown in Fig. 1c, can be fit to an Airy pattern, suggesting that the junction is circular rather than rectangular, yielding a junction size consistent with the plate thickness.

We measured the junction resistance, R_J as a function of current repeatedly at a fixed temperature and obtained a set of R_J *vs.* I curves. From the fitting to a shifted data we obtains a set of offset currents, a histogram can then be constructed, from which we obtained an average off-set of 0.7 μA. Given that the width and the height of the Sr_2RuO_4 is 8 and 2 μm, the magnetic field corresponding to the total current is calculated in the London approximation assuming an infinitely long slab geometry. The final result gives

a maximal value of field that used to cancel the chiral edge field to be ~1 mG, four orders of magnitude smaller than the original Motsmoto-Sigrist calculation but nonzero. A manuscript is being prepared and will be submitted soon.

We also fabricated mesoscopic superconducting rings of Sr_2RuO_4 and carried out Little-Parks resistance oscillation measurements. The Little-Parks experiment will provide not only additional evidence for the presence of a half-flux states but also insight into its physical origin by tracing out the landscape for the system. We found anomalously large resistance oscillation of full-flux quantum (h/2e) without the presence of an in-plane field. However, so far, the application of an in-plane field aiming at obtaining additional evidence for the half flux states has generated one set of data that suggests the presence of two sets od resistance oscillations that are consistent with the h/4e oscillations, but the measurements have not been reproduced in another sample.

The enhanced T_c seen in the eutectic phase of Ru-Sr_2RuO_4 was attributed originally to the capillary effect at the Ru/Sr_2RuO_4 interface. In a recent study, we found that dislocations in Sr_2RuO_4, which can form easily near the Ru/Sr_2RuO_4 interface, may also be able to produce an enhancement in T_c in this material system (Y. A. Ying, N. E. Staley, Y. Xin, K. Sun, X. Cai, D. Fobes, T. J. Liu, Z. Q. Mao, and Y. Liu, **Nature Communications** 4, 2596 (2013).). This is surprising for Sr_2RuO_4 as it was found previously that superconductivity in Sr_2RuO_4 is particularly sensitive to the presence of disorder. We worked on tunneling into the interface region in the Ru-Sr_2RuO_4 eutectic phase by pressed In junction to search for mixed pairing states. Single junction tunneling data obtained so far is not conclusive.

Strontium ruthenates in the Roddlesden-Popper (R-P) series of $Sr_{n+1}Ru_nO_{3n+1}$ with a layered perovskite structure have attracted much attention since the discovery of superconductivity in the single-layer (n = 1) member of the series, Sr_2RuO_4 and the subsequent demonstration of spin-triplet pairing in this material. The study of other members in the R-P series would provide insight into the mechanism of spin-triplet superconductivity in Sr_2RuO_4. It was shown theoretically that local noncentrosymmetricity resulting from the rotation of RuO_6 octahedral in $Sr_3Ru_2O_7$ will also give rise to a spin-orbital coupling (SOC) for itinerant electrons. Here we report results of our in-plane magnetoresistivity and magnetothermopower measurements on single crystals of $Sr_3Ru_2O_7$ with an electrical or a thermal current applied along specific crystalline directions and a magnetic field rotating in the *ab* plane, showing a minimal value for field directions predicted by the local noncentrosymmetricity theory. We also found the thermopower, and therefore, the electron entropy, were found to be suppressed as the field was applied perpendicular to the thermal current and argue to result from spin-momentum locking in $Sr_3Ru_2O_7$, which imply that SOC may also be relevant to superconductivity in Sr_2RuO_4.

3. Future Plan

Our top priority is to complete the experiment on the detection of half flux states in mesoscopic rings of Sr_2RuO_4 through the Little-Parks resistance oscillation measurements. The main focus now is to measure a new set of rings we just fabricated that will minimize the spin-orbital coupling energy of spin supercurrent and enhance the stability of the half-flux quantum state. We're also in the process of setting up a ^{3}He scanning SQUID that will measure directly the flux trapped in a mesoscopic ring of Sr_2RuO_4 and image half-flux Abrikosov vortices. The PI arranged an Agreement for Joint Study between IBM and Penn State that has allowed the scanning SQUID built by Dr. John Kirtley to be on loan to PI's lab.

Domains and domain walls expected in a chiral *p*-wave superconductor have not yet been observed directly in this material. Therefore, further experimental studies that can detect and manipulate domains and domain walls are highly desired. We plan to carry out experiments on microstructures of Sr_2RuO_4 and detect the presence of domains and domain walls in Sr_2RuO_4 using Josephson effect based phase-sensitive measurements. We plan to prepare $Au_{0.5}In_{0.5}/Sr_2RuO_4$ SQUIDs for controlling and detecting domains in Sr_2RuO_4. Small magnetic field coils prepared by photo lithography can be used to create conditions favoring the formation of two domains opposite chiralities during a slow field cool. Quantum oscillation patterns obtained in zero-field and finite-field cools will be compared to see if there are signs for the present of domains. Essentially, with and without the presence of the domain correspond to a 180-degree intrinsic phase shift, which will in turn lead to a shift in the minimum position in the quantum oscillation. In addition, we will also explore the physical behavior of the flakes when their sizes become smaller and smaller. In sufficiently small flakes only a single domain exist as the domain wall is expected to be around 1 μm wide, which will show feature not present in flakes that can host multiple domains.

Ru islands in the Ru-containing Sr_2RuO_4 single crystal, may host a mixed pairing state. We plan to prepare tunnel junctions of $Au/Ru/Sr_2RuO_4$ or $In/Ru/Sr_2RuO_4$ with minimal amount of the disorder on the surface of Ru island by FIB followed by low-energy ion milling to remove the damaged surface layer to search for evidence for the mixed pairing state through both single-particle and Josephson tunneling measurement.

We will extent the angle-dependent magnetothermoelectric measurements carried out on $Sr_3Ru_2O_7$ to single crystals of Sr_2RuO_4 to search for signs of spin-momentum locking in the normal state, which will have strong implications for the mechanism of superconductivity in this material.

4. Publications resulting from DOE sponsored research (2011-2013)

1) Shaun A. Mills, Neal E. Staley, Jacob J. Wisser, Chenyi Shen, Zhuan Xu, and Ying Liu, "Ultra-thin, single-crystal superconducting nanowires of $NbSe_2$ fabricated by reactive plasma etching," **Appl. Phys. Letts.** 104, 052604 (2014); doi: 10.1063/1.4864158. arXiv:1311.1773.

2) Conor P. Puls, X. Cai, Y. Zhang, and Y. Liu, "Structural and metal-insulator transitions in ionic liquid-gated $Ca_3Ru_2O_7$ surface", **App. Phys. Lett.** 104, 253503 (2014); doi: 10.1063/1.4884277. arXiv:1312.5340.

3) Ying Liu and Zhi-Qiang Mao, "Unconventional superconductivity in Sr_2RuO_4," (Invited Review. *Physica C Special Issue on Superconducting Materials*, editors: Jorge Hirsch, Brian Maple, Frank Marsiglio). **Physica C** 514, 339–353 (2015). doi:10.1016/j.physc.2015.02.039.

4) Shaun A. Mills, Chenyi Shen, Zhuan Xu, and Y. Liu "Vortex crossing and trapping in doubly connected mesoscopic loops of a single-crystal type II superconductor," submitted to **Phys. Rev. B Rapid Comm.** (2015). arXiv:1410.8469.

5) He Wang, Weijian Lou, Jiawei Luo, and Jian Wei, Y. Liu, J. E. Ortmann and Z. Q. Mao, "Enhanced superconductivity at the interface of W/Sr_2RuO_4 point contacts," **Phys. Rev. B** 91, 184514 (2015).

6) Chenyi Shen, Hui Xing, Xinxin Cai, David Fobes, Mingliang Tian, Zhiqiang Mao, Zhuan Xu, and Ying Liu "Local noncentrosymmetricity and possible spin-momentum locking in $Sr_3Ru_2O_7$," out for an in-depth review at **Nature Comms.** (2015). ArXiv:1507.00229.

7) Xinxin Cai, Brian M. Zakrzewski, Yiquan Ying, David Fobes, Tijiang Liu, Zhiqiang Mao, and Ying Liu, "Constraints on the observation of half-flux-quantum of Sr_2RuO_4 in the presence of an in-plane magnetic field," submitted to **Phys. Rev. B** (2015). ArXiv:1507.00326.

Program Title: Understanding topological pseudospin transport in van der Waals' materials

Principle Investigator: Kin Fai Mak
Mailing Address: Department of Physics, The Pennsylvania State University, University Park, PA 16802
E-mail: kzm11@psu.edu

Program Scope

The goals of the program are to develop a fundamental understanding of the mechanisms of the valley pseudospin transport and to identify regimes for quantized valley Hall conductivity and pure valley pseudospin currents. Successful implementation of the program will help develop techniques to control pseudospin transport and design new pseudospin-based device concepts that may have an impact on the next-generation information technology. Two-dimensional (2D) van der Waals' materials of hexagonal structure including group-VI transition metal dichalcogenides, bilayer graphene, and graphene on hexagonal boron nitride (hBN) are the major materials of interest.

The main strategy that we use to achieve our goals consists of direct measurements of the pseudospin currents or valley Hall conductivity that is required to access the contribution to the valley Hall effect (VHE) from all the filled electronic states and the direction of the pseudospin current flow. The approach can overcome the deficiencies of the initial experiments on the VHE in monolayer molybdenum disulfide (MoS_2) [1], graphene on hBN [2] and bilayer graphene [3, 4] that measure either the change in the valley Hall conductivity induced by photoexcited carriers of given pseudospin state or the nonlocal voltage arisen from the combined VHE and inverse VHE. The direct measurement of the valley conductivity relies on the simultaneous determination of both the pseudospin polarization accumulated on the channel edges of the transistors driven by the VHE and the electron intervalley scattering time. The former can be probed by the Kerr rotation microscopy and the latter by the femtosecond two-pulse correlation of the anomalous Hall voltage generated by circularly polarized laser pulses.

The projects also involve fabrication of 2D vdW materials and their heterostructures by micromechanical exfoliation and transfer, and nanofabrication of electronic and optoelectronic devices based on these materials and structures.

Recent Progress

<u>Kerr rotation microscopy of valley polarization</u>

Since electrical methods do not directly probe the presence of a valley Hall current (equal flow of the K and K' electrons in opposite direction in MoS_2 or graphene produces zero Hall voltage), we developed Kerr rotation (KR) microscopy to image the valley polarization near the channel edges driven by the valley Hall current. The method has been used in similar studies of the spin

Hall effect (SHE), for instance, in GaAs [5,6]. In this method, linearly polarized light is focused onto a sample under normal incidence. The polarization of the reflected beam is rotated by an amount that is proportional to the net magnetization of the sample in the out-of-plane direction (Fig. 1a). Instead of detecting the spin magnetization in the SHE, here we measure the valley (or orbital) magnetization [7]. More specifically, under steady-state conditions, the valley Hall current density is balanced by intervalley relaxations at the sample boundaries. As a result, net valley polarizations of opposite sign are accumulated at the two edges of the device channel and are detected as KR of opposite sign (Fig. 1b, for a bilayer MoS_2 with broken inversion symmetry as discussed below).

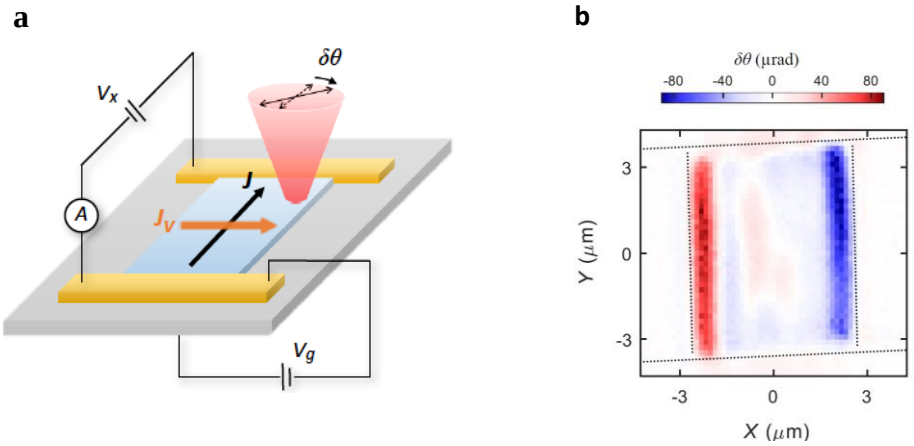

Figure 1. (a) Schematics of a MoS_2 field-effect transistor with bias voltage (V_x) applied on the source-drain electrodes and gate voltage (V_g) applied through the Si/SiO_2 substrate. In the valley Hall effect, a valley current J_V (orange arrow) in the transverse direction is induced by a longitudinal electrical current J (black arrow). The VHE is detected by focusing a linearly polarized probe beam onto the device under normal incidence and measuring the Kerr rotation angle δθ of the reflected beam. (b) Kerr rotation image of the device provides a 2D map of the valley polarization in a bilayer MoS_2 transistor with broken inversion symmetry. The dashed lines are the boundaries of the device. The source drain electrodes are along the X-direction at Y = -3 and 3 μm.

<u>Electrical control of the valley Hall effect in bilayer MoS_2 transistors</u>

Recent experimental demonstrations of the optical orientation of the valley polarization [8-11] and generation of the valley current through the valley Hall effect in monolayer MoS_2 [1] have shown the potential of 2D semiconductor transition metal dichalcogenides for valley based electronic and optoelectronic applications. The direction of the valley Hall current in monolayer MoS_2, a non-centrosymmetric crystal, however, cannot be easily tuned, presenting a challenge for valley-based applications. We demonstrated the electrical control of the valley Hall current in *bilayer* MoS_2 transistors through an electrostatic gate [7]. The inversion symmetry present in bilayer MoS_2 was broken by the gate electric field perpendicular to the plane. The valley polarization near the edges of the device channel induced by a transverse valley current was imaged by use of Kerr rotation microscopy. The polarization is out-of-plane, has opposite sign for the two edges, and is strongly dependent on the gate voltage (Fig. 2). The observation is consistent with the symmetry dependent Berry curvature and valley Hall conductivity in bilayer

MoS_2. Our results are another step towards information processing based on the valley degree of freedom.

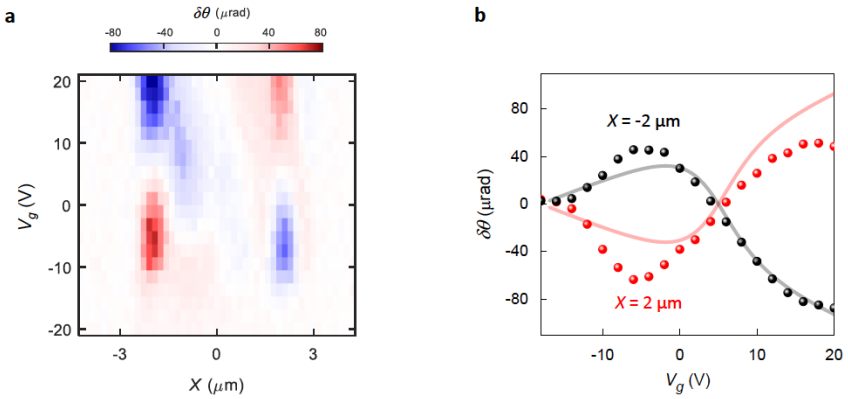

Figure 2. Electrical control of the valley Hall effect in bilayer MoS2. (a) Kerr rotation δθ map as a function of X position and gate voltage V_g. (b) Gate dependence of δθ on the left edge (X = -2 μm, black symbols) and right edge (X = 2 μm, red symbols). Solid lines are fit to the gate dependent VHE predicted by a $K \cdot P$ model.

Future Plans

<u>VHE as a function of doping density</u>

We plan to investigate the role of intrinsic Berry curvature effect and extrinsic disorder effect in driving the pseudospin currents. While the former is independent of the electron scattering time τ, the latter is in general dependent on τ. We will investigate the relation of valley Hall conductivity on τ in transition metal dichalcogenides and to identify regimes where the intrinsic topological currents dominate. The sample scattering time τ will be varied through the electrostatic doping density and the choice of substrate. Monolayer WSe2 will be used in the initial study since tuning of the doping density in a large range (from hope doping to electron doping) has been achieved.

<u>Time-resolved measurements of the electron intervalley relaxation time</u>

The valley polarization revealed by the KR is a product of the valley Hall conductivity and the electron/hole intervalley relaxation time τ_V. Independent measurement of τ_V on the same sample is therefore required to determine the valley Hall conductivity from the KR measurement. We plan to measure the free carrier intervalley relaxation time by femtosecond two-pulse correlation of the photo-induced anomalous Hall effect in the same device under the same conditions as the KR measurement. The anomalous Hall voltage will be measured as a function of delay time between a pair of circularly polarized femtosecond pulses, from which the free carrier intervalley relaxation time can be determined.

References

1. Mak, K. F., McGill, K. L., Park, J. & McEuen, P. L. The valley Hall effect in MoS_2 transistors. *Science* **344,** 1489–1492 (2014).
2. Gorbachev, R. V. *et al.* Detecting topological currents in graphene superlattices. *Science* **346,** 448–451 (2014).
3. Sui, M. *et al.* Gate-tunable topological valley transport in bilayer graphene. *arXiv*:1501.04685 (2015).
4. Shimazaki, Y. *et al.* Generation and detection of pure valley current by electrically induced Berry curvature in bilayer graphene. *arXiv:*1501.04776 (2015).

5. Kato, Y. K., Myers, R. C., Gossard, A. C. & Awschalom, D. D. Observation of the spin Hall effect in semiconductors. *Science* **306,** 1910–1913 (2004).
6. Sih, V. *et al.* Spatial imaging of the spin Hall effect and current-induced polarization in two-dimensional electron gases. *Nat. Phys.* **1,** 31–35 (2005).
7. J. Lee, K. F. Mak, and J. Shan, Electrical control of the valley Hall effect in bilayer MoS_2 transistors. *submitted* (2015).
8. Mak, K. F., He, K., Shan, J. & Heinz, T. F. Control of valley polarization in monolayer MoS_2 by optical helicity. *Nat. Nanotech.* **7,** 494–498 (2012).
9. Zeng, H., Dai, J., Yao, W., Xiao, D. & Cui, X. Valley polarization in MoS_2 monolayers by optical pumping. *Nat. Nanotech.* **7,** 490–493 (2012).
10. Cao, T. *et al.* Valley-selective circular dichroism of monolayer molybdenum disulphide. *Nat. Comm.* **3,** 887 (2012).
11. Sallen, G. *et al.* Robust optical emission polarization in MoS_2 monolayers through selective valley excitation. *Phys. Rev. B* **86,** 081301(R) (2012).

Publications

1. J. Lee, K. F. Mak, and J. Shan, Electrical control of the valley Hall effect in bilayer MoS_2 transistors. *submitted* (2015).
2. X. Xi, Z. Wang, W. Zhao, J.-H. Park, K. T. Law, H. Berger, L. Forro, J. Shan, and K. F. Mak, Evidence of Ising pairing in superconducting $NbSe_2$ atomic layers. *submitted* (2015).

Program Title: Emerging Materials

Principal Investigator: J.F. Mitchell; Co-PI: D. Phelan; SA: H. Zheng
Mailing Address: Materials Science Division, Argonne National Laboratory, 9700 S. Cass Avenue, Argonne, IL 60430
Email: Mitchell@anl.gov

Program Scope

Emerging Materials regards discovery and understanding of materials as the gateway to new science and as a means to advance knowledge of the incompletely understood physics of transition metal oxides. Our program pursues materials synthesis and single crystal growth combined with foundational scientific research on these materials, identifying important science issues, developing specific questions or testable hypotheses, and mapping these questions onto materials control strategies designed to answer them. Such strategies include manipulation of structural dimensionality or geometric frustration, control of electronic structure via doping, or atomic substitution to control composition, structure, and behavior. Importantly, pursuing this approach requires knowledge of both the relevant physics and of the materials themselves. *Emerging Materials* selects and develops its personnel and deploys its resources to achieve and to cultivate this essential, complementary understanding. We also enable and depend on an international network of collaborators who share our interests and who add value through key measurements or theoretical insights.

Transition metal oxide science is both broad and deep, requiring focused efforts to yield meaningful results. Our current program emphasizes three areas that we consider as high-impact opportunities: *Iridates and Spin-Orbit Coupling Physics*, *Random Fields in Complex Oxides*, and *Crystal Synthesis at High Pressure.* The second of these is a developing area under the purview of an early career physicist, Daniel Phelan, hired in July 2014 jointly with the Argonne Neutron and X-ray Scattering program.

Recent Progress

(1) *Iridates and SOC Physics* Since the early work by Kim asserting that the j_{eff}=1/2 state underpins the Mott insulating physics of Sr_2IrO_4, research has been driven by (i) prospects that iridates could be the next high-T_c superconductor, or at the very least tell us more about cuprates, (ii) potential routes to a quantum spin liquid in 'honeycomb' lattice materials like Na_2IrO_3, and (iii) predictions of topologically protected states of matter, for instance topological insulators (TI), in iridate pyrochlores. Our work has focused on the first two of these possibilities. In particular, we have explored how to dope the surface of canonical Sr_2IrO_4 using in situ potassium atom sputtering in an ARPES chamber. This provides an attractive alternative to bulk crystal doping, which appears to be limited and suffers from irreproducibility. Using this technique, we were able to identify the fingerprint of 'fermi arcs' in the spectrum and a 'nodal-antinodal dichotomy' as found in cuprate superconductors. Combined with our existing understanding of the magnetic exchange as 2D Heisenberg, a stronger analogy to cuprates was developed. Definitive proof of superconductivity remains an open question. In the search for QSL behavior, we have grown and studied magnetic diffuse scattering in Na_2IrO_3 (see 'Fingerprints of Kitaev Interactions in Honeycomb Iridates' below for details), a material targeted as a potential model

of a Kitaev QSL. While this material orders antiferromagnetically, our results show the signature of bond-dependent anisotropy that is a necessary condition for Kitaev physics. We have also used both chemical and electrochemical means to remove Na from the lattice, stabilizing a number of phases, including $Na_{1.5}IrO_3$ and $NaIrO_3$. Characterization of these phases is underway. We have also succeeded to grow large (~1 mm^3) single crystals of another QSL candidate, $Na_4Ir_3O_8$ ('hyperkagome lattice'). This material has been analyzed theoretically, resulting in phase diagrams that include the QSL as well as neighboring ordered states.

Highlight: Fingerprints of Kitaev Interactions in Honeycomb Iridates

Bond-directional interactions create a novel alternative to Heisenberg exchange and provide the building blocks of the Kitaev model, which has a quantum spin liquid (QSL) as its ground state. Honeycomb iridates, A_2IrO_3 (A=Na,Li), offer potential realizations of the Kitaev magnetic exchange coupling, and their reported magnetic behaviors may be interpreted within the Kitaev framework. However, the extent of their relevance to the Kitaev model remains unclear, as evidence for bond-directional exchange interactions remains indirect or conjectural. We presented direct evidence for dominant bond-directional interactions in antiferromagnetic Na_2IrO_3 and showed that they lead to strong magnetic frustration.[3] Diffuse magnetic x-ray scattering (Fig. 1) revealed broken spin rotational symmetry, with the three spin components exhibiting nano-scale correlations along distinct crystallographic directions. This spin-space and real-space entanglement directly manifests the bond-directional interactions, provides the missing link to `Kitaev' physics in honeycomb iridates, and establishes a new design strategy toward frustrated magnetism.

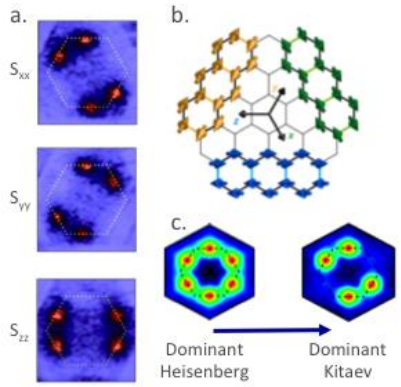

Fig. 1 Diffuse magnetic x-ray scattering (a) reveals three distinct nanoscale magnetic domains related by 120° rotations in real and spin-space, (b). Comparison of diffuse magnetic scattering to model calculations establishes the dominance of directional (Kitaev) exchange, (c).

(2) *Random Fields in Complex Oxides* Random fields, both electric and magnetic, can be seeded by intrinsic randomness and quenched disorder present in many complex oxides, ranging from strongly correlated systems that possess magneto-electronic phase separation to certain dielectrics and ferroelectrics that exhibit "relaxor" behavior. Currently, our program focuses on how random fields influence the strongly frequency-dependent dielectric susceptibility and ultrahigh electromechanical coupling present in relaxors. As an example, we recently revised the phase diagram of PMN-PT (Fig. 2(a)),[5] contrasting the evolution of ground-states of single crystals with those of polycrystalline specimens, the disparity arising from a skin effect; proper knowledge of these symmetries is critical for understanding the piezoelectric coupling at the morphotropic phase boundary. Materials control strategies that emphasize compositions with varying degrees of quenched random fields combine with structural and dynamical investigations at state-of-the-art scattering instruments, such as the recently commissioned diffuse neutron scattering instrument, *Corelli*, located at the SNS (Fig 2(b)). By providing unprecedented data

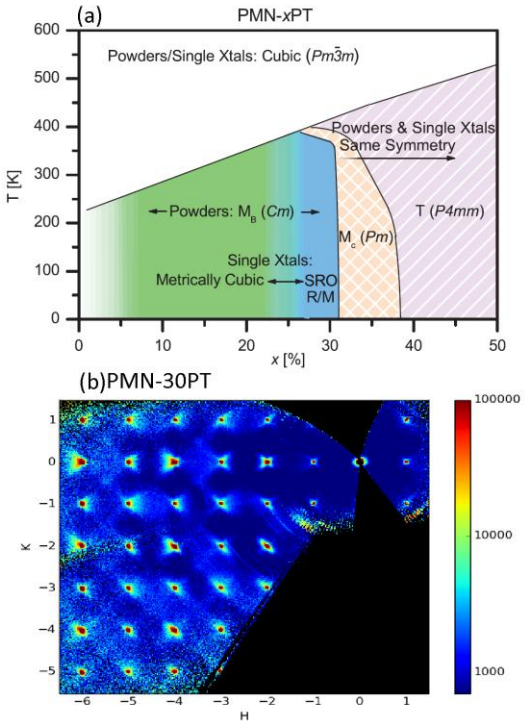

Fig. 2. (a) Phase diagram of PMN-PT determined from high resolution powder and single crystal neutron diffraction (after [5]). (b) *Corelli* measurement of PMN-30PT showing elastic diffuse neutron scattering in an unprecedented number of zones.

for modeling microscopic displacements and forces, our methodology seeks to quantify the connection between random fields, their strengths, and their impact on relaxor behavior.

(3) *Crystal Synthesis at High Pressure* Using a high pressure (150 bar) floating zone furnace installed in mid-2013, we have been growing new materials only accessible from the melt at high oxygen fugacity. Our guiding principle is to target materials that have no tie-line to a liquid under ambient pressure conditions. As an example, we have succeeded in stabilizing the heretofore unknown brownmillerite $Ca_2Co_2O_5$ phase, which adopts a rare structure in which CoO_4 tetrahedra within and between layers are all coherently ordered.[6] Surprisingly, $Ca_2Co_2O_5$ does not adopt the usual $\boldsymbol{q}$=0 ('3D checkerboard') antiferromagnetism, but rather a $\boldsymbol{q}$=(0,0,1/2) structure at intermediate temperatures and an even more complex $\boldsymbol{q}$=(0,1/3/1/6) structure as its ground state. Representation analysis suggests the possibility of a novel type of frustration in which one of the octahedrally coordinated Co ions is disordered. The frustration can be resolved by a *b*-axis field and indeed the intermediate phase is susceptible to a field-induced transition into a ferro- or canted antiferromagnetic configuration (See Fig. 7 of Ref. 6).

Future Plans

Iridates: We will concentrate on exploring Kitaev physics in the Na_2IrO_3 and $Na_4Ir_3O_8$ systems. The key questions in the latter include understanding of the short-range order observed below a 'freezing' temperature ~5.5 K and making contact to several theoretical predictions of the ground state order. Our single crystals will make this possible via x-ray and neutron scattering experiments in collaboration with both the Argonne group and that of Stephen Wilson (UCSB).

Random Fields: In relaxors, our effort will concentrate on emerging classes of Pb-free perovskites. Relaxor behavior here has been reported with isovalent B-site substitution, allowing us to interrogate a regime of weak random fields not accessible in the Pb-based compounds. In strongly correlated materials, we are pursuing magnetically phase-separated cobalt perovskites, which possess strongly varying local magnetic fields due to the co-existence of ferromagnetic, metallic regions with non-ferromagnetic, insulating regions. A focus of future work includes extending crystal growth efforts to lower-bandwidth systems, such as Pr-based cobaltites which possess unique a unique 1st-order valence transition and a highly inhomogeneous ground-state. The tendency of such materials to form oxygen vacancies necessitates oxygen-rich growth conditions – a natural candidate high pressure growth.

Crystal Synthesis at High Pressure: In addition to the cobaltites just mentioned, we will focus on layered materials in unusually high oxidation states. One target is the 'gap' region in the phase diagram of bilayer manganites, where no long-range magnetic order is observed. We will grow crystals from this region and use them to test our hypothesis that nanoscale frustration of orbital order is the underlying cause.

Selected Publications (out of 25 during 09/2013-08/2015; FWP members underlined):

(1) "Neutron-scattering-based evidence for interacting magnetic excitons in $LaCoO_3$," S. El-Khatib, D. Phelan, J.G. Barker, H. Zheng, J.F. Mitchell, and C. Leighton, Phys. Rev. B **92**, 060404 (2015).

(2) "Sr_2IrO_4: Gateway to Cuprate Superconductivity?" J.F. Mitchell, APL Mater. **3**, 062404 (2015). **INVITED ARTICLE**

(3) "Direct evidence for dominant bond-directional interactions in a honeycomb lattice iridate Na_2IrO_3," S.H. Chun, J.-W. Kim, J. Kim, H. Zheng, C.C. Stoumpos, C.D. Malliakas, J.F. Mitchell, K. Mehlawat, Y. Singh, Y. Choi, T. Gog, A. Al-Zein, M.M. Sala, M. Krisch, J. Chaloupka, G. Jackeli, G. Khaliullin, and B.J. Kim, Nature Phys. **11**, 462 (2015).

(4) "Antiferromagnetic Kondo lattice in the layered compound $CePd_{1-x}Bi_2$ and comparison to the superconductor LaPd1−*x*Bi2," F. Han, X. Wan, D. Phelan, C. C. Stoumpos, M. Sturza, C. D. Malliakas, Q. Li, T.-H. Han, Q. Zhao, D. Y. Chung, and M. G. Kanatzidis, Phys. Rev. B **92**, 045112 (2015).

(5) "Phase diagram of the relaxor ferroelectric $(1 - x)Pb(Mg_{1/3}Nb_{2/3})O_{3+x}PbTiO_3$ revisited: a neutron powder diffraction study of the relaxor skin effect," D. Phelan, E. E. Rodriguez, J. Gao, Y. Bing, Z. –G. Ye, Q. Huang, J. S. Wen, G. Xu, C. Stock, M. Matsuura, and P. M. Gehring, Phase Transitions **88**, 283 (2015).

(6) "Brownmillerite $Ca_2Co_2O_5$: Synthesis, Stability, and Re-entrant Single Crystal to Single Crystal Structural Transitions," J. Zhang, H. Zheng, C.D. Malliakas, J.M. Allred, Y. Ren, Q. Li, T.-H. Han, and J.F. Mitchell, Chem. Mater. **26**, 7172 (2014).

(7) "Prediction and Experimental Evidence for Thermodynamically Stable Charged Orbital Domain Walls," Q. Li, K.E. Gray, S B Wilkins, M. García-Fernández, S. Rosenkranz, and J.F. Mitchell, Phys. Rev. X **4**, 031028 (2014).

(8) "In situ studies of a platform for metastable inorganic crystal growth and materials discovery," D.P. Shoemaker, Y.-J. Hu, D.Y. Chung, G.J. Halder, P.J. Chupas, L. Soderholm, J.F. Mitchell, and M.G. Kanatzidis, Proc. Natl. Acad. Sci. **11**, 10922 (2014).

(9) "Fermi arcs in a doped pseudospin-1/2 Heisenberg antiferromagnet," Y.K. Kim, O. Krupin, J.D. Denlinger, A. Bostwick, E. Rotenberg, Q. Zhao, J.F. Mitchell, J.W. Allen, and B.J. Kim, Science **345**, 187 (2014).

(10) "Spin ordering and dynamics in the frustrated antiferromagnet $YBaCo_4O_{7.1}$," S. Yuan, X. Hu, P.L. Kuhns, A.P. Reyes, J.S. Brooks, T. Besara, T. Siegrist, H. Zheng, J.F. Mitchell, and M.J.R. Hoch, Phys. Rev. B **89**, 094416 (2014).

(11) "$Cu(Ir_{1-x}Cr_x)_2S_4$: a model system for studying nanoscale phase coexistence at the metal-insulator transition," E.S. Božin, K.R. Knox, P. Juhás, Y.S. Hor, J.F. Mitchell, and S. Billinge, Sci. Rep. **4**, (2014).

(12) "Oxygen Stoichiometry in the Geometrically Frustrated Kagomé System $YBaCo_4O_{7+\delta}$: Impact on Phase Behavior and Magnetism," S. Avci, O. Chmaissem, H. Zheng, A. Huq, P. Manuel and J.F. Mitchell, Chem. Mater. **25**, 4188 (2013).

Program title: Spectroscopic investigations of novel electronic and magnetic materials

Principle Investigator: Janice L. Musfeldt
Affiliation: Department of Chemistry, University of Tennessee, Knoxville TN 37996
Contact: (865) 974-3392 or musfeldt@utk.edu

Program scope

The goal of our research program is to develop a fundamental understanding of the mechanisms underlying the interplay between charge, structure, and magnetism in complex materials. This insight facilitates the development of tunable multifunctional solids and nanomaterials, which are scientifically and technologically important. Our main strategy involves investigating the dynamic response of functional materials like multiferroics, quantum magnets, frustrated systems, and compounds containing domain walls or 4- and 5*d* centers, and we perform these measurements under external stimuli (like high magnetic fields and pressures) and at very small sizes where quantum confinement becomes apparent. By so doing, we learn about the relationships between different ordered and emergent states, explore the dynamic aspects of coupling, and gain insight into the generality of these phenomena and their underlying mechanisms. In addition to broadening the understanding of novel solids under extreme conditions, multifunctional materials and their assemblies are of interest for light harvesting, spintronic, and solid state lubrication applications.

Recent progress

Several exciting discoveries were made under the auspices of our Department of Energy-supported program during the past year. Briefly, they include (i) revealing the spectroscopic signatures of structural domain walls in hexagonal $ErMnO_3$, (ii) testing the size-dependence of vibronic coupling in α-Fe_2O_3, and (iii) uncovering the electronic structure and band gaps of *h*-$LuFeO_3$. What brings these findings together is the interplay between charge, structure, and magnetism and the spectroscopic techniques with which we investigate these phenomena. A broad range of educational, outreach, and service activities also took place under the auspices of this Department of Energy grant. The majority were in the area of conference organization (for instance, the 2015 Telluride workshop on spin-orbit coupling in 4- and 5d materials and the 2014 Gordon Research Conference on multiferroic and magnetoelectric materials) and service to the National High Magnetic Field Laboratory and National Synchrotron Light Source.

Spectroscopic signatures of structural domain walls in hexagonal $ErMnO_3$: Domain walls are fascinating. In multiferroics like BiFeO3, they appear in a variety of patterns, are both insulating and conducting, and can be rearranged by external stimuli like electric field and strain. Recently, domain walls were discovered in hexagonal rare earth manganites (*R*MnO3, *R* = rare earth), where they take on either stripe or Z2 × Z3 vortex patterns depending upon the growth temperature and whether the crystals are cooled slowly or quenched. We investigated the spectroscopic response of stripe- and vortex-containing $ErMnO_3$. Because these crystals have such contrasting domain wall concentrations, the difference spectrum corresponds to the dynamic signature of the domain walls (Fig. 1). Analysis of the lattice behavior reveals differences in the Born effective charge and polarization, effectively linking microscopic texture with macroscopic properties. At the same time, fine structure and intensity variations in the *f* manifold excitations expose identical rare earth environments but changes in chemical bonding. Finally, blue shifts in the on-site and charge transfer excitations modify both the Mn crystal field and the charge gap. We bring these findings together with a discussion of hybridization and domain wall density effects, the former of which emanates from the modified local structure of the domain walls as compared to the bulk. This work advances the understanding chemical bonding in mesoscale topologies and raises a number of important questions that merit further investigation in $ErMnO_3$ and several other materials. The strong frequency dependence also holds out the promise that domain wall engineering will offer unique prospects for controlling functionality.

Fig. 1: (a) TEM images and infrared mapping at 465 cm^{-1}. (b) Vibrational properties of stripe-and vortex-containing $ErMnO_3$ from which we extract Born charge and polarization changes. These changes scale with the number of domain walls and are consistent with greater ionicity. (c) Analysis of f-manifold excitations uncovers identical local Er environments. The reduced oscillator strength in the vortex crystal is due to decreased hybridization. (d) The band gap increases from 2.5 to 3.1 eV due to decreased hybridization. The optical properties of the domain walls are strongly frequency dependent. The boundaries are lossy because this is where the domains are flipping.

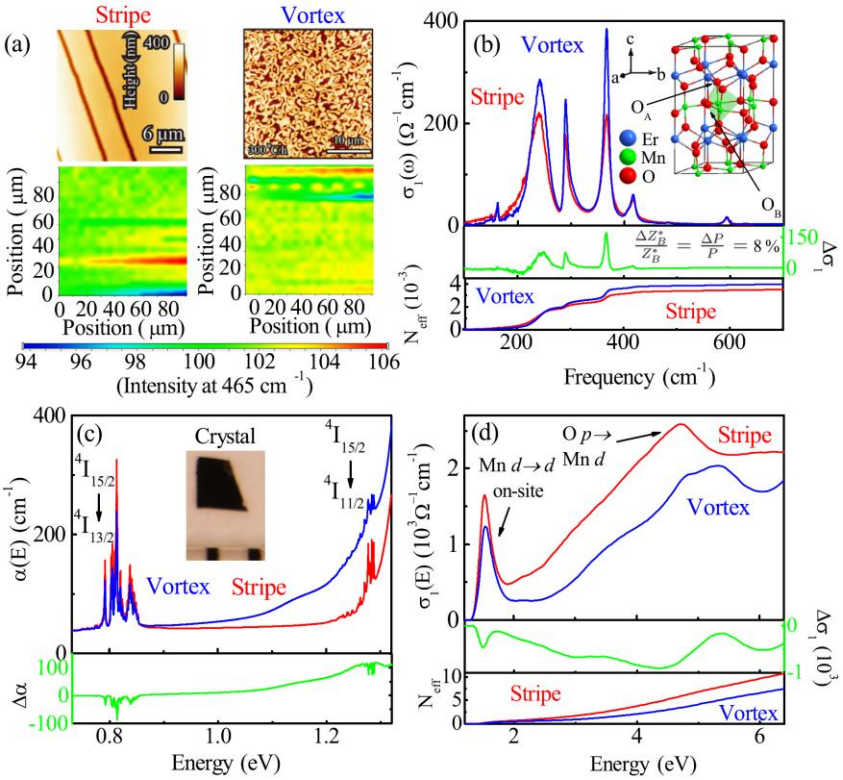

Size-dependent vibronic coupling in α-Fe_2O_3: Charge-lattice coupling is one of the most celebrated interactions in functional materials. The mechanism underlies a wide variety of scientifically and technologically important processes including superconductivity, charge density wave formation, vibronic coupling, and photochemical reactions, just to name a few. Each expresses itself in different ways. One important instance of vibronic coupling is the activation of *d*-manifold excitations in transition metal-containing molecules and materials. This mechanism, in which an odd parity phonon interacts with an on-site *d-d* excitation to break inversion symmetry, has been investigated in a number of bulk oxides like $CuGeO_3$, $LiNbO_3$, and $BiFeO_3$. Excitations of this type probe the crystal field environment and are often called color bands when they appear in the visible range. The mechanism is relatively unexplored in

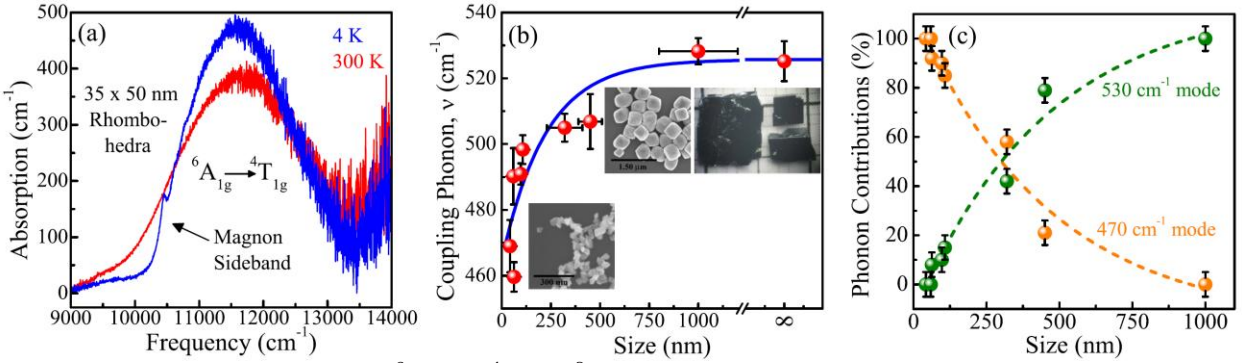

Fig. 2: (a) Close-up view of the $^6A_{1g} \rightarrow {}^4T_{1g}$ Fe^{3+} on-site excitation of α-Fe_2O_3 nano-rhombohedra. (b) Coupling phonon frequency vs. particle size in α-Fe_2O_3. Images of the single crystals, nano-cubes, and nano-tetrahedra are shown for comparison. (c) Cross-over from coupling with the 530 cm^{-1} stretching mode (solely ab-plane motion) to the 470 cm^{-1} bending mode (which also contains c-directed displacements. These findings highlight the flexibility of mixing processes in nanoscale oxides.

nanomaterials. We recently reported the discovery of finite length scale effects on vibronic coupling innanoscale α-Fe_2O_3 as measured by the behavior of vibronically-activated on-site Fe^{3+} excitations (Fig. 2). An oscillator strength analysis reveals that the frequency of the coupled symmetry-breaking phonon changes with size, a crossover that we analyze in terms of increasing three-dimensional character to the displacement pattern. We confirm these findings via direct vibrational property measurements and comparison with prior lattice dynamics calculations and, at the same time, uncover a two-state mixing process at intermediate sizes. These findings demonstrate the remarkable flexibility of mixing processes in confined systems and suggest a strategy for both enhancing and controlling energy transfer processes in other materials. They also motivate our continuing work on charge-lattice interactions in functional nanoscale oxides.

Uncovering the electronic structure and band gaps in *h*-$LuFeO_3$: The dream of room temperature ferroelectric ferromagnets is at the heart of the field of multiferroics and magnetoelectrics. Interface engineering is gaining traction in this regard. The idea is that by controlling composition and strain, room temperature exotic properties might emerge. One candidate for ferroelectric ferrimagnetism is a set of superlattices of the form $(LuFeO_3)_n$:$(LuFe_2O_4)_m$. Here, n and m are layer indices that run from 0 to 4. In order to place our investigations of the superlattices on a firm foundation, we began by studying the properties of the parent compounds, $LuFe_2O_4$ and $LuFeO_3$. Recently, we measured the optical properties of epitaxial thin films of the metastable hexagonal polymorph of $LuFeO_3$ by absorption spectroscopy, magnetic circular dichroism, and photoconductivity. Comparison with complementary electronic structure calculations reveals a 1.1 eV direct gap involving hybridized Fe $3d_{z2}$ + O $2p_z \rightarrow$ Fe *d* excitations at the Γ and A points, with a higher energy direct gap at 2.0 eV. Both charge gaps nicely overlap the solar spectrum. This work supports on on-going interest in the development of room temperature ferroelectric ferromagnets via $(LuFeO_3)_n$:$(LuFe_2O_4)_m$ super-lattice formation. The need to understand the electronic structure of these engineered materials and complement susceptibility measurements with microscopic evidence for high temperature magnetism invites our continued work in this area.

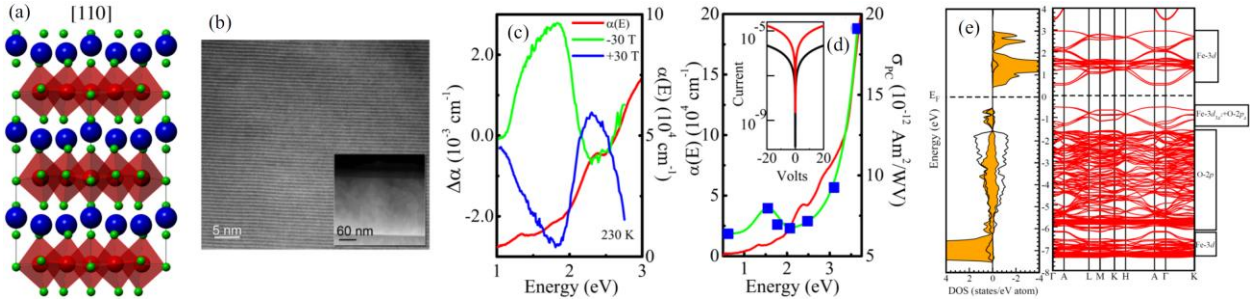

Fig. 3: (a, b) Crystal structure of $LuFeO_3$ and transmission electron microscopy of an epitaxial thin film. (c,d,e) Optical absorption, magnetic circular dichroism, photoconductivity, and first principles calculations. This data resolved the controversy about the electronic structure of $LuFeO_3$ below 2 eV.

Future plans

Several exciting efforts are planned for the coming year. Briefly, they include (i) investigating the single sheet properties of $CrSiT_3$ and $CrGeTe_3$ with a focus on band gap trends and determining the magnetic state via magnetic circular dichroism, (ii) probing the spectroscopic signatures of various topological structures like stripes and vortices on the dynamics of TaS_2 and Fe-substituted TaS_2 to understand the dynamics of topological domains in heavy chalcogenides, (iii) measuring the optical properties of spinel ferrites with a focus on magnetic circular dichroism and photoconductivity, and (iv) investigating nanoscale $CuGeO_3$ to explore finite length scale effects on vibronic coupling.

Publications emanating from this grant (2014 – 2015)

1. *Magnetic field-induced shift of the optical band gap in $Ni_3V_2O_8$*, P. Chen, B. S. Holinsworth, K. R. O'Neal, T. V. Brinzari, D. Mazumdar, Y. Q. Wang, S. McGill, R. J. Cava, B. Lorenz, and J. L. Musfeldt, Phys. Rev. B. **89**, 165120 (2014).

2. *Size-dependent vibronic coupling in α-Fe_2O_3*, K. R. ONeal, J. M. Patete, P. Chen, B. S. Holinsworth, J. Smith, N. Lee, Sang-Wook Cheong, Stanislaus S. Wong, and J. L. Musfeldt, J. Chem. Phys., **141**, 044710 (2014).

3. *Transition metal dichalcogenides for spintronic applications*, N. Zibouche, A. Kuc, J. L. Musfeldt, and T. Heine, Ann. Phys. **526**, 395 (2014).

4. *Spectroscopic signatures of domain walls in hexagonal $ErMnO_3$*, Q. -C. Sun, X. Xi, N. Lee, D. Mazumdar, R. J. Smith, G. L. Carr, S. -W. Cheong, and J. L. Musfeldt, Phys. Rev B. **90**, 121303R, (2014).

5. *Direct band gaps in multiferroic $LuFeO_3$*, B. S. Holinsworth, D. Mazumdar, C. M. Brooks, J. A. Mundy, H. Das, J. G. Cherian, S. A. McGill, C. J. Fennie, D. G. Schlom, and J. L. Musfeldt, Appl. Phys. Lett. **106**, 082902 (2015).

6. *Strong spin-lattice coupling in $CrSiTe_3$*, L. D. Casto, A. J. Clune, J. L. Musfeldt, T. J. Williams, H. L. Zhuang, R.G. Henning, K. Xiao, M.-W. Lin, B. C. Sales, J. -Q. Yan, and D. Mandrus, Appl. Phys. Lett. Mater. **3**, 041515 (2015).

7. *Magnetochromic effect in multiferroic $RIn_{1-x}Mn_xO_3$ (R=Tb, Dy)*, P. Chen, B. S. Holinsworth, K. R. O'Neal, T. V. Brinzari, C. V. Topping, X. Luo, S. -W. Cheong, J. Singleton, S. McGill, and J. L. Musfeldt, Phys. Rev. B. **91**, 205130 (2015).

Program Title: Nanostructure Studies of Strongly Correlated Materials

Principal Investigator: Douglas Natelson
Mailing Address: Department of Physics and Astronomy, MS 61, Rice University, 6100 Main St., Houston, TX 77005
E-mail: natelson@rice.edu

Program Scope: The current program applies nanostructure methods to investigate particular open questions in the physics underlying certain strongly correlated materials. Systems with strong electron-electron and electron-lattice interactions often exhibit competing ground states with varied broken symmetries, leading to rich phenomena (metal-insulator transitions; unusual magnetic or charge order; unconventional superconductivity). In some of these systems, there is experimental evidence that the standard Fermi liquid (FL) description of metals, with low energy excitations being long-lived, weakly interacting, electron-like quasiparticles, breaks down.

For example, a number of materials (most famously, the high temperature superconducting cuprates) exhibit a resistivity that varies linearly in T over a broad range down to low temperatures, rather than showing the T^2 dependence expected in the low-T limit of a Fermi liquid. This *strange metal* response is sometimes observed in proximity to a putative quantum phase transition of the ground state as a function of a tuning parameter. One interpretation of the strange metal is that the low energy electronic excitations of the system are no longer well-defined electron-like (charge $-e$, spin ½) quasiparticles with lifetimes long enough that they are energetically distinct from the Fermi sea. Some other correlated materials are *bad metals*, having a resistivity sufficiently high that a naïve interpretation in terms of traditional Drude transport implies a carrier mean free path shorter than the lattice parameter; this is the so-called Mott-Ioffe-Regel (MIR) limit. Bad metallicity at sufficiently high temperatures is perhaps unsurprising. However, some systems appear to exhibit bad metallicity even at low temperatures, when conventional expectations would predict a transition to a strong localization and an insulating ground state as $T \rightarrow 0$. In the absence of strong localization, and in putative non-Fermi liquids in general, it is unclear how to think about the long-lived, charge-carrying excitations in these systems as $T \rightarrow 0$.

With the phase of this program beginning this past June, we specifically seek to examine the nature of charge excitations in the strange metal, and the mesoscopic, quantum corrections to conduction in low temperature bad metals and non-Fermi liquids. In the strange metal, we are going to perform broad band, rf measurements of **shot noise** in tunnel junctions and nanoscale constrictions between macroscopic strange metal leads. Shot noise probes the effective charge of carriers, and comparisons with analogous structures in Fermi liquids can reveal the effects of correlations through their alteration of the current- and voltage-scaling of the noise. We have begun a collaboration with Prof. R. Dynes and Dr. S. Cybart at UC San Diego, who have high quality cuprate thin films and a unique helium ion beam tool capable of creating single-nm-width tunnel junctions with minimal ancillary damage of surrounding material[1]. In bad metals and

non-Fermi liquids, we are fabricating micro- and nanoscale device structures to examine magnetotransport on the mesoscopic scale, particularly looking at weak localization and conductance fluctuations. Initial investigations employ the hydrogen-stabilized bad metal state of H_xVO_2 established and explored in prior support periods. In a continuation of our collaboration with Prof. S. Stemmer at UC Santa Barbara, we are also preparing devices based on $SrTiO_3$ quantum wells embedded in $SmTiO_3$, a system known to exhibit either Fermi liquid or non-Fermi liquid (NFL) response depending on quantum well thickness[2].

Recent Progress: Mesoscopic quantum effects in a bad metal, hydrogen-doped vanadium dioxide (in review, Phys. Rev. B)

Background: Vanadium dioxide exhibits a first-order transition at around 65 C between a low temperature, monoclinic, insulating phase and a high temperature, tetragonal, bad metal phase. The phase transition is modified in the presence of strain, such that epitaxial films on, e.g., tetragonal TiO_2 substrates have comparatively suppressed transition temperatures. Understanding the metal-insulator transition requires accounting for both electron-electron interactions (the on-site repulsion in the half-filled vanadium *d* band) and electron-lattice interactions (the lattice distortion that dimerizes the 1d vanadium chains going into the monoclinic state). In previous work we have found that intercalation of atomic hydrogen, either through catalytic spillover[3] or direct exposure[4], suppresses the insulating state[3] and stabilizes an orthorhombic structure very close to the metallic tetragonal phase[5]. This newly accessible, low temperature bad metal has a high resistivity (milliohm-cm), and depending on strain can show little or no sign of apparently incipient strong localization as $T \rightarrow 0$. This makes it a good candidate to examine mesoscopic effects in a correlated, possible non-Fermi liquid. In this recent work, we examine low temperature magnetotransport in (a) single crystal epitaxial films (collaboration with Prof. D. Schlom at Cornell); (b) single-crystal nanobeams; and (c) single-crystal micron-scale plates. These systems were hydrogenated via exposure to H produced by a hot filament.

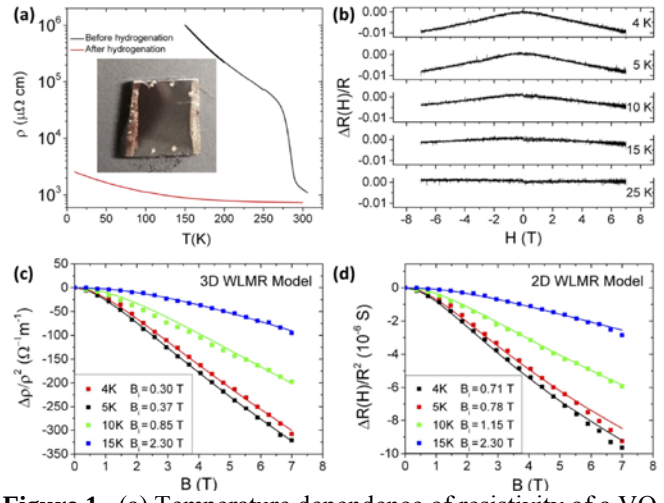

Figure 1. (a) Temperature dependence of resistivity of a VO_2 film device, before (black) and after (red) atomic hydrogenation process. The resistivity was measured during warming. Inset: photo of the device, with 6 contacts to form a hall bar structure. (b) Magneto-resistance measurement of the film device at different temperature with an external field perpendicular to film surface. (c), (d) Fits to quasi-3d and 2d weak localization.

Discussion of findings: All of these material systems exhibited magnetoresistive effects that appeared at low temperatures, growing in magnitude as T is decreased. For the films, which had resistivity increasing slightly with decreasing T at low temperatures, we find a nearly isotropic *negative* magnetoresistance consistent with quasi-3d weak localization. However, a consistent quantitative analysis is difficult because the relevant theoretical expressions assume $k_F l >> 1$, a limit apparently violated because of the high resistivity of the material. Note that in the films the current necessarily flowed transverse to the (tetragonal/orthorhombic) c axis, due to the film growth direction.

In contrast, in both nanobeams and micron-scale single-crystal flakes, the hydrogenated material had a slightly decreasing resistivity with decreasing temperature. Moreover, in these systems magnetotransport on multi-micron scales revealed a nearly isotropic *positive* magnetoresistance, growing in magnitude with decreasing temperature, qualitatively consistent with quasi-3d weak *anti*-localization. The micron-scale plates allowed confirmation that this positive magnetoresistance persisted when the current was directed (as it had been in the film devices) transverse to the tetragonal/orthorhombic c-axis. As in the film devices, quantitative analysis of this magnetoresistive effect is complicated by the high resistivity of the material.

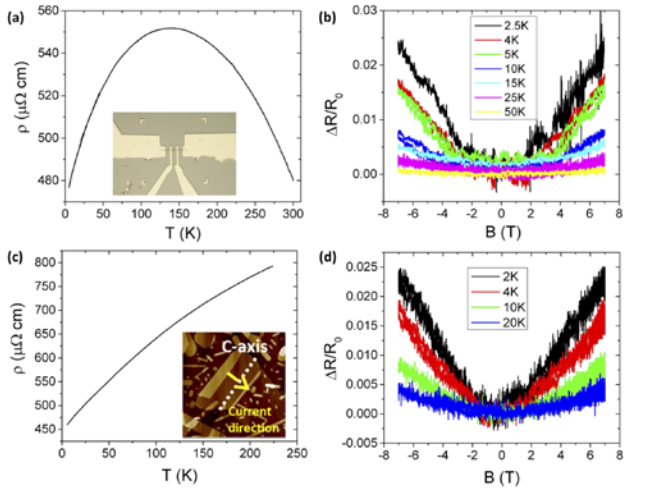

Figure 2. (a) Temperature dependence of resistivity of a VO_2 nanobeam device. Inset is its photo taken under an optical microscope. (b) Positive MR response of VO_2 nanobeam device. (c) Temperature dependence of resistivity of a VO_2 micron-size flake device, with the inset of theatomic force microscope (AFM) image of the device, and (d) its MR responses.

In sub-micron-scale structures in these systems, we further observe seemingly random but sample- and cooldown-specific magnetoresistive fluctuations. These have a magnetic field scale comparable to that of the weak localization/antilocalization seen in larger devices, grow in amplitude as T is reduced, and are on the order of 0.1 e^2/h in magnitude if modeled as a parallel conductance. This is consistent with universal conductance fluctuations.

These observations suggest that mesoscopic quantum corrections to classical conduction are present in this newly accessible low-T bad metal, even when a standard quantitative analysis suggests that conventional long-lasting quasiparticles may not be well-defined in this system. We hope that these initial results will spur theoretical investigations of the mesoscopic regime in such systems.

Future Plans: We are in the process of fabricating new samples and setting up for forthcoming measurements. With STO/SmTO quantum well samples from the Stemmer group at UCSB, we are testing lithography, dry etching, and contact metallization to prepare samples for magnetotransport examination of the mesoscopic regime. By a direct comparison between Fermi liquid and apparent non-Fermi liquid samples that are otherwise prepared identically, it should be possible to gain insights into the nature of the long-lived, low energy excitations in the NFL regime. The magnetotransport experiments will be similar in spirit to those reported in VO_2, looking at magnetoresistive effects over various device scales and field orientations.

We have completed a new rf probe for use in our Quantum Design physical property measurement system (PPMS). We are awaiting samples from UCSD in the next couple of weeks made from $YBa_2Cu_3O_7$ epitaxial films prepared by pulsed laser deposition, patterned through a combination of photolithography and helium ion beam etching. These will contain 1 nm tunnel barriers of various widths, for initial attempts at shot noise measurements. We will examine dc transport and noise of these junctions down to and through the superconducting transition.

References:

1. S. A. Cybart, E. Y. Cho, T. J. Wong, B. H. Wehlin, M. K. Ma, C. Huynh and R. C. Dynes, Nat Nano **10** (7), 598-602 (2015).
2. C. A. Jackson, J. Y. Zhang, C. R. Freeze and S. Stemmer, Nat Commun **5**, 4258 (2014).
3. J. Wei, H. Ji, W. H. Guo, A. H. Nevidomskyy and D. Natelson, Nat Nanotechnol **7** (6), 357-362 (2012).
4. J. Lin, H. Ji, M. W. Swift, W. J. Hardy, Z. Peng, X. Fan, A. H. Nevidomskyy, J. M. Tour and D. Natelson, Nano Lett. **14** (9), 5445-5451 (2014).
5. Y. Filinchuk, N. A. Tumanov, V. Ban, H. Ji, J. Wei, M. W. Swift, A. H. Nevidomskyy and D. Natelson, Journal of the American Chemical Society **136** (22), 8100-8109 (2014).

Publications in the last two years (with acknowledged DOE support):

1. Y. Filinchuk, N. A. Tumanov, V. Ban, H. Ji, J. Wei, M. W. Swift, A. H. Nevidomskyy, and D. Natelson, *J. Amer. Chem. Soc.* **136**, 8100-8109 (2014).
2. W. J. Hardy, H. Ji, E. Mikheev, S. Stemmer, and D. Natelson, *Phys. Rev. B* **90**, 205117 (2014).
3. J. Lin, H. Ji, M. W. Swift, W. J. Hardy, Z. Peng, X. Fan, A. H. Nevidomskyy, J. M. Tour, and D. Natelson, *Nano Lett.* **14**, 5445-5451 (2014).
4. B. Huber-Rodriguez, Siu Yi Kwang, W. J. Hardy, H. Ji, C.-W. Chen, E. Morosan, and D. Natelson, *Appl. Phys. Lett.* **105**, 131902 (2014).
5. W. J. Hardy, C.-W. Chen, A. Marcinkova, J. Sinova, D. Natelson, and E. Morosan, *Phys. Rev. B* **91**, 054426 (2015).
6. Jin Hu, Xue Liu, Chunlei Yue, Jinyu Liu, Huiwen Zhu, Jibao He, Jiang Wei, Z.Q. Mao, Liubov Antipina, Zakhar Popov, Pavel Sorokin, Tijiang Liu, Philip Adams, Seyed Radmanesh, Leonard Spinu, Heng Ji, and Douglas Natelson, *Nature Phys.* **11**, 471-476 (2015).

Mapping the Electron Response of Artificial 2D Heterostructures

R. M. Osgood, Jr.
Columbia University
osgood@columbia.edu

Project Scope:
This program has the goal of understanding the physics of the emergent properties in artificial 2D materials – these have been newly realized due to advances in monolayer synthesis. In our case, emergent behavior in complex systems is due to the role of confinement, both lateral and vertical, in evolving new and unexpected materials response. Our specific focus is the electronic properties of these 2D surface and near-surface systems, which when properly prepared enable the use of the powerful tools of momentum-resolved and time-resolved photoemission (ARPES) for probing electron motion and electronic structure. Our current program, which will be addressed during the CMP meeting, is artificial 2D crystals or materials. These materials allow tuning of their properties by altering surface composition, reconstruction, or confinement. Our program also has key components involving *in situ* probes and theory (via collaboration with colleagues at Columbia or international laboratories).

In our recent prior work we have answered such fundamental CMP questions such as:

- What is the electronic structure of 2D crystals in the presence of their reduced dimensionality or in more practical terms; what is the effect of layer-number and layer orientation on their electronic structure?
- What are the emergent crystal properties arising from confinement in 2D systems? Can these properties thus be "tuned" via dimensionality (or layer number) and other parameters such as voltage?
- Can we probe many-body effects in exfoliated freestanding TMDC and in other new exfoliated materials such as mono-elemental crystals, e.g., monolayer black phosphorous?
- What is the degree of coupling of vdW layers to a nearby supporting crystal substrate?
- How can we design new electronic structure using heterostructures of 2D/layered materials?

In addition, these fundamental questions can be addressed of course only in the presence of new materials handling, materials synthesis, and materials/electrode patterning methods, which are also under development in our program,. To cite one specific question for example, "What are the limits to the current *ex situ* surface preparation and how can these be overcome?"

Recent Progress:
While our program is now focused on 2D van der Waals heterostructure materials, recent research in our program has thus far resulted in significant results in other reduced dimension materials systems. Briefly these results include:

- Atomic spin chains
  - Experimental observation of spin-exchange-induced dimerization of an atomic one-dimensional system.
  - Investigating the failure of DFT-based computations for a stepped-substrate-supported Co wire.
- Understanding the complete occupied-state bandstructure of 2D *single-monolayer* van der Waals crystals/materials such as graphene and transitional metal dichalcogenides
  - Direct measurement of the thickness-dependent electronic band structure of MoS_2 using angle-resolved photoemission spectroscopy.
  - Elucidating the substrate interactions in suspended and supported *monolayer* MoS_2.

    - Probing the substrate-dependent long-range surface structure of single- and multi-layered MoS_2 by low-energy electron microscopy and microprobe diffraction.
    - Measuring the layer-dependent electronic structure of an atomically heavy two-dimensional dichalcogenide.
- Quasiparticle interference and the origin of charge density waves in 2H-$NbSe_2$
    - Interpreting the experimental evidence for a Bragg glass density wave phase in a transition-metal dichalcogenide.

A New Direction to Investigate the Electronic Structure of 2D van der Waals Heterostructures: This new direction builds upon Columbia's strength in synthesizing new 2D materials via flexible layer stacking of multiple vdW layers. In order to illustrate our work in this area, we have selected two examples of our current research in these new *heteromaterials*; but before discussing these two examples, we will first introduce this exciting, rapidly developing area.

Introduction: The interest in two-dimensional (2D) materials and materials physics has grown dramatically over the past decade. The family of 2D materials, which includes graphene (Gr), transition metal dichalcogenides (TMDCs), hexagonal boron nitride (hBN), *etc*., can be fabricated into atomically thin films since their intralayer bonding arises from their strong covalent character, while the interlayer interaction is mediated by weak van der Waals(vdW) forces. Now using the synthesis methods and physics of *homogenous* 2D materials, vdW *heterostructures* have recently emerged as a novel class of materials, in which different 2D atomic planes are vertically stacked to give rise to distinctive properties and exhibit new structural, chemical, and electronic phenomena. These artificial heterostructures, in contrast with traditional heterostructures, can be designed and assembled by stacking individual 2D layers without lattice parameter constraints. Also, the weak electron coupling at the interface of vdW heterostructures offers the possibility of combining the intrinsic electronic properties of the individual 2D layers into a new artificial material with its own distinct preoperties. For example, it has recently been shown that Gr/MoS_2 vdW heterostructures show *graphene's* high carrier mobility and broadband absorption, in combination with monolayer MoS_2's direct bandgap and thus its strong light-matter interactions. The combination of these unusual characteristics has led to potential nanodevice applications. Despite the relatively weak interactions at the Gr/MoS_2 interface, density functional theory (DFT) calculations on Gr/MoS_2 heterostructure have predicted the crossover between a direct and indirect bandgap of MoS_2 induced by the modification of interlayer orientation and photoluminescence experiments have suggested charge transfer between Gr and TMDC layers. Very recently, photoemission measurements of Gr/MoS_2 interface have been undertaken to unravel the role of electronic structure in such phenomena; however, despite these important studies, experiments on the electronic structure of stacked true-monolayer structures are lacking due in large part to complexity of sample size and preparation methods.

Tuning the Electronic Structure of Graphene/MoS_2 van der Waals Heterostructures via Interlayer Twist (Collaborators- Hone Group [Columbia] and Locatelli Beam Line [Elettra]): With the above introduction in mind, we now report our direct measurement of the electronic structure of twisted graphene/MoS_2 van der Waals heterostructures, in which both graphene and MoS_2 are of monolayer thickness. We have used cathode lens microscopy and microprobe angle-resolved photoemission spectroscopy measurements to image the surface, determine twist angle, and map the electronic structure of these artificial heterostructures. We have now found that for monolayer graphene on monolayer MoS_2, the resulting band structure reveals the absence of hybridization between the graphene and MoS_2 electronic states. Further, the graphene-derived electronic structure in the heterostructures remains intact, irrespective of the twist angle between the two materials. In contrast, the electronic structure associated with the MoS_2 layer is found to be twist-angle dependent; in particular, the relative difference in the energy of the valence band maximum at $\bar{\Gamma}$ and $\bar{K}$ of the MoS_2 layer varies from approximately 0 to 0.2 eV. Our results suggest that monolayer MoS_2 within the heterostructure becomes predominantly an

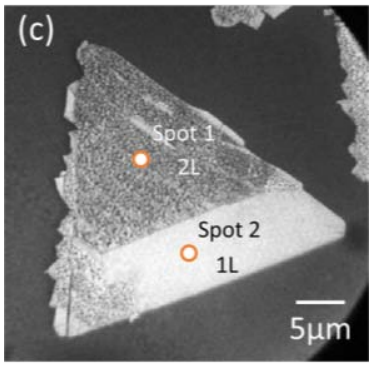

Fig.1: Bright-field LEEM measurement of a bilayer MoS_2 stack; spots indicate locations of the nano-LEED and -ARPES measurements needed our electronic structure determination.

indirect bandgap system for all twist angles except in the proximity of 30 degrees. This result enables potential bandgap engineering in vdW heterostructures simply by variation of single-layer twist angle.

Direct measurement of the tunable electronic structure of bilayer MoS_2 by interlayer twist (Collaborators: Hone Group, Jens Kunstmann [Dresden], Jerzy Sadowski and Peter Sutter[BNL]): Using angle-resolved photoemission, we have now directly measured the interlayer twist angle-dependent electronic band structure of bilayer molybdenum-disulfide (MoS_2). Our measurements, performed on arbitrarily stacked bilayer MoS_2 flakes, prepared by chemical vapor deposition, have provided direct evidence for the downshift of the quasiparticle energy of the valence-band at $\bar{\Gamma}$, the Brillouin zone center, with an interlayer twist angle by up to 200 meV at an interlayer twist angle of ~40°. Our direct measurements of the valence band structure have demonstrated the evolution of the electronic structure with twist angle, and thus have enabled the extraction of the effective hole mass as a function of the interlayer twist angle. While our results at $\bar{\Gamma}$ agree with recently published photoluminescence reports, our measurements of the quasiparticle spectrum over the full 2D Brillion zone have revealed a richer and more complicated change in the electronic structure than was initially theoretically predicted. This directly measured electronic structure mapping, including the evolution of the effective mass with twist-angle, should provide a better insight into understanding of dichalcogenide twisted-bilayer device physics and serve as a guideline for practical design of MoS_2 optoelectronic and spin-valley devices.

Future Plans:

Our near-term-future research will consist of mapping the electronic structure of 2D heterostructures of vdW materials. As explained above, these materials are at the cutting edge of DOE's interest in correlated electron and spintronics physics in condensed matter research; they offer new physics and new energy-device applications. Our overall interest here is mapping accurately the electronic and crystal structure of these new materials, which can be most readily formed by both wet and dry lift-off followed by placement of monolayer sheets. Our experiments will have the goals of understanding the electronic structure of different heterolayer stacks using electron and UV nanoprobes and investigating the variation in the electronic structure via tuning of parameters such as layer rotation or layer spacing. Finally we continue to have interest in the monolayer and layer dependence of electronic structure in alternative 2D systems, such as complex metal oxides. Due to their very small sizes we will use SPLEEM nanoprobes instruments at BNL and Elettra, as well as the higher-energy-resolution nanospectroscopy beam line at Elettra. We will also use unoccupied-state structure and dynamical behavior via nonlinear photoemission.

Publications (2012-2015):

1. Junichi Okamoto, A. J. Millis, "One-Dimensional Physics in Transition-Metal Nanowires: Renormalization Group and Bosonization Analysis." **Phys. Rev. B** 85, 115406 (2012)

2. D. Niesner, Th. Fauster, J. I. Dadap, N. Zaki, K. R. Knox, P.-C. Yeh, R. Bhandari, R. M. Osgood, M. Petrovic, and M. Kralj "Trapping Surface Electrons On Graphene Layers and Islands." **Phys. Rev. B – Rapid Comm**. 85, 081402(R (2012)

3. M. B. Yilmaz, J. I. Dadap, K. R. Knox, N. Zaki, Zhaofeng Hao, P. D. Johnson,R. M. Osgood, Jr., "Photoemission Band Mapping With A Tunable Femtosecond Source Using Nonequilibrium Absorption Resonances." **J. Vac. Sci. Technol. A** 30, 041403 (2012) – **Cover Article**

4. N. Zaki, C. A. Marianetti, D. P. Acharya, P. Zahl, P. Sutter, J. Okamoto, P. D. Johnson, A. J. Millis, R. M. Osgood, "Experimental Observation of Spin-Exchange-Induced Dimerization of an Atomic One-Dimensional System." **Phys. Rev.-B Rapid Comm.** 87, 16, 161406 (2013)

5. W. Jin, P.-C. Yeh, N.r Zaki, D. Zhang, J. T. Sadowski, A. Al-Mahboob, A. M. van der Zande, D. A. Chenet, J. I. Dadap, I. P. Herman, P. Sutter, J. Hone, and R. M. Osgood Jr. "Direct Measurement of the Thickness-Dependent Electronic Band Structure of Mos_2 Using Angle-Resolved Photoemission Spectroscopy." **Phys. Rev. Lett. 111**, 106801 (2013) – **Highly Cited Paper: ISI Web of Science**

6. P.-C. Yeh, W. Jin, N. Zaki, D. Zhang, J. T. Sadowski, A. Al-Mahboob, A. M. van der Zande, D. A. Chenet, J. I. Dadap, I. P. Herman, P. Sutter, J. Hone, R. M. Osgood, Jr., "Probing Substrate-Dependent Long-Range Surface Structure of Single- and Multi-Layered Mos_2 by Low-Energy Electron Microscopy and Microprobe Diffraction." **Phys. Rev. B.** 89, 155408 (2014)

7. N. Zaki, H. Park, R. M. Osgood, A. J. Millis, C. A. Marianetti, "The Failure of DFT-Based Computations for a Stepped-Substrate-Supported Correlated Co Wire." **Phys. Rev. B** 89, 205427-205432 (2014)

8. P.-C. Yeh, W. Jin, N. Zaki, D. Zhang, J. T. Sadowski, A. Al-Mahboob, J.I. Dadap, I.P. Herman, P. Sutter, R. M. Osgood, Jr., "Layer-Dependent Electronic Structure of an Atomically Heavy Two-Dimensional Dichalcogenide." **Phys. Rev. B.** 91, 041407(**R**) (**2015) - Editors Suggestion**

9. W. Jin, P.-C. Yeh, N. Zaki, D. Zhang, J. T. Liou, J. I. Dadap, I. P. Herman, R. M. Osgood, Jr., "Substrate Interactions in Suspended and Supported Monolayer Mos_2: Angle-Resolved Photoemission Spectroscopy." **Phys. Rev. B.** 91, 121409(R) (2015)

10. C. J. Arguello, E. P. Rosenthal, E. F. Andrade, W. Jin, P. C. Yeh, N. Zaki, S. Jia, R. J. Cava, R. M. Fernandes, A. J. Millis, T. Valla, R. M. Osgood Jr., A. N. Pasupathy, "Quasiparticle Interference and the Origin of Charge Density Waves in 2H-$Nbse_2$." **Phys. Rev. Lett.** 114, 037001 (2015) – **Cover Article, Editor's Suggestion**

11. J. Okamoto, C. J. Arguello, E. Rosenthal, A. Pasupathy, A. J. Millis "Experimental Evidence for A Bragg Glass Density Wave Phase in A Transition-Metal Dichalcogenide." **Phys. Rev. Lett.** 114, 026802 (2015)

12. J. Okamoto, A. J. Millis, "Effect of dilute strongly pinning impurities on charge density waves." **Phys. Rev. B.** 91, 184204 **(**2015)

13. Wencan Jin, Po-Chun Yeh, Nader Zaki, Daniel Chenet, Ghidewon Arefe, Yufeng Hao, Alessandro Sala, Tevfik Onur Mentes, Jerry I. Dadap, Andrea Locatelli, James Hone, and Richard M. Osgood, Jr. "Tuning the Electronic Structure of Graphene/MoS_2 van der Waals Heterostructures via Interlayer Twist" (submitted to **PRX**)

14. Rui Lou, Zhonghao Liu, Wencan Jin, Haifeng Wang, Zhiqing Han, Kai Liu, Xueyun Wang, Tian Qian, Yevhen Kushnirenko, Sang-Wook Cheong, Richard M. Osgood, Jr., Hong Ding, and Shancai Wang "Sudden gap-closure across the topological phase transition in $Bi_{2-x}InxSe_3$ (Under review in PRB)

15. Po-Chun Yeh, Wencan Jin, Nader Zaki, Jens Kunstmann, Daniel Chenet, Ghidewon Arefe, Jerzy T. Sadowski, Jerry I. Dadap, Peter Sutter, James Hone, and Richard M. Osgood, Jr."Direct measurement of the tunable electronic structure of bilayer MoS_2 by interlayer twist" (submitted)

Synthesis and Observation of Emergent Phenomena in Heusler Compound Heterostructures

Principal Investigator: C. J. Palmstrøm; Co-PIs: A. Janotti (Univ. of Delaware)
Mailing Address: Electrical and Computer Engineering, University of California at Santa Barbara, Santa Barbara, CA 93106-9560
Email: cpalmstrom@ece.ucsb.edu

Program Scope

The goal of the program is to grow and investigate the electronic and magnetic properties of Heusler compound heterostructures through experiment and theory. By merging the two, we hope to use theory to guide experiment and experiment to refine theory. This program aims to investigate the stability, and electronic band structure, and influence of defects and strain in half-Heusler compounds. Particular focus will be given to the subset of half-Heusler compounds which have been predicted to be topologically insulating[1-3]. These topologically non-trivial materials exhibit a metallic surface and insulating bulk and should have surface states that are spin-momentum locked with an odd number of Dirac points[4,5].

To achieve these goals, molecular beam epitaxy (MBE) will be used to grow the Heusler compounds. Characterization will be conducted using *in-situ* scanning tunneling microscopy/spectroscopy (STM/STS), x-ray photoelectron spectroscopy, Auger electron spectroscopy, magneto optic Kerr spectroscopy, reflected high-energy electron diffraction (RHEED), and low-energy electron diffraction (LEED) as well as *ex-situ* angle-resolved photoemission spectroscopy (ARPES), temperature dependent magnetotransport, and superconducting quantum interference device magnetometry. These experimental techniques will then be paired with first-principle calculations with special attention being made to understand the influence of surface reconstructions, strain, and point defects.

Recent Progress*

Growth and characterization of MBE grown PtLuSb (001) thin films by first-principles calculations and angle-resolved photoemission spectroscopy

Recently, we have examined the MBE growth of PtLuSb thin films on lattice matched $Al_xIn_{1-x}Sb$ buffers on GaAs (001) substrates. To establish a baseline, we have focused on the unstrained and unintentionally doped material first. While optimizing

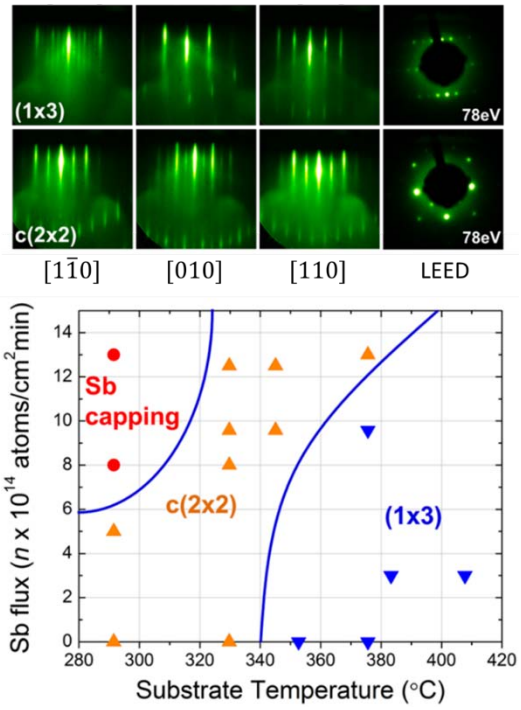

Figure 1. RHEED and LEED patterns of PtLuSb (001) for various growth conditions along with corresponding reconstruction map[7].

the growth conditions, we have discovered several surface reconstruction regimes, similar to III-V materials. As seen in figure 1, for antimony rich conditions (high antimony overpressure and/or low substrate temperature) a c(2x2) reconstruction is apparent while for antimony poor conditions (low antimony overpressure and/or high substrate temperature) a (1x3) reconstruction is apparent. Furthermore, by conducting STM of quenched samples[6], these reconstructions may be seen in real space.

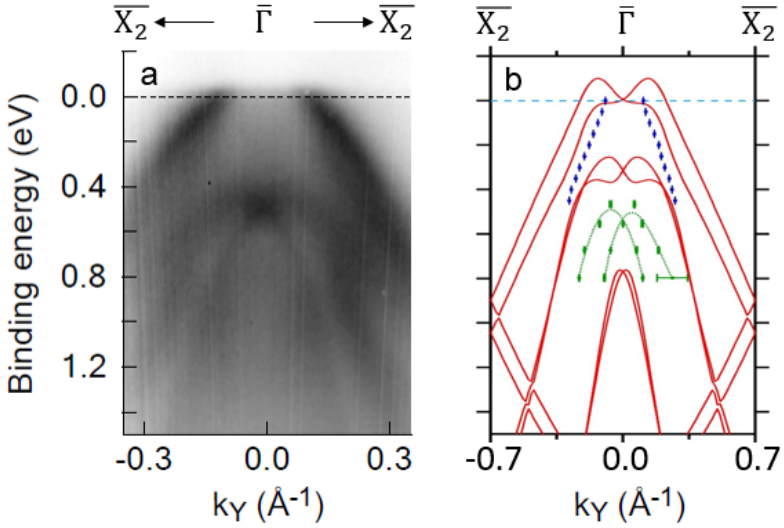

Figure 2. (a) ARPES in-plane intensity map and (b) corresponding first-principles bulk band structure calculation (red) with overlaid surface state positions (blue and green).

In order to examine the electronic structure, ARPES measurements were taken at MAX-Lab beamline I4 in Lund, Sweden. Considering that PtLuSb is a topological insulator candidate, ARPES is particularly well-suited for this investigation due to its inherent surface sensitivity. As see in figure 2, the measured electronic band structure is dominated by surface state behavior. Although not shown here, by examining the photon energy dependence, the bulk band motion can also be seen. To confirm that these strong states are surface states, figure 3 shows the k_z

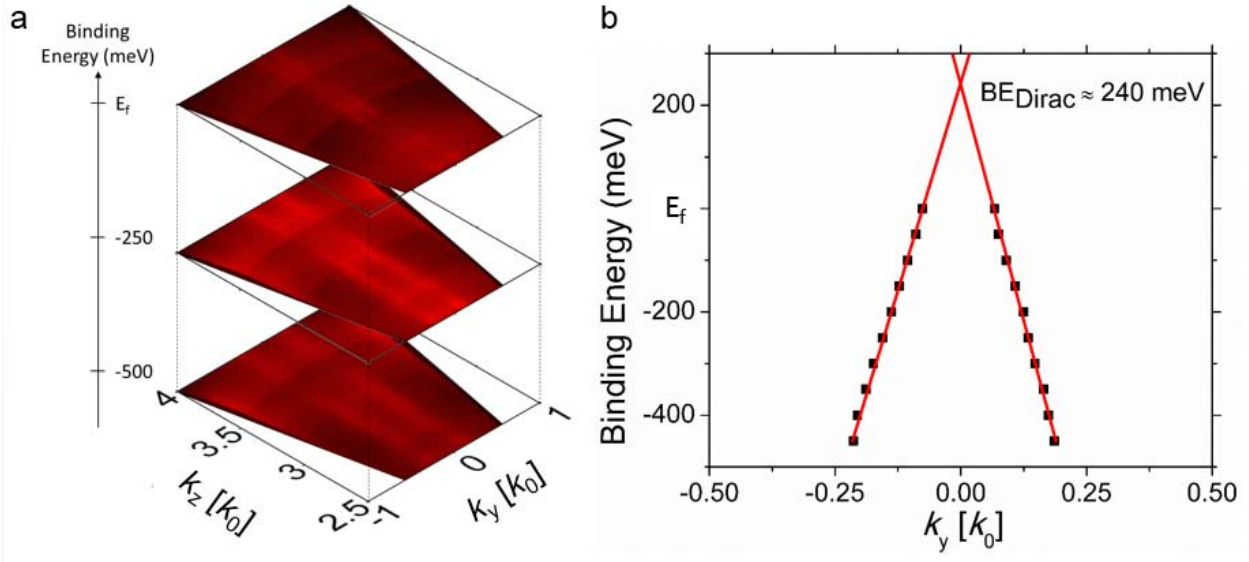

Figure 3. (a) ARPES k_z dependence confirming that the blue state in figure 2b is a surface state. (b) Linear fit to surface state position (error bars are one standard deviation) suggesting a Dirac-like crossing approximately 240 meV above the Fermi level.

dependence. We immediately note a lack of dispersion, consistent with expectation of the confined nature of a surface state. By extrapolating the upper surface state (blue) above the Fermi level, we find a Dirac-like feature with a crossing approximately 240 meV above the experimental Fermi level. These promising results suggest the presence of a surface state with linear dispersion and projected crossing above the Fermi level in PtLuSb, which agrees well with the theory expectations of topological behavior. Presently, we are further pursuing spin-ARPES measurements that can reveal the presence of spin-textures (a key element in topologically non-trivial materials).

Future Plans

(1) Explore the influence of strain and doping/alloying on the growth and electronic properties of PtLuSb

To date, we have conducted angle-resolved photoemission spectroscopy measurements (ARPES) of unstrained and undoped PtLuSb thin films. While we observe the expected zero bandgap semiconducting density of states, to effectively use any topological behavior in a device, a true bandgap is needed. Previous theory calculations have suggested that introducing biaxial tension may both increase the strength of the topological character (by increasing the Γ_6- Γ_8 band inversion) but also open a bulk bandgap[1,2]. In principle, by tuning the strain environment it should be possible to tune the apparent band-inversion across the trivial to non-trivial transition to turn on and off the topological behavior. Secondly, some previous work on $Co_xNi_{1-x}TiSb$ has suggested by introducing dopants it may be possible to tune the Fermi level position. If possible in PtLuSb, by combining strain and doping the Dirac point may be centered at the Fermi level and within the bandgap. However, even if such a configuration proves infeasible for PtLuSb, understanding the nature of how dopants and strain interact with the band structure in half-Heusler compounds would prove invaluable. With a large number of candidate half-Heusler topologically insulators, such knowledge could be translated to other materials where the energetics are more favorable.

(2) Theory-Experiment comparison

First-principles calculations based on the density functional theory (DFT) within the generalized gradient approximation (GGA) and the screened hybrid functional of Heyd, Scuseria, and Enrzerhof (HSE) will be used to identify low energy atomic surface and interface arrangements that are consistent with the in-situ STM and XPS studies. The calculated electronic band structures and the orbital composition of the bands near the Fermi level will provide fundamental understanding on optical and transport properties and will be compared with STS and ARPES measurements.

(3) Develop a vacuum suitcase for sample transfer from UCSB-MBE to ALS-Spin-ARPES

An atomically clean and well-ordered sample surface is required for high quality ARPES data. In order to transfer samples grown in the UCSB-MBE that cannot be capped and decapped, an ultra-high vacuum suitcase will be designed and developed to allow transfer to the ALS-ARPES system without air exposure.

*This DOE project funding has just started (8/1/2015). The experimental Progress Reported here was supported by ARO W911NF-12-1-0459, which ends 10/9/2015, and the theoretical progress was supported by this DOE grant.

References

1 S. Chadov, X. Qi, J. Kuebler, G. H. Fecher, C. Felser, and S. C. Zhang, *Tunable multifunctional topological insulators in ternary Heusler compounds,* Nature Materials **9,** 541 (2010).

2 H. Lin, L. A. Wray, Y. Q. Xia, S. Y. Xu, S. A. Jia, R. J. Cava, A. Bansil, and M. Z. Hasan, *Half-Heusler ternary compounds as new multifunctional experimental platforms for topological quantum phenomena,* Nature Materials **9,** 546 (2010).

3 W. Al-Sawai, H. Lin, R. S. Markiewicz, L. A. Wray, Y. Xia, S. Y. Xu, M. Z. Hasan, and A. Bansil, *Topological electronic structure in half-Heusler topological insulators,* Physical Review B **82,** 125208 (2010).

4 Y. Ando, *Topological Insulator Materials,* Journal of the Physical Society of Japan **82,** 102001 (2013).

5 X.-L. Qi and S.-C. Zhang, *Topological insulators and superconductors,* Reviews of Modern Physics **83,** 1057 (2011).

6 S. J. Patel, J. K. Kawasaki, J. Logan, B. D. Schultz, J. Adell, B. Thiagarajan, A. Mikkelsen, and C. J. Palmstrom, *Surface and electronic structure of epitaxial PtLuSb (001) thin films,* Appl. Phys. Lett. **104,** 201603 (2014).

Publications

None

Development of NV-centers-in-diamond optical sensing at the nanoscale

R. Prozorov, V. V. Dobrovitski, M. Hupalo, Y. Lee, M. Tringides, D. Vaknin, J. Wang

Ames Laboratory, Ames, Iowa 50011

Program Scope

Magnetic NanoSystems: Making, Measuring, Modeling, Manipulation.

The scientific goal of this program is to investigate pathways that connect quantum mechanical mechanisms governing nano-scale magnetism with macroscopic magnetic properties emerging as the system size increases from nano- to macro- length scales. We are interested in studying the effects of quantum confinement and reduced dimensionality in magnetic nano- and meso-scale structures, study quantum coherence and spin coupling to the environment, investigate charge and spin currents in topologic insulators and examine out of equilibrium dynamics of quantum magnetism in these systems. Advanced experimental probes, such as novel optical magnetic field sensor based on nitrogen–vacancy centers in diamond and spin-polarized scanning tunneling spectroscopy will be used to map magnetic and electronic responses, while x-ray magnetic circular dichroism and ultra-fast optical spectroscopies will provide information on element-resolved local moment and non-equilibrium charge and spin dynamics, respectively. Theoretical analysis of the collected data will provide details of static and dynamic spin and charge distributions as a function of external parameters and this information will be coupled with numerical calculations of spin - resolved electronic structure and simulation of quantum spin dynamics to obtain microscopic picture of quantum magnetism in the systems of interest, such as magnetic nanoislands and topological insulators.

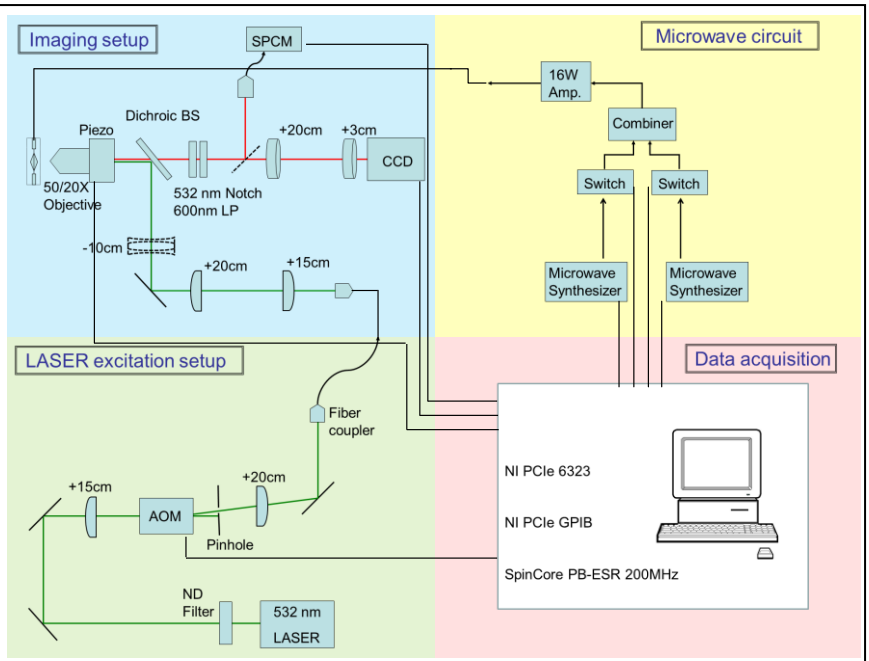

Fig. 1 principle schematics of the NV-sensing apparatus.

Recent Progress

Here we focus only on one aspect of our program – the development of nanoscale sensing based on NV-centers in diamond color centers whose optical fluorescence levels depend sensitively on local magnetic field. Other types of sensing (e.g., temperature or local NMR) are also possible. This novel technique has just graduated from the research labs with only a few instruments available in the world. For the description of the physical principles behind this technique, please see Refs. [1-3]. The setup is shown schematically in Fig. 1. For the low-temperature operation, the imaging part is to be replaced by the low-temperature (4.2 K) version. An example of the first test data, Fig. 1, shows optically detected electron spin resonance (ESR) of an ensemble of NV centers embedded in a single crystalline diamond substrate. The inset in the upper panel shows hyper-fine structure due to the (field-independent) interaction between NV electronic spin and ^{14}N nuclear spin (I=1). An applied magnetic field was measured from the frequency shift compared to B=0 spectra (bottom panel). In this continuous wave (CW) mode, the field sensitivity is about 30 μT/√Hz. In a CW experiment, the florescence is measured under continuous excitation of a 532 nm laser light and, simultaneously, sweeping - frequency microwave radiation. A more versatile approach leading to a better sensitivity and reduction of the data acquisition time is to use pulse-ESR, which is currently being implemented. For the low – temperature operation a combo system incorporating two XYZ scanners and a confocal microscope inside a helium dewar was acquired from Attocube (Germany). Figure 3 shows the primary components of this system. We are currently developing a single – NV center scanning with this system, which will require the development of AFM tips functionalized with NV centers.

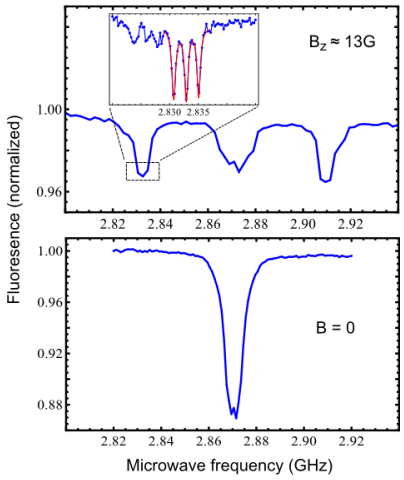

Fig. 2 Magnetic field – sensitive optical ESR spectra of NV centers embedded in a single crystalline diamond substrate.

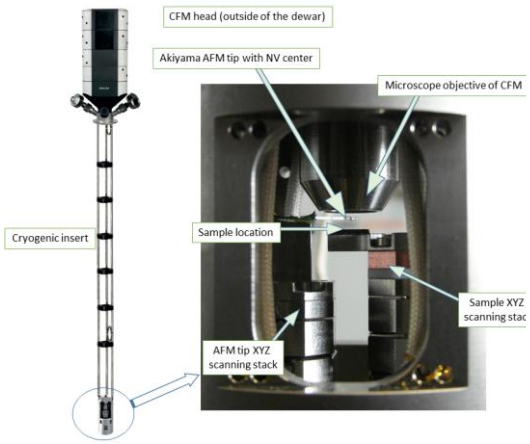

Fig. 3 Cryogenic insert (left) and sample space of our low-temperature Attocube atomic force microscope (AFM) / confocal microscope (CFM) setup also showing two XYZ scanning piezo stacks.

Concurrently with the instrumentation development we performed several important studies focused on the spin dynamics of NV centers in diamond. In particular, we have studied in detail the dynamics of the electronic spin of the NV center in diamond under strong Rabi driving in the

presence of environmental magnetic noise. While the case of simple Rabi oscillations has been studied by us before [4], we now considered the strong driving signal whose phase is periodically switched in time by 180º. This regime, known as rotary echo, ensures good stability in the case of slowly fluctuating driving strength, which often happens in real experiments [5-7]. We have shown more importantly, that the rotary echo provides excellent protection of the NV spin from decoherence created by the environmental magnetic noise [8]. We addressed the problem analytically and confirmed our conclusions with direct numerical simulations. It also provided important insights into the quantum spin dynamics under time-varying strong driving. Next, we investigated quantum dynamics of the NV spin coupled to a bath of nuclear spins in the presence of the rotary-echo driving [9]. We have discovered that by fine-tuning the time between the phase changes of the driving field, the coupling between the NV spin and an arbitrary nuclear spin in the neighborhood of the NV center can be selectively preserved, while the coupling to all other nuclear spins is turned off (decoupled) by the rotary echo driving. Besides providing important insights into the joint electron-nuclear spin dynamics, this effect is very important for sensing individual nuclear spins and thus allowing highly selective one-by-one detection (nanoscale tomography) of the nuclear spins in the nanometer vicinity of the NV center. Our direct numerical simulations confirmed selective addressing of each of fourteen ^{13}C spins located near NV center in diamond, with spectral resolution improved 10-100 times compared to previously developed methods, - a significant improvement in the field of the NV-based sensing at nanoscale. In addition to magnetic field sensing, we have investigated the quantum dynamics of the NV centers beyond the two-level approximation [10], taking into account all three levels of the electronic spin S=1. We have developed the scheme for measurement of temperature using the zero-field splitting of the NV spin as a probe. Together with the experimental group of Prof. D. Awschalom (U. Chicago), we developed a method which allows high precision (<0.5 K error) temperature measurement at the nanoscale and at ambient conditions [10].

Future Plans

Our immediate goal is to focus on fabricating diamond AFM probes for NV magnetometry as well as investigating ways to functionalize AFM probes with nano-diamonds containing single NV centers. We will continue working on adaptation of the Attocube AFM/CFM system to become a complete low-temperature NV-magnetoScope. This includes the modification of optics in CFM for magnetometry and introduction of microwave to the probe region for NV magnetometry. In addition, we will develop advanced data acquisition routines for magnetic imaging and experiment on novel techniques for fast acquisition. Once achieved, the following scientific studies will be undertaken: (1) magnetic phenomena in superconductors, such as resolution of individual Abrikosov vortices, their periodic arrangement, and interaction with structural defects. This will be done in bulk crystals and compared to nano-islands of Pb on various substrates to study the confinement (or even parity) effects. (2) distribution of magnetization in magnetic nanoislands and nanoparticles. For example, Dy deposited epitaxially on graphene is found to grow fcc (111) instead of hcp (0001) islands expected from its bulk structure. Preliminary magnetic measurements using x-ray circular dichroism indicate that Dy

nanoislands do not exibit long – range magnetic order. With NV-sensing we will investigate magnetization of the individual nanoislands in order to understand such a pronounced size effect. Over the longer term, we will attempt to functionalize the islands, for example, by placing various molecules between them and trying to attach meso-scale electric leads, and to detect the induced changes with the NV-magnetoScope. (3) topologically non-trivial systems with nano- and meso- scale magnetic modulations. Specifically, we are interested in attempting to detect nano- and meso- scale magnetism related effects in electronic systems with topologically protected states. For example, to study electric current- induced spin polarization due to spin-momentum locking in Bi_2Se_3 films of different thickness. Similarly, imaging of the magnetic fields of the ballistic (dissipassionless) edge channels in HgTe quantum wells in the quantum spin Hall regime recently was demonstrated with scanning SQUID [11]. There is also a possibility of net charge current without applied magnetic or electric fields in the presence of ferromagnetic order on the edges of quantum spin Hall insulator. Another example of interest is a possibility of spontaneous currents due to Andreev bound states. Finally, exotic magnetic structures, such as skyrmions, can be studied with the NV-sensing.

References

1. J. R. Maze *et al.*, *Nature* **455**, 644 (2008).
2. L. Rondin *et al.*, *Rep. Prog. Phys.* **77**, 056503 (2014).
3. D. Le Sage *et al.*, *Nature* **496**, 486 (2013).
4. V. V. Dobrovitski *et al.*, *Phys. Rev. Lett.* **102**, 237601 (2009)
5. C. D. Aiello *et al.*, *Nature Comm.* **4**, 1419 (2013).
6. A. Laraoui and C. A. Meriles, *Phys. Rev. B* **84**, 161403 (2011).
7. J. Cai *et al.*, *New J. Phys.* **15**, 013020 (2013).
8. V. V. Mkhitaryan and V. V. Dobrovitski, *Phys. Rev. B* **89**, 224402 (2014).
9. V. V. Mkhitaryan *et al.*, arXiv:1503.06811 (2015).
10. D. M. Toyli *et al.*, *PNAS* **110**, 8417-8421 (2013).
11. K. C. Nowack *et al.*, *Nat. Mat.* **12**, 787 (2013).

Publications (select from the 26 papers published by this project in the last two years.

Y. Lee and B. N. Harmon, *J. App. Phys.* **113**, 17e145 (2013).

D. Vaknin and F. Demmel, *Phys. Rev. B* **89**, 2180411R (2014).

X. Liu *et al.*, *Phys. Rev. B* **90**, 155444 (2014).

R. S. Dhaka *et al.*, *Phys. Rev. Lett.* **110**, 067002 (2013).

V. V. Dobrovitski *et al.*, *Annual Reviews (Cond. Mat.)* **4**, 23-50 (2013).

D. M. Toyli *et al.*, *PNAS* **110**, 8417-8421 (2013).

M. S. Blok *et al.*, *Nature Phys.* **10**, 189 (2014).

T. H. Taminiau *et al.*, *Nature Nanotech.* **9**, 171 (2014).

A. Patz *et al.*, *Nature Comm.* **5**, 3229 (2014).

Program Title: Engineering topological superconductivity towards braiding Majorana excitations

Principle Investigator: Leonid P. Rokhinson
Mailing Address: Department of Physics, Purdue University, West Lafayette, IN 47906
E-mail: leonid@purdue.edu

Program Scope

The goal of the program is to develop systems which support excitations with non-Abelian statistics and to study properties of these new unconventional states of matter. In such matter some quantum numbers of a many-particle condensate are encoded in the topology of the state and protected from small local perturbations. These protected degrees of freedom can be used to encode quantum information and are the basis of fault-tolerant topological quantum computer proposals, which presents a robust alternative to the conventional quantum computation where decoherence poses the major technological challenge.

With DOE support we explored different systems where topologically non-trivial phases can be realized and, most importantly, exchange statistics of non-Abelian excitations can be probed experimentally. Over the last two years we studied superconductivity in topological insulator nanoribbons and developed a new system where helical states, precursors of topological superconductivity, can be formed in quantum Hall regime. Most importantly, we worked with crystal growers to improve InSb-based heterostructures and to develop new InAsSb materials, where we expect enhancement of the parameter space for topological superconductivity. In the proposed research program we will continue development and characterization of InAsSb materials, investigate proximity-induced superconductivity in one-dimensional nanostructures, and measure spectroscopic signatures of Majorana fermions, including ac fractional Josephson effect. The major objective of the proposed research is to develop quasi-one dimensional structures where non-Abelian statistics of topological excitations can be tested. We propose experiments to demonstrate a σ_x gate with a rotating magnetic field.

Recent Progress

A. Development of a new system with gate-defined helical domain walls. One of the major research achievements over the last 2 years is devising and development of a new platform where Majorana fermions and higher order non-Abelian excitations can be created, braided, manipulated and fused in a controllable fashion. At the heart of the platform is a high mobility 2D gas where Lange *g*-factor changes sign at high magnetic fields. This unusual behavior is realized in CdTe/CdMgTe quantum well heterostructures with paramagnetic impurities. A unique advantage of this material is a possibility to substitute some Cd atoms with Mn, which forms a spin-5/2 neutral paramagnetic impurity (there are no atoms with a partially filled d-shell and three valence electrons to make an analogous substitution in GaAs). Presence of paramagnetic impurities drastically changes energy splitting of spin-up and spin-down subbands in magnetic fields: the splitting is large at small fields, decreases as the field increases, and

changes sign at critical field B^* (as shown in Fig. 1 for $|0\uparrow\rangle - |1\downarrow\rangle$ crossing)! Moreover, proper Mn placement and heterostructure engineering allows electrostatic control of the spin-subband crossing field $B^*(V_G)$. When 2D gas is in a quantum Hall effect (QHE) regime and spin polarization changes sign under the gate, there are exactly two counter-propagating channels with opposite spin polarization formed along the edge of the gate. These edge states form a 1D helical domain wall (*h*-DW), analogous to helical edge states in the quantum spin Hall effect. These helical channels are robust and enjoy topological protection of the QHE regime. Coupled to superconducting contacts, *h*-DW will support non-Abelian excitations which can be localized at the phase boundary between superconducting and spin-orbit-induced gaps. These particles will be non-Abelian Majorana fermions for $\nu = 1$ and parafermions (fractional Majorana fermions) for $\nu = 1/3$. The presence of non-Abelian particles will alter the fundamental Josephson current-flux relation and can be detectable via ac Josephson effect; it will be 4π-periodic in the presence of Majorana fermions and 12π-periodic in the presence of parafermions.

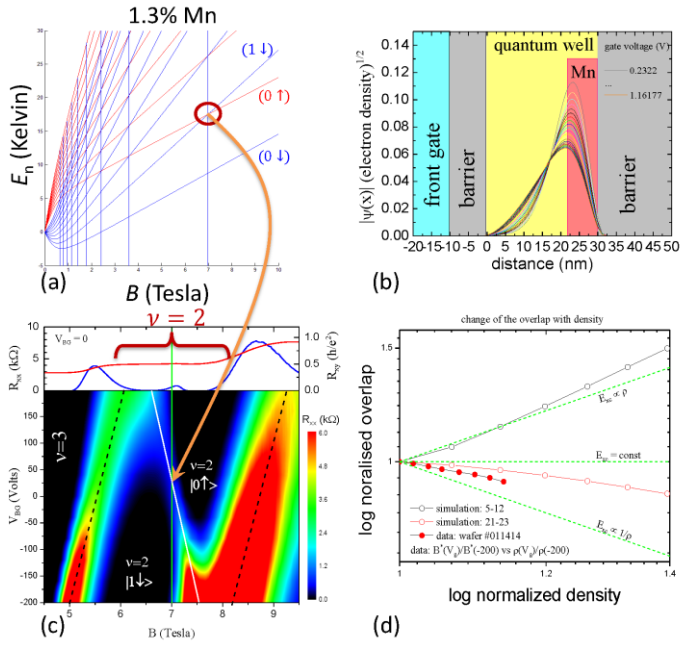

Figure 1: Wavefunction engineering for the controllable s-d exchange. (a) Energy diagram for a 2D gas with 1.5% Mn. (b) Modeling of an electron wavefunction in a QW at different gate voltages. s-d exchange is proportional to the overlap of the wavefunction with the Mn-doped region (magenta) (c) experimental data for an asymmetrically doped QW with 1.5% Mn. The peak within the ν=2 region is due to the crossing of $|0\uparrow\rangle$ and $|1\downarrow\rangle$ states. The shift of this crossing is gate dependent, it is plotted as filled dots in (d), dependence is in a good agreement with calculations (open dots). Note that a green vertical line at 7 Tesla crosses regions of opposite spin polarization for -200 and 200 Volts on the back gate. Submitted to Nature Materials (2015)

Quantum Hall effect in one of the samples is shown in Fig. 1. A small peak at B^*=7 Tesla in the middle of the $\nu = 2$ state is a phase transition between $|0\uparrow\rangle$ and $|1\downarrow\rangle$ states which changes polarization of the top filled energy level. In the color plots magnetoresistance is plotted as a function of voltage on the front and back gates. For both gates density increases with gate voltage and the peak between ν and ν+1 shifts to higher *B*. The spin transition B^* shifts in opposite directions as a function of V_{bg}, consistent with the modelling. Note that for *B*=7 Tesla polarization of the top level can be tuned between $|0\uparrow\rangle$ and $|1\downarrow\rangle$ states by electrostatic gating, thus realizing the theoretical concept required for a *h*-DW formation.

B. Another notable achievement is demonstration of induced superconductivity in high-mobility two-dimensional electron gas in gallium arsenide heterostructures and development of highly transparent semiconductor–superconductor ohmic contacts. Supercurrent with characteristic temperature dependence of a ballistic junction has been observed across 0.6 μm, a regime previously achieved only in point contacts but essential to the formation of well separated non-Abelian states. High critical fields (>16 T) in NbN contacts enables investigation of an interplay between superconductivity and strongly correlated states in a two-dimensional electron gas at high magnetic fields.

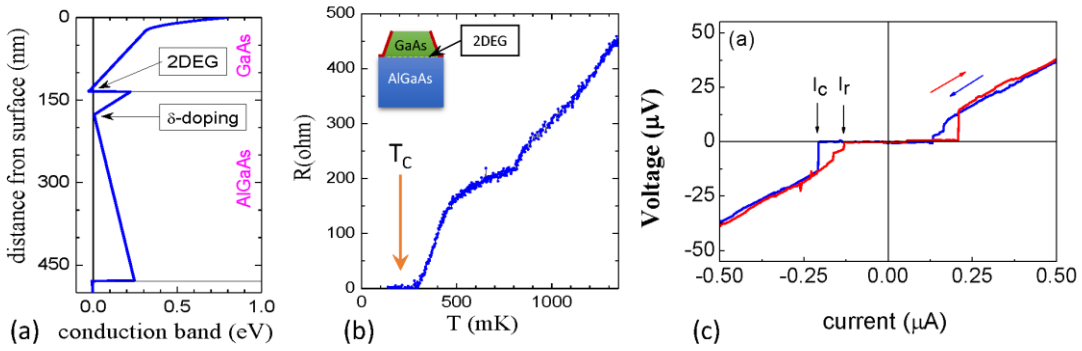

Figure 2: (a) Simulation of the conduction band energy profile in the inverted single heterointeface heterojuncion. (b) *T*-dependence of resistance across a 0.6 μm-wide 2DEG measured with 10 nA ac excitation. Induced superconductivity is observed for T<290 mK. (c) Current-voltage characteristic of a superconducting junction with 2DEG measured at 30 mK. Published in Nature Communications, **6** 7426 (2015).

C. Development of high quality epitaxial growth of InSb heterostructures is the key to achieve the proposed goals. Growth of strained InSb layers is challenging and we performed several iterations of growth/characterizations sequence with our collaborators to improve buffer quality and reduce density of dislocations. For InSb grown on GaAs substrates we reduced roughness from 30nm to 5-6nm, which is still too large for 20nm-thick InSb layers and inferior to monolayer plateaus we have grown on InSb substrates (InSb substrates are highly conductive and, as such, cannot be used for device fabrication).

Future Plans

Physics demonstration goals. Investigation of InSb/superconductor one-dimensional systems, search for the signatures of Majorana fermions and investigation of non-Abelian excitations.

Development of materials and measurement techniques:

We continue working on the growth improvement of InSb heterostructures. Recently we obtained semi-insulating GaSb substrates, which reduce lattice mismatch by 50% compared to GaAs. With semi-insulating GaSb substrates we are planning to achieve 1-2nm roughness.

AFM-lithography (a low energy alternative to electron beam lithography) of InSb will be characterized. We will also characterize oxidation and post-oxidation stability of thin Nb and NbN films and reproducibility of AFM-fabricated Josephson junctions and work on subsequent oxidation of multi-layer semiconductor/superconductor structures.

We designed and assembled most components for the development of a sensitive heterodyne rf detection system which, ideally, should allow us to measure single photon absorption in a Josephson junction. We will work on the assembly and characterization of the system in the dilution refrigerator, as well as the design of the coupling scheme for the actual device measurements.

Fabrication of single electron transistors for sensitive charge sensing will be developed. These charge sensors will be used to detect results of Majorana manipulation.

Publications

Zhong Wan, Aleksandr Kazakov, Michael J. Manfra, Loren N. Pfeiffer, Ken W. West, and Leonid P. Rokhinson, *"Induced superconductivity in high mobility two dimensional electron gas in GaAs heterostructures"*; Nature Communications, **6** 7426 (2015).

Aleksandr Kazakov, George Simion, Yuli Lyanda-Geller, V. Kolkovsky, Z. Adamus, G. Karczewski, Tomasz Wojtowicz, and Leonid P. Rokhinson, *"Development of electrostatically controlled quantum Hall ferromagnet, a new platform to realize high order non-Abelian excitations"*; submitted to Nature Materials (2015)

Luis A. Jauregui, Michael T. Pettes, Leonid P. Rokhinson, Li Shi, and Yong P. Chen, *"Magnetic field induced helical mode and topological transitions in a quasi-ballistic topological insulator nanoribbon with circumferentially quantized surface state sub-bands"*; submitted to Nature Materials (2015)

Tzu-ging Lin, George Simion, John D. Watson, Michael J. Manfra, Gabor A. Csathy, Yuli Lyanda-Geller, and Leonid P. Rokhinson, *"Evidence of new topological excitations in the reentrant quantum Hall effect"*; submitted to Physical Review Letters (2015)

George Simion, Tzu-ging Lin, John D. Watson, Michael J. Manfra, Gabor A. Csathy, Yuli Lyanda-Geller, and Leonid P. Rokhinson, *"Theory of topological excitations and melting transitions in reentrant integer quantum Hall effect"*; submitted to Physical Review Letters (2015)

Program Title: Quantum Coherence and Random Fields at Mesoscopic Scales

Principal Investigator: Thomas F. Rosenbaum
Institution: The University of Chicago / California Institute of Technology
E-mail: tfr@caltech.edu

Program Scope

We seek to explore and exploit model, disordered and geometrically frustrated magnets where coherent spin clusters stably detach themselves from their surroundings, leading to extreme sensitivity to finite frequency excitations and the ability to encode information. Global changes in either the spin concentration or the quantum tunneling probability via the application of an external magnetic field can tune the relative weights of quantum entanglement and random field effects on the mesoscopic scale. These same parameters can be harnessed to manipulate domain wall dynamics in the ferromagnetic state, with technological possibilities for magnetic information storage. Finally, extensions from quantum ferromagnets to antiferromagnets promise new insights into the physics of quantum fluctuations and effective dimensional reduction. A combination of ac susceptometry, dc magnetometry, noise measurements, hole burning, non-linear Fano experiments, and neutron diffraction as functions of temperature, magnetic field, frequency, excitation amplitude, dipole concentration, and disorder address issues of stability, overlap, coherence, and control. We have been especially interested in probing the evolution of the local order in the progression from spin liquid to spin glass to long-range-ordered magnet.

Recent Progress

(A) Quantum Annealing and Optimization: We have performed a proof-of-concept experiment on a crystal containing 10^{20}, rather than hundreds, of quantum spins, which replicates some of the features of the current generation of much smaller specialized computers. The experiment looked at the valleys found after annealing with different weights of thermal excitation over barriers and quantum tunneling through them in the crystalline quantum magnet, $LiHo_xY_{1-x}F_4$. In this material, at temperatures near absolute zero, the speed and strength of thermal annealing can be controlled by rods of sapphire attached to a helium dilution refrigerator with more or less contact with the crystal. At the same time, the rate of quantum annealing can be controlled by means of a (transverse) magnetic field that acts to set the rate of quantum tunneling in the magnetic sample.

We find that when the system reaches its final valley via thermal annealing alone, it was dramatically different from the state reached when the thermal annealing was weakened and quantum annealing was turned on. The key difference involves the collective nature of the relaxation process. The small values of transverse field are orders of magnitude smaller than the field scales required to produce single-ion effects. Describing this system using the Hamiltonian for the Ising Model in transverse field,

$$H = -\sum_{i,j}^{N} J_{ij}\sigma_i^z\sigma_j^z - \Gamma\sum_{i}^{N}\sigma_i^x \qquad (1)$$

where the σ's are Pauli spin matrices and the J_{ij}'s are longitudinal couplings, permits a quantitative evaluation of the pertinent energies. Experiments and mean-field theory calculations find the mixing term Γ to be approximately quadratic in H_t for $H_t < 20$ kOe, with Γ(1 kOe) = 30 mK. Clearly, in the single ion picture only transverse fields on the order of 1 kOe or more will be relevant at temperatures of order 1 K; however, we have observed unmistakable effects on the evolution of the magnetic system for transverse cooling fields as small as 10 Oe. We argue that in order for the interaction energy between a magnetic

moment and a transverse field this small to be relevant at T ~ 0.1 K, the moment must be comprised of order 100 spins adding coherently.

(B) Geometric Frustration: We have extended our studies of coherent clusters of spins effectively decoupled from the surrounding magnetic environment (so-called "quantum protectorates") in spin liquids to geometrically-frustrated systems. In the case of GGG ($Gd_3Ga_5O_{12}$), spin freezing is suppressed classically by geometrical frustration, without the need for dilution. We have investigated the effects of up to 1% Neodymium substitution for Gallium on the ac magnetic response at temperatures below 1 K in both the linear and nonlinear regimes. Substitutional disorder actually drives the system towards a more perfectly frustrated state, depressing any signatures of ordering such as a plateau in the low frequency dissipative response. The magnetic Nd substitution apparently compensates for the effects of imperfect Gadolinium/Gallium stoichiometry and, at the same time, more closely demarcates the boundaries of isolated, coherent clusters composed of hundreds of spins. Optical measurements of the local Nd environment substantiate the picture of an increased frustration index with doping. Correlating the linear ac magnetic susceptibility with the non-linear response should provide insights into the continuum of frustrated states as well as the nature of the quantum-mechanically isolated degrees of freedom.

(C) Tunable Domain Pinning in Ferromagnets: We adopt a new tactic to regulate isothermal magnetization reversal in real materials by exploiting the random-field Ising model (RFIM), where a site-random magnetic field acts to orient magnetization locally in competition with the underlying exchange couplings that favor homogeneous magnetism. Random fields act on ferromagnets via their pinning of domain walls, creating barriers to motion that increase with random field amplitude. The rising barrier height decreases the probability of reversal at a given applied field, and if the amplitude of the random field contribution can be controlled continuously, then the pinning potential can be increased or decreased on demand.

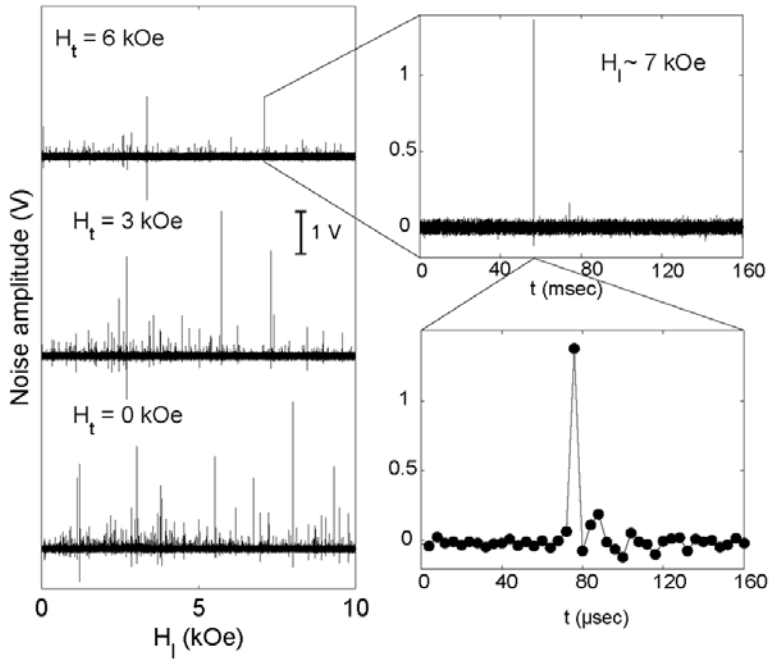

Fig. 1: Barkhausen noise recorded on sweeping the longitudinal magnetic field through a hysteresis loop in the ferromagnet $Nd_2Fe_{14}B$. All data are taken at fixed temperature. The noise decreases with increasing transverse magnetic field as the transverse field induces local random magnetic fields that pin the domains. The ability to alter the pinning potential in this manner may have applications in magnetic storage (From Publication 9).

We have extended earlier (DOE-supported) work at milliKelvin temperatures on dipolar ferromagnets by considering a rare-earth ferromagnet, $Nd_2Fe_{14}B$, with high crystalline anisotropy and a tendency to form elongated grains. Within a grain, the individual spins are exchange-coupled, yielding a strong interaction energy that magnetizes the entire grain and yields a Curie temperature of order 300° C. Each grain acts like a single effective spin with a moment equivalent to millions of Bohr magnetons because of the crystalline and shape anisotropy, and couples to neighboring grains via the dipolar interaction. The dynamics of the domain walls can be elucidated through Barkhausen noise, the noise generated by switching domains occurring at audio frequencies under the influence of a changing longitudinal field. We have demonstrated that the Barkhausen noise can be suppressed by the application of a transverse field (Fig. 1), reinforcing the interpretation of isothermal hardening of the magnet. Measurements at a series of longitudinal magnetic fields, transverse magnetic fields, and temperatures have permitted comparisons to scaling theories for the RFIM.

Future Plans

Spin Liquids: The existence of coherent clusters of spins effectively decoupled from the surrounding magnetic environment can be interrogated using a magnetic hole-burning technique. The excited spins are removed from the magnetic relaxation spectrum in a process analogous to optical bleaching experiments, but we use an inductance loop at a few Hertz rather than a laser at TeraHertz frequency, with an excitation field of order the earth's magnetic field. The presence of interference between the discrete transition inside the resonant state and the weaker pathway to the continuum of spin-bath states gives rise to a Fano resonance in the absorption spectrum, with a functional form $\chi'' \propto \frac{\left(q\Gamma_r/2 + f - f_r\right)^2}{\left(\left(f - f_r\right)^2 + \Gamma_r/2\right)}$, where Γ_r is the linewidth of the discrete transition centered at frequency f_r. The Fano parameter q measures the asymmetry of the lineshape, and parameterizes the strength of the interference between the two transition pathways.

Remarkably, it is possible to drive the Fano parameter q to zero in $LiHo_{0.045}Y_{0.955}F_4$. The relative energies of the effective two-level system that characterizes the coherent spin modes can be tuned by external magnetic fields. This is illustrated by the set of energy levels illustrated in Fig. 2a. The phase of the Fano resonance, parameterized by the magnitude and sign of q, reverses depending on which energy level is lower; when q=0, the levels are degenerate. The behavior of the Fano phase is also correlated with the shape of the nonlinear susceptibility $\chi = dM/dH$. In particular, as shown in Fig. 2b, the phase angle of the susceptibility approaches zero when q approaches zero. Nearly dissipationless oscillations occur when the energy levels are tuned to be equal. The ability to tune the energy levels and move in and out of a near-dissipationless regime offers the prospect of performing detailed lifetime and decay measurements on such states. Magnetic ring down of the Fano resonance should be extended to longer times as dissipation decreases, permitting us to manipulate the state and perhaps even mix multiple states at different frequencies with transverse magnetic field. We also plan to employ thermodynamic boundary conditions to test the universality of the behavior shown in Fig. 2b. The weaker the thermal connection to the external world, the more quantum the character of the state, favoring tunneling of blocks of spins rather than excitations of individual spins over activation barriers. Pump-probe Fano measurements in the presence of a continuously-variable thermal linkage would provide a powerful way to interrogate the fundamental behavior of the quantum protectorates.

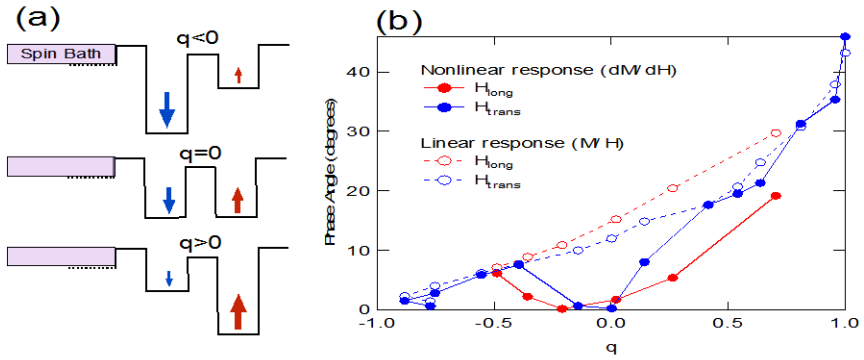

Fig. 2: (a) The excitation spectrum of the coherent spin clusters can be represented by a two-level system with coupling to a spin bath. Quantum interference leads to Fano resonances. (b) For both longitudinal (excitation amplitude) and transverse (quantum tunneling) fields the nonlinear response becomes almost dissipationless when the Fano parameter *q* approaches 0. This effect cannot be seen in the linear response.

Recent Publications (Supported by BES)

1. "Continuous and Discontinuous Quantum Phase Transitions in a Model Two-Dimensional Magnet," S. Haravifard, A. Banarjee, J.C. Lang, G. Srajer, D.M. Silevitch, B.D. Gaulin, H. Dabkowska, and T.F. Rosenbaum, Proc. Nat. Acad. Sci. **109**, 2286 (2012).

2. "Contribution of Spin Pairs to the Magnetic Response in a Dilute Dipolar Ferromagnet," C.M.S. Gannarelli, D.M. Silevitch, T.F. Rosenbaum, G. Aeppli, and A.J. Fisher, Phys. Rev. B **86**, 014420 (2012).

3. "Dipolar Antiferromagnetism and Quantum Criticality in $LiErF_4$," C. Kraemer *et al.*, Science **336**, 1416 (2012).

4. "Sub-Kelvin ac Magnetic Susceptometry," M.A. Schmidt, D.M. Silevitch, N. Woo, and T.F. Rosenbaum, Rev. Sci. Instrum. **84**, 013901 (2013).

5. "Using Thermal Boundary Conditions to Engineer the Quantum State of a Bulk Magnet," M.A. Schmidt, D.M. Silevitch, G. Aeppli, and T.F. Rosenbaum, Proc, Nat. Acad. Sci. **111**, 3689 (2014).

6. "Reversible Disorder in a Room Temperature Ferromagnet," S.L. Tomarken, D.M. Silevitch, G. Aeppli, B.A.W. Brinkman, J. Xu, K. A. Dahmen, and T.F. Rosenbaum, Advanced Functional Materials **24**, 2986 (2014).

7. "Quantum Tunneling vs. Thermal Effects in Experiments on Adiabatic Quantum Computing," D.M. Silevitch, T.F. Rosenbaum, and G. Aeppli, Eur. Phys. J. Special Topics **224**, 25 (2015).

8. "Interplay of Disorder and Geometrical Frustration in Doped Gadolinium Gallium Garnet," N. Woo, D.M. Silevitch, C. Ferri, S. Ghosh, and T.F. Rosenbaum, J. Phys.: Cond. Matt. **27**, 296001 (2015).

9. "Barkhausen Noise in the Random Field Ising Magnet $Nd_2Fe_{14}B$," J. Xu, D.M. Silevitch, K.A. Dahmen, and T.F. Rosenbaum, Phys. Rev. B **92**, 024424 (2015).

10. "Sub-Kelvin Magnetic and Electrical Measurements in a Diamond Anvil Cell with *in situ* Tunability," A. Palmer, D.M. Silevitch, Y. Feng, Y. Wang, R. Jaramillo, A. Banerjee, Y. Ren, and T.F. Rosenbaum, Rev. Sci. Instrum., in press.

11. A. Dutta, G. Aeppli, B.K. Chakrabarti, U. Divakaran, T.F. Rosenbaum, and D. Sen, *Quantum Phase Transitions in Transverse Field Models: From Statistical Physics to Quantum Information* (Cambridge University Press, New Delhi, 2015), ISBN 978-1-107-06879-7.

Thermalization of artificial spin ice and related frustrated magnetic arrays

Principal Investigator: Peter Schiffer, University of Illinois at Urbana-Champaign, Urbana, IL (pschiffe@illinois.edu)

Co-Investigators: Vincent Crespi and Nitin Samarth, Pennsylvania State University, University Park, PA

Program Scope

This program encompasses studies of lithographically fabricated "artificial spin ice" arrays of nanometer-scale single-domain ferromagnetic islands in which the array geometry results in frustration of the magnetostatic interactions between the islands. These systems are analogs to a class of magnetic materials in which the lattice geometry frustrates interactions between individual atomic moments, and in which a wide range of novel physical phenomena have been observed. The advantage to studying lithographically fabricated samples is that they are both designable and resolvable: i.e., we can control all aspects of the array geometry, and we can also observe how individual elements of the arrays behave. In previous work, we have designed frustrated lattices, controlled the strength of interactions by changing the spacing of the islands, and demonstrated that the island magnetic moment orientation is controlled by the inter-island interactions. Current work is focusing on three areas: thermal annealing of these arrays at temperatures above the Curie point of the ferromagnetic permalloy, a technique that allows better access to the low-energy ground state of these many-body systems, PEEM studies of very thin islands that exhibit thermal fluctuations near room temperature, and electrical transport studies of connected networks of ferromagnetic nanowires.

Recent Progress

The past two years of this program has focused on several projects within the scope described above. All work has been done in close collaboration with the group of Chris Leighton at the University of Minnesota and that of Cristiano Nisoli at Los Alamos National Laboratory.

Thermal annealing of artificial spin ice: Because of the large magnetic energy scales of the ferromagnetic islands in artificial spin ice, workers in the field were originally unable to find a technique to thermally anneal artificial spin ice into desired thermodynamic ensembles. Early studies of artificial spin ice have either applied alternating magnetic fields or focused on the as-grown state of the systems, neither of which allowed consistent study of the ground state of the arrays (such as ordering of effective charges). We have now demonstrated a method for thermalizing artificial spin ice arrays by heating them above the Curie temperature of the

constituent material. This effectively allows us to reach the ground state of square ice and see charge ordering in kagome ice. We find excellent agreement between experimental data and Monte Carlo simulations of emergent charge–charge interactions [1]. We also have used this technique to make the first study of a vertex-frustrated system, the so-called "shakti lattice", a structure that does not directly correspond to any known natural magnetic material. On the shakti lattice, none of the near-neighbor interactions are locally frustrated, but instead the lattice topology frustrates the interactions leading to a high degree of degeneracy. We demonstrate that the shakti system achieves a physical realization of the classic six-vertex model ground state. Furthermore, we observe that the mixed coordination of the shakti lattice leads to crystallization of effective magnetic charges and the screening of magnetic charge excitations, underscoring the importance of magnetic charge as the relevant degree of freedom in artificial spin ice and opening new possibilities for studies of its dynamics. This work has been published as a long

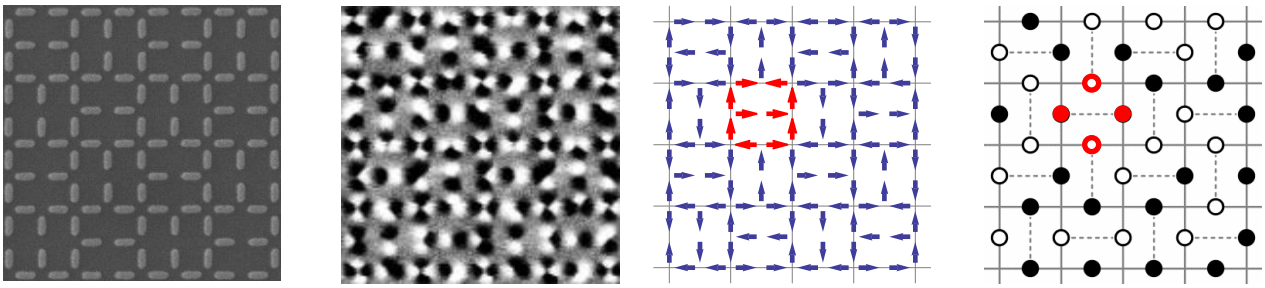

Figure 1 The skakti lattice. From left to right: SEM image, MFM image, mapping of moments from MFM image, and mapping of ground state and excited state vertices from MFM image [3].

article in Nature Physics [3].

Thermal fluctuations in artificial spin ice: To explore thermal behavior in these systems, we have used photoemission electron microscopy with x-ray magnetic circular dichroism contrast (XMCD-PEEM). This imaging technique shows black/white contrast on the islands (which indicates whether the island magnetization has a positive or negative projection on the polarization of the incident x-rays) allowing the experiments to unambiguously identify the exact microstate of an array. The advantage of PEEM is that it can be employed with very thin islands whose moments are extremely soft and would be unmeasurable with MFM. Such thin islands can be grown such that their moments fluctuate thermally at room temperature but then freeze into a static configuration upon cooling. While these studies require access to a synchrotron facility, they allow the examination of moment fluctuations in artificial spin ice by comparing successive images. In collaboration with Andreas Scholl at LBNL, we have employed this technique to study another vertex-frustrated lattice unavailable in nature, the "tetris" lattice (figure 2). This lattice shows quasi-one dimensional behavior that maps onto a one-dimensional Ising model, and through a temperature-dependent study, we can see the development of thermal fluctuations associated with the vertex frustration.

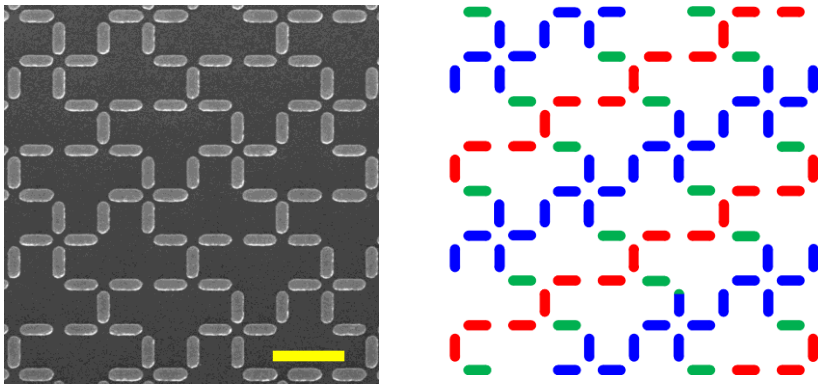

Figure 2 The tetris lattice. Right: SEM image of artificial spin ice in the tetris lattice (scale bar is 1 micron). Left: color-coded image showing the different quasi one-dimensional structures within the lattice.

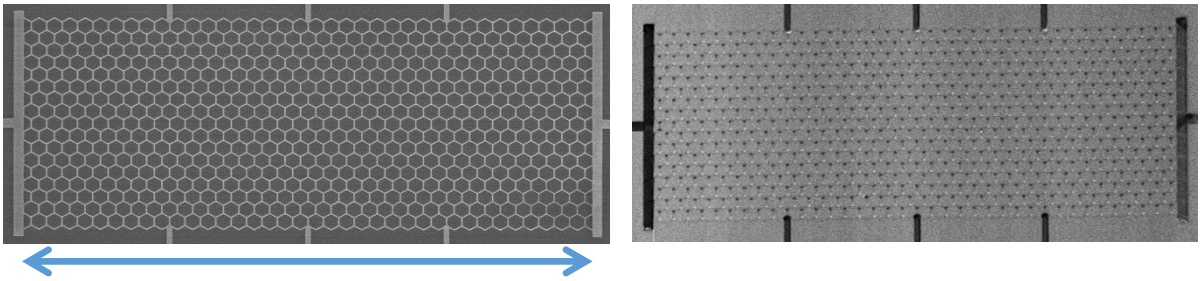

Figure 3. SEM and MFM images of connected artificial spin ice network for electrical magnetotransport studies. The black and white dots on the MFM image correspond to effective magnetic charges at the lattice vertices, and the scale bar corresponds to 50 microns.

Memory effects in artificial spin ice: We experimentally demonstrated that square artificial spin ice develops reproducible microstates upon cycling an applied magnetic field, exhibiting memory effects analogous to those seen in other magnetic systems but with the important difference that we can track the microstates leading to memory effects. The onset of this repeatability is determined by the strength of the applied field relative to the array coercivity. Specifically, when the applied field strength is very close to the array coercivity, several training cycles are required before the array achieves a nearly completely repeatable microstate, whereas when the applied field strength is considerably larger or smaller than the array coercivity, a repeatable microstate is achieved after the first minor loop. We show through experiment and simulation that this memory exhibited by artificial spin ice is due to a ratchet effect on interacting, magnetically-charged vertices and to the complexity of the network of strings of reversed moments that forms during magnetization reversal.

Transport studies of connected artificial spin ice structures: We are examining the electrical transport properties of artificial spin ice networks (figure 3). Our data showed clear evidence of magnetic switching among the wires, both in the longitudinal and transverse magnetoresistance that we attribute largely to planar hall effects and anisotropic magnetoresistance, although the details remain to be explored. An unusual asymmetry with field sweep direction appeared at

temperatures below about 20 K that appears to be associated with exchange bias resulting from surface oxidation of permalloy, and that disappears in alumina-capped samples. These results demonstrate that exchange bias is a phenomenon that must be considered in understanding the physics of such artificial spin ice systems, and that opens up new possibilities for their control. Further studies of the transport as a function of magnetic field show exquisite sensitivity to the angle of the field relative to the lattice structure.

Future Plans

Future plans for this research program include a number of different thrusts, in particular exploration of the consequences of thermalization for a range of different lattices and the nature of thermal fluctuations in those lattices. These studies will include the tetris and the shakti lattices that we have already begun to explore, but also others proposed by our collaborator Cristiano Nisoli as well as simpler lattices that now can be studied in more detail thanks to improved experimental techniques. We also plan more detailed magnetotransport studies of different connected artificial spin ice networks, looking for anomalous effects that we have observed in preliminary studies of the honeycomb samples of the sort shown in figure 3.

References and Publications

1. "Crystallites of magnetic charges in artificial spin ice," Sheng Zhang, Ian Gilbert, Cristiano Nisoli, Gia-Wei Chern, Michael J. Erickson, Liam O'Brien, Chris Leighton, Paul E. Lammert, Vincent H. Crespi and Peter Schiffer, Nature 500, 553–557 (2013).

2. "Artificial Spin Ice: Controlling Geometry, Engineering Frustration," Cristiano Nisoli, Roderich Moessner, and Peter Schiffer, Reviews of Modern Physics 85, 1473-1490 (2013).

3. "Emergent ice rule and magnetic charge screening from vertex frustration in artificial spin ice," Ian Gilbert, Gia-Wei Chern, Sheng Zhang, Liam O'Brien, Bryce Fore, Cristiano Nisoli, and Peter Schiffer, Nature Physics 10, 670–675 (2014).

4. "Effects of exchange bias on magnetotransport in permalloy kagome artificial spin ice," B. L. Le, D. W Rench, R. Misra, L. O'Brien, C. Leighton, N. Samarth and P. Schiffer, New Journal of Physics 17, 023047-1-7 (2015).

PROJECT TITLE: Tuning Phase Transformations for Designed Functionality

PRINCIPLE INVESTIGATORS: Athena S. Sefat, David Parker, Zheng Gai, Miaofang Chi

INSTITUTION: Oak Ridge National Laboratory

EMAIL ADDRESS: sefata@ornl.gov

PROJECT SCOPE:

Recent, often serendipitous, discoveries of functional materials have demonstrated great potential for a wide variety of applications, including magnetic sensors, permanent magnets, magnetocaloric refrigerators, and superconducting wires. The functionality of these materials are based upon exotic phase transitions which are thermally-driven via atomic, electronic or spin correlations; however, these behaviors are generally poorly understood. This project seeks to understand the foundations for these behaviors to enable the design of a new generation of functional materials. This project's scope is to understand the fundamental chemical and physical phenomena underpinning exotic thermal phase transformations in materials that yield specific functionalities (**Fig. 1**). To achieve this goal we will pursue three specific aims: (1) elucidate of the effects of atomic interactions; (2) understand the effect of dimensionality within crystal structures; and (3) clarify the role of atomic clustering. Specifically, we will probe behaviors near the exotic phase transitions where there is close competition between atomic, electronic and spin orders that ultimately trigger different functionalities. Through tightly-integrated feedback between *synthesis*, *computation*, and *characterization* of materials across a broad range of length scales (cm to pm), we will ultimately enable the a priori prediction of functionality at relevant temperatures.

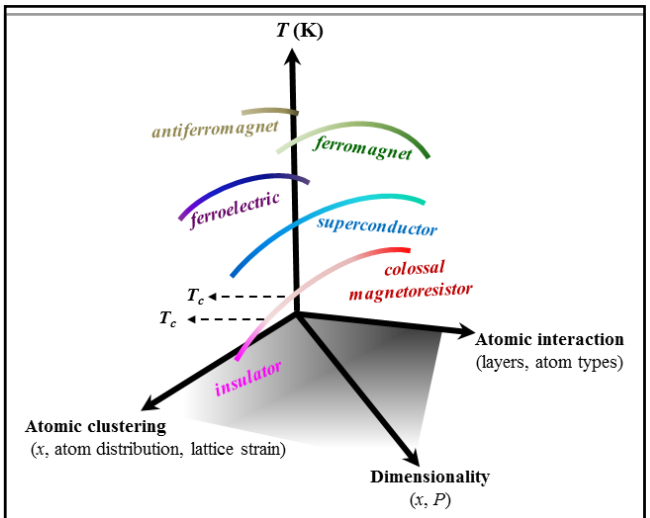

Fig. 1: Schematic of the intimate relationship between materials' structural details (atomic interaction; dimensionality; clustering) & property emergence (types; finite critical temperature T_c).

RECENT PROGRESS:

This project is new and is just funded (late-August 2015). Hence, we present notes are on the Recent Progress from PI's ECA (ended in mid-April 2015), and as they relate to this new FWP.

Highlight 1: Evidence for non-uniform superconductivity in a 'high-T_c' 122 crystal

Reference: Gofryk, K.; Pan, M.; Cantoni, C.; Saparov, B.; Mitchell, J.E.; Sefat, A.S., "Local inhomogeneity and filamentary superconductivity in Pr-Doped $CaFe_2As_2$," *Phys. Rev. Lett.* **112**, 047005 (2014).

The issues of doping and inhomogeneity are exemplified in this $Pr_{0.14}Ca_{0.86}Fe_2As_2$ study, in

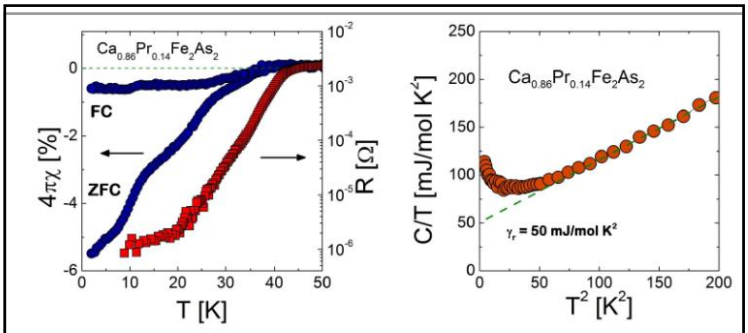

Fig. 2. (Left) Magnetic susceptibility and electrical resistance showing non-bulk superconductivity marked by weak diamagnetism (~ 6% at 2 K) and non-vanishing resistance (~10^{-6} ohm at 10 K). (Right) Heat capacity plot showing non-zero, large, Sommerfeld coefficient.

which bulk superconductivity has been under debate. Our measurements on these single crystals have revealed that the non-bulk nature of the high-temperature superconducting state (**Fig. 2**) is a consequence of non-uniform praseodymium distribution that develops localized, isolated regions within the crystals. STEM/EELS analyses show real-space inhomogeneous state and clustering of Pr. STM/S results show the 'clover-like defects' for $Pr_{0.14}Ca_{0.86}Fe_2As_2$ and a spatial distribution of gaps with up to 30% in the non-superconducting state.

Highlight 2: Clues for absence of superconductivity in collapsed-tetragonal 122

Reference: Gofryk, K.; Saparov, B.; Durakiewicz, T.; Chikina, A.; Danzenbacher, S.; Vyalikh, D.V.; Graf, M.J.; Sefat, A.S., "Fermi-surface reconstruction and complex phase equilibria in $CaFe_2As_2$," *Phys. Rev. Lett.* **112**, 186401 (2014).

The electronic properties of $CaFe_2As_2$ single crystals using a combination of bulk transport measurements (**Fig. 3**), x-ray diffraction, theoretical modeling and surface photoemission spectroscopy, have revealed reasons for its lack of magnetism. We show evidence for a large modification of the electronic properties when the structure changes on cooling and modification of the Fermi surface in $CaFe_2As_2$ at the transition from high-temperature tetragonal to low-temperature collapsed-tetragonal phase, different from the typical superconducting phase.

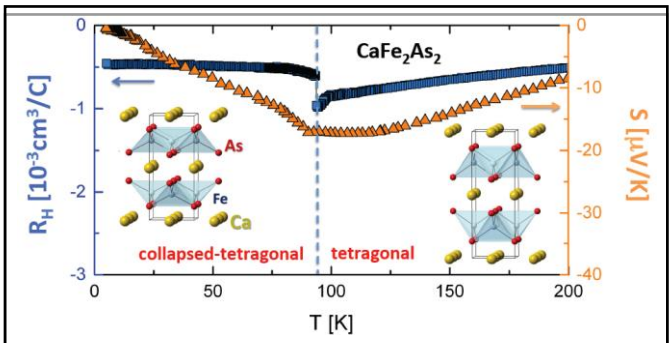

Fig. 3: Temperature-dependence of Hall effect and Seebeck are associated with a large Fermi surface modification at the structural transition (dashed line) between collapsed-tetragonal to tetragonal phase, preventing superconductivity of $CaFe_2As_2$.

Highlight 3: Importance of diminished structural distortions and magnetism in superconductivity

Reference: Takeda, H.; Imai, T.; Tachibana, M.; Gaudet, J.; Gaulin, B.D.; Saparov, B.I.; Sefat, A.S., "Cu substitution effects on the local magnetic properties of $Ba(Fe_{1-x}Cu_x)_2As_2$: A site-selective ^{75}As and ^{63}Cu NMR study," *Phys. Rev. Lett.* **113**, 117001 (2014).

By analyzing role of structural variation and magnetism of Cu dopants in FeAs planes, we demonstrate the absence of large superconducting dome in the phase diagram of Cu-doped $BaFe_2As_2$. This study used a combination of crystal synthesis, temperature dependence of single-crystal x-ray diffraction, electrical resistance and magnetic susceptibility, and NMR. Undoped $BaFe_2As_2$ has a simultaneous tetragonal-to-orthorhombic and spin-density-wave transition below $T_s = T_N = 132$ K. Although dopants of Co and Ni were found to support the rigid band picture to give high-T_c superconductivity, Cu-doped crystals give a nearly magnetically ordered FeAs plane and orthorhombic distortions. In fact, the strength of spin fluctuations

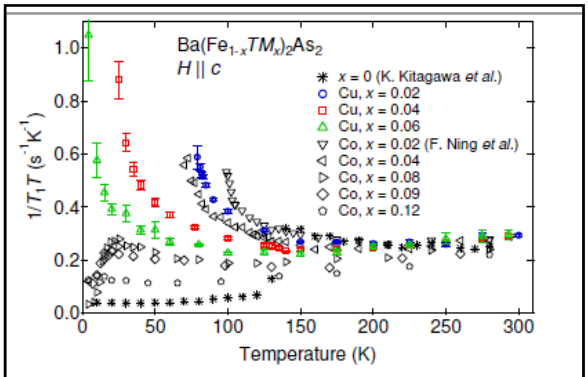

Fig. 4: Temperature-dependence ofthe strength of spin fluctuation ($1/T_1T$), where T_1 is ^{75}As nuclear spin-lattice relaxation rate and T is temperature for $Ba(Fe_{1-x}Cu_x)_2As_2$ and $Ba(Fe_{1-x}Co_x)_2As_2$.

($1/T_1T$), where T_1 is the ^{75}As nuclear spin-lattice relaxation rate, remains high for Cu-doped crystals (**Fig. 4**), even though greatly reduced upon Co doping. These results extend our understanding of bulk vs. local structure effects, finding that the orthorhombic distortion below T_s leads to magnetically ordered state of FeAs planes, hence minimal superconductivity.

FUTURE PLAN: Two of our immediate upcoming plans are below.

(I) Effects of interlayer spacing (*X*) on Magnetism in 122 FeAs-based Structures: We hypothesize that the size of the *X* directly impacts atomic interactions, and therefore the spin structures, overall magnetic order and strength. For $B Fe_2As_2$ materials, *X* will be tuned through choice and size of intercalant (*e.g. B*= Ba, Sr, Tl, Bi, etc.). Key questions that drive this research plan include the following: Can the spin ordering along different crystal axes be predicted with change in *X*? What is the critical ordering temperature? What is the effect of the intercalated *B* on the effective dimensionality? This research will develop a predictive capability of the types and strengths of magnetic order of 122 structures, and how they are affected by interlayer spacing.

(II) Effects of layer thickness (*n*) on magnetic ordering in CuS-based structures: We hypothesize that the type and strength of magnetism is due to Fermi level nesting, which will change as we change the layer thickness (*e.g. n* = 1, vs 2, vs 3). To test this, we will examine magnetism in copper sulfide-based systems, with different *n*. For CuS-based systems of '122,' '143,' and '164,' magnetic order may arise from Fermi-nesting effects, similar to many conclusions on the FeAs-based 122 materials. The role of nesting will be examined by controlling the number of CuS-based layers through chemistry and synthesis, moving from a single layer to multiple layers, as a stage toward moving toward 3D structures.

A LIST OF PUBLICATION: FY2015 (Oct 2014- Sept 2015)

(1) Li, L.; Cao, H.B.; McGuire, M.A.; Kim, J.S.; Stewart, G.R.; Sefat, A.S., "Role of magnetism in superconductivity of $BaFe_2As_2$: Study of 5*d* Au-doped crystals," *Physical Review B*, accepted August (2015).

(2) Khasanov, R.; Guguchia, Z.; Luetkens, H.; Amato, A.; Biswas, P.K.; Ruegg, C.; Susner, M.A.; Sefat, A.S.; Zhigadlo, N.D.; Morenzoni, E., "Pressure-induced electronic phase separation of magnetism and superconductivity in CrAs," *Scientific Reports*, accepted August (2015).

(3) Shipra, R.; Idrobo, J.C.; Sefat, A.S., "Structural and superconducting features of Tl-1223 prepared at ambient pressure," *Superconducting Science & Technology*, accepted August (2015). [PTS#: 58345]

(4) Li, L.; Parker, P.; Babkevich, P.; Yang, L.; Ronnow, H.M.; Sefat, A.S., "Superconductivity in semimetallic $Bi_3O_2S_3$," *Physical Review B* **91**, 104511 (2015).

(5) Keller, L.; White, J. S.; Frontzek, M.; Babkevich, P.; Susner, M.A.; Sims, Z.C.; Sefat, A.S.; Ronnow, H.M.; Ruegg, Ch., "Pressure dependence of the magnetic order in CrAs: A neutron diffraction investigation," *Physical Review B* **91**, 020409(R) (2015).

(6) Kim, J.; Haberkorn, N.; Gofryk, K.; Graf, M.J.; Ronning, F.; Sefat, A.S.; Movshovich, R.; Civale, L., "Superconducting properties in heavily overdoped $Ba(Fe_{0.86}Co_{0.14})_2As_2$ single crystals," *Solid State Communications* **201**, 20 (2015).

(7) Mitchell, J.E., Hillesheim, D.A.; Bridges, C.A.; Paranthaman, M.P.; Gofryk, K.; Rindfleisch, M.; Tomsic, M.; Sefat, A.S. "Optimization of a non-arsenic iron-based superconductor for wire fabrication," *Superconductor Science & Technology* **28**, 045018 (2015).

(8) Hillesheim, D.; Gofryk, K.; Sefat, A.S., "On the nature of filamentary superconductivity in metal-doped hydrocarbon organic materials," *Novel Superconducting Materials* **1**, 2299 (2015).

(9) Wu, S.F.; Richard, P.; Roekeghem, A.v.; Nie, S.M.; Miao, H.; Xu, N.; Qian, T.; Saparov, B.; Fang, Z.; Biermann, S.; Sefat, A.S.; Ding, H., "Direct spectroscopic evidence for completely filled Cu 3d shell in $BaCu_2As_2$ and α-$BaCu_2Sb_2$," *Physical Review B* **91**, 235109 (2015).

(10) Haberkorn, N.; Kim, J.; Gofryk, K.; Ronning, F.; Sefat, A.; Welp, U.; Fang, L.; Kwok, W.K.; Civale, L., "Enhancement of the critical current density by increasing collective pinning energy in heavy ion irradiated Co-doped $BaFe_2As_2$ single crystals," *Superconductor Science & Technology* **28**, 055011 (2015).
(11) Susner, M.A.; Parker, D.S.; Sefat, A.S., "Importance of doping and frustration in itinerant Fe-doped Cr_2Al," *Journal of Magnetism and Magnetic Materials* 392, **68** (2015).
(12) Moseley, D.A.; Yates, K.A.; Mandrus, D.; Sefat, A.S.; Branford, W.R.; Cohen, L.F., "Magnetotransport of proton-irradiated $BaFe_2As_2$ and $BaFe_{1.985}Co_{0.015}As_2$ single crystals," *Physical Review B* **91**, 054512 (2015).
(13) Cantoni, C.; McGuire, M.A.; Saparov, B.; May, A.F.; Keiber, T.; Bridges, F.; Sefat, A.S.; Sales, B.C., "Room-temperature $Ba(Fe_{1-x}Co_x)_2As_2$ is not tetragonal: Direct observation of magnetoelastic interactions in pnictide superconductors," *Advanced Materials* **27**, 2715 (2015).
(14) Mohanty, D.; Sefat, A.S.; Payzant, E.A.; Li, J.; Wood, D.L.; Daniel, C., "Unconventional irreversible structural changes in a high-voltage Li-Mn-rich oxide for lithium-ion battery cathodes," *Journal of Power Sources* **283**, 423 (2015).
(15) Mirmelstein, A.; Podlesnyak, A.; Santos, A.M.; Ehlers, G.; Kerbel, O.; Matvienko, V.; Sefat, A.S.; Saparov, B.; Halder, G.J.; Tobin, J.G. "Pressure-induced structural phase transition in CeNi: X-ray and neutron scattering studies and first-principles calculations," *Physical Review B* **92** (2015), 054102.
(16) Belianinov, A.; Ganesh, P.; Lin, W.; Sales, B. C.; Sefat, A. S.; Jesse, S.; Pan, M.; Kalinin, S. V. "Research update: Spatially resolved mapping of electronic structure on atomic level by multivariate statistical analysis," *APL Materials* **2** (2014), 120701.
(17) Gu, D.; Dai, X.; Le, C.; Sun, L.; Wu, Q.; Saparov, B.; Guo, J.; Gao, P.; Zhang, S.; Zhou, Y.; Zhang, C.; Xiong, L.; Li, R.; Li, Y.; Li, X.; Liu, J.; Sefat, A.S.; Hu, J.; Zhao, Z. "Robust antiferromagnetism preventing superconductivity in pressurized $Ba_{0.61}K_{0.39}Mn_2Bi_2$," *Scientific Reports* **4** (2014), 7342.
(18) Kim, J.; Haberkorn, N.; Gofryk, K.; Graf, M. J.; Ronning, F.; Sefat, A.S.; Movshovich, R.; Civale, L. "Superconducting properties in heavily overdoped $Ba(Fe_{0.86}Co_{0.14})_2As_2$ single crystals," *Solid State Communications* **201** (2014), 20.
(19) Shi, H.; Saparov, B.; Singh, D. J.; Sefat, A.S.; Du, M. H. "Ternary chalcogenides $Cs_2Zn_3Se_4$ and $Cs_2Zn_3Te_4$: Potential *p*-type transparent conducting materials," *Physical Review B* **90** (2014), 184104.
(20) Belianinov, A.; Ganesh, P.; Lin, W.; Sales, B. C.; Sefat, A.S.; Jesse, S.; Pan, M.; Kalinin, S. V. "Research update: Spatially resolved mapping of electronic structure on atomic level by multivariate statistical analysis," *APL Materials* **2** (2014), 120701.
(21) Gu, D.; Dai, X.; Le, C.; Sun, L.; Wu, Q.; Saparov, B.; Guo, J.; Gao, P.; Zhang, S.; Zhou, Y.; Zhang, C.; Xiong, L.; Li, R.; Li, Y.; Li, X.; Liu, J.; Sefat, A.S.; Hu, J.; Zhao, Z. "Robust antiferromagnetism preventing superconductivity in pressurized $Ba_{0.61}K_{0.39}Mn_2Bi_2$," *Scientific Reports* **4** (2014), 7342.
(22) Kim, J.; Haberkorn, N.; Gofryk, K.; Graf, M. J.; Ronning, F.; Sefat, A.S.; Movshovich, R.; Civale, L. "Superconducting properties in heavily overdoped $Ba(Fe_{0.86}Co_{0.14})_2As_2$ single crystals," *Solid State Communications* **201** (2014), 20.
(23) Shi, H.; Saparov, B.; Singh, D. J.; Sefat, A.S.; Du, M. H. "Ternary chalcogenides $Cs_2Zn_3Se_4$ and $Cs_2Zn_3Te_4$: Potential *p*-type transparent conducting materials," *Physical Review B* **90** (2014), 184104.

Program Title: Magneto-transport in GaAs Two-dimensional Hole Systems

Principal Investigator: M. Shayegan

Mailing Address: Department of Electrical Engineering, Princeton University, Princeton, NJ, 08544

E-mail: shayegan@princeton.edu

Program Scope

Two-dimensional (2D) carrier systems confined to modulation-doped semiconductor hetero-structures provide a nearly ideal testing ground for exploring new physical phenomena. At low temperatures and in the presence of a strong magnetic field, these systems exhibit fascinating, often unexpected, many-body states, arising from the strong electron-electron interaction. Examples include the fractional quantum Hall liquid, the Wigner solid, and the newly discovered striped and bubble phases in the higher Landau levels.

Much of the work on the clean 2D systems has been performed on 2D *electrons* confined to a remotely-doped GaAs quantum well. The goal of this project is to study the materials science and physics of 2D *holes* confined to such wells. Compared to the 2D electrons in GaAs, the 2D holes possess a more complex energy band structure which not only depends on the quantum well width and 2D hole density, but it can also be tuned via perpendicular electric field (gate bias), parallel magnetic field, and strain. These characteristics add new twists and allow for insight into fundamental phenomena in confined, low-disorder carrier systems.

In our project we study 2D hole samples which are grown via state-of-the-art molecular beam epitaxy, and use low-temperature magneto-transport measurements to explore their novel physics. Among the problems we are addressing are the shapes of Fermi contours of 2D holes and of flux-hole composite fermions as a function of parameters such as parallel magnetic field and/or strain. Also of interest are the fractional quantum Hall states, including the state at the even-denominator filling $\nu = ½$, in 2D hole systems confined to wide GaAs quantum wells. In our work, we collaborate closely with Prof. Roland Winkler (Univ. of Northern Illinois), who is an expert in calculating the energy band structure and Landau levels in 2D hole systems, and Dr. Loren Pfeiffer who is a world expert in molecular beam epitaxy.

Recent Progress

A hallmark of the GaAs 2D holes is their complex band structure. Thanks to the spin-orbit interaction, the 2D hole bands are often split at finite values of wave vector (k) and also become anisotropic as k grows in different in-plane directions (Fig. 1). One goal of our proposed research is to quantitatively probe these dispersions, both experimentally and theoretically. Experimental determination of the 2D hole dispersions has long been a subject of interest. It continues to be a subject of active research, thanks partly to the interest in spintronic devices and also the possibility that holes in confined structures might have a long spin coherence time (because of the lack of overlap of holes' p-type wave function with the nuclei) and be useful in quantum computing. Here we describe our recent efforts in two areas.

A. Tuning and probing Fermi contours of hole-flux composite Fermions

The composite fermion (CF) formalism provides an extremely powerful yet very simple description of the interacting particles at high perpendicular magnetic fields. In the CF picture,

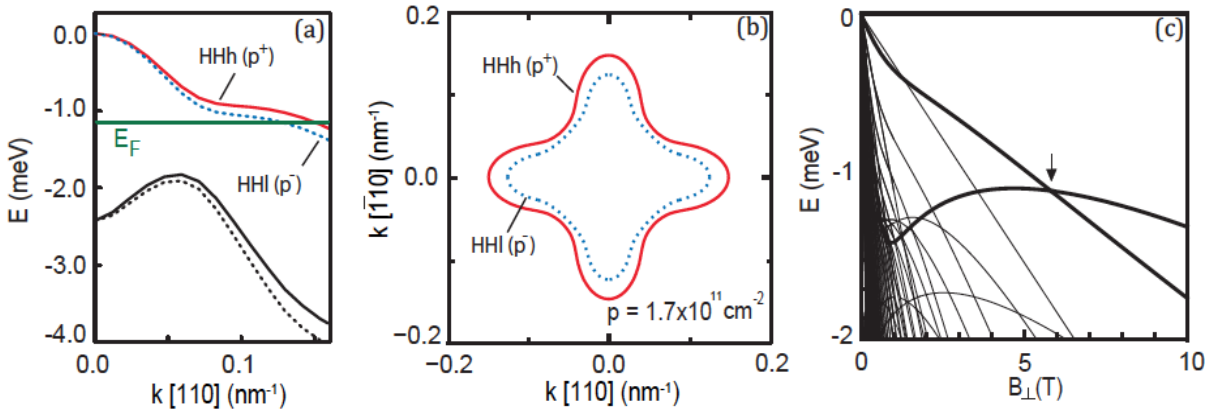

Fig. 1. (a) Energy vs. wave vector (k) dispersions, and (b) Fermi contours, calculated for 2D holes confined to a 25-nm-wide, (001) GaAs quantum well at a density of $p = 1.7 \times 10^{11}$ cm^{-2}. At this density, only the heavy (p+) and light (p-) heavy-hole (HH) bands of the ground-state electric subband are occupied. These correspond to the majority and minority spin-subbands and the splitting between them (at finite values of k) is caused by the spin-orbit interaction. Note the pronounced warping of both p+ and p- Fermi contours. In (c) the calculated Landau levels are shown for this 2DHS, indicating a crossing of the lowest two levels at around 6 T. (After Refs. 5 & 11)

an even number of flux quanta pair up with each carrier at high magnetic field to form quasi-particles which, at Landau level filling factor ν = ½, occupy a Fermi sea with a well-defined Fermi contour. The existence of a CF Fermi contour raises the question whether fermionization preserves any low-field Fermi contour anisotropy (Fig. 1(b)). To answer this fundamental question we determined, via measurements of commensurability oscillations, the shape of the hole-flux CF Fermi contour near filling factor ν = ½ in a wide GaAs quantum well where the low-field holes have a significant *warping* in their Fermi contour (Fig. 1(b)). These are very challenging measurements as they require samples with extremely high quality 2D holes, as well as a very gentle and well-ordered periodic potential. Our experiments (Fig. 2) reveal that the CFs are strongly influenced by the characteristics of the Landau level in which they are formed [11]. In particular, their Fermi contour is warped when their Landau level originates from hole band with significant warping.

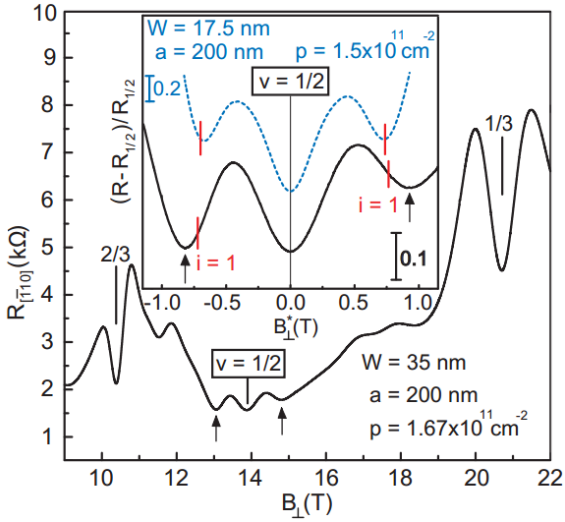

Fig. 2. Magneto-resistance trace for 2D holes confined to a GaAs quantum well of width W = 35 nm and subjected to a small one-dimensional potential modulation with period 200 nm. The two prominent minima seen near filling factor ν = 1/2 are signatures of commensurability of CF cyclotron orbit diameter with the period of the density modulation. Inset: Enlarged trace near ν = 1/2 shows that the positions of the minima are measurably farther from $B^*_\perp = 0$ than expected for a circular Fermi contour of fully spin-polarized CFs (marked by vertical red tick marks); $B^*_\perp$ is the effective magnetic field felt by the CFs. For comparison, we also include data (dotted blue trace) from a narrower 2D hole system (W = 17.5 nm). In this case, similar to their 2D hole counterparts near zero magnetic field, CFs also show no warping in their Fermi contour, as illustrated by commensurability minima near ν = 1/2, which agree well with the red tick marks that are based on a circular Fermi contour. (After Ref. 11)

B. Even-denominator fractional quantum Hall effect in wide GaAs quantum wells

When electrons at sufficiently high density are confined to a high-quality *wide* GaAs quantum-well, they occupy two electric subbands and possess a bilayer-like charge distribution. Under appropriate conditions, the additional layer and/or subband degree of freedom stabilizes a special fractional quantum Hall state (FQHS) at the *even-denominator* Landau level filling factor $\nu = ½$. This state is generally believed to be the two-component, Halperin-Laughlin (Ψ_{331}) state, a FQHS with strong inter-layer and intra-layer correlations. Although the $\nu = ½$ state was discovered over 20 years ago, its observation was only reported in high quality GaAs electron systems until now.

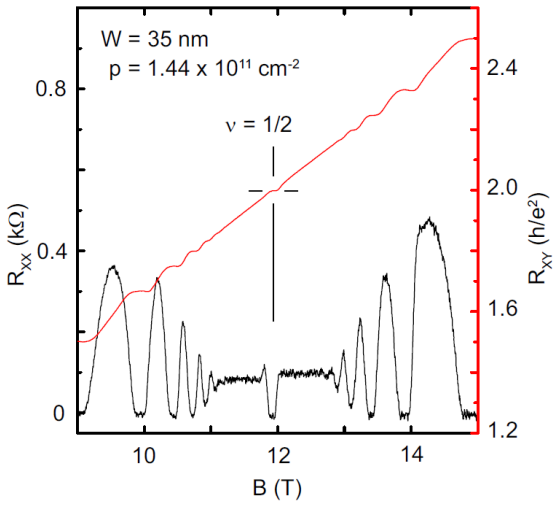

Fig. 3. An example of fractional quantum Hall effect observed at the *even-denominator* fractional filling in a 2D hole system confined to a 2D hole system in a symmetric 35-nm-wide GaAs quantum well. Data shown here are the longitudinal (R_{xx}) and Hall (R_{xy}) resistances. (After Refs. 4 and 5)

In our laboratory, we made the first observation of the $\nu = ½$ FQHS in GaAs *hole* systems [4,5]. Figure 3 shows the longitudinal and Hall resistances measured in a symmetric 35-nm-wide GaAs quantum well at density $p = 1.44 \times 10^{11}$ cm^{-2}. At filling factor $\nu = 1/2$, we observe a deep minimum in the longitudinal resistance (R_{xx}) and a clear plateau in the Hall resistance (R_{xy}) quantized at $2h/e^2$. The evolution of this $\nu = ½$ FQHS as a function of hole density in the quantum well is quite unexpected and qualitatively different from what is seen in 2D electron systems. In particular, we observe an unusual crossing of the two, lowest-energy, hole Landau levels as we tune the 2D hole density (Fig. 1(c)) [5]. The crossing leads to a weakening or disappearance of the commonly seen odd-denominator FQHSs in the filling range $1/3 \leq \nu \leq 2/3$. But, surprisingly, a new FQHS at the even-denominator filling $\nu = 1/2$ comes to life at the crossing.

Future plans

We plan to concentrate in several areas. First, we will continue our study of 2D holes confined to relatively wide GaAs quantum wells, with a focus on tilting the sample in the magnetic field. Our preliminary data show that we can tune the crossing of the lowest two Landau levels (leading, again to a $\nu = 1/2$ FQHS) using the in-plane component of the magnetic field ($B_{||}$) instead of changing the density. We also see other, unusual anisotropic many-body states as we tilt the sample and we plan to explore their origin. Second, we would like to continue our experiments on tuning and probing the CF Fermi contours using $B_{||}$ (see, e.g., publications 1 and 3?). In particular, we plan to study the relation between the anisotropies of transport and the Fermi contours. We will measure the resistance at $\nu = 1/2$ as a function of $B_{||}$. Combined with our Fermi contour measurements, the data should shed light on CFs' scattering time and effective mass. We also plan to utilize uniaxial strain, rather than $B_{||}$, to induce Fermi contour anisotropy. The main advantage of using strain is that it eliminates the coupling of CFs' out-of-plane motion with $B_{||}$.

Publications (which acknowledge DOE support; since 2013)

1. D. Kamburov, Yang Liu, M. Shayegan, L.N. Pfeiffer, K.W. West, and K.W. Baldwin, "Composite Fermions with Tunable Fermi Contour Anisotropy," Phys. Rev. Lett. **110**206801 (2013).
2. D. Kamburov, M. A. Mueed, M. Shayegan, L. N. Pfeiffer, K. W. West, K. W. Baldwin, J. J. D. Lee, and R. Winkler, "Anisotropic Fermi Contour of (001) GaAs Electrons in Parallel Magnetic Fields," Phys. Rev. B **88**, 125435 (2013).
3. D. Kamburov, M.A. Mueed, M. Shayegan, L. N. Pfeiffer, K. W. West, K. W. Baldwin, J. J. D. Lee, R. Winkler, "Fermi Contour Anisotropy of GaAs Electron-Flux Composite Fermions in Parallel Magnetic Fields," Phys. Rev. B **89**, 085304 (2014).
4. Yang Liu, A.L. Graninger, S. Hasdemir, M. Shayegan, L.N. Pfeiffer, K.W. West, K.W. Baldwin, and R. Winkler "Fractional Quantum Hall Effect at ν = ½ in Hole Systems Confined to GaAs Quantum Wells," Phys. Rev. Lett. **112**, 046804 (2014).
5. Yang Liu, S. Hasdemir, A.L. Graninger, D. Kamburov, M. Shayegan, L.N. Pfeiffer, K.W. West, K.W. Baldwin, and R. Winkler, "Even-denominator Fractional Quantum Hall Effect at a Landau Level Crossing," Phys. Rev. B **89**, 165313 (2014).
6. Yang Liu, S. Hasdemir, A. Wojs , J.K. Jain, L.N. Pfeiffer, K.W. West, K.W. Baldwin, and M. Shayegan, "Spin Polarization of Composite Fermions and Particle-hole Symmetry Breaking," Phys. Rev. B **90**, 085301 (2014).
7. D. Kamburov, Yang Liu, M.A. Mueed, M. Shayegan, L.N. Pfeiffer, K.W. West, K. Baldwin, "What Determines the Fermi Wave Vector of Composite Fermions?" Phys. Rev. Lett. **113**, 196801 (2014).
8. D. Kamburov, M.A. Mueed, I. Jo, Y. Liu, M. Shayegan, L.N. Pfeiffer, K.W. West, K.W. Baldwin, J.J. Lee, R. Winkler, "Determination of Fermi Contour and Spin Polarization of ν = 3/2 Composite Fermions via Ballistic Commensurability Measurements," Phys. Rev. B **90**, 235108 (2014).
9. Yang Liu, D. Kamburov, S. Hasdemir, M. Shayegan, L.N. Pfeifer, K.W. West, and K.W. Baldwin, "Fractional Quantum Hall Effect and Wigner Crystal of Interacting Composite Fermions," Phys. Rev. Lett. **113**, 246803 (2014).
10. S. Hasdermir, Yang Liu, H. Deng, M. Shayegan, L.N. Pfeiffer, K.W. West, and K.W. Baldwin, "ν = ½ Fractional Quantum Hall Effect in Titled Magnetic Fields," Phys. Rev. B **91**, 045113 (2015).
11. M.A. Mueed, D. Kamburov, Y. Liu, M. Shayegan, L.N. Pfeiffer, K. West, K. Baldwin, R. Winkler, "Composite Fermions with a Warped Fermi Contour," Phys. Rev. Lett. **114**, 176805 (2015).
12. M.A. Mueed, D. Kamburov, M. Shayegan, L.N. Pfeiffer, K.W. West, K.W. Baldwin, and R. Winkler, "Splitting of the Fermi Contour of Quasi-2D Electrons in Parallel Magnetic Fields," Phys. Rev. Lett. **114**, 236404 (2015).
13. M.A. Mueed, D. Kamburov, S. Hasdemir, M. Shayegan, L.N. Pfeiffer, K.W. West, K.W. Baldwin, "Geometric Resonance of Composite Fermions Near the ν = 1/2 Fractional Quantum Hall State," Phys. Rev. Lett. **114,** 236406 (2015).

Program Title: Photonic Systems

PI: J. Shinar; Co-PIs: R. Biswas, K.M. Ho, C.M. Soukoulis, S. Dobrovitski
Mailing Address: Ames Laboratory, Iowa State University, Ames, Iowa 50010.

Program Scope

The Ames Laboratory has pioneered the development of 3D photonic crystals (PCs), developed forefront organic light-emitting diodes (OLEDs) and procedures for characterizing them, and conducted pioneering optically and electrically detected magnetic resonance studies on organic semiconductors and OLEDs since ~1990. These research areas are combined into interrelated tasks that will be performed in the next three years. Besides continuing the studies in each of these areas, we will use our vast expertise in them to enhance light emission from OLEDs, thereby combining the PC expertise with (organic) light-emitting structures. These will include, inter alia, top-emitting microcavity OLEDs that will be fabricated on glass and plastic substrates coated with a thick metal electrode. This architecture will dramatically enhance heat sinking in the devices and consequently their stability as well. Importantly, the FWP has been expanded to include quantum dynamics and control of spins in organic semiconductors, i.e., organic spintronics. While this task is driven by theoretical work, it includes experiments to verify the theoretical results. In another task, we will build on our strengths to achieve new functionalities of PCs, including surface beaming, supertransmission, and PC lasing. Finally, we will utilize low-cost methods to design and fabricate large-area PC structures relevant to energy-related applications. There will be a close synergy between theory, simulation, fabrication and experimental studies in these inter-related tasks.

Recent Progress

Energy harvesting in OPVs: Bulk heterojunction OPVs have advanced rapidly in recent years. However, due to free carrier recombination the active layer thickness is limited to < 200 nm, significantly less than the NIR photon absorption length, so ~ 50% of the incident sunlight is not absorbed. Using scattering matrix simulations we developed a novel photonic/plasmonic architecture, with an anode corrugated in a periodic nanocone array that traps photons in the BHJ layer; that layer and the metal cathode grow conformally on this anode. By optimizing the array pitch and corrugation height we increased light absorption by ~40% and the simulated photocurrent by ~50% [14]. The periodic nanostructure strongly diffracts light creating a mesh of waveguiding modes. The corrugated metal cathode also yields propagating surface plasmons at the organic/metal interface, which aids in harvesting long-wavelength

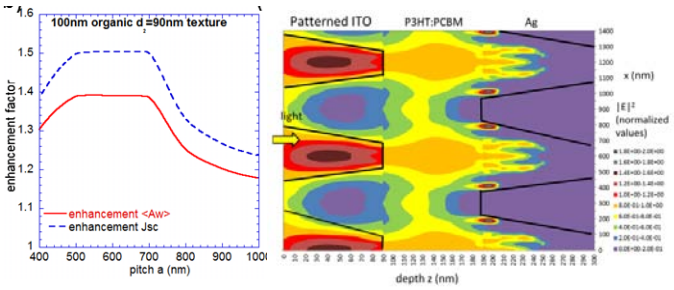

Fig. 1. *Left: Enhancement factor of light absorption and photocurrent, as a function of the pitch, for the conformally corrugated organic solar architecture. Right: Electric field intensity $|E|^2$ in the cross-section of the cell at λ =620nm.*

photons.

Enhanced efficiency of OPVs and OLEDs using microlens arrays (μLAs): OPVs and OLEDs require structures to enhance light absorption and extraction, respectively. Different periods and heights of μLAs were simulated and then fabricated from polyurethane (PU) with soft lithography (Fig. 2) and attached to the "blank" side of the glass substrate. The optical path in the active OPV layer increased by diffraction resulting in enhanced optical absorption. The μLAs increased the power conversion efficiency (PCE) of PCDTBT:$PC_{71}BM$ OPVs (active layer thickness t_{act} ~ 70nm) by 5.6%-13% and of PTB_7:$PC_{71}BM$ OPVs (t_{act} ~ 90nm) by 5.3%-10.6%, depending on the μLA structure [4, 15], in agreement with our simulations. μLAs can also be used to improve light extraction in OLEDs by eliminating the total internal reflection (TIR) and waveguiding in the glass substrate, which is seen in the edge emission. If the μLA is much larger than the OLED pixel, it enhances light extraction by ~100%. A single lens also improves extraction but it is not practical for large area luminaires.

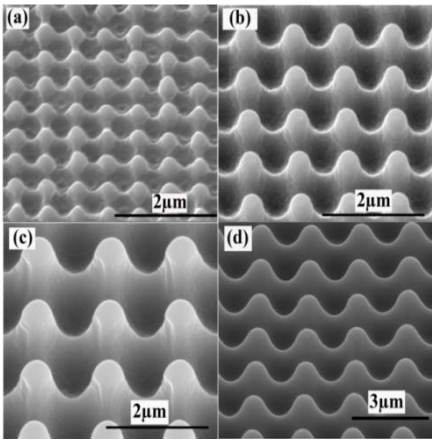

Fig. 2. *SEM images of MLAs: (a) period 0.6μm, height 250nm, (b) p=1μm and h=350 nm, (c) p=1.5 μm and h=900 nm, and (d) p=2 μm and h=1000 nm.*

Beam collimation and directional emission using dielectric surface states: We demonstrated, experimentally and theoretically, 2-layer dielectric structures that collimate and enhance transmission of a Gaussian beam passing through it [13]. This demonstrates that low-loss purely dielectric resonant surface states can be leveraged for low loss beam collimation. A system of multiple cascading bilayers can sustain the beam for large propagation distances. Grating coupled surface modes fed by a matched waveguide allow for efficient in/out coupling of nanostructures, beaming and beam steering as well as frequency splitters [10]. We demonstrate dielectric surface mode based beaming, directional emission and frequency splitters (Fig. 3).

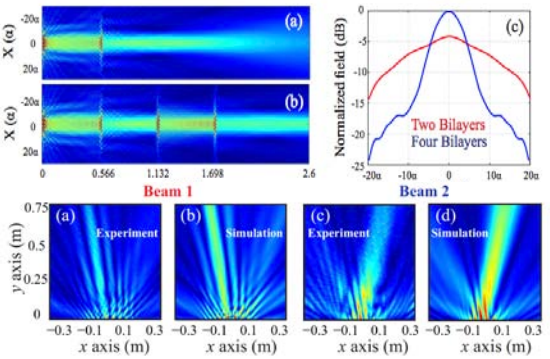

Fig. 3. *Collimating a microwave beam by discrete dielectric double layers (top); Directional emission from a photonic crystal surface mode (bottom).*

Lasing threshold in Photonic Crystal slabs: We derived and demonstrated a simple analytic Q factor model that elucidates the lasing threshold of a PC slab vs interface reflectivities (impedance), group velocity (band structure), and intrinsic loss [14]. It shows how the lasing threshold may be dramatically altered inside a band or, most importantly, close to the band edge. Our simple model enables understanding and optimizing the design of PC-based lasing structures.

Future Plans

Future work will focus partly on the microscopic polaron, exciton, and spin dynamics in organic light-emitting systems and on the science underlying their macroscopic behavior: light extraction and emission profiles from OLEDs and other active surfaces, OLED and OPV efficiency and stability, and beaming and lasing from PCs and related surface structures.

Photonic structures low threshold lasers or smasers with directional emission: We will develop a self-consistent method to incorporate gain in metamaterials photonic crystals and plasmonics and perform simulations also for 3D photonic crystals with gain materials to obtain low-threshold lasers. Our experimental colleagues (M. Farsari) at FORTH developed a new bulk polymer with gain and nonlinearity that supports two-photon polymerization to create the woodpile photonic crystal of CdS nanoparticles-polymer nanocomposities, which can be used to develop low-threshold lasers. We will design, simulate, and fabricate PCs with surface modes as the resonant feedback with gain ultrathin surface lasers ("SMASER": Surface Mode [L]ASER). We propose to demonstrate smasers with highly directional emission.

Nanostructured plasmonic reflectors for efficient thin film solar cells: We designed thin absorbers utilizing both electrical and magnetic impedance matching in the near-IR using two artificial layers that provide electric and magnetic resonances, yielding perfect polarization-independent broadband absorption. We will fabricate updated designs and measure the thin absorbers. Such structures can also lead to a rich variety of non-linear phenomena.

High aspect metallic transparent electrodes on flexible substrate: We have demonstrated high aspect metallic transparent electrodes as a replacement of conventional ITO-coated glass. Metal thin films are more flexible than metal-oxides making high aspect metallic electrodes more suitable for flexible devices. The electrodes can be made on flexible substrates as flexible devices electrodes in OLEDs, solar cells, and touchpad. Our electrodes can be made on flexible substrate without substantial heating on flexible substrates.

Large area 3D PCs: For proof of concept, 3D multilayer wood pile PCs from a few hundred microns to 4 mm have been made in our FWP. Large area PCs are required for practical use in many applications. Scaling up the sample size is another major breakthrough in applications. We developed the 2P-μTM to reduce the process time from month to days for mm size woodpile PCs. Large area wood pile PCs of few inches square or larger are beneficial in developments requiring large area as well as short process time.

Publications

1. W. P. Cui, R. Liu, E. Manna, J. M. Park, F. Fungura, J. Shinar, and R. Shinar, "Oxygen and Relative Humidity Monitoring with Films Tailored for Enhanced Photoluminescence," Analytica Chimica Acta, 853, 563-571 (2015).

2. E. Manna, F. Fungura, R. Biswas, J. Shinar, and R. Shinar, "Tunable near Uv Microcavity Oled Arrays: Characterization and Analytical Applications," Advanced Functional Materials, 25, 1226-1232 (2015).
3. C. M. Soukoulis, T. Koschny, P. Tassin, N. H. Shen, and B. Dastmalchi, "What Is a Good Conductor for Metamaterials or Plasmonics," Nanophotonics, 69-74 (2014).
4. Y. Q. Chen, M. Elshobaki, R. Gebhardt, S. Bergeson, M. Noack, J. M. Park, A. C. Hillier, K. M. Ho, R. Biswas, and S. Chaudhary, "Reducing Optical Losses in Organic Solar Cells Using Microlens Arrays: Theoretical and Experimental Investigation of Microlens Dimensions," Physical Chemistry Chemical Physics, 17, 3723-3730 (2015).
5. Z. X. Huang, S. Droulias, T. Koschny, and C. M. Soukoulis, "Mechanism of the Metallic Metamaterials Coupled to the Gain Material," Optics Express, 22, 28596-28605 (2014).
6. W. R. Lindemann, W. Wang, F. Fungura, J. Shinar, and D. Vaknin, "The Effect of Cesium Carbonate on 1-(3-Methoxycarbonyl)Propy-L-Phenyl[6,6]C61 Aggregation in Films," Applied Physics Letters, 105, 5 pages (2014).
7. S. Pattnaik, N. Chakravarty, R. Biswas, V. Dalal, and D. Slafer, "Nano-Photonic and Nano-Plasmonic Enhancements in Thin Film Silicon Solar Cells," Solar Energy Materials and Solar Cells, 129, 115-123 (2014).
8. T. K. Djidjou, Y. Chen, T. Basel, J. Shinar, and A. Rogachev, "Magnetic Field Enhancement of Generation-Recombination and Shot Noise in Organic Light Emitting Diodes," Journal of Applied Physics, 117, 115501 (2015).
9. E. S. Hellerich, E. Manna, R. Heise, R. Biswas, R. Shinar, and J. Shinar, "Deep Blue/Ultraviolet Microcavity Oleds Based on Solution-Processed PVK:CBP Blends," Organic Electronics, 24, 246-253 (2015).
10. A. C. Tasolamprou, L. Zhang, M. Kafesaki, T. Koschny, and C. M. Soukoulis, "Frequency Splitter Based on the Directional Emission from Surface Modes in Dielectric Photonic Crystal Structures," Optics Express, 23, 13972-13982 (2015).
11. Z. Y. Wang, R. J. Zhang, S. Y. Wang, M. Lu, X. Chen, Y. X. Zheng, L. Y. Chen, Z. Ye, C. Z. Wang, and K. M. Ho, "Broadband Optical Absorption by Tunable Mie Resonances in Silicon Nanocone Arrays," Scientific Reports, 5, 7810 (2015).
12. X. K. Xin, B. Li, J. H. Jung, Y. J. Yoon, R. Biswas, and Z. Q. Lin, "Ab Initio Simulation of Charge Transfer at the Semiconductor Quantum Dot/TiO2 Interface in Quantum Dot-Sensitized Solar Cells," Particle & Particle Systems Characterization, 32, 80-90 (2015).
13. A. C. Tasolamprou, L. Zhang, M. Kafesaki, Th. Koschny and C. M. Soukoulis, “Experimentally experiment beaming in a two-layer dielectric structure,” Opt. Express 22, 23147 (2014).
14. S. Droulias, C. Fietz, P. Zhang, Th. Koschny and C.M. Soukoulis, “Lasing threshold control in 2D photonic crystals with gain,” Opt. Express 22, 19242 (2014).
15. Y. Chen, M. Elshobaki, Z. Ye, J. M. Park, M. A. Noack, K. M. Ho and S. Chaudhary, “Microlens array induced light absorption enhancement in polymer solar cells”, *Phys. Chem. Chem. Phys.* **15**, 4297 (2013).
16. R. Biswas, E. Timmons, “Nano-photonic light trapping near the Lambertian limit in organic solar cell architectures,” Optics Express 21 Iss. S5, pp. A841–A846 (2013)

Project Title: Magneto-optical study of correlated electron materials in high magnetic fields

Principal Investigator: Dmitry Smirnov; Co-PI: Zhigang Jiang
Address: National High Magnetic Field Laboratory, Tallahassee, FL 32312
Email: smirnov@magnet.fsu.edu

Program Scope

Probing energy, symmetry and dispersion of low-lying excitations and studying many-body effects in novel electronic materials via magneto-optical spectroscopy is a longstanding goal of this program. The remarkable properties of graphene have generated a great interest in other inorganic, two-dimensional (2D) crystalline materials or Dirac-like surface-state materials with unique electronic and optical properties. Among those "graphene-inspired" materials, two- and three- dimensional topological insulators and transition metal dichalcogenides are of great interest due to their extraordinary range of new properties and new functionalities.

Our prior DOE supported work was focused on Landau level spectroscopy of graphene and graphite. The main earlier findings include magneto-infrared (IR) studies of cyclotron resonance (CR) in mono- and bi-layer graphene, coupled plasmon-CR modes in graphene nano-ribbons, and magneto-Raman spectroscopy of magneto-phonon resonances in graphene and graphite. In our recent studies, we employed optical spectroscopy to study electronic states and correlations in graphite in very strong magnetic fields up to 45 T [1], and probe electronic structure of 2D and 3D topological insulators [2-5].

Recent Progress

Landau level spectroscopy study of 2D topological insulators (quantum spin Hall insulators): HgTe/CdHgTe and InAs/GaSb quantum wells

Background: Recently topological insulators (TIs) have emerged as a new class of quantum matter in which gapless Dirac-like surface states are protected by time-reversal symmetry. TIs can be realized in systems with opposite parity of the conduction and the valence bands when the band inversion occurs, for example, in HgTe/CdHgTe semiconductor quantum wells (QWs). This 2D system can be tuned from the trivial band insulator to a 2D TI phase, or a quantum spin Hall phase, by changing the QW thickness [7]. A topological phase transition occurs at the critical QW thickness where the band gap vanishes and the low-energy band structure can be described by the linear dispersions of massless Dirac fermions. In 2011, a new type of quantum spin Hall insulator has been realized in inverted InAs/GaSb quantum wells [8], following the initial theoretical prediction of Ref. [9]. This quantum well system exhibits a unique band alignment: the bottom of the conduction band in InAs lies below the top of the valence band in GaSb. Consequently, a hybridization gap forms in the inverted region, leading to a topologically

protected quantum spin Hall phase when the Fermi level lies inside the gap. Band structure engineering of this material is a cornerstone for its future development.

Discussion of Findings:

(i) HgTe/CdHgTe quantum wells. We performed low-temperature IR cyclotron resonance (CR) studies on a series HgTe QWs at and near the critical QW thickness. In a gapless HgTe QW, we observed a characteristic $B^{1/2}$ dependence of CR energies, a signature of massless 2D Dirac fermions, also enabling direct and accurate measurements of the band velocity. In a small gap QW with the width that slightly deviates from the critical thickness, the dominant fundamental CR line also follows the $B^{1/2}$ dependence, though its splitting indicates the existence massive Dirac fermions. We show that the low-energy CR transitions of HgTe QWs near or at the critical thickness can be quantitatively described by an effective Dirac model, making it a valuable tool for future band-gap engineering of similar materials [2].

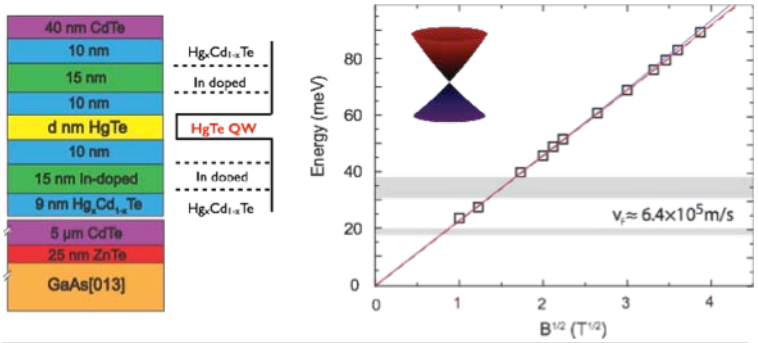

FIG. 1: (a) Schematic view of studied HgTe/CdHgTe quantum well structures. (b) The CR energies plotted as a function of $B^{1/2}$ for a gapless sample. The linear slope is the direct measure of the band velocity of the Dirac cone [2].

(ii) InAs/GaSb quantum wells. Here we employ Landau level spectroscopy (experimental) and eight-band k·p calculation to determine the critical widths of quantum wells separating the quantum spin Hall phase from the normal phase. Collaborating with the Sandia Labs (Drs. Wei Pan and John Klem), we studied a series of InAs/GaSb quantum well bilayers with 5nm-wide GaSb (fixed) and various widths of InAs, as shown in Fig. 2(a). We find that, by changing the relative thickness of each quantum well layer, one can band-engineer the material from the normal region to the inverted region (quantum spin Hall region) through a phase transition (critical region). We further demonstrate that in the normal and critical region (for 8nm- and

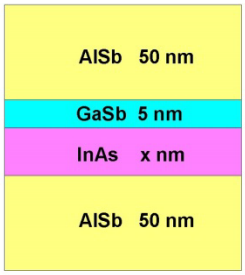

Sample	InAs width (x)
1	8nm
2	10nm
3	11nm
4	13nm
5	15nm

(a)

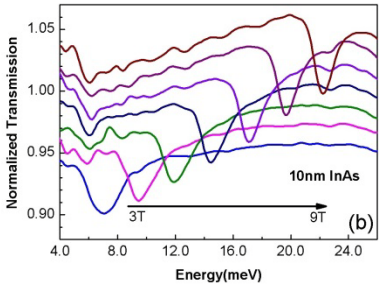

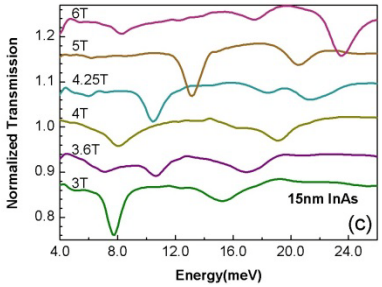

FIG. 2: (a) Quantum well structure of InAs/GaSb material system. (b,c): Normalized transmission spectra (with respect to zero field spectra) in the normal/critical (b) and inverted (c) regions at selected magnetic fields.

10nm-wide InAs) only single cyclotron resonance can be observed, while in the inverted region (for 11nm-, 13nm- and 15nm-wide InAs) multiple cyclotron resonances, as well as anti-crossing behavior, occur.

To quantitatively understand our experimental results, we performed eight-band k·p calculation of the electronic band structure of the quantum wells. We confirm that the critical width of InAs (given 5nm-wide GaSb) is 10.2 nm, indeed between 10 nm and 11 nm where multiple cyclotron resonances and anti-crossing behavior start to appear. Currently, we are collaborating with Prof. Chris Stanton at the University of Florida to calculate the Landau fan diagrams of the materials with realistic conditions, considering Zeeman effect, strain effect, self-consistency, the Fermi level position, and the barrier strength between the InAs layer and the GaSb layer. The outcome of this work will provide a powerful prediction tool for band-engineering the intriguing InAs/GaSb system.

Future Plans

(1) Landau level spectroscopy study of InAs/GaSb quantum wells at critical thickness. We plan to continue the IR magneto-spectroscopy study of InAs/GaSb quantum wells, crossing the quantum phase transition between the quantum spin Hall phase and the normal insulator phase. Recent low-temperature electronic transport measurements have indicated that InAs/GaSb quantum wells at critical thickness is an excitonic insulator. We will develop an IR transparent gate (made of ITO or transition metal thin films) to tune the carrier density in the quantum wells towards charge neutrality, and look for the IR evidence (e.g., an energy gap) of such an intriguing state.

(2) Magneto-IR study of graphene in a periodically modulated magnetic field (PMMF). We plan to continue the IR spectroscopy study of magneto-plasmons in graphene structures. Specifically, we will fabricate a corrugated surface on silicon carbide substrate and grow epitaxial graphene (following the corrugated surface profile) using the confinement controlled sublimation method. During the measurement, the component of an externally applied magnetic field perpendicular to the graphene is spatially modulated. New electronic band structure, as well as new optical mode, is expected to arise from the PMMF-induced coupling between the magneto-plasmons in graphene. The strength of the coupling can be engineered via varying the dimensionality and periodicity of the corrugated surface structure, and can be tuned externally by rotating the magnetic field with respect to the graphene surface.

(3) Magneto-optical study of semiconducting, atomically thin transition metal dichalcogenides (TMDs). 2D semiconducting TMD compounds ($MoSe_2$, WSe_2, …). are direct-gap semiconductors in a monolayer with two degenerate valleys per Brillouin zone. This valley degree of freedom can be selectively accessed by optical helicity, providing a unique platform to probe and manipulate the charge carriers in the two valleys. Recently, in collaboration with Prof. Tony F. Heinz at Columbia University, we demonstrated lifting of the valley degeneracy in

monolayer $MoSe_2$ by valley-resolved magneto-photoluminescence (PL) spectroscopy in magnetic field up to 10T [10]. We plan to carry out a series of higher field magneto-PL experiments in the presence of gate-controlled electric field to probe spin-valley coupling, valley polarization, excitonic effects, and, possibly Landau level physics. Another research direction aims at performing similar magneto-optical experiments on gated bilayer TMD structures, in which the intrinsic inversion symmetry can be broken by applying a perpendicular electric field.

References (which acknowledge DOE support)

1. *"Effects of Electron-Electron Interactions on Electronic Raman Scattering of Graphite in High Magnetic Fields,"* Y. Ma, Y. Kim, N.G. Kalugin, A. Lombardo, A.C. Ferrari, J. Kono, A. Imambekov, and D. Smirnov, Physical Review B, **89**(12), 121402(R) (2014).
2. *"Cyclotron Resonance of Single-valley Dirac Fermions in Nearly Gapless HgTe Quantum Wells,"* J. Ludwig, Y.B. Vasilyev, N.N. Mikhailov, J.M. Poumirol, Z. Jiang, O. Vafek, and D. Smirnov, Physical Review B, **89**(24), 241406(R) (2014).
3. *"Magneto-infrared Spectroscopic Study of Ultrathin Bi_2Te_3 Single Crystals,"* L.-C. Tung, W. Yu, P. Cadden-Zimansky, I. Miotkowski, Y.P. Chen, D. Smirnov, and Z. Jiang, arXiv:1508.04704.
4. *"Magneto-infrared Study of Topological Insulator Bi_2Se_3,"* W. Yu, X. Chen, Z. Jiang, I. Miotkowski, H. Cao, Y.P. Chen, D. Smirnov, and L.-C. Tung, arXiv:1508.04363.
5. *"Unraveling photoinduced spin dynamics in topological insulator Bi_2Se_3,"* M. C. Wang, S. Qiao, Z. Jiang, S. N. Luo, and J. Qi, submitted to Physical Review Letters.
6. *"High Photoresponsivity and Short Photoresponse Times in Few-Layered WSe_2 Transistors"*, N. R. Pradhan, J. Ludwig, Z. Lu, D. Rhodes, M.M. Bishop, K. Thirunavukkuarasu, K., S. McGill, D. Smirnov, and L. Balicas, ACS Applied Materials & Interfaces, **7**, 12080 (2015)

Other references

7. *"Quantum Spin Hall Effect and Topological Phase Transition in HgTe Quantum Wells"*, B.A. Bernevig, T.L. Hughes, and S.C. Zhang, Science **314**(5806), 1757–1761 (2006).
8. *"Evidence for Helical Edge Modes in Inverted InAs/Gasb Quantum Wells,"* I. Knez, R.-R. Du, and G. Sullivan, Physical Review Letters **107**, 136603 (2011).
9. *"Quantum Spin Hall Effect in Inverted Type-Ii Semiconductors,"* C. Liu, T. L. Hughes, X.-L. Qi, K. Wang, and S.-C. Zhang, Physical Review Letters **100**, 236601 (2008).
10. *"Valley Splitting and Polarization by the Zeeman Effect in Monolayer $MoSe_2$,"* Li, Y.; Ludwig, J.; Low, T.; Chernikov, A.; Cui, X.; Arefe, G.; Kim, Y. D.; van der Zande, A. M.; Rigosi, A.; Hill, H. M.; Kim, S. H.; Hone, J.; Li, Z.; Smirnov, D.; Heinz, T. F. Phys. Rev. Lett., **113**, 266804 (2014).

Project Title: Fermi Gases in Bichromatic Superlattices

Principal Investigator: John E. Thomas (Award # DE-SC0008646)

Mailing Address: Physics Department, North Carolina State University, Raleigh, NC 27695

E-mail: jethoma7@ncsu.edu

Program Scope

The purpose of the proposed program is the broad study of designer materials made of ultra-cold atoms and light, which provides new paradigms for emulating exotic layered systems. Bichromatic superlattices enable control and study of both dimensionality and dispersion in layered, strongly correlated Fermi gases, offering new opportunities in the search high-temperature superfluidity/superconductivity.

Most layered materials are quasi-two-dimensional, neither two-dimensional, like a sheet, nor three-dimensional, like a gas, but somewhere in between. In quasi-2D layers with an unequal number of spin-up and spin-down electrons, particularly strong attraction between pairs of electrons with opposite spins is predicted to achieve the highest possible superconducting transition temperatures. To understand these materials, we emulate them with a layered, ultra-cold Fermi gas of ^{6}Li atoms, magnetically tuned near a collisional (Feshbach) resonance, where precise control of the attraction, spin-composition, dimensionality and dispersion provides new tests of theory.

The primary goals are of the program are: (1) Elucidation of the effects of dimensionality and confining potential shape on the enhancement of high-temperature superfluidity in a layered, strongly correlated Fermi gases; (2) Control of dispersion and the study of tunable Dirac points in one dimension.

Recent Progress

In the past year, we made two major breakthroughs in our experiments on layered Fermi gases:

- We performed the first precision measurements on a spin-imbalanced quasi-2D Fermi gas, confined in a CO_2 laser standing wave, Fig. 1. Our measurements, Fig. 2, provide the first benchmarks for predictions of the phase diagram of imbalanced 2D gases and demonstrate the failure of 2D-BCS mean field theory in the quasi-2D regime. We developed a 2D polaron model of the thermodynamics that captures much of the behavior, but the model fails to predict a transition to a balanced core that we observe as the minority fraction is increased.

- Using a newly constructed red optical lattice, we have observed the transition from true 2D to quasi-2D behavior in the radiofrequency spectra, as the transverse Fermi energy is tuned from small to comparable to the energy level spacing in the tightly confined

direction. As the Fermi energy is increased, the spectra reveal a transition from 2D-dimer to polaron behavior.

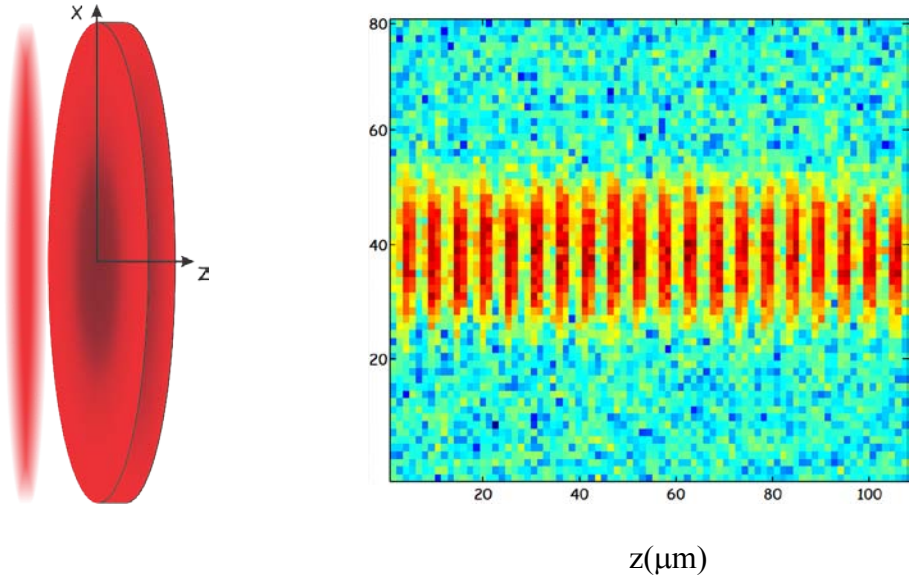

Fig.1. Image of ^{6}Li atoms in a CO_2 laser standing wave trap (right). Each site (left) is a quasi-2D Fermi gas, containing N_1 = 800 spin-up (majority) atoms, where the Fermi energy for motion in the x-direction is comparable to the harmonic oscillator energy level spacing $h\nu_z$ in the tightly confined direction. The number N_2 of spin-down (minority) atoms is variable between 0 and 800. The temperature $T \approx 0.2T_F$.

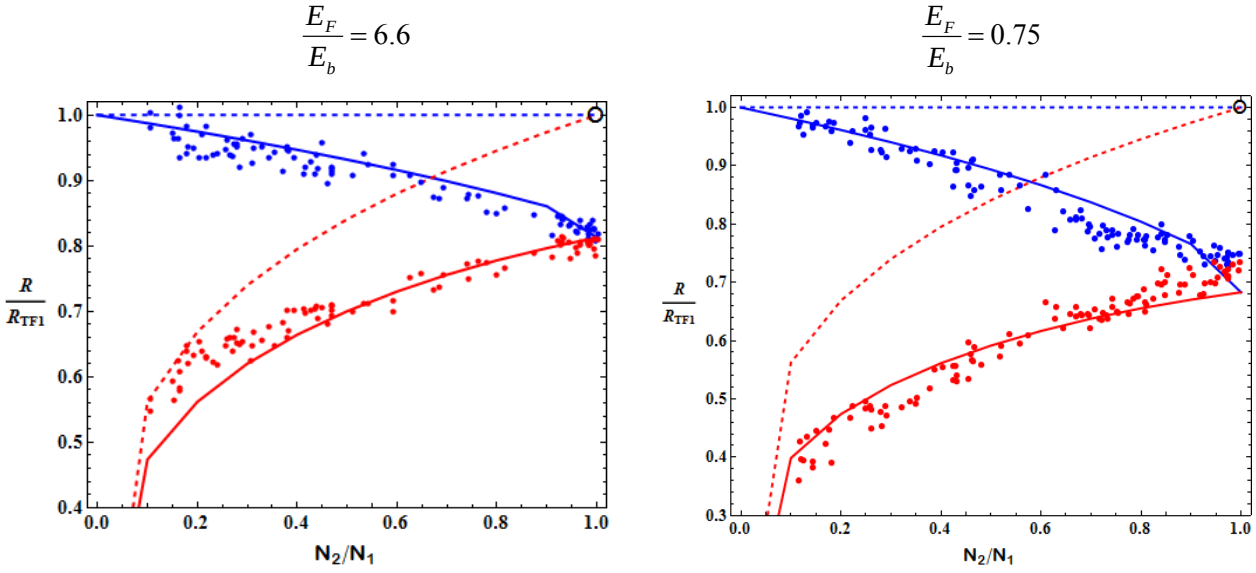

Fig.2. Minority and majority cloud radii as a function of spin-imbalance N_2/N_1 for two different interaction strengths, parameterized by the ratio of the marjority transverse Fermi energy E_F to the 2D dimer binding energy E_b. Dotted lines: ideal gas model; Black circle: 2D-BCS theory for balanced mixture; Solid lines: polaron thermodynamic model.

Future Plans

Our immediate plan is to measure radio-frequency spectra as a function of lattice depth, chemical potential and interaction strength in a combined red lattice-CO_2 laser confining potential to fully characterize the 2D to quasi-2D transition. We plan to study spin-imbalance in the true 2D regime, for which there are many predictions of the phase diagram, but no experimental tests. We also plan to use our current bichromatic (red-green) lattice system to control the potential shape in the tightly confined direction, to create bi-layer sites. Additional experiments will explore thermodynamics in a Fermi gas with 1D relativistic dispersion.

References (which acknowledge DOE support).

1) E. Elliott, J. A. Joseph, and J. E. Thomas, "Observation of Conformal Symmetry Breaking and Scale Invariance in Expanding Fermi Gases," Phys. Rev. Lett. **112**, 040405 (2014).

2) E. Elliott, J. A. Joseph, and J. E. Thomas, "Anomalous Minimum in the Shear Viscosity of a Fermi Gas," Phys. Rev. Lett. **113**, 020406 (2014).

3) W. Ong, Chingyun Cheng, I. Arakelyan, and J. E. Thomas, "Spin-Imbalanced Quasi-Two-Dimensional Fermi Gases," Phys. Rev. Lett. **114**, 110403 (2015).

4) J. A. Joseph, E. Elliott, and J. E. Thomas, "Shear viscosity of a unitary Fermi gas near the superfluid phase transition," Phys. Rev. Lett. **115**, 020401 (2015), selected as an *Editor's Suggestion*.

Electron Spectroscopy of Novel Materials

Tonica Valla, Christopher C. Homes and Peter D. Johnson

valla@bnl.gov, homes@bnl.gov, pdj@bnl.gov

Condensed Matter Physics & Materials Science Department

Brookhaven National Laboratory, Upton, NY 11973-5000

Program Scope

The focus of this program is the exploration of the electronic structure and electrodynamics of strongly correlated electron systems, with particular attention to emergent phenomena, such as superconductivity and magnetism, using angle-resolved photoemission (ARPES) and optical spectroscopy. A central goal of the program is to discover the mechanism of superconductivity in the high-temperature superconductors and iron-based superconductors and to better understand the role of spin- and charge-orders and nematicity that shape the phase diagrams of these materials. The studies also include other modern materials such as topological insulators, topological crystalline insulators, 3D Dirac and Weyl semimetals and materials with extremely large magnetoresistance (WTe_2 and $ZrTe_5$). Interactions of topological insulators with materials displaying magnetism and superconductivity, have been also studied, as the proximity of these two distinct types of matter is expected to produce exotic new phenomena, some of which could be applied in devices.

Recent Progress

Novel phase diagram of an iron-based superconductor. The discovery of iron-based superconductors has prompted an intense investigation of this class of materials in order to determine if the superconductivity originates from a conventional phonon-mediated mechanism, or if, as in the case of the high-temperature cuprate superconductors, it is due to an exotic mechanism that evolves out of a normal state usually characterized as a "bad metal". The iron-based superconductors are multiband materials that can be structurally complicated; however, LiFeAs is relatively simple, consisting of an iron-arsenic layer separated by lithium atoms. We have measured the detailed optical properties of $LiFe_{1-x}Co_xAs$ for Co concentrations of up to 40%. These measurements have been supplemented by transport, ARPES, and nuclear magnetic resonance (NMR) measurements. In its stoichiometric form, LiFeAs has a maximum critical temperature of T_c=18 K; however, T_c decreases monotonically with increasing cobalt content, and superconductivity is destroyed for x>0.18. The real part of the optical conductivity has been determined from a Kramers-Kronig analysis of the reflectance. Because LiFeAs is a multiband material consisting of electron and hole pockets, a minimal description of the optical conductivity consists of two (non-interacting) electronic subsystems, which are modeled as simple Drude components; one narrow and one broad. The narrow term is strongly temperature dependent, while the broad term is essentially temperature independent [8,12,21]. An open question is: what is the nature of the normal state from which superconductivity emerges? In a single-band material, the generalized Drude model is used to calculate the frequency-dependent

scattering rate – if it displays a quadratic form, the material is a Fermi liquid (FL). However, the generalized Drude model does not work for multiband materials [21]; instead, the detailed temperature dependence of the narrow scattering rate for the stoichiometric material, shows quadratic behavior, indicating a FL, in agreement with transport. As cobalt is introduced, T_c decreases and the normal state deviates from a Fermi liquid, with the most profound non-Fermi liquid (NFL) behavior occurring for x ≈ 0.12. As the cobalt concentration continues to increase, the normal state reverts back to a Fermi liquid behavior, but the superconductivity is quickly destroyed and does not re-emerge, again in good agreement with transport measurements. ARPES measurements suggest that this FL-NFL-FL behavior is related to the nesting between the electron and hole Fermi surfaces, which is optimized for x ≈ 0.12. NMR measurements indicate that at this doping low-energy spin fluctuations (LESFs) are maximized, leading to the surprising conclusion that the LESFs disrupt the SC in this material and that the pairing likely relies on high-energy spin fluctuations. This work has led us to propose the phase diagram for this system, shown in Fig. 1.

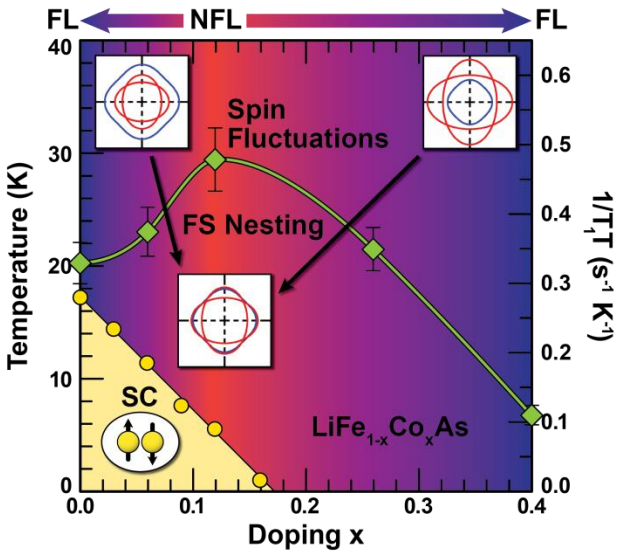

Figure . The phase diagram of $LiFe_{1-x}Co_xAs$, where SC (yellow) is decreasing with increasing Co concentration. In addition, this material shifts from a Fermi liquid to a non-Fermi liquid and back. The green diamonds denote the NMR spin-lattice relaxation rate ($1/T_1T$) at 20 K which reaches a maximum at $x \approx 0.12$, signifying that low-energy spin fluctuations (LESF) are optimized. The three inset panels depict the extracted Fermi surfaces for three representative Co concentrations: x=0 (left), x=0.12 (middle), and x=0.4 (right). The Fermi surface nesting is optimal for x=0.12.

Electronic structure basis for enormous magnetoresistance in WTe_2. Recently, an enormous ("titanic") positive magneto-resistance (MR) was discovered in several non-magnetic materials including WTe_2, $NbSb_2$ and Cd_3As_2 [1–3]. In each of these compounds, an increase in resistivity of several orders of magnitude was found at low temperatures, with no evidence of saturation in very high fields. This is in strong contrast with the conventional behavior observed in simple metals, where MR is usually very small and quadratic in low fields, while it saturates in high fields. To better understand such an enormous MR in these new materials, their electronic structure has to be explored. Our high-resolution ARPES studies of the low energy electronic structure of WTe_2 show that the configuration and the temperature dependence of its Fermi surface, as well as band dispersion along the direction coinciding with the direction of the metallic chains can explain the main features of the "titanic " MR effect [17]. Our results suggest that the large unidirectional MR originates from small and, at low-T, perfectly balanced electron and hole Fermi pockets that are very near each other and aligned along the most conductive (chain) direction (Fig. 2). In the semi-classical picture, the prefect balance between electrons and holes gives a quadratic, non-saturating MR. WTe_2 is the only perfectly balanced material known so far. With increasing temperature, the balance is lost as electrons start to dominate and, consequently, MR disappears.

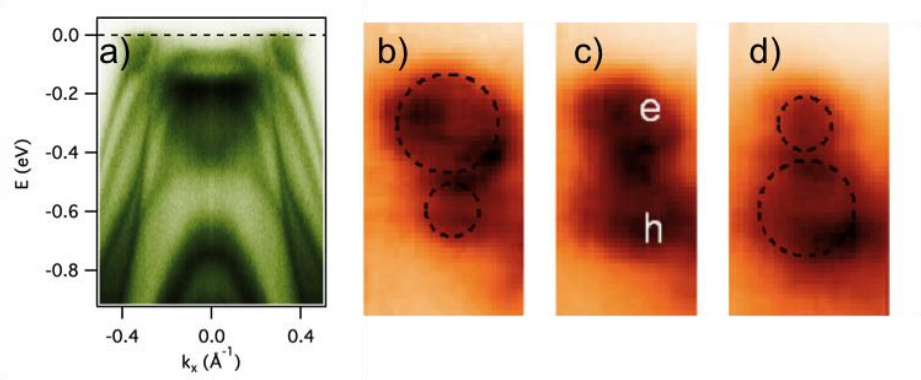

Figure . The measured electronic structure of WTe_2 along the G-X direction of the surface Brillouin zone (a) shows tiny electron and hole pockets (b-d) of exactly the same size at low temperature (c) – an origin of extreme MR.

Future Plans

The group's contribution in design/construction of the Electron Spectro-Microscopy (ESM) and the infrared MET beamlines at NSLS II will allow ARPES and infrared studies of complex materials at the microscopic level. The group is also leading the OASIS project – the integration of precise Oxide Molecular Beam Epitaxy (OMBE) synthesis of correlated oxides with ARPES and state-of-the-art SI-STM in a single instrument. OASIS will be a science-driven facility, enabling in-situ SI-STM and ARPES studies of single-crystal films of a dramatically wider variety of correlated oxides, oxide heterostructures and topological materials than heretofore. The group is also developing a laser-based time-of-flight ARPES facility that will enable studies of transient phenomena and the dynamics of carriers in correlated materials.

References

[1] M. N. Ali, J. Xiong, S. Flynn, J. Tao, Q. D. Gibson, L. M. Schoop, et al., Large, non-saturating magnetoresistance in WTe_2, Nature (London) **514**, 205 (2014).
[2] Kefeng Wang, D. Graf, Lijun Li, C. Petrovic, Anisotropic giant magnetoresistance in $NbSb_2$, Scientific Reports **4**, 7328 (2014).
[3] Tian Liang, Quinn Gibson, Mazhar N. Ali, Minhao Liu, et al., Ultrahigh mobility and giant magnetoresistance in the Dirac semimetal Cd3As2, Nature Materials 14, 280–284 (2015).

Publications

[4] M. Petrovic, I.S. Rakic, S. Runte, C. Busse, J.T. Sadowski, P. Lazic, et al., The mechanism of caesium intercalation of graphene, Nat. Commun. **4** (2013) 2772.
[5] C.C. Homes, T. Vogt, COLOSSAL PERMITTIVITY MATERIALS Doping for superior dielectrics, Nat. Mater. **12** (2013) 782.
[6] A. Gyenis, I.K. Drozdov, S. Nadj-Perge, O.B. Jeong, et al., Quasiparticle interference on the surface of the topological crystalline insulator $Pb_{1-x}Sn_xSe$, Phys. Rev. B. **88** (2013) 125414.
[7] Q.D. Gibson, L.M. Schoop, A.P. Weber, H. Ji, S. Nadj-Perge, I.K. Drozdov, et al., Termination-dependent topological surface states of the natural superlattice phase Bi_4Se_3, Phys. Rev. B. **88** (2013) 081108.
[8] Y.M. Dai, B. Xu, B. Shen, H. Xiao, H.H. Wen, X.G. Qiu, et al., Hidden T-Linear Scattering Rate in $Ba_{0.6}K_{0.4}Fe_2As_2$ Revealed by Optical Spectroscopy, Phys. Rev. Lett. **111** (2013) 117001.
[9] C.C. Homes, J.J. Tu, J. Li, G.D. Gu, A. Akrap, Optical conductivity of nodal metals, Sci. Rep. **3** (2013) 3446.

[10] S.K. Kushwaha, Q.D. Gibson, J. Xiong, I. Pletikosic, A.P. Weber, A. V Fedorov, et al., Comparison of Sn-doped and nonstoichiometric vertical-Bridgman-grown crystals of the topological insulator Bi_2Te_2Se, J. Appl. Phys. **115** (2014) 143708.
[11] A. Akrap, Y.M. Dai, W. Wu, S.R. Julian, C.C. Homes, Optical properties and electronic structure of the nonmetallic metal FeCrAs, Phys. Rev. B. **89** (2014) 125115.
[12] Y.M. Dai, A. Akrap, J. Schneeloch, R.D. Zhong, T.S. Liu, G.D. Gu, et al., Spectral weight transfer in strongly correlated $Fe_{1.03}Te$, Phys. Rev. B. **90** (2014) 121114.
[13] S. V Dordevic, D. van der Marel, C.C. Homes, Fate of quasiparticles in the superconducting state, Phys. Rev. B. **90** (2014) 174508.
[14] J.D. Rameau, S. Freutel, L. Rettig, I. Avigo, M. Ligges, Y. Yoshida, et al., Photoinduced changes in the cuprate electronic structure revealed by femtosecond time- and angle-resolved photoemission, Phys. Rev. B. **89** (2014) 115115.
[15] J.D. Rameau, T.J. Reber, H.-B. Yang, S. Akhanjee, G.D. Gu, P.D. Johnson, Nearly perfect fluidity in a high-temperature superconductor, Phys. Rev. B. **90** (2014) 134509.
[16] C. Ma, L. Wu, W.-G. Yin, H. Yang, H. Shi, et al., Strong Coupling of the Iron-Quadrupole and Anion-Dipole Polarizations in $Ba(Fe_{1-x}Co_x)_2As_2$, Phys. Rev. Lett. **112** (2014) 077001.
[17] I. Pletikosic, M.N. Ali, A. V Fedorov, R.J. Cava, T. Valla, Electronic Structure Basis for the Extraordinary Magnetoresistance in WTe_2, Phys. Rev. Lett. **113** (2014) 216601.
[18] I. Pletikosic, G.D. Gu, T. Valla, Inducing a Lifshitz Transition by Extrinsic Doping of Surface Bands in the Topological Crystalline Insulator Pb1-xSnxSe, Phys. Rev. Lett. **112** (2014) 146403.
[19] T. Yilmaz, I. Pletikosic, A.P. Weber, J.T. Sadowski, G.D. Gu, A.N. Caruso, et al., Absence of a Proximity Effect for a Thin-Films of a Bi_2Se_3 Topological Insulator Grown on Top of a $Bi_2Sr_2CaCu_2O_{8+\delta}$ Cuprate Superconductor, Phys. Rev. Lett. **113** (2014) 067003.
[20] J. Buhot, M.A. Measson, Y. Gallais, M. Cazayous, A. Sacuto, F. Bourdarot, et al., Lattice dynamics of the heavy-fermion compound URu_2Si_2, Phys. Rev. B. **91** (2015) 035129.
[21] C.C. Homes, Y.M. Dai, J.S. Wen, Z.J. Xu, G.D. Gu, $FeTe_{0.55}Se_{0.45}$: A multiband superconductor in the clean and dirty limit, Phys. Rev. B. **91** (2015) 144503.
[22] R.P.S.M. Lobo, J. Buhot, M.A. Measson, D. Aoki, G. Lapertot, et al., Optical conductivity of URu_2Si_2 in the Kondo liquid and hidden-order phases, Phys. Rev. B. **92** (2015) 045129.
[23] B. Xu, Y.M. Dai, B. Shen, H. Xiao, Z.R. Ye, A. Forget, et al., Anomalous phonon redshift in K-doped $BaFe_2As_2$ iron pnictides, Phys. Rev. B. **91** (2015) 104510.
[24] R. Zhong, X. He, J.A. Schneeloch, C. Zhang, T. Liu, I. Pletikosic, et al., Surface-state-dominated transport in crystals of the topological crystalline insulator In-doped $Pb_{1-x}Sn_xTe$, Phys. Rev. B. **91** (2015) 195321.
[25] C.J. Arguello, E.P. Rosenthal, E.F. Andrade, W. Jin, P.C. Yeh, N. Zaki, et al., Quasiparticle Interference, Quasiparticle Interactions, and the Origin of the Charge Density Wave in 2H-$NbSe_2$, Phys. Rev. Lett. **114** (2015) 037001.
[26] P.D. Johnson, H.-B. Yang, J.D. Rameau, G.D. Gu, et al., Spin-Orbit Interactions and the Nematicity Observed in the Fe-Based Superconductors, Phys. Rev. Lett. **114** (2015) 167001.
[27] A.P. Weber, Q.D. Gibson, H. Ji, A.N. Caruso, A. V Fedorov, R.J. Cava, et al., Gapped Surface States in a Strong-Topological-Insulator Material, Phys. Rev. Lett. **114** (2015) 256401.
[28] I. Lee, C.K. Kim, J. Lee, S.J.L. Billinge, R. Zhong, J.A. Schneeloch, et al., Imaging Dirac-mass disorder from magnetic dopant atoms in the ferromagnetic topological insulator $Cr_x(Bi_{0.1}Sb_{0.9})_{2-x}Te_3$, Proc. Natl. Acad. Sci. U. S. A. **112** (2015) 1316.

Project Title: Electronic complexity of epitaxial rutile heterostructures

Principal Investigator: H.H. Weitering
Co-PIs: P.C. Snijders, P.R.C. Kent, and T. Berlijn

Mailing Address: Oak Ridge National Laboratory, PO Box 2008 MS-6056
Oak Ridge, TN 37831-6056

Email: hanno@utk.edu

Program scope

This is a new program that commenced in FY 2014. The overarching goal is to understand and tailor the electronic complexity of epitaxial rutile heterostructures. The presence of edge-shared MO_6 octahedra (M=metal cation) and formation of direct cation-cation bonds in the rutile structure tends to lower the effective dimensionality of the electronic structure, compared to corner-shared perovskite systems. Our focus will center on exploiting quantum mechanical confinement to tailor the electronic structure and orbital order of epitaxial rutile heterostructures. The existence of the two (001) and (110) growth orientations, along with the extreme anisotropy of the metal-metal σ-bonds, offers a unique opportunity to vary the occupation of selected $3d$-t_{2g} orbitals via quantum confinement, and their coupling to the other degrees of freedom. Tuning parameters include film thickness, substrate orientation, dielectric properties of the boundary materials, and chemical doping. Our approach involves epitaxial synthesis via Molecular Beam Epitaxy (MBE), *in situ* photo-electron spectroscopy, scanning tunneling microscopy (or spectroscopic STM), *ab initio* density functional theory (DFT) and post-DFT calculations.

Recent progress

1. **New oxide MBE system –** We have designed and constructed an ultrahigh vacuum (UHV) oxide molecular beam epitaxy system, connected to an existing UHV sample characterization facility that includes a variable temperature scanning tunneling microscope and low energy electron diffraction. The MBE chamber features thermal as well as electron beam evaporation sources for cation evaporation, an oxygen plasma source to control cation oxidation states at low oxygen pressures, a fast laser-based sample heater, and reflection high energy electron diffraction. An Auger spectrometer capable of operating in high oxygen pressures during sample growth is currently being commissioned. It will allow for real time monitoring of surface chemical composition during thin film growth.

2. **Film growth –** We succeeded in growing epitaxial RuO_2(110) films on TiO_2 (110). The corresponding STM image is shown in the left panel below. Besides the (110) orientation,

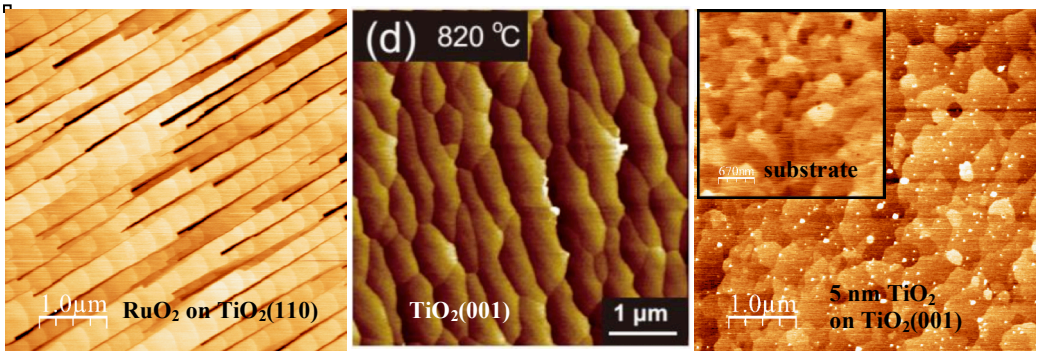

kinetic stabilization of the (001) orientation is critically important for this project. It would allow for quantum confinement studies in (001) oriented rutile films where the electronic structure is confined along the rutile c-axis. TiO_2(001) has a large surface energy, however, and its surface easily facets, thus hindering efforts to grow atomically flat (001) rutile films. We succeeded preparing atomically-smooth TiO_2(001) substrates through an elaborate process of chemical etching and ex-situ furnace annealing. The AFM image in the middle panel clearly reveals the presence of smooth (001) terraces. Interestingly, the atomically-flat morphology remains stable up 500 °C. Hence, it is possible to grow atomically smooth TiO_2(001) films with PLD (right panel). This homo-epitaxial growth experiment was done in collaborations with H.N. Lee.

3. **Antiferromagnetic RuO_2 –** Our DFT(+U) studies unexpectedly indicate that bulk RuO_2 (Ru $4d^4$) is an itinerant antiferromagnet for a large range of U (see table). The magnetic structure predicted by DFT does not increase the size of the rutile unit cell. Rather, it features ferromagnetic Ru chains that run parallel to the rutile c-axis, where the moments on the two Ru atoms

PBE+U=2eV	M-Ru$_1$(μ_B)	M-Ru$_2$(μ_B)	E_{tot}(meV)
AFM	1.173	-1.074	0
NM	0.000	0.000	61

PBE+U=3eV	M-Ru$_1$(μ_B)	M-Ru$_2$(μ_B)	E_{tot}(meV)
AFM	1.442	-1.414	0
NM	0.000	0.000	209
FM	1.437	1.545	428

PBE+U=4eV	M-Ru$_1$(μ_B)	M-Ru$_2$(μ_B)	E_{tot}(meV)
AFM	1.575	-1.564	0
NM	-0.008	-0.008	389
FM	1.646	1.742	452

HSE06	M-Ru$_1$(μ_B)	M-Ru$_2$(μ_B)	E_{tot}(meV)
AFM	1.438	-1.424	0
NM	0.000	0.000	293

inside the rutile unit cell are antiparallel (see figure, inset left panel). Guided by these theory results, we grew bulk single crystal RuO_2 samples (collaboration H. Zhou, UTK), measured their magnetic susceptibility, and performed neutron scattering experiments (collaboration with O. Delaire). The temperature dependence of the susceptibility resembles that of Cr (figure, right panel), and suggests a Néel temperature of 925 K. Neutron diffraction

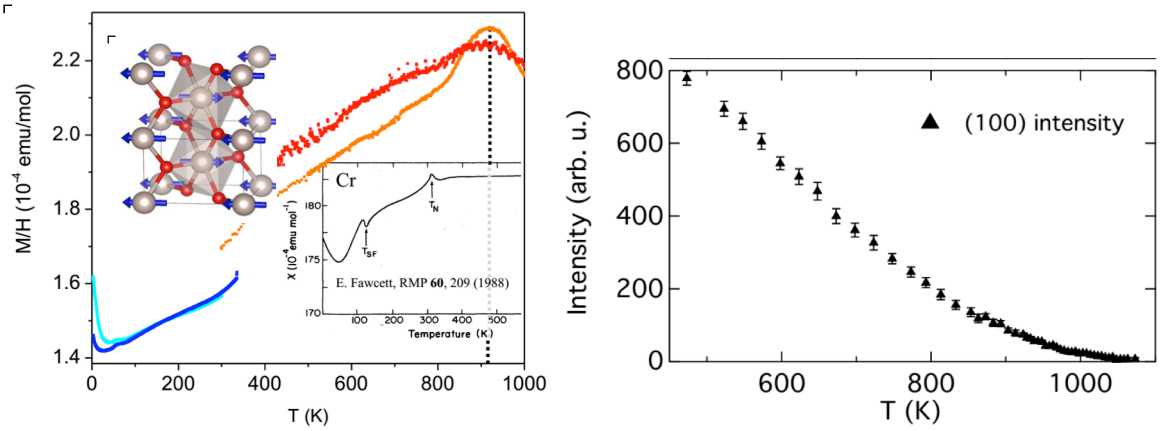

experiments reveal structurally "forbidden" peaks that are absent in x-ray diffraction from the same crystal. The intensity of the structurally forbidden (100) peak, measured with neutron scattering (right panel), decreases gradually with temperature, suggesting that magnetic ordering vanishes near 1000 K. The structural Bragg peaks only loose ~25% of their integrated intensity in this temperature range.

Future plans

Antiferromagnetism in bulk RuO_2. We will further analyze the antiferromagnetic order in bulk RuO_2. This will include expanding the temperature range accessed in neutron scattering to low temperatures, so as to determine the full temperature dependence of the magnetic order parameter, and possibly elucidate the origins of the concave temperature dependence of the order parameter above room temperature. We will also attempt a neutron structural refinement to extract the specific type of antiferromagnetic order, as well as the magnetic moment per Ru atom.

RuO_2 is clearly metallic and its 4d-bands are quite delocalized. Hence, RuO_2 represents a novel itinerant antiferromagnet. Our RPA calculations of the static susceptibility of the nonmagnetic phase reveals clear peaks at $\boldsymbol{q} = (2\pi,0)$ and $(0,2\pi)$, consistent with the predicted magnetic order. Here, the dominating contributions to the susceptibility arise from cusp-like parts of the Fermi surface. The magnetic transition wipes out large sections of the Fermi surface, while the calculated density of states is still metallic and resembles published low-resolution photoelectron spectroscopy data. These theoretical observations call for detailed investigation of the electronic structure by means of high-resolution ARPES.

We will grow a thick RuO_2 film in order to perform *in situ* ARPES on a 'bulk' sample with a well-defined atomically clean stoichiometric surface. The existence of fluctuating local moments will be investigated by examining possible multiplet splittings in the Ru core level spectra.

Quantum confined (001) rutile films. In rutile oxides, there is direct metal-metal bonding along the crystallographic c-axis. This is made possible by the edge-sharing of the metal-oxygen octahedra along this direction, allowing the metal cations to interact without having an oxygen ion in between. In bulk VO_2 this results in a structural dimerization in the M-phase below the metal-insulator transition at 340 K. Quantizing the anisotropic *d*-bands resulting from the metal-metal interaction along the c-axis by quantum confinement is expected to destabilize this ground state, and create novel electronic phases not present in the bulk. Theoretical calculations indeed indicate that a novel semi-Dirac phase can be formed in 3 ML thick VO_2 films [1]. We plan to grow such confined VO_2 films on TiO_2(001), i.e. with the rutile c-axis out of plane, and measure their electronic structure focusing on *in situ* electron spectroscopy, as a function of confinement.

In contrast to VO_2, RuO_2 does not dimerize in the bulk. Its large 4*d* band width is however susceptible to quantization upon confinement. This selective quantization of the orbitals with a component along the confinement direction will lead to a redistribution of electron occupancy over the different *d*-orbitals [2], and subband dependent electronic correlation strengths. Our preliminary DFT calculations of the magnetic structure of 3 ML RuO_2 films sandwiched between TiO_2(001) predict that the ground state is, like the bulk, antiferromagnetic, but with a different magnetic order: Ru atoms along the c-axis exhibit antiparallel moments, meaning that the magnetic unit cell has doubled. As experimental verification of antiferromagnetism in ultrathin films is extremely challenging, we will initially focus on consistency between the theoretical band structure and experimental electron spectroscopy data obtained using scanning tunneling and photoelectron spectroscopy.

References

[1] V. Pardo, and W.E. Pickett, "Metal-insulator transition through a semi-Dirac point in oxide nanostructures: VO_2(001) layers confined within TiO_2," Phys. Rev. B **81**, 035111 (2010).
[2] K. Yoshimatsu, K. Horiba, H. Kumigashira, T. Yoshida, A. Fujimori, and M. Oshima, "Metallic quantum well states in artificial structures of strongly correlated oxide," Science **333**, 319 (2011).

List of publications from this project

There are no accepted publications yet, due to the recent start of this project, and the design, acquisition and build-up of the oxide growth facility. One paper is under revision, and one paper is in preparation.

Charge inhomogeneity in correlated electron systems: charge order or not

Principal Investigator: Barrett O. Wells
Mailing Address: Department of Physics, University of Connecticut, Storrs, CT 06269-3046
E-mail: wells@phys.uconn.edu

Program Scope

The goal of this program is to develop an understanding of how and why conduction electrons arrange themselves in correlated electron systems, with particular emphasis on superconducting and closely related materials. Our strategy is to explore materials in which dopants can be controlled in a manner that leads to interesting properties. This primarily means comparing the properties of similar compounds doped with highly mobile oxygen defects compared to static cation substitutions. The different dopants lead to differences in charge ordering and in some cases electronic phase separation. In the cases we study, oxygen can be incorporated topotactically, at lower temperatures within an already formed crystalline network.

The systems we study include both materials related to copper-oxide superconductors and Fe-based superconductors. In the cuprate-like materials we focus on unique properties of those compounds doped with mobile excess oxygen, including $La_{2-x}Sr_xCuO_{4+y}$ (LSCO+O) and nickelate compounds such as $Pr_2NiO_{4.25}$ (PNO+O). In both compounds the excess, interstitial oxygen is highly mobile. Compounds with such mobile charge dopant ions tend to phase separate over long length scales. This phase separation may include differing crystal structures but often involves primarily the local charge density. As an example, superoxygenated LSCO+O at sufficiently high hole doping levels electronically phase separates to large regions with optimally doped superconductivity and other regions with no superconductivity but a well-developed spin density wave. [1,2]

Our study of Fe-based superconductors aims to understand the exact role of dopants in producing a superconductor from a parent compound. Generally, both isovalent and heterovalent dopants can be used to create a superconductor from a parent compound, and sometimes pressure without doping will do the same. While one role of the doping process involves suppressing ordered magnetism, just how that happens is unclear; so, for example, exactly why FeTe is a parent compound while FeSe is a superconductor is not well understood. We study the co-doped system $FeTe_{1-x}Se_xO_y$. Either isovalent doping of Se onto Te sites or charge doping with excess oxygen will produce a superconductor from the parent FeTe. Oxygen doping of FeTe is difficult as oxygen mobility is very low, but can be accomplished in films. [3] Superconductivity in these films is robust with considerable Meissner signals. Superconducting $FeTeO_y$ has some intriguing properties. Of particular note is that FeTeOx not only retains magnetism similar to FeTe, but the superconducting form has stronger magnetic neutron scattering than does the parent FeTe compound. There are a variety of curious properties in the Fe valence, conductivity, and magnetism.

Recent Progress

Charge order modeled as stripes separating similarly striped magnetic regions was discovered in using neutron scattering in 214-type cuprates, most notably in compounds such as

$La_{1.875}Ba_{0.125}CuO_4$ where superconductivity is suppressed.[4] More recently, the charge-order nature of the scattering was confirmed with resonant soft x-ray scattering. [5] The resonance process leads to a dramatic increase of the charge order scattering intensity. Using this technique charge order has now been found in most every family of cuprate superconductors, though in most systems without the obvious connection to incommensurate magnetic order.[6]

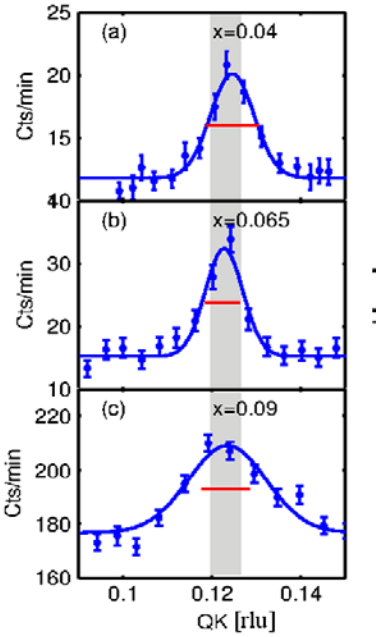

Figure 1. Magnetic neutron scattering profiles from a set of $La_{2-x}CuO_{4+y}$ samples co-doped with O and Sr. The value listed for x gives the Sr concentration only. The total hole concentration is approximately equal in all three samples and near n_h=0.14. The red bar represents the resolution.

La_2CuO_4 can be doped to be a superconductor using cation substitution for La, the addition of excess oxygen, or co-doped with a mixture of both. The oxygen doped system is less studied as incorporating sufficient amount of excess oxygen takes unusual techniques and long preparation times. However, the oxygen doped system has several interesting properties including large length scale electronic phase separation between a magnetic phase and a superconducting phase. Our recent work established that the magnetic phase matches the 1/8th doped LBCO material while the superconducting phase matches optimally doped $La_{1.84}Sr_{0.16}CuO_4$. Of particular note is that the magnetic phase gives rise to elastic magnetic neutron scattering peaks at least as strong and sharp as has been reported in any cuprate. Thus if the model of charge stripes as antiphase domain boundaries to magnetic regions were to hold, we expect strong, sharp charge order peaks as well.

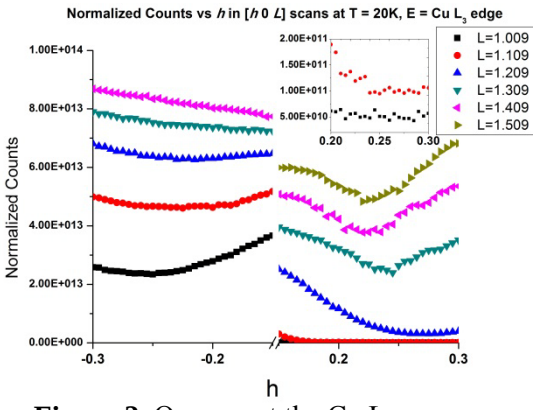

Figure 2. Q-scans at the Cu L_3 absorption energy searching for charge order peaks at the expected (0.25,0,L) position. Nothing is detected.

Our group has performed several searches for such peaks. We have employed neutron scattering, high energy x-ray scattering, and most recently resonant soft x-ray scattering. Based upon the known magnetic scattering profile and results from similar compounds, we expect the charge order scattering near the Q position (0.25,0,1.5) and symmetry equivalent positions. The L position does depend upon layer by layer stacking, which may vary from other samples, though the charge order scattering is typically broad in L. A typical set of spectra for the resonant scattering search is shown in figure 2, showing nothing but a varying background. Occasionally we find trace signals, however none

have had the temperature dependence or symmetry partners appropriate for charge order peaks. In addition, none have intensity and width expected based upon the magnetic scattering.

The lack of charge order peaks in this very robust 214-type cuprate superconductor despite the presence of very strong, sharp magnetic order would seem to pose a powerful challenge to the popular stripe model. In addition, it would appear to counter the emerging view that charge order near $1/8^{th}$ doping is ubiquitous in cuprate superconductors. Of course proving a negative is difficult and our challenge is to determine what comprises adequate evidence.

In a similar vein we have undertaken a study of 214-nickelate compounds with doping provided by interstitial oxygen ions. The 214-nickelates, particularly $La_{2-x}Sr_xNiO_4$ with x=1/3 have been the canonical material for combined charge and spin order into stripes. We have begun a study of Pr_2NiO_{4+y}, where the Pr ion promotes higher oxygen concentrations and allows us to look at high doping levels and the effect of mobile dopants. Our first studies are on samples with oxygen concentration near $Pr_2NiO_{4.25}$, or doped near ½ hole per Ni ion. These higher doping levels are mostly unexplored. We have found likely charge order peaks at q=(0.35,0.35,0). Scattering at this position extends to the surprisingly high temperature of 200K, coincident to the LTO-LTT transition. Perhaps more interestingly, we have found strong scattering on resonance of the nominally disallowed (001) peak. This peak can become allowed on resonance associated with orbital order. We find strikingly different temperature dependence of the (001) peak on the in-plane Ni L_3 resonance compared to the Pr M-edge resonance, as shown in figure 3. This behavior is nominally similar to that recently found in $La_{1.875}Ba_{0.125}CuO_4$ by Achkar et al. and associated with an extra nematic order parameter in the sample. Whether a similar explanation can be extended to the nickelate requires further study.

Figure 3

Temperature dependence on resonance of the nominally disallowed (001) peak. The peak is only visible at resonance, with drasticlaly different temperature dependence on the Ni L and Pr M absorption edges.

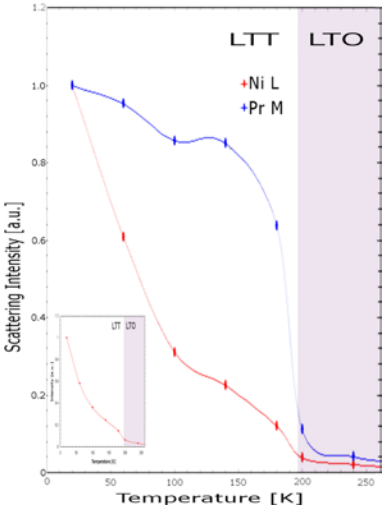

Future Plans

Our immediate plans are to confirm the results described above. In particular we are currently attempting to determine what constitutes acceptable evidence for a lack of charge order in phase separated, $La_{2-x}Sr_xCuO_{4+y}$. Future experiments include exploring whether these compounds have any signs of the nematic behavior that has been reported for samples such as $La_{1.875}Ba_{0.125}CuO_4$ even though they seem to only show magnetic stripe order without clear charge order. For example, we have preliminary results that the (001) peak does become allowed at resonance even without charge order – which may reflect upon the nematicity. This could shed light on the driving force for such effects.

The Pr_2NiO_{4+y} experiments have just begun. The first order of business is to establish a clear identification of the various peaks we have measured on and off resonance. We also need to

explore the oxygen concentration phase diagram, and begin to look at co-doping with oxygen and cation substitution. There is some indication for a similar electronic phase separation as reported in the oxygenated cuprates, but differences between insulating (nickelate) and conducting (cuprate) samples remain to be explored.

References

1. A.Savici "Muon spin relaxation studies of incommensurate magnetism and superconductivity in stage-4 $La_2CuO_{4.11}$ and $La_{1.88}Sr_{0.12}CuO4$" Phys. Rev. B **66**, 014524 (2002)
2. Hashini E. Mohottala, et al, "Phase Separation in Superoxygenated $La_{2-x}Sr_xCuO_{4+y}$" Nature Materials **5**, 377 (2006)
3. Y. Nie, Y., et al, "Superconductivity induced in iron telluride films by low-temperature oxygen incorporation." *Phys. Rev. B* **82**, 020508 (2010)
4. J. M. Tranquadaet al., " Evidence for stripe correlations of spins and holes in copper oxide superconductors" *Nature* **375**, 561 (1995).
5. P. Abbamonte, "Spatially modulated 'Mottness' in $La_{2-x}Ba_xCuO_4$" *Nature Phys* **1**, 155 (2005)
6. G. Ghiringhelli, et al."Long-range incommensurate charge fluctuations in $(Y,Nd)Ba_2Cu_3O_{6+x}$". *Science* **337**, 821–825 (2012); R.A. Comin et al, "Charge Order Driven by Fermi-Arc Instability in $Bi_2Sr_{2-x}La_xCuO_{6+\delta}$" Science **343**, 390 (2014); da Silva Neto et al, "Ubiquitous Interplay Between Charge Ordering and High-Temperature Superconductivity in Cuprates" *Science* **24**, 393 (2014). W. Tabis et al, "Charge order and its connection with Fermi-liquid charge transport in a pristine high-T_c cuprate" Nature Comm **5**, 5875 (2014).

Publications

1. L.K. Narangammana, Z.W. Zhang, J.I. Budnick, W.A. Hines, J.W. Lynn, Ch. Niedermayer, E.E. Alp, W. Bi, M.Y. Hu, J. Zhao, D.G. Hinks, D.E. Brown, B.O. Wells, "Excess magnetism in superconducting films of FeTeOx" in preparation
2. L. K. Narangammana, Y. F. Nie, F. J. Rueckert, J. I. Budnick, W. A. Hines, G. Gu, and B. O. Wells, "Control of crystalline morphology and superconductivity in growth of $FeTeO_x$ superconducting films" in preparation.
3. F. J. Rueckert, F. He, B. Dabrowski, W.A. Hines, B. O. Wells, Charge order in $SrCoO_3$ investigated through resonant soft x-ray scattering" submitted to *Physical Review Letters*.
4. L. Udby, J. Larsen, N. B. Christensen, M. Boehm, Ch. Niedermayer, H. E. Mohottala, T. B. S. Jensen, R. Toft-Petersen, F. C. Chou, N. H. Andersen, K. Lefmann, B. O. Wells "Measurement of unique magnetic and superconducting phases in superoxygenated high-Tc cuprates" *Phys. Rev. Lett*. **111**, 227001 (2013).
5. L. K. Narangammana, X. Liu, Y. F. Nie, F. J. Rueckert, J. I. Budnick, W. A. Hines, G. Gu, and B. O. Wells, "Low temperature crystal structure and large lattice discontinuity at Tc in superconducting $FeTeO_x$ films" *Appl. Phys. Lett*. **103**, 102604 (2013).
6. D. Telesca, Y. Nie, J.I. Budnick, B.O. Wells, B. Sinkovic "Surface valence states and stoichiometry of non-superconducting and superconducting FeTe films" *Surf. Sci*. **606**, 1056-1061 (2012).
7. D. Telesca, Y. Nie, J. I. Budnick, B. O. Wells, and B. Sinkovic, "Impact of valence states on the superconductivity of iron telluride and iron selenide films with incorporated oxygen" *Phys. Rev. B* **85**, 214517 (2012).

Author Index

Author Index

Participant List

Participant List

Adams, Philip	Louisiana State University	adams@phys.lsu.edu
Analytis, James	University of California, Berkeley	analytis@berkeley.edu
Ashoori, Raymond	Massachusetts Institute of Technology	ashoori@mit.edu
Balicas, Luis	National High Magnetic Field Laboratory	balicas@magnet.fsu.edu
Basov, Dmitri	University of California, San Diego	dbasov@ucsd.edu
Bawendi, Moungi	Massachusetts Institute of Technology	mgb@mit.edu
Beach, Geoffrey	Massachusetts Institute of Technology	gbeach@mit.edu
Bhattacharya, Anand	Argonne National Laboratory	anand@anl.gov
Bird, Jonathan	University at Buffalo, SUNY	jbird@buffalo.edu
Birge, Norman	Michigan State University	birge@pa.msu.edu
Buchanan, Kristen	Colorado State University	kbuchan@colostate.edu
Butov, Leonid	University of California, San Diego	lvbutov@physics.ucsd.edu
Cha, Judy	Yale University	judy.cha@yale.edu
Civale, Leonardo	Los Alamos National Laboratory	lcivale@lanl.gov
Csathy, Gabor	Purdue University	gcsathy@purdue.edu
Davenport, James	US DOE– Office of Basic Energy Sciences	james.davenport@science.doe.gov
Davidovic, Dragomir	Georgia Institute of Technology	dragomir.davidovic@physics.gatech.edu
Dessau, Dan	University of Colorado	dessau@colorado.edu
DiTusa, John	Louisiana State University	ditusa@phys.lsu.edu
Eom, Chang-Beom	University of Wisconsin-Madison	eom@engr.wisc.edu
Fecko, Christopher	US DOE– Office of Basic Energy Sciences	Christopher.Fecko@science.doe.gov
Field, Stuart	Colorado State University	stuart.field@colostate.edu
Finkelstein, Gleb	Duke University	gleb@phy.duke.edu
Fischer, Peter	Lawrence Berkeley National Laboratory	PJFischer@lbl.gov
Fisher, Ian	Stanford University	irfisher@stanford.edu
Graf, Matthias	US DOE– Office of Basic Energy Sciences	matthias.graf@science.doe.gov
Guyot-Sionnest, Philippe	University of Chicago	pgs@uchicago.edu
Haglund, Richard	Vanderbilt University	richard.haglund@vanderbilt.edu
Halperin, Bill	Northwestern University	w-halperin@northwestern.edu
Harrison, Neil	Los Alamos National Laboratory	nharrison@lanl.gov
Hellman, Frances	Lawrence Berkeley National Lab, UC Berkeley	fhellman@berkeley.edu
Henderson, Craig	US DOE– Office of Basic Energy Sciences	craig.henderson@science.doe.gov
Heremans, Jean J.	Virginia Tech	heremans@vt.edu
Hla, Saw Wai	Ohio University	hla@ohio.edu
Hoffmann, Axel	Argonne National Laboratory	hoffmann@anl.gov
Horwitz, Jim	US DOE– Office of Basic Energy Sciences	james.horwitz@science.doe.gov
Hsieh, David	Caltech	dhsieh@caltech.edu
Hwang, Harold	Stanford & SLAC	hyhwang@stanford.edu
Jarillo-Herrero, Pablo	Massachusetts Institute of Technology	pjarillo@mit.edu
Jiang, Zhigang	Georgia Institute of Technology	zhigang.jiang@physics.gatech.edu
Kaminski, Adam	Ames Laboratory	kaminski@ameslab.gov
Ketterson, John	Northwestern University	j-ketterson@northwestern.edu
Kim, Philip	Harvard University	pkim@physics.harvard.edu
Kono, Junichiro	Rice University	kono@rice.edu
Koschny, Thomas	Ames Laboratory, Iowa State University	koschny@ameslab.gov
Krivorotov, Ilya	University of California, Irvine	ikrivoro@uci.edu
Kunchur, Milind	University of South Carolina	kunchur@sc.edu
Kwok, Wai-Kwong	Argonne National Laboratory	wkwok@anl.gov
Lau, Chun Ning (Jeanie)	University of California, Riverside	lau@physics.ucr.edu
Lee, Ho Nyung	Oak Ridge National Laboratory	hnlee@ornl.gov
Lee, Minhyea	University of Colorado Boulder	minhyea.lee@colorado.edu
Lemberger, Thomas	The Ohio State University	trl@physics.osu.edu
Levy, Jeremy	University of Pittsburgh	jlevy@pitt.edu

Li, Lu	University of Michigan	luli@umich.edu
Li, Qi	Pennsylvania State University	qil1@psu.edu
Litchinitser, Natalia	University at Buffalo, SUNY	natashal@buffalo.edu
Luepke, Gunter	College of William and Mary	Luepke@wm.edu
MacDougall, Gregory	University of Illinois at Urbana-Champaign	gmacdoug@illinois.edu
Mak, Kin Fai	Penn State University	kzm11@psu.edu
Manfra, Michael	Purdue University	mmanfra@purdue.edu
Mani, Ramesh	Georgia State University	rmani@gsu.edu
Mao, Jinhai	Rutgers University	jhmao@physics.rutgers.edu
Maple, M. Brian	University of California, San Diego	mbmaple@ucsd.edu
Maracas, George	US DOE– Office of Basic Energy Sciences	george.maracas@science.doe.gov
Mason, Nadya	University of Illinois at Urbana-Champaign	nadya@illinois.edu
McGuire, Michael	Oak Ridge National Laboratory	mcguirema@ornl.gov
Mitchell, John	Argonne National Laboratory	Mitchell@anl.gov
Musfeldt, Janice	University of Tennessee	musfeldt@utk.edu
Natelson, Douglas	Rice University	natelson@rice.edu
Ni, Ni	University of California, Los Angeles	nini@physics.ucla.edu
Orenstein, Joseph	Lawrence Berkeley National Laboratory	jworenstein@lbl.gov
Osgood, Richard	Columbia University	osgood@columbia.edu
Ouyang, Min	University of Maryland - College Park	mouyang@umd.edu
Paglione, Johnpierre	University of Maryland	paglione@umd.edu
Palmstrøm, Chris	University of California, Santa Barbara	cpalmstrom@ece.ucsb.edu
Pan, Wei	Sandia National Laboratories	wpan@sandia.gov
Pechan, Michael	US DOE– Office of Basic Energy Sciences	michael.pechan@science.doe.gov
Perry, Kelly	U. S. Department of Energy	kelly.perry@science.doe.gov
Phelan, Daniel	Argonne National Laboratory	dphelan@anl.gov
Pinczuk, Aron	Columbia University	aron@physics.columbia.edu
Prozorov, Ruslan	Ames Laboratory	prozorov@ameslab.gov
Rhyne, James	US DOE– Office of Basic Energy Sciences	james.rhyne@science.doe.gov
Rokhinson, Leonid	Purdue University	leonid@purdue.edu
Rosenbaum, Thomas	University of Chicago / Caltech	tfr@caltech.edu
Schiffer, Peter	University of Illinois at Urbana-Champaign	chamber1@illinois.edu
Schuller, Ivan	University of California, San Diego	ischuller@ucsd.edu
Sefat, Athena	Oak Ridge National Laboratory	sefata@ornl.gov
Sellmyer, David	University of Nebraska	dsellmyer@unl.edu
Severs, Linda	Oak Ridge Institute for Science & Education	Linda.Severs@orau.org
Shayegan, Mansour	Princeton University	shayegan@princeton.edu
Smirnov, Dmitry	National High Magnetic Field Laboratory	smirnov@magnet.fsu.edu
Thomas, John	North Carolina State University	jethoma7@ncsu.edu
Valla, Tonica	Brookhaven National Laboratory	valla@bnl.gov
Valls, Oriol	University of Minnesota	otvalls@umn.edu
Weitering, Hanno	University of Tennessee, Oak Ridge National Lab	hanno@utk.edu
Wells, Barrett	University of Connecticut	wells@phys.uconn.edu
Welp, Ulrich	Argonne National Laboratory	welp@anl.gov
Westervelt, Robert	Harvard University	westervelt@seas.harvard.edu
Wilson, Lane	US DOE–Basic Energy Sciences, DMSE	lane.wilson@science.doe.gov
Yang, Fengyuan	The Ohio State University	fyyang@physics.osu.edu
Yazdani, Ali	Princeton University	yazdani@princeton.edu
Zettl, Alex	Lawrence Berkeley National Lab, UC Berkeley	azettl@physics.berkeley.edu
Zudov, Michael	University of Minnesota	zudov@physics.umn.edu